MM

Transport Canada
Development

Transports Canada
Développement

TP 5702E

# Segmented Model Testing in Ice
# Development of Techniques

*Summary Report*

Prepared for

Transportation
Development Centre

**SEPTEMBER 1984**

CA1
DTC 845
84
S25S
c.2

Canada

ARCTEC CANADA LIMITED SR 566C

# SEGMENTED MODEL TESTING IN ICE - DEVELOPMENT OF TECHNIQUES

SUMMARY REPORT
TP 5702E

SEPTEMBER 1984

A.M. Nawwar
D. Howard

Prepared for:

Transportation Development Centre,
1000 Sherbrooke Street West,
Montreal, Quebec.
H3A 2R3

Prepared by:

Arctec Canada Limited,
311 Legget Drive,
Kanata, Ontario.
K2K 1Z8

## DISCLAIMER

The contents of this report reflect the views of the contractor and not necessarily the official views or policies of the Transportation Development Centre.

## PROJECT TEAM

The project team consisted of:

A.M. Nawwar,
D. Howard,
M. Steele,
H. Blount,
C. Daley,
and others.

Egalement disponible en français.

"APPROVED BY ____________________

## REPORT DOCUMENTATION FORM

| | | |
|---|---|---|
| 1. Transport Canada Report No.<br>TP 5702E | 2. TDC Project No.<br>4847, 4848 | 3. Recipient's Catalogue No. |
| 4. Title and Subtitle<br>**SEGMENTED MODEL TESTING IN ICE - DEVELOPMENT OF TECHNIQUES**<br>**Summary Report** | | 5. Report Date<br>September 1984<br>6. Performing Organization Report No.<br>SR 566C |
| 7. Author(s)<br>Dr. A. Nawwar and Mr. D. Howard | | 8. Transport Canada File No.<br>D1460-194 |
| 9. Performing Organization Name and Address<br>Arctec Canada Limited<br>311 Leggett Drive<br>Kanata, Ontario<br>K2K 1Z8 | | 10. DSS File No.<br>10SD.T8200-2-2547<br>11. DSS or Transport Canada Contract No.<br>1SD82-00153 |
| 12. Sponsoring Agency Name and Address<br>Transportation Development Centre (TDC)<br>1000 Sherbrooke Street West<br>Suite 2421<br>Montreal, Quebec H3A 2R3 | | 13. Type of Report and Period Covered<br>Summary; Jan. 83-84<br>14. Sponsoring Agency Code<br>TDC 4847, 4848 |
| 15. Supplementary Notes | | 16. TDC Project Officer<br>Ian M. Bayly |

17. Abstract

This report describes the development of a new technique for testing model ships in ice. The technique consists of creating independent segments within the hull. Each segment is instrumented to monitor and define ice forces acting on the segment. The method of segmentation was developed with a view of the existing analytical models and components of ice resistance. The instrumentation system was designed and implemented to enable the complete definition of normal and frictional components of the ice load. The model was subjected to calibration and preliminary resistance testing in order to identify and correct its deficiencies. Preliminary results showed that the system is capable of measuring ice load location and magnitude; agreement with analytical expectations is good in terms of location, but the magnitude of ice load exhibits some difference. This finding indicates the capability of the model to examine and verify analytical models of ice forces and resistance. Further work is necessary to fine-tune the system and automate the data analysis process.

| | | | |
|---|---|---|---|
| 18. Key Words<br>Ships, Icebreaking, Model Tests, Hull Segments | | 19. Distribution Statement<br>Limited number of copies available from Transportation Development Centre | |
| 20. Security Classification (of this report)<br>Unclassified | 21. Security Classification (of this page)<br>Unclassified | 22. No. of Pages<br>28 | 23. Price<br>-- |

TDC CDT 79-005

# FORMULE DE DOCUMENTATION POUR RAPPORT

1. Nº du rapport Transports Canada
TP 5702E

2. Nº de l'étude — CDT
4847, 4848

3. Nº de catalogue du destinataire

4. Titre et sous-titre
SEGMENTED MODEL TESTING IN ICE -
DEVELOPMENT OF TECHNIQUES
Summary Report

5. Date du rapport
septembre 1984

6. Nº du rapport de l'organisme exécutant
SR 566C

7. Auteur(s)
Dr. A. Nawwar et M. D. Howard

8. Nº de dossier Transports Canada
D1460-194

9. Nom et adresse de l'organisme exécutant
Arctec Canada Limitée
311 Leggett Drive
Kanata, Ontario
K2K 1Z8

10. Nº de dossier — ASC
10SD.T8200-2-2547

11. Nº de contrat — ASC ou Transports Canada
1SD82-00153

12. Nom et adresse de l'organisme parrain
Centre de développement des transports (CDT)
1000 ouest, rue Sherbrooke
Suite 2421
Montréal, Québec H3A 2R3

13. Genre de rapport et période visée
Sommaire; jan. 83-84

14. Code de l'organisme parrain
CDT 4847, 4848

15. Remarques additionnelles

16. Agent de projet — CDT
Ian M. Bayly

17. Résumé

Ce rapport fait le compte rendu d'une technique nouvelle dans le domaine des essais de résistance à l'avancement sur maquettes de navires. Cette technique consiste à découper la maquette de la coque en sections amovibles, de les doter d'instruments de mesure et de déterminer la charge des glaces qui s'exerce sur chacune d'elles. Le découpage de la coque en sections est fondé sur les modèles analytiques existants et sur les composantes de la résistance à l'avancement. Quant à l'appareillage de mesure, il a été conçu et mis en place de manière à permettre une définition complète des deux composantes de cette résistance: une normale à la surface de la coque et l'autre parallèle, appelée frottement. La maquette, préalablement étalonnée, a subi les premiers essais de résistance, permettant ainsi de connaître ses faiblesses et de les corriger. Les résultats préliminaires demontrent que cette technique permet de localiser les charges et d'en mesurer l'amplitude; une bonne corrélation a pu être obtenue avec les calculs théoriques quant à la localisation des charges, mais pas quant à l'amplitude. Cette technique a permis de vérifier les calculs de charge et de résistance. Une étude plus poussée est nécessaire pour affiner la technique et permettre le traitement automatique des données.

18. Mots-clés
Navires, brise-glace, essais sur maquettes, coque segmentée

19. Diffusion
Le Centre de développement des transports dispose d'un nombre limité d'exemplaires

20. Classification de sécurité (de ce rapport)
non-classifié

21. Classification de sécurité (de cette page)
non-classifiée

22. Nombre de pages
28

23. Prix
--

CDT TDC 79-005

# ACKNOWLEDGEMENT

The authors gratefully acknowledge the constant guidance, encouragement and valuable suggestions of Mr. Ian Bayly of Transport Canada, Transportation Development Centre, during the course of this study.

## TABLE OF CONTENTS

1. INTRODUCTION 1

2. RATIONALE OF MODEL SEGMENTATION 2

3. DEVELOPMENT OF TECHNIQUE 6
   3.1 Segmentation Technique 6
   3.2 Instrumentation 8
   3.3 Data Reduction Methods 10

4. TESTING PROGRAM 14
   4.1 Calibration Testing 14
   4.2 Model Testing in Ice 14

5. ANALYSIS AND DISCUSSION 16
   5.1 Quality of Results 16
      5.1.1 Validation of Model Resistance 16
      5.1.2 Segment Calibrations 16
      5.1.3 Transducer Response 16
      5.1.4 Effects of Ship Motion 16
      5.1.5 Effects of Pretension Loads 16
   5.2 Detailed Analysis of Segment Forces and Responses 17
      5.2.1 Resistance Breakdown 17
      5.2.2 Analysis of Force Components 17

6. TECHNIQUE EVALUATION AND CONCLUSIONS 18
   6.1 Evaluation of System Performance 18
      6.1.1 Segmented Model and Icebreaking Mechanisms 18
      6.1.2 Instrumentation System 19
      6.1.3 Data Acquisition and Reduction System 20
      6.1.4 Data Analysis Methodology 20
   6.2 Conclusions 21

REFERENCES 22

## 1. INTRODUCTION

The prediction of icebreaking resistance of ships has been the focus of interest of many research efforts since Runeburg in 1888. Despite this early start, it was 80 years later when Kashteljan and Russian co-investigators published the first attempt to rationalize the various mechanisms involved in the icebreaking resistance and their contribution to the total ice resistance forces. Several attempts followed and may be categorized in three distinct groups:

a) Empirical approach: Describes the resistance performance of a given ship under a finite range of conditions. This type cannot be extended beyond the range of determination and has limited value in extrapolation to other ship shapes or sizes.

b) Analytical approach: Modelling is based on certain assumptions relating to the components of icebreaking resistance and the development of forces by various mechanisms with verification usually by comparison to experimental data.

c) Semi-empirical approach: This is essentially an empirical development which takes into account ship and ice variables. It can be extended, for prediction purposes, in a wider range but would still be limited in scope to the range of determination.

In all the above methods, extrapolation is risky since the verification of any one model is often based on limited experimental data. The consolidation of analytical or semi-empirical models can be accomplished by the verification of the contribution of the various mechanisms involved in icebreaking to the total resistance. A proposal to develop a new experimental approach to investigate the resistance components and mechanisms associated with icebreaking has been pursued. Since different icebreaking components affect different zones on the hull surface, it was thought feasible to build a segmented model which enables the measurement of such forces individually. Such a technique would provide an excellent tool to improve the present state of understanding of the icebreaking resistance and associated mechanisms and components and in turn, the capability to predict the total ice resistance, as well as to optimize the hull shape.

The immediate objective of this project was to develop and demonstrate the feasibility of the technique including a strategy for model segmentation, and the various technical problems associated with its use.

## 2. RATIONALE OF MODEL SEGMENTATION

Segmented models have been used in the past for testing ship model forms. The earliest reported attempt to utilize segmented ship models for experimental purposes is credited to Lewis in 1954 [1]. He developed a two-segment model of the T-2 tanker and used deflection measuring devices to monitor bending loads. Since that time several other investigators reported the use of models segmented and joined in different ways to measure hydrodynamic loads on the model hulls. The latest attempt was reported by Beukelman and Gerritsma in 1982 [2]. The common element among previous experiments was the complete transverse segmentation of the hull into a number of segments which were connected to a rigid or flexible girder. The loads transferred to the girder or through it were measured using a variety of dynamometers or strain gauged elements.

This method of segmentation and associated instrumentation were not suitable for the measurement of ice loads, because ice loads are different in nature than hydrodynamic loads. Therefore, the first step in the present investigation was to develop the rationale for segmentation.

It is generally recognized that the resistance of ice to ship motion consists of several components due to bending and breaking of ice cusps, acceleration and moving of broken ice pieces, and gravitational resistance due to the buoyancy of submerged ice. A review and implementation of the most recent mathematical prediction model has been carried out and reported in several Transport Canada publications [3]. The model was used to study the breaking patterns of a selected icebreaking ship, and access certain regions associated with the icebreaking mechanisms.

The ship hull selected for this study was that of the Canadian Coast Guard icebreaker PIERRE RADISSON. This selection was made for the availability of both model test and full scale data on the ship performance which will be available to corroborate the present results.

Four major regions have been identified, as a result of studying successive ice cusp action on the advancing hull in different ice thicknesses, Figure 2.1(a). The four regions have been identified as shown in Figure 2.1(b) and may be characterized as follows:

°REGION I: which is mainly subjected to icebreaking forces at the stem and the foremost row of cusps. No significant turning and submergence loads are to be expected here.

°REGION II: which will experience icebreaking forces due to the second row of cusps as well as an increasing level of turning and submergence forces.

°REGION III: which will experience icebreaking forces only in thin ice, but will mainly be subjected to turning and submergence forces.

FIGURE 2.1 (a)

SCHEMATIC PRESENTATION OF SUCCESSIVE
ICE CUSP ACTION ON SHIP HULL

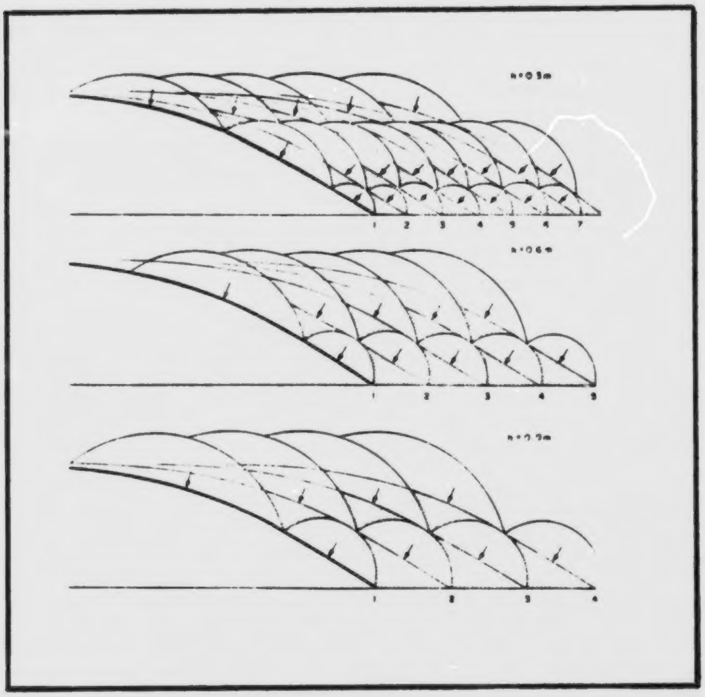
h=0.3m
1
2
3
4
5
6
7
h=0.6m
1
2
3
4
5
h=0.9m
1
2
3
4

FIGURE 2.1 (b)

DEFINITION OF HULL REGIONS

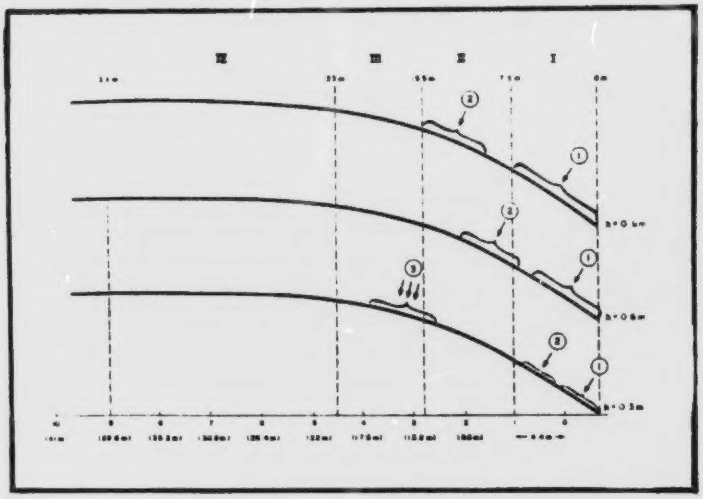
IV
III
II
I
23m
0m
②
①
h=0.6m
③
h=0.3m

°REGION IV will primarily experience turning, submergence and associated friction forces.

Experimental investigation of the breaking pattern was conducted on a 20th scale model of the PIERRE RADISSON in 30 mm thick ice (0.6 m full scale) to verify the foregoing conclusions. The observed breaking patterns were in general agreement with the analytical patterns illustrated in Figure 2.1.

The rationale for segmentation was based on the contribution of hull geometric areas to the total resistance. The four regions identified may be used as a basis of segmentation since they represent balanced combinations of icebreaking components of varying proportions. Most breaking forces are expected to occur in the vicinity of waterline. As soon as the ice fails, it is moved downwards and away from the hull and forces could act below the waterline.

However, estimates of the proportions of breaking, turning and other forces for different speeds, indicated the dominance of breaking forces at lower speeds. As the speed increases the proportions change but typical values may be given for 1 m/s (2 kts):

°Breaking and friction - 70%
°Turning and friction - 20%
°Others (submergence) - 10%.

While the ratios of the first two components will vary at higher speeds, the third component should not vary significantly.

Considering the relative importance of force components and in order to maintain the segmented model simple and inexpensive, it was decided that no segments will be assigned to the submergence component and only three segments extending sufficiently above and below the waterline would be most adequate for the purposes of this study.

The model segmentation plan is shown in Figure 2.2 (a) and a photograph illustrating the model under construction is also shown in Figure 2.2(b). The three selected segments are expected to cover the most significant icebreaking forces which are the breaking, turning and associated frictional components.

Realizing the current state-of-the-art of designing, building, instrumenting and testing of segmented models, it was felt that the segmentation plan is a step ahead and rather than increasing the number of segments it would be more desirable, at this stage, to develop a better instrumentation system for model measurements.

FIGURE 2.2 (a)

SEGMENTATION PLAN

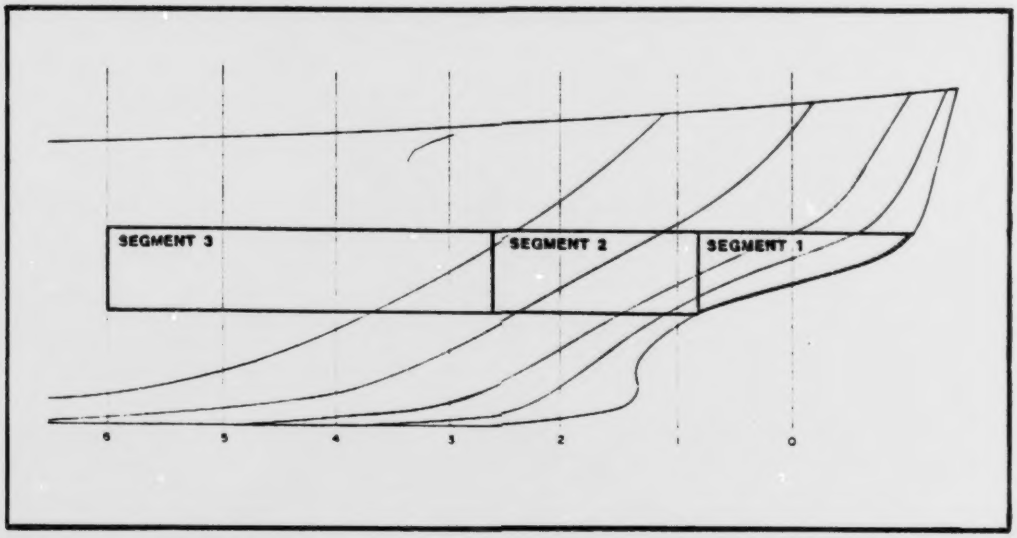
SEGMENT 3
SEGMENT 2
SEGMENT 1
6
5
4
3
2
1
0

FIGURE 2.2 (b)

SEGMENTED MODEL UNDER CONSTRUCTION

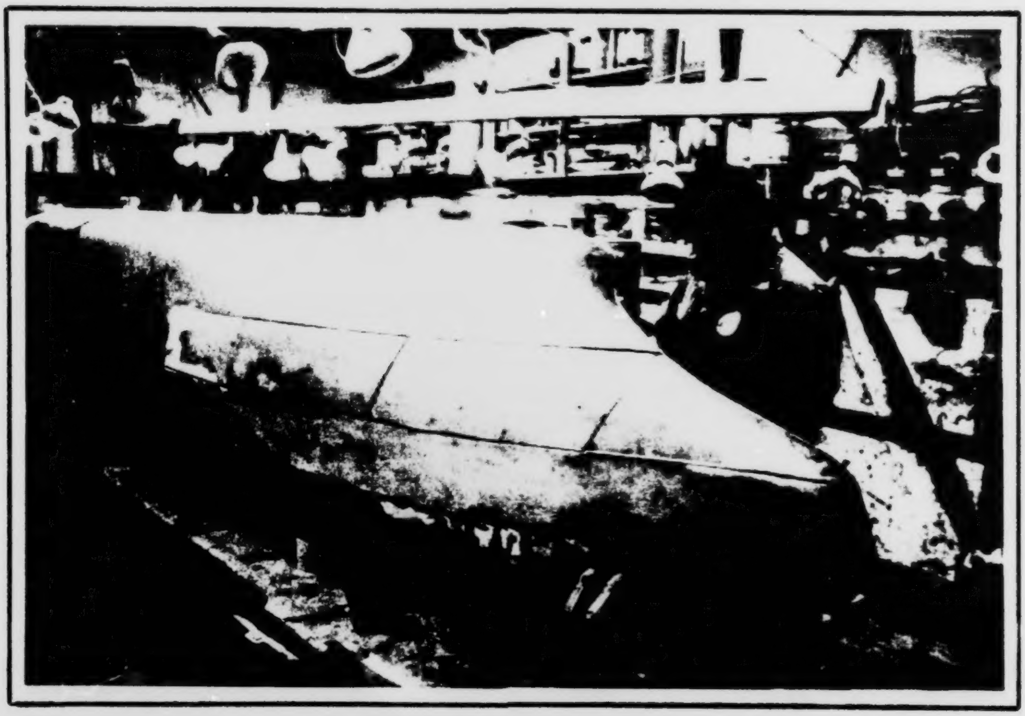

# 3. DEVELOPMENT OF TECHNIQUE

## 3.1 Segmentation Technique

Several methods for segmentation of the model were examined to allow independent sensing of loads on the hull as identified in Figure 2.2. Such methods included the creation of a core hull which supports three shell segments on load cells, piezo-electric sheets or buttons to be placed between the core hull and shell segments and the possibility of full transverse segmentation.

Discussions with the model builder resulted in adopting the method illustrated in Figure 3.1. This technique involved cutting the outer shell as projected for each segment. Each shell was integrated in a box-like structure which fits into a corresponding cavity in the hull. The inter-segment cavities were separated by water tight coffer dams which were created to permit easy access to all sides of the segments necessary for fitting the support and load measuring devices.

Each segment was ballasted to be neutrally buoyant to minimize the requirements for its support under no load conditions.

The segment support requirements were based on the minimum number of measurements to be obtained and the typical force (Figure 3.2.) The support system comprises:

- one support point, $R_1$ along the x-direction (resistance direction)
- two support points, $H_1$ and $H_2$ in the y-direction (transverse direction)
- four support points, $V_1$ through $V_4$ in the z-direction (vertical direction)

Pretension wires to preload all segment support points in compression were fitted so that if the loading is such that negative forces occur, contact would still be maintained.

The design of the load cells, shown in Figure 3.3, was developed to:

a) Provide unidirectional sensitivity along the axis of the cell with practically negligible lateral or cross sensitivity.

b) Ensure high stiffness so that the lowest natural frequency of each supported segment was well removed from the ice load frequencies.

c) Ensure ease of assembly and repair since the load cells will be immersed in urea doped water and may be subjected to overloads.

d) Allow sealing of load cells to eliminate strain gauge failures.

FIGURE 3.1

METHOD OF MODEL SEGMENTATION

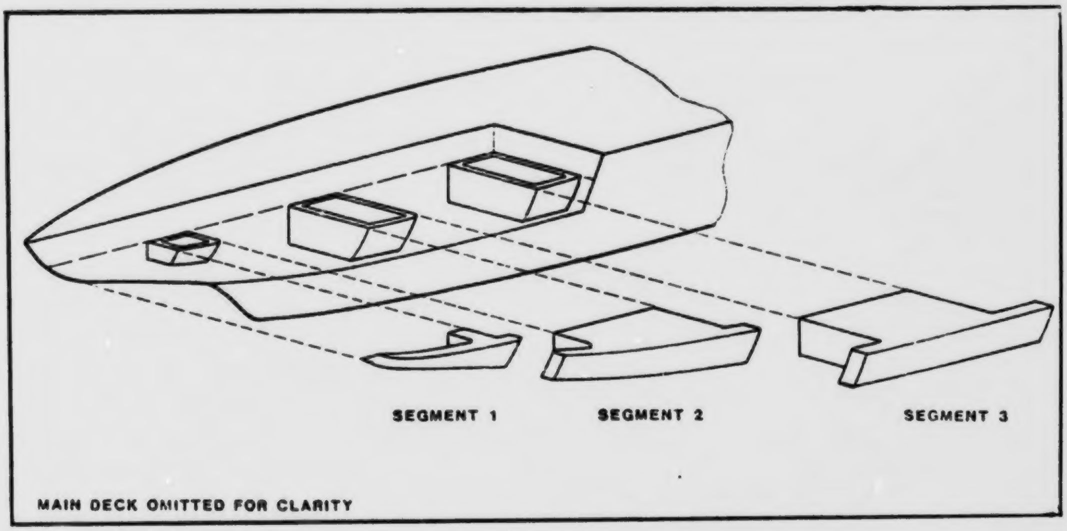
SEGMENT 1
SEGMENT 2
SEGMENT 3
MAIN DECK OMITTED FOR CLARITY

FIGURE 3.2

TYPICAL SEGMENT SUPPORT SYSTEMS

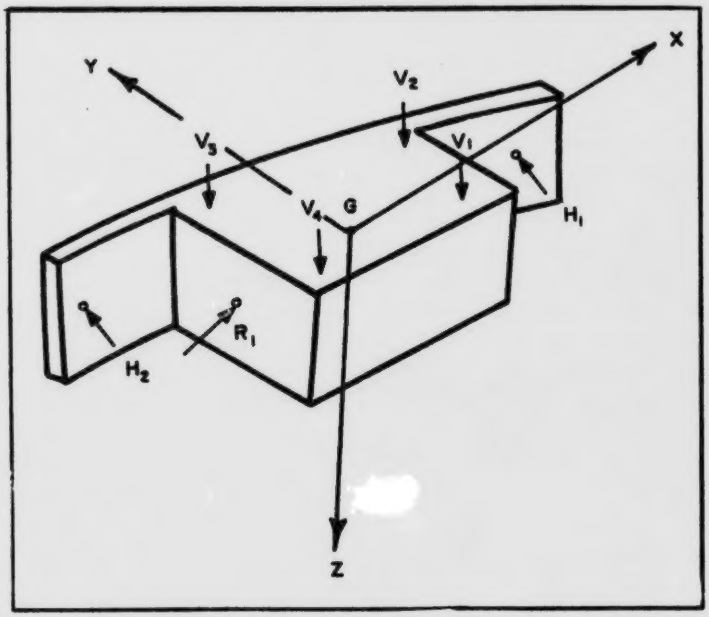
Y
X
$V_2$
$V_1$
$V_3$
$V_4$
G
$H_1$
$H_2$
$R_1$
Z

FIGURE 3.3

PHOTOGRAPH OF LOAD CELLS

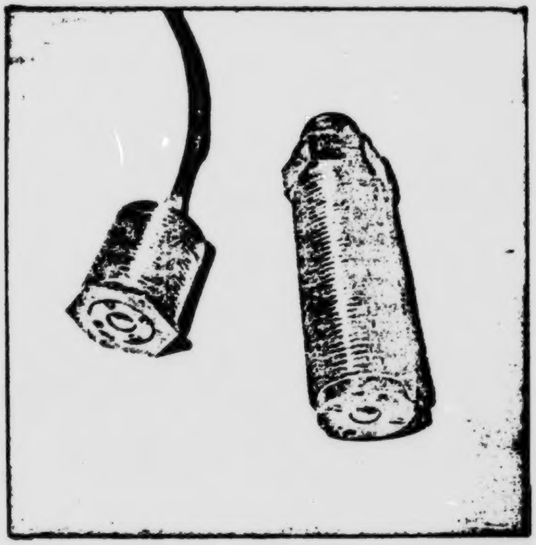

e) Provide individual selection of range of measurement.

f) Provide a level of precision of each load cell matched to purpose and cost.

g) Be self-temperature compensated to minimize thermal response.

Load cell capabilities were determined on the basis of the maximum reactions at load support points due to maximum dynamic loading on each segment calculated by the proprietary ice resistance component program "RICE".

The final configuration of each load cell was also influenced by geometric constraints such as location, and accessibility and other practical considerations.

## 3.2 Instrumentation

The instrumentation package of the segmented model consisted of:

- five load cells on segment 1 to measure force components,
- seven load cells on segment 2 to measure force components,
- seven load cells on segment 3 to measure force components,
- one force block to measure the total resistance of the model,
- two pendula to measure pitch and roll,
- three accelerometers to measure linear acceleration components near the centre of gravity of the model (only surge to be further processed),
- other channels to monitor position of the model, instantaneous speed, and to record events signifying model progress during the test.

Figure 3.4 is a schematic representation of the data acquisition system. All signals were recorded in magnetic tape using a 28 channel FM tape recorder. All channels were then filtered as necessary and digitized, then further processed using an HP 9816 microcomputer. The digitized data were stored on micro disc and plotted in engineering units along with the statistics obtained during the test interval.

FIGURE 3.4 SEGMENTED MODEL INSTRUMENTATION

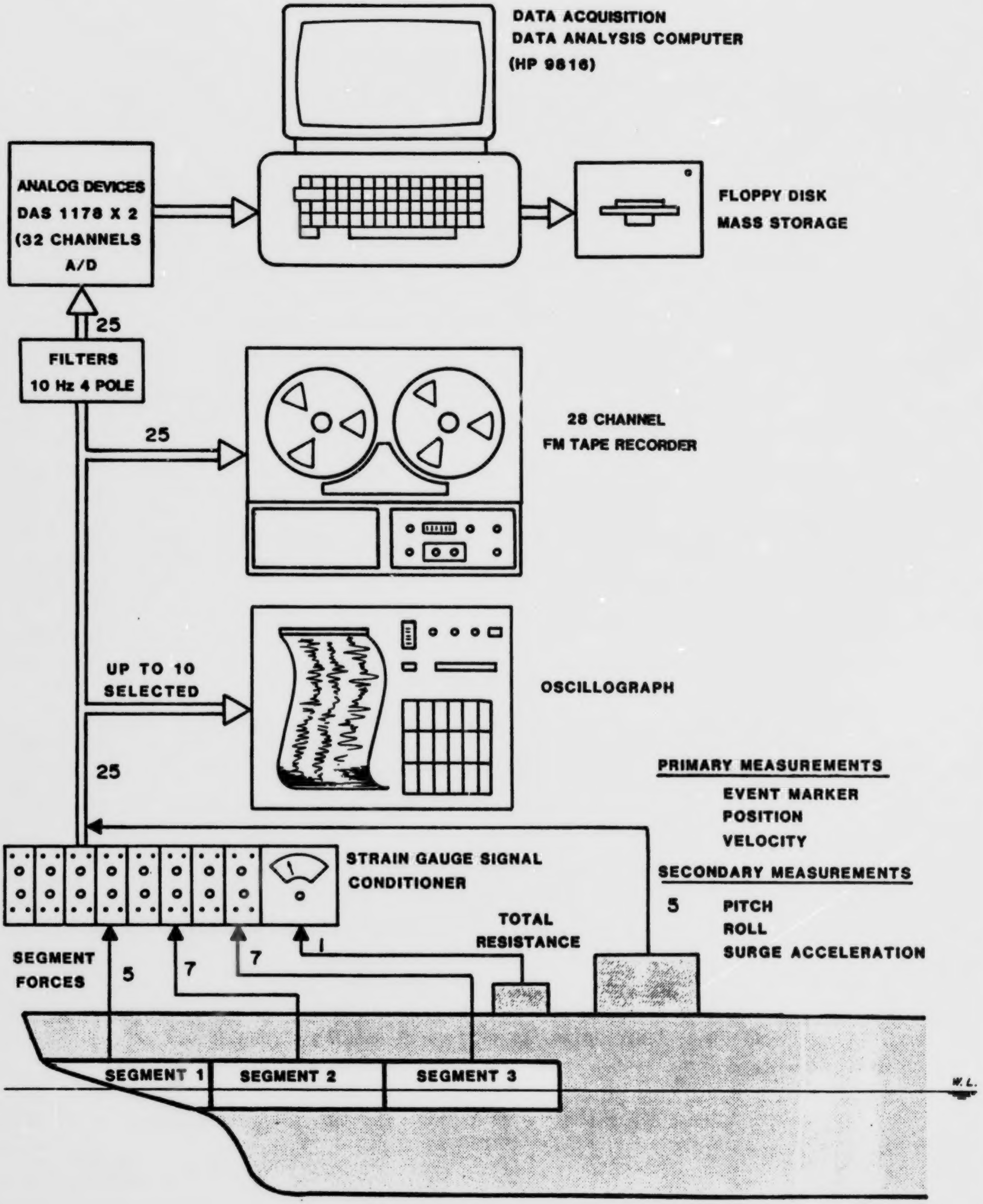
DATA ACQUISITION
DATA ANALYSIS COMPUTER
(HP 9816)
ANALOG DEVICES
DAS 1178 X 2
(32 CHANNELS
A/D
FLOPPY DISK
MASS STORAGE
25
FILTERS
10 Hz 4 POLE
25
28 CHANNEL
FM TAPE RECORDER
UP TO 10
SELECTED
OSCILLOGRAPH
25
PRIMARY MEASUREMENTS
EVENT MARKER
POSITION
VELOCITY
STRAIN GAUGE SIGNAL
CONDITIONER
SECONDARY MEASUREMENTS
5
PITCH
ROLL
SURGE ACCELERATION
TOTAL
RESISTANCE
SEGMENT
FORCES
5
7
7
1
SEGMENT 1
SEGMENT 2
SEGMENT 3
W.L.

### 3.3 Data Reduction Methods

Data reduction algorithms have been developed to analyze measured load components and reduce them into the required descriptions of ice load location and magnitude (including friction force). The contribution of each segment to the total resistance can be evaluated directly from the load components measured.

Figure 3.5 schematically illustrates an ice load F acting at some point on the hull O' which is defined by coordinates (x', y', z'). This force may be analyzed into its normal component which always acts perpendicular to the hull and a frictional component which will act along an unknown direction parallel to the hull surface.

The total ice force components may be written:

$$\begin{aligned} F_x &= - F_n (n_1 + \mu e_1) \\ F_y &= - F_n (n_2 - \mu e_2) \qquad (4.5)^1 \\ F_z &= - F_n (n_3 - \mu e_3) \end{aligned}$$

Using the three force components applied at point O' on the shell of a segment, and applying the six equilibrium conditions one obtains six equations relating the external loads to the reactions measured at various support points. These six equations contain ten unknown quantities being:

$$F_n, n_1, n_2, n_3, e_1, e_2, e_3, x', y', z',$$

assuming that the friction factor is known.

Through recognition of other relationships between the unknowns and the constraint that the point of load application is always on the surface of the hull, the number of unknowns can be reduced to four.

A summary of the method of solution described in detail in the main report is given below.

a) For each segment calculate the sum of measured load cell reactions $R_i$ , $\Sigma H_{ij}$ and $\Sigma V_{ij}$.

c) Select an active waterline and consider the ice loads to act close to it.

c) Determine the x-coordinate of ice force.

d) Use lines plans to find corresponding y' and adjust x' if necessary.

---

[1] Equation numbers used in the main report are maintained here for ease of cross reference.

FIGURE 3.5

BASIC FORCE ANALYSIS

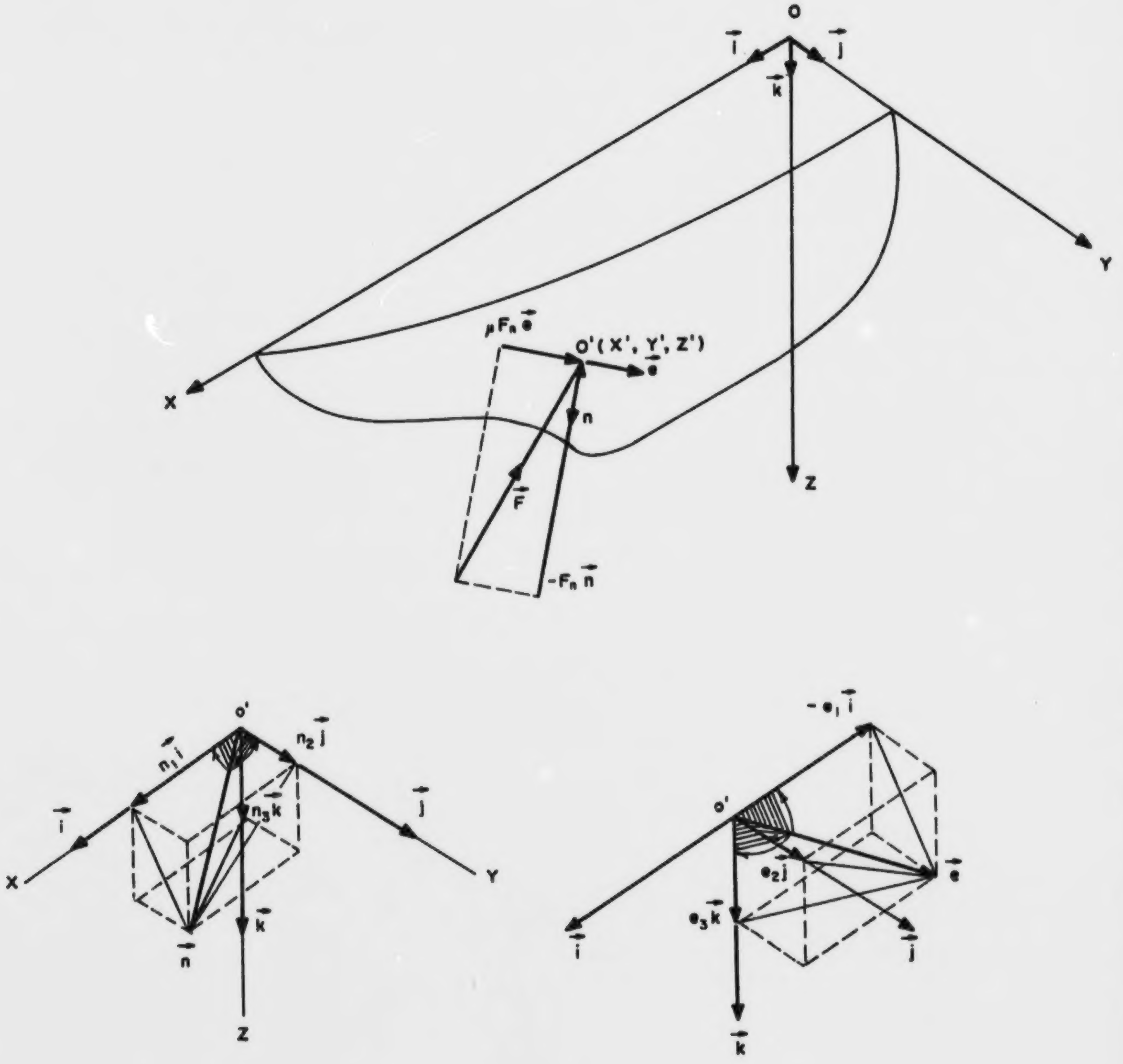
O
$\vec{i}$
$\vec{j}$
$\vec{k}$
Y
X
Z
$\mu F_n \vec{e}$
O'(X', Y', Z')
$\vec{e}$
n
$\vec{F}$
$-F_n \vec{n}$
o'
$n_1 \vec{i}$
$n_2 \vec{j}$
$n_3 \vec{k}$
$\vec{i}$
$\vec{j}$
X
Y
$\vec{n}$
$\vec{k}$
Z
$-e_1 \vec{i}$
o'
$e_2 \vec{j}$
$\vec{e}$
$e_3 \vec{k}$
$\vec{i}$
$\vec{j}$
$\vec{k}$

**NORMAL UNIT VECTOR**

$\vec{n} = n_1 \vec{i} + n_2 \vec{j} + n_3 \vec{k}$

**FRICTION UNIT VECTOR**

$\vec{e} = -e_1 \vec{i} + e_2 \vec{j} + e_3 \vec{k}$

e) Assess the errors involved in the moment equilibrium equations (4.15) a, b and c. Correct if necessary.

f) Determine ($n_1$, $n_2$, $n_3$) at the location (x' , y', z').

g) Calculate the normal ice load on the segment.

h) Estimate the friction coefficient and compare with measured factor.

i) Calculate the indices of the friction vector ($e_1$, $e_2$, $e_3$).

j) Compare the direction with hull lines i.e. waterline, buttock angles, etc.

The present method utilizes an analytic iterative procedure to determin the position of ice load. It is also possible to use a graphical procedure as illustrated in Figure 3.6 to provide a simultaneous solution for x', y' and z' in one step. While the first method is preferred for ease of automation of the solution it would require some interactive output to verify that the point O' exists on the hull surface. An attempt to input the hull geometry of the ship and use interpolation programs has its merits and should be considered for future work.

FIGURE 3.6

GRAPHICAL DETERMINATION OF THE ICE LOAD POSITION

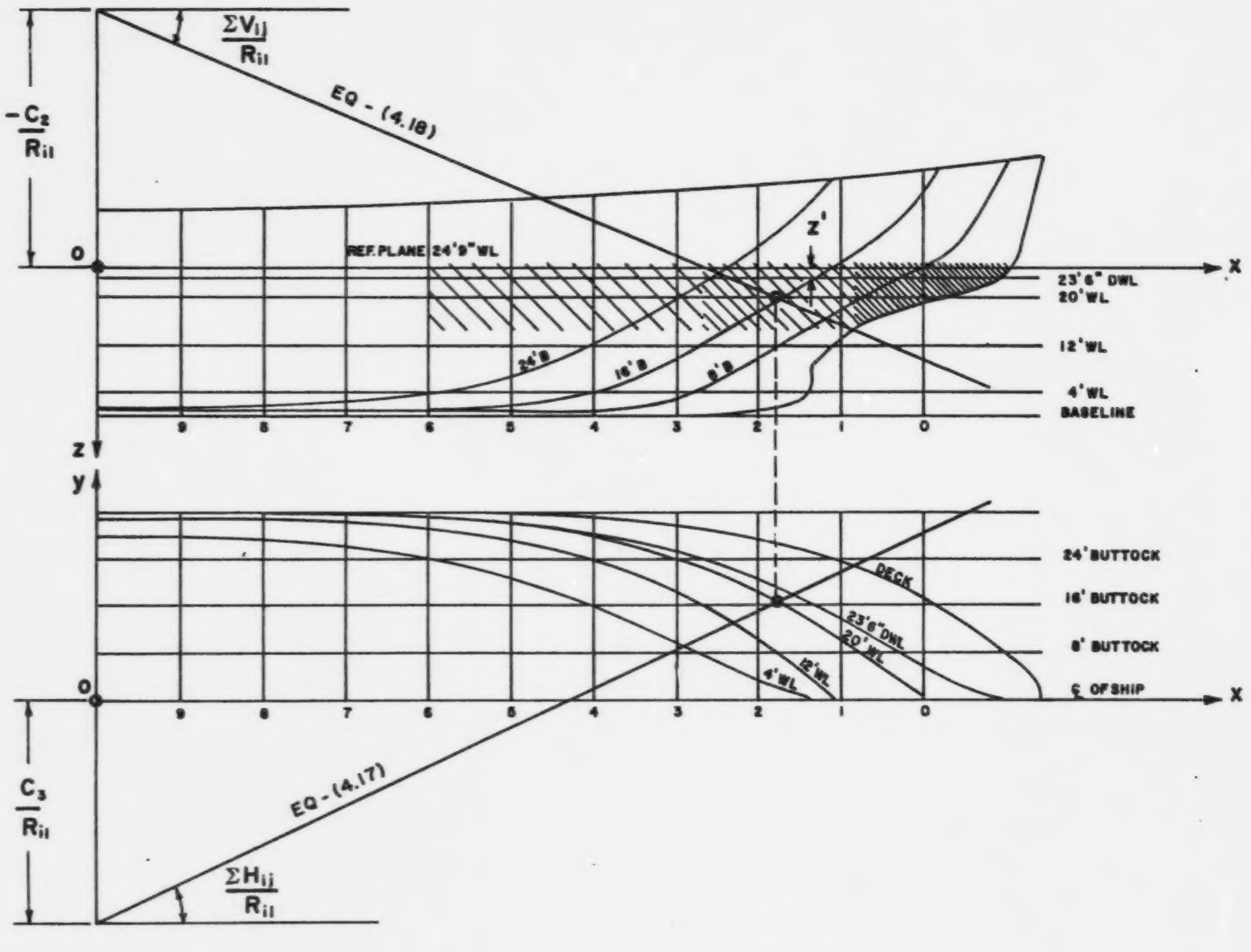

$\frac{\Sigma V_{ij}}{R_{ii}}$
$-\frac{C_2}{R_{ii}}$
EQ - (4.18)
REF. PLANE 24'9" WL
Z'
O
X
23'6" DWL
20' WL
12' WL
4' WL
BASELINE
24' B
16' B
8' B
9
8
7
6
5
4
3
2
1
0
z
y
24' BUTTOCK
16' BUTTOCK
8' BUTTOCK
℄ OF SHIP
DECK
23'6" DWL
20' WL
12' WL
4' WL
O
X
EQ - (4.17)
$\frac{C_3}{R_{ii}}$
$\frac{\Sigma H_{ij}}{R_{ii}}$

## 4. TESTING PROGRAM

The testing program of the segmented model included two major parts: calibration testing, and model testing in ice.

### 4.1 Calibration Testing

Calibration testing was performed to assess the model response to applied loads and determine calibration constants or correction factors to be used in data interpretation. The following calibration tests were conducted.

(a) Load Cell Calibrations: in which each load cell was calibrated in a closed loop test system under dynamic loading and the calibration constant for each load cell was determined.

(b) Segment Response Calibration: in which a known load was applied at the outer hull of each segment and the response measured. A finite element model was also built for segment 2 to study the segment response and load transfer under external ice load. The finite element analysis was used to examine possible causes for lack of transfer of the full load.

(c) System Response to Model Motions: in which the effect of model motions on the measured response of the system was determined. This test included a number of open water tests at various speeds to determine the bow wave effect as well as roll and pitch tests.

(d) Standard calibrations were performed on the force block and the other sensors used to monitor the segmented model's performance.

### 4.2 Model Testing in Ice

A total of eight tests were conducted on the segmented model in ice sheets of 25 and 45 mm and speeds from 1 knot to 5 knots full scale. After the first two ice sheets, the tests were stopped and the results examined to determine their quality and identify problems in the operations of the segments. All tests were conducted on carbamide-doped ice grown in accordance with standard procedures at Arctec.

The model was removed from the basin after the initial testing of two ice sheets and some modifications made to the short version of load cells and preloading arrangements to solve lack of contact which was identified in some segment support points.

A typical summary of ice test results is given in Table 4.1.

## TABLE 4.1

## ICE TEST SUMMARY SHEET

ICE SHEET NO. 4
RUN NO. 2
TEST DATE: AUG-12-83
DIGITIZING DATE: AUG-17,25-83

| | MEAN | STANDARD DEVIATION | MAXIMUM VALUE | MINIMUM VALUE |
|---|---|---|---|---|
| ICE: | | | | |
| THICKNESS (mm) | 43.80 | 1.83 | 48.30 | 41.90 |
| STRENGTH (kPa) | 21.79 | 4.71 | 28.20 | 14.20 |
| MODULUS (MPa) | 18.55 | - | - | - |
| CHANNEL WIDTH (m) | 1.21 | 0.14 | 1.43 | 1.03 |
| $R_{11}$ (N) | 0.01 | 0.02 | 0.05 | -0.05 |
| $H_{11}$ (N) | -11.44 | 7.51 | 5.07 | -38.33 |
| $H_{12}$ (N) | -1.37 | 2.39 | 4.22 | -6.65 |
| $V_{11}$ (N) | -12.37 | 6.13 | -1.00 | -31.77 |
| $V_{12}$ (N) | 7.08 | 1.77 | 9.93 | 2.08 |
| $R_{21}$ (N) | -10.51 | 2.14 | -5.44 | -15.37 |
| $H_{21}$ (N) | -7.79 | 2.30 | -1.56 | -13.97 |
| $H_{22}$ (N) | -20.47 | 6.18 | -6.96 | -34.33 |
| $V_{21}$ (N) | 0.86 | 0.93 | 2.38 | -2.69 |
| $V_{22}$ (N) | -4.49 | 3.53 | 4.03 | -10.61 |
| $V_{23}$ (N) | -2.94 | 3.43 | 5.46 | -10.51 |
| $V_{24}$ (N) | 2.39 | 1.17 | 5.94 | -0.13 |
| $R_{31}$ (N) | -6.96 | 6.00 | 2.48 | -21.46 |
| $H_{31}$ (N) | -8.08 | 12.80 | 22.92 | -44.65 |
| $H_{32}$ (N) | -29.70 | 16.23 | -5.13 | -70.39 |
| $V_{31}$ (N) | -10.34 | 17.49 | 9.47 | -54.20 |
| $V_{32}$ (N) | 20.08 | 11.70 | 40.44 | -4.24 |
| $V_{33}$ (N) | 9.56 | 1.10 | 10.88 | 4.57 |
| $V_{34}$ (N) | 22.66 | 1.49 | 24.28 | 19.23 |
| RESISTANCE (N) | -69.40 | 50.45 | 35.13 | -166.45 |
| SURGE ACCL (mm/sec$^2$) | 4.91 | 4.85 | 16.27 | -5.21 |
| PITCH (DEGREES) | -0.26 | 0.27 | 0.67 | -0.98 |
| ROLL (DEGREES) | -4.71 | 4.78 | 1.52 | -15.30 |
| POSITION (m) | 9.49 | 2.19 | 13.25 | 5.69 |
| SPEED (m/sec) | 0.59 | 0.01 | 0.60 | 0.56 |

# 5. ANALYSIS AND DISCUSSION

## 5.1 Quality of Results

### 5.1.1 Validation of Model Resistance

The first step in the analysis conducted was to validate the present experimental results by comparing the present total resistance set of data with previous results obtained using other models of the CCGS PIERRE RADISSON.

Since no common set of testing conditions existed, the various data sets were compared by regressing a "best fit" equation and then normalized to correct for ice strength. The normalized data from the present test series compared extremely well with the results from two other test series even though a slightly different hull friction and hull draft was used. It was concluded that the segmentation of the model did not appear to produce significant differences in the measured total resistance.

### 5.1.2 Segment Calibrations

As noted earlier segment calibrations were performed to determine the transfer response of the load to the load cells. These were performed with the model out of the water by applying a load at a given point in a known direction. This load was then separated into components and compared with the measured output, to provide a mean segment correction factor for each component, albeit a 'dry' state.

### 5.1.3 Transducer Response

The quality of the nineteen load cell signals was assessed per run and, with the results of the previous section, used to select test 4-2 as the appropriate test to verify the analysis procedure.

### 5.1.4 Effects of Ship Motion

During most tests, it was observed that large ship motions occurred. Therefore, the first step in the data analysis was to eliminate the effect of ship motions on the recorded force components. This was determined from open water tests. These tests were used to algebraically remove the measured force component due to model motion to obtain the component due to ice loading.

### 5.1.5 Effects of Pretension Loads

The effect of the pretension wires for segment 2 was estimated using the average measurements from test 4-2, to be 1% or less and has been neglected throughout this analysis. However, if a stiffer pretension arrangement is used in the future, a tension bolt (or similar device) would be necessary to record pretension wire effect.

## 5.2 Detailed Analysis of Segment Forces and Responses

### 5.2.1 Resistance Breakdown

For test 4-2, segments 2 and 3 contribute 30.6% and 20.1% respectively to half the total resistance. The resistance component of segment 1 was not functioning during this test, so no conclusion can be drawn regarding the resistance of segment 1. However, this reflects a trend of decreasing resistance contribution of the aftmost segments despite the possibility that the normal force on the hull could have an opposite trend.

Examining the variation of the resistance components during test 4.2 indicated a dominant frequency of 0.31 Hz on segment 2 and 0.23 Hz on segment 3. On segment 3, there were two dominant levels of peaks: the lower peaks being approximately 60% of the maximum peaks. The lower peaks were likely associated with the turning components. Also the maximum breaking resistance associated with segment 3 was 41% higher than the corresponding resistance associated with breaking in segment 2. This corroborates the assumption that the hull flare plays an important role in reducing the resistance contribution of the aft-bow region.

Although a higher maximum peak resistance was measured on segment 3 than on segment 2, the reverse was true with regards to the mean resistance. The standard deviation of the resistance components may be used to identify the predominant forces associated with icebreaking. For instance, segment 2 exhibited a standard deviation of 20% of the mean compared to 87% for segment 3. This may be interpreted as an indication to the dominance of ice cusp bending and breaking occurring on segment 2. As the cusps break they move aftwards relative to the model and the turning mechanism and associated forces affect segment 3. The higher standard deviation on segment 3 indicated a greater variation and more frequent occurrence of lower magnitude ice loads.

### 5.2.2 Analysis of Force Components

The analysis of force components was conducted according to the procedures outlined earlier. The analysis was performed with the mean forces on segment 2 during test 4-2. The results of the analysis using the force components as measured predicted a hull friction factor of 0.071 which was reasonably close to the present model friction. While the order of magnitude of the friction factor was correct, the direction was not. The obvious reason is the sensitivity of the friction components to the measured force components.

Analysis has shown that by using the mean segment calibration factors (MSCF), the direction of friction was reversed and was more adequate, thus indicating that correction is required for the measurements.

However, the present analysis suggests that the application of MSCF's as obtained from dry calibration tests result in over correction. Better MSCF values for each segment could be obtained from in-water calibration.

## 6. TECHNIQUE EVALUATION AND CONCLUSIONS

### 6.1 Evaluation of System Performance

An evaluation of the following major aspects of the program have been made:

a) A segmented model,

b) An associated instrumentation system,

c) A data acquisition, reduction and analysis system.

### 6.1.1 Segmented Model and Icebreaking Mechanisms

The present attempt at ship model segmentation is the first of its kind in the following respects:

- Testing of thoroughly segmented, and fully instrumented ship models in ice.
- Segmentation of only one side of the hull instead of full transverse segmentation, which permits the measurement of lateral loads (rather than differential lateral loads).
- The segmentation system provides the only available method to date which can be used to measure local ice loads on a ship model hull to a high accuracy.

Overall, it appears that segmentation of the model does not influence or interfere with the icebreaking process. Therefore, the ice force measurements on the various segments should be compared to the expected ice loads to verify the success of the segmentation plan or lack of it.

Comparing the results obtained in this study to calculated ice loads, has shown that the location of the loads on the segments is as expected.

The magnitudes of ice loads agree in general with the trend suggested by analytical methods. However, the results do not appear to agree with the basic premise proposed by Russian investigators [4] that the normal force at any position along the hull is proportional to the cosine of the waterline angle. Nonetheless, the trend appears to be similar indicating increasing normal force with decreasing waterline angle, but it is nonlinear.

To sum up, it may be stated that the segmentation of the model of the PIERRE RADISSON has been successful in reproducing the expected positions of the ice forces. With regards to magnitudes of the ice loads there appears to be some differences in maximum load values among the present tests, the computer code RICE and empirical formulation. These differences should be fully investigated in future tests to identify their causes and their implications on the mathematical modelling of the icebreaking phenomenon.

### 6.1.2 Instrumentation System

During this phase of development, an instrumentation system has been designed to enable the determination of the following for each segment:

- magnitude of the normal component of ice load,
- position of centre of ice load,
- magnitude of the frictional component of ice load (friction factor),
- absolute direction along which frictional forces act.

This, in turn, provides the information necessary for one to trace:

- How does the direction of frictional forces vary with the progress of ice crushing, bending, fracturing, turning and sliding?
- How does the position of ice forces change during the various phases of icebreaking?
- How does the magnitude of normal force change along the hull?
- How does the value of friction factor change?

and other aspects of icebreaking which could result in the revision of the assumptions usually made in the course of mathematical modelling.

The system in principal is shown to be capable of providing this information. However, there have been a number of problems which affected the proper operation of the system and the interpretation of the results. These problems may be summarized in the following:

a) The system was found to be sensitive to minor manufacturing defects relating to the seating of the load cells on the segments. Such defects result in a less than 100% transfer of loads to the sensor. In-water calibration of segments should be performed in future trials.

b) The load cells were purposely designed to sense load in one direction. In order to maintain contact with the segments, a preload was applied using flexible wire ropes which were adjustable. The stiffness of the pretension wires was kept as low as possible to ensure that their effect on measurements could be neglected. However, contact between the segments and load cells was frequently lost during the testing and caused a zero shift of the load cell output. In order to eliminate such problems it is essential to redesign the pretensioning system to increase its rigidity. This could possibly be accomplished by using the finite element model to design and select the pretensioning elements and determine their required stiffnesses.

c) Segment 1 is the least stable and its pretension support arrangements must be re-examined, probably using a finite element model to assess its requirements under the most extreme loading condition.

d) The measurement of pitch and roll angles during the tests, though regarded as secondary measurements have been instrumental in including the effects of model motions in calculating the ice loads.

e) Acceleration was also measured in the surge direction to monitor model motions. The effect of inertial forces have been shown to be negligible for the three segments.

### 6.1.3 Data Acquisition and Reduction System

The data acquisition system was successfully used to monitor and record all the information collected during the test. All data has been recorded on FM tape recorder and further processed into digital form where each signal was filtered at a frequency of 1 Hz and then digitized at a rate of 32 Hz. All test data is now available on micro-disc medium which is in engineering units.

In general, the data acquisition system performed well and it would only require minor adjustments for future work. The addition of a complete data analysis software should also be considered after necessary modifications are carried out on the model and instrumentation to ensure trouble-free operation.

### 6.1.4 Data Analysis Methodology

The method of solution developed assumed that all measurements were available and correct. However, if the load cell was out of contact and not measuring, solution was not possible - a weakness in the method of solution. It might be possible to develop other methodologies which can accept partial data and produce the necessary output even with lower reliability.

Other aspects of the methodology are discussed in detail in the main report and summarized here. For low values of friction coefficient the relative error in estimating the frictional ice load increases. Let us assume an experimental error in measurement ranging between $\underline{+}$ 10 percent. It can be shown that the error in estimating the total or normal force is relatively small for randomly occuring errors, but for systematic errors in one direction the error increases. For ±5 percent error, the resulting deviation in calculating the normal force is well within ± 0.2 percent.

The experimental errors in measuring the force components produce a friction coefficient which is approximately equal to the experimental error, that is 0.055 for ±5% error and 0.101 for 10% error. This results in a small frictional force component of a few Newtons, which seems to change direction in an erratic manner.

We believe that the range of experimental errors, may be minimized by necessary segment support system modifications and more detailed calibration of secondary effects such as roll and pitch motions.

Another solution is to increase the friction factor of the model hull. It has been shown that as the friction factor was increased from 0.1 to 0.5, the direction of the friction force stabilizes and becomes much less sensitive to experimental errors. The trade off is obviously accepting lower accuracy in predicting the normal force in favour of better estimates of the frictional force magnitude and direction.

It may be suggested that the friction factor be set according to the objectives of a given experiment. The major emphasis, though, should remain on improving the overall experimental accuracy.

## 6.2 Conclusions

Based on the work undertaken in this project and summarised in this document the following conclusions may be drawn:

(1) The basic scheme for model segmentation for ice testing has been successfully developed to address the measurement requirements for ice loads on ship hulls.

(2) The instrumentation system has been successfully developed to completely define the instantaneous ice loads and associated friction forces.

(3) The system has been shown to be capable of detecting the correct position and magnitude of ice loads.

(4) The friction component detection is sensitive to experimental errors and further work is required to fine tune the system.

(5) Preliminary results and analysis suggest that extensive in-water calibration and completely automated data analysis systems are needed.

## REFERENCES

[1] Lewis, E.V., "Ship Model Tests to Determine Bending Moments in Waves", Transactions Society of Naval Architects and Marine Engineers, Vol. 62 (1954).

[2] Beukelman, W., and Gerritsma, J., "The Distribution of Hydrodynamic Mass and Damping of an Oscillating Ship Form in Shallow Water", Intl. Shipbuilding Progress, Vol. 29, No. 339, November 1982, p. 297-315.

[3] Lewis, J.W., Bulat, V., Glen, I., and Kotras, T., "A Semi-Empirical Ice Resistance Model", ACL FR 444C.4, April 1983, submitted to TDC:

Volume I - Main Report - TP4376E
Volume II - Appendices - TP4375E
Volume III - Principles and Assumptions, by A.M. Nawwar - TP4374E

[4] Kashteljan, V.I., Ryvlin, A.Ya., Feddeyev, O.V., and Yagodkin, V.Ya., "Icebreakers", Translation, CRREL TL 418, August 1973.

ARCTEC CANADA LIMITED FR 566C

# SEGMENTED MODEL TESTING IN ICE - DEVELOPMENT OF TECHNIQUES

FINAL REPORT
TP 5701E

JUNE 1984

A.M. Nawwar
D. Howard

Prepared for:

Transportation Development Centre,
1000 Sherbrooke Street West,
Montreal, Quebec.
H3A 2R3

Prepared by:

Arctec Canada Limited,
311 Legget Drive,
Kanata, Ontario.
K2K 1Z8

Library and Information Centre
RECEIVED
FEB 1985
Transport Canada | Transports Canada

## DISCLAIMER

The contents of this report reflect the views of the contractor and not necessarily the official views or policies of the Transportation Development Centre.

## PROJECT TEAM

- A. M. NAWWAR
- D. HOWARD
- M. STEELE
- H. BLOUNT
- C. DALEY

and others

"APPROVED BY ______________________ "

## REPORT DOCUMENTATION FORM

| | | |
|---|---|---|
| 1. **Transport Canada Report No.**<br>TP 5701E | 2. **TDC Project No.**<br>4847, 4848 | 3. **Recipient's Catalogue No.** |
| 4. **Title and Subtitle**<br>**SEGMENTED MODEL TESTING IN ICE - DEVELOPMENT OF TECHNIQUES** | | 5. **Report Date**<br>June 1984<br>6. **Performing Organization Report No.**<br>ACL FR566C |
| 7. **Author(s)**<br>Dr. A. Nawwar and Mr. D. Howard | | 8. **Transport Canada File No.**<br>D1460-194 |
| 9. **Performing Organization Name and Address**<br>Arctec Canada Limited<br>311 Leggett Drive<br>Kanata, Ontario<br>K2K 1Z8 | | 10. **DSS File No.**<br>10SD.T8200-2-2547<br>11. **DSS or Transport Canada Contract No.**<br>1SD.82-00153 |
| 12. **Sponsoring Agency Name and Address**<br>Transportation Development Centre (TDC)<br>1000 Sherbrooke Street West<br>Suite 2421<br>Montreal, Quebec H3A 2R3 | | 13. **Type of Report and Period Covered**<br>Final; Jan. 83-84<br>14. **Sponsoring Agency Code**<br>TDC 4847, 4848 |
| 15. **Supplementary Notes** | | 16. **TDC Project Officer**<br>Ian M. Bayly |

17. **Abstract**

This report describes the development of a new technique for testing model ships in ice. The technique consists of creating independent segments within the hull. Each segment is instrumented to monitor and define ice forces acting on the segment. The method of segmentation was developed with a view of the existing analytical models and components of ice resistance. The instrumentation system was designed and implemented to enable the complete definition of normal and frictional components of the ice load. The model was subjected to calibration and preliminary resistance testing in order to identify and correct its deficiencies. Preliminary results showed that the system is capable of measuring ice load location and magnitude; agreement with analytical expectations is good in terms of location, but the magnitude of ice load exhibits some difference. This finding indicates the capability of the model to examine and verify analytical models of ice forces and resistance. Further work is necessary to fine-tune the system and automate the data analysis process.

| | | | |
|---|---|---|---|
| 18. **Key Words**<br>Ships, Icebreaking, Model Tests, Hull Segments | | 19. **Distribution Statement**<br>Limited number of copies available from Transportation Development Centre | |
| 20. **Security Classification (of this report)**<br>Unclassified | 21. **Security Classification (of this page)**<br>Unclassified | 22. **No. of Pages**<br>154 | 23. **Price**<br>-- |

TDC/CDT 79-005

# FORMULE DE DOCUMENTATION POUR RAPPORT

| | | |
|---|---|---|
| 1. N° du rapport Transports Canada<br>TP 5701E | 2. N° de l'étude — CDT<br>4847, 4848 | 3. N° de catalogue du destinataire |

| | |
|---|---|
| 4. Titre et sous-titre<br>SEGMENTED MODEL TESTING IN ICE - DEVELOPMENT OF TECHNIQUES | 5. Date du rapport<br>juin 1984<br>6. N° du rapport de l'organisme exécutant<br>ACL FR566C |
| 7. Auteur(s)<br>Dr. A. Nawwar et M. D. Howard | 8. N° de dossier Transports Canada<br>D1460-194 |
| 9. Nom et adresse de l'organisme exécutant<br>Arctec Canada Limitée<br>311 Leggett Drive<br>Kanata, Ontario<br>K2K 1Z8 | 10. N° de dossier — ASC<br>10SD.T8200-2-2547<br>11. N° de contrat — ASC ou Transports Canada<br>1SD82-00153 |
| 12. Nom et adresse de l'organisme parrain<br>Centre de développement des transports (CDT)<br>1000 ouest, rue Sherbrooke<br>Suite 2421<br>Montréal, Québec H3A 2R3 | 13. Genre de rapport et période visée<br>Final;jan 83-84<br>14. Code de l'organisme parrain<br>CDT 4847, 4848 |
| 15. Remarques additionnelles | 16. Agent de projet — CDT<br>Ian M. Bayly |

17. Résumé

Ce rapport fait le compte rendu d'une technique nouvelle dans le domaine des essais de résistance à l'avancement sur maquettes de navires. Cette technique consiste à découper la maquette de la coque en sections amovibles, de les doter d'instruments de mesure et de déterminer la charge des glaces qui s'exerce sur chacune d'elles. Le découpage de la coque en sections est fondé sur les modèles analytiques existants et sur les composantes de la résistance à l'avancement. Quant à l'appareillage de mesure, il a été conçu et mis en place de manière à permettre une définition complète des deux composantes de cette résistance: une normale à la surface de la coque et l'autre parallèle, appelée frottement. La maquette, préalablement étalonnée, a subi les premiers essais de résistance, permettant ainsi de connaître ses faiblesses et de les corriger. Les résultats préliminaires demontrent que cette technique permet de localiser les charges et d'en mesurer l'amplitude; une bonne corrélation a pu être obtenue avec les calculs théoriques quant à la localisation des charges, mais pas quant à l'amplitude. Cette technique a permis de vérifier les calculs de charge et de résistance. Une étude plus poussée est nécessaire pour affiner la technique et permettre le traitement automatique des données.

| | |
|---|---|
| 18. Mots-clés<br>Navires, brise-glace, essais sur maquettes, coque segmentée | 19. Diffusion<br>Le Centre de développement des transports dispose d'un nombre limité d'exemplaires |

| | | | |
|---|---|---|---|
| 20. Classification de sécurité (de ce rapport)<br>non-classifié | 21. Classification de sécurité (de cette page)<br>non-classifiée | 22. Nombre de pages<br>154 | 23. Prix<br>-- |

CDT/TDC 79-005

## ACKNOWLEDGEMENT

The authors gratefully acknowledge the constant guidance, encouragement and valuable suggestions of Mr. Ian Bayly of Transport Canada, Transportation Development Centre, during the course of this study.

## TABLE OF CONTENTS

1. INTRODUCTION ....................................................2

2. MODEL SEGMENTATION; ANALYSIS AND RATIONALE........................6

- 2.1 Primary Sources of Ice Resistance ..............................6
- 2.2 Contribution of Hull Geometric Areas ...........................8
- 2.3 Segmentation Rationale .........................................18
- 2.4 PIERRE RADISSON Characteristics.................................20

3. DEVELOPMENT OF SEGMENTATION AND INSTRUMENTATION TECHNIQUES.........24

- 3.1 Model Segmentation Plan ........................................24
- 3.2 Review of Earlier Work .........................................26
- 3.3 Segmentation Technique .........................................32
- 3.4 Analysis of Segment Support System .............................36
- 3.5 Load Cell Design Development ...................................40
    - 3.5.1 Determination of Load Cell Capacities.....................42
    - 3.5.2 Geometric Constraints.....................................48
    - 3.5.3 Load Cell Design..........................................48
    - 3.5.4 Friction Effects..........................................52
    - 3.5.5 Diaphragm Sizing..........................................53
    - 3.5.6 Dynamic Response..........................................56
- 3.6 Prototype Calibration...........................................58
- 3.7 Data Acquisition System.........................................60

4. DATA REDUCTION ALGORITHM.........................................64

- 4.1 Total Resistance and Components.................................64
- 4.2 Analysis of Force Components....................................68
- 4.3 Method of Solution..............................................74
    - 4.3.1 Normal Ice Force .........................................74
    - 4.3.2 Friction Coefficient......................................74
    - 4.3.3 Direction of Friction Force...............................75
    - 4.3.4 The Ice Load Location.....................................75
    - 4.3.5 Summary ..................................................79

5. TESTING PROGRAM .................................................82

- 5.1 Introduction....................................................82
- 5.2 Calibration Testing ............................................82
    - 5.2.1 Calibration of Load Cells..................................82
    - 5.2.2 Calibration of Segment Response ...........................82
    - 5.2.3 Calibration of System Response to Model Motions............82
    - 5.2.4 Other Calibrations.........................................82
- 5.3 Model Testing...................................................84
    - 5.3.1 Test Plan and Procedure...................................84
    - 5.3.2 Test Results .............................................86

6. ANALYSIS AND DISCUSSION ........ 96

6.1 Validation of Model Resistance ........ 96
6.2 Assessment of Transducer Response ........ 100
6.3 Segment Calibration Factors ........ 103
6.4 Detailed Analysis of Segment Forces ........ 106
    6.4.1 Effects of Ship Motions ........ 106
    6.4.2 Effects of Pretension Loads ........ 106
    6.4.3 Resistance Breakdown ........ 108
    6.4.4 Analysis of Force Components ........ 111
    6.4.5 Application of Segment Calibrations ........ 113
    6.4.6 Other Segments ........ 116

7. TECHNIQUE EVALUATION AND CONCLUSIONS ........ 118

7.1 Evaluation of System Performance ........ 118
    7.1.1 Segmented Model and Icebreaking Mechanisms ........ 118
    7.1.2 Instrumentation System ........ 122
    7.1.3 Data Acquisition and Reduction System ........ 124
    7.1.4 Data Analysis Methodology ........ 125

7.2 Conclusions ........ 129

8. REFERENCES AND BIBLIOGRAPHY ........ 132
8.1 References ........ 132
8.2 Bibliography ........ 134

APPENDIX A - CALIBRATION OF LOAD CELLS
APPENDIX B - CALIBRATION OF SEGMENTS
APPENDIX C - SYSTEM RESPONSE TO MODEL MOTION
APPENDIX D - MISCELLANEOUS TRANSDUCER CALIBRATIONS
APPENDIX E - MODEL ICE PROPERTIES MEASUREMENT
APPENDIX F - DETAILED TEST RESULTS
APPENDIX G - FINITE ELEMENT CALIBRATION OF SEGMENT NO. 2

## LIST OF FIGURES

| NO. | TITLE | PAGE # |
|---|---|---|
| 1.1 | The Development of Icebreaking Theory and Modelling | 3 |
| 2.1 | Forces Exerted by a Single Cusp Moving Along the Ship Hull | 10 |
| 2.2 | Two Cusp Breaking Pattern | 10 |
| 2.3 | Calculated Breaking Patterns | 11 |
| 2.4 | Schematic Presentation of Successive Ice Cusp Action on Ship Hull | 13 |
| 2.5 | Definition of Hull Regions | 15 |
| 2.6 | Experimental Investigation of Breaking Patterns | 16 |
| 2.7 | Overall Breaking Pattern | 17 |
| 2.8 | Segmentation Plan | 19 |
| 2.9 | Hull Lines of the PIERRE RADISSON | 22 |
| 3.1 | The PIERRE RADISSON Model with Three Bow Segments During Model Manufacturing | 25 |
| 3.2 | First Segmented Model of T-2 Tanker | 27 |
| 3.3 (a) | Internal Arrangement and Towing Gear of Segmented Model [10] | 27 |
| (b) | Instrumented Flexure | 27 |
| 3.4 | Segmented Model with Steel Box Girder Support [13] | 29 |
| 3.5 (a) | Arrangement of Model Segments [11] | 29 |
| (b) | Dynamometers | 29 |
| 3.6 | Above-Water Bow Segment and Associated Apparatus as used for a Pilot Experiment at NSRDC | 31 |
| 3.7 | Method of Model Segmentation | 35 |
| 3.8 | Ice Load Analysis on a Segment | 37 |
| 3.9 | Typical Segment Support Systems | 39 |
| 3.10 | Assembly Drawings for Load Cells | 49 |
| 3.11 | Photograph of Load Cells | 51 |
| 3.12 | Diaphragm Model | 55 |
| 3.13 | Prototype Calibration Results | 59 |
| 3.14 | Segmented Model Instrumentation | 61 |
| 4.1 | Typical Resistance Breakdown | 65 |
| 4.2 | Typical Speed and Acceleration Records | 67 |
| 4.3 | Measured Force Components for All Segments | 69 |
| 4.4 | Basic Force Analysis | 71 |
| 4.5 | Graphical Determination of the Ice Load Position | 77 |
| 5.1 | Finite Element Model Geometry | 83 |
| 6.1 | Measured vs Predicted Model Resistance | 97 |
| 6.2 | Dimensional Resistance Comparison | 97 |
| 6.3 | Measured vs Predicted Nondimensional Resistance | 99 |
| 6.4 | Nondimensional Resistance Comparison | 99 |
| 6.5 | Dry Calibrations of Segment 2 | 105 |
| 6.6 | Load Definition of Ice Load Cycles | 109 |

## LIST OF TABLES

NO. TITLE PAGE #

2.1 Typical Input and Output Requirements........................7
2.2 Segmented PIERRE RADISSON MODEL @ 23' Draft................21
3.1 Some Segmentation Options...................................33
3.2 Inertia Loads on Segments...................................43
3.3 (a) Reference Test Conditions...............................43
3.3 (b) Resistance Components for Reference Test Conditions........43
3.4 (a) CAlculated Impact Force.................................45
3.4 (b) Maximum Reactions at Segment Support Points..............45
3.5 Load Cell Ratings...........................................47
3.6 (a) Load Cell Stiffness.....................................57
3.6 (b) Frequency Response (Hz).................................57
4.1 Summary of Equations........................................80
5.1 Details of Tests............................................85
5.2 Ice Test Summary Sheet 1-1..................................87
5.3 Ice Test Summary Sheet 1-2..................................88
5.4 Ice Test Summary Sheet 2-1..................................89
5.5 Ice Test Summary Sheet 2-2..................................90
5.6 Ice Test Summary Sheet 3-1..................................91
5.7 Ice Test Summary Sheet 3-2..................................92
5.8 Ice Test Summary Sheet 4-1..................................93
5.9 Ice Test Summary Sheet 4-2..................................94
6.1 Quality of Transducer Response.............................101
6.2 Load Cell Registration Ratios and Mean Segment Correction Factors ..............................................104
6.3 The Effects of Ship Motions on Mean Values.................107
6.4 Comparison of Results......................................115
7.1 Comparison of Measured and Expected Ice Loads Segment 2, Test No.4-2.................................121
7.2 Effect of Experimental Errors on Friction Measurement Zero Friction Case.........................................127
7.3 Effect of Experimental Errors on Friction Measurement Higher Friction Cases.....................................128

# NOMENCLATURE

| | |
|---|---|
| $a$ | radius |
| $b$ | length of zone of ice crushing |
| $D$ | depth of broken floe |
| $E$ | Elastic Modulus |
| $F$ | force |
| $f_n$ | natural frequency |
| $H_c$ | horizontal extent of ice crushing |
| $h$ | ice thickness |
| $K$ | stiffness |
| $L$ | length |
| $M$ | vibrating mass |
| $P_n$ | maximum normal force |
| $R_i$ | ice resistance |
| $R_T$ | total resistance |
| $r$ | radius |
| $r_o$ | radius of applied load |
| $t$ | thickness |
| $v$ | ship speed |
| $\alpha$ | waterline angle |
| $\beta$ | transverse section flare angle |
| $\epsilon_r$ | maximum radial strain |
| $\ell_c$ | characteristic length |
| $\sigma_c$ | compressive strength |
| $\sigma_f$ | flexural strength |
| $\sigma_r$ | maximum normal stress |
| $\sigma_y$ | yield strength |
| $\rho_c$ | density of water |
| $\rho_g$ | weight density |
| $\rho_i$ | density of ice |
| $\mu F$ | external friction force |
| $\mu m$ | maximum deflection |
| $\nu$ | Poisson's ratio |

## SOME USEFUL CONVERSION FACTORS

| | |
|---|---|
| Mass (kilograms) | 1 kg = 2.2046 lb.m |
| Length (meters) | 1 m = 39.370 in. |
| Force (Newtons) | 1 N = 0.2248 lb.f |
| Stress (Mega Pascals) | 1 MPa = 145 psi |
| Pressure (kilo Pascals) | 1 kPa = 20.88 psf |
| (bars) | 1 ba. = 14.5 psi |
| Power (kilo Watts) | 1 kW = 1.341 hp |
| Speed (knots) | 1 kt = 1.699 fps (0.515 m/s) |

## COMMON MULTIPLES

| PREFIX | SYMBOL | FACTOR | EXAMPLE |
|---|---|---|---|
| giga | G | $10^9$ | GPa for Elastic Modulus |
| mega | M | $10^6$ | MN for force |
| kilo | k | $10^3$ | km for distance |
| centi | c | $10^{-2}$ | cm for length |
| milli | m | $10^{-3}$ | mbar for pressure |
| micro | $\mu$ | $10^{-6}$ | $\mu\varepsilon$ for strain |

# 1.
# INTRODUCTION

## 1. INTRODUCTION

Ships navigating in ice covered waters must be designed and powered to cope with environmental conditions which vary significantly in severity depending on the geographic zone and the time of year. While safety and hull structural integrity are of prime concern, the ability of a ship to proceed in ice and accomplish its mission is determined by its ability to overcome the resistance of ice and advance at an economic rate. A better ship would be one which offers a lower ice resistance thus requiring less power and energy.

The prediction of icebreaking resistance of ships has been the focus of interest of many research efforts since Runeburg in 1888. Figure 1.1 depicts the development of icebreaking theory and modelling. Despite this early start, it was 80 years later when Kashteljan and Russian co-investigators published the first attempt to rationalize the various mechanisms involved in the icebreaking resistance and their contribution to the total ice resistance forces. Several attempts followed and may be categorized in three distinct groups:

a) Empirical approach: Describes the resistance performance of a given ship under a finite range of conditions. This type cannot be extended beyond the range of determination and has limited value in extrapolation to other ship shapes or sizes.

b) Analytical approach: Modelling is based on certain assumptions relating to the components of icebreaking resistance and the development of forces by various mechanisms. The total resistance is either determined by mechanics or energy methods. Verification is usually made by comparison of total resistance to experimental data.

c) Semi-empirical approach: This is an intermediate level between empirical and analytical techniques. It is essentially an empirical development which takes into account ship and ice variables. It can be extended, for prediction purposes, in a wider range but would still be limited in scope to the range of determination.

In all the above methods, extrapolation is risky since the verification of any one model is often based on limited experimental data. However, analytical type models hold the promise of possible extension to the prediction of ice resistance to longer, and larger ships envisaged for Arctic Transportation routes and of better accuracy. The consolidation of analytical or semi-empirical models can be accomplished by the verification of the contribution of the various mechanisms involved in icebreaking. The lack of information on the contribution of various elements and mechanisms of the icebreaking process was noted. Furthermore, the lack of universal agreements between predictions made by various types of models and experimental (full or model scale) data have underscored the need for further study.

The identification of such a need has resulted in the structuring of a new approach to investigate the resistance components and

FIGURE 1.1

THE DEVELOPMENT OF ICEBREAKING THEORY AND MODELLING

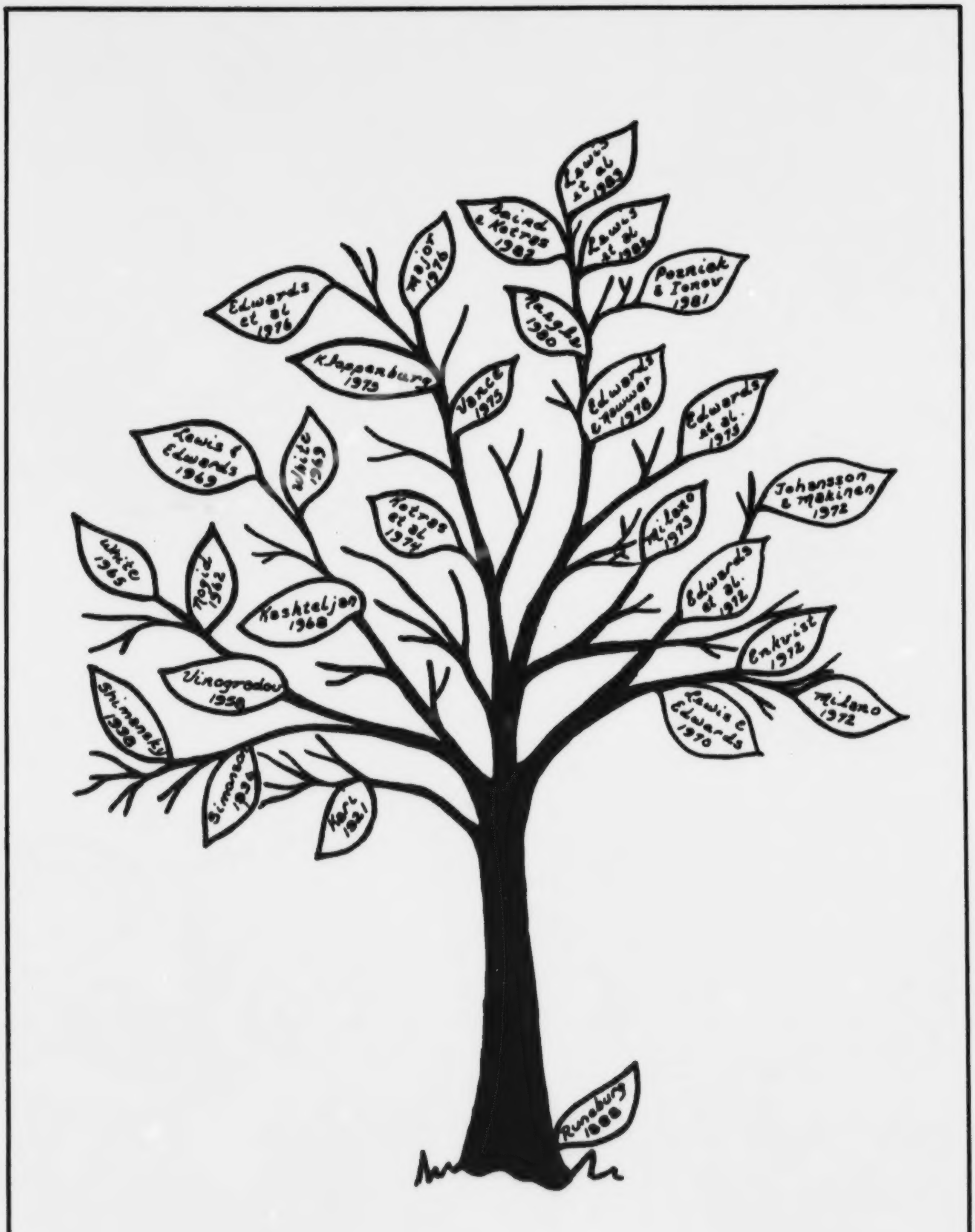
Lewis et al 1983
Saeid & Kotras 1982
Lewis et al 1982
Poznjak & Ionov 1981
Naegle 1980
Major 1976
Edwards et al 1976
Kloppenburg 1975
Vance 1975
Edwards & Rouwer 1978
Edwards et al. 1975
Lewis & Edwards 1969
White 1969
Kotras et al 1974
Milano 1973
Johansson & Makinen 1972
White 1965
Nogid 1962
Kashteljan 1968
Edwards et al. 1972
Enkvist 1972
Vinogradov 1959
Lewis & Edwards 1970
Milano 1972
Shimansky 1938
Simonson 1936
Kari 1921
Runeberg 1888

mechanisms associated with icebreaking. Since different icebreaking components affect different zones on the hull surface, it would therefore be feasible to build a segmented model which enables the measurement of such forces individually. The success in developing this testing technique would provide an excellent tool which can be devised to improve the present state of understanding of the icebreaking resistance and associated mechanisms and components. This, in turn, would improve the capability to predict the total ice resistance, as well as to optimize the hull shape to minimize the resistance and possibly power requirements.

The immediate objective of the present study was to develop and to use a segmented model, to establish the technique and to provide an initial amount of data and analysis of icebreaking mechanisms and processes.

## 2.

# MODEL SEGMENTATION, ANALYSIS AND RATIONALE

## 2. MODEL SEGMENTATION: ANALYSIS AND RATIONALE

### 2.1 Primary Sources of Ice Resistance

> *It is generally recognized that the resistance of ice to ship motion consists of several components due to bending and breaking of ice cusps, acceleration and moving of broken ice pieces and gravitational resistance due to the buoyancy of submerged ice. The forces caused by these effects are assumed to be additive.*

Earlier analytical models developed by Milano [1], Enkvist [2], Naegle [3], and most recently, Carter [4] acknowledged the additive nature of various components and follow different approaches. While Milano advocated an energy concept to sum up the various energies expended by the force components, both Enkvist and Naegle used a mechanics approach which analyzes the forces associated with each of the successive mechanisms observed during icebreaker progress in ice. Enkvist developed a number of coefficients which described the hull form effects on transformation of forces acting on the hull. On the other hand, Naegle treated the ship as a responsive rigid body, thus by setting its surge acceleration to zero continuous forward motion could be analyzed and the effects of ship motions were incorporated in the analysis. Carter's approach was entirely different. He formulated the problem in closed form rather than a time-step solution used by others. Carter made some basic assumptions in his analysis which have not been verified. Nonetheless, his equation was shown to provide agreeable correlations with limited experimental data.

Details of the primary features of the state-of-the-art models may be found in several of Transport Canada technical publications as noted in the reference list.

Only analytical models were inherently capable of predicting the distribution of forces along the hull and hence, those empirical or semi-empirical models, though capable of representing the overall effects of hull geometric characteristics on the resistance, could be used to provide grounds for model segmentation as anticipated in the present study.

For instance the RICE computer code which was developed on analytical grounds and adjusted by field data available on a number of ships is available. Typical input and output requirements are listed in Table 2.1.

In this present study, recent developments of the semi-empirical model based on Naegle's analytical approach were used to assess force components and their distribution on the hull.

## TABLE 2.1

## TYPICAL INPUT AND OUTPUT REQUIREMENTS FOR RESISTANCE PREDICTOR MODEL

### INPUT REQUIREMENTS

Waterline offsets, in metres
Waterline angles
Particulars: LBP, Beam, Draft, in metres
Coefficients: Block, Waterline, Midships
Number of Propellers
Center Shaft: Power (KW), Diameter (m), Speed (RPS)
Wing Shafts: Power (KW), Diameter (m), Speed (RPS)
Friction Factor
Operating parameters for the program

Ice thickness, metres
Elastic Modulus (MPa)
Flexural strength (kPa)
Ship Speed, m/s

### OUTPUT

Total Resistance
Water Resistance
Breaking resistance, Breaking Friction
Turning resistance, Turning Friction
Sliding resistance, Sliding Friction

(All resistance values in Newtons)

## 2.2 Contribution of Hull Geometric Areas

*The total resistance to ship motion at any time is the sum of all force components acting on the hull at this time resolved in the direction of ship motion. The variation in magnitude and locations of these individual forces during ship progress in ice reflects on the variation in total measured resistance with time. Therefore, the average resistance is the sum of average resolved forces acting on all hull zones and calculated over the same time interval.*

The forces generated on any geometric hull zone are imposed by the contacting ice. As the ice moves along the hull it deflects, bends, breaks, gets turned around and submerged until it is either displaced away from the ship or until it clears the hull. For a ship moving at constant speed, the moving force exerted by a specific cusp (or point on the ice) may be demonstrated by the trace given in Figure 2.1. It is anticipated that the maximum force will correspond to the breaking of ice and that the relative magnitudes of forces corresponding to events (3), (5) and (6) as noted in the figure will depend on ice characteristics as well as the ship speed and the hull geometry at the point of contact. For instance if hull angles promote crushing and preclude flexural mode of deflection and failure, the force will be higher. However, the contribution to the total resistance will depend again on local hull angles which determine the resolved component. Generally, the ice fails in the bending mode at the stem and the forward part of the bow. As the ice moves aftwards, the contribution of friction forces associated with ice failure increases.

If the ice continuously broke in a repeated pattern, a fixed point on the hull would experience a load which varied as the ice moved past this particular point. For instance, consider Figure 2.2 which schematically illustrates a two cusp breaking pattern and at fixed position 2 at the cusp centre of contact, an ice load will be experienced which could be expected to vary between levels (3) and (5) as shown in Figure 2.1. The frequency of variation would be determined by the speed of the ship. Another point on the hull located at the intersection between the first and second cusps would likely experience lesser loads because as the first cusp breaks and moves aft, it would be turning and submerging. Therefore, maximum loads in this area of the hull would probably be as high as level (5), Figure 2.1.

When the ice thickness or properties change the pattern may also change and the locations which experience maximum forces will shift. Nonetheless, the cyclic nature will be maintained, unless ice fails at random.

Therefore, the understanding of the contribution of different hull geometric areas to the total resistance can aid in hull optimization for resistance minimization. The expected locations of maximum force for a given pattern of icebreaking will constitute a major criterion in developing the segmentation rationale.

Differences will exist in force locations among different hull forms. At this early state of technique development it was justified to confine the study to a single hull form. The hull of the CCGS PIERRE RADISSON[1] was selected because of the availability of a large database which could make further interpretation of test results easier.

For the PIERRE RADISSON hull, the breaking patterns and hull areas subjected to maximum loads were investigated experimentally and analytically.

The analytical examination was based on recent analytical model developments [5,6]. Figure 2.3 illustrates the calculated breaking patterns of ice ranging in thickness from 0.3 to 0.9 m. The calculations were based on the following assumptions:

- Ice properties; Elastic modulus $E = 3$ GPa
  Poisson's ratio $\nu = 0.3$
  Weight density $\rho_g = 10$ kN/m³
- The characteristic length was calculated from:

$$\ell_c = \left[\frac{Eh^3}{12\,(1-\nu^2)\rho_g}\right]^{0.25} = 12.87\ h^{0.75}$$

- The depth of the first cusp was dependent on the characteristic length and the average third direction cosine over 20% of the ship length ($\bar{n}_3 = 0.437$ for the RADISSON).

$$D_1 = \ell_c[0.0247 + 0.5439\ \bar{n}_3] = 0.262\ \ell_c$$

- The first row of cusps had a length/depth ratio of 3.
- The second row of cusps had a length/depth ratio of 4.
- The third row of cusps had a length/depth ratio of 5.

All calculations were based on procedures used by Naegle and were further modified by Arctec. It was shown that the ship would likely break two rows of cusps for thicker ice and three rows or more for thin ice.

---

[1] Basic characteristics of the CCGS PIERRE RADISSON hull are given in Section 2.4. Please note that all line diagrams presented in this report are based on 20 station subdivisions.

## FIGURE 2.1

## FORCES EXERTED by a SINGLE CUSP MOVING ALONG the SHIP HULL

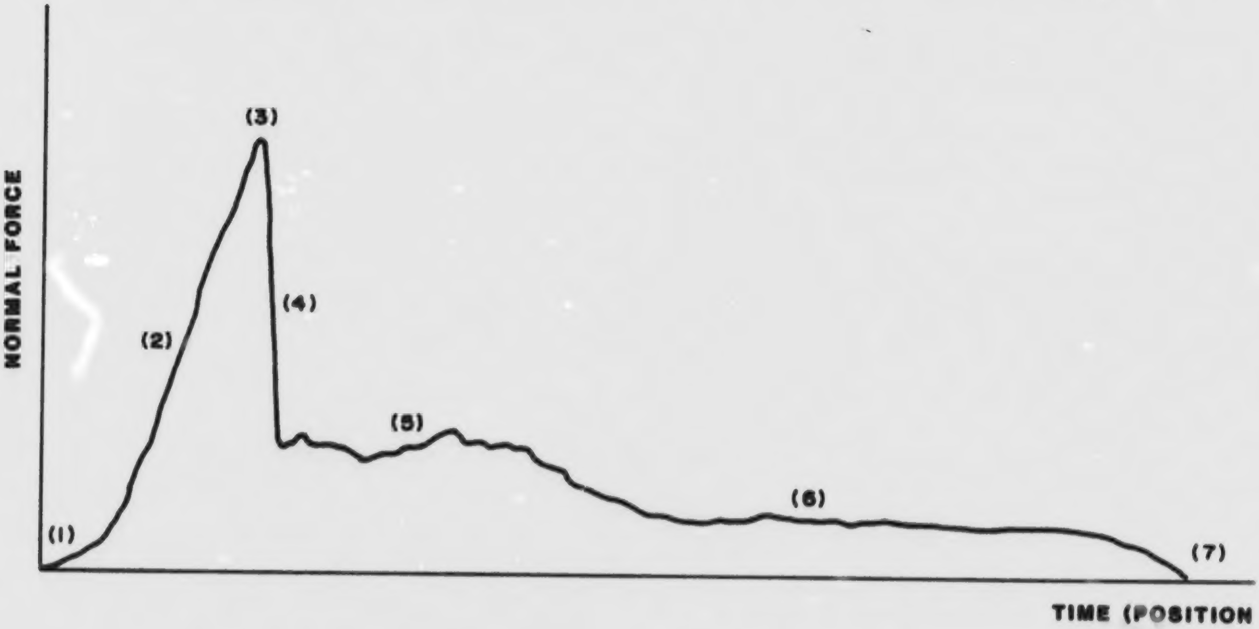

(1) CONTACT STARTS

(2) ICE BENDING AND DEFLECTION, LOAD AREA DEVELOPED BY CRUSHING.

(3) FLEXURAL FAILURE AT MAXIMUM FORCE.

(4) RELEASE OF ELASTIC ENERGY.

(5) ICE TURNING AND SUBMERGENCE.

(6) ICE SLIDING ALONG HULL (BUOYANCY FORCES).

(7) ICE CLEARING.

## FIGURE 2.2 TWO CUSP BREAKING PATTERN

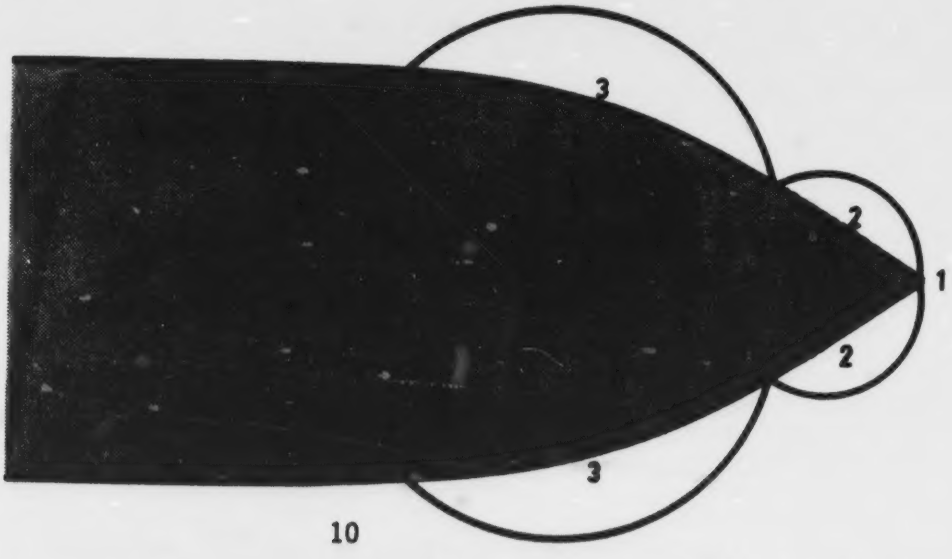

**FIGURE 2.3 CALCULATED BREAKING PATTERNS**

h = 0.3 m

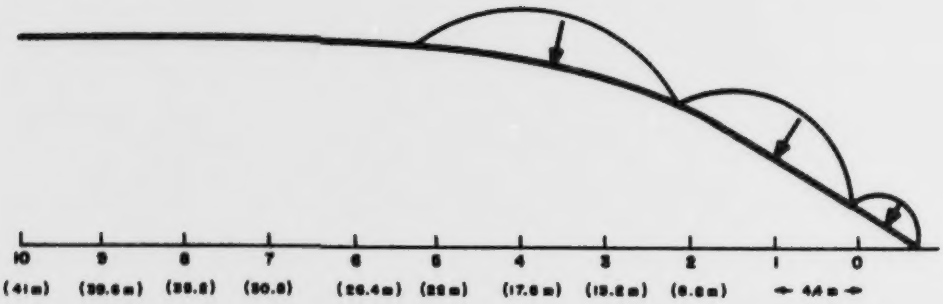
10
9
8
7
6
5
4
3
2
1
0
(41m)
(39.6m)
(35.2)
(30.8)
(26.4m)
(22m)
(17.6m)
(13.2m)
(8.8m)
← 4.4m →

h = 0.6 m

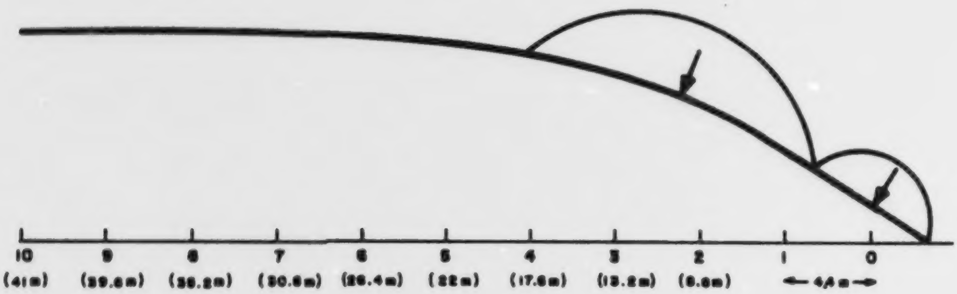
10
9
8
7
6
5
4
3
2
1
0
(41m)
(39.6m)
(35.2m)
(30.8m)
(26.4m)
(22m)
(17.6m)
(13.2m)
(8.8m)
← 4.4m →

h = 0.9 m

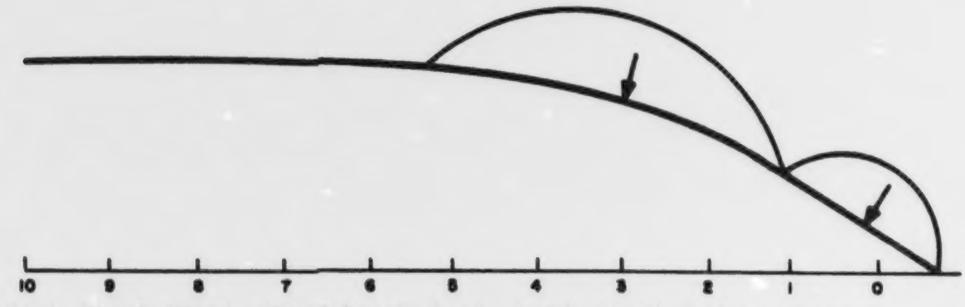
10
9
8
7
6
5
4
3
2
1
0
(41m)
(39.6m)
(35.2m)
(30.8m)
(26.4m)
(22m)
(17.6m)
(13.2m)
(8.8m)
← 4.4m →

Based on the cusp breaking patterns illustrated in Figure 2.3, one can assume that the forces acting on the hull occur at the center of the cusp as shown by pointed arrows. This indicates that the locations subjected to maximum ice forces on the hull will be dependent on ice thickness. They would also be affected by the stochastic aspects of the icebreaking process which causes some random variations in the cusp size and length to depth ratio. However, the indicated positions can be assumed to represent locations where maximum forces on ice fracture would most likely occur. That is, most incidences would be observed in the close vicinity of these locations.

As the ship moved forward, the ice crushing, bending and failure and subsequent displacement of broken ice continued. Figure 2.4 is a schematic representation of the progressive development of cusps. The shaded areas represent continued crushing and contact area development. As the contact area grows larger the centre of contact (where the resultant force acts) also moves outwards. It is shown that once a repeated pattern is developed the positions of maximum forces shift slightly inwards for the second and third rows of cusps. In this graphical analysis it is assumed that the first row of cusps governs the pitch of breaking the ice.

It should be noted that while the first row of cusps in a repeated pattern is symmetric, the second and following rows are non-symmetric. This is caused by the geometry of the breaking and expected stress patterns within the ice sheet. The shape of the cusps in reality is triangular with curved edges, which very closely resembles the broken shapes as noted in Figure 2.4. It should also be mentioned that the patterns indicated are those of primary breaking. Large cusps could further break into smaller segments as they get turned and submerged. The presence of cracks in ice promote such occurrences.

Using these repeated patterns it is possible to determine the area of the hull along the waterline where maximum forces will occur by projection of the action of successive cusp rows on the hull. It is interesting to observe that a steady-state cusp breaking pattern will be repeated with some differences due to the inhomogeneity of ice.

If model tests were conducted on a 20th scale model, the thin ice in model scale would be 15 mm. We do not recommend this low thickness for preliminary developments to avoid problems which may arise due to improper scaling of ice properties. Therefore, testing was limited to 0.6 and 0.9 m and possibly thicker ice. It is the two-row pattern in all cases which makes the division of the hull into segments more rational as it would cover a wide and practical range of thicknesses.

Figure 2.5 gives a summary of Figure 2.4 and proposed demarkation lines for three bow regions which are likely to see the maximum ice forces. A fourth region was also identified to cover the remainder of the bow length.

**FIGURE 2.4**

**SCHEMATIC PRESENTATION of SUCCESSIVE ICE CUSP ACTION on SHIP HULL**

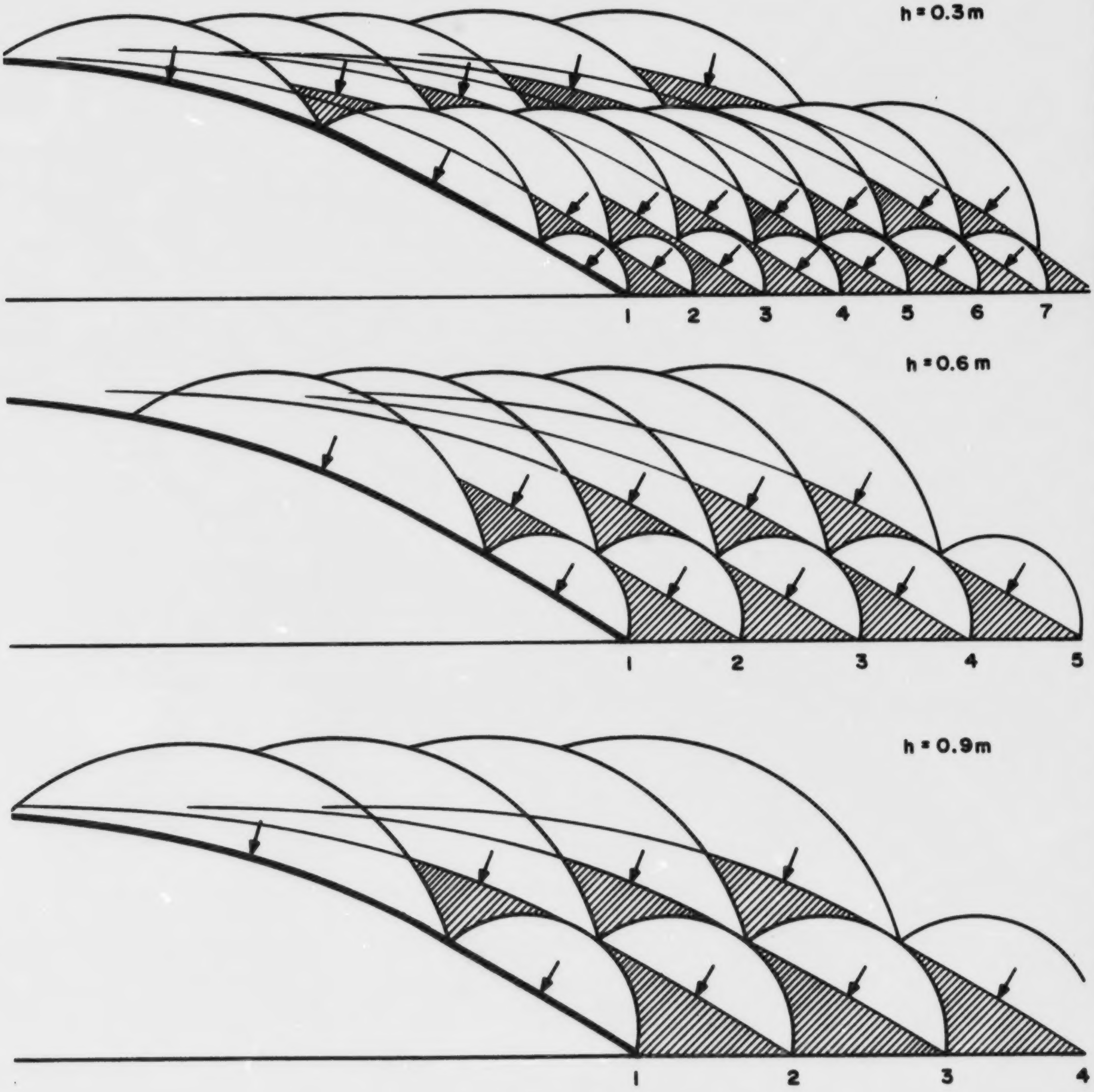
h = 0.3m
1
2
3
4
5
6
7
h = 0.6m
1
2
3
4
5
h = 0.9m
1
2
3
4

These regions are characterized by the following:

- Region I: (0 to 7.5m) will mainly experience icebreaking and associated friction forces due to the stem and first row of cusps. Turning and submergence loads are minor.

- Region II: (7.5 to 15.5m) will experience icebreaking and associated friction forces due to the 2nd row of cusps, as well as an increased level of turning and submergence forces.

- Region III: (15.5 to 23.0m) will experience icebreaking forces only in thin or extremely thick ice but is expected to sense only turning and submergence forces due to the second row of cusps in medium (0.6m) and thick (0.9m) ice.

- Region IV: (23.0 to 39.0m) will primarily experience turning, submergence and associated friction forces. Therefore, it will not be subjected to maximum breaking forces.

Experimental investigation of the breaking pattern was conducted by running a 20th scale model of the PIERRE RADISSON in 30mm thick ice and observing the breaking patterns. Figure 2.6 is a series of photographs which were taken by a spatially fixed camera on the side of the basin. The photographs were shot automatically at constant time intervals and represent the development of the breaking patterns. The red marks on the hull represent stations 1, 2 and 3 and the yellow colour ends approximately at station 3 3/4. Examination of the series of photographs revealed that:

- The test was done at shallow draft.

- Photo #1 showed initial crushing at the stem, and cracks of the first row of cusps become visible in photo #2. As the ship progressed the cusp gets turned, up-ended and submerged as illustrated in photo #'s 3,4, and 5.

- Photo #6 is an excellent shot of two cusps being broken and turning simultaneously which depicts what was suggested in the idealized pattern. The first cusp is broken forward of station #1 while the second seems to be centered about station #1 3/4. This very well corroborates the projections made in Figure 2.5. As the second cusp moves aftward and turns as shown in Photo #7, we notice the presence of the previous row being up-ended.

- Photo #8 through #12 illustrates the continuation of the failure process with different levels of clarity as the ship moves ahead and the relative position of the camera changes.

Figure 2.7 illustrates the overall pattern of broken ice. It was noted that larger cusps may break in smaller pieces during the submergence and sliding against the hull. The ice thickness was 30 mm or (0.6m full scale).

It may be concluded that general agreements were observed between the analytical predictions and experimental results and, hence, the analytical model could be used as a basis for segmentation.

FIGURE 2.5

DEFINITION OF HULL REGIONS

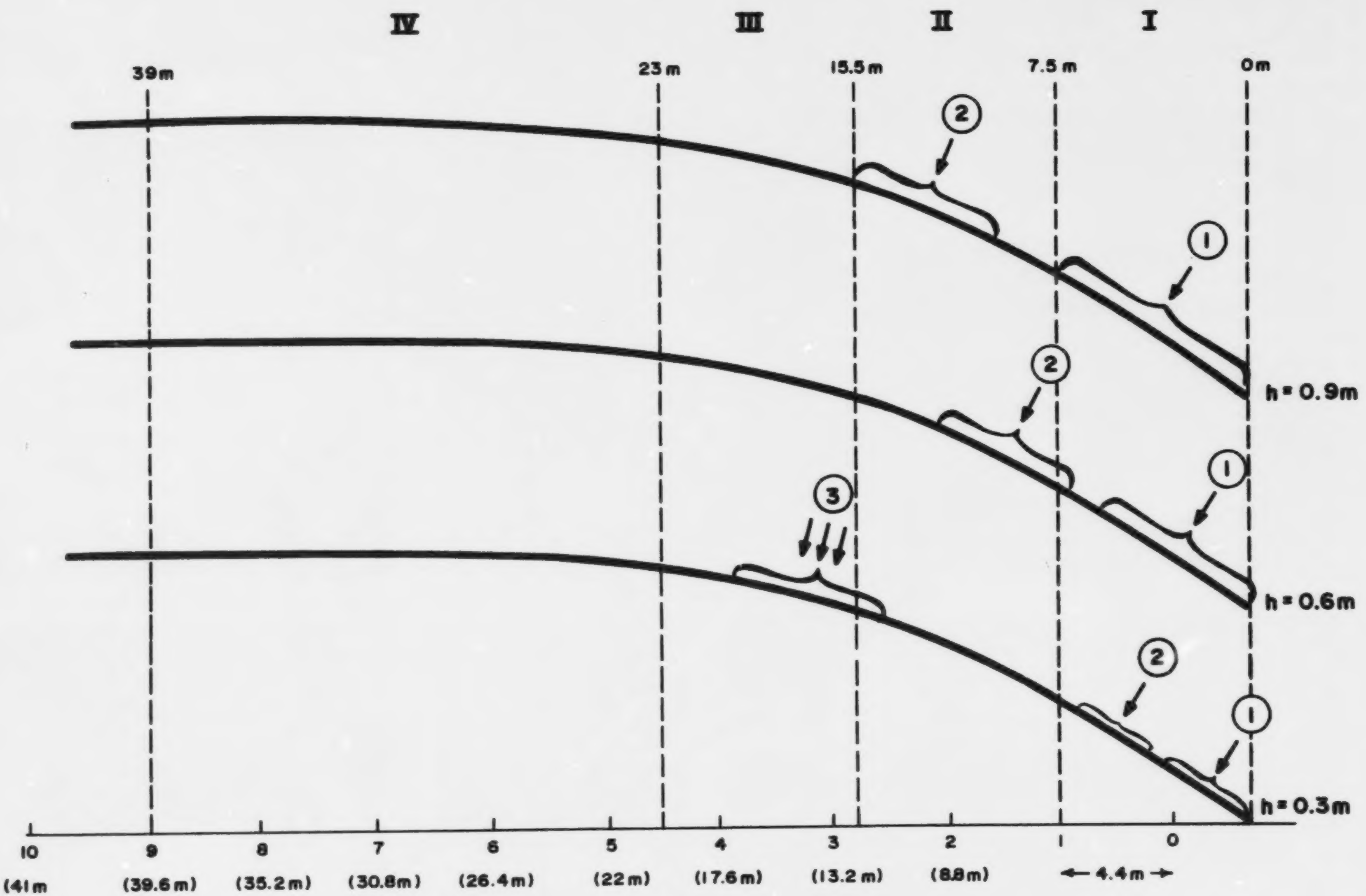
IV
III
II
I
39m
23 m
15.5 m
7.5 m
0m
①
②
③
h = 0.9m
h = 0.6m
h = 0.3m
10
9
8
7
6
5
4
3
2
0
(41m
(39.6 m)
(35.2 m)
(30.8m)
(26.4 m)
(22 m)
(17.6 m)
(13.2 m)
(8.8m)
← 4.4m →

FIGURE 2.6 EXPERIMENTAL INVESTIGATION OF BREAKING PATTERNS

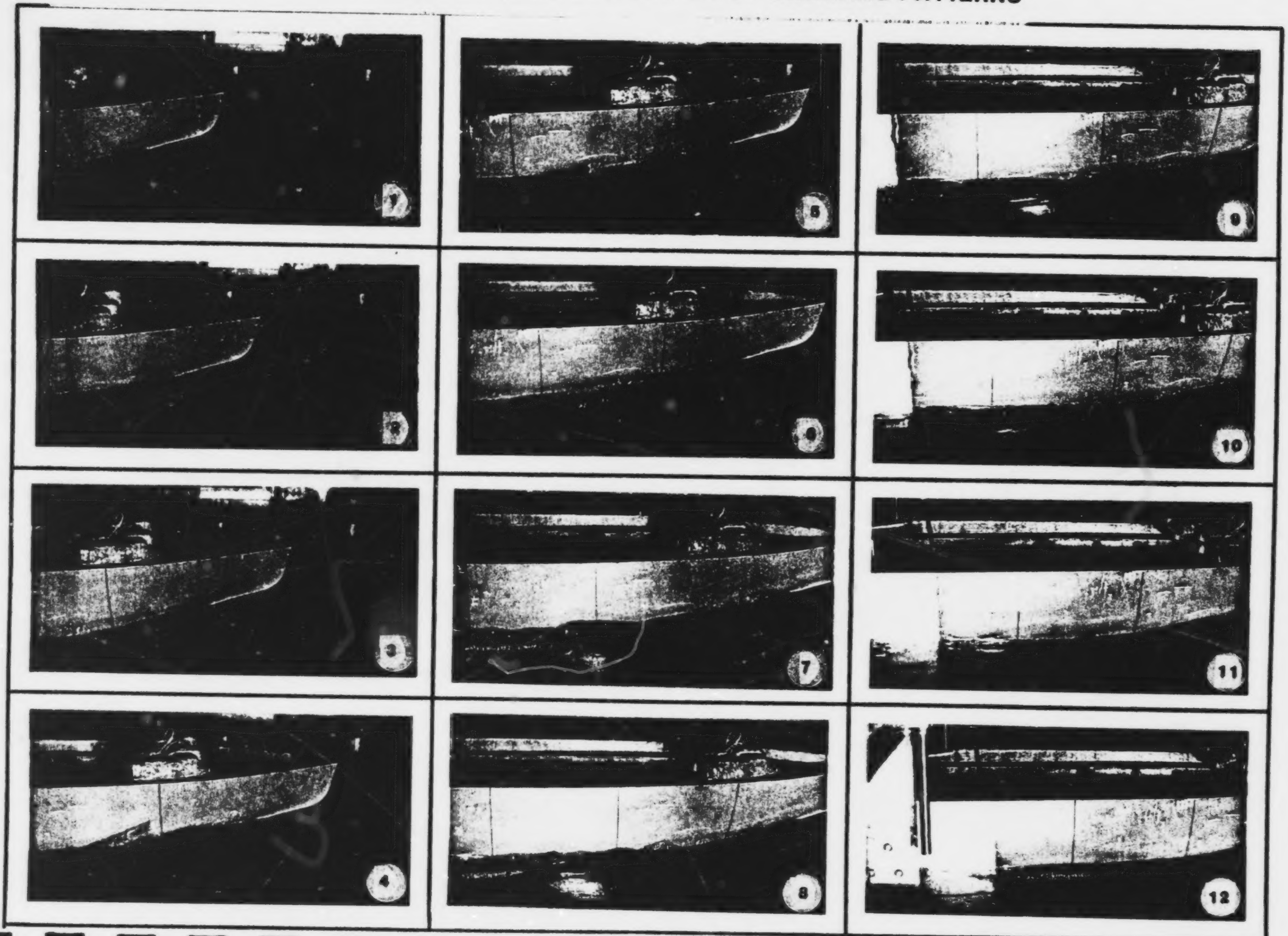
1
2
3
4
5
6
7
8
9
10
11
12

FIGURE 2.7
OVERALL BREAKING PATTERN

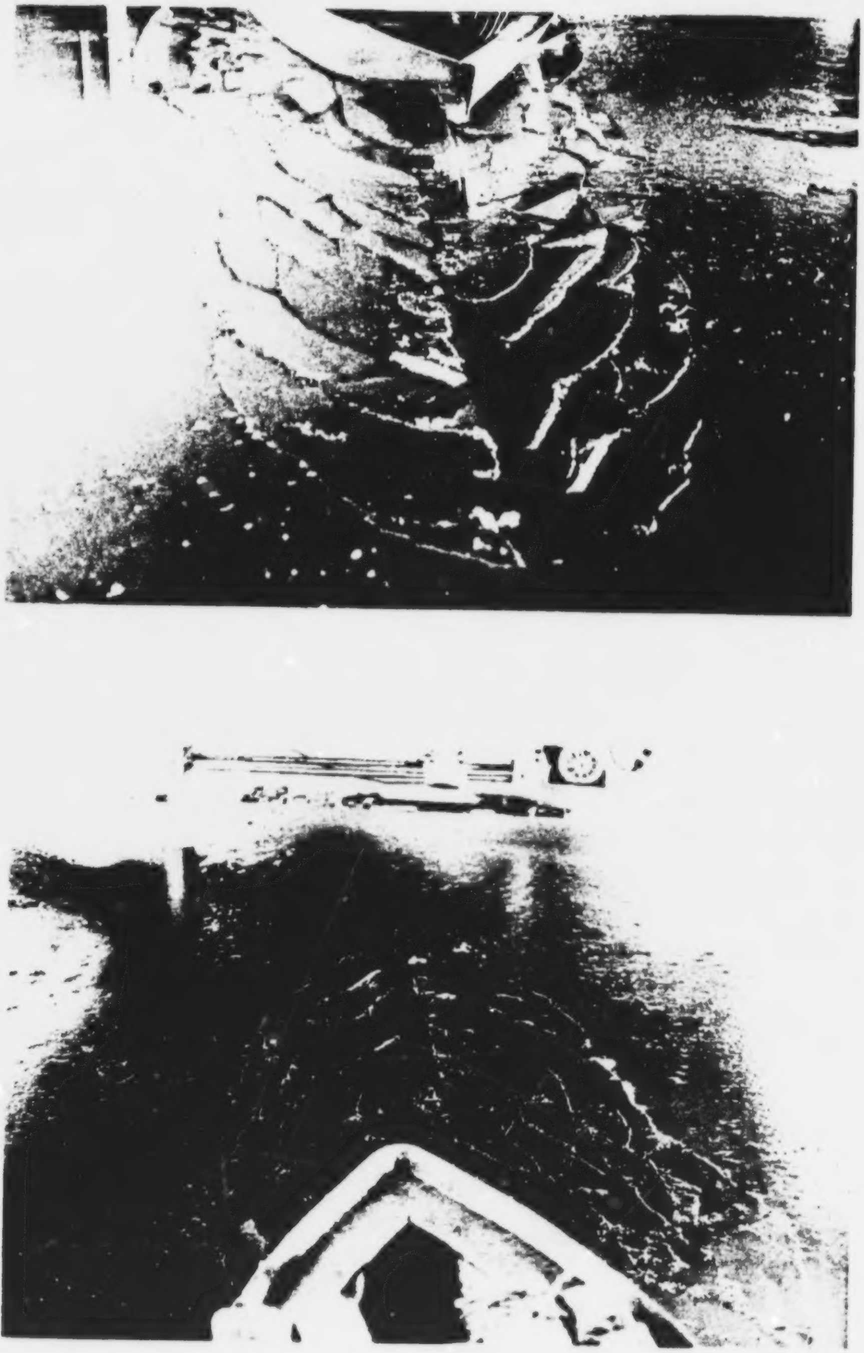

## 2.3 Segmentation Rationale

> *The rationale for segmentation was based on the contribution of hull geometric areas to the total resistance. From the foregoing analysis it was shown that there were four regions which could be identified at the waterline which were relevant to the breaking pattern. Therefore, if the hull was divided into segments which sufficiently extend above and below the waterline, these segments would be exposed to breaking and turning forces exerted by the generated rows of cusps.*

Figure 2.8 illustrates three bow segments based on the above justification. Segment 1 is the stem segment which primarily monitors breaking force and friction at the stem and the immediate vicinity forward of Station #1. The second segment would likely be subjected to breaking forces from the second row of cusps in addition to some turning forces arising from the first row. The third segment would be the turning force and friction segment. It is not likely to be subjected to maximum breaking forces except in thin or very thick ice or when direct ice crushing occurs on the segment.

No segments were placed in region IV as it was felt unnecessary at this stage of development. However, the contribution of this region to total resistance under normal operating conditions was judged to be small. This applied only to the present study since the contribution of this region to impeding ship progress could greatly increase under certain conditions such as build up of pressure in the ice cover.

Forces contributed by the lower hull were mainly due to submergence components. The latter was estimated to range between 10 and 15 percent of the total resistance.

It was estimated that at low speeds of the order of 2 kts (1 m/s), breakdown of resistance would be approximately given by:

| | |
|---|---|
| ° Breaking and friction | 70% |
| ° Turning and friction | 20% |
| ° Other (submergence) | 10% |

At higher speeds the turning component becomes more significant due to dynamic effects and the relative significance of the breaking component decreases and becomes comparable to the turning component. These figures may vary but they represent a reasonable distribution of resistance by source.

Due to the relative significance of icebreaking force components and in order to maintain the model simple and inexpensive, it was decided that no additional segments would be assigned to the submergence components.

FIGURE 2.8

SEGMENTATION PLAN

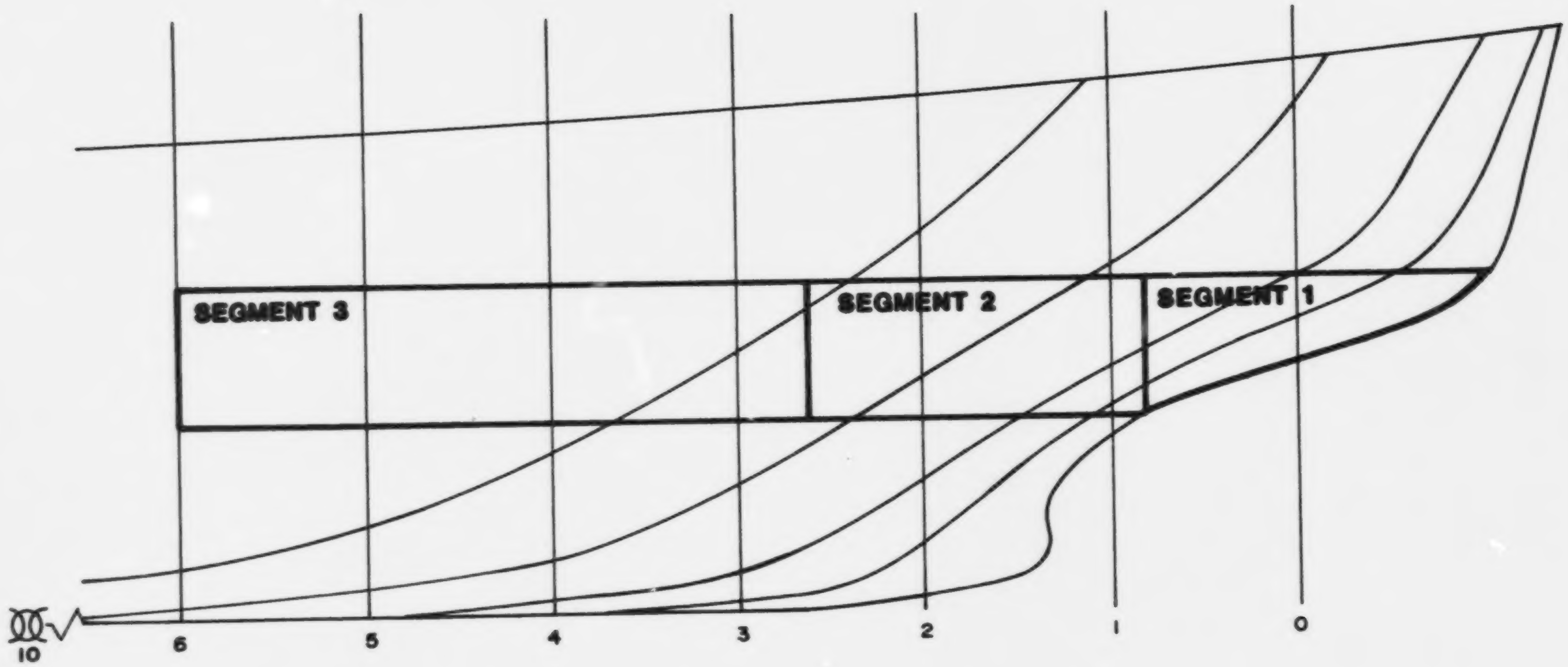
SEGMENT 3
SEGMENT 2
SEGMENT 1
6
5
4
3
2
1
0
10

## 2.4 PIERRE RADISSON Characteristics

The characteristics of the PIERRE RADISSON 20th scale model are given in Table 2.2 which is a standard data sheet used by Arctec to document all models or ships tested.

Figure 2.9 gives the hull lines of the ship for reference purposes.

The model surface was prepared to a friction factor of 0.095 ± 0.007. All three segments had a friction coefficient of 0.1.

| SERIAL # | TABLE 2.2 | DESIGNATION<br>566C |
|---|---|---|
| VESSEL NAME<br>&<br>HULL FORM | SEGMENTED PIERRE RADISSON<br>MODEL (@ 23' Draft) | SCALE<br>1:20 |

***DIMENSIONAL PARAMETERS**

$L_{OA} = 4.916$ m
$L_{pp} = 4.397$ m
$L_{WL} = 4.575$ m
$B = 0.966$ m
$T = 0.351$ m
$\nabla = 0.967$ m³
Roll period = 2.0 sec
Pitch Radius of gyration = ¼ L

$C_b = 0.623$
$C_{bf} = 0.540$
$C_p = 0.679$
$C_w = 0.798$
$C_{wf} = 0.796$
$C_m = 0.918$
$\gamma_0 = 36°$
$\beta_5 = 5.5°$

****NONDIMENSIONAL PARAMETERS**

$L/B = 4.736$ $\textcircled{M} = 4.446$
$B/T = 2.752$ $\sqrt{\textcircled{M}} = 2.109$
$\nabla/(0.1L)^3 = 11.38$

$\mu_0 = 1.582$
$\eta_2 = 2.915$

**FRICTION FACTORS, $f$:**

$f = .095 \pm .007$

**GEOMETRY-FRICTION COEFFICIENTS**

| $f$ | $\mu_1$ | $\mu_2$ |
|---|---|---|
| 0.000 | .582 | .343 |
| 0.100 | .780 | .479 |
| 0.200 | .978 | .628 |
| 0.300 | 1.176 | .791 |
| 0.400 | 1.373 | .971 |
| 0.500 | 1.571 | 1.170 |

**FOREBODY WATERPLANE ANGLES**

| STATION | 0 | 1 | 2 | 3 | 4 | 5 | 6 | 7 | 8 | 9 | 10 |
|---|---|---|---|---|---|---|---|---|---|---|---|
| α ° | 29 | 28 | 23 | 14.5 | 8.5 | 5.5 | 3.5 | 2.5 | 1 | 0 | 0 |
| β ° | 50 | 43 | 33 | 22 | 12.5 | 10 | 7 | 6.5 | 5.5 | 5.5 | 5.5 |

FIGURE 2.9

HULL LINES OF THE PIERRE RADISSON

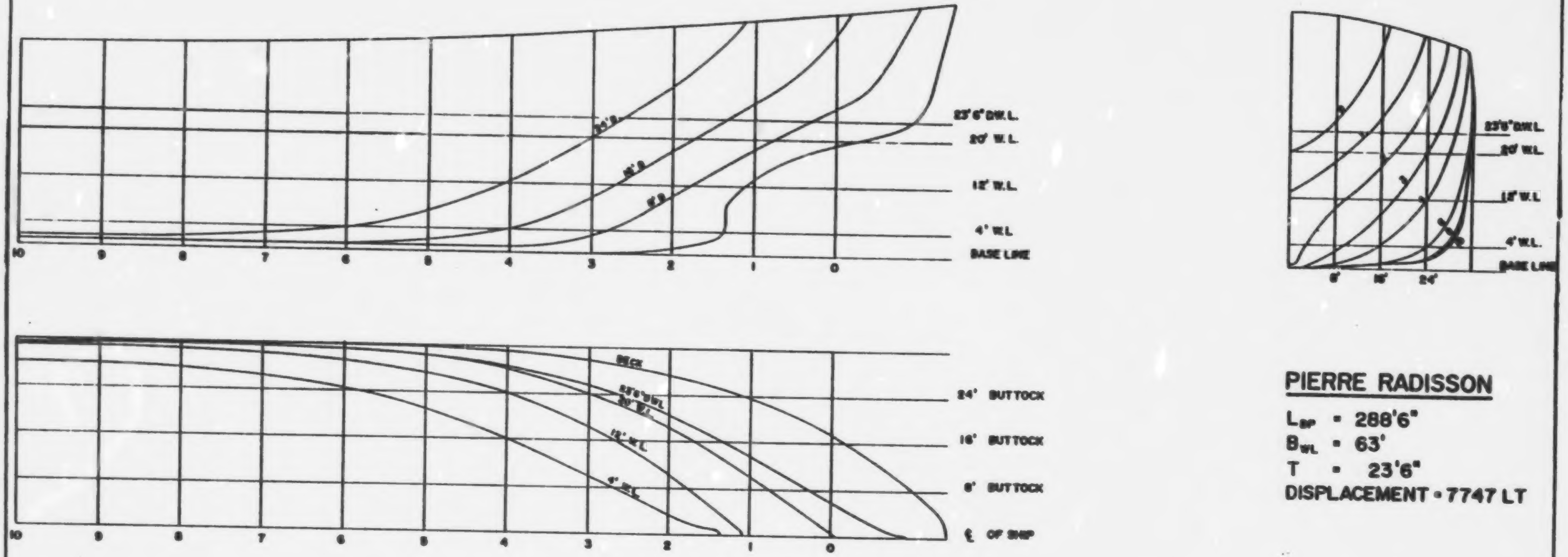
24' B
16' B
8' B
23'6" DWL
20' W.L.
12' W.L.
4' W.L.
BASE LINE
10
9
8
7
6
5
4
3
2
1
0
DECK
23'6" DWL
20' W.L.
12' W.L.
4' W.L.
24' BUTTOCK
16' BUTTOCK
8' BUTTOCK
℄ OF SHIP
8'
16'
24'

**PIERRE RADISSON**

$L_{BP}$ = 288'6"
$B_{WL}$ = 63'
T = 23'6"
DISPLACEMENT = 7747 LT

# 3.

# DEVELOPMENT OF SEGMENTATION AND INSTRUMENTATION TECHNIQUES

# 3. DEVELOPMENT OF SEGMENTATION AND INSTRUMENTATION TECHNIQUES

## 3.1 Model Segmentation Plan

Ideally several segments at the bow would be required to separate the significant components of ice forces which contribute most to the resistance of the ship. Such a segmentation plan should coincide with the action zones identified in Figure 2.8. Obviously, compliance with this standard of detail required compatible efforts in the design of supporting and force measuring systems as well as those required for manufacturing the models.

Upon extensive consultation with the model builder to determine the implication of the number of segments and their location, with due consideration of the available resources, and due consultation with TDC, it was decided that:

a) A model with three segments covering the bow at water line would provide a means for investigating the most significant forces associated with icebreaking, namely; breaking and turning forces and their frictional components.

b) A fourth segment covering zone 4 would likely be subjected to the less significant submersion component of resistance. The expected return of technical information, at this state of development, does not warrant the complications resulting from the addition of this segment.

c) The simplicity of the segmentation plan was desirable for this exploratory work as it permitted the devotion of efforts to achieve higher quality rather than quantity. Once this technique is well developed, the segmentation plan could be expanded and improved to cover other aspects of hull-ice interaction.

d) Realizing the current state-of-the-art of building and testing of segmented models, it was felt that this attempt to segment the bow and provide for 3-D force measurement was sufficiently advanced. Thus, efforts were to be directed to solving the problems of instrumentation rather than those arising from increasing the number of segments.

Therefore, the segmentation plan of the model was finally approved as illustrated in Figure 3.1.

FIGURE 3.1

THE PIERRE RADISSON MODEL WITH THREE BOW SEGMENTS

DURING MODEL MANUFACTURING

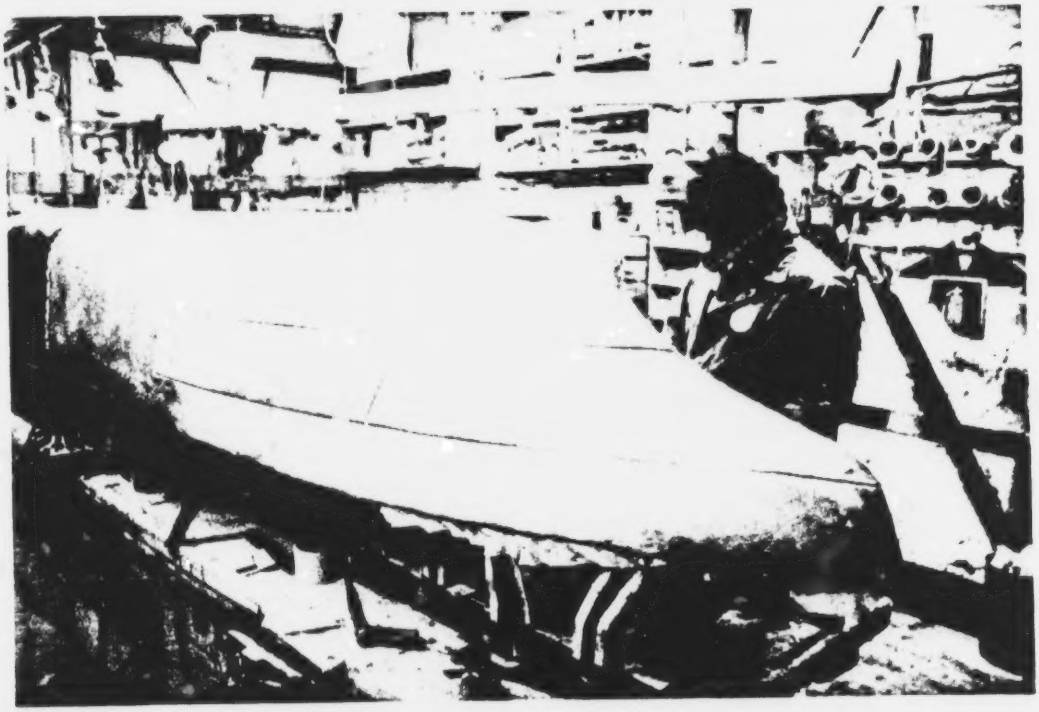

## 3.2 Review of Earlier Work

In the process of developing the segmentation technique for the present study, earlier efforts to utilize segmented models of ships were reviewed. None of the earlier tests were conducted in ice.

The earliest reported attempt to utilize segmented ship models for experimental purposes is credited to Lewis in 1954 [7]. Lewis developed a two-segment model of T-2 tanker in which the model was cut at midship and the two segments were joined in such a manner that small measurable deflections could be mechanically amplified and picked up. A sketch of his technique is shown in Figure 3.2. The two segments were considered as rigid bodies connected by flexure bars. The rigidity of the flexures was selected such that:

- The deflection was measurable.
- The natural frequency of the system was well removed from the frequency of applied loads (wave frequency).
- The flexibility of the model corresponded to the natural frequency of vertical two-noded vibrations of the full scale elastic hull in order to account for the effects of vibratory phenomena on the bending moment (approximately).

Based on experimental results it was found that inertia effects were significant and actually affected the accuracy of measurements. Later, Lewis improved his measurement technique by using an improved dynamometer to measure bending moments and shear forces at the plane of segmentation amidships [8].

In 1956, another approach to measure bending moments using segmented models was developed by Wachnik and Robinson [9]. They divided a five-foot long model of a cargo/passenger vessel into three segments separated at the midship section and at the forward quarter point. The segments were interconnected by an aluminum bar which was strain gauged to measure the bending moment at each connection.

In 1963, this technique was further refined by Wachnik and Schwartz [10]. They developed a ten-foot long self-propelled model of a MARINER Class ship which was segmented longitudinally at seven locations as illustrated in Figure 3.3(a). The eight segments were interconnected by an aluminum flexure beam instrumented with strain gauges to measure bending moments and shear forces. The flexure EI modulii at each section were the scaled down values of the ship. Figure 3.3 (b) illustrates the strain gauging arrangement for a typical flexure. The beam was calibrated statically by using deadweights at discrete points along its length and the calibration constants were calculated from the beam properties and associated instrumentation.

The results obtained using this technique were shown to offer general similarities to data obtained by other investigators using different techniques. However, some differences were observed under different conditions and they were attributed to differences in loading distributions.

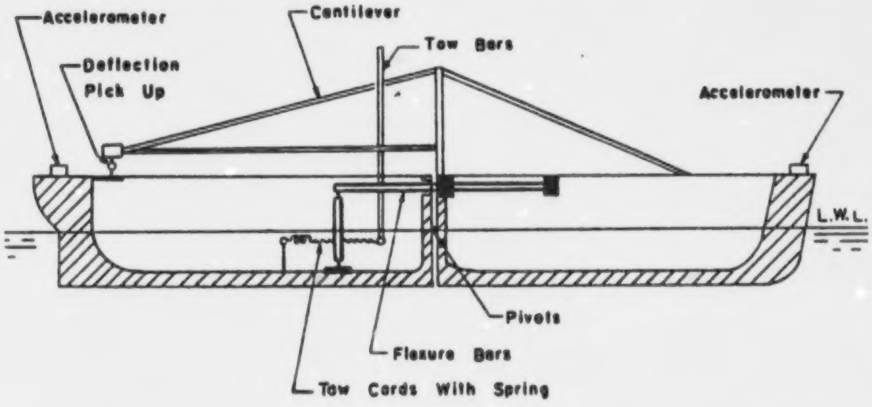
Accelerometer
Cantilever
Tow Bars
Deflection Pick Up
Accelerometer
L.W.L.
Pivots
Flexure Bars
Tow Cords With Spring

FIGURE 3.2

FIRST SEGMENTED MODEL OF T-2 TANKER

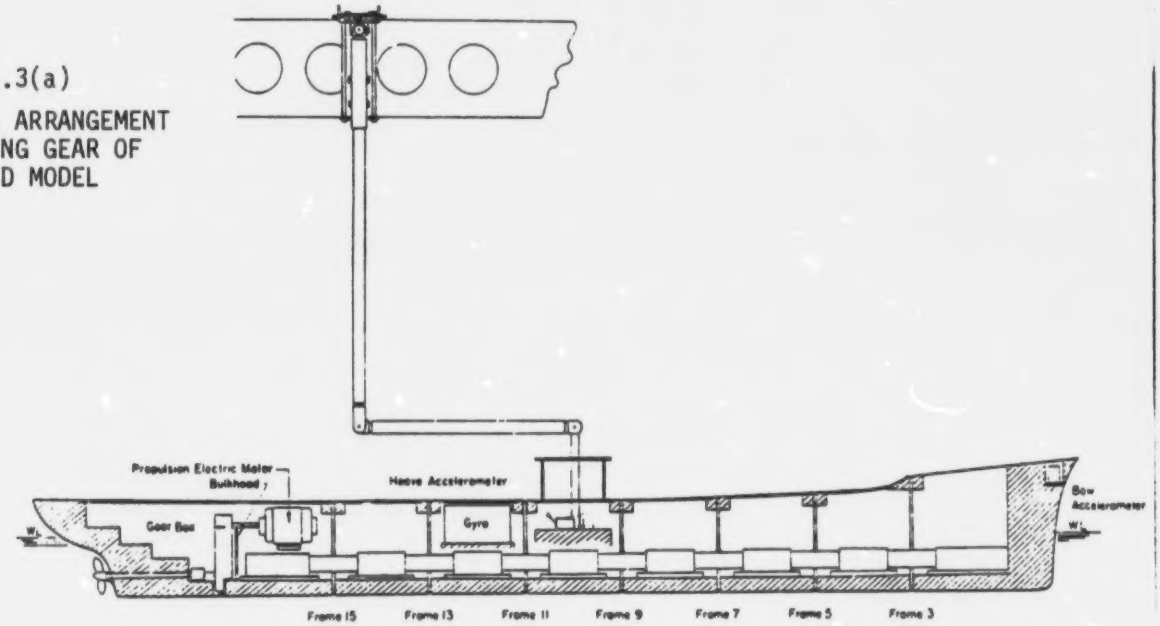
Propulsion Electric Motor
Bulkhead
Heave Accelerometer
Gear Box
Gyro
Bow Accelerometer
Frame 15
Frame 13
Frame 11
Frame 9
Frame 7
Frame 5
Frame 3

FIGURE 3.3(a)

INTERNAL ARRANGEMENT AND TOWING GEAR OF SEGMENTED MODEL [10]

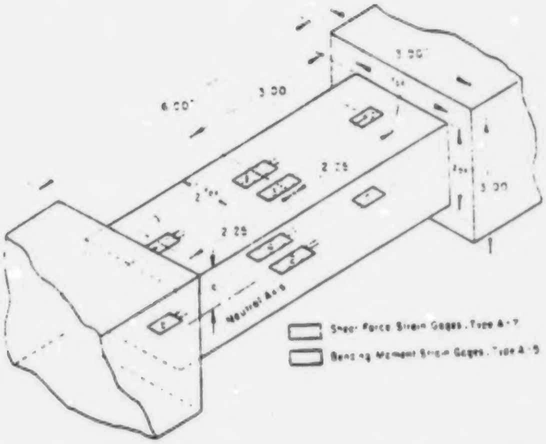
3.00"
6.00"
3.00
2.25
2.25
3.00
Neutral Axis
Shear Force Strain Gages, Type A-7
Bending Moment Strain Gages, Type A-5

FIGURE 3.3(b)

INSTRUMENTED FLEXURE

A similar technique was later used at NSRDC to measure loads and motions in segmented models.

In 1965, Gerritsma and Beukelman [13] developed a segmented model of the Sixty Series ($C_B = 0.70$) with seven separate segments of equal length. The model was developed for investigating the distribution of hydrodynamic forces along the model hull for heaving and pitching motions. Each segment had two transverse bulkheads and was connected to a longitudinal steel box girder, as illustrated in Figure 3.4. The vertical forces transmitted to the girder were measured by a stiff strain-gauge dynamometer. The results obtained using the segmented model were reported to agree satisfactorily with theory.

The technique developed by Gerritsma and Benkelman was different from that used by Wachnik and co-investigators in that the box girder was infinitely stiff and there was no allowance of model flexibility. This represented a rigid ship hull (since the dynamometers were also stiff) in which only one component of load was of interest. In this case the natural frequency of the segments will be high and vibratory effects could be of secondary significance and may be neglected if the frequency of excitation, in this case, pitching and heaving oscillation, were far below the resonance frequency of the model structure.

In their investigation the influence of gaps between the segments on model behaviour and measurements would be negligible due to the high stiffness of the segment supports. This was verified by testing and comparing a non-segmented model under the same conditions.

In 1979, Lloyd, et al [11] reported on a study of motions and loads on warships using segmented models and a different instrumentation method. In this case the model was subdivided into four segments as illustrated in Figure 3.5(a). The segments were separated by 2mm wide transverse cuts and closed by webbed aluminum bulkheads to provide rigidity and accurate base fixings for the dynamometers which joined each two neighbouring segments. The gaps between segments were either sealed by flexible tape or left open.

The dynamometers used are shown in Figure 3.5(b) and they were designed to measure vertical and horizontal (lateral) bending moments as well as torsional moments. To protect the gauges from water splash, the dynamometers were encased in water tight flexible rubber elbows. In comparison to theory, the results of vertical plane motions and loads were found to be reasonable. On the other hand, lateral motions and loads were less well predicted and torsional moments were very poorly predicted. This was attributed to a deficient theoretical solution rather than a shortcoming of the experimental technique.

It should be noted that the segmentation of ship models so far has been limited to transversely sectioning the model into a number of segments (2 to 8) and some method of instrumentation was used to measure the bending moments and shear forces at the various sections as a primary requirement. Both towed or self-propelled models have been used with varying levels of success. The evaluation process of

FIGURE 3.4
SEGMENTED MODEL WITH STEEL BOX GIRDER SUPPORT [13]

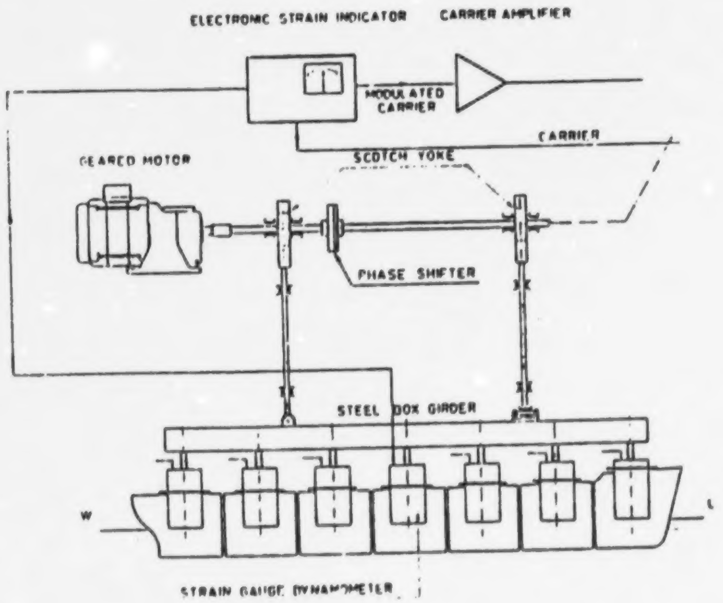
ELECTRONIC STRAIN INDICATOR
CARRIER AMPLIFIER
MODULATED CARRIER
CARRIER
SCOTCH YOKE
GEARED MOTOR
PHASE SHIFTER
STEEL BOX GIRDER
W
L
STRAIN GAUGE DYNAMOMETER

FIGURE 3.5 (a)
ARRANGEMENT OF MODEL SEGMENTS [11]

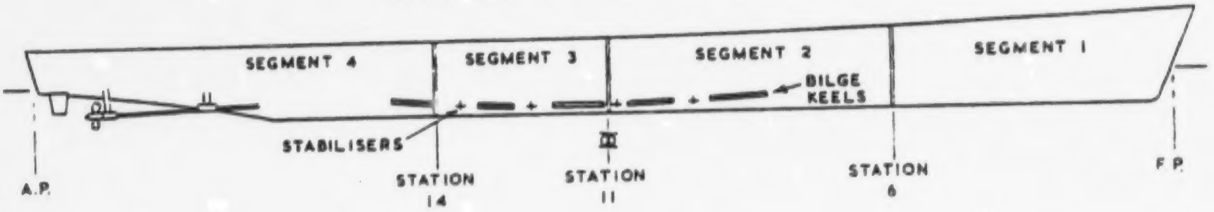
SEGMENT 4
SEGMENT 3
SEGMENT 2
SEGMENT 1
BILGE KEELS
STABILISERS
A.P.
STATION 14
STATION 11
STATION 6
F.P.

FIGURE 3.5 (b)
DYNAMOMETERS

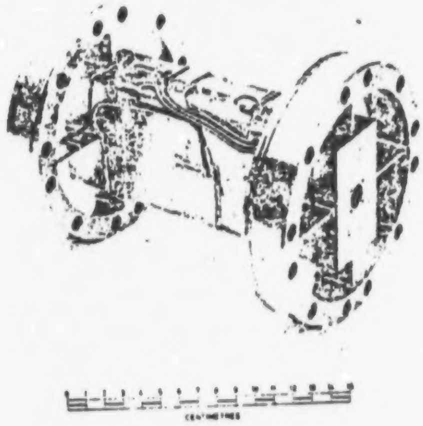
CENTIMETRES

Strain Gauged Dynamometer

instrumentation methods illustrated the feasibility of many suitable schemes which may be adopted for this purpose.

In 1980, the most recent work we have identified, was that conducted at NSRDC by Bales and Jones [12] in which they used a single bow segment to measure flare slamming forces. The segment was designed to measure the vertical force acting on the above-water bow. The measurement system consisted of a triangular array of force gauges as illustrated in Figure 3.6. During the pilot experiments vibration problems were encountered due to the high compliance of force transducers as well as some mechanical failures of flexures and accelerometers. These problems were to be corrected before further experiments.

The latest work which has been cited was reported by Beukelman and Gerritsma in 1982 [16] on the use of the same segmentation technique they had developed earlier in the mid-sixties to determine the distribution of hydrodynamic mass and damping of an oscillating shipform in shallow water.

Based on this review which covered the major developments in segmented model tesing it is worthy of note to mention that this work represented the first attempt to apply segmented models to ice testing. Furthermore, considering the method of segmentation and instrumentation, it was felt that the successful completion of the present study would be a major contribution to the state-of-the art of this frontier technology. It is needless to emphasize the additional complications introduced to the technique by the very nature of ice forces and the low temperature at which tests have to be conducted.

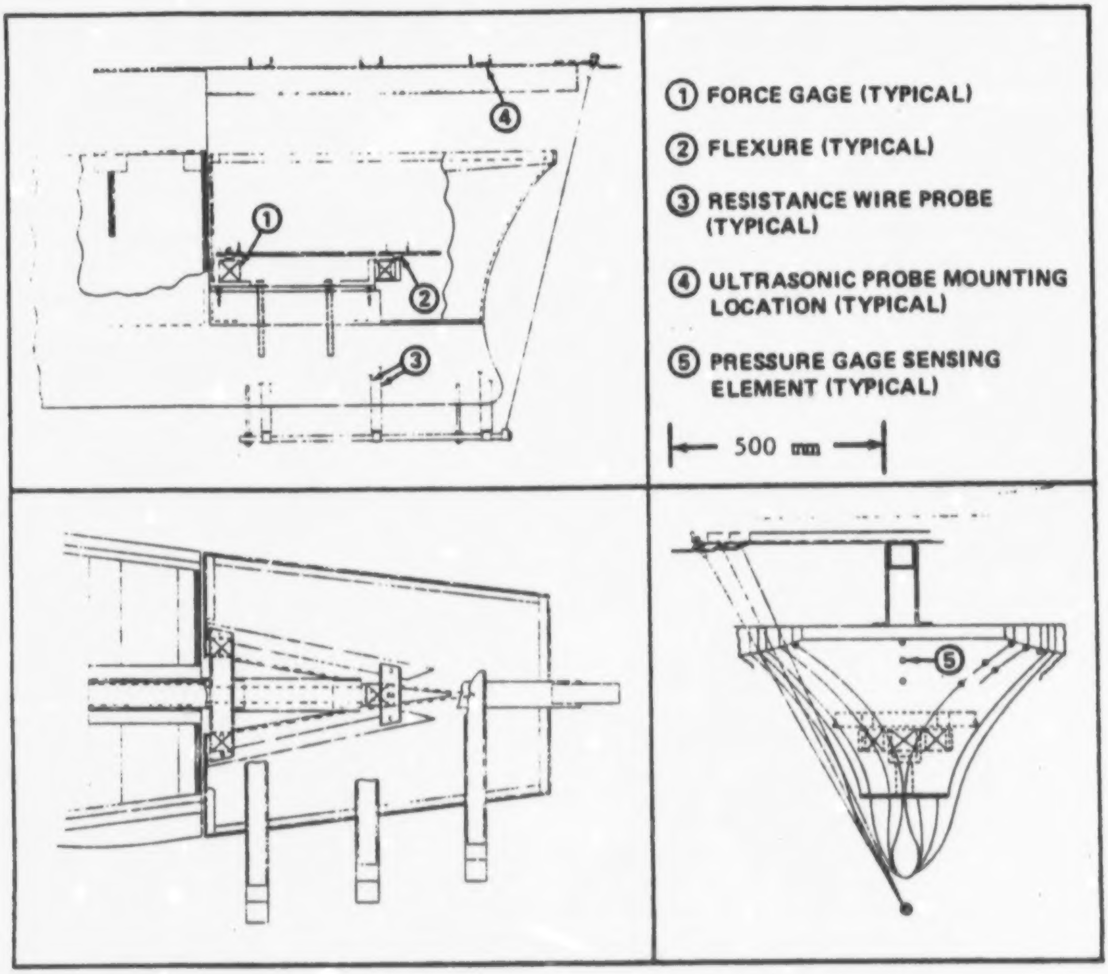

FIGURE 3.6

ABOVE-WATER BOW SEGMENT AND ASSOCIATED APPARATUS
AS USED FOR A PILOT EXPERIMENT AT NSRDC

① FORCE GAGE (TYPICAL)
② FLEXURE (TYPICAL)
③ RESISTANCE WIRE PROBE (TYPICAL)
④ ULTRASONIC PROBE MOUNTING LOCATION (TYPICAL)
⑤ PRESSURE GAGE SENSING ELEMENT (TYPICAL)
500 mm
①
②
③
④
⑤

### 3.3 Segmentation Technique

Several methods of segmentation and model instrumentation have been examined. Some of the options examined are described in Table 3.1.

In evaluating these alternatives it was soon realized that in order to be able to determine the contribution of frictional forces on the total breaking or turning components it would be necessary to design the instrumentation system to accomplish this objective. Some of the above methods are inherently limited with respect to this requirement. For instance, a piezo electric sensor will sense only the normal pressure acting on its surface and it would not be simple to attempt to measure the frictional component acting parallel to the surface. This is further complicated by hull curvature, dynamic requirements and accuracy.

A basic requirement was to determine whether to cut the model into complete transverse segments or only use half body segments. Due to the stochastic nature of icebreaking at either side of the hull, a complete transverse segment would be subjected to three forces in the thrust, vertical and horizontal directions in addition to three moments created by the unbalanced forces acting in the horizontal and longitudinal directions as well as the net vertical load. These six net forces and moments are caused by two sets of forces acting on either side of the hull, and each set consists of a normal force of unknown magnitude and position and a frictional force of unknown direction. This creates a total of ten unknown quantities and necessitates ten measurements to be taken to facilitate a complete analysis. It was concluded that the instrumentation of this scheme of complete transverse segments would be extremely difficult and costly despite the apparent simplicity in supporting segments.

On the other hand, a port (or equally; a starboard) segment would reduce the number of unknowns to five. It was felt that it would be quite feasible to instrument and support each segment to provide at least five force measurements which are sufficient for analysis.

Discussions with the model builder have resulted in the segmentation method illustrated schematically in Figure 3.7. Each segment consists of an outer shell which is cut out from the hull form in the specified segment location. The shell is supported by a box like structure which fits into a corresponding cavity in the hull. Each box was made smaller in size than the outer shell of the segment to permit the provision of water tight coffer dams interstitial to the segments. These coffer dams were created to permit easy access to all sides of the box for purposes of fitting supports and load measuring devices. The model structure was modified internally to create a water-tight centreline bulkhead and a number of transverse bulkheads which perform two functions:

- Increase the stiffness of the model and compensate for the weakening effect of segmenting the shell.
- Provide water tight coffer dams between the segments.

TABLE 3.1

SOME SEGMENTATION OPTIONS

| | | |
|---|---|---|
| 1. | ° Transverse segmentation with interconnecting dynamometers capable of measuring transmitted thrust, vertical shear and differential lateral load on each segment. | 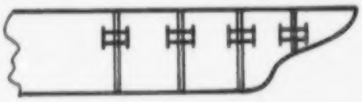 |
| 2. | ° Transverse segments connected independently to a rigid top beam (or main deck) which enables the direct measurement of forces acting on each segment. | 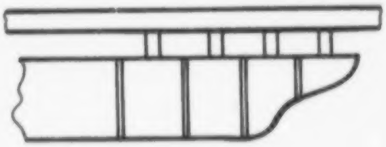 |
| 3. | ° Creating a core hull which supports shell segments. Each shell segment would be supported by a number of load cells to measure the total forces acting on it. | 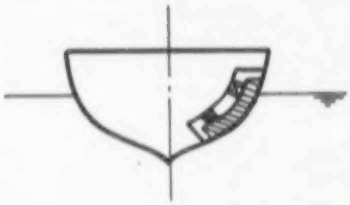 |
| 4. | ° Using piezo-electric material between the core hull and external hull shell segments. | 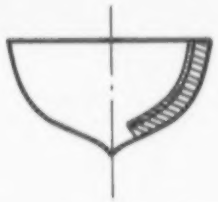 |
| 5. | ° Segmenting only port or starboard bow with different means of support of segments in a cage or skeleton frame or others. | 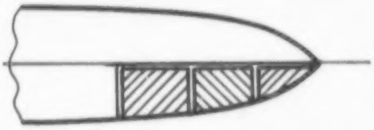 |

Access to the segments for support purposes can be made from the main deck on top, the centreline bulkhead on the starboard cavity, and the coffer dam cavities forward and aft of each segment. No access is possible from the bottom.

Each segment was to be neutrally buoyant to minimize the requirements for its support under no load condition.

The segmentation of the port side was selected for ease of observation during tests in the basin.

FIGURE 3.7

METHOD OF MODEL SEGMENTATION

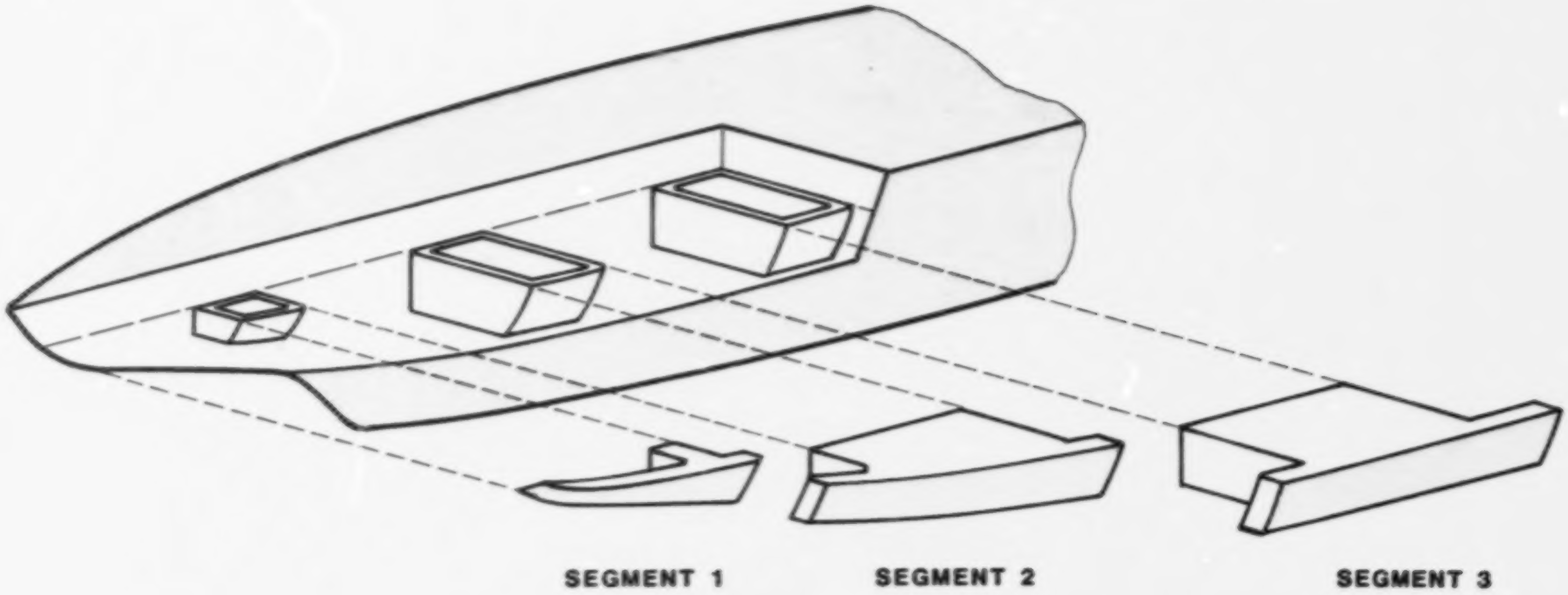
SEGMENT 1
SEGMENT 2
SEGMENT 3

MAIN DECK OMITTED FOR CLARITY

## 3.4 Analysis of Segment Support System

Each segment must be supported in such a manner to ensure its stability under ice load conditions. Consider a segment as shown in Figure 3.8(a) which is essentially subjected to a normal force and a frictional component of load. These forces are variable in nature and can occur at any point along the waterline as well as below the waterline for submersion and turning components. Therefore, these forces can be replaced at the centre of gravity of the segment by an equivalent force system, as shown in Figure 3.8(b). This system consists of three linear components along the x, y, z axes and three moments about the three coordinate directions.

In order to provide support for the segment subjected to such loading conditions the following are required:

° 3 support points along the x, y and z directions,

° 1 extra support point in the x-y plane to support the moment $M_z$, this point will provide a reaction in either the x- or y-direction.

° 1 extra support point in the x-z plane to support the moment component $M_y$.

° 1 extra support point in the y-z plane to support the moment component $M_x$.

The provision of these support points creates a stable segment which will not rotate or distort under load. Since the load is of a traversing nature the support points must be set farther apart to create the largest possible balancing moments on each segment.

If load cells can be placed at all these locations then sufficient measurements will be available to determine the unknown forces acting on the segment. If space limitations do not permit placement of load cells at all support points, a pretension support system may be devised to stabilize the segment. It should be emphasized that the minimum number of measurements which are required to determine a solution are five and this condition is implied by the number of unknowns. These are:

a) The position of load centre on the hull, which can be defined by two coordinates,

b) The magnitude of the normal force component at the specified point of action,

c) The direction of the frictional force component which can be completely defined by two direction cosines with respect to the ship coordinate system. It is assumed that the friction coefficient will be measured independently.

FIGURE 3.8

ICE LOAD ANALYSIS ON A SEGMENT

(a) EXTERNAL FORCES ON A SEGMENT

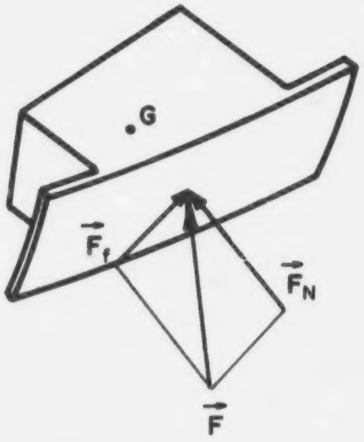
G
$\vec{F}_f$
$\vec{F}_N$
$\vec{F}$

(b) EQUIVALENT FORCE SYSTEM

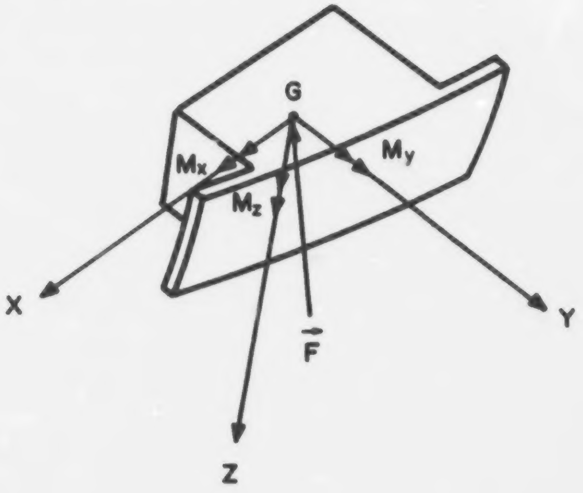
G
$M_x$
$M_y$
$M_z$
X
Y
$\vec{F}$
Z

The force system proposed for the support of a typical segment is illustrated schematically in Figure 3.9 and it consists of:

- One support point $R_1$ in the x-direction
- Two support points $H_1$ and $H_2$ in the y-direction and they are located as far apart as possible.

These three points will support the force projection in the x and y directions as well as the moment component $M_z$. They provide a single measurement of the resistance component as well as highest stabilization effects in the x-y plane. These locations will be easily accessible from inside the model cavity and without having to perforate the centreline bulkhead.

- Additional support points are then located on the top surface of the segment:
    - $V_1$ and $V_2$ support the moment $M_x$
    - $V_2$ and $V_3$ support the moment $M_y$
    - the vertical force component will be distributed over the three support points.

This system of support points is sufficient with one reservation. When the load is located such that the reactions at support points are negative, contact at these points may be lost. To overcome this problem an additional vertical support point $V_4$ is added.

This support system was implemented on segments 2 and 3. For segment 1, the forward most segment,it was not possible to fit more than two vertical supports due to the lack of space. Therefore, only $V_2$ and $V_3$ supports were used and additional preload arrangements were added to stabilize the segment.

Since all segments were neutrally buoyant, it was necessary to provide a vertical pretension mechanism to apply a preload on the segment to ensure continuous contact even if negative reactions occur. The problem of loss of contact was not to be expected in the horizontal (transverse direction). In the longitudinal or resistance direction a small preload arrangement was made to ensure contact at $R_1$ support at all times.

## FIGURE 3.9

## TYPICAL SEGMENT SUPPORT SYSTEMS

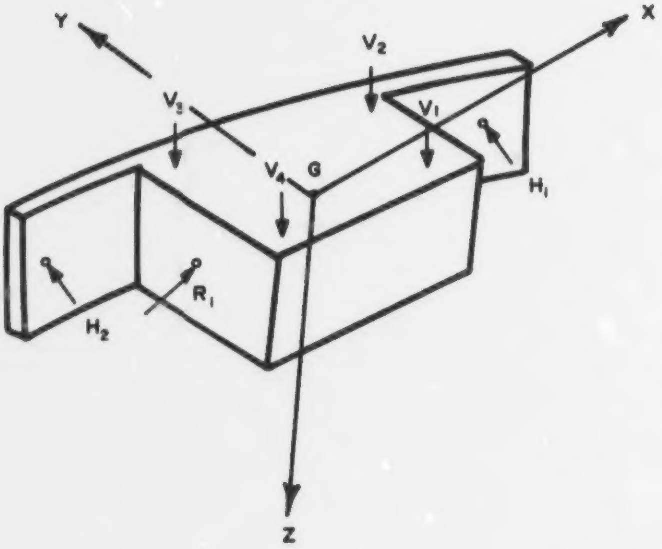

Y
X
V2
V3
V1
V4
G
H1
H2
R1
Z

## 3.5 Load Cell Design Development

A total of nineteen load cells were designed and built for supporting the three segments. Due to different load ratings and geometric restraints at each support point the load cells were manufactured in groupings as will be discussed later.

The basic design requirements of the load cells are listed in the following:

a) Load cells should provide unidirectional sensitivity along the axis of the cell with practically negligible lateral or cross sensitivity.

b) High stiffness to ensure that the lowest natural frequency of each supported segment is well removed from the ice load frequencies. This will also ensure that no ringing effects will be observed on load cell signals.

c) Ease of assembly and repair is essential since the load cells will be immersed in urea doped water and may be subjected to overloads.

d) Sealing of load cells must be good to eliminate strain gauge failures.

e) The range of measurement for each load cell must be selected to ensure highest possible sensitivity. For instance if a 500N rated load cell is used to measure 50N loads the sensitivity will be low and the accuracy will be reduced. Therefore, the rating of each load cell must be carefully selected to ensure the highest sensitivity and accuracy.

f) The level of precision of each load cell should be determined on the basis of purpose and cost. For measurement of ice loads in segmented models for the first time it is felt that high precision load cells are not desirable. The cost increases exponentially with the load cell precision requirements for higher precision implies the use of much more expensive materials, strain gauges which are more difficult to handle and install, and more elaborate strain gauge circuitry. Considering the nature of this program, the stochastic nature and repeatability of ice loads, and the cost it was justifiable to target for an ordinary precision load cell which must be calibrated and evaluated prior to installation.

g) Since operations of the load cells will be subjected to variable temperature, each load cell must be self-temperature compensated to minimize thermal response.

Keeping the above requirements in mind the load cell design was developed. The development steps are discussed in the following sections, and summarized opposite.

## DESIGN PROCEDURE OF LOAD CELLS

1. Determination of individual load cell ratings based on maximum expected dynamic loads during testing.

2. Determination of implications of the geometric constraints of the locations of points of support on dimensional requirements of load cells.

3. Design details of load cells.

4. Diaphragm sizing based on load rating.

5. Examination of the dynamic response of the load cells.

6. Examination of the effect of friction and lateral sensitivity of the load cell.

7. Calibration of Prototype

### 3.5.1 Determination of Load Cell Capacities

From our experience in model testing of ships, it was observed that maximum loads registered by a force block were associated with acceleration of the model to the test speed. For instance for a model of the CCGS PIERRE RADISSON having a mass of 1000 kgs and accelerating at a rate of 0.08 $m/s^2$ to test speed the force block registers a peak load of 80N. On deceleration at a rate of 0.16 $m/s^2$ the force is negative and it amounts to 160N.

However, on smaller segments the inertia forces will be proportional to their mass. Table 3.2 gives details of inertial forces for each segment. It is shown that the forces are negligible for the first two segments but much higher for segment 3. These forces act in the (thrust) x-direction and represent the worst case of inertia effects since all this load is carried by one load cell. In the vertical or lateral (horizontal) directions the inertial effects will be smaller and will be distributed among four or two load cells, respectively.

Therefore, load rating of each cell has to be determined on the basis of maximum expected loads during icebreaking and not on the basis of inertial effects. For this purpose reference test conditions, as listed in Table 3.3(a) were used. Using RICE computer program to calculate resistance components under these conditions the results are given in Table 3.3(b).

The maximum normal force which is calculated during cusp breaking is 195.4 kN which corresponds to 24.4N in model scale. This force occurs at Station 9 where the direction cosines are given by (0.335, 0.790, 0.513). Considering dynamic load effects, and using a dynamic load factor of 3.0, the estimated maximum dynamic force components in the x, y and z directions are:

$$F_x = 25N, \quad F_y = 59N, \quad F_z = 38N$$

These are the maximum forces to be expected on Segment 2. The normal force on the other two segments are lower.

To corroborate the above estimates of force components, Naegle's approach was followed. This is described in reference [6] entitled "Ice Resistance Prediction Model for Icebreaking Ships - Principles and Assumptions". The static breaking force is a calculated output of the RICE computer program. It is based on the following equation:

$$P_n = \sigma_c \cdot \frac{H_c \cdot b}{\sin \beta'} \qquad (3.1)$$

where $\sigma_c$ = crushing strength of ice

$H_c$ = horizontal extent of ice crushing (calculated at every time step).

b = length of the zone of ice crushing taken equal to cusp length

$\beta$ = normal section flare angle

## TABLE 3.2

## INERTIA LOADS ON SEGMENTS

| SEGMENT NO. | MASS kg | MAX. INERTIA LOAD, N |
|---|---|---|
| 1 | 1.0 | 0.08 |
| 2 | 6.0 | 0.48 |
| 3 | 28.0 | 2.24 |

## TABLE 3.3(a)
## REFERENCE TEST CONDITIONS

| VARIABLE | FULL SCALE | MODEL SCALE |
|---|---|---|
| Ice Thickness, h | 0.6 m | 30 mm |
| Elastic Modulus, E | 3.0 GPa | 150 MPa |
| Flexural Strength, $\sigma_f$ | 500 kPa | 25 kPa |
| Compressive Strength, $\sigma_c$ | 1.5 MPa | 75 kPa |
| Ship Speed, v | 4 m/s | 0.894 m/s |

## TABLE 3.3(b)
## RESISTANCE COMPONENTS FOR REFERENCE TEST CONDITIONS

| COMPONENT | F.S. kN | M.S. N | PERCENTAGE OF TOTAL ICE RESISTANCE | |
|---|---|---|---|---|
| Total Ice Resistance | 610.8 | 76.4 | | 100% |
| Water Resistance | 53.9 | 6.7 | | |
| Breaking Resistance | 154.9 | 19.4 | 25.4% | |
| Breaking Friction | 110.9 | 13.9 | 18.2% | |
| Total Breaking | 265.8 | 33.2 | | 43.6% |
| Turning Resistance | 166.3 | 20.8 | 27.2% | |
| Turning Friction | 72.5 | 9.1 | 11.9% | |
| Total Turning | 238.8 | 29.9 | | 39.1% |
| Sliding Resistance | 68.9 | 8.6 | 11.3% | |
| Sliding Friction | 37.3 | 4.7 | 6.1% | |
| Total Submersion | 106.2 | 13.3 | | 17.4% |

Normal Force Distributions

| | | | | | |
|---|---|---|---|---|---|
| Distance from Midship in Metres | 0 | 23.2 | 29.7 | 36.7 | 41.8 |
| Maximum Normal Force, $P_n$, kN | 0 | 132.9 | 190.0 | 195.4 | 123.0 |

The maximum values of $P_n$ are given in Table 3.3(b). In addition to this static component, the acceleration force (dynamic component) may be calculated on the basis of energy loss averaging. Therefore, the mean dynamic component may be given by [6]:

$$R_m = \frac{v^2 \tan^2 \alpha \sin \alpha}{4 \tan^2 \beta} \left[\pi \rho_i h L + \frac{\pi}{6} \rho_w D L\right] \qquad (3.2)$$

where $v$ = ship speed,
$\alpha$ = waterline angle
$\beta$ = transverse section flare angle
$\rho_i$ = density of ice
$\rho_c$ = density of water
$h$ = ice thickness
$L$ = length of broken floe
$D$ = depth of broken floe

For the reference test conditions at Station 9 (Segment #2):

$$R_m = 46{,}097 \text{ N} \quad (\text{F.S.}) \quad = \quad 5.76 \text{ N} \quad (\text{M.S.})$$

Considering the cusp breaking frequency at 4 m/s is approximately 4.2 seconds and assuming that the dynamic force rises linearly to a maximum value in approximately one second followed by a sudden drop on ice failure, the maximum dynamic force may be calculated by equating the energy losses:

$$\text{Max dynamic force} = \frac{5.76 \times 4.2}{0.5 \times 1} = 48.4\text{N}$$

This is almost twice as much as the static icebreaking force and, therefore, it is reasonable to use a dynamic factor of 3.0.

Another approach to justify this for the purpose of defining load cell capacities may be based on the following empirical ice impact force equation [18]:

$$\frac{F_i}{\rho_w g h^3} = 0.385 \left(\frac{1}{a_3}\right)^{1.31} \left[a_1 \frac{v}{\sqrt{gh}} \cdot \frac{\sigma_f}{\rho_w g h}\right]^{1.17} \qquad (3.3)$$

where $a_1$, $a_3$ are the first and third direction cosines at the point of impact. For the reference test conditions and at various positions obtained in model scale the impact force is calculated in Table 3.4(a). These values appear to be lower than previously calculated values and it would be adequate (in fact more conservative and desirable in this study) to use a dynamic load factor of 3.0.

Therefore, it was decided to use a maximum normal ice force of 75N as a design load for any segment. With this normal load applied at the centre of each segment the reactions at each load support point were determined by equilibrating all the forces and moments acting on each segment. Table 3.4(b) lists the results of calculation. It has been assumed that the friction coefficient is 0.1 and that the friction force acts in the waterplane, so that the third direction cosine of the friction vector is always zero.

## TABLE 3.4(a)

## CALCULATED IMPACT FORCE

| STATION NO. | $F_i$, N (Ref. Conditions) | $F_i$, N ($\sigma_f$ = 1124 kPa) |
|---|---|---|
| 8 | 26 | 31.5 |
| 9 | 22 | 49.5 |
| 10 | 14 | 58.5 |

## TABLE 3.4 (b)

## MAXIMUM REACTIONS AT SEGMENT SUPPORT POINTS

| | SEGMENT #1 | SEGMENT #2 | SEGMENT #3 |
|---|---|---|---|
| Coordinates of Load Point | | | |
| X', m | 2.20 | 1.76 | 1.32 |
| Y', m | 0.08 | 0.31 | 0.44 |
| Z', m | 0.02 | 0.02 | 0.02 |
| Direction Cosines | | | |
| normal force, l | 0.336 | 0.335 | 0.144 |
| m | 0.606 | 0.790 | 0.966 |
| n | 0.722 | 0.513 | 0.214 |
| friction force, $e_1$ | 0.870 | 0.920 | 0.99 |
| $e_2$ | 0.480 | 0.390 | 0.15 |
| $e_3$ | 0.0 | 0.0 | 0.0 |
| Calculated Reactions | | | |
| $R_{i_1}$, N | 18.58 | 18.23 | 3.38 |
| $H_{i_1}$, N | 27.25 | - 4.78 | 31.61 |
| $H_{i_2}$, N | 14.60 | +61.11 | 39.72 |
| $\Sigma H$, N | 41.85 | 56.33 | 71.33 |
| $V_{i_1}$, N | 40.97 | -17.15 | -12.94 |
| $V_{i_2}$, N | 13.18 | 42.09 | 22.80 |
| $V_{i_3}$, N | - | 34.32 | 17.96 |
| $V_{i_4}$, N | - | -20.77 | -11.70 |
| $\Sigma V$, N | 54.15 | 38.48 | 16.05 |

From the calculated reactions the following observations may be made:

(a) The negative reactions in some cases necessitate the application of a sufficient initial preload to ensure that the segments are always in contact with the support points and that all measurements are unidirectional. While it would be possible to preset the zero level of the load cells while under preload, the load cell must be rated according to the maximum possible load plus the initial load.

(b) Since the loads are moving loads and may occur at any position along the length of the segment, the condition when the normal force occurs directly on $H_1$ or $H_2$ position should be considered. In this case the total horizontal force component has to be carried by a single load cell. A reasonable approximation of this load is the total horizontal force $\Sigma H$.

(c) The vertical support points in segments 2 and 3 are always subjected to high negative load. This means that a high preload will be necessary. This preload should be distributed over the four vertical support points for practical reasons.

Again for practical considerations each segment was designed with two independent pretension lines in the vertical direction and in the horizontal plane at 45° with ship centreline. Therefore, the second pretension line would imply a preload equally applied in the thrust and the transverse directions.

Based on maximum expected dynamic load and the preload requirements, the load ratings for each load cell have been established. Table 3.5 lists the load ratings and the minimum and maximum preload levels. The reason for setting up a preload range is mainly to simplify the actual adjustments of the segments in the test basin.

These load ratings have a built-in overload protection since the selection was based on maximum dynamic load occuring at relatively high speed. In selecting the rating levels the merits of standardization of the load cell capacities were favourably considered. It should also be noted that, in the determination of load cell ratings it was assumed that the ice load was applied directly on load cell position so that no load sharing was used. This was done to cover extreme load conditions on any one load cell.

TABLE 3.5

LOAD CELL RATINGS

| SEGMENT NO. | LOAD CELL DESIGNATION | RATINGS N | TYPE | PRELOAD, N | |
|---|---|---|---|---|---|
| | | | | MINIMUM | MAXIMUM |
| 1 | $R_{11}$ | 50 | T | 0 | 30 |
| | $H_{11}$ | 100 | T | 10 | 40 |
| | $H_{12}$ | 100 | T | 10 | 40 |
| | $V_{11}$ | 100 | L | 20 | 40 |
| | $V_{12}$ | 100 | S | 20 | 40 |
| 2 | $R_{21}$ | 50 | T | 0 | 30 |
| | $H_{21}$ | 100 | T | 10 | 40 |
| | $H_{22}$ | 100 | L | 10 | 30 |
| | $V_{21}$ | 50 | S | 20 | 30 |
| | $V_{22}$ | 100 | S | 0 | 30 |
| | $V_{23}$ | 100 | S | 0 | 30 |
| | $V_{24}$ | 50 | S | 20 | 30 |
| 3 | $R_{31}$ | 50 | S | 0 | 30 |
| | $H_{31}$ | 100 | L | 10 | 30 |
| | $H_{32}$ | 100 | S | 10 | 30 |
| | $V_{31}$ | 50 | S | 15 | 25 |
| | $V_{32}$ | 50 | S | 0 | 25 |
| | $V_{33}$ | 50 | S | 0 | 25 |
| | $V_{34}$ | 50 | S | 15 | 25 |

### 3.5.2 Geometric Constraints

The load cells geometric constraints such as location and accessibility were considered during the design stage and their implications on the design of load cells were determined. Using the prototype design and the RADISSON model it was possible to select three types of load cells:

a) STANDARD SIZE "S",

b) LONG VERSION "L",

c) SHORT VERSION "T".

The three types are variations of the same basic design which will be presented in the following subsection. The type designations for each load cell are given in the type column in Table 3.5.

### 3.5.3 Load Cell Design

The standard design of the load cell was developed in compliance with the basic requirements stated earlier in this section. The resulting design is illustrated schematically in Figure 3.10 (b) which describes the basic components of the load cell. The long version is identical to the standard design except for stem length and the short version is illustrated in Figure 3.10 (a). The latter is specially designed to be fitted from external cavity instead of the internal cavity of the model.

The final design was selected after comparison of several options for load transfer, sensing element, and type of strain gauge to be used. The selection was based on:

° simplicity of design,

° reliability of design which increases with decreasing number of elements,

° manufacturing considerations which are basically reflected on the total cost of manufacturing,

° availability of materials as standard stock items for shorter lead time,

in addition to the satisfactory compliance with the basic requirements.

FIGURE 3.10 ASSEMBLY DRAWINGS FOR LOAD CELLS

a) SHORT VERSION

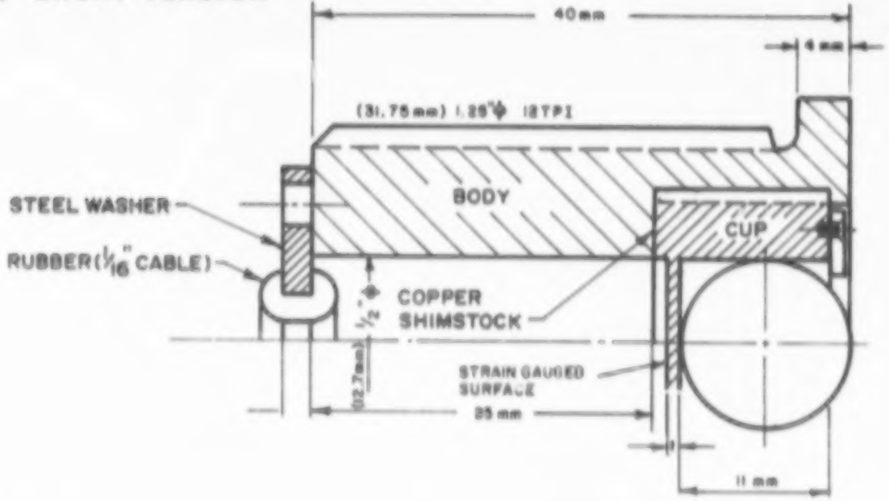
40mm
4mm
(31.75mm) 1.25"Φ 12TPI
BODY
CUP
STEEL WASHER
RUBBER(1/16" CABLE)
1/2"Φ
COPPER SHIMSTOCK
(12.7mm)
STRAIN GAUGED SURFACE
25 mm
t
11 mm

b) STANDARD and LONG VERSIONS

STANDARD : $L_1$ = 45mm, $L_2$ = 60mm

LONG : $L_1$ = 80mm, $L_2$ = 95mm

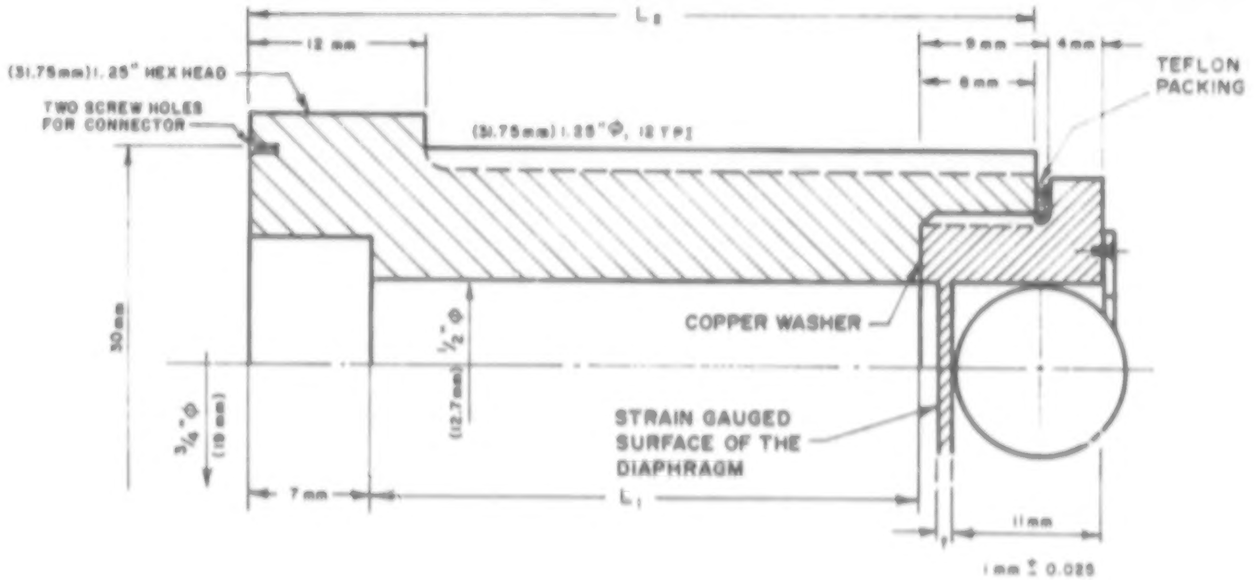
L2
12 mm
9mm
4mm
6mm
TEFLON PACKING
(31.75mm) 1.25" HEX HEAD
TWO SCREW HOLES FOR CONNECTOR
(31.75mm) 1.25"Φ, 12 TPI
COPPER WASHER
30mm
1/2"Φ
(12.7mm)
3/4"Φ (19mm)
STRAIN GAUGED SURFACE OF THE DIAPHRAGM
7mm
L1
t
11mm
1mm ± 0.025

DIAPHRAGM THICKNESS

t = 1.00 ± 0.025mm for 100N RATED CELLS

t = 0.70 ± 0.020mm for 50N RATED CELLS

Dimensions given in inches are for the convenience of the manufacturer.

All parts of the load cell were made of stainless steel 416 except the balls which were standard corrosion resistant hardened alloy steel used in precision applications of ball bearings. The S.S. 416 has the following advantages:

- ° good machinability, which permits precision cutting,
- ° high strength to yield of 276 MPa (40 ksi)
- ° it is martensitic type which has a thermal expansion coefficient of 6.0 ppm/°F, this provides an excellent match with standard temperature compensated strain gauges and therefore permits the best level of temperature stability without having to resort to more expensive alternatives.

However, martensitic stainless steels have slightly lower general corrosion resistance than austenitic stainless steels. In view of the short exposure of load cells to corrosive environment during the testing periods, this differential corrosion behaviour cannot be used as grounds for preference of one type of stainless steel over the other. Therefore, the foregoing selection was judged optimum for the application.

The type of strain gauge selected was the full-bridge diaphragm gauge. This type is specially designed for diaphragm strain measurements and provides highest sensitivity since it has four active bridge arms. This feature also provides excellent temperature compensation provided that the STC number of the gauges is selected properly. To match S.S. 416 the gauges used had an STC-06 temperature compensation number.

Figure 3.11 shows a photograph of the completed load cells used in the present study.

FIGURE 3.11

PHOTOGRAPH OF LOAD CELLS

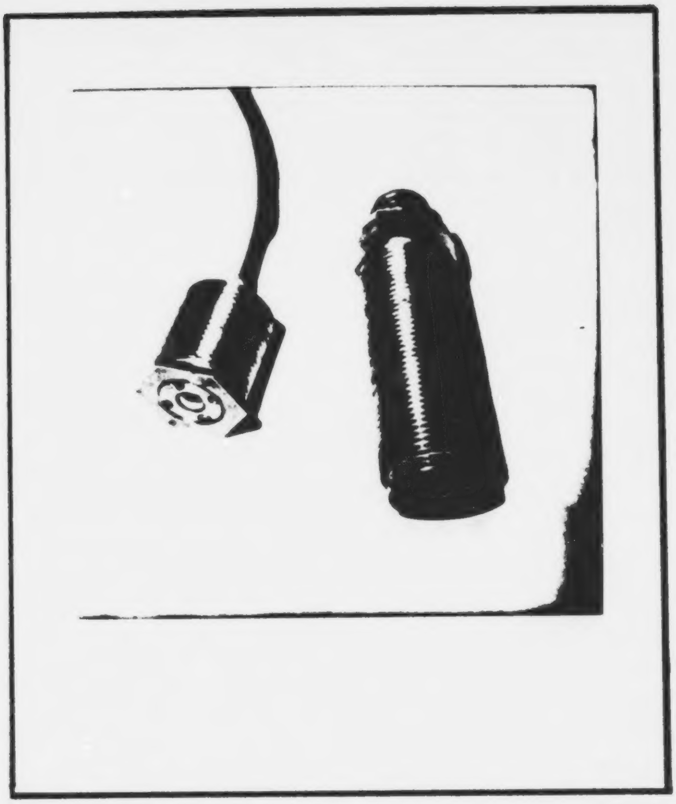

### 3.5.4 Friction Effects

Friction between the load cell and the segment can produce a lateral force component which depends on the friction coefficient. The design of the load cell minimizes the sensitivity of measurement to lateral loads. This is done by minimizing the internal friction between the surfaces of the ball and the retainer. The balls were made to a precision ball bearing standard (Class 3) and the retainers were fine turned. The quality of roundness of the ball will not permit wedging effects and will promote rolling and sliding of the ball in the retainer if the lateral load exceeds a limiting value. The other limiting condition depends on the friction factor between the ball element of the load cell and corresponding contact surface on the segment.

There are two cases to be considered. The first is for a vertically aligned load cell in which the weight of the ball acts in the same direction as the load and will be automatically counterbalanced during preload adjustments. The second case is that for a horizontal load cell in which the weight of the ball will always be active. Both cases have been analyzed with the objective of calculating the error in measurement to be expected due to frictional effects and it was concluded that the lateral sensitivity of the load cell design is within acceptable levels.

### 3.5.5 Diaphragm Sizing

The diaphragm size was calculated for the selected standard sizes according to the following procedure. The rim surrounding the diaphragm is thick enough relative to the diaphragm thickness that the latter could be considered as a circular thin plate rigidly fixed at the circumference.

The solution for this problem may be found in Roark [14] for the case illustrated in Figure 3.12. This is complimented by Timoshenko's solution [15] for the radius of contact area for a ball pressed against a plane surface.

The maximum stresses and strains of the diaphragm occur at the centre due to biaxial bending and it can be shown that the radial and tangential components at the centre may be given by:

$$\sigma_r\,(\max) = \sigma_\theta(\max) = \frac{6\,(1+\nu)}{4\,\pi\,t^2}\cdot\left[W \ln \frac{a}{r_o}\right] \tag{3.4}$$

$$\varepsilon_r\,(\max) = \varepsilon_\theta(\max) = \frac{6\,(1-\nu^2)}{4\,\pi\,Et^2}\cdot\left[W \ln \frac{a}{r_o}\right] \tag{3.5}$$

Also

$$W \,.\, \ln \frac{a}{r_o} = W\left[\ln\left(\frac{a}{1.109}\right) + \frac{1}{3}\ln\left(\frac{E}{WR}\right)\right] \tag{3.6}$$

or

$$= W\left[\ln\left(\frac{a}{1.109}\right) + \frac{1}{3}\ln\left\{\frac{E}{WR}\,.(1 - \frac{WR}{4D}\,[1 + \ln \frac{a}{r_o}])\right\}\right] \tag{3.7}$$

Equation (3.7) is more precise as it takes into account the diaphragm curvature under load. However, it only results in a small difference from Equation (3.6) of not more than 0.6% for 100N rated diaphragm.

The size of the diaphragm may be determined from considerations of allowable stress or strain at the centre of the diaphragm so that no permanent deformation occurs during load application. This permanent deformation will usually cause an offset of the load cell output when the overload is removed.

An acceptable level of stress would be that based on the elastic limit of the material and maximum normal stress theory which may be expressed:

$$\sigma_r \leq \sigma_y \tag{3.8}$$

where $\sigma_y$ is the yield strength of the material. The maximum strain based on Equation (3.8) may then be given by:

$$\varepsilon_r \leq \frac{(1 - \nu)}{E} \sigma_y \tag{3.9}$$

For stainless steel S.S.416 with $\sigma_y$ = 275 MPa (40 ksi), Poisson's ratio $\nu$ = 0.29 and Elastic modulus E = 307 GPa, obtain the maximum strain to be 943 microstrain. Therefore, using Equations (3.5) and (3.7) obtain:

$$t^2 = \frac{6(1 - \nu^2)}{4\pi E.\varepsilon_r} \cdot W \cdot \left[\ln\left(\frac{a}{1.109}\right) + \frac{1}{3} \ln \left\{\frac{E}{WR} \left[1 - \frac{WR}{4D}\left(1 + \ln \frac{a}{r_o}\right)\right]\right\}\right] \tag{3.10}$$

Equation (3.10) can only be solved by iteration since D is a function of thickness. Therefore, if WR/4D is eliminated for the first step t may be calculated and then an estimate of D can be made and used to correct t. This procedure may be repeated until sufficient accuracy is achieved. Also r has to be calculated using either of expressions (a) or (b) in Figure 3.12, and has to be corrected for every iteration step. One or two iteration steps would normally suffice for conversion.

The following minimum thickness estimates of the diaphragm have been calculated:

For 100N rating: $t_{min}$ = 0.905 mm

For 50N rating: $t_{min}$ = 0.659 mm

These minimum requirements justify the design values given in Figure 3.10.

FIGURE 3.12

DIAPHRAGM MODEL

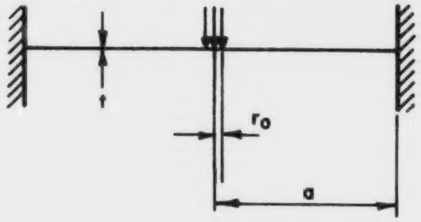

Diaphragm thickness = t
Maximum Moment at r = 0,

$$M_r = M_t = \frac{W}{4\pi}(1 + \nu)\ \ln\frac{a}{r_o}$$

where $r_o$ = radius of applied load or contact zone with ball
$a$ = radius of diaphragm

From Timoshenko:

(a) $r_o = 1.109\sqrt[3]{\frac{WR}{E}}$ for a ball of Radius, R, pressed against flat surface of same elasticity, E

(b) $r_o = 1.109\sqrt[3]{\frac{W}{E}\cdot\frac{1}{\frac{1}{R} - \frac{W}{4D}\left(1 + \ln\frac{a}{r}\right)}}$

when the curvature of the diaphragm under deflection is taken into consideration.

$D = \frac{Et^3}{12(1 - \nu^2)}$ = flexural rigidity of diaphragm

### 3.5.6 Dynamic Response

The natural frequency, $f_n$, of the load cell may be calculated from:

$$f_n = \frac{1}{2\pi} \sqrt{\frac{K}{M}}, \text{ (Hz)} \tag{3.11}$$

where K = the total stiffness of the load cell

M = the vibrating mass supported by the load cell

The natural frequency of the diaphragm itself is naturally very high and is higher than 80 kHz for both standard sizes selected for the present work.

The stiffness of the diaphragm may be calculated from:

$$K = \frac{W}{\delta_{max}} = \frac{16\ \pi\ D}{a^2} .$$

where a = the radius of the diaphragm

D = its flexural rigidity

The natural frequencies were calculated for all segments with the following assumptions:

- linear vibration in three coordinates are independent
- all load cells are expected to actively share the load
- damping effects ignored
- effects of pretension lines and their stiffness ignored

The results are tabulated in Table 3.6. The natural frequency levels as determined are sufficiently high and are not expected to interfere with the frequencies of the physical action of icebreaking. Therefore, there will be no requirements for signal correction.

## TABLE 3.6

### (a) LOAD CELL STIFFNESS

| RATING, N | 50 | 100 |
|---|---|---|
| Thickness, t, mm | 0.7 | 1.0 |
| Radius, a, mm | 6.35 | 6.35 |
| Flexural Rigidity, D, N.m | 5.45 | 14.1 |
| Stiffness, K, MN/m | 6.79 | 18.0 |
| Max, Deflection, μm | 7.36 | 5.57 |

### (b) FREQUENCY RESPONSE (Hz)

| Segment No. | 1 | 2 | 3 |
|---|---|---|---|
| Mass, Kg | 1 | 6 | 28 |
| Longitudinal Direction | 415 | 169 | 78 |
| Lateral Direction | 954 | 389 | 180 |
| Vertical Direction | 954 | 457 | 157 |

### 3.6 Prototype Calibration

A prototype load cell was built and its performance was tested in the laboratory. The prototype was then modified to the final design presented in Section 3.5.3. The objective of testing the prototype was to verify the linearity, sensitivity and identify any design problems in manufacturing, gauging and assembly and test for drifting and water leakage by immersion for at least 24 hours to assess the adequacy of sealing of the cell.

A special calibration rig was built to permit calibration using either deadweights or a dynamic load applied by a closed loop testing system under controlled conditions. More details of this calibration system may be found in Appendix A. The results of prototype calibration are shown in Figures 3.13 (a) and (b) for both loading and loading/unloading conditions. It is shown that the design provides good linearity and little hysterises under continuous loading/unloading calibration conditions. The zero intercept indicates some nonlinearity at the lower load end. However, the application of a preload will eliminate this problem.

Calibrations of all 19 load cells used in the segmented model are reported in Appendix A.

It should be noted that the loading rate of the load cells during calibration was only limited by the distortion in the ramp load when higher frequencies were used. Comparisons of the reference and test load cells were generally good at various rates. Selected ramp load durations were 120 and 60 seconds for the 100 and 50 N load cells, respectively.

## FIGURE 3.13 PROTOTYPE CALIBRATION RESULTS

### (DYNAMIC CALIBRATION)

PROTOTYPE CALIBRATION

TRANSDUCER S/N: 100 JUN-20-83

(A)

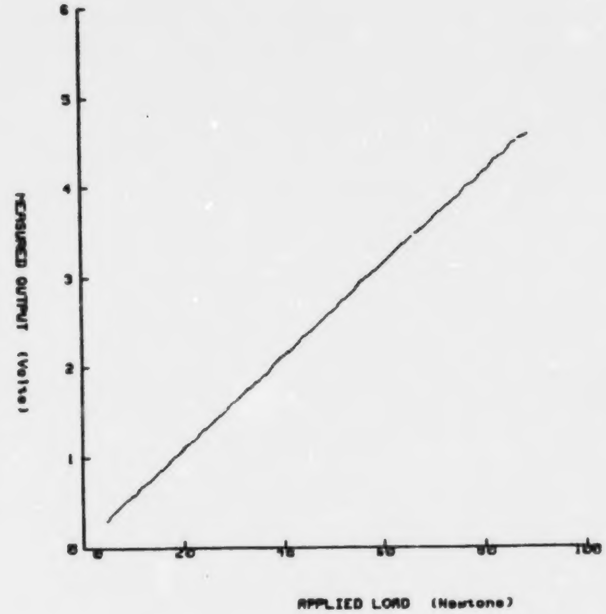

```
EXCITATION = 5.00 Volts
      GAIN = 2000 Volts/Volts

  SENSITIVITY= .5126 mV/V @ 100 Newtons

REGRESSION ANALYSIS :
                SLOPE  = .0513  Volts/Newton
            INTERCEPT  = .0708  Volts
 CORRELATION COEFF. = 1.0000
```

PROTOTYPE CALIBRATION

TRANSDUCER S/N: 100 JUN-20-83

(B)

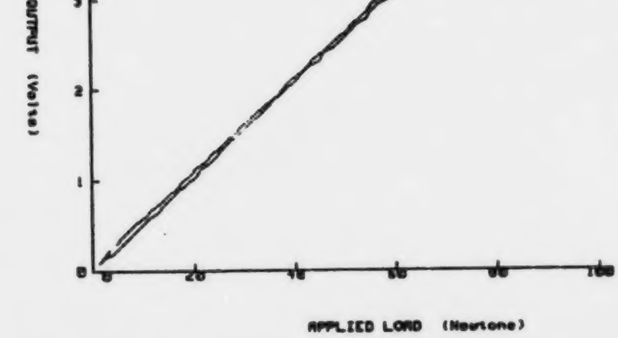

```
EXCITATION = 5.00 Volts
      GAIN = 2000 Volts/Volts

  SENSITIVITY= .5155 mV/V @ 100 Newtons
NON-LINEARITY= 2.5540 %
   HYSTERESIS= 1.7223 %

REGRESSION ANALYSIS :
                SLOPE  = .0516  Volts/Newton
            INTERCEPT  = .0332  Volts
 CORRELATION COEFF. = .9998
```

## 3.7 Data Acquisition System

Figures 3.14 describes the segmented model instrumentation and main components of the data acquisition system. The following measurements were acquired:

a) Total resistance of the ice measured by a standard force block. The location of the force block, however, has to be shifted into the stern half of the model due to lack of room in the bow half. However, this did not affect the model tendency to yaw.

b) All force components of segment loads as measured by the 19 load cells. Each channel is signal conditioned prior to further processing using Vishay 2100 series signal conditioning amplifiers.

c) Model speed and position.

d) Model pitch, roll and yaw rate. These measurements were obtained as secondary input to provide back-up information if required.

e) Accelerations of the model were also monitored near the centre of mass of the model. It was not spatially possible to locate the x-y-z accelerometers at the centre of gravity due to the structural reinforcements and design of the bow half of the model.

All signals were recorded on magnetic tape using a 28-channel Honeywell Model 5600E FM tape recorder and selected channels were simultaneously reproduced using an oscillograph chart recorder for immediate inspection of the measurements.

The data acquisition system was originally designed to provide simultaneous filtering of the signals, conversion to digital form and analysis using an HP9816 computer. The digitized data was stored on disc for later retrieval and further processing. However, the computer analysis was not done simultaneously in order to permit proper selection of the filtering frequencies.

The filtering frequency was selected by experimentation to study the effect of the cut-off frequency on the output signals. A low pass filter frequency of 1 Hz was selected on the basis of the results presented in Appendix A.

FIGURE 3.14 SEGMENTED MODEL INSTRUMENTATION

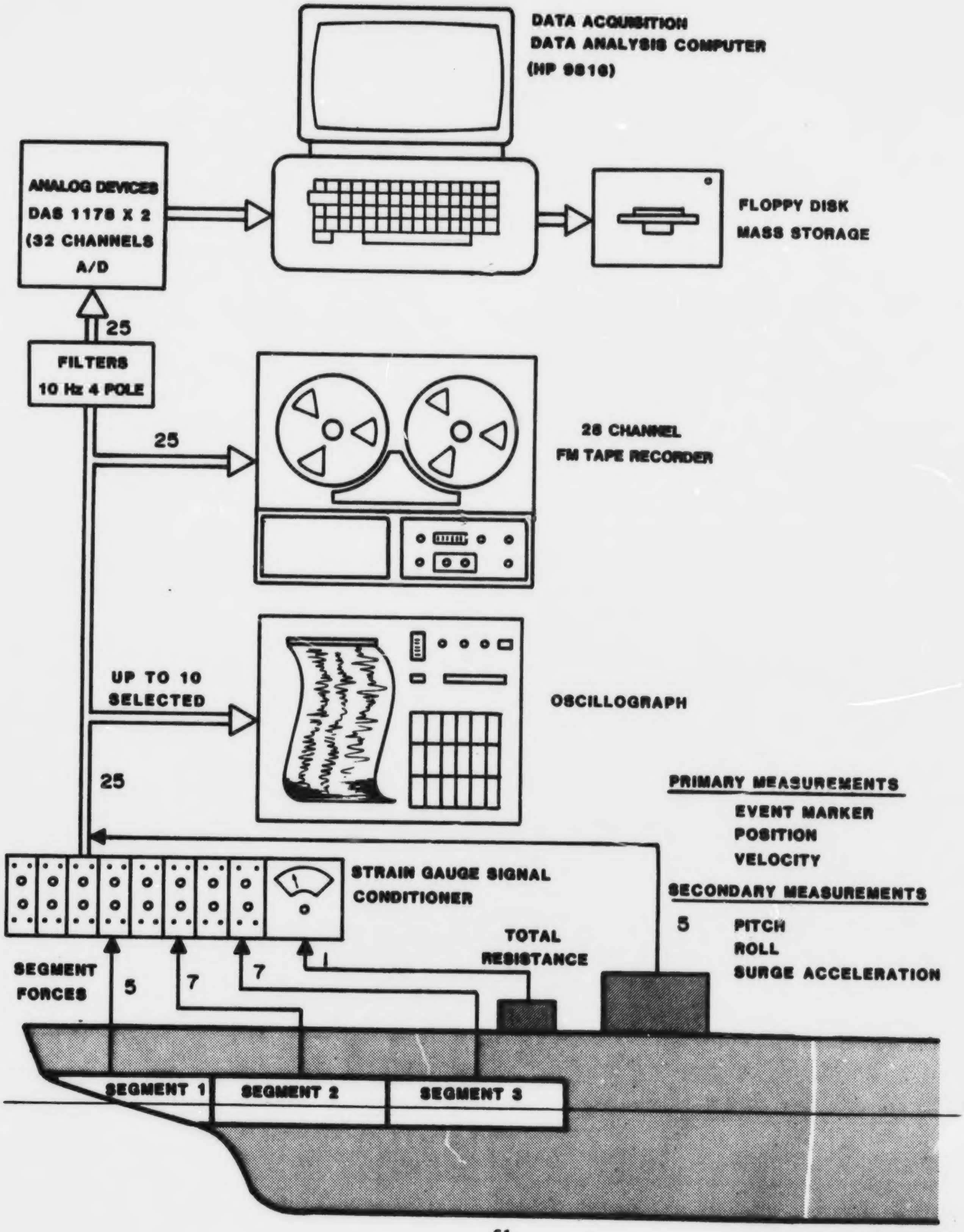
DATA ACQUISITION
DATA ANALYSIS COMPUTER
(HP 9816)
ANALOG DEVICES
DAS 1178 X 2
(32 CHANNELS
A/D
FLOPPY DISK
MASS STORAGE
25
FILTERS
10 Hz 4 POLE
25
28 CHANNEL
FM TAPE RECORDER
UP TO 10
SELECTED
OSCILLOGRAPH
25
PRIMARY MEASUREMENTS
EVENT MARKER
POSITION
VELOCITY
STRAIN GAUGE SIGNAL
CONDITIONER
SECONDARY MEASUREMENTS
5
PITCH
ROLL
SURGE ACCELERATION
TOTAL
RESISTANCE
SEGMENT
FORCES
5
7
7
SEGMENT 1
SEGMENT 2
SEGMENT 3
W.L.

THIS PAGE INTENTIONALLY LEFT BLANK

# 4.

# DATA REDUCTION ALGORITHM

# 4. DATA REDUCTION ALGORITHMS

## 4.1 Total Resistance and Components

The total resistance of the model was measured by a standard force block. The resistance components on each one of the three segments were directly measured by load cells.

A sample output is shown in Figure 4.1 in which the time histories of the total resistance and resistance components measured by the three sensors $R_{11}$, $R_{21}$, $R_{31}$ are plotted. It can be seen that the effect of inertia forces on the segments are negligible and that the response of the segments appears to be well represented within the measurement interval.

This interval was set according to a systematic procedure. That is when the event marker indicated that contact with the ice began the ship model was allowed to advance a distance equal to the entrance length of the PIERRE RADISSON bow. The starting point of resistance calculation was set at that point and identified by ST1 on the plots. At the end of the run and before the speed was reduced to stop the model the event marker was pressed again to identify the end of the steady progress interval. At this point the end curser was established and designated EN1 on the plots. The event marker, model speed, position and surge acceleration were plotted for every test run as part of the standard output format as illustrated in Figure 4.2 for the same test results of Figure 4.1.

The duration of the run was established such that at least one ship model length of data could be collected. For the example shown the duration of the test was approximately 10.3 seconds and the average velocity was 0.576 m/s thus yielding a constant velocity interval of approximately 5.95 m. This distance could also be obtained directly from the position signal by subtracting the "minimum" value at the beginning of the interval from the "maximum" value at the end of the interval, which gives 6.02 m. This penetration was approximately equivalent to 1.3 Ship model lengths. The total ship penetration for the run was about 7.85 m or 1.7 model lengths.

The filtering frequency of 1 Hz was selected so that only the higher frequency components extraneous to the icebreaking process are removed. This was done by trying several filtering frequencies namely 0.5, 1, 2 and 4 Hz. The results of this analysis are given in Appendix F.

FIGURE 4.1

TYPICAL RESISTANCE BREAKDOWN

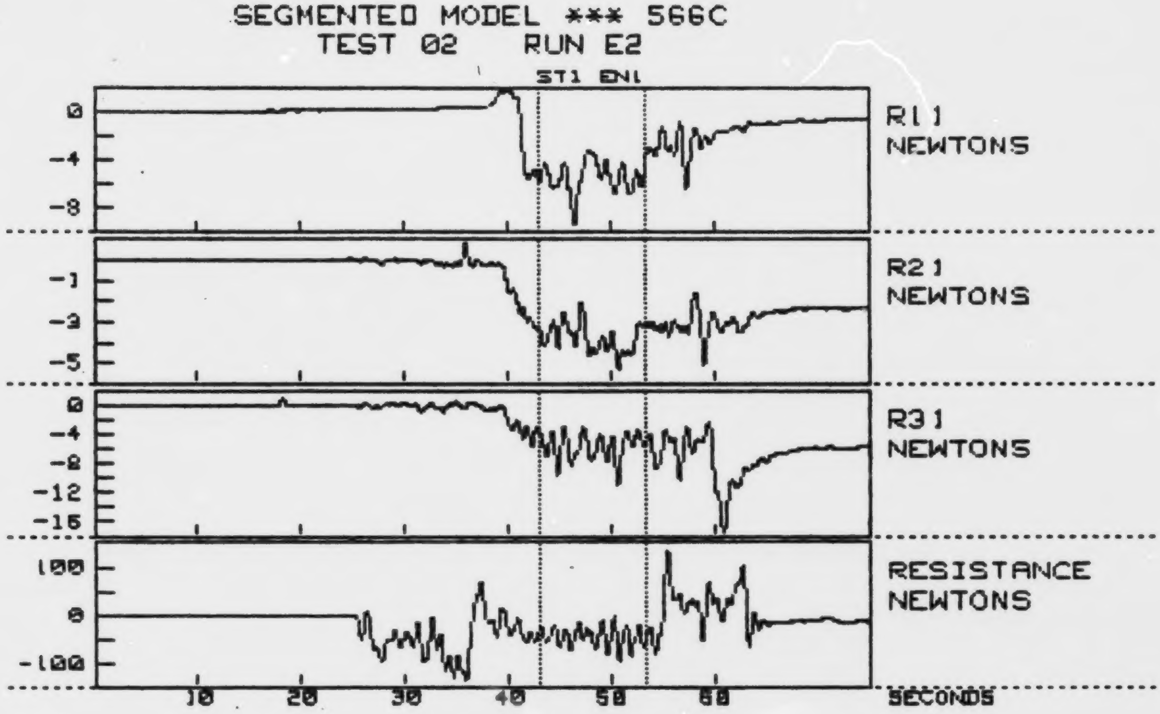

DATA DIGITIZED ON: 22 AUG 1983
DIGITIZING RATE: 32 Hz/CHANNEL
FILTER FREQUENCY: 1 HZ

INTERVAL STATISTICS

INTERVAL 1 START: 42.90625 END: 53.40625

| CHANNEL | MINIMUM | MAXIMUM | MEAN VALUE | STAN. DEV. |
|---|---|---|---|---|
| R11 | -9.406 | -3.11 | -5.384 | 1.27 |
| R21 | -5.282 | -2.12 | -3.78 | .678 |
| R31 | -10.74 | -2.93 | -5.633 | 1.71 |
| RESISTANCE | -94.163 | -1.35 | -44.519 | 19.18 |

For each signal standard statistics were obtained as shown in Figures 4.1 and 4.2.

As a check the total resistance should always satisfy this condition:

$$R_T > 2(\overline{R}_{11} + \overline{R}_{21} + \overline{R}_{31}) \tag{4.1}$$

Inequality (4.1) was based on a fundamental assumption that the ice on both sides of the hull broke in the same statistical fashion. This assumption may somewhat be violated since the model has to be laterally fixed and not permitted to sway. Due to variations in the ice thickness or strength along the path some error in applying (4.1) may be observed and it has to be interpreted with due consideration of the ice characteristics. For instance in the example shown:

$R_T =$ 44.52 N

$\Sigma R_{i_1} =$ 14.80 N

$2\Sigma R_{i_1} =$ 29.59 N = 66% of Total Resistance

FIGURE 4.2

TYPICAL SPEED AND ACCELERATION RECORDS

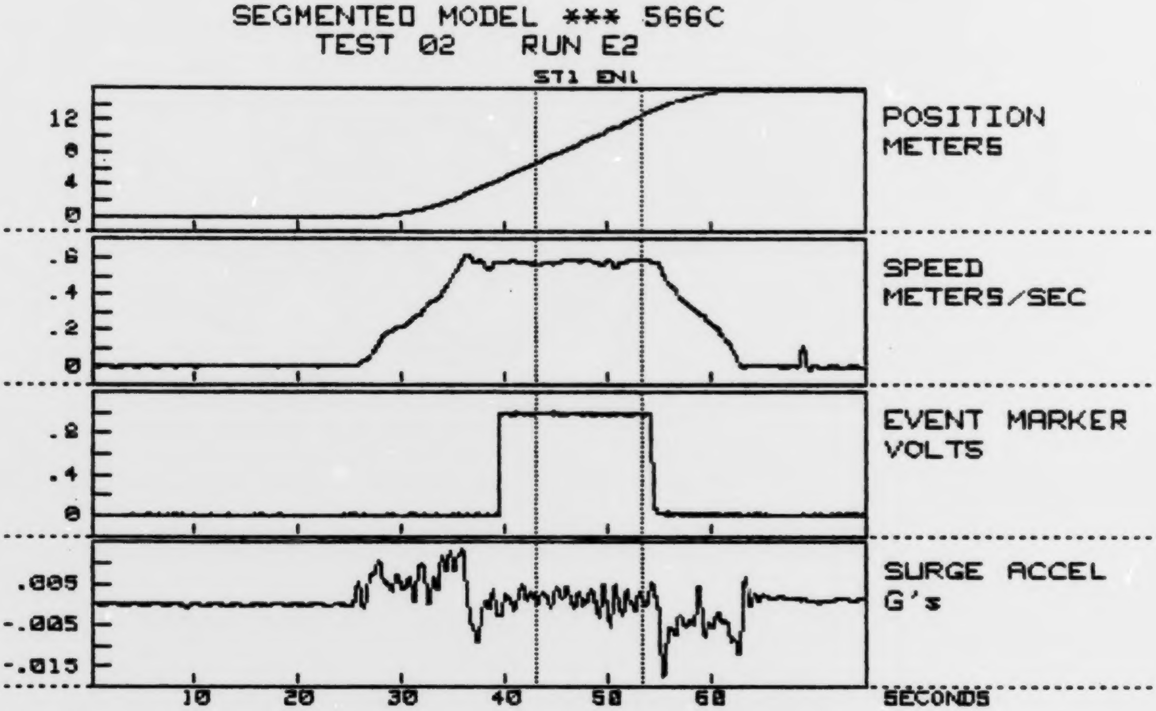

DATA DIGITIZED ON: 22 AUG 1983
DIGITIZING RATE: 32 Hz/CHANNEL
FILTER FREQUENCY: 1 HZ

INTERVAL STATISTICS

INTERVAL 1 START: 42.90625 END: 53.40625

| CHANNEL | MINIMUM | MAXIMUM | MEAN VALUE | STAN. DEV. |
|---|---|---|---|---|
| POSITION | 6.63 | 12.65 | 9.656 | 1.75 |
| SPEED | .543 | .591 | .576 | .010638 |
| EVENT MARKER | .972 | 1 | .987 | .0061895 |
| SURGE ACCEL | -.0052981 | .0049558 | .0011894 | .00208583 |

## 4.2 Analysis of Force Components

The objective of the analysis of force components on each segment was to determine the magnitude and centre of action of ice load on each segment. The ice load consisted of normal and frictional components. The point (centre) of ice load occurred at different positions on the segment depending on the cusp breaking pattern, ship speed, etc. Therefore, the position on the hull was unknown. Once the position was determined the direction of the normal force vector can be defined by the hull angles at this point. The frictional component of force was proportional to the normal force since the process was dynamic and continuous but the direction of this force remains unknown. Therefore, if the kinematic friction coefficient was known, the objective of the analysis would be to determine:

a) Position of ice load.
b) Magnitude of normal force.
c) Direction of friction force.

The load measurements made for each segment are shown in Figure 4.3 along with the coordinates of the support points in a left hand coordinate system with its origin located at the intersection of centreline bulkhead, the main deck and the midship plane. All the zero values indicate that no measurement was made nor required for calculations since this coordinate will occur along the line of action of a load cell reaction. The coordinate directions were consistent with previous definitions.

### 4.2.1 Equilibrium Equations

Due to the small mass of each segment, inertia effects can be neglected. Therefore, the equilibrium equations may be written in terms of instantaneous or average forces and may be solved as such. For each segment the force system consisted of:

a) External normal force to the hull, $-F_n\vec{n}$ which acts at point (x', y', z') on the hull surface, which has direction cosines ($n_1$, $n_2$, $n_3$). This force is always negative since it always opposes the normal unit vector n. (See Figure 4.4).

# FIGURE 4.3

## MEASURED FORCE COMPONENTS FOR ALL SEGMENTS

DIRECTION OF MEASUREMENT $V_{ij}$

SEGMENT No. ($i$) — LOAD CELL No. ($j$)

### POSITIONS of LOAD CELLS

| | X | Y | Z |
|---|---|---|---|
| $R_{11}$ | 0 | 0.050 | 0.020 |
| $R_{21}$ | 0 | 0.122 | 0.080 |
| $R_{31}$ | 0 | 0.320 | 0.080 |
| $H_{11}$ | 2.219 | 0 | 0.020 |
| $H_{12}$ | 2.055 | 0 | 0.083 |
| $H_{21}$ | 2.005 | 0 | 0.075 |
| $H_{22}$ | 1.653 | 0 | 0.080 |
| $H_{31}$ | 1.603 | 0 | 0.080 |
| $H_{32}$ | 0.920 | 0 | 0.080 |
| $V_{11}$ | 2.240 | 0.025 | 0 |
| $V_{12}$ | 2.056 | 0.153 | 0 |
| $V_{21}$ | 1.875 | 0.040 | 0 |
| $V_{22}$ | 2.005 | 0.179 | 0 |
| $V_{23}$ | 1.653 | 0.337 | 0 |
| $V_{24}$ | 1.795 | 0.040 | 0 |
| $V_{31}$ | 1.467 | 0.040 | 0 |
| $V_{32}$ | 1.603 | 0.346 | 0 |
| $V_{33}$ | 0.920 | 0.406 | 0 |
| $V_{34}$ | 1.105 | 0.040 | 0 |

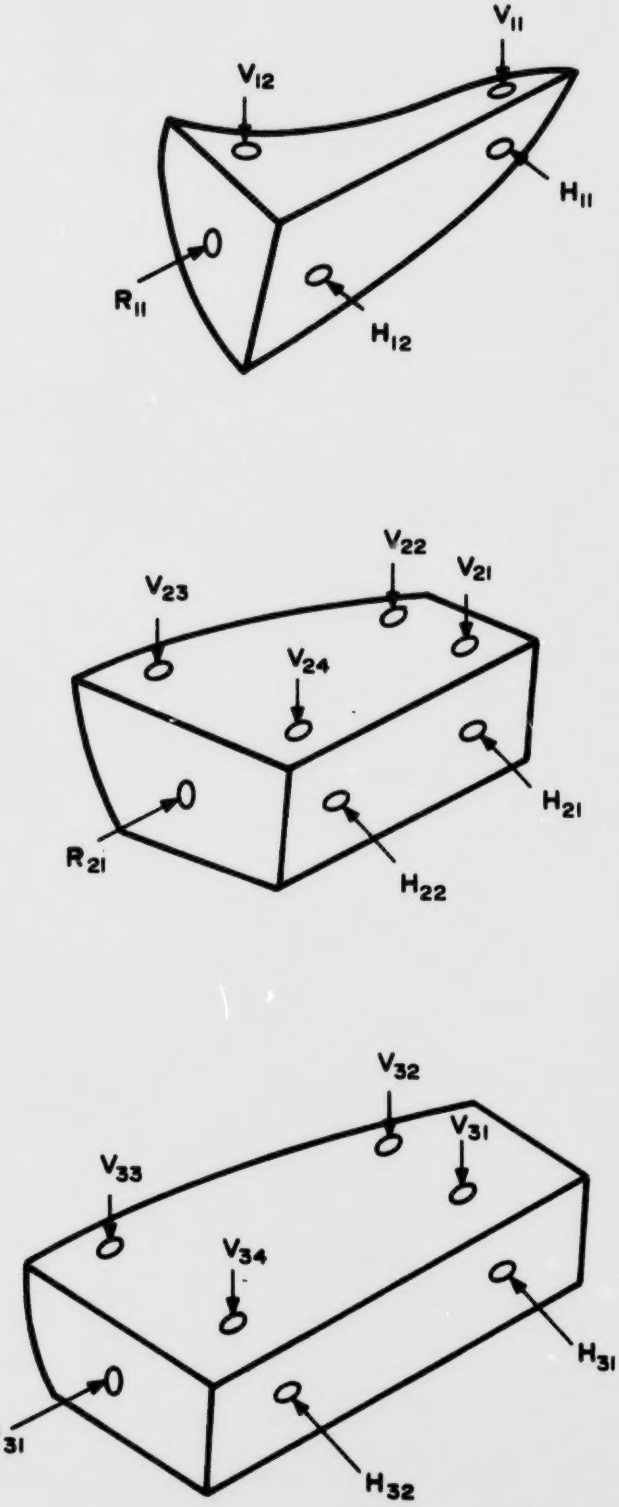
V11
V12
H11
R11
H12
V22
V21
V23
V24
H21
R21
H22
V32
V31
V33
V34
H31
R31
H32

b) External frictional force $\mu F_n . \vec{e}$, where $\vec{e}$ is the unit friction vector which may be expressed by:

$$\vec{e} = -e_1 \vec{i} + e_2 \vec{j} \pm e_3 \vec{k} \qquad (4.2)$$

This unit vector is always normal to $\vec{n}$ and could take any direction in the normal plane (tangential to the hull at the point of action). Practically, in the ahead motion of the ship in continuous icebreaking it will assume the direction indicated by Equation (4.2).

c) Reaction vectors or load cell reactions on the segments as depicted in Figure 4.3. All these components are always positive in the L.H. coordinate system. In index notation these measured reactions can be expressed by $R_{i_1} . \vec{i}$, $H_{ij} . \vec{j}$ and $V_{ij} . \vec{k}$ .

The external forces may be expressed in terms of its components in the x, y, z system as follows:

$$\vec{F} = -F_n . \vec{n} + \mu F_n . \vec{e} = F_x \vec{i} + F_y \vec{j} + F_z \vec{k} \qquad (4.3)$$

Substituting for the unit vectors obtain:

$$\vec{F} = -(F_n n_1 \vec{i} + F_n n_2 \vec{j} + F_n n_3 \vec{k})$$

$$+(-\mu F_n e_1 \vec{i} + \mu F_n e_2 \vec{j} + \mu F_n e_3 \vec{k})$$

$$\vec{F} = -F_n(n_1 + \mu e_1)\, \vec{i} - F_n(n_2 - \mu e_2)\, \vec{j} - F_n(n_3 - \mu e_3)\, \vec{k} \qquad (4.4)$$

or in scalar form:

$$\begin{aligned} F_x &= -F_n(n_1 + \mu e_1) \\ F_y &= -F_n(n_2 - \mu e_2) \\ F_z &= -F_n(n_3 - \mu e_3) \end{aligned} \qquad (4.5)$$

Since all these forces were in equilibrium for each segment, the following equilibrium conditions should be satisfied:

$$\begin{aligned} \Sigma \vec{F} &= 0 \\ \Sigma \vec{M}_0 &= 0 \end{aligned} \qquad (4.6)$$

**FIGURE 4.4**

**BASIC FORCE ANALYSIS**

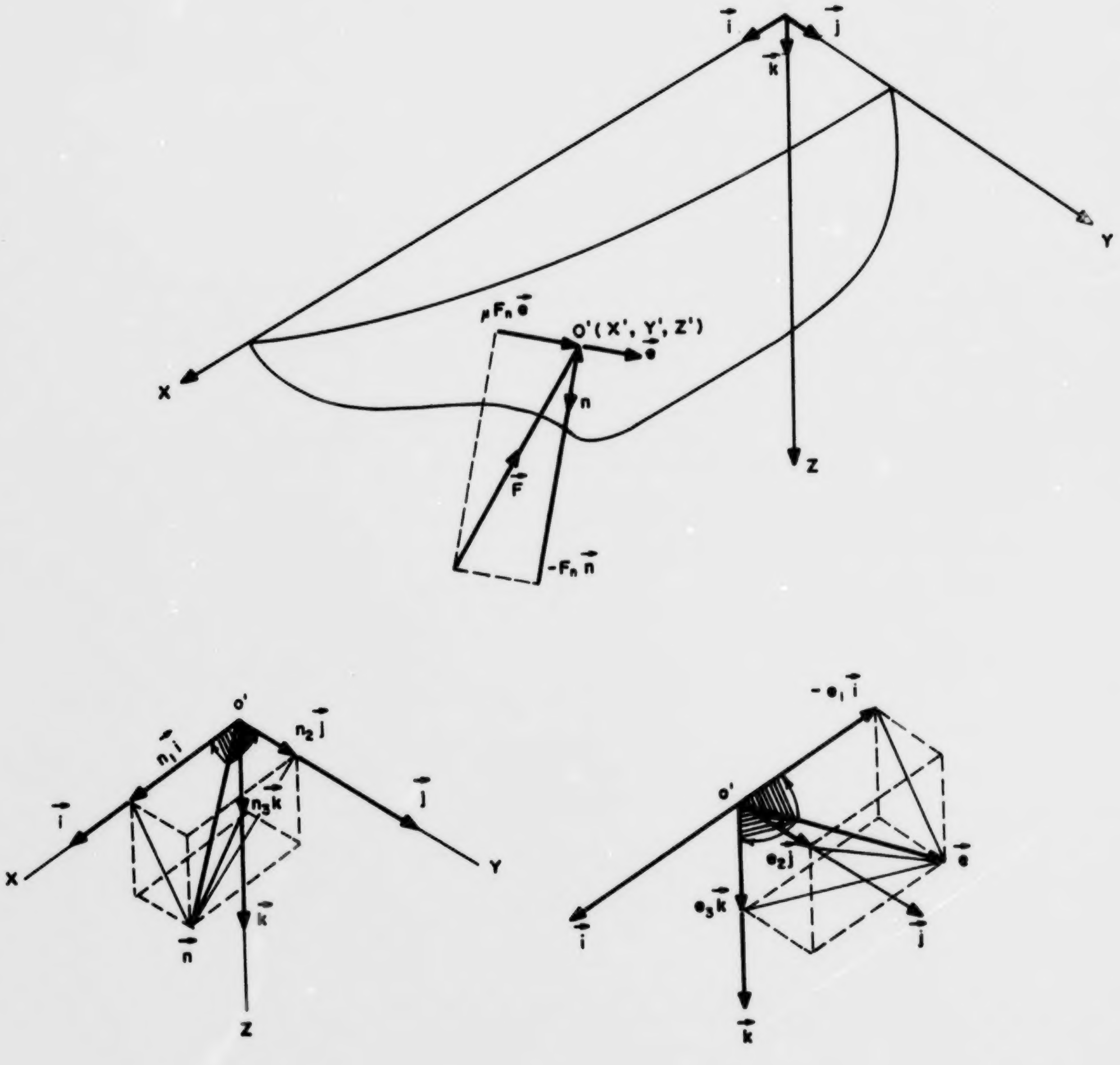
O
$\vec{i}$
$\vec{j}$
$\vec{k}$
Y
X
Z
$\mu F_n \vec{e}$
O'(X', Y', Z')
$\vec{e}$
n
$\vec{F}$
$-F_n \vec{n}$
o'
$n_1\vec{i}$
$n_2\vec{j}$
$n_3\vec{k}$
$\vec{i}$
$\vec{j}$
$\vec{k}$
$\vec{n}$
X
Y
Z
$-e_1\vec{i}$
o'
$e_2\vec{j}$
$\vec{e}$
$e_3\vec{k}$
$\vec{i}$
$\vec{j}$
$\vec{k}$

NORMAL UNIT VECTOR

$\vec{n} = n_1\vec{i} + n_2\vec{j} + n_3\vec{k}$

FRICTION UNIT VECTOR

$\vec{e} = -e_1\vec{i} + e_2\vec{j} + e_3\vec{k}$

These fundamental equations can be expanded into six equations which may be written as follows for any segment:

$$(\Sigma F)_x = 0 : \quad -F_n(n_1 + \mu e_1) + R_{i1} = 0 \qquad (4.7.a)$$

$$(\Sigma F)_y = 0 : \quad -F_n(n_2 - \mu e_2) + H_{ij} = 0 \qquad (4.7.b)$$

$$(\Sigma F)_z = 0 : \quad -F_n(n_3 - \mu e_3) + V_{ij} = 0 \qquad (4.7.c)$$

$$(\Sigma M_0)_x = 0 : +F_n(n_2 - \mu e_2) \,.\, z' - F_n(n_3 - \mu e_3) \,.\, y' + \Sigma V_{ij} .\, Y_{ij} - \Sigma H_{ij} . z_{ij} = 0 \qquad (4.8.a)$$

$$(\Sigma M_0)_x = 0 : +F_n(n_3 - \mu e_3) \,.\, x' - F_n(n_1 + \mu e_1) \,.\, z' + R_{i1} .\, z_{i1} - \Sigma V_{ij} .\, X_{ij} = 0 \qquad (4.8.b)$$

$$(\Sigma M_0)_z = 0 +F_n(n_1 + \mu e_1) \,.\, y' - F_n(n_2 - \mu e_2) \,.\, x' + \Sigma H_{ij} .\, x_{ij} - R_{i1} .\, y_{i1} = 0 \qquad (4.8.c)$$

These equations must be supplemented by the following known relationships:

a) The direction cosines $n_1$, $n_2$, $n_3$ are related by:

$$n_1^2 + n_2^2 + n_3^2 = 1 \qquad (4.9.a)$$

also

$$e_1^2 + e_2^2 + e_3^2 = 1 \qquad (4.9.b)$$

Therefore if any two direction cosines are known, the third can be calculated using the above rules.

b) Since $\vec{n}$ and $\vec{e}$ are orthogonal, therefore their cross product must vanish. Therefore:

$$\vec{n} \,.\, \vec{e} = 0$$

$$(n_1\vec{i} + n_2\vec{j} + n_3\vec{k}) \,.\, (-e_1.\vec{i} + e_2.\vec{j} + e_3\vec{k}) = 0$$

but since the square of a unit vector is unity and the product of orthogonal unit vectors must vanish obtain:

$$- n_1e_1 + n_2e_2 + n_3e_3 = 0 \qquad (4.10)$$

c) The position of the point of action ($x'$, $y'$, $z'$) and its direction cosines ($n_1$, $n_2$, $n_3$) are related by the hull shape and angles. Therefore, if these six unknowns reduce to three, also if two coordinates on the ship hull are known the third coordinate must have a unique value which is defined by the hull surface. Therefore, if $x'$, and $y'$ are known, the other four unknowns are automatically defined by the hull geometry.

As a result of the above discussions, the number of unknowns in Equations (4.7) and (4.8) are originally ten:

$F_n$, $n_1$, $n_2$, $n_3$, $e_1$, $e_2$, $e_3$, $x'$, $y'$, $z'$

Using (c) above the unknowns can be reduced to six

$F_n$, $e_1$, $e_2$, $e_3$, $x'$, $y'$

Further employing Equations (4.9.b) and (4.10) these will be reduced to four:

$F_n$, $e_1$, $x'$, $y'$

Therefore, theoretically one would require only four of Equations (4.7) and (4.8) to solve the problem. In simple terms there are thirteen equations and ten unknowns thus rendering any three equations redundant.

However, from a practical engineering point of view, some of the relationships listed above were difficult to formulate (item (c) above) in closed form thus limiting their usefulness in providing a solution.

Several methods can be developed to solve the above system of equations, for each segment independently. One preferred approach will be discussed in the following section which attempts to structure the data analysis in levels to minimize the effects of experimental errors and enable the identification of such errors in due course.

It should be noted that due to the inherent scatter in ice force and resistance data (observed both in model and full scale tests), the approach presented in this report is probably more suited for this type of analysis. It should also be mentioned that the solution is valid whether instantaneous or corresponding average force measurements are used.

## 4.3 Method of Solution

If the location of the point of action of ice loads is known, the vector $\vec{n}$ is readily determined and Equations (4.7) can be treated as follows:

### 4.3.1 Normal Ice Force

Multiply equations (4.7) a, b and c by $n_1$, $n_2$ and $n_3$, respectively and add the resulting equations. Then substitute the definitions expressed by equations (4.9) b and (4.10) to obtain:

$$F_n = n_1 R_{i1} + n_2 \Sigma H_{ij} + n_3 \Sigma V_{ij} \qquad (4.11)$$

Therefore, equation (4.11) can be used directly to calculate the normal force component.

### 4.3.2 Friction Coefficient

The coefficient of friction can be measured before the experiment. Nevertheless if an error occurred in its measurement, or for other reasons, the direct calculation of the direction of the friction components could result in significant errors in their direction cosines. Therefore, this step was essential for two reasons:

a) to verify the friction factor,
b) to identify any experimental errors in measurement or conversion of the load cell reactions.

Equations (4.7) may be rewritten in the form:

$$\mu e_1 = \frac{R_{i1}}{F_n} - n_1 = \frac{F_x}{F_n} - n_1 = \mu_1 \qquad (4.12.a)$$

$$- \mu e_2 = \frac{\Sigma H_{ij}}{F_n} - n_2 = \frac{F_y}{F_n} - n_2 = \mu_2 \qquad (4.12.b)$$

$$- \mu e_3 = \frac{\Sigma V_{ij}}{F_n} - n_3 = \frac{F_z}{F_n} - n_3 = \mu_3 \qquad (4.12.c)$$

Therefore, the sum of square of the L.H.S. combined with equation (4.9) b yields:

$$\boxed{\mu = \sqrt{\mu_1^2 + \mu_2^2 + \mu_3^2}} \qquad (4.13)$$

where $\mu_1$, $\mu_2$ and $\mu_3$ were defined by Equations (4.12). Generally, the deviation of the calculated friction coefficient from the measured one may be considered a measure of the degree of experimental error. The consistent and biased deviation from measured friction can also be construed as evidence of the effect of the techniques used to measure friction as compared to the actual friction mechanism associated with the icebreaking.

### 4.3.3 Direction of Friction Force

Once the friction coefficient is determined, the direction cosines of the friction vector may be calculated using equations (4.12) in the form:

$$e_1 = \mu_1/\mu = \frac{1}{\mu}\left[\frac{F_x}{F_n} - n_1\right] \qquad (4.14.a)$$

$$e_2 = -\mu_2/\mu = -\frac{1}{\mu}\left[\frac{F_y}{F_n} - n_2\right] \qquad (4.14.b)$$

$$e_3 = -\mu_3/\mu = -\frac{1}{\mu}\left[\frac{F_z}{F_n} - n_3\right] \qquad (4.14.c)$$

The calculated direction cosines will automatically satisfy both equations (4.9)b and (4.10) since the former equation has been a necessary condition in calculating friction factor and the latter has been satisfied in calculating the normal ice force.

It is shown that once the coordinates of the point of ice action are known all other unknowns can readily be determined regardless of the numbers of load cells. The solution was developed on the basis of the sums of measured load cell reactions in the x, y and z directions; respectively. The accurate determination of the location of ice action will be examined in the following section.

### 4.3.4 The Ice Load Location

Substituting equations (4.7) into (4.8) gives the following simpler form:

$$(\Sigma H_{ij}).\ z' - (\Sigma V_{ij})\ .\ y' = \Sigma(H_{ij}.\ Z_{ij}) - \Sigma(V_{ij}\ .\ Y_{ij}) = C_1 \qquad (4.15.a)$$

$$(\Sigma V_{ij}).\ x' - R_{i_1}\ .\ z' = \Sigma(V_{ij}.\ X_{ij}) - R_{i_1}\ .\ Z_{i_1} = C_2 \qquad (4.15.b)$$

$$R_{i_1}.\ y' - (\Sigma H_{ij}).\ x' = R_{i_1}\ .\ Y_{i_1} - \Sigma(H_{ij}\ .\ X_{ij}) = C_3 \qquad (4.15.c)$$

Equations (4.15) represent the moments of external ice loads about the x, y, and z axes; respectively. These equations contain only three unknowns and may be expressed in a matrix form as follows:

$$\begin{bmatrix} 0 & -\Sigma V_{ij} & \Sigma H_{ij} \\ \Sigma V_{ij} & 0 & -R_{i1} \\ -\Sigma H_{ij} & R_{i1} & 0 \end{bmatrix} \begin{bmatrix} x' \\ y' \\ z' \end{bmatrix} = \begin{bmatrix} C_1 \\ C_2 \\ C_3 \end{bmatrix} \qquad (4.16)$$

A solution is possible if the determinant of the square matrix of measured force components is non-zero. Unfortunately this is not the case and the square matrix is singular. Therefore, there is one redundant equation[1] and the solution can only be determined on the basis of model hull characteristics. The following procedure is proposed.

a) Use Equation (4.15.c) and rearrange in the following linear format:

$$y' = \left(\frac{C_3}{R_{i1}}\right) + \left(\frac{\Sigma H_{ij}}{R_{i1}}\right) x' \qquad (4.17)$$

This linear equation will in most cases under consideration have a negative intercept and a positive slope. This linear relationship can then be plotted on the ship hull lines plan, as illustrated in Figure 4.5.

b) The intersection with the proper waterline will provide a corresponding z' coordinate of the point of impact which satisfies all conditions of occuring on the hull surface. In order to determine the proper waterline another condition must be satisfied which may be given by re-arranging equation (4.15)b:

$$z' = -\left(\frac{C_2}{R_{i1}}\right) + \left(\frac{\Sigma V_{ij}}{R_{i1}}\right) . x' \qquad (4.18)$$

This condition is similar to that of equation (4.17) and may be also plotted on Figure 4.5 as illustrated. Based on these two lines a solution which satisfies both equations may be found graphically.

---

[1] This redundancy can be shown by eliminating x', y' and z' from equations (4.15) thus resulting in the following condition:

$$C_1 R_{i1} + C_2 . \Sigma H_{ij} + C_3 \Sigma V_{ij} = 0$$

FIGURE 4.5

GRAPHICAL DETERMINATION OF THE ICE LOAD POSITION

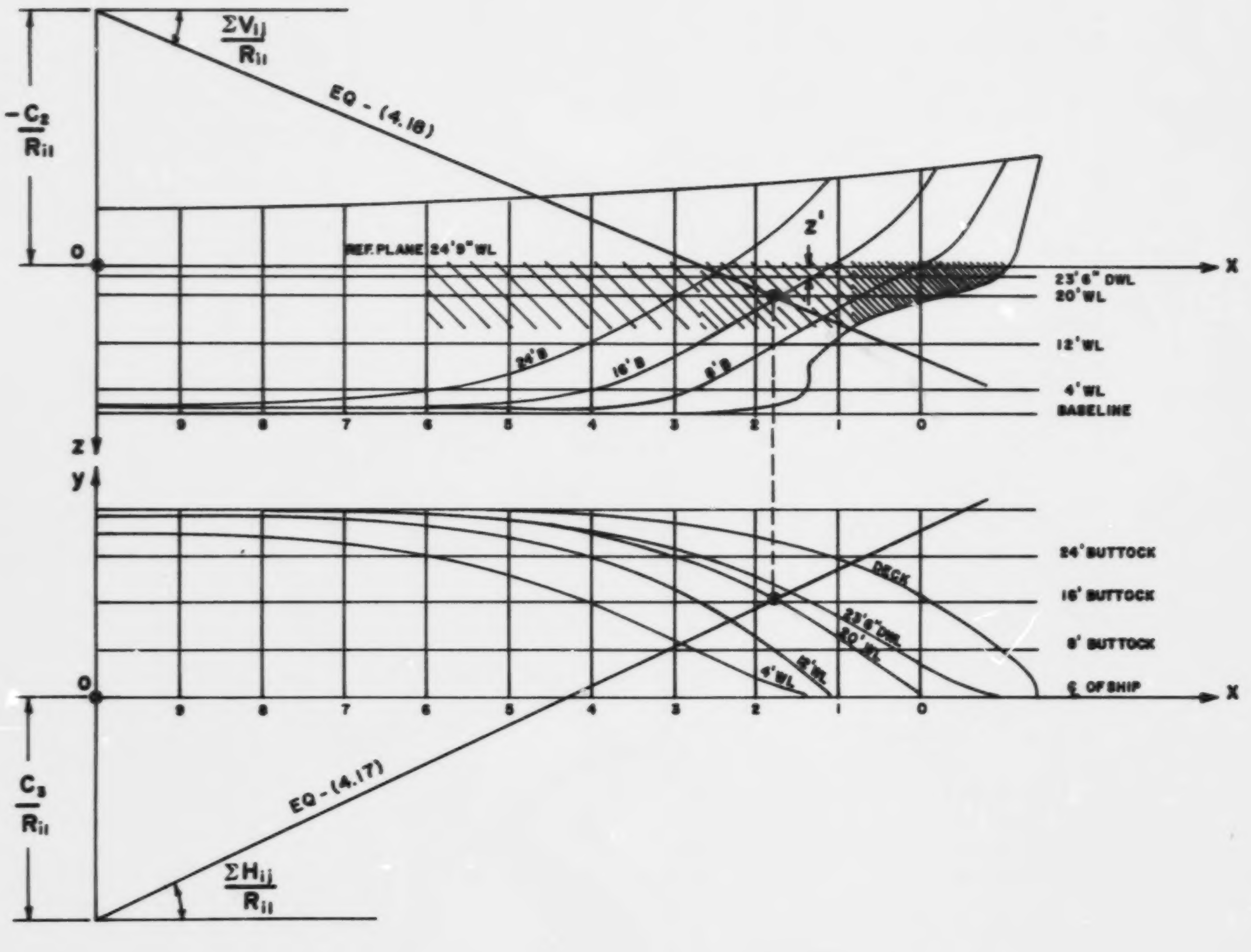
$\frac{\Sigma V_{ij}}{R_{ii}}$
$-\frac{C_2}{R_{ii}}$
EQ - (4.18)
REF. PLANE 24'9" WL
Z'
0
X
23'6" DWL
20' WL
12' WL
4' WL
BASELINE
24' B
16' B
8' B
9
8
7
6
5
4
3
2
1
0
z
y
24' BUTTOCK
16' BUTTOCK
8' BUTTOCK
℄ OF SHIP
DECK
23'6" DWL
20' WL
12' WL
4' WL
X
$\frac{C_3}{R_{ii}}$
EQ - (4.17)
$\frac{\Sigma H_{ij}}{R_{ii}}$

c) Once the coordinates of the ice load point are determined for a given segment, a check must be made to ensure that this point occurs, not only on the hull, but within the surface area of the segment. This could be made by laying the segment boundaries on the lines plans as shown by the light shade in Figure 4.5.

It should be noted that the resolved x-component of the ice force is generally smaller than the lateral loads. Also the moment of ice forces about the z-axis, $C_3$ is primarily influenced by the H-components of load and their relatively long arm of moment. The contribution of the smaller R-component with its smaller moment arm will be much smaller, resulting in a predominantly negative $C_3$. As a first approximation of solution, equation (4.15.c) may be solved for x' with the variation of y' neglected and a fixed average y' used for each segment, i.e. the location of ice load may be determined on the basis of the following equation:

$$x' = \frac{-C_3}{\Sigma H_{ij}} + \frac{R_{i1} y'_{iav}}{\Sigma H_{ij}} = \frac{\Sigma(H_{ij} \cdot x_{ij})}{\Sigma H_{ij}} - \frac{R_{i1} . (y_{i1} - y'_{iav})}{\Sigma H_{ij}} \quad (4.19)$$

The last term in the R.H.S. makes little contribution to the value of x' and may be neglected. This is mainly because the difference in $y'_{i1}$ and $y'_{iav}$ was minimized by design. Equation (4.19) may, therefore, be simplified to:

$$x' = \frac{\Sigma H_{ij} \, . \, x_{ij}}{\Sigma H_{ij}} \quad (4.20)$$

This estimate may be adjusted once y' is obtained.

It is obvious that the graphical solution is possible but it requires manual processing. There are two alternative solutions to this time consuming process which limits the value of a completely computerized processing of test data. The first is to make some assumptions regarding the value of z' and accept some error in calculation. This solution can be justified if the value of z' is only going to vary in a narrow range. From RICE it was found that the vertical deflection of the ice sheet before its breaking was of the order of 0.3 m (1 ft). Therefore, making an estimate for the value of z, it would be simpler to calculate the x-y coordinates of the point of load for a given waterline. It would also be possible to digitize the waterline and enter hull direction cosines along the waterline for possible interpolation.

The second alternative would require the digitization of the entire hull form. This process would require a great deal of computational capabilities in terms of memory and processing.

### 4.3.5 Summary

The summary of the procedures discussed in previous sections is given as follows:

a) For each segment calculate the sum of measured load cell reactions $R_{i_1}$, $\Sigma H_{ij}$ and $\Sigma V_{ij}$.

c) Select an active waterline and consider the ice loads to act close to it.

c) Determine the x-coordinate of ice force according to Equation (4.20).

d) Use lines plans to find corresponding y' and adjust x' if necessary.

e) Assess the errors involved in the moment equilibrium equations (4.15) a, b and c. Correct if necessary.

f) Determine $(n_1, n_2, n_3)$ at the location (x' , y', z').

g) Calculate the normal ice load on the segment using equation (4.11).

h) Estimate the friction coefficient from equation (4.13) and compare with measured factor.

i) Calculate the indices of the friction vector $(e_1, e_2, e_3)$.

j) Compare the direction with hull lines i.e. waterline, buttock angles, etc.

Table 4.1 assembles all the equations necessary for the analysis.

## TABLE 4.1

## SUMMARY OF EQUATIONS

$$\Sigma H_{ij} = H_{i_1} + H_{i_2}$$

$$\Sigma V_{ij} = V_{i_1} + V_{i_2} + V_{i_3} + V_{i_4}$$

$$x' = \frac{\Sigma H_{ij} \cdot x_{ij}}{\Sigma H_{ij}} \qquad (4.20)$$

$$(\Sigma H_{ij}) . \; z' - (\Sigma V_{ij}) \; . \; y' = \Sigma(H_{ij} . \; Z_{ij}) - \Sigma(V_{ij} \; . \; Y_{ij}) = C_1 \qquad (4.15.a)$$

$$(\Sigma V_{ij}) . \; x' - R_{i_1} \; . \; z' = \Sigma(V_{ij} . \; X_{ij}) - R_{i_1} \; . \; Z_{i_1} = C_2 \qquad (4.15.b)$$

$$R_{i_1} . \; y' - (\Sigma H_{ij}) . \; x' = R_{i_1} \; . \; Y_{i_1} - \Sigma(H_{ij} \; . \; X_{ij}) = C_3 \qquad (4.15.c)$$

$$F_n = n_1 R_{i_1} + n_2 \; \Sigma H_{ij} + n_3 \; \Sigma V_{ij} \qquad (4.11)$$

$$\mu e_1 = \frac{R_{i_1}}{F_n} - n_1 = \frac{F_x}{F_n} - n_1 = \mu_1 \qquad (4.12.a)$$

$$-\mu e_2 = \frac{H_{ij}}{F_n} - n_2 = \frac{F_y}{F_n} - n_2 = \mu_2 \qquad (4.12.b)$$

$$-\mu e_3 = \frac{V_{ij}}{F_n} - n_3 = \frac{F_z}{F_n} - n_3 = \mu_3 \qquad (4.12.c)$$

$$\boxed{\mu = \sqrt{\mu_1^2 + \mu_2^2 + \mu_3^2}} \qquad (4.13)$$

$$e_1 = \mu_1/\mu = \frac{1}{\mu}\left[\frac{F_x}{F_n} - n_1\right] \qquad (4.14.a)$$

$$e_2 = -\mu_2/\mu = -\frac{1}{\mu}\left[\frac{F_y}{F_n} - n_2\right] \qquad (4.14.b)$$

$$e_3 = -\mu_3/\mu = -\frac{1}{\mu}\left[\frac{F_z}{F_n} - n_3\right] \qquad (4.14.c)$$

# 5.

# TESTING PROGRAM

# 5. TESTING PROGRAM

## 5.1 Introduction

The objectives of the testing program were to experimentally investigate the ice forces on specific areas of the hull surface and to determine the ice resistance component breakdown using the segmented model developed for this purpose.

The testing program was divided into two major parts:

a) Calibration testing
b) Model testing

## 5.2 Calibration Testing

In the first part aimed at verifying the response of the model and providing calibration constants to be used in data reduction, various calibration tests were conducted.

### 5.2.1 Calibration of Load Cells

This provided the basic set of calibration data for all nineteen load cells used to measure segment loads. The results may be found in Chapter 3 and Appendix A of this report.

### 5.2.2 Calibration of Segment Response

This was necessary to ensure that the segments were responding as anticipated. The details of this testing, as reported in Appendix B, have demonstrated some attenuation of response and have further shown that in some cases the measured response will be dependent on the location of load.

This observation prompted further investigation of the reasons behind this behaviour and this was accomplished by using the finite element method. Figure 5.1 illustrates the finite element model geometry for Segment 2. The details of this investigation are reported in Appendix G and have resulted in further segment calibration factors to be used in adjusting the load cell independent calibration constants.

### 5.2.3 Calibration of System Response to Model Motions

This consisted of investigating the effects of model motions in open water on the output of load cells. This included model towing at various speeds as well as model rolling, heaving and pitching. The detailed results of the various tests may be found in Appendix C.

### 5.2.4 Other Calibrations

These were also conducted on force block and other sensors used to monitor the segmented model, as detailed in Appendix D.

FIGURE 5.1 FINITE ELEMENT MODEL GEOMETRY

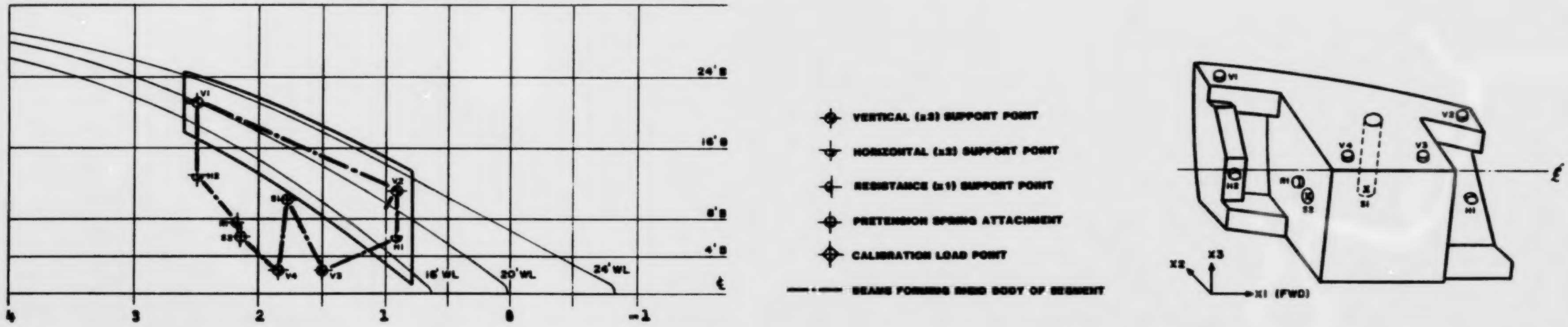

24'B
16'B
8'B
4'B
16'WL
20'WL
24'WL
℄
4
3
2
1
0
-1
V1
V2
V3
V4
H1
H2
S1
S2
R1
VERTICAL (x3) SUPPORT POINT
HORIZONTAL (x2) SUPPORT POINT
RESISTANCE (x1) SUPPORT POINT
PRETENSION SPRING ATTACHMENT
CALIBRATION LOAD POINT
BEAMS FORMING RIGID BODY OF SEGMENT
X1 (FWD)
X2
X3

(b) WATERLINES of THE RADISSON SHOWING THE OUTLINE of SEGMENT No. 2 LOADCELL POSITIONS SHOWN

(a) ISOMETRIC VIEW of LOADCELL POSITIONS on SEGMENT No. 2

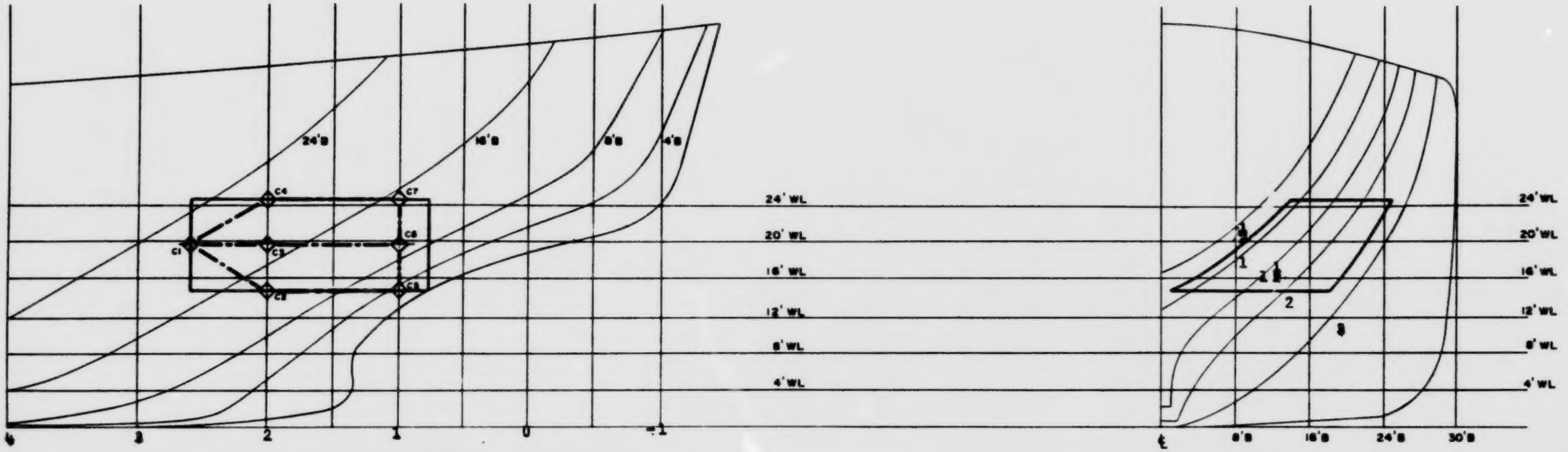

24'B
16'B
8'B
4'B
C1
C2
C3
C4
C5
C6
C7
C8
24' WL
20' WL
16' WL
12' WL
8' WL
4' WL
4
3
2
1
0
-1
1
2
3
℄
8'B
16'B
24'B
30'B

(c) BUTTOCKS of RADISSON SHOWING THE OUTLINE OF SEGMENT No. 2 CALIBRATION LOADING POINTS SHOWN

(d) BODY PLAN of RADISSON SHOWING OUTLINE of SEGMENT No. 2

## 5.3 Model Testing

In this part, towed resistance tests of the segmented model were conducted with the objective of collecting experimental data for further analysis.

Due to the high sensitivity and limited capacity of the load cells used to instrument each segment, extra precaution was taken during these ice tests. Such precaution, combined with rigid test constraints such as the test length and time, have reduced the quantity of data that can be obtained during these tests. For standard resistance tests of the 20th scale model of the CCGS PIERRE RADISSON, it is usually possible to obtain three runs per ice sheet up to a maximum speed of 9 knots full scale. For the segmented model, only two runs per ice sheet up to a maximum speed of 5 knots were performed. The reduction in speed and number of tests should result in better quality data.

A primary constraint which reduced the available basin length is acceleration and deceleration levels. Ordinarily for a resistance test, the total force measured by the force block during acceleration and deceleration intervals is as high as five to ten times the mean ice resistance. However, inertia forces acting on each segment are expected to be proportional to its mass and angular moment characteristics. To minimize such effects on the load cells, the acceleration and deceleration lengths were increased to lower the maximum acceleration forces. For this reason, most high speed tests were performed following a lower speed test. The model between each test was backed to the beginning of the basin. The model was gradually accelerated to speed in the previously broken channel, eliminating any loss of basin length due to the slower acceleration.

### 5.3.1 Test Plan and Procedure

The original plan of testing required a pause and report on quality of data after three ice sheets had been tested. In the actual testing program tests were stopped after the first two ice sheets, the model was removed and some adjustments were made. Following this, two more ice sheets were tested. Details of the four ice sheets and eight test runs are given in Table 5.1.

The ice sheets were prepared in accordance with Arctec's standard procedures and the properties of ice were measured and reported using the procedures described in Appendix E.

Following each of the four freezes, the ice sheet was allowed to slowly decay in strength while being monitored. During this "come down" period, the segments were all washed with warm water to ensure that any ice build-up between segments would melt. Once it was certain that any build-up was eliminated and that all load cells were working, then the segments were adjusted and properly preloaded.

It should be noted that in this type of model there is a requirement for some adjustment of the segments prior to a test, such as setting the preloads and ensuring the proper operation of each load cell. The time penalty imposed by this requirement make it more diffi-

# TABLE 5.1
# DETAILS OF TESTS

| TEST DATA | SHEET NO. | RUN NO. | ICE THICKNESS (mm) | FULL SCALE VELOCITY (knots) | MODEL VELOCITY (m/sec) | RUN LENGTH (m) | RUN TIME (sec) |
|---|---|---|---|---|---|---|---|
| July | 1 | 1 | 25 | 1.0 | 0.12 | 8.5 = 1.86 $L_{WL}$ | 71 |
| 18/83 | 1 | 2 | 25 | 1.7 | 0.20 | 8.5 = 1.86 $L_{WL}$ | 43 |
| July | 2 | 1 | 25 | 2.9 | 0.33 | 7.8 = 1.70 $L_{WL}$ | 24 |
| 19/83 | 2 | 2 | 25 | 5.0 | 0.58 | 7.8 = 1.70 $L_{WL}$ | 13 |
| August | 3 | 1 | 25 | 1.0 | 0.12 | 7.0 = 1.53 $L_{WL}$ | 58 |
| 9/83 | 3 | 2 | 25 | 5.0 | 0.58 | 8.7 = 1.90 $L_{WL}$ | 15 |
| August | 4 | 1 | 45 | 1.0 | 0.12 | 9.0 = 1.97 $L_{WL}$ | 75 |
| 12/83 | 4 | 2 | 45 | 5.0 | 0.58 | 9.3 = 2.03 $L_{WL}$ | 16 |

cult to control the warm up period and this resulted in greater variation in ice thickness, strength and modulus from target values. This problem can be eliminated by reducing the time required to set the model for testing, which could only improve either by practice or by implementing some design and procedural changes at a later stage of the program.

As soon as the model was ready to test, the ice decay process was allowed to continue and the elastic modulus test described in Appendix E was performed. When the average ice strength reached approximately 25 kPa, the ice resistance test was performed. Immediately following the ice resistance tests, a minimum of eight flexural strength measurements were taken for each of the two resistance tests. These flexural strength measurements were taken to coincide with approximately the beginning and end of each run as well as both sides of the channel. These measurements were taken as close as possible to the broken channel edge and averaged for each resistance test. The average strength was then multiplied by the modulus ratio to estimate the elastic modulus of the ice for that specific test.

Following the flexural strength test, the ice thickness and channel width profile were measured at one metre intervals along the length of the basin. These values were then averaged to give the mean thickness and channel width for each test.

During the resistance tests, a total of twenty-five transducers were monitored and recorded as described in Section 3.7. The signals from these transducers were later digitized and processed to give the mean and other relevant statistics for each of the twenty-five transducers.

### 5.3.2 Test Results

While details of the test results are given in Appendix F, a summary sheet for each test has been prepared. These summary sheets are given in Tables 5.2 through 5.9. Each sheet contains summaries of ice data and measurements obtained during the tests being:

- Segment loads [19 load cells]
- Total Resistance
- Surge Acceleration
- Pitch and Roll
- Position and speed of the model

For all measurements the mean, standard deviation, maximum and minimum values obtained during the test interval are provided.

## TABLE 5.2

## ICE TEST SUMMARY SHEET

ICE SHEET NO. 1
RUN NO. 1
TEST DATE: JUL-18-83
DIGITIZING DATE:AUG-18,22,23-83

| | MEAN | STANDARD DEVIATION | MAXIMUM VALUE | MINIMUM VALUE |
|---|---|---|---|---|
| ICE: | | | | |
| THICKNESS (mm) | 23.50 | 2.60 | 27.50 | 19.20 |
| STRENGTH (kPa) | 22.07 | 4.33 | 28.50 | 15.20 |
| MODULUS (MPa) | 24.13 | - | - | - |
| CHANNEL WIDTH (m) | 1.06 | 0.04 | 1.11 | 1.02 |
| $R_{11}$ (N) | -0.11 | 0.39 | 1.12 | -1.31 |
| $H_{11}$ (N) | 0.03 | 0.05 | 0.17 | -0.03 |
| $H_{12}$ (N) | 0.01 | 0.02 | 0.09 | -0.08 |
| $V_{11}$ (N) | -0.77 | 1.30 | 2.21 | -5.41 |
| $V_{12}$ (N) | 0.13 | 1.84 | 5.06 | -7.66 |
| $R_{21}$ (N) | 0.01 | 0.05 | 0.27 | -0.12 |
| $H_{21}$ (N) | -1.53 | 1.39 | 0.90 | -7.06 |
| $H_{22}$ (N) | -3.51 | 2.57 | 0.91 | -13.16 |
| $V_{21}$ (N) | -0.24 | 0.34 | 0.67 | -1.53 |
| $V_{22}$ (N) | -1.65 | 1.47 | 1.66 | -7.69 |
| $V_{23}$ (N) | -0.94 | 1.53 | 1.95 | -6.22 |
| $V_{24}$ (N) | 1.07 | 0.45 | 2.52 | 0.08 |
| $R_{31}$ (N) | -4.90 | 2.43 | -1.35 | -14.53 |
| $H_{31}$ (N) | -6.02 | 3.31 | -1.36 | -18.77 |
| $H_{32}$ (N) | -9.86 | 9.37 | -0.50 | -47.54 |
| $V_{31}$ (N) | 4.25 | 1.74 | 9.79 | 1.53 |
| $V_{32}$ (N) | -1.06 | 1.52 | 2.78 | -6.22 |
| $V_{33}$ (N) | 0.43 | 1.11 | 2.68 | -2.03 |
| $V_{34}$ (N) | 0.01 | 0.01 | 0.04 | -0.03 |
| RESISTANCE (N) | -20.82 | 18.38 | 37.27 | -78.02 |
| SURGE ACCL (mm/sec$^2$) | 1.37 | 2.01 | 7.04 | -5.41 |
| PITCH (DEGREES) | -0.03 | 0.03 | 0.04 | -0.10 |
| ROLL (DEGREES) | 0.09 | 0.28 | 0.77 | -0.86 |
| POSITION (m) | 18.58 | 1.94 | 21.90 | 15.19 |
| SPEED (m/sec) | 0.14 | 0.00 | 0.15 | 0.12 |

TABLE 5.3

ICE TEST SUMMARY SHEET

ICE SHEET NO. 1
RUN NO. 2
TEST DATE: JUL-18-83
DIGITIZING DATE:AUG-18,23-83

| | MEAN | STANDARD DEVIATION | MAXIMUM VALUE | MINIMUM VALUE |
|---|---|---|---|---|
| ICE: | | | | |
| THICKNESS (mm) | 24.59 | 1.28 | 27.00 | 23.00 |
| STRENGTH (kPa) | 18.80 | 5.85 | 28.50 | 12.50 |
| MODULUS (MPa) | 20.55 | - | - | - |
| CHANNEL WIDTH (m) | 1.04 | 0.04 | 1.09 | 1.00 |
| $R_{11}$ (N) | 0.05 | 0.33 | 1.15 | -0.72 |
| $H_{11}$ (N) | 0.02 | 0.05 | 0.25 | -0.05 |
| $H_{12}$ (N) | 0.00 | 0.02 | 0.09 | -0.08 |
| $V_{11}$ (N) | -0.97 | 1.35 | 1.63 | -4.94 |
| $V_{12}$ (N) | 0.24 | 1.39 | 3.16 | -3.69 |
| $R_{21}$ (N) | -0.10 | 0.10 | 0.48 | -0.30 |
| $H_{21}$ (N) | -1.74 | 1.22 | 0.80 | -5.26 |
| $H_{22}$ (N) | -3.94 | 2.43 | -0.15 | -10.69 |
| $V_{21}$ (N) | -0.20 | 0.31 | 0.62 | -1.17 |
| $V_{22}$ (N) | -1.67 | 1.46 | 1.39 | -6.20 |
| $V_{23}$ (N) | -1.22 | 1.57 | 1.69 | -5.47 |
| $V_{24}$ (N) | 0.99 | 0.47 | 2.21 | 0.06 |
| $R_{31}$ (N) | -5.96 | 2.07 | -2.08 | -12.61 |
| $H_{31}$ (N) | -6.15 | 3.36 | -0.34 | -18.86 |
| $H_{32}$ (N) | -12.95 | 10.08 | 0.80 | -47.85 |
| $V_{31}$ (N) | 5.25 | 1.44 | 9.33 | 2.07 |
| $V_{32}$ (N) | -1.10 | 1.61 | 3.69 | -5.11 |
| $V_{33}$ (N) | 0.22 | 2.13 | 5.48 | -4.30 |
| $V_{34}$ (N) | -0.01 | 0.01 | 0.03 | -0.04 |
| RESISTANCE (N) | -24.79 | 19.74 | 42.73 | -83.43 |
| SURGE ACCL ($mm/sec^2$) | 1.58 | 2.19 | 8.80 | -5.61 |
| PITCH (DEGREES) | -0.02 | 0.08 | 0.30 | -0.38 |
| ROLL (DEGREES) | -0.06 | 0.59 | 1.14 | -1.64 |
| POSITION (m) | 8.26 | 2.03 | 11.75 | 4.73 |
| SPEED (m/sec) | 0.21 | 0.01 | 0.22 | 0.20 |

## TABLE 5.4

## ICE TEST SUMMARY SHEET

ICE SHEET NO. 2
RUN NO. 1
TEST DATE: JUL-19-83
DIGITIZING DATE:AUG-18,23-83

| | MEAN | STANDARD DEVIATION | MAXIMUM VALUE | MINIMUM VALUE |
|---|---|---|---|---|
| ICE: | | | | |
| THICKNESS (mm) | 22.74 | 2.04 | 26.00 | 19.80 |
| STRENGTH (kPa) | 24.19 | 3.30 | 29.60 | 18.50 |
| MODULUS (MPa) | 25.02 | - | - | - |
| CHANNEL WIDTH (m) | 1.12 | 0.13 | 1.38 | 1.02 |
| $R_{11}$ (N) | -7.98 | 3.05 | -4.17 | -16.15 |
| $H_{11}$ (N) | 0.05 | 0.17 | 0.89 | -0.21 |
| $H_{12}$ (N) | 0.07 | 0.03 | 0.16 | -0.01 |
| $V_{11}$ (N) | -3.93 | 2.83 | 3.08 | -10.36 |
| $V_{12}$ (N) | -3.31 | 1.57 | -0.35 | -7.02 |
| $R_{21}$ (N) | -1.78 | 0.79 | -0.26 | -3.42 |
| $H_{21}$ (N) | 0.05 | 0.10 | 0.35 | -0.17 |
| $H_{22}$ (N) | -4.70 | 2.06 | -1.86 | -9.29 |
| $V_{21}$ (N) | 0.15 | 0.32 | 0.84 | -0.71 |
| $V_{22}$ (N) | -2.59 | 1.69 | 0.28 | -8.01 |
| $V_{23}$ (N) | -2.04 | 0.67 | -0.77 | -3.43 |
| $V_{24}$ (N) | 1.12 | 0.71 | 2.66 | -0.30 |
| $R_{31}$ (N) | -5.10 | 2.07 | -1.87 | -10.26 |
| $H_{31}$ (N) | -9.00 | 4.26 | -2.72 | -19.72 |
| $H_{32}$ (N) | -6.56 | 5.03 | -0.74 | -20.91 |
| $V_{31}$ (N) | 1.90 | 1.08 | 4.35 | 0.17 |
| $V_{32}$ (N) | -1.97 | 2.53 | 3.58 | -7.82 |
| $V_{33}$ (N) | -2.13 | 2.08 | 3.41 | -7.45 |
| $V_{34}$ (N) | 3.27 | 1.69 | 7.03 | -0.05 |
| RESISTANCE (N) | -31.64 | 20.64 | 9.68 | -78.79 |
| SURGE ACCL (mm/sec$^2$) | 1.58 | 2.20 | 6.55 | -3.22 |
| PITCH (DEGREES) | -0.10 | 0.09 | 0.12 | -0.42 |
| ROLL (DEGREES) | 0.33 | 0.74 | 1.88 | -1.71 |
| POSITION (m) | 19.86 | 1.51 | 22.45 | 17.27 |
| SPEED (m/sec) | 0.33 | 0.01 | 0.34 | 0.31 |

## TABLE 5.5

## ICE TEST SUMMARY SHEET

ICE SHEET NO. 2
RUN NO. 2
TEST DATE: JUL-19-83
DIGITIZING DATE:AUG-22,23-83

| | MEAN | STANDARD DEVIATION | MAXIMUM VALUE | MINIMUM VALUE |
|---|---|---|---|---|
| ICE: | | | | |
| THICKNESS (mm) | 26.74 | 1.60 | 30.30 | 24.30 |
| STRENGTH (kPa) | 30.80 | 7.33 | 43.30 | 22.40 |
| MODULUS (MPa) | 31.86 | - | - | - |
| CHANNEL WIDTH (m) | 1.11 | 0.05 | 1.16 | 1.04 |
| $R_{11}$ (N) | -5.28 | 1.35 | -2.92 | -9.42 |
| $H_{11}$ (N) | 0.00 | 0.04 | 0.07 | -0.03 |
| $H_{12}$ (N) | -7.24 | 2.16 | -2.23 | -10.79 |
| $V_{11}$ (N) | -10.73 | 2.53 | -5.76 | -18.33 |
| $V_{12}$ (N) | -5.33 | 1.99 | -2.23 | -10.98 |
| $R_{21}$ (N) | -3.79 | 0.69 | -2.09 | -5.25 |
| $H_{21}$ (N) | 0.00 | 0.07 | 0.34 | -0.18 |
| $H_{22}$ (N) | -4.68 | 1.71 | -1.11 | -8.34 |
| $V_{21}$ (N) | -0.25 | 0.47 | 0.74 | -1.14 |
| $V_{22}$ (N) | -5.18 | 2.07 | -0.36 | -9.53 |
| $V_{23}$ (N) | -3.15 | 0.90 | -1.00 | -5.03 |
| $V_{24}$ (N) | 1.48 | 0.63 | 2.64 | -0.32 |
| $R_{31}$ (N) | -5.63 | 1.71 | -2.94 | -10.71 |
| $H_{31}$ (N) | -5.96 | 4.24 | 0.24 | -16.96 |
| $H_{32}$ (N) | -4.50 | 4.02 | 0.61 | -15.23 |
| $V_{31}$ (N) | 2.26 | 1.26 | 4.68 | -0.14 |
| $V_{32}$ (N) | -5.60 | 4.40 | 3.73 | -13.06 |
| $V_{33}$ (N) | -5.41 | 5.44 | 3.98 | -14.75 |
| $V_{34}$ (N) | 3.66 | 1.60 | 6.65 | 0.10 |
| RESISTANCE (N) | -44.52 | 19.18 | -1.35 | -94.16 |
| SURGE ACCL (mm/sec$^2$) | 1.19 | 2.09 | 4.96 | -5.30 |
| PITCH (DEGREES) | -0.15 | 0.10 | 0.16 | -0.44 |
| ROLL (DEGREES) | 1.94 | 2.01 | 5.83 | -0.95 |
| POSITION (m) | 10.34 | 1.75 | 13.37 | 7.35 |
| SPEED (m/sec) | 0.58 | 0.01 | 0.59 | 0.54 |

## TABLE 5.6

## ICE TEST SUMMARY SHEET

ICE SHEET NO. 3
RUN NO. 1
TEST DATE: AUG-09-83
DIGITIZING DATE:AUG-10,23-83

| | MEAN | STANDARD DEVIATION | MAXIMUM VALUE | MINIMUM VALUE |
|---|---|---|---|---|
| ICE: | | | | |
| THICKNESS (mm) | 24.66 | 2.11 | 27.80 | 22.00 |
| STRENGTH (kPa) | 34.50 | 10.32 | 60.60 | 24.90 |
| MODULUS (MPa) | 16.40 | - | - | - |
| CHANNEL WIDTH (m) | 1.13 | 0.07 | 1.24 | 1.04 |
| $R_{11}$ (N) | 1.86 | 0.58 | 2.75 | 0.05 |
| $H_{11}$ (N) | -3.84 | 2.48 | -0.43 | -12.23 |
| $H_{12}$ (N) | -1.17 | 1.73 | 2.87 | -5.09 |
| $V_{11}$ (N) | -1.9 | 1.77 | 0.96 | -7.05 |
| $V_{12}$ (N) | -0.83 | 1.69 | 2.83 | -6.46 |
| $R_{21}$ (N) | -2.33 | 1.02 | -0.40 | -5.28 |
| $H_{21}$ (N) | -30.59 | 1.48 | -27.20 | -33.57 |
| $H_{22}$ (N) | -5.89 | 4.62 | 0.37 | -21.22 |
| $V_{21}$ (N) | 0.53 | 0.39 | 1.82 | -0.17 |
| $V_{22}$ (N) | -1.90 | 2.32 | 1.75 | -9.42 |
| $V_{23}$ (N) | -1.61 | 2.39 | 2.54 | -9.94 |
| $V_{24}$ (N) | 0.00 | 0.02 | 0.01 | -0.02 |
| $R_{31}$ (N) | -3.20 | 2.38 | -0.27 | -10.26 |
| $H_{31}$ (N) | -0.16 | 2.07 | 4.23 | -6.25 |
| $H_{32}$ (N) | -9.97 | 10.99 | 2.67 | -43.86 |
| $V_{31}$ (N) | 1.96 | 1.50 | 6.05 | -0.58 |
| $V_{32}$ (N) | -0.87 | 2.86 | 3.48 | -9.70 |
| $V_{33}$ (N) | 0.01 | 0.02 | 0.05 | -0.03 |
| $V_{34}$ (N) | 3.62 | 1.40 | 7.09 | 0.67 |
| RESISTANCE (N) | -26.52 | 19.85 | 23.63 | -80.78 |
| SURGE ACCL (mm/sec$^2$) | 1.79 | 2.27 | 7.83 | -3.89 |
| PITCH (DEGREES) | -0.15 | 0.08 | 0.22 | -0.33 |
| ROLL (DEGREES) | -0.19 | 0.75 | 1.28 | -1.99 |
| POSITION (m) | 20.63 | 1.10 | 22.55 | 18.72 |
| SPEED (m/sec) | 0.15 | 0.00 | 0.16 | 0.14 |

## TABLE 5.7

## ICE TEST SUMMARY SHEET

ICE SHEET NO. 3
RUN NO. 2
TEST DATE: AUG-09-83
DIGITIZING DATE:AUG-23,25-83

| | MEAN | STANDARD DEVIATION | MAXIMUM VALUE | MINIMUM VALUE |
|---|---|---|---|---|
| ICE: | | | | |
| THICKNESS (mm) | 24.95 | 1.81 | 28.50 | 22.30 |
| STRENGTH (kPa) | 31.91 | 5.18 | 42.60 | 25.60 |
| MODULUS (MPa) | 15.14 | - | - | - |
| CHANNEL WIDTH (m) | 1.06 | 0.03 | 1.10 | 1.02 |
| $R_{11}$ (N) | -0.80 | 0.52 | 0.22 | -2.18 |
| $H_{11}$ (N) | -7.24 | 2.25 | -2.47 | -12.04 |
| $H_{12}$ (N) | -0.90 | 1.09 | 1.67 | -3.63 |
| $V_{11}$ (N) | -5.82 | 1.48 | -2.64 | -9.31 |
| $V_{12}$ (N) | -1.61 | 1.00 | 0.84 | -3.40 |
| $R_{21}$ (N) | -5.36 | 0.91 | -3.45 | -7.38 |
| $H_{21}$ (N) | -16.54 | 0.46 | -15.72 | -17.43 |
| $H_{22}$ (N) | -8.69 | 2.43 | -2.23 | -13.98 |
| $V_{21}$ (N) | 0.26 | 0.23 | 0.77 | -0.29 |
| $V_{22}$ (N) | -5.47 | 2.18 | -1.16 | -10.21 |
| $V_{23}$ (N) | -2.76 | 1.48 | 0.83 | -6.15 |
| $V_{24}$ (N) | 0.00 | 0.01 | 0.04 | 0.00 |
| $R_{31}$ (N) | -4.36 | 1.83 | -1.83 | -8.67 |
| $H_{31}$ (N) | -0.63 | 1.36 | 2.35 | -4.67 |
| $H_{32}$ (N) | -12.13 | 9.08 | 1.24 | -33.42 |
| $V_{31}$ (N) | 2.88 | 1.16 | 6.66 | 0.75 |
| $V_{32}$ (N) | 0.47 | 2.32 | 4.15 | -7.73 |
| $V_{33}$ (N) | 0.00 | 0.02 | 0.03 | -0.04 |
| $V_{34}$ (N) | 4.72 | 0.81 | 7.20 | 3.40 |
| RESISTANCE (N) | -41.04 | 26.18 | 12.66 | -89.58 |
| SURGE ACCL (mm/sec$^2$) | 1.95 | 2.59 | 7.28 | -3.22 |
| PITCH DEGREES | -0.19 | 0.18 | 0.34 | -0.43 |
| ROLL (DEGREES) | -0.50 | 0.95 | 0.98 | -2.28 |
| POSITION (m) | 12.04 | 1.97 | 15.45 | 8.68 |
| SPEED (m/sec) | 0.59 | 0.01 | 0.61 | 0.56 |

## TABLE 5.8

## ICE TEST SUMMARY SHEET

ICE SHEET NO. 4
RUN NO. 1
TEST DATE: AUG-12-83
DIGITIZING DATE:AUG-15,16,25-83

| | MEAN | STANDARD DEVIATION | MAXIMUM VALUE | MINIMUM VALUE |
|---|---|---|---|---|
| ICE: | | | | |
| THICKNESS (mm) | 43.66 | 2.08 | 50.00 | 40.80 |
| STRENGTH (kPa) | 19.83 | 3.40 | 25.60 | 15.80 |
| MODULUS (MPa) | 16.89 | - | - | - |
| CHANNEL WIDTH (m) | 1.21 | 0.09 | 1.40 | 1.14 |
| $R_{11}$ (N) | 0.00 | 0.01 | 0.04 | -0.03 |
| $H_{11}$ (N) | -17.29 | 10.38 | -1.58 | -46.92 |
| $H_{12}$ (N) | -4.47 | 4.18 | 3.18 | -16.08 |
| $V_{11}$ (N) | -7.47 | 7.16 | 4.17 | -25.27 |
| $V_{12}$ (N) | -0.01 | 0.34 | 1.07 | -3.62 |
| $R_{21}$ (N) | -3.92 | 3.02 | 0.36 | -13.82 |
| $H_{21}$ (N) | -1.58 | 4.41 | 7.19 | -17.91 |
| $H_{22}$ (N) | -9.42 | 13.01 | 4.76 | -70.66 |
| $V_{21}$ (N) | 0.47 | 1.10 | 5.05 | -2.61 |
| $V_{22}$ (N) | -2.15 | 6.30 | 6.94 | -26.55 |
| $V_{23}$ (N) | -2.02 | 6.16 | 6.12 | -31.15 |
| $V_{24}$ (N) | 1.09 | 2.07 | 9.59 | -5.28 |
| $R_{31}$ (N) | -3.33 | 2.45 | -0.38 | -17.36 |
| $H_{31}$ (N) | -4.62 | 7.07 | 3.44 | -47.85 |
| $H_{32}$ (N) | -8.09 | 9.97 | 1.07 | -62.16 |
| $V_{31}$ (N) | 2.16 | 1.83 | 9.26 | -3.91 |
| $V_{32}$ (N) | 2.24 | 8.84 | 20.95 | -28.39 |
| $V_{33}$ (N) | 3.16 | 6.30 | 12.06 | -13.77 |
| $V_{34}$ (N) | 7.31 | 3.99 | 17.87 | -0.68 |
| RESISTANCE (N) | -55.41 | 26.68 | 28.34 | -136.98 |
| SURGE ACCL (mm/sec$^2$) | 4.50 | 2.65 | 14.02 | -4.53 |
| PITCH (DEGREES) | -0.12 | 0.12 | 0.22 | -0.64 |
| ROLL (DEGREES) | -0.95 | 2.09 | 3.23 | -4.85 |
| POSITION (m) | 19.46 | 1.94 | 22.80 | 16.08 |
| SPEED (m/sec) | 0.15 | 0.00 | 0.16 | 0.13 |

## TABLE 5.9

## ICE TEST SUMMARY SHEET

ICE SHEET NO. 4
RUN NO. 2
TEST DATE: AUG-12-83
DIGITIZING DATE:AUG-17,25-83

| | MEAN | STANDARD DEVIATION | MAXIMUM VALUE | MINIMUM VALUE |
|---|---|---|---|---|
| ICE: | | | | |
| THICKNESS (mm) | 43.80 | 1.83 | 48.30 | 41.90 |
| STRENGTH (kPa) | 21.79 | 4.71 | 28.20 | 14.20 |
| MODULUS (MPa) | 18.55 | - | - | - |
| CHANNEL WIDTH (m) | 1.21 | 0.14 | 1.43 | 1.03 |
| $R_{11}$ (N) | 0.01 | 0.02 | 0.05 | -0.05 |
| $H_{11}$ (N) | -11.44 | 7.51 | 5.07 | -38.33 |
| $H_{12}$ (N) | -1.37 | 2.39 | 4.22 | -6.65 |
| $V_{11}$ (N) | -12.37 | 6.13 | -1.00 | -31.77 |
| $V_{12}$ (N) | 7.08 | 1.77 | 9.93 | 2.08 |
| $R_{21}$ (N) | -10.51 | 2.14 | -5.44 | -15.37 |
| $H_{21}$ (N) | -7.79 | 2.30 | -1.56 | -13.97 |
| $H_{22}$ (N) | -20.47 | 6.18 | -6.96 | -34.33 |
| $V_{21}$ (N) | 0.86 | 0.93 | 2.38 | -2.69 |
| $V_{22}$ (N) | -4.49 | 3.53 | 4.03 | -10.61 |
| $V_{23}$ (N) | -2.94 | 3.43 | 5.46 | -10.51 |
| $V_{24}$ (N) | 2.39 | 1.17 | 5.94 | -0.13 |
| $R_{31}$ (N) | -6.96 | 6.00 | 2.48 | -21.46 |
| $H_{31}$ (N) | -8.08 | 12.80 | 22.92 | -44.65 |
| $H_{32}$ (N) | -29.70 | 16.23 | -5.13 | -70.39 |
| $V_{31}$ (N) | -10.34 | 17.49 | 9.47 | -54.20 |
| $V_{32}$ (N) | 20.08 | 11.70 | 40.44 | -4.24 |
| $V_{33}$ (N) | 9.56 | 1.10 | 10.88 | 4.57 |
| $V_{34}$ (N) | 22.66 | 1.49 | 24.28 | 19.23 |
| RESISTANCE (N) | -69.40 | 50.45 | 35.13 | -166.45 |
| SURGE ACCL (mm/sec$^2$) | 4.91 | 4.85 | 16.27 | -5.21 |
| PITCH (DEGREES) | -0.26 | 0.27 | 0.67 | -0.98 |
| ROLL (DEGREES) | -4.71 | 4.78 | 1.52 | -15.30 |
| POSITION (m) | 9.49 | 2.19 | 13.25 | 5.69 |
| SPEED (m/sec) | 0.59 | 0.01 | 0.60 | 0.56 |

# 6.

# ANALYSIS AND DISCUSSION

# 6. ANALYSIS AND DISCUSSION

## 6.1 Validation of Model Resistance

The first step in the analysis conducted was to validate the present experimental results. That is to verify whether the segmentation of the model had any effect on its total resistance. This was accomplished by comparing the present set of data with previous data obtained using other models of the CCGS PIERRE RADISSON.

However, each time the CCGS PIERRE RADISSON was tested there were different objectives and therefore no common set of testing conditions existed. For example, during the present program there was concern about damaging the sensitive segment load cells, thus the model velocity and ice thickness were kept low. Of the previous three model test programs using the twentieth scale model, there was a total of 131 data points. Of these 131 data points, there were six points within the thickness and strength range that coincides with the present tests performed at a thickness of about 25mm. Of these six data points, there were two points within the velocity test range used during this program and another two within ten percent of the velocity test range. Comparing model conditions such as hull friction and ballast draft, there were no two sets of data using the same conditions. Therefore, no direct comparison can be made and indirect comparison with fitted data was possible.

First, the present resistance data points were regressed into a well known model ice resistance equation. This equation was selected because of insufficient data points to determine the 'best fit' relationship. The resulting equation from the regression analysis is given below.

$$R = 8.55 + 840vh + 989\,\sigma_f h^2 \qquad (6.1)$$

Figure 6.1 is a plot of measured resistance versus values predicted by equation (6.1). The figure shows reasonable scatter about the prediction line.

Regression analysis was also performed on each of the three data sets for the 20th scale model tests of the PIERRE RADISSON. The results are illustrated in Figure 6.2 in comparison with the present data for two ice thicknesses and a single ice strength. Although the variation in slope is evident among the four sets of data, the order of magnitudes are comparable and the cross over points indicate the resemblance of the models. The differences, however, can be explained by the differences in test drafts and friction factors. Some of the differences also arise from the extrapolation of other data sets to the range of the present results.

FIGURE 6.1 MEASURED VS PREDICTED MODEL RESISTANCE

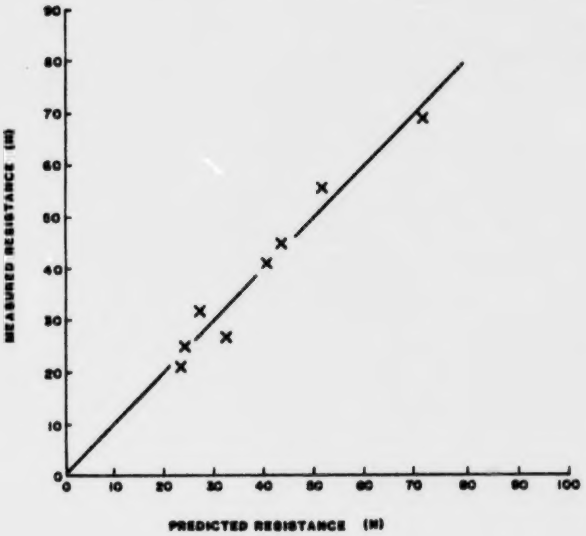

FIGURE 6.2 DIMENSIONAL RESISTANCE COMPARISON

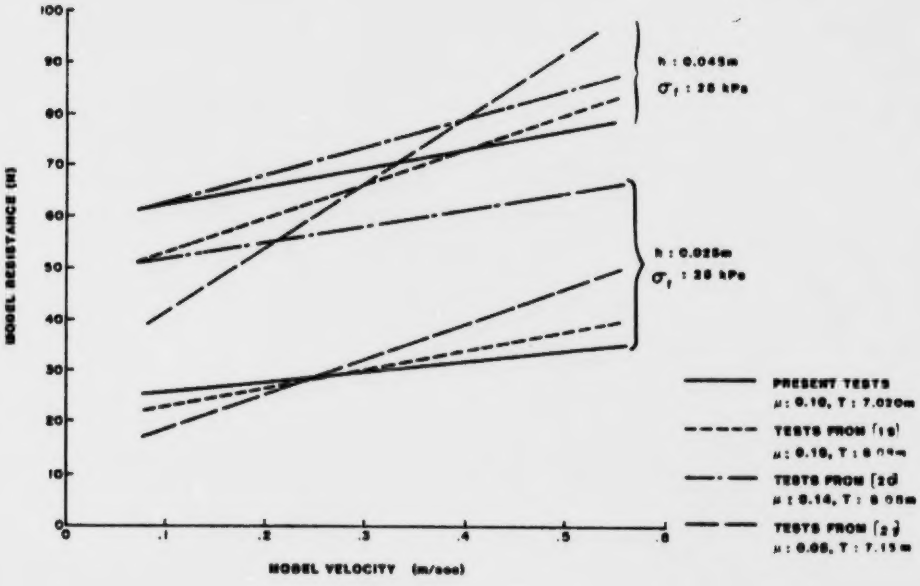

To partially eliminate the discrepancy due to the differences in model test range, nondimensional analysis was performed. The nondimensional form of the four prime variables of thickness, strength, velocity and resistance was:

Nondimensional Resistance $R/\rho_g Bh^2$ (6.2)

Nondimensional Stength $\sigma_f/\rho_{gh}$ (6.3)

Nondimensional Velocity $v/\sqrt{gh}$ (6.4)

Regressing the present model test series using the above three combinations produced:

$$R/\rho_g Bh^2 = 1.304 + 2.291\, v/\sqrt{gh} + 0.0227\sigma_f/_g h \quad (6.5)$$

If a resistance correction term is now introduced to normalize the effect of ice strength to 25 kPa:

$$(R/\rho_g Bh^2)' = R/\rho_g Bh^2 - \frac{0.0227}{\rho_{gh}} (\sigma_f - 25000) \quad (6.6)$$

where $(R/\rho_g Bh^2)'$ is the nondimensional resistance for a base strength value of 25 kPa

Regressing the normalized nondimensional resistance term versus the nondimensional velocity produces:

$$(R/\rho_g bh^2)' = 3.390 + 2.321\, v/\sqrt{gh} \quad (6.7)$$

Figure 6.3 shows the quality of fit of the above equation to the measured results.

FIGURE 6.3 MEASURED VS PREDICTED NONDIMENSIONAL RESISTANCE

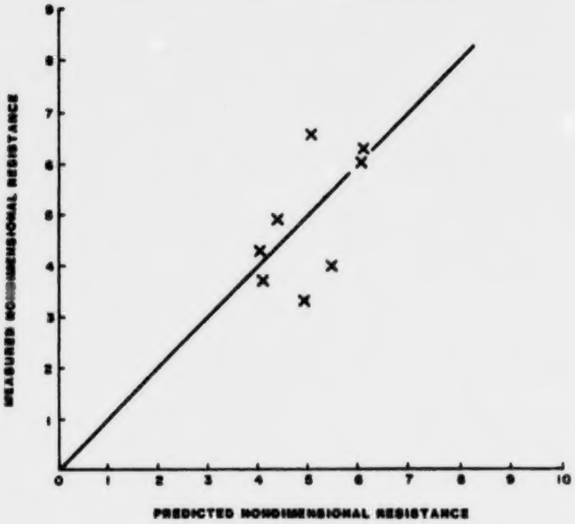

FIGURE 6.4 NONDIMENSIONAL RESISTANCE COMPARISON

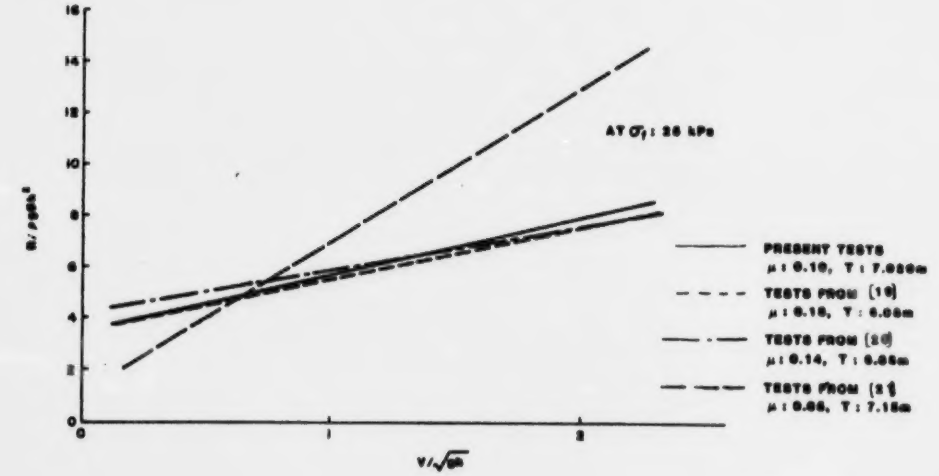

Despite the increased scatter in the predictions of ice resistance over the experimental range in non-dimensional form, the resulting equation (6.7) appeared to provide better correlation with previous test results as illustrated in Figure 6.4. The only data set which is obviously out of the range is the one for the deepest draft. Close examination of this particular data set revealed that the velocities considered were in a higher range, this combined with the low friction factor may have resulted in a bias in the slope when extrapolated to the lower speed range and higher friction.

In conclusion, it may be stated that in all likelihood the segmentation of the model of the CCGS PIERRE RADISSON did not appear to produce significant differences in the measured total resistance of the model. Therefore, the breakdown of the components of the resistance by segments may be generalized since the segmentation results in neither augmentation nor reduction of the total ice resistance.

## 6.2 Assessment of Transducer Response

Table 6.1 provides an overall assessment of the transducers' responses during the entire resistance testing program. The rating of the signal was based on five categories:

- = No signal which would occur for a number of reasons including lack of contact, insufficient preload or others. The quality points assigned to this category were nil. Most occurrences of this category were observed in segment #1 and least occurrences in segment No. 3.

P = Poor signal in which a zero offset in excess of 3% of the load cell rating was observed after the test. It was verified by examination of the load cells that the offset did not mean load cell plasticity but rather readjustment of the segments and preload wires after the load had been applied and removed. It is possible that the offset could be caused by friction between the segments and the main hull or a small misalignment of the load cell seats. The quality point assigned to this category was 1 point. The occurrences of poor signals were recorded three times in segment 1 for signal $R_{11}$ and once in segment 2 and four times in segment 3 only during the last test.

F = Fair signal in which a zero offset less than 3% but greater than 1.5% of the rated load cell capacity remained after the test. The quality points assigned to this category were 2 points. More frequent occurrences than the poor category were observed.

G = Good signal in which the zero offset did not exceed 1.5% of rated cell capacity. The quality points assigned were 3 points. Most of the data can be categorized here.

## TABLE 6.1

## QUALITY OF TRANSDUCER RESPONSE

| | | Test - Run Number | | | | | | | | Percent of Time in Operation & Quality | | Overall Segment Operation and Quality Points | | | |
|---|---|---|---|---|---|---|---|---|---|---|---|---|---|---|---|
| | | 1-1 | 1-2 | 2-1 | 2-2 | 3-1 | 3-2 | 4-1 | 4-2 | | | 1-1<br>1-2 | 2-1<br>2-2 | 3-1<br>3-2 | 4-1<br>4-2 |
| SEGMENT #1 | $R_{11}$ | G | G | P | F | P | P | - | - | 75%, | 1.4 | 60% | 70% | 100% | 70% |
| | $H_{11}$ | - | - | - | - | G | G | F | F | 50%, | 1.3 | | | | |
| | $H_{12}$ | - | - | - | G | E | F | G | G | 63%, | 1.9 | Overall: 75% | | | |
| | $V_{11}$ | G | G | G | G | E | G | G | F | 100%, | 3.0 | 1.8 | 1.8 | 2.7 | 1.7 |
| | $V_{12}$ | G | G | G | G | G | G | - | F | 88%, | 2.5 | Quality Points: 8.0 | | | |
| SEGMENT #2 | $R_{21}$ | - | - | G | G | E | G | G | G | 75%, | 2.4 | 86% | 86% | 71% | 100% |
| | $H_{21}$ | E | E | - | - | - | - | G | G | 50%, | 1.8 | | | | |
| | $H_{22}$ | E | E | P | F | G | E | G | G | 100%, | 3.0 | Overall: 86% | | | |
| | $V_{21}$ | G | G | G | G | E | E | G | G | 100%, | 3.3 | | | | |
| | $V_{22}$ | G | G | G | G | E | G | G | G | 100%, | 3.1 | 2.9 | 2.4 | 2.6 | 3.0 |
| | $V_{23}$ | G | G | G | G | E | E | G | G | 100%, | 3.3 | | | | |
| | $V_{24}$ | G | G | G | G | - | - | G | G | 75%, | 2.3 | Quality Points: 10.9 | | | |
| SEGMENT #3 | $R_{31}$ | G | G | G | G | G | G | G | P | 100%, | 2.8 | 86% | 100% | 86% | 100% |
| | $H_{31}$ | F | G | F | F | G | G | G | P | 100%, | 2.4 | | | | |
| | $H_{32}$ | G | E | F | F | G | G | G | P | 100%, | 2.8 | Overall: 93% | | | |
| | $V_{31}$ | G | E | G | G | G | G | G | G | 100%, | 3.1 | | | | |
| | $V_{32}$ | G | G | G | G | G | G | F | F | 100%, | 2.8 | 2.6 | 2.7 | 2.4 | 2.1 |
| | $V_{33}$ | G | G | G | G | - | - | F | P | 75%, | 1.9 | | | | |
| | $V_{34}$ | - | - | G | G | F | F | F | P | 75%, | 1.6 | Quality Points: 9.9 | | | |

Key: - = No signal
P = Poor signal, zero offset > 3.0% of Rated Capacity (>3.0 N for 100 N Cell)
F = Fair signal, large offset < 3.0% of Rated Capacity (< 3.0 N for 100 N Cell)
G = Good signal, small offset < 1.5% of Rated Capacity (< 1.5 N for 100 N Cell)
E = Excellent signal, no offset.

E = Excellent signal in which no zero offset was detected. The highest quality value of 4 points was given to this category. Approximately 20% of segment #2 load cells were categorized at this quality, compared to 5% of segment #1 and 4 % for segment #3.

Some general observations can be made based on the results given in Table 6.1. These are:

a) The overall best quality of data can be obtained from measurements on Segment 2.

b) Segments 2 and 3 responded more often than Segment 1.

c) Complete data sets are available as follows:

for Segment 1: Tests 3-1 and 3-2 with quality level: 2.7
for Segment 2: Tests 4-1 and 4-2 with quality level: 3.0
for Segment 3: Tests 2-1 and 2-2 with quality level: 2.7
and Tests 4-1 and 4-2 with quality level: 2.1

d) Therefore, the most suitable data set for complete analysis is that of Segment #2 during Tests 4-1 and 4-2.

e) The average overall quality of the resistance, horizontal and vertical groups of load cells were: 2.2, 2.2, and 2.7, respectively. Segment #2 being above average for resistance and vertical components while Segment #3 above average in resistance and horizontal components and Segment #1 being on or below average in quality.

f) The three components of resistance were obtained simultaneously during the following tests: 2-1, 2-2, 3-1, and 3-2. Therefore resistance breakdown on 3 segments would be feasible for these tests. During the first two tests Segment 2 resistance was absent and during the last two tests Segment 1 resistance was not measurable due to loss of contact in both tests.

## 6.3 Segment Calibration Factors

Based on the results obtained from segment calibrations, as reported in Appendix B, and finite element validation as reported in Appendix G, it was found that the measured responses of the segments do not agree with the calculated responses for a given load. Figure 6.5, reproduced from Appendix B, illustrates this deviation for segment 2. In fact this segment has exhibited the most reasonable response when compared to the other two segments.

The results clearly demonstrate the need for segment calibration or correction factors. These factors will be used to correct the measurements registered by load cells to account for the segment behaviour which results in loss of registration at each load support point. These factors may be considered as segment constants. Nonetheless, they exhibit limited variable dependency on the magnitude and position of applied load. This is particularly true for the resistance load cell which exhibits the largest dependency on position of applied load.

It should be stated that the dry calibration results have been obtained with increased pretension to support the weights of the segments. When free floating, the segments are neutrally buoyant and would require smaller preloads to support it in position. Therefore, the in-water calibration may produce less dependencies as observed here and will probably be better behaved. While this underscores the need for a rigorous in-water calibration of the segments, the present data will be used for the purposes of this analysis with discretion. That is when such corrections may be required.

There are two possible methods for correcting the measurements to account for the segment behaviour:

1. By using average segment correction factors to be obtained from experimental measurements and to be based on average positions of load.

2. By using the measurements to determine the approximate position and magnitude of normal loading on the segment, then using the experimental calibration to determine the corresponding corrections to be applied to the data.

Either method may be used in order to provide reasonable corrections for load cell readings. In case of low scatter of the results, particularly for horizontal and vertical forces the first method may be preferred, while for cases of greater scatter the second method may be applied.

Table 6.2 lists the mean values of the segment calibration factors (MSCF) to be applied according to the first method, along with the standard deviations of load registration ratios. It is felt that if the standard deviation exceeds 10-12% of the mean value it would be more appropriate to use the second method and refer directly to the data given in Appendix B. However, for approximate analysis these values may be used.

From the data presented in this table, it is confirmed that segment 2 is most suited for detailed analysis since the measurements exhibit the least scatter as compared to other segments. The lowest scatter levels in the entire dry calibration testing were observed on segment 2 horizontal and vertical load cells. Of all components, the horizontal component was the best while the worst scatter was associated with the vertical component of segments 1 and 3 and with the resistance component of both segments. This would be expected in segment 3, however, because the hull angles tend to promote the horizontal resolution of applied ice loads with small force components to be expected in vertical or resistance direction. If the scatter band is the same due to similar level of experimental errors, the percentage deviations can be high, as can be verified by calculated values in Table 6.2. The horizontal component of segment 3, as may be expected exhibits the lowest value of standard deviation of all sensors. Therefore, they can be used reliably in determining the position of impact.

The MSCF values listed in Table 6.2 will be used in further analysis unless otherwise indicated. However, since these values were obtained from dry calibration runs, their relationship to in-water calibration cannot be determined on the basis of present information. For the time being, they may be exercised with caution until better segment calibration factors can be determined for a floating model.

TABLE 6.2

LOAD CELL REGISTRATION RATIOS
AND MEAN SEGMENT CORRECTION FACTORS

| FORCE COMPONENT | | SEGMENT 1 | SEGMENT 2 | SEGMENT 3 |
|---|---|---|---|---|
| Resistance (R) | mean | 0.636 | 0.558 | 0.727 |
| | s.d. | 0.531 | 0.208 | 0.612 |
| | s.d.% | 83.5% | 37.2% | 84.2% |
| | MSCF | 1.573 | 1.792 | 1.376 |
| Horizontal (H) | mean | 1.327 | | |
| | s.d. | 0.324 | | |
| | s.d.% | 24.4% | | |
| | MSCF | 0.754 | | |
| Vertical (V) | mean | 0.347 | | |
| | s.d. | 0.659 | | |
| | s.d.% | 189.8% | | |
| | MSCF | 2.880 | | |
| No. of Data Points each set | | 25 | 35 | 40 |

mean = average registration ratio over experimental range
s.d. = standard deviation of above mean
s.d.% = standard deviation expressed as a percentage of mean
MSCF = mean segment correction factor = 1/mean

FIGURE 6.5 DRY CALIBRATIONS of SEGMENT 2

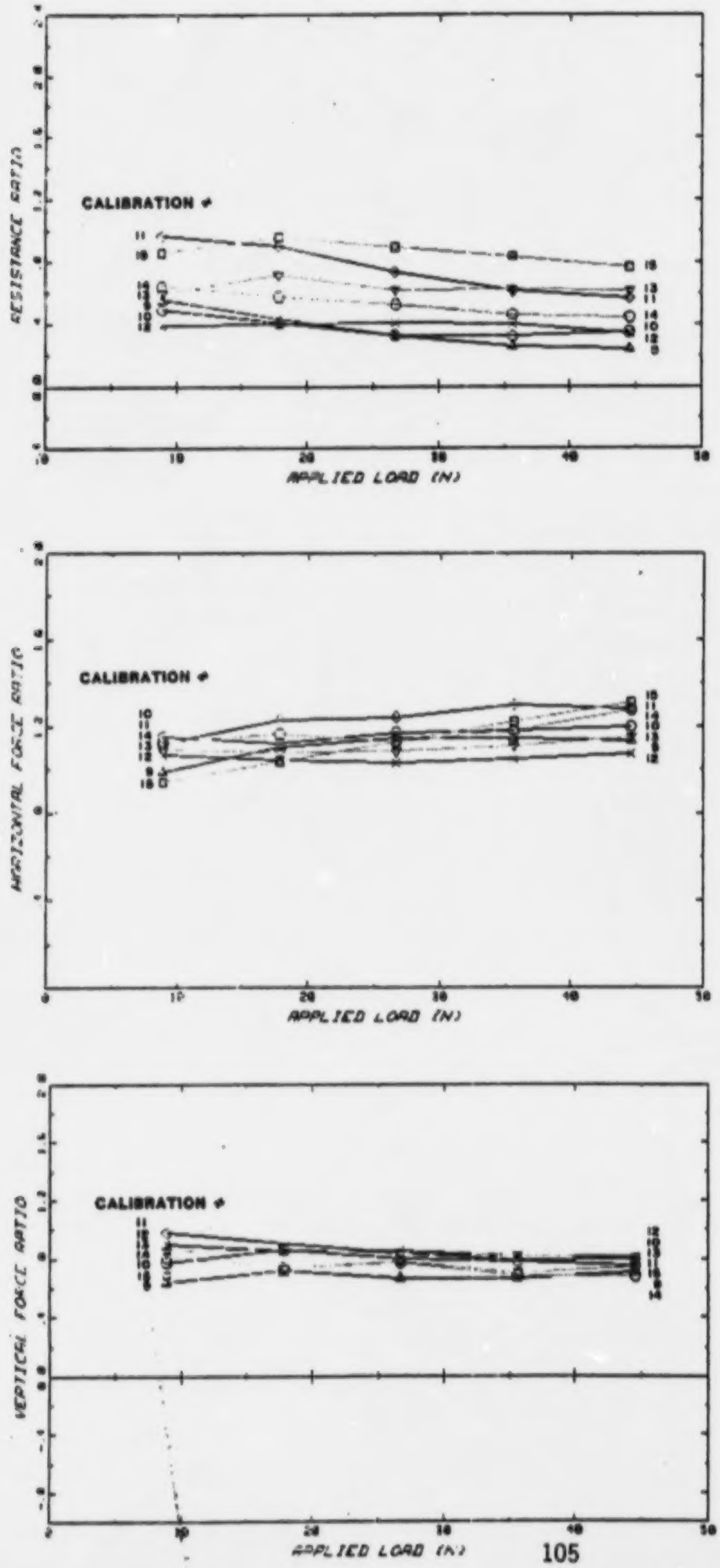

### 6.4 Detailed Analysis of Segment Forces

The last test No.4-2 was used to provide a model analysis of the segment forces for purposes of verifying the analysis procedures and assessing the potential of the present system. Mean values will be used in the following analysis.

#### 6.4.1 Effects of Ship Motions

Using the mean values of all measurements as summarized in Table 5.9, it may be observed that large ship motions persist during the test run. Ship model pitch and roll appear to have high values on the average and high standard deviation. The latter indicates their continuous variability during the test which can primarily be caused by variable characteristics of the ice throughout the run. While variations in strength and thickness are generally within acceptable levels in model testing, their effect on local forces on the hull can be large.

Therefore, the first step in the data analysis would be to eliminate the effect of ship motions on the recorded force components. For this purpose, the calibration results of Appendix C will be used. The calibration data, as summarized in Table C.2 are limited and therefore, they will be used with proper understanding of their limits. Some linear interpolation or extrapolation will have to be applied to estimate the effects of roll and pitch independently from one another. Since heave was not routinely measured during the resistance tests, no correction for heave will be possible.

From the test results, the pitch and roll were -0.26 and -4.71 degrees, respectively, thus indicating bow up in pitch and port up in roll. In order to eliminate these effects we must subtract the contributions of these motions (algebraically) from the measured force components to obtain the actual effect of ice loading. This is done in Table 6.3. The pitch and roll effects were determined by assuming linear dependence on the tangent of pitch or roll angles, respectively. For small angles, this is equivalent to direct proportion with the angles. It is shown that the net load cell responses due to applied loads and after accounting for ship motions effects can be quite different particularly when the effects of motion are pronounced. Now, the net forces can be used in further analysis.

#### 6.4.2 Effects of Pretension Loads

The preloads on the segments were applied such that the load cells were to remain in contact with the segments during interaction. This was obviously not maintained during some of the tests where contact was lost during the run. The solution to this would be to increase the pretension loads and in this case they should be measured. The present design allows for relatively compliant tension wires which may be neglected in the analysis. To demonstrate this, let us consider Segment 2 which has a vertical tension wire approximately at the centre of the four vertical load support points.

## TABLE 6.3

## THE EFFECTS OF SHIP MOTIONS ON MEAN VALUES

| RESISTANCE COMPONENT | MEASURED VALUE, N | PITCH EFFECT N | ROLL EFFECT N | NET FORCE COMPONENT, N |
|---|---|---|---|---|
| $R_{11}$ | 0.01 | -0.073 | +0.064 | 0.019 |
| $H_{11}$ | -11.44 | 0 | -0.255 | -11.185 |
| $H_{12}$ | -1.37 | -0.104 | -0.255 | -1.011 |
| $V_{11}$ | -12.37 | +0.728 | +0.637 | -13.735 |
| $V_{12}$ | 7.08 | +0.312 | +0.892 | 5.876 |
| $R_{21}$ | -10.51 | +0.416 | -0.319 | -10.607 |
| $H_{21}$ | - 7.79 | +0.104 | -0.127 | - 7.767 |
| $H_{22}$ | -20.47 | +0.520 | 0 | -20.990 |
| $V_{21}$ | 0.86 | +0.052 | +1.529 | - 0.721 |
| $V_{22}$ | - 4.49 | +1.560 | +3.695 | - 9.745 |
| $V_{23}$ | - 2.94 | +0.832 | +6.370 | -10.142 |
| $V_{24}$ | 2.39 | +0.042 | -0.051 | + 2.399 |
| $R_{31}$ | - 6.96 | 0 | 0 | - 6.960 |
| $H_{31}$ | - 8.08 | +1.560 | +0.446 | -10.086 |
| $H_{32}$ | -29.70 | +1.248 | -1.274 | -29.674 |
| $V_{31}$ | -10.37 | 0 | +6.370 | -16.740 |
| $V_{32}$ | 20.08 | -1.560 | +11.467 | +10.173 |
| $V_{33}$ | 9.56 | 0 | +16.563 | - 7.003 |
| $V_{34}$ | 22.66 | -1.248 | + 5.733 | +18.175 |

| | | | |
|---|---|---|---|
| pitch | -0.25 | -0.25 | 0 |
| roll | -4.71 | 0 | -4.71 |

The tension wire was a double 1.6 mm diameter wire rope having an elastic modulus of 96.6 GPa, according to Spotts [17] and having a length of 0.2 m. The calculated stiffness of the wire was 0.94 MN/m. for test No. 4-2, this compares to 6.79 MN/m for load cells $V_{21}$ and $V_{24}$ and 18.00 MN/m for $V_{22}$ and $V_{23}$. Considering the measured net forces, the deflections at the load points may be calculated:

$$\Delta Z_{21} = -0.721/6.79 \times 10^6 = -0.106\ \mu m$$

$$\Delta Z_{22} = -9.745/18.00 \times 10^6 = -0.541\ \mu m$$

$$\Delta Z_{23} = -10.142/18.00 \times 10^6 = -0.564\ \mu m$$

$$\Delta Z_{24} = +2.399/6.79 \times 10^6 = +0.353\ \mu m$$

Approximating the deflection of the tension wire by the average obtain a slack of 0.214 $\mu m$ which is equivalent to 0.202 N. This should be used to correct the net vertical load $\Sigma F_Z$ and this correction amounts to about 1% of this force and may be neglected to avoid complication of the analysis. For earlier tests, Series 1 and 2 a flexible rubber line was used to support the segments instead of a steel strand. For the horizontal and resistance components a lower stiffness would apply due to length of wire and its angle of application, which renders the effect of pretension less significant.

In the future, stiffer pretension arrangements may be treated as a load measuring position which necessitates the addition of an extra load cell (or tension bolt) at each pretension position. For the present analysis pretension effects may be considered secondary.

### 6.4.3 Resistance Breakdown

a) The total model resistance in ice as measured by the force block was 69.4N on the average. The responses of resistance components of the three segments were: (see Figure 6.6).

$\bar{R}_{11}$ = no reading

$\bar{R}_{21}$ = 10.607 N

$\bar{R}_{31}$ = 6.960 N

The contributions of segments 2 and 3 to one half of the total resistance are 30.6% and 20.1%; respectively. This reflects a trend of decreasing resistance contribution of the aftmost segments, despite the possibility that the normal force on the hull could have an opposite trend. It should be noted that the effects of roll and pitch on resistance components of force are negligible.

FIGURE 6.6

LOAD DEFINITION OF ICE LOAD CYCLES

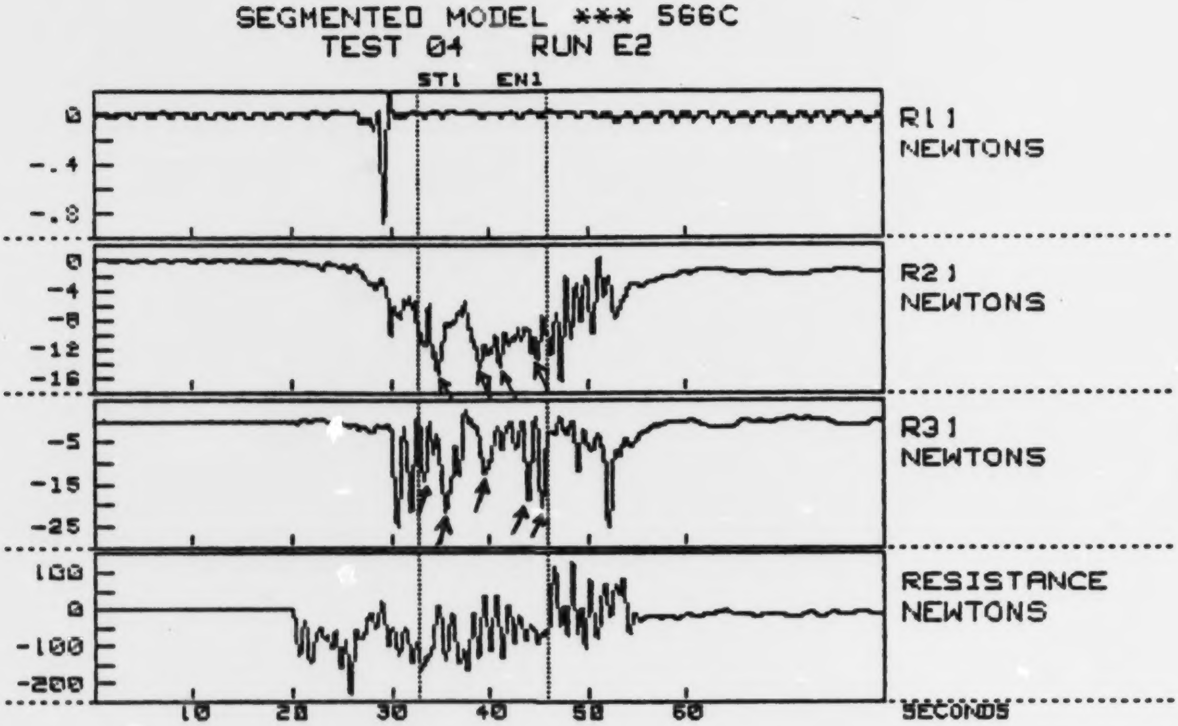

```
DATA DIGITIZED ON:   17 AUG 1983
  DIGITIZING RATE:   32  Hz/CHANNEL
 FILTER FREQUENCY:    1  HZ

                         INTERVAL STATISTICS

INTERVAL 1       START: 32.8125     END: 45.8125

CHANNEL          MINIMUM          MAXIMUM          MEAN VALUE       STAN. DEV.
R11              -.019734          .04591           .013954         .019066
R21              -15.32           -5.385           -10.47           2.14
R31              -21.54            2.52            -6.933           6.02
RESISTANCE       -166.45           35.13           -69.399          50.449
```

P.S. Values listed above do not include roll and pitch adjustments.

b) Examination of the variation of the resistance components during the test, as illustrated in Figure 6.6, shows that:

° On Segment 2 the maximum and minimum values were 15.32 N and 5.39 N implying a variation range of 95% of the mean resistance and approximately ± 50% of the mean resistance. The peak occurrences of segment 2 precede those of segment 3 by 0.7 - 0.8 seconds. At a test speed of 0.587 m/s this means a model advance distance of 0.41 - 0.47 m which, in turn, means that the peak force location moves gradually from segment 2 to segment 3. The peak occurrences correspond to a cusp breaking frequency of 0.31 Hz.

° On segment 3 the peak resistance fluctuates up to a maximum of 21.54 N which is more than 300% of the mean. While five peaks may be identified in the resistance trace, Figure 6.6, only three approach the maximum resistance. This ties in with a lower frequency of cuspbreaking of 0.23 Hz, to indicate that the lower peaks are likely to be associated with turning components. The lower peaks reach only 60 percent or lower values than the maximum resistance associated with the breaking. Also the maximum breaking resistance associated with segment 3 is 41% higher than the corresponding resistance associated with breaking in Segment 2. This corroborates the assumption that the hull flare plays an important role in reducing the resistance contribution of the aft-bow region in particular.

c) The standard deviation of the resistance component may be used to identify the predominant forces associated with icebreaking. For instance, $R_{21}$ exhibits a standard deviation of 20% of the mean compared to 87% for $R_{31}$. This may be interpreted as indication of the dominance of ice cusp bending and breaking occuring on Segment 2. As the cusps break they move aftwards relative to the model and the turning mechanism and associated forces affect segment 3. The higher standard deviation of $R_{31}$ indicates greater variation and more frequent occurrences of lower magnitude ice loads.

This argument is corroborated by the ratios of maximum to mean resistance component - for Segments 2, and 3 being 1.46 and 3.11; respectively.

It should be noted that the trim angle of the model during the test was -0.26 degrees on the average with 100% standard deviation.

### 6.4.4 Analysis of Force Components

The analysis of force components was conducted according to the procedures outlined in Chapter 4 and summarized in Table 4.1. The implications of applying segment calibration factors as discussed in Section 6.3 were considered, and are discussed in Section 6.4.5. In this section only the net force components as measured and corrected were used. The model analysis is performed in detail on segment No. 2.

a) The total components in the x, y and z directions:

$$\Sigma R_{zj} = -10.607 \text{ N}$$

$$\Sigma H_{zj} = -28.757 \text{ N}$$

$$\Sigma V_{zj} = -18.209 \text{ N}$$

b) Using Equation (4.20) the horizontal position of the centre of ice action on the segment is calculated:

$$x' = \frac{7.767 \times 2.005 + 20.990 \times 1.653}{28.757} = 1.748 \text{ m}$$

This position coincides with station #9 and for the 23 foot waterline, its offset $y' = 0.312$ m. Now, Equation (4.19) may be used to get a better convergence to the position:

$$x' = 1.748 - \frac{10.607}{28.757}(0.122 - 0.312) = 1.818 \text{ m}$$

This yields $y' = 0.29$ and the following iteration of $x' = 1.810$ m which is a significantly accurate positioning of the load action location on segment No.2.

c) At this position $x' = 1.81$ m, $y' = 0.29$ m, the hull angles are $\alpha = 24.5°$ and $\beta = 35°$ thus the direction cosines will be given by:

$$(n_1, n_2, n_3) = 0.350, 0.767, 0.537$$

d) Using Equation (4.11) obtain the normal force:

$$F_n = 0.350 \times 10.607 + 0.767 \times 28.757 + 0.537 \times 18.209$$
$$= 35.563 \text{ N}$$

e) The next step determines the friction components:

$$\mu e_1 = \frac{10.607}{35.563} - 0.350 = - 0.051$$

$$- \mu e_2 = \frac{28.757}{35.563} - 0.767 = 0.041$$

$$- \mu e_3 = \frac{18.209}{35.563} - 0.573 = -0.025$$

and the friction factor $\mu = 0.071$ which is reasonably close to the preset friction factor of the model hull. Therefore, the friction force would have the direction cosines:

$$(e_1, e_2, e_3) = - 0.729, -0.583, +0.359$$

This indicates a friction force which is approximately equal to 2.525 N acting in the direction given by $\vec{e}$. While the order of magnitude of friction factor and, thus the friction force component, are correct the direction does not seem to be right. The obvious reason is the sensitivity of the friction components $\mu e_1$, $\mu e_2$, and $\mu e_3$ to errors in the measured force components . It is therefore, possible to improve these estimates by improving the measurement accuracy or exploring the effect of segment calibration factors.

f) A check on the success of the solution may be made by using Equations (4.15) to calculate the moments of external ice loads as discussed previously in Section 4.3.4. This yields for Z' = 0.027 m;

$$C_1 = (-28.757) \times 0.027 - (-18.209) \times 0.29 = +4.504$$

$$C_2 = (-18.209) \times 1.81 - (-10.607) \times 0.027 = -32.672$$

$$C_3 = (-10.607) \times 0.29 - (-28.757) \times 1.81 = +48.974$$

From actual load cell measurements obtain:

$$\begin{aligned} C_1 = {} & (-7.767 \times 0.075) + (-20.99 \times 0.080) - (-0.721 \times 0.04) \\ & - (-9.745 \times 0.179) - (-10.142) \times 0.337) \\ & - (2.399 \times 0.040) = +2.833 \end{aligned}$$

$$\begin{aligned} C_2 = {} & (-0.721 \times 1.875) + (-9.745 \times 2.005) + (-10.142 \times 1.653) \\ & + (2.399 \times 1.795) - (-10.607 \times 0.08) = -32.501 \end{aligned}$$

$$\begin{aligned} C_3 = {} & (-10.607 \times 0.122) - (-7.767 \times 2.055) - (-20.99 \times 2.005) \\ & + 56.836 \end{aligned}$$

The above sets of calculated C-values compare favourably and it may be concluded the position of ice load given by:

$$(x', y', z') = 1.81,\ 0.29,\ 0.027$$

is reasonably accurate. However, in an iterative solution (or graphical solution) a better value could be obtained. When the above values are plotted such as in Figure 4.5 it will be noted that a solution can be obtained which brings closer agreements between the above estimates. Also more accurate measurements of the forces could accurately determine the position of ice load.

### 6.4.5 Application of Segment Calibrations

a) Using the average segment calibration factors of 1.792, 0.880 and 1.280 for resistance, horizontal and vertical force components; these components would become:

$$\Sigma R_{zj} = -19.008 \text{ N}$$

$$\Sigma H_{zj} = -25.306 \text{ N}$$

$$\Sigma V_{zj} = -23.308 \text{ N}$$

b) The implication of these changes on the position of load is the modification of the correction of x' giving

$x' = 1.891$ m , $y' = 0.246$ in the first iteration

$x' = 1.841$ m , $y' = 0.285$ in the second iteration

which is close enough to the position identified in Section 6.4.4.

c) This results in change of the hull angles to:

$$\alpha = 25.3°, \quad \beta = 36.7°$$

and the direction cosines become:

$$(n_1\ ,\ n_2\ ,\ n_3) = (0.354,\ 0.750,\ 0.559)$$

which represents a minor change from previous analysis.

d) The normal force becomes $F_n = 38.734$ N which is about 9% greater than previous analysis.

e) The coefficients of the friction component become

$$(\mu e_1, \mu e_2, \mu e_3) = 0.136, + 0.096, -0.043$$

thus yielding a friction factor $\mu = 0.172$ and direction cosines for the friction force of:

$$(e_1, e_2, e_3) = +0.791, +0.559, -0.249)$$

Comparing the results, the effect of applying the full value of segment calibration factors may be summarized in Table 6.4. The table also illustrates the effect of applying 50% of the correction due to MSCF. It may be observed that there is complete reversal in the direction of friction when the full MSCF is applied. This reversal occurs in the right direction although it is obvious that it overshoots in the other direction. The friction force here tends to indicate a falling bow (vertical components acts upwards).

The expected answer for the direction of friction is three positive values for $e_1$, $e_2$ and $e_3$. These values may range between two most likely limits:

- ° The first is determined by assuming the friction force to act in the waterplane, i.e. for the present case the values would be (0.85, 0, 0.52).

- ° The second limit is determined by assuming the friction force to act along buttocks, which gives the e-values: (0.91, 0.42, 0).

Therefore, reasonable estimates of the friction unit vector components would be:

$e_1 = 0.85 \rightarrow 0.91$

$e_2 = 0 \rightarrow 0.42$

$e_3 = 0 \rightarrow 0.52$

Going in a reverse procedure the ratio of force components to normal force may be calculated as follows, for a friction factor of 0.1, and compared to actual mesurements:

$$\frac{\Sigma R}{F_n} = 0.439 \rightarrow 0.441 \text{ (compare to 0.298)}$$

$$\frac{\Sigma H}{F_n} = 0.767 \rightarrow 0.809 \text{ (compare to 0.809)}$$

$$\frac{\Sigma V}{F_n} = 0.537 \rightarrow 0.589 \text{ (compare to 0.512)}$$

## TABLE 6.4

## COMPARISON OF RESULTS

| VARIABLE | WITHOUT MSCF | FULL VALUE OF MSCF | HALF VALUE OF MSCF |
|---|---|---|---|
| $\Sigma R_{zj}$ | -10.607 | -19.008 | -14.807 |
| $\Sigma H_{zj}$ | -28.757 | -25.306 | -27.032 |
| $\Sigma V_{zj}$ | -18.209 | -23.308 | -20.758 |
| $x'$ | 1.818 | 1.841 | 1.83 |
| $y$ | 0.29 | 0.285 | 0.29 |
| $z$ | 0.027 | 0.027 | 0.027 |
| $\alpha$ | 24.5 | 25.3° | 25.0 |
| $\beta$ | 35.0 | 36.7° | 35.9 |
| $n_1$ | 0.350 | 0.354 | 0.353 |
| $n_2$ | 0.767 | 0.750 | 0.758 |
| $n_3$ | 0.537 | 0.557 | 0.549 |
| $F_n$ | -35.563 | -38.734 | -37.103 |
| $\mu e_1$ | - 0.051 | + 0.136 | + 0.046 |
| $\mu e_2$ | - 0.041 | + 0.096 | + 0.029 |
| $\mu e_3$ | + 0.025 | - 0.043 | - 0.011 |
| $\mu$ | 0.071 | 0.172 | 0.055 |
| $e_1$ | - 0.729 | + 0.791 | + 0.826 |
| $e_2$ | - 0.583 | + 0.559 | + 0.528 |
| $e_3$ | + 0.359 | - 0.249 | - 0.197 |

Note that $\vec{e} = = e_1\vec{i} + e_2\vec{j} + e_3\vec{k}$

These comparisons with the net measured load components suggest that we have been over correcting when we applied the full value or even half value of the MSCF. According to the foregoing comparison and in order to maintain the friction force within the bounds described above one would expect to adjust the measured force components by the following ratios:

| | | |
|---|---|---|
| R | 1.472 → 1.479 | (compare to 1.792) |
| H | 0.948 → 1.000 | (compare to 0.880) |
| V | 1.049 → 1.150 | (compare to 1.280) |

It should be noted that while the magnitudes of average MSCF factors are high compared to what they should be, their trend is absolutely consistent with what should be expected. That is an increase of R and V and a decrease of H.

It appears from the above discussions that the MSCF values based on dry calibration are high and should not be used to correct the measurements. It is further suggested that more realistic values should be obtained from in-water calibration.

### 6.4.6 Other Segments

Similar analysis was conducted on Segment 3. However, the results have not been possible due to the zero shifting of signals after the test which implies segment adjustments. The symptom of this shifting appears as a positive net force in the vertical direction. Examination of segment 3 results (in Appendix F) have shown that the aft load cells lost contact during the test run and remained in a noncontact position after the test run. This points out to the necessity of improving the preloading arrangements for this segment, to ensure that contact is maintained during the entire test.

In segment 1, contact was also lost on the first impact with the resistance load cell and was not regained during the test. The horizontal and vertical load cell readings clearly indicate the concentration of load in the vicinity of H11 and V11.

It should be pointed out that the segment movements necessary to cause loss of contact are rather small. For a preload of 30N, the relative motion which is sufficient to cause a loss of contact is of the order of 4 microns (0.17 mils). Such movements cannot be detected by mere observation of the model during the test.

# 7.

# TECHNIQUE EVALUATION AND CONCLUSIONS

# 7. TECHNIQUE EVALUATION AND CONCLUSIONS

## 7.1 Evaluation of System Performance

The work conducted in this phase of the program has resulted in:

a) A segmented model,

b) An associated instrumentation system,

c) A data acquisition, reduction and analysis system.

At this state of technique development it is essential to validate the technique and associated systems. Many questions have to be answered as to their performance and efficiency. The focus of the evalution should be directed toward the identification and assessment of the problems and weaknesses as well as the capabilities of the system. This is to provide for their rectification in the following phase of the program. This evaluation will determine the operating characteristics of the segmented model testing technique and its performance so that its potential and limitations are defined.

The above mentioned features of the test technique have been evaluated independently on the basis of the current results. Furthermore, an outline of the modification beyond the scope of the present study but deemed necessary for the future program has been prepared.

### 7.1.1 Segmented Model and Icebreaking Mechanisms

The segmentation technique developed and implemented in this study represents the state-of-the-art of segmentation or sectioning of ship models. As discussed in Section 3.2, the current procedures for segmenting ship models for purposes of hydrodynamic studies has been limited to transverse sections with rigid or flexible interconnecting beams. The present attempt is the first of its kind in the following respects:

° Testing of thoroughly segmented, and fully instrumented ship models in ice.

° Segmentation of only one side of the hull instead of full transverse segmentation, which permits the measurement of lateral loads (rather than differential lateral loads).

° The segmentation system provides the only available method to date which can be used to measure local ice loads on a ship model hull to a high accuracy. This characteristic permits open ended opportunities for validation in model scale of ice impact loads during ship encounter with ice features.

In order to assess the success of the segmentation scheme, measured loads should be compared to what was expected. Overall, it appears that segmentation of the model does not influence or interfere with the icebreaking process. This has been discussed in Section 6.1. Therefore, the ice force measurements on the various segments should be compared to the expected ice loads to verify the success of the segmentation plan or lack of it.

Based on the results obtained and discussed in Section 6.4, it is observed that the loads on Segment 1 occur in the very close vicinity of load cells $H_{11}$ and $V_{11}$, that is at a distance 2.2 to 2.4 m from midship. For Segment 2 the loads appear to be centred about station #9, while for Segment 3, and based on the reliable horizontal load cells, the load is centred about a region 1.09 m from midship. The ice thickness for this test was 45 mm (0.9 m full scale), and test speed was 0.58 m/s (5.0 kts full scale).

Comparing these results to the information presented in Figure 2.5 reveals that:

- The loads on segment 2 are exactly where they were expected. This is in region II of the analysis.

- The loads on segment 1 occur forward of the FP for the test draft. This again agrees in general with the expectation that ice loads due to the first cusp occur very near the stem point of the ship.

- The load on segment 3 occurs in the vicinity of station #5. No breaking forces were expected on this segment. This implies that these forces are associated either with ice turning and friction or minor crushing force at the end of the second cusp.

The above appears to corroborate the segmentation rationale in terms of the extensions of each segment.

The next question relates to the magnitude of normal ice loads. The normal components of ice force were estimated for the three segments:

- for segment 1: $F_n$ = 19.0 N (est. from $\Sigma H$)
- for segment 2: $F_n$ = 35.6 N (calculated)
- for segment 3: $F_n$ = 40.6 N (est. from $\Sigma H$)

These values agree in general with the trend suggested by the analysis described in Section 3.5.1. However the results, do not appear to agree with basic premise proposed by Russian investigators [22] that the normal force at any position along the hull is proportional to the cosine of the waterline angle. Nonetheless the trend appears to be similar indicating increasing normal force with decreasing waterline angle, but it is nonlinear.

While the results of the computer model RICE as presented in Table 3.3 for reference test conditions suggest that the normal force has a maximum value near station #9, there are no data for the thickness under consideration. However, it is worthwhile to compare the present measurements of ice load on Segment 2 with expected values. This comparison is made in Table 7.1. It is shown that there is reasonable agreement between the model experimental results and the empirical equation (3.3) and the computer model of Ice Resistance "RICE". However, the experimental values seem to be greater than those obtained earlier in Chapter 3, which should be corroborated by further experimentation and then carefully analyzed to determine its implications on the mechanisms associated with icebreaking as may be found necessary.

To sum up, it may be stated that the segmentation of the model of the PIERRE RADISSON has been successful in reproducing the expected positions of the ice forces. With regards to magnitudes of the ice loads there appears to be some differences in maximum load values among the present tests, the computer code RICE and empirical formulation. These differences should be fully investigated in future tests to identify their causes and their implications on the mathematical modelling of the icebreaking phenomenon.

## TABLE 7.1

## COMPARISON OF MEASURED AND EXPECTED ICE LOADS
## SEGMENT 2, TEST NO.4-2

| | Test 4-2 | Equ.(3.3) Ref.Cond. | Equ.(3.3) Test Cond. | RICE Ref. Cond. | RICE(1) Test Cond. |
|---|---|---|---|---|---|
| Model Scale | | | | | |
| Ice Thickness, mm | 44 | 30 | | | |
| Ice Strength, kPa | 22 | 25 | | | |
| Elastic Modulus, MPa | 18.6 | 150 | | | |
| Model Speed, m/s | 0.59 | 0.894 | | | |
| $F_n$, N | 35.6 | 22 | | | |
| Projected Full Scale | | | | | |
| Ice Thickness, m | 0.88 | 0.6 | 0.88 | 0.6 | 0.88 |
| Ice Strength, kPa | 440 | 500 | 440 | 500 | 440 |
| Elastic Modulus, GPa | 0.37 | 3.0 | - | 3.0 | |
| Model Speed, kts | 5.1 | 7.8 | 5.1 | 7.8 | 5.1 |
| $F_n$, kN | 284.8<br>(2)(415.8) | 176.5 | 244.0 | 243.8 | 337.0 |
| Other Information | | | | | |
| $n_1$ | 0.350 | 0.335 | 0.350 | 0.335 | |
| $n_2$ | 0.767 | 0.790 | 0.767 | 0.790 | |
| $n_3$ | 0.537 | 0.513 | 0.537 | 0.537 | |

(1) Estimated values based on the ratio proportions of Equ. (3.3).

(2) Peak normal force ≅1.46 Average Force, based on resistance comparison Section 6.4.3.

### 7.1.2 Instrumentation System

During this phase of development, the instrumentation system has been designed to enable the determination of the following for each segment:

- magnitude of the normal component of ice load,
- position of centre of ice load,
- magnitude of the frictional component of ice load (friction factor),
- absolute direction along which frictional forces act.

The system has been designed so that sufficient measurements would be taken to enable the calculation of the above variables at any moment during the test. This ensures that a record on the progress of loading of each segment would be maintained on a continuous basis. This, in turn, provides the information necessary for one to trace:

- How does the direction of frictional forces vary with the progress of ice crushing, bending, fracturing, turning and sliding.
- How does the position of ice forces change during the various phases of icebreaking,
- How does the magnitude of normal force change along the hull,
- How does the value of friction factor change,

and other aspects of icebreaking which could result in the revision of the assumptions usually made in the course of mathematical modelling.

The system in principle is shown to be capable of providing this information as discussed in Section 6.4.4. However, there has been a number of problems which affected the proper operation of the system and the interpretation of the results. These problems may be summarized in the following:

a) The system was found to be sensitive to minor manufacturing defects which must be ironed out prior to further testing. Such defects relate to the seating of the load cells on the segments. As demonstrated by finite element analysis, Appendix G, such defects account for segment calibration constants different from unity. Ideally, the segments will transfer 100 percent of the ice loads without attenuation. At the present time this is not the case. Attempts made to calibrate the segments out of water have produced large scatter and apparent nonlinearity. The use of such factors (mean values of segment calibration factors) to correct measurements have resulted in over-correction evidenced by reversal in the friction force components. This points to the necessity of conducting a thorough in-water calibration of the segment response to determine more adequate MSCF values. This does not preclude the need for increasing the accuracy of load cell seating on the segment to eliminate any wedging effects.

b) The load cells were purposely designed to sense load in one direction. They are not sensitive to lateral load and the friction between the ball and seat has negligible effect on their accuracy. The load cells were made in two load ratings, being 50 and 100N and are capable of measuring only compressive loads. In order to maintain contact with the segments, a preload was applied using flexible wire ropes which were adjustable. The stiffness of the pretension wires was kept as low as possible to ensure that their effect on measurements could be neglected. Based on the present experimental program it was found that contact between the segments and load cells was frequently lost during the tesing and that some adjustments of the segments in position would cause a zero shift of the load cell output and this made it extremely difficult to interpret the signals. The order of magnitude of such adjustments and movements is very small and cannot be detected by eye.

In order to eliminate such problems it is essential to redesign the pretensioning system to increase its rigidity. This will mean a change in philosophy since a stiffer pretension mechanism should be taken into account when calculating the ice loads. Fortunately, this provision will not require any changes in the data analysis algorithms nor procedures but it would necessitate the measurement of the pretension wire (or element) load in order to incorporate it into the analysis. This transition to more rigid pretensioning system must be undertaken with due care so that the ice loads will be transferred along the three principal axes without coupling effects. In simpler terms, this means that the pretension arrangement should remain unidirectional. This could possibly be accomplished by using the finite element model to design and select the pretensioning elements and determine their required stiffnesses.

c) Segment 1 is the least stable and its pretension support arrangements must be re-examined, probably using a finite element model to assess its requirements under the most extreme loading condition.

d) The measurement of pitch and roll angles during the tests, though regarded as secondary measurements, have been quite useful in data interpretation. They have been instrumental in including the effects of model motions in calculating the ice loads, as described in section 6.4.1. The calibration testing conducted to evaluate the effects of model motions, as reported in Appendix C, should be expanded to produce accurate calibration curves for each load cell in pure pitch, roll and heave to be used in correcting the load cell records. This is equivalent to eliminating model motions relative to the ice and compensating for the changes in buoyancy during the ice test run.

e) Acceleration was also measured in the surge direction to monitor model motions. As shown in chapter 3, the effect of inertial forces seems to be negligible for the three segments. During the present tests, the model acceleration and deceleration were kept to a minimum and hence the inertia forces were kept within the estimates provided in table 3.2. It would be desirable to instrument Segment 3 with accelerometers to determine whether the inertia forces are significant or not. However, the priority level of such undertaking should be low since the accelerometers (particularly in the range considered) will be sensitive to variations in pitch and roll. This is confirmed by the consistent mean surge acceleration which is recorded during the constant speed part of the run and which can be correlated to model motions, e.g. mean trim angle during the same interval.

### 7.1.3 Data Acquisition and Reduction System

The data acquisition system described in Section 3.7 was successfully used to monitor and record all the information collected during the test. All data has been recorded on FM tape recorder and further processed into digital form where each signal was filtered at a frequency of 1 Hz and then digitized at a rate of 32 Hz. The data was then formatted in the series of graphs given for each test in Appendix F. Basic statistics were calculated for each signal in the test length interval. The latter has been determined from the time the bow length of the model is fully penetrated in the ice sheet until the end of the test run, which occurs prior to deceleration and stopping of the model. This interval is automatically identified by built-in software in the data reduction system. All test runs are now available on micro-disc medium which is easily accessible and is a more friendly medium. All data stored on micro-disc were converted to engineering units.

Due to the difficulties we experienced in interpretation of data, it was not possible to write the software for the remaining analysis algorithms as described in Chapter 4. The zero shift of the signals must be resolved prior to implementation of the analysis software. As discussed earlier, this would be possible by increasing the rigidity of segment supports. Should more channels of measured signals be added as a result of further modification it would be necessary to select 27 channels for permanent recording on tape and assign other channels containing secondary information to the oscillograph recorder. Up to 32 channels, however, may be accommodated through the A/D devices and processed simultaneously using the microcomputer.

In general, the data acquisition system performed well and it would only require minor adjustments for future work. The addition of a complete data analysis software should also be considered after necessary modifications are carried out on the model and instrumentation to ensure trouble-free operation.

### 7.1.4 Data Analysis Methodology

The data analysis algorithms were described in Chapter 4 and applied in Chapter 6. The method of solution has been made on the assumption that all measurements were available and correct. However, if the resistance cell was out of contact and not measuring, the solution was not possible.

This may be considered a weakness in the method of solution. It might be possible to develop other solutions which can accept partial data and produce the necessary output even with lower reliability.

It should be pointed out that for low values of friction coefficient the relative error in estimating the frictional ice load increases. To illustrate this a calibration case was considered, where a known load was applied normal to the hull surface and we therefore assumed that the measured responses of the segment were exact. The values are listed in the first column in Table 7.2. Applying the calculation algorithms, one would obtain zero frictional force component and zero friction coefficient. Now let us assume an experimental error in measurement ranging between ±10 percent. It is obvious that:

- The error in estimating the total or normal force is relatively small for randomly occuring errors. For systematic errors in one direction the error increases as shown in the last case. It is shown that for ±5 percent error, the resulting deviation in calculating the normal force is well within ±0.2 percent.

- The friction factor estimates are off by a greater margin. While no friction forces exist in this case ($\mu = 0$). The experimental errors in measuring the force components produce a friction coefficient which is approximately equal to the experimental error. That is 0.055 for ±5% error and 0.101 for 10% error.

- This results in a small frictional force component of a few Newtons, which seems to change direction in an erratic manner.

This idealized example of zero friction coefficient illustrates that the errors associated with the definition of the friction force components can be large. However, if we know beforehand that the friction factor is going to be small, we know that it has a minor effect on the ice forces, resistance, etc. and it would automatically be placed in a low priority category.

The obvious solution to this problem is to minimize the range of experimental errors, which we feel can be accomplished by necessary segment support system modifications and more detailed calibration of secondary effects such as roll and pitch motions.

Another solution is to increase the friction factor of the model hull. To explore this method let us consider two cases:

a) A hull - ice friction factor of 0.1 (present study)
b) A hull - ice friction factor of 0.5 (rough surface)

In both cases we will assume that the friction force acts in the waterplane, thus having components in the x- and y- directions only. Now we assume that the normal force in the base case, Table 7.2 is complimented with the frictional force (limiting or sliding friction is considered) and the readings of the load cells produce three principal components as listed in table 7.3. It is shown that as the friction factor was increased from 0.1 to 0.5, the direction of the friction force stabilizes and becomes much less sensitive to experimental errors. The trade off is obviously accepting lower accuracy in predicting the normal force in favour of better estimates of the frictional force magnitude and direction.

It may be suggested that the friction factor be set according to the objectives of a given experiment. The major emphasis, though, should remain on improving the overall experimental accuracy by following the course of action suggested earlier.

## TABLE 7.2

## EFFECT OF EXPERIMENTAL ERRORS ON FRICTION MEASUREMENT
## ZERO FRICTION CASE

| VARIBLE | BASE | ERROR BAND | | | |
|---|---|---|---|---|---|
| $\Sigma R$, N | -15.57 | -5% | +5% | -10% | -10% |
| $\Sigma H$, N | -31.99 | +5% | -5% | +10% | 0 |
| $\Sigma V$, N | -26.79 | -5% | +5% | -10% | 0 |
| $F_{TOTAL}$, N | 44.563 | 44.663 | 44.521 | 44.900 | 44.016 |
| % Deviation | 0 | +0.29% | -0.03% | +0.82% | -1.17% |
| $F_n$, N | 44.536 | 44.612 | 44.463 | 44.686 | 43.992 |
| % Deviation | 0 | +0.17% | -0.19% | +0.34% | -1.22% |
| $\mu$ (est) | n/a | 0.048 | 0.052 | 0.098 | 0.034 |
| $F_f$, N | n/a | 2.16 | 2.30 | 4.38 | 1.48 |
| $e_1$ | n/a | -0.382 | +0.343 | -0.371 | -0.936 |
| $e_2$ | n/a | 0.694 | +0.695 | -0.694 | -0.231 |
| $e_3$ | n/a | -0.611 | -0.632 | +0.616 | -0.267 |

(1) For above analysis $(n_1, n_2, n_3)$ = 0.350, 0.7194, 0.600

(2) The friction factor in this case is set at zero.

## TABLE 7.3

## EFFECT OF EXPERIMENTAL ERRORS ON FRICTION MEASUREMENTS HIGHER FRICTION CASES

| VARIABLE | $\mu$ = 0.1 | | $\mu$ = 0.5 | |
|---|---|---|---|---|
| | BASE CASE (NO ERROR) | EXP. ERROR (-10,+10,-10%) | BASE CASE (NO ERROR) | EXP. ERROR (-10,+10,-10%) |
| $\Sigma R$, N | -19.573 | -10% | -35.584 | -10% |
| $\Sigma H$, N | -30.038 | +10% | -22.228 | +10% |
| $\Sigma V$, N | -26.790 | -10% | -26.790 | -10% |
| $F_{TOTAL}$, N | 44.756 | 44.536 | 49.780 | 46.956 |
| % Deviation | - | -0.5% | - | -5.7% |
| $F_n$, N | 44.534 | 44.402 | 44.519 | 43.265 |
| % Deviation | - | -0.3% | - | -2.8% |
| $\mu$(est) | 0.1002 | 0.078 | 0.5003 | 0.422 |
| % Error | - | -22.3% | - | 15.6% |
| $e_1$ (3) | +0.894 | +0.601 | 0.898 | 0.925 |
| $e_2$ | +0.448 | -0.318 | 0.440 | 0.366 |
| $e_3$ | -0.016 | +0.733 | -0.004 | 0.101 |

(1) The waterline angle at the point of action ≅ 26°.

(2) Direction cosines are at the same point as in Table 7.2

(3) $\vec{e} = -e_1\vec{i} + e_2\vec{j} + e_3\vec{k}$

## 7.2 Conclusions

Based on the work undertaken in this project and reported in this document the following conclusions may be drawn:

1. The basic scheme for model segmentation for ice testing has been successfully developed to address the measurement requirements for ice loads on ship hulls.
2. The instrumentation system has been successfully developed to completely define the instantaneous ice load and associated frictional forces.
3. The system has been shown to be capable of detecting the correct position and magnitude of ice loads.
4. The friction component detection is sensitive to experimental errors and further work is required to fine tune the system.
5. Some problems associated with the segment support and preload have yet to be solved to attain a perfect working order.
6. Preliminary results and analysis suggest that extensive in-water calibration and completely automated data analysis systems are needed.

THIS PAGE INTENTIONALLY LEFT BLANK

## 8.

# REFERENCES AND BIBLIOGRAPHY

## 8.1 References

[1] MILANO, V.R., "Ship Resistance to Continuous Motion in Ice", Proc. SNAME Annual Meeting, New York, N.Y., November 15-17, 1973.

[2] ENKVIST, E., "On the Ice Resistance Encountered by Ships Operating in the Continuous Mode of Icebreaking", the Swedish Academy of Engineering Sciences in Finland, Report No. 24, Helsinky, 1972.

[3] NAEGLE, J.N., "Ice Resistance Prediction and Motion Simulation for Ships Operating in the Continuous Mode of Icebreaking", Ph.D. Thesis, University of Michigan, 1980.

[4] CARTER, D., "Ship Resistance To Continuous Motion in Level Ice", Transport Canada Report No. TP.3679.E, March 1983.

[5] LEWIS, J., BULAT, V., GLEN, I.F. and KOTRAS, T. "A Semi-Empirical Ice Resistance Model", submitted to Transportation Development Centre, April 1983, Arctec Canada Limited Report No. FR444C.

[6] NAWWAR, A.M. "Ice Resistance Prediction Model for Icebreaking Ships - Principles and Assumptions", submitted to Transportation Development Centre, March 1983, Arctec Canada Limited Report No. 1172C. Transport Canada Publication TP 4374E, April 1983.

[7] LEWIS, E.V., "Ship Model Tests to Determine Bending Moments in Waves", Transactions Society of Naval Architects and Marine Engineers, Vol. 62 (1954).

[8] LEWIS, E.V. and DALZELL, J.R., "Motions, Bending Moment and Shear Measurements on a Destroyer Model in Waves". Stevens Institute of Technology, Report 656 (April 1958).

[9] WACHNIK, Z.G. and ROBINSON, D.R., "A Study of Bending Moments in a Ship Model, Moving in Waves", B.S.Thesis, Massachusetts Inst. of Technology (May 1956).

[10] WACHNIK, Z.G. and SCHWARTZ, F.M., "Experimental Determination of Bending Moments and Shear Forces in a Multi-Segmented Ship Model Moving in Waves", International Shipbuilding Progress, Vol.10,n.101, January 1963, pp 12-24. Also DTMB Report No. 1743, July 1963.

[11] LLOYD, A.R.J.M., BROWN, J.C., and ANSLOW, J.F.W., "Motions and Loads on Ship Models in Regular Oblique Waves", Trans. of RINA, 1979, pp.21-33.

[12] BALES, N.K. and JONES, H.D., "Measurement and Reduction of Model-Scale Data on Flare Slamming and Deck Wetness", Paper Pres. at 19th ATTC, University of Michigan, July 9-11, 1980.

[13] GERRITSMA, J. and BEUKELMAN, W., "The Distribution of the Hydrodynamic Forces on a Heaving and Pitching Ship Model in Still Water", Proc. 11th Symposium on Naval Hydrodynamics, Bergen, Norway, 1964, p.219. Also Report PUB-124, Technische Hogeschool, Shipbuilding Lab, Delft, Netherlands, Feb.1965.

[14] ROARK, R.J., and YOUNG, W.C., "Formulas for Stress and Strain", 5th ed., McGrawHill, 1975.

[15] TIMOSHENKO, S.P. and GOODIER, J.N., "Theory of Elasticity", 3rd ed., McGrawHill, 1970.

[16] BEUKELMAN, W., and GERRITSMA, J., "The Distribution of Hydrodynamic Mass and Damping of an Oscillating Shipform in Shallow Water", Intl. Shipbuilding Progress, V.29, No. 339 November 1982, p.297-315.

[17] SPOTTS, M.F., "Design of Machine Elements, 5th ed., Princtce Hall, 1978, p.546.

[18] Internal work at ARCTEC based on Full Scale observations.

[19] HOWARD, D. and ABDELNOUR, R., "Results of the Interpretation of Carbamide Doped Ice in Arctic's Refrigerated Basin", Submitted to NRC, April 22, 1983.

[20] BULAT, V. and HOWARD, D., "Model Tests in Ice of POLAR 8 Icebreaker Development Study", Submitted to German and Milne, March 1980.

[21] BULAT, V., and GLEN I.F. "The Testing of a Ship Model in Ice" for National Research Council, August 1981.

[22] KASHTELJAN, V.I., POZNJAK, I.I. and RYULIN, A.Ja., "Ice Resistance to Motion of Ships", Sudostroeniy, Leningrad, 1968.

## 8.2 Bibliography

We have conducted a brief literature survey on the subjects of this study and related areas of interest. The survey was conducted using our own resources at ARCTEC as well as the CISTI on-line search facility. All references have been classified into three categories:

1. Segmented Models and Instrumentation Techniques.
2. Model Scale and Full Scale Icebreaking Tests.
3. Mathematical Models of Icebreaking.

These categories are broad enough so that some references are repeated in various categories. Some references which contain proprietary information are also listed for completeness. For instance, ARCTEC has conducted tests on segmented offshore structures during icebreaking - for commercial organizations but none of the details of the models, instrumentation or results are available in the public domain. It should be noted that the third category includes both analytical and semi-empirical models of relevance to the study.

Following is the bibliographic list.

## 1. SEGMENTED MODELS AND INSTRUMENTATION TECHNIQUES

[1] Manders, C., and Steele, M.A., ARCTEC CANADA LIMITED Report FR264C, 1978, Proprietary.

[2] Glen, I.F., Steele, M.A., and Bulat, V., "Ice Worthiness of HMCS CORMORANT", ARCTEC CANADA LTD. Report FR298C, 1981.

[3] Chabot, L. and Noble, P., ARCTEC CANADA LTD. Report DR 867C-1, 1981, Proprietary.

[4] Daley, M. and Abdelnour, R., ARCTEC CANADA LIMITED Report FR 901C-5, 1981, Proprietary.

[5] Chabot, L., Sayed, M., and Abdelnour, R., ARCTEC CANADA LIMITED Report, FR 938C, 1982, Proprietary.

[6] Chute, G.M. and Chute, R.D., "Electronics in Industry, 1971.

[7] Cerni, R.H., and Foster, L.E., "Instrumentation for Engineering Measurement", 1962.

[8] Perry, C.C. and Lissner, H.R., "The Strain Gauge Primer", 1962.

[9] Anonymous, "Buyers Guide - Mass/Force Transducers", Measurements and Control, Issue 95, October 1982.

[10] Beukelman, W., "Bottom Impact Pressures due to Forced Oscillation", Delft University of Technology, Report #479, 1979.

[11] Kloppenburg, M., "Ice Resistance of a Cargo Vessel in the Continuous Mode of Icebreaking. Tests of Three Geosim Models in Ice", SNAME, Ice Tech Symposium, Montreal, Canada, April 9-11, 1975.

[12] Malecke,, J., Vrhel, J., "Some Problems of Modelling Aeroelastic Phenomena in a Transonic Tunnel", 1975.

[13] Belleman, G.W., June, R.R., "Design and Fabrication of an Aeroelastic Flap Element for a Short Takeoff and Landing (STOL) Aircraft Model", 1973.

[14] Templin, J.T., Cooper, K.R., "Design and Performance of a Multi-Degree of-Freedom Aeroelastic Building Model", National Research Council of Canada, Ottawa.

[15] Otsuki, Y., Washizu, K., Ohya, A., "Wind Tunnel Experiments on the Aeroelastic Instability of a Prismatic Model with a Rectangular Section", 1975.

[16] Burkham, J.E., Miao, W.L., "Exploration of Aeroelastic Stability Boundaries with a Soft-in-Plane Hingeless-Rotor Model", 1972.

[17] Lewis, E.V., "Ship Model Tests to Determine Bending Moments in Waves", SNAME, Vol. 62, 1954.

[18] Wachnik, Z.G. and Schwartz, F.M. "Experimental Determination of Bending Moments and Shear Forces in a Multi-Segmented Ship Model Moving in Waves", DTMB Report 1743 July 1963 and Int'l Shipbuilding Progress Vol. 10, 1963.

[19] Dinsenbacker, A.L. and Andrews, J.N., "Vertical and Transverse Loads and Motions of a Segmented Model in Regular Waves", NSRDC Report 3152, August 1969.

[20] Akita, Y. and Sohda, K., "Experimental Determination of Bending Moments for T2-SE-A1 Tanker Model in Regular Waves", TTRI, Tokyo, March 1961.

[21] Gerritsma, J. and Beukelman, W., "The Distribution of the Hydrodynamic Forces on a Heaving and Pitching Ship Model in Still Water".

[22] Lloyd, A.R.J.M., Brown, J.C., and Anslow, J.F.W., "Motions and Loads on Ship Models in Regular Oblique Waves", The Naval Architect, January 1980.

[23] Bales, N.K. and Jones H.D., "Measurement and Reduction of Model Scale Data on Flare Slamming and Deck Wetness", 19th ATTC July 1980.

## 2. MODEL SCALE AND FULL SCALE ICEBREAKING TESTS

[1] Edwards, R.Y., Jr., German, J.G., & Lawrence, R.G.A., Comparative Model Tests on the Icebreaker Performance of Two Canadian Coast Guard Icebreakers", Proc. Second Int. Conf. on Port & Ocean Engineering under Arctic Conditions, Univ. of Iceland, Reykavik, Iceland, 1973.

[2] Major, R., "Ice Worthiness of Two Candidate Hulls for a Cabot Strait Ferry", ARCTEC CANADA LIMITED, FR91C, August 13, 1975.

[3] Lecourt, E.J., & Deslaurier, P.C., "Icebreaking Model Tests of the USCG POLAR STAR", Report No. 0278C-2, ARCTEC, Inc., November 1976.

[4] Nawwar, A.M., & Edwards, R.Y., Jr., "Compilation and Analysis of Recent Icebreaking Model Test Data of a World-Wide Variety of Hull Forms", 3 volumes, FR 211C, by ARCTEC CANADA LIMITED, submitted to Transport Canada R&D Center, Montreal, January, 1978.

[5] Anonymous, Extracts from "Model Tests on Canadian Icebreaker POLAR VII", Report #E8617 by HSVA, Hamburg, prepared for Canadian Ministry of Transport, 1976.

[6] Kotras, T.V., Benze, D.L. & Blanton, W.J., "Length/Beam Effect of an Icebreaking Resistance", presented in Eastern Canada, SNAME Meeting 1974.

[7] Johansson, B.M., & Makinen, E., "Great Lakes Ore Carrier Series: Ice Resistance Model Test Program", Wartsila Icebreaking Model Basin (WIMB), Test Report No. 18, December 29, 1972.

[8] Edwards, R.Y., Jr., Lewis, J.W., Wheaton, J.W., & Coburn, J., Jr., "Full Scale and Model Tests of a Great Lakes Icebreaker", SNAME Paper No. 5, presented at the Annual Meeting, New York, November 1972.

[9] Kloppenburg, M., "Ice Resistance of a Cargo Vessel in the Continuous Mode of Icebreaking. Tests of Three Geosim Models in Ice", SNAME, Ice Tech Symposium, Montreal, Canada, April 9 - 11, 1975.

[10] Vance, G.P., "A Scaling System for Vessels Modelled in Ice", Paper H, Presented at the Ice Tech Symposium, SNAME, Montreal April 1975.

[11] Makinen, E., & Roos, A., "Ice Resistance in Level Ice of Ships with Main Dimensions Typical for the Great Lakes Bulk Carriers", Supplement to WIMB Test Report No. A18, September 28, 1973.

[12] Laini, A., et al "Great Lakes Ore Carrier Series Ice Resistance Model Tests in Ballast Conditions", WIMB Report No. 24, September 25, 1975.

[13] Virtamen, J., et al, "Great Lakes Ore Carrier Series - Ice Resistance Model Tests Draft Variations", WIMB Report No. 34, April 15, 1975.

[14] Roos, A., et al, "Great Lakes Ore Carrier Series - Ice Resistance Model Test Program", WIMB Report No. A41, November 21, 1974.

[15] Voelker, R.P., & Kim, J.K., "Summary Results of Ice Resistance Tests for Great Lakes Bulk Carriers from the Wartsila Model Test Series", ARCTEC Inc., Report No. 160C-1, submitted to Maritime Admin., U.S. Dept. of Commerce, December 3, 1976.

[16] Allen, R.J., "Results of Full Scale Trials in Ice to Further Assess the Icebreaking Capability of the CCGS WOLFE", ARCTEC CANADA LIMITED DFR 202C, June 30, 1977.

[17] Makinen, E. & Johansson, B.M., "Great Lakes Ore Carrier Series - Ice Resistance Model Test Program", WIMB Test Report A41 for Maritime Admin., U.S. Dept of Commerce, November 21, 1974.

[18] Kashteljan, V.I., Ryvlin, A.Ya., Feddeyev, O.V., & Yagodkin, V.Ya., "Icebreakers", Translation, CRREL TL 418, August 1973.

[19] Lewis, J.W., DeBord, F.W., and Bulat, V., "Resistance and Propulsion of Iceworthy Ships", to be presented at the Annual Meeting, SNAME, New York, N.Y., 1982.

[20] DeBord, F.W., Voelker, R.P., Geisel, F.A., Coburn, J.L., and Dane, K.E., "Winter 1981 Trafficability Tests of the USCGC POLAR SEA; Volume V - Bollard and Tow Rope Pull Tests", ARCTEC INCORPORATED Report No. 583C-3, Columbia, Md., 1981.

[21] Noble, P., Bulat, V., "Icebreaker Bow Form - A Parametric Variation", SNAME, Ice Tech '81, Ottawa.

[22] Bulat, V., Glen, I., "The Testing of a Ship Model in Ice for the NRC", ACL, August 1981, Submitted to National Research Council, Ottawa.

[23] Lewis, J.W., Benze, D.L., "Model Ice Resistance Tests of the USCGC MACKINAW in Uniform Thick Ice Cover", ARCTEC Inc., Report 293, December 1971.

[24] Michailidis, M., Murdey, D., "Performance of CCGS FRANKLIN in Lake Melville, 1980", SNAME Ice Tech '81.

[25] Vance, G.P., Grocewski, A.S., Goodwin, M.J., "Full Scale Icebreaking Tests of USCGC KATMAI BAY", SNAME Ice Tech '81.

[26] Edwards, R.Y., Johnson, B., Dunne, M., Comfort, G., Bulat, V., "Results of Full Scale Trials in Ice of CCGS PIERRE RADISSON", SNAME Ice Tech '81.

[27] Noble, P., Comfort, G., "Ice Trials to Evaluate Low Friction Coating on CCGS LOUIS S. ST. LAURENT", ACL FR 357C, November 1979.

[28] Glen, I., Dunne, M., "After Action Report Fall Probe 1980 CCGS LOUIS S. ST. LAURENT", ACL Report 737C-2.

[29] German, R., Lawrence R.G.A., "Full Scale Testing in Ice of Three Icebreakers", ICE TECH '75, Montreal, SNAME.

[30] Nadreau, J.P., Dunne, M., "Results of Full Scale Field Trials of ACT 100 with CCGS ALEXANDER HENRY", ACL Report 150C, May 1976. Submit to Transportation Development Centre, Montreal.

[31] Edwards, R.Y., Abdelnour, R., "Model Tests in Support of ALEXANDER HENRY/ACT 100 Concept Development", ACL Report 122C, May 1977, Submitted to Transportation Development Centre, Montreal.

[32] Edwards, R.Y., Allan, R.J., Dunne, M.A., "Results of Full Scale Trials in Ice of the CCGS WOLFE", Volume I and II, ARCTEC CANADA LIMITED Final Report 45C, December 31, 1976.

[33] Allan, R.J., "Results of Full Scale Trials in Ice to Further Assess the Icebreaking Capabiity of the CCGS WOLFE, ACL Report 202C for Transport Canada R&D Centre, June 30, 1977.

[34] Edwards, R.Y., German, G., Lawrence, R., "Comparative Model Tests of the Icebreaker Performance of Two CCG Icebreakers", Second POAC Conference, 1973.

[35] Edwards, R.Y., Lewis, J.W., "Modelling the Motion of Ships through Polar Ice Fields using Unconstrained Self Propelled Models", IAHR Symposium, Reykjavik, 1970.

[36] Kawervinski, L.I., "Trial Procedures and Torsionmeter Calibrations, MV ARCTIC Saguenay River", NRC Report, LTRSH266, January 1980.

[37] Enkvist, E., "Full Scale Icebreaking Tests with the Icebreaking Tug JELPARRI in 1971", WHI 1971 (Unpublished).

[38] Hilden, S., "Report on Full Scale Icebreaking Tests with Varme and Vladivostok on the Gulf of Finland in March 1969", WHT 1969 (Unpublished).

[39] Selminen, O., "Report of Full Scale Icebreaking Tests with RoRo Cargo Ferry Finncarrier int he Gulf of Finland in March 1979", WHT 1970 (Unpublished).

[40] Glen, I.F., Steele, M.A., and Bulat, V., "Ice Worthiness of HMSC CORMORANT", ARCTEC CANADA LTD. Report No. FR298C, 1981.

## 3. MATHEMATICAL MODELS OF ICEBREAKING

[1] White, R.M., "Prediction of Icebreaker Capability", Royal Institute of Naval Architects, Paper W8, 1969.

[2] Lewis, J.W., & Edwards, R.Y., Jr., "Methods of Predicting Icebreaking and Ice Resistance Characteristics of Icebreakers", Paper #5, SNAME Annual Meeting, New York, November 1970.

[3] Shimansky, J.A., "Conditional Standards of Ice Qualitites of a Ship", Trans. of the Arctic Institute of the Chilf Administration of the Northern Sea Route, V. 130, Leningrad, 1938 (translation).

[4] Kashteljan, V.I., & Ryvlin, A. Ja., "The Influence of Natural Characteristics of Solid Ice in Evaluation of its Resistance to Icebreaker Passage", Problemy Artiki I Antartiki, V. 22, 1966, pp. 77 (Translation).

[5] Enkvist, E., "On the Ice Resistance Encountered by Ships Operating in the Continuous Mode of Icebreaking", the Swedish Academy of Engineering Sciences in Finland, Report No. 24, Helsinky, 1972.

[6] Edwards, R.Y., Jr., German, J.G., & Lawrence, R.G.A., Comparative Model Tests on the Icebreaker Performance of Two Canadian Coast Guard Icebreakers", Proc. Second Int. Conf. on Port & Ocean Engineering under Arctic Conditions, Univ. of Iceland, Reykavik, Iceland, 1973.

[7] Milano, V.R., "Ship Resistance to Continuous Motion in Ice", Proc. SNAME Annual Meeting, New York, N.Y., November 15-17, 1973, pp. 274-299. Discussions by R. White, G.P. Vance, E. Makinen, pp. 300-302. (Paper evolved from Ph.D. Dissertation, Stevens Institute of Technology, N.J. 1972).

[8] Major, R., "Ice Worthiness of Two Candidate Hulls for a Cabot Strait Ferry", ARCTEC CANADA LIMITED, FR91C, August 13, 1975.

[9] Nawwar, A.M., & Edwards, R.Y., Jr., "Compilation and Analysis of Recent Icebreaking Model Test Data of a World-Wide Variety of Hull Forms", 3 volumes, FR 211C, by ARCTEC CANADA LIMITED, submitted to Transport Canada R&D Center, Montreal, January, 1978.

[10] Anonymous, Extracts from "Model Tests on Canadian Icebreaker POLAR VII", Report #E8617 by HSVA, Hamburg, prepared for Canadian Ministry of Transport, 1976.

[11] Kotras, T.V., Benze, D.L. & Blanton, W.J., "Length/Beam Effect of an Icebreaking Resistance", presented in Eastern Canada, SNAME Meeting 1974.

[12] Johansson, B.M., & Makinen, E., "Great Lakes Ore Carrier Series: Ice Resistance Model Test Program", Wartsila Icebreaking Model Basin (WIMB), Test Report No. 18, December 29, 1972.

[13] Edwards, R.Y., Jr., Lewis, J.W., Wheaton, J.W., & Coburn, J., Jr., "Full Scale and Model Tests of a Great Lakes Icebreaker", SNAME Paper No. 5, presented at the Annual Meeting, New York, November 1972.

[14] Kloppenburg, M., "Ice Resistance of a Cargo Vessel in the Continuous Mode of Icebreaking. Tests of Three Geosim Models in Ice", SNAME, Ice Tech Symposium, Montreal, Canada, April 9 - 11, 1975.

[15] Edwards, R.Y., Jr., Major, R.A., Kim, J.K., German, J.G., Lewis, J.W., & Miller, D.M., "Influence of Major Characteristics of Icebreaker Hulls on their Powering Requirements and Maneuverability in Ice", Paper No. 12, SNAME Annual Meeting, New York, November 1976.

[16] Vance, G.P., "A Scaling System for Vessels Modelled in Ice", Paper H, Presented at the Ice Tech Symposium, SNAME, Montreal April 1975.

[17] Roos, A., et al, "Great Lakes Ore Carrier Series - Ice Resistance Model Test Program", WIMB Report No. A41, November 21, 1974.

[18] Makinen, E., Discussion Contribution to "Ship Resistance to Continous Motion in Ice", By V.R. Milano, Proc. SNAME, November 1973, pp. 300-302.

[19] Enkvist, E., Discussion Contribution to "Ship Resistance to Continuous Motion in Ice", by V.R. Milano, Proc. SNAME November 1973, pp. 300-302.

[20] Milano, V.R., "Variation of Ship/Ice Parameters on Ship Resistance to Continuous Motion in Ice", Paper B1, ICE TECH '75, Symposium on Icebreaking and Related Technologies, Montreal, 1975.

[21] Kashteljan, V.I., "Methods of Estimating the Ice Navigating Capability of a Ship in Solid Ice", The Navigation Qualities of Ships, ed. by Kheisin, D.Ie., and Popov, Iu.N., Translation CRREL TL 417, August 1973, pp. 3-18.

[22] Kashteljan, V.I., Ryvlin, A.Ya., Feddeyev, O.V., & Yagodkin, V.Ya., "Icebreakers", Translation, CRREL TL 418, August 1973.

[23] Poznyak, I.I. and Ionov, B.P., "The Division of Icebreaker Resistance into Components", SNAME Ice Tech '81, Paper No. 19.

[24] Naegle, J.N., "Ice Resistance Prediction and Motion Simulation for Ships Operating in the Continuous Mode of Icebreaking", Ph.D. Thesis, University of Michigan, 1980.

[25] Lewis, J.W., DeBord, F.W., and Bulat, V., "Resistance and Propulsion of Iceworthy Ships", to be presented at the Annual Meeting, SNAME, New York, N.Y., 1982.

[26] Noble, P., Bulat, V., "Icebreaker Bow Form - A Parametric Variation", SNAME, Ice Tech '81, Ottawa.

[27] Bulat, V., Glen, I., "The Testing of a Ship Model in Ice for the NRC", ACL, August 1981, Submitted to National Research Council, Ottawa.

[28] Vance, G.P., Grocewski, A.S., Goodwin, M.J., "Full Scale Icebreaking Tests of USCGC KATMAI BAY", SNAME Ice Tech '81.

# APPENDIX A

# CALIBRATION OF LOAD CELLS

## A.1 Calibration System and Procedure

A special calibration rig was designed and built for this purpose. Figure A.1 illustrates the main features of the rig which can be adapted easily to either of the following types of calibration:

a) Dead weight static calibration, in which an attachment to the loading beam is used to support the weights. To set up the zero load condition a counterbalancing weight mounted on a long threaded rod at the opposite end is used. The rig can be placed on the edge of a table and adjusted so that the load cell remains in a vertical position with the loading arm in the horizontal position.

b) Dynamic calibration, in which the rig is mounted on the platen of a closed loop testing frame. The load is then applied through an alignment ball which ensures coaxial loading of the load cell. The loading frame is controlled to apply repeated loading cycles while measurements are obtained.

In either case the load is measured with a reference force transducer which measures the load to within $15 \times 10^{-6}$ N for 100 N load.

The dynamic calibration was conducted under controlled frequencies and wave forms using the closed loop control system. The system controls a hydraulic ram to which the bottom platen of the test frame was fixed. The top platen was fixed to the frame. The control system available at Arctec consists of:

- An MTS Model 410-31 Digital function generator
- An MTS Model 406-11 Controller
- A servo-hydraulic valve

Figure A.2 is a schematic illustration of the system. The digital function generator produces a load function (sinusoidal, square, or ramp) at the given frequency and amplitude level. The controller is responsible for issuing the necessary control signal to the servo valve to control the oil flow rate and quantity to the hydraulic ram. A feed back signal is measured at the frame and returned to the controller which compares it to the reference signal input by the function generator and issues the necessary corrections to the control signal to correct the response of the hydraulic ram. The feedback signal could be any measured physical quantity depending on the required type of control. Examples are:

- pressure control
- load control
- deflection or displacement control
- strain control

In the present calibration load control was desired and feedback signal was that of the reference Mini Beam load cell.

FIGURE A.1

LOAD CELL CALIBRATION RIG
INSTALLED IN CLOSED LOOP TESTING MACHINE

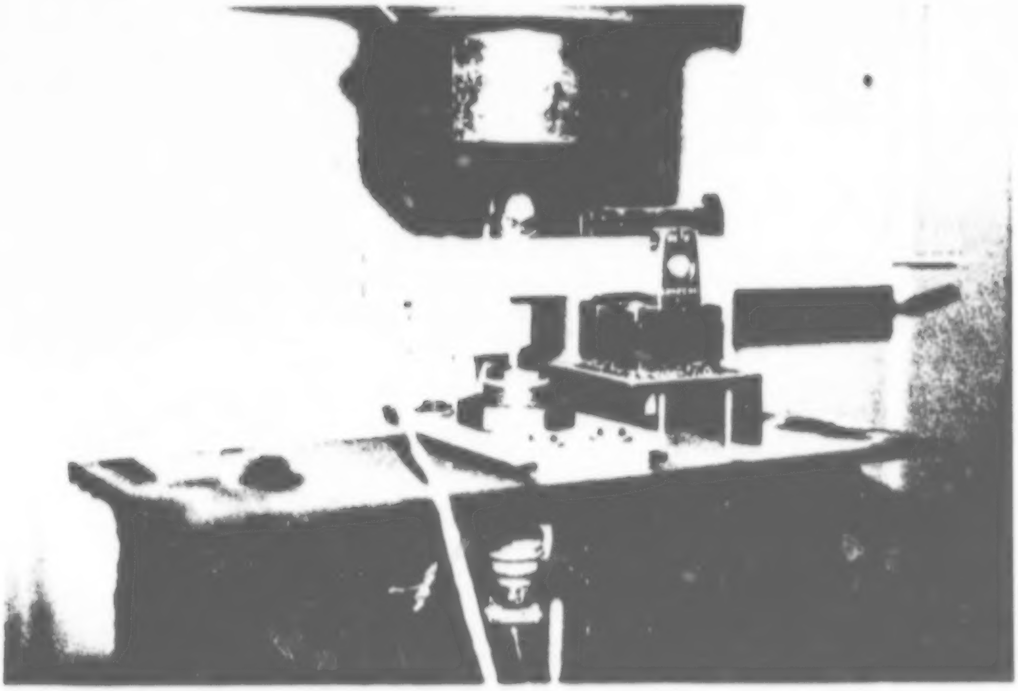

Prior to calibration, the procedure was developed by subjecting a prototype load cell to a wide range of sinusoidal and ramp signals of different frequencies. The objective was to determine the best period for which minimum signal distortion can be obtained. It is usual to conduct this type of test to ensure that the response of the hydromechanical components corresponds to the much faster electronic control commands. It was found that the best cycle periods for 100 N and 50 N load cells were 120 and 60 seconds, respectively.

The data was collected by the standard data acquisition system and analyzed on line using an HP 9845 computer.

The calibration procedure may be summarized in the following:

- Start up system

- Install load cell in the calibration frame and adjust its position such that the load beam is horizontal - check with spirit level.

- Tighten load cell in positon with lock nut.

- Move the ram into contact position and apply a small preload of approximately 2 Newtons for the 100 N load cells and 1.4 Newtons for the 50 N rated cells. Check seating of load cell.

- Set the function generator and apply the test load continuously.

- Affect computer scan for two cycles after permitting a few load cycles.

- Run data analysis which plots calibration curves and calculation its characteristics.

- Examine both the loading curve and the loading/unloading curve as well as the calculated linear regression results, sensitivity, linearity, and hysterises.

## FIGURE A.2

## CLOSED LOOP CALIBRATION SYSTEM

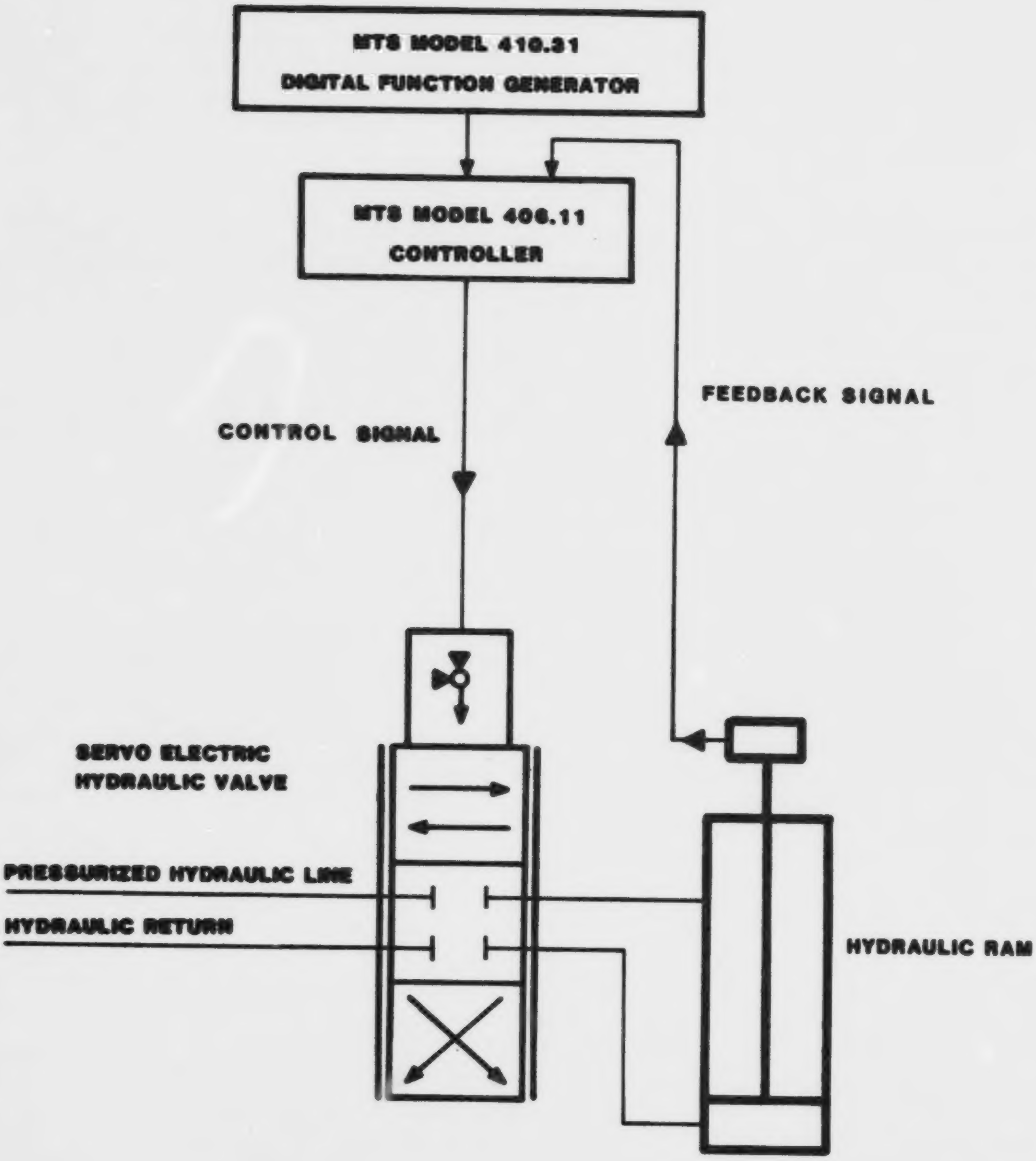
MTS MODEL 410.31
DIGITAL FUNCTION GENERATOR
MTS MODEL 406.11
CONTROLLER
FEEDBACK SIGNAL
CONTROL SIGNAL
SERVO ELECTRIC
HYDRAULIC VALVE
PRESSURIZED HYDRAULIC LINE
HYDRAULIC RETURN
HYDRAULIC RAM

## A.2 Calibration Results

A summary of calibration results is given in Table A.1 for all load cells and all the calibration curves are given at the end of this section.

It should be noted that the accuracy of the present design is generally lower than comparable commercially available products. However, this was acceptable for the following reasons:

- The cost of home made cells was less than half what one would pay for comparable ordinary precision cells. In fact, a commercial order would have costed more because of the special geometric requirements for the present application.

- In view of the exploratory nature of this study, it was felt that the resources would be better used to verify the concept and develop the procedures of segmented model testing than to invest in expensive load cells and reduce the efforts in other areas of investigation.

- The method utilized in calibration considers the maximum deviation in a continuous record for the calculation of either nonlinearity or hysterises. This deviation, in fact, is partly due to some signal noise as can be observed in most of the calibration lines. Therefore, while the calibration constant which is based on the average quality of the line can be determined with confidence and with a correlation coefficient better than 0.999 ( $r > 0.9995$), the estimates of the quality of excursions from this line must be interpreted with caution due to extraneous effects.

It is desirable to conduct a detailed study on the characteristics of the dynamic calibration using the closed loop system. However, for the purposes of this study it would suffice to obtain the calibration coefficients. The value of the intercept as noted in the regression analysis will usually be eliminated by a slight preload and hence will not likely have any effect on the calibration constants.

The calibration results for each load cell are given in the following pages:

TABLE A.1

LOAD CELL CALIBRATION SUMMARY

| SERIAL NUMBER | VISHAY GAIN (volts) | VISHAY EXCITATION (volts) | RANGE (N) | INITIAL CALIBRATION (N/v) | COMMENTS | SECOND CALIBRATION (N/v) | COMMENTS |
|---|---|---|---|---|---|---|---|
| 100 | 2000 | 5.00 | 100 | 20.28 | | - | Not calculated |
| 101 | 2000 | 5.00 | 100 | 18.49 | | 18.8 | |
| 102 | 2000 | 5.00 | 50 | 8.66 | | 8.6 | |
| 103 | 2000 | 5.00 | 100 | 18.71 | | 19.2 | |
| 104 | 2000 | 5.00 | 100 | 18.77 | | 19.1 | |
| 105 | 2000 | 5.00 | 50 | 7.58 | | 7.8 | |
| 106 | 2000 | 5.00 | 50 | 7.14 | | 7.6 | |
| 107 | 2000 | 5.00 | 100 | 17.34 | | 17.9 | |
| 108 | 2000 | 5.00 | 100 | 18.62 | Calibrated to 50N | 18.6 | Calibrated to 100N |
| 109 | 2000 | 5.00 | 50 | 8.31 | | 7.8 | |
| 110 | 2000 | 5.00 | 100 | 19.53 | | 19.44* | |
| 111 | 2000 | 5.00 | 100 | 20.73 | | 19.3 | |
| 112 | 2000 | 5.00 | 100 | 20.80 | | 20.1 | |
| 113 | 2000 | 5.00 | 50 | 6.72 | | 6.8 | |
| 114 | 2000 | 5.00 | 100 | 20.55 | | 19.03** | Regauged |
| 115 | 2000 | 5.00 | 100 | 17.55 | | 16.9 | |
| 116 | 2000 | 5.00 | 100 | 18.39 | | - | Not functioning |
| 117 | 2000 | 5.00 | 50 | 7.64 | | 7.8 | |
| 118 | 2000 | 5.00 | 50 | 7.96 | | 8.1 | |
| 119 | 2000 | 5.00 | 100 | - | Not yet functioning | 19.11** | Regauged |
| 120 | 2000 | 5.00 | 50 | 8.20 | | 8.29* | |

* Dead weight calibration performed half way through test program as a check (only 3 different applied loads).

** A precise dead weight calibration performed.

TRANSDUCER S/N: 100 JUL-07-83

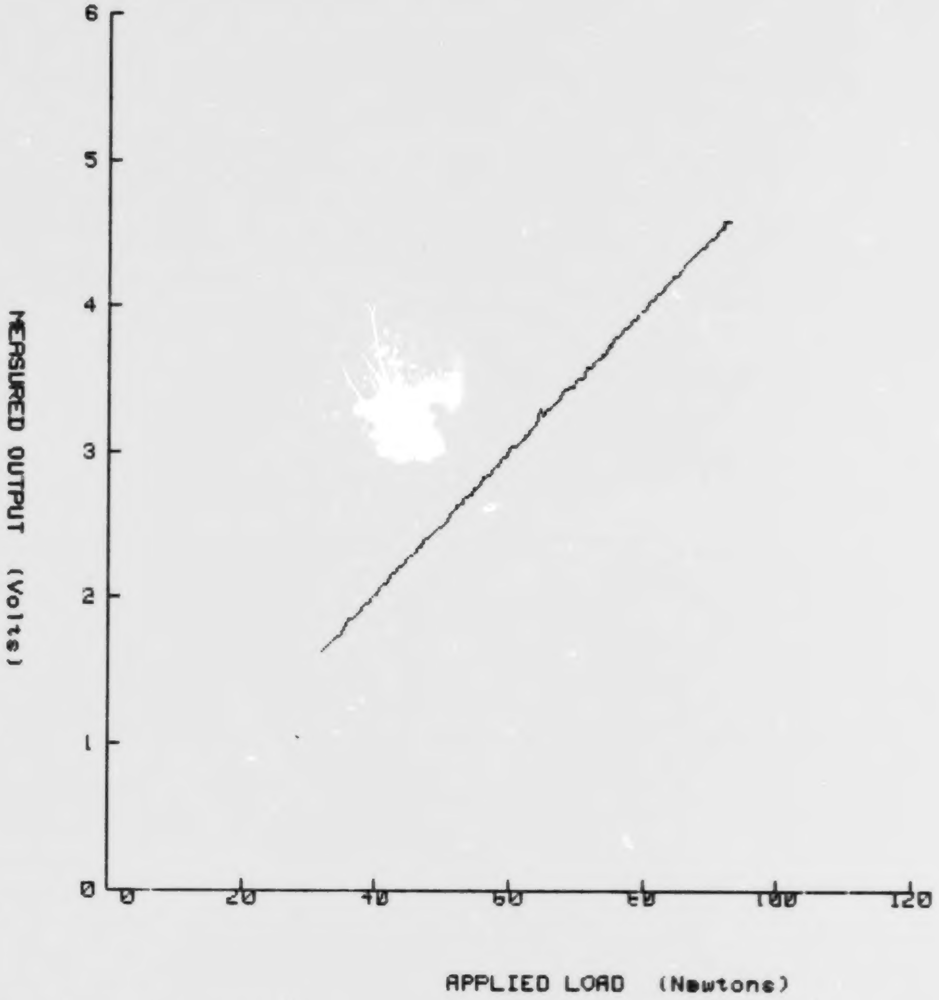

EXCITATION = 5.00 Volts
GAIN = 2000 Volts/Volts

SENSITIVITY= .4875 mV/V @ 100 Newtons

REGRESSION ANALYSIS :
SLOPE = .0487 Volts/Newton
INTERCEPT = .0795 Volts
CORRELATION COEFF. = .9999

CALIBRATION = 20.51 Newtons/Volt

TRANSDUCER S/N: 100 JUL-07-83

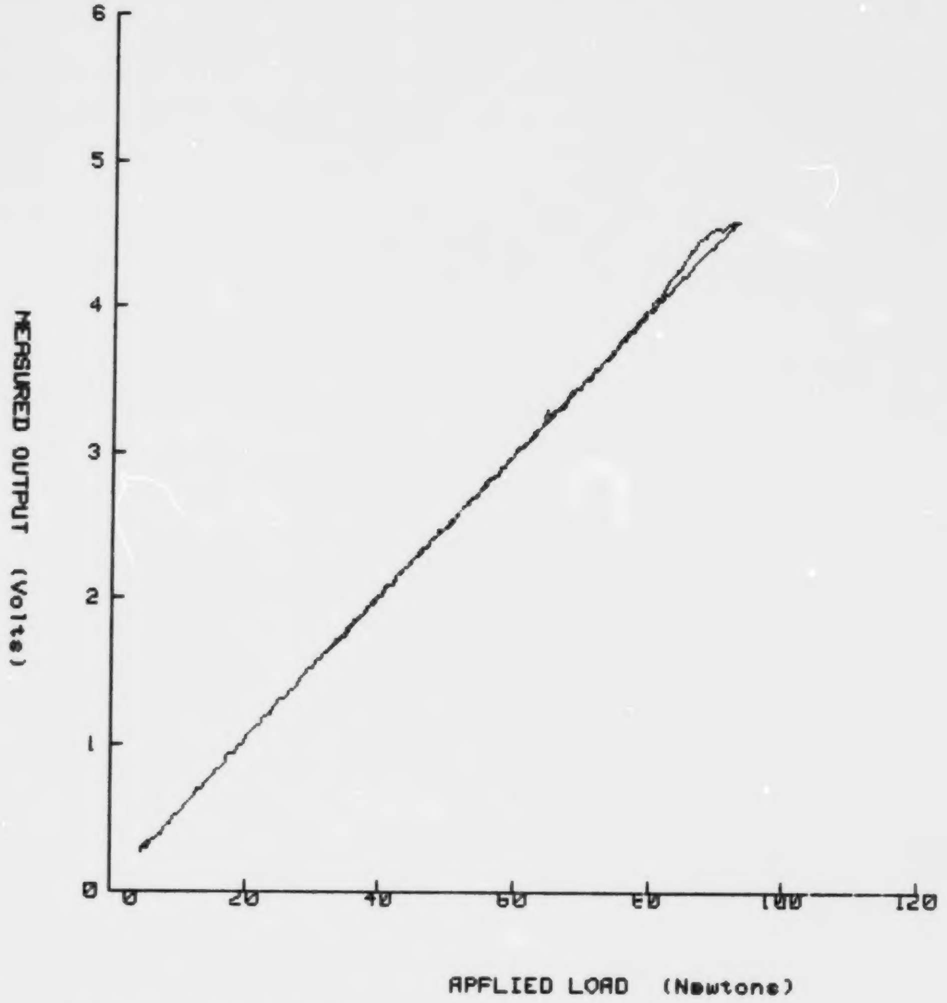

```
EXCITATION = 5.00 Volts
      GAIN = 2000 Volts/Volts

  SENSITIVITY= .4931 mV/V @ 100 Newtons
NON-LINEARITY= 1.8880 %
   HYSTERESIS= 2.5430 %

REGRESSION ANALYSIS :
             SLOPE    = .0493  Volts/Newton
         INTERCEPT    = .0540  Volts
 CORRELATION COEFF.   = .9998

       CALIBRATION    = 20.28  Newtons/Volt
```

TRANSDUCER S/N: 101 JUL-07-83

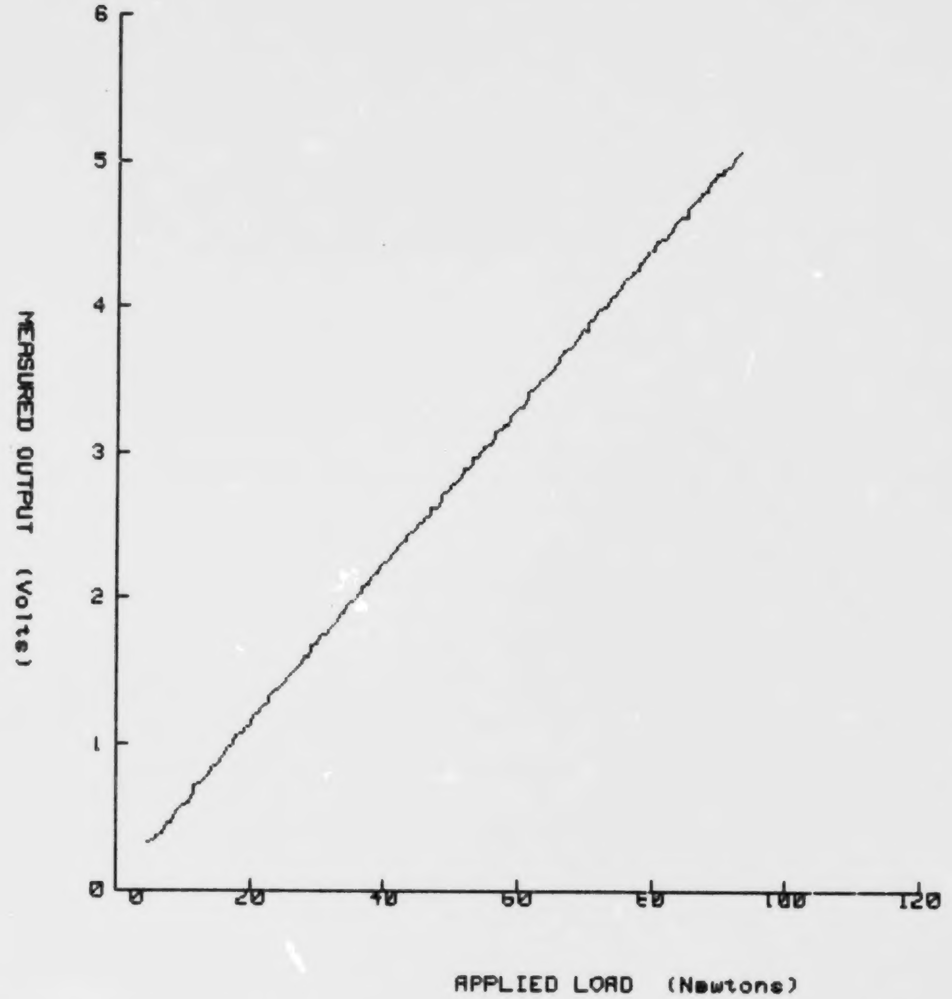

```
EXCITATION = 5.00 Volts
      GAIN = 2000 Volts/Volts

  SENSITIVITY= .5407 mV/V @ 100 Newtons

REGRESSION ANALYSIS :
             SLOPE   = .0541  Volts/Newton
         INTERCEPT   = .0695  Volts
 CORRELATION COEFF. = .9999

      CALIBRATION   = 18.49  Newtons/Volt
```

TRANSDUCER S/N: 101 JUL-07-83

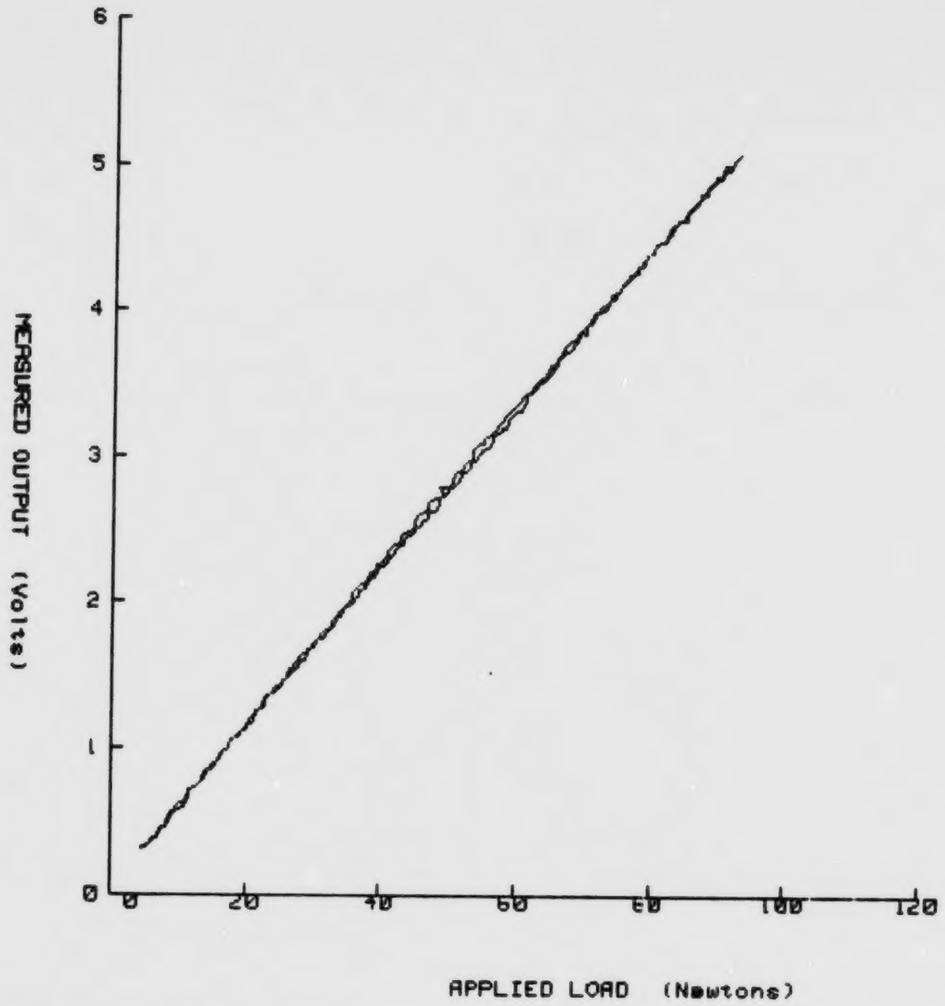

```
EXCITATION = 5.00 Volts
      GAIN = 2000 Volts/Volts

  SENSITIVITY= .5409 mV/V @ 100 Newtons
NON-LINEARITY= 1.2633 %
   HYSTERESIS= 1.6249 %

REGRESSION ANALYSIS :
              SLOPE  = .0541  Volts/Newton
          INTERCEPT  = .0811  Volts
 CORRELATION COEFF. = .9998

       CALIBRATION  = 18.49  Newtons/Volt
```

TRANSDUCER S/N: 102

JUL-09-83

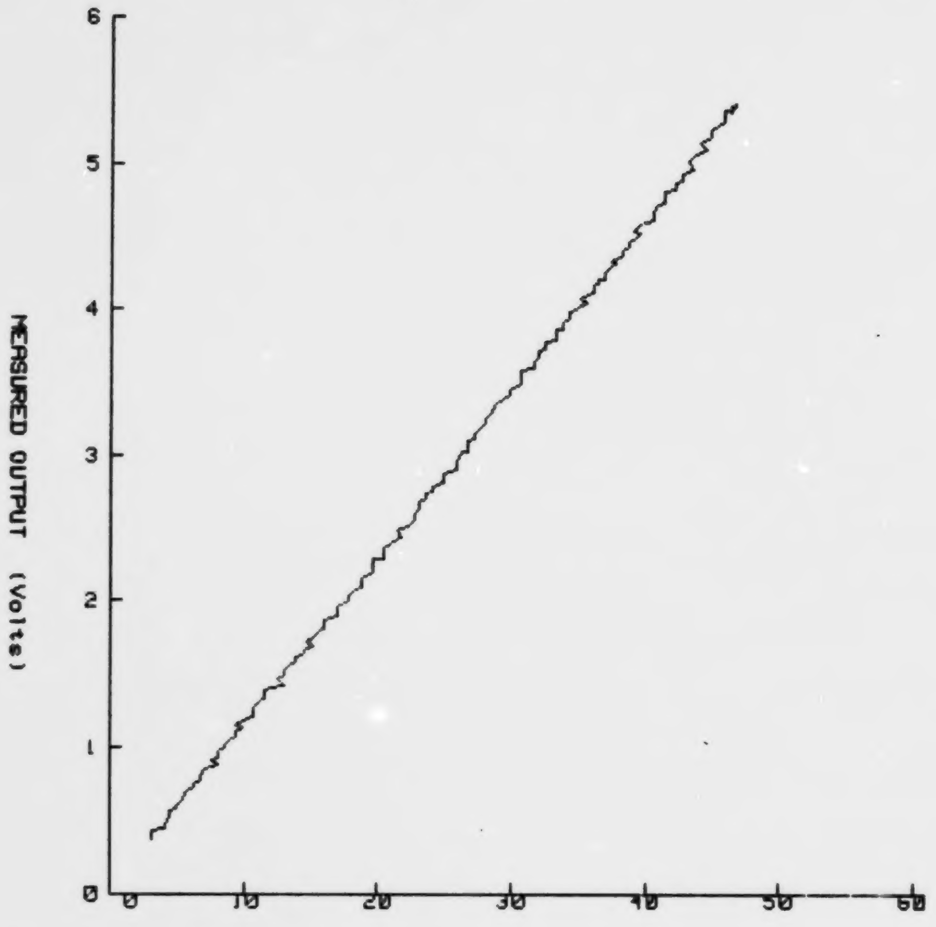

APPLIED LOAD (Newtons)

EXCITATION = 5.00 Volts
GAIN = 2000 Volts/Volts

SENSITIVITY= .5756 mV/V @ 50 Newtons

REGRESSION ANALYSIS :
SLOPE = .1151 Volts/Newton
INTERCEPT = .0062 Volts
CORRELATION COEFF. = .9998

CALIBRATION = 8.69 Newtons/Volt

TRANSDUCER S/N: 102 JUL-09-83

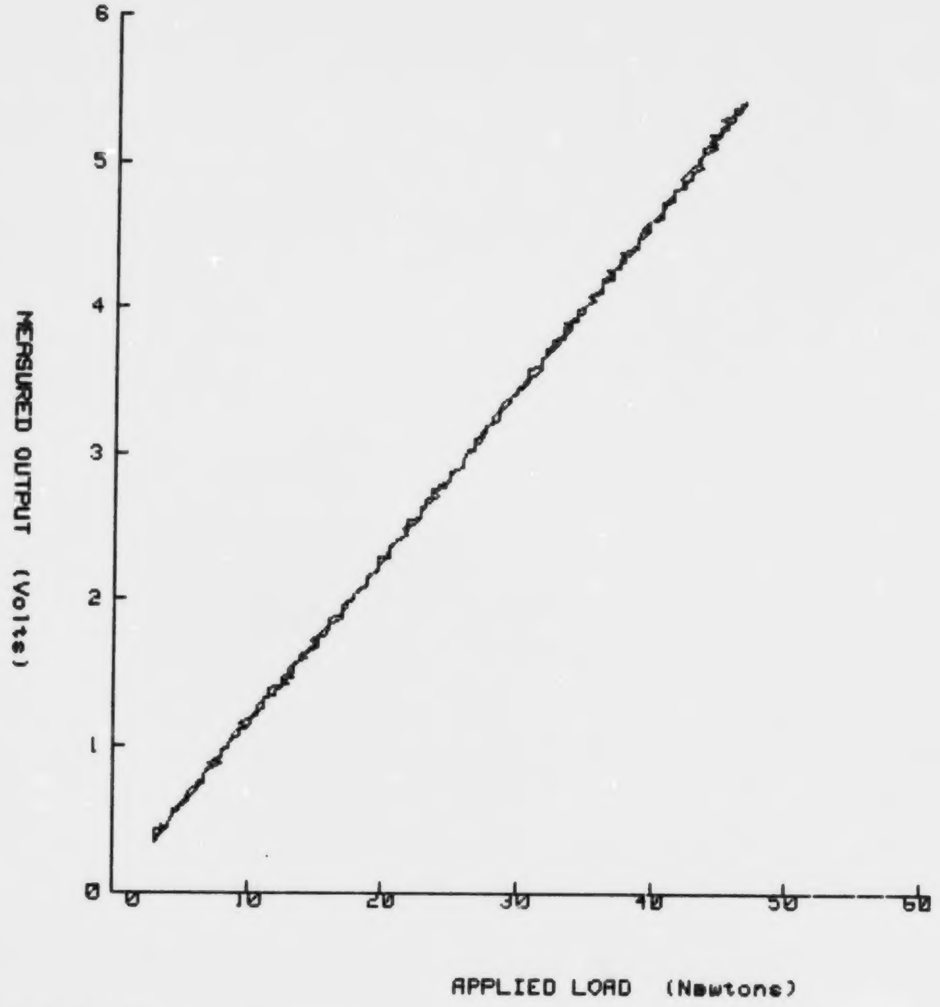

EXCITATION = 5.00 Volts
GAIN = 2000 Volts/Volts

SENSITIVITY= .5772 mV/V @ 50 Newtons
NON-LINEARITY= 1.4028 %
HYSTERESIS= 1.2991 %

REGRESSION ANALYSIS :
SLOPE = .1154 Volts/Newton
INTERCEPT =-.0059 Volts
CORRELATION COEFF. = .9997

CALIBRATION = 8.66 Newtons/Volt

TRANSDUCER S/N: 103 JUL-09-83

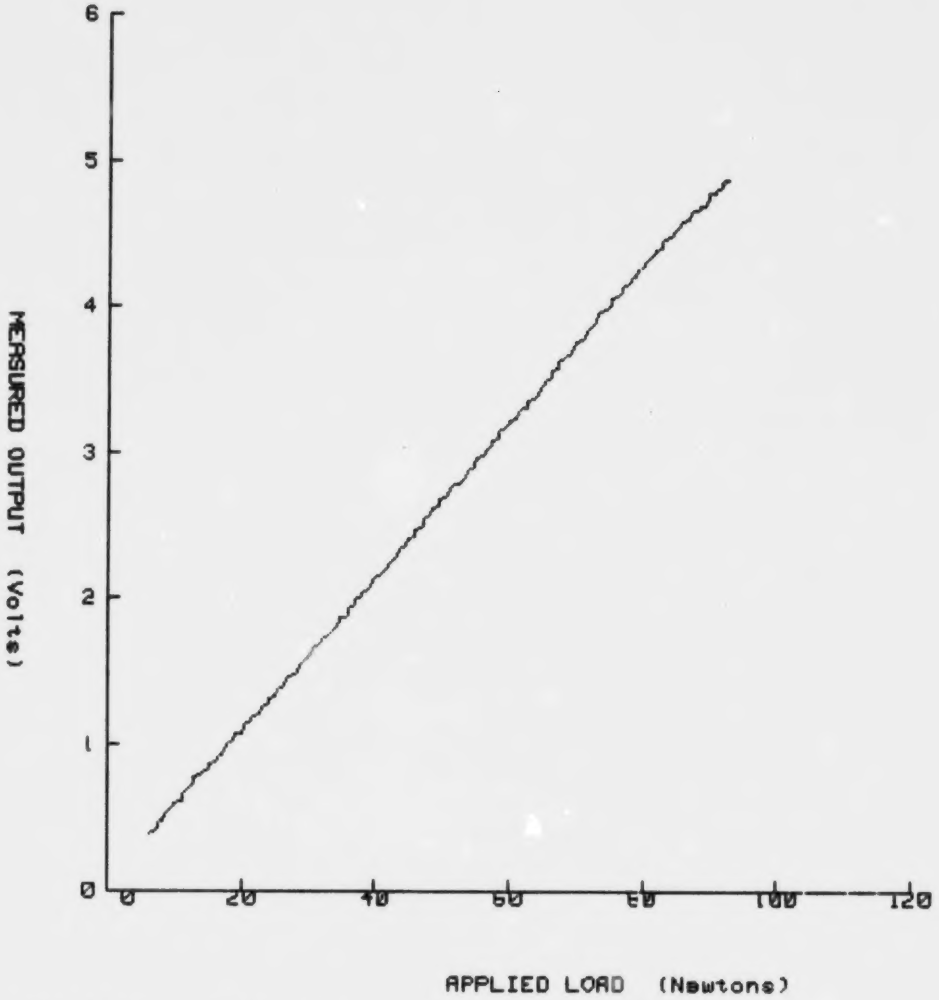

```
EXCITATION = 5.00 Volts
      GAIN = 2000 Volts/Volts

  SENSITIVITY= .5276 mV/V @ 100 Newtons

REGRESSION ANALYSIS :
             SLOPE  = .0528  Volts/Newton
         INTERCEPT  = .0416  Volts
 CORRELATION COEFF. = .9999

       CALIBRATION  = 18.95  Newtons/Volt
```

TRANSDUCER S/N: 103 JUL-09-83

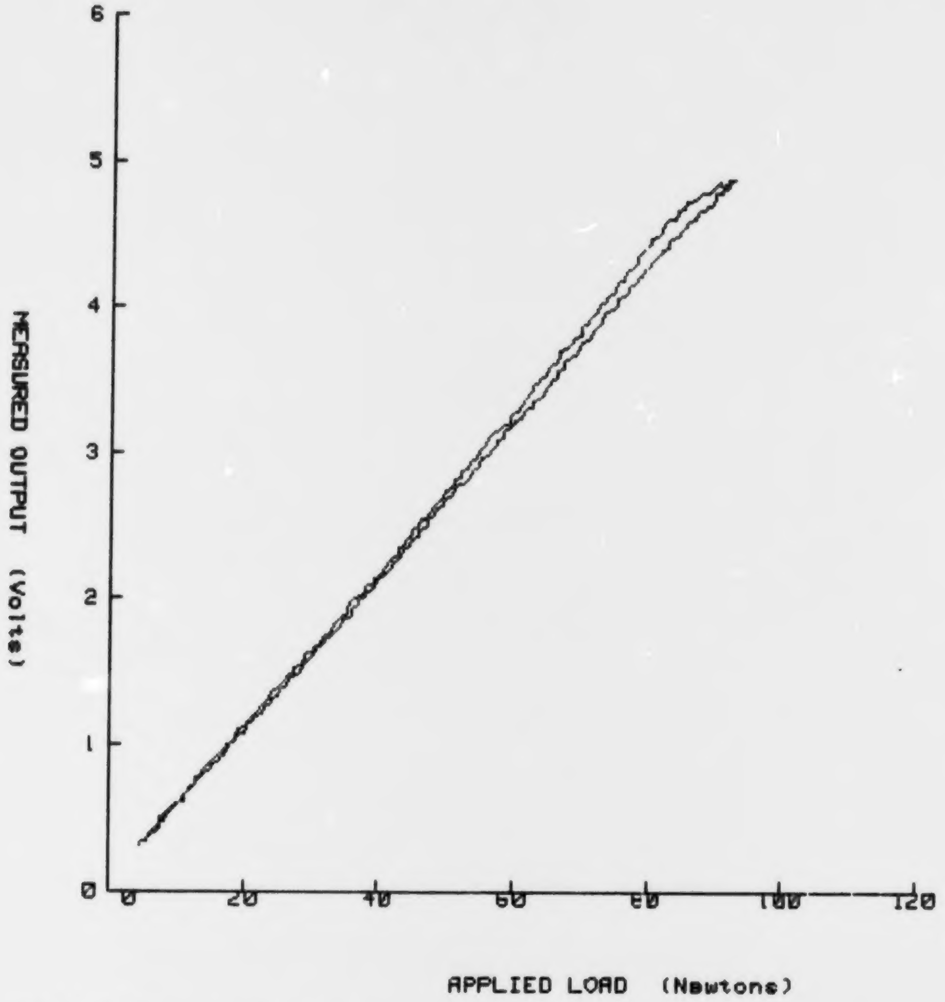

EXCITATION = 5.00 Volts
GAIN = 2000 Volts/Volts

SENSITIVITY= .5346 mV/V @ 100 Newtons
NON-LINEARITY= 1.3717 %
HYSTERESIS= 2.8494 %

REGRESSION ANALYSIS :
SLOPE = .0535 Volts/Newton
INTERCEPT = .0417 Volts
CORRELATION COEFF. = .9993

CALIBRATION = 18.71 Newtons/Volt

TRANSDUCER S/N: 104 JUL-11-83

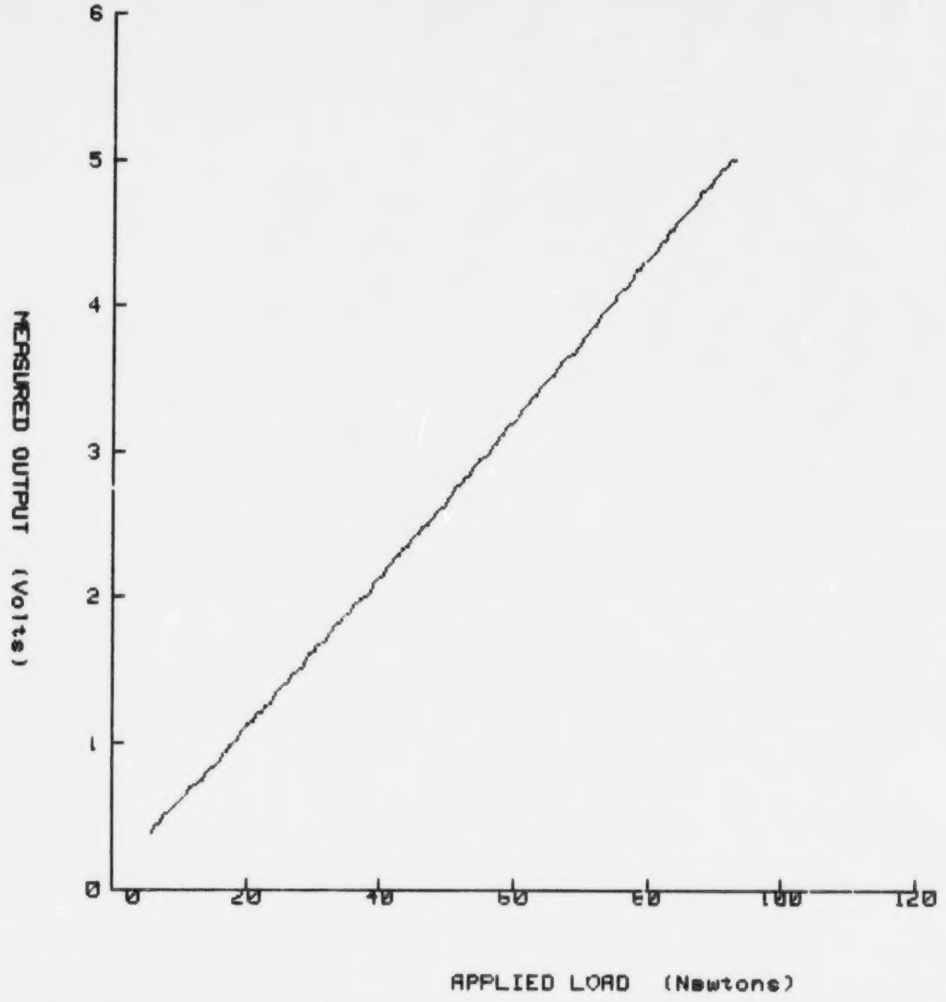

EXCITATION = 5.00 Volts
GAIN = 2000 Volts/Volts

SENSITIVITY= .5348 mV/V @ 100 Newtons

REGRESSION ANALYSIS :
SLOPE = .0535 Volts/Newton
INTERCEPT = .0323 Volts
CORRELATION COEFF. = .9998

CALIBRATION = 18.70 Newtons/Volt

TRANSDUCER S/N: 104 JUL-11-83

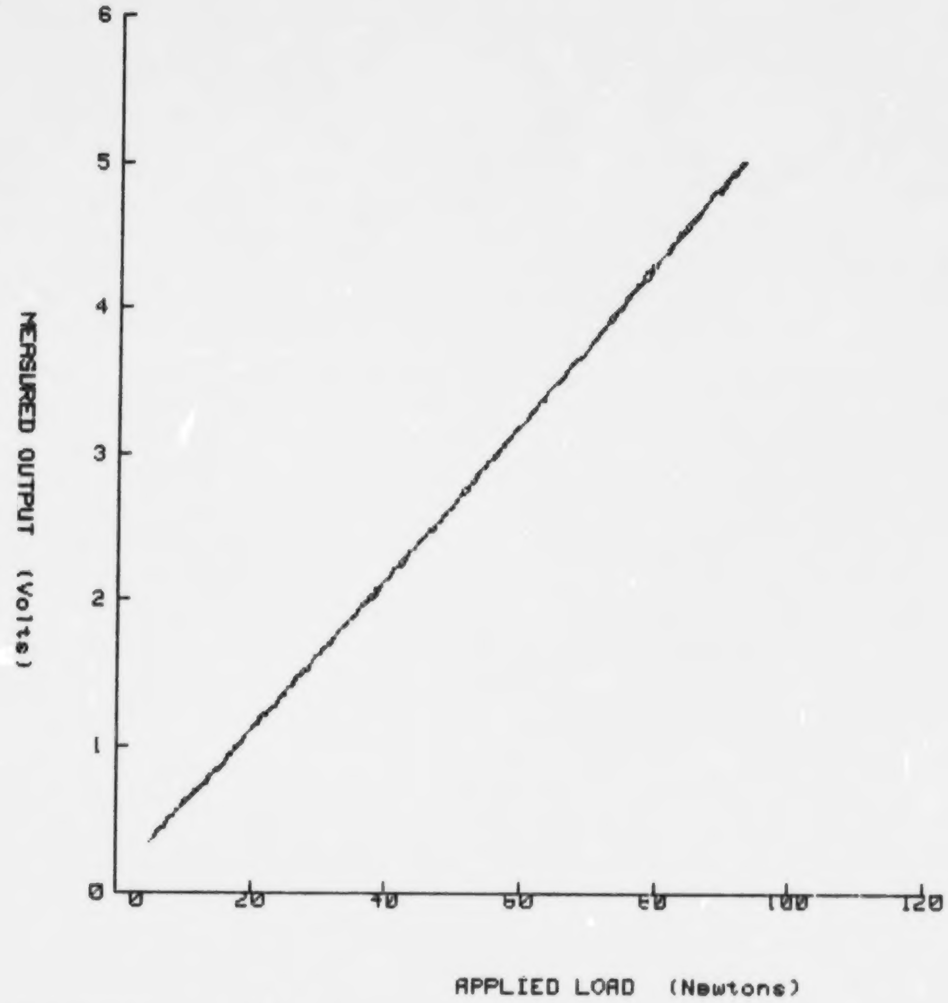

```
EXCITATION = 5.00 Volts
      GAIN = 2000 Volts/Volts

  SENSITIVITY= .5326 mV/V @ 100 Newtons
NON-LINEARITY= 1.6258 %
   HYSTERESIS= 1.0610 %

REGRESSION ANALYSIS :
              SLOPE   = .0533  Volts/Newton
          INTERCEPT   = .0404  Volts
 CORRELATION COEFF. = .9998

       CALIBRATION  = 18.77  Newtons/Volt
```

TRANSDUCER S/N: 105 JUL-11-83

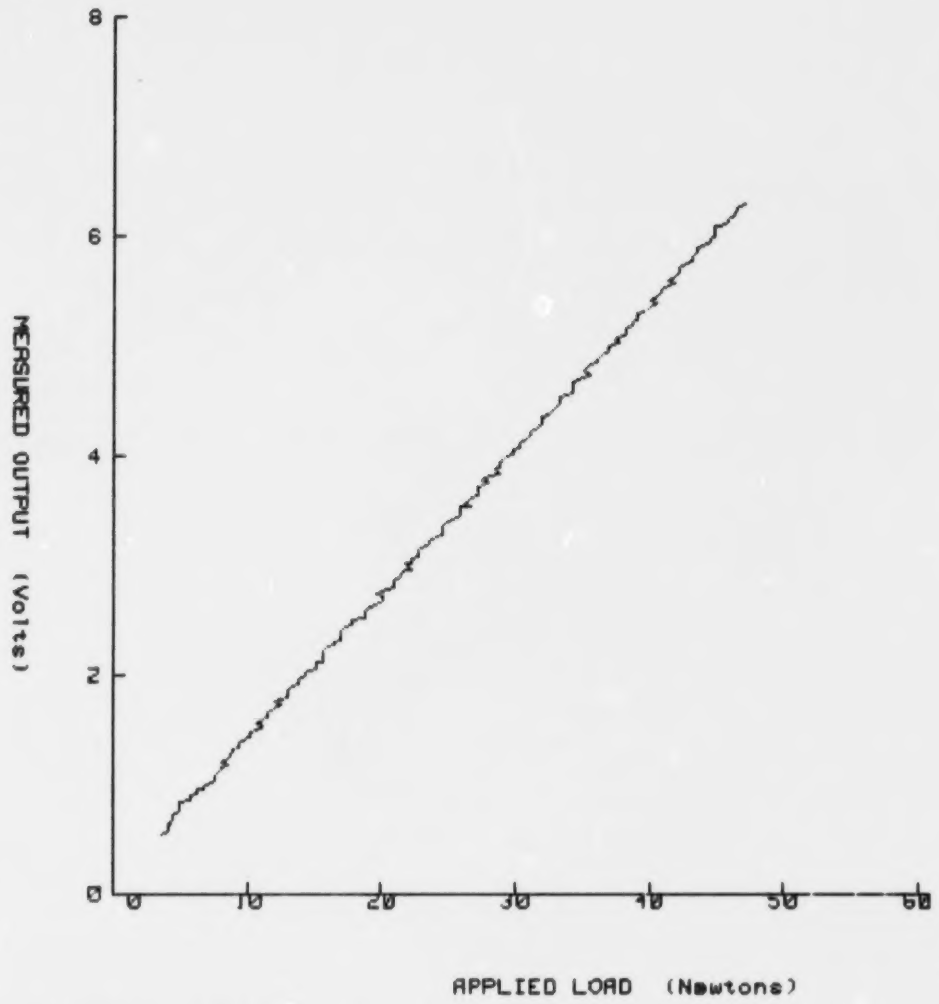

EXCITATION = 5.00 Volts
GAIN = 2000 Volts/Volts

SENSITIVITY= .6595 mV/V @ 50 Newtons

REGRESSION ANALYSIS :
SLOPE = .1319 Volts/Newton
INTERCEPT = .1021 Volts
CORRELATION COEFF. = .9998

CALIBRATION = 7.58 Newtons/Volt

TRANSDUCER S/N: 105

JUL-11-83

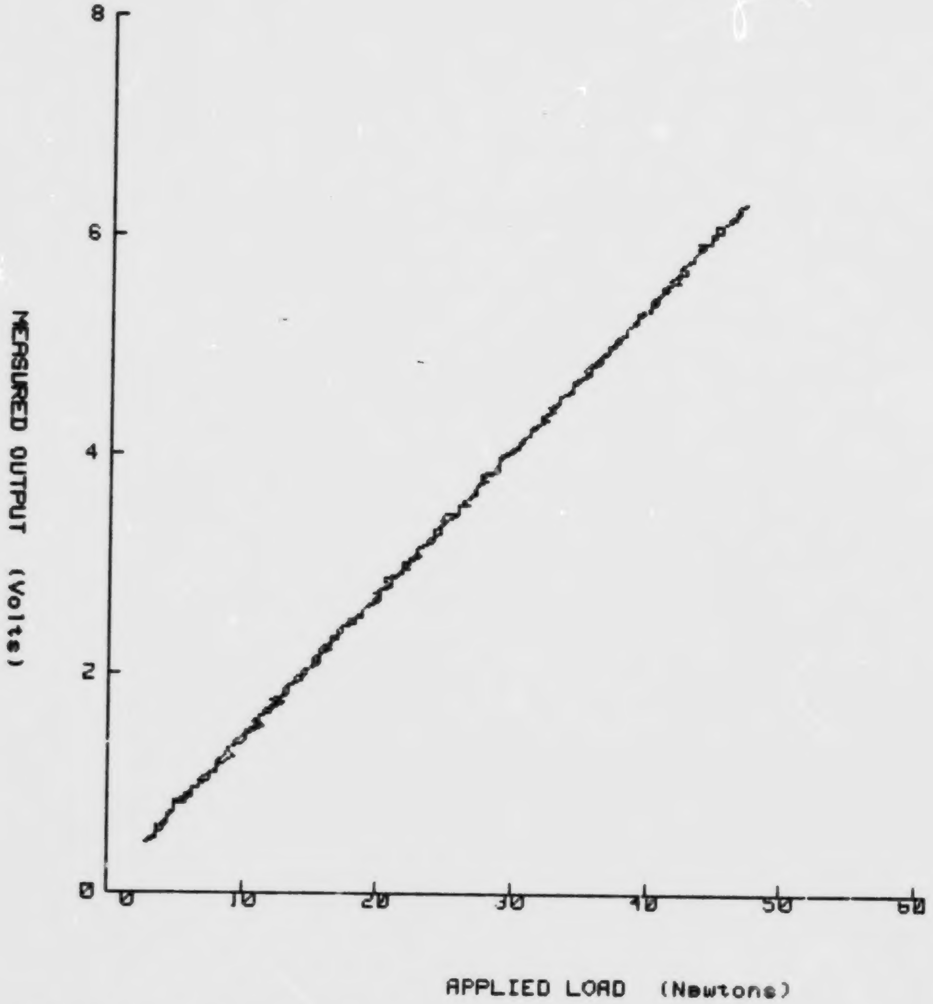

EXCITATION = 5.00 Volts
GAIN = 2000 Volts/Volts

SENSITIVITY= .6599 mV/V @ 50 Newtons
NON-LINEARITY= 1.2388 %
HYSTERESIS= 1.0626 %

REGRESSION ANALYSIS :
SLOPE = .1320 Volts/Newton
INTERCEPT = .0943 Volts
CORRELATION COEFF. = .9998

CALIBRATION = 7.58 Newtons/Volt

TRANSDUCER S/N: 106

JUL-09-83

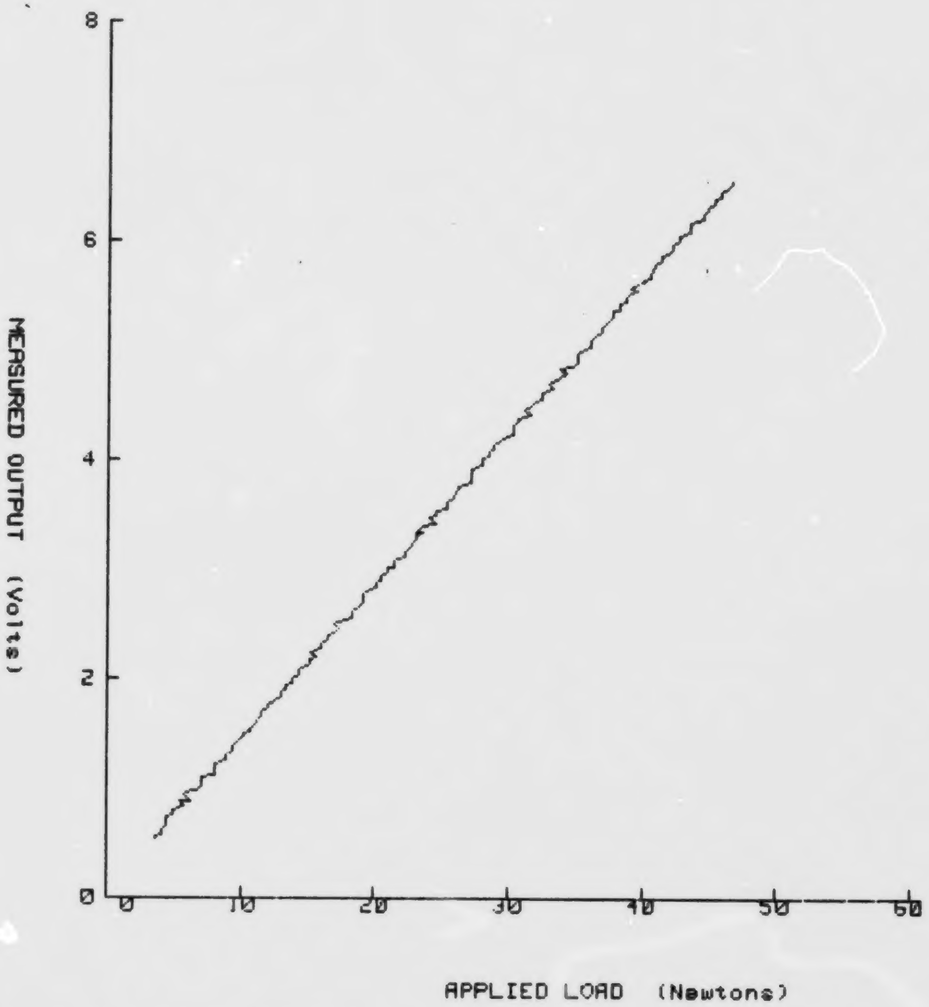

EXCITATION = 5.00 Volts
GAIN = 2000 Volts/Volts

SENSITIVITY= .6968 mV/V @ 50 Newtons

REGRESSION ANALYSIS :
SLOPE = .1394 Volts/Newton
INTERCEPT = .0642 Volts
CORRELATION COEFF. = .9998

CALIBRATION = 7.18 Newtons/Volt

TRANSDUCER S/N: 106 JUL-09-83

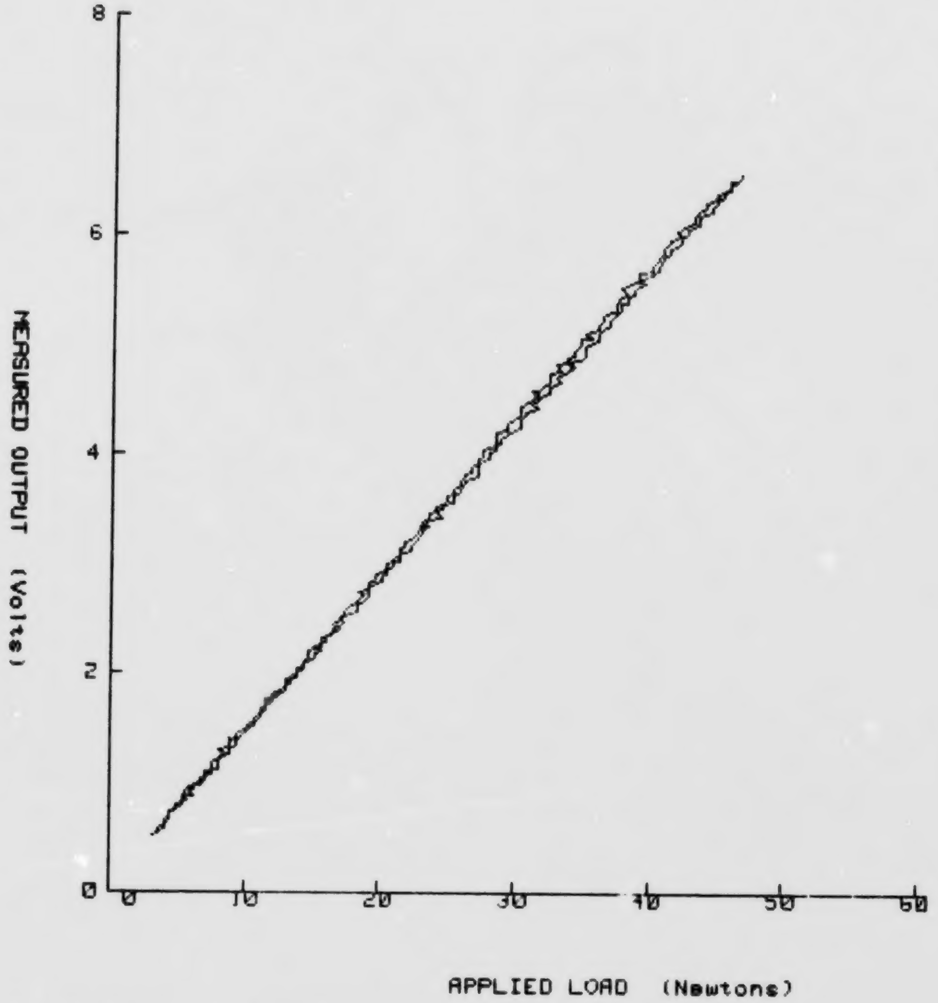

```
EXCITATION = 5.00 Volts
      GAIN = 2000 Volts/Volts

  SENSITIVITY= .7004 mV/V @ 50 Newtons
NON-LINEARITY= 1.9846 %
   HYSTERESIS= 1.8437 %

REGRESSION ANALYSIS :
             SLOPE  = .1401  Volts/Newton
         INTERCEPT  = .0775  Volts
 CORRELATION COEFF. = .9996

       CALIBRATION  = 7.14  Newtons/Volt
```

TRANSDUCER S/N: 107 JUL-08-83

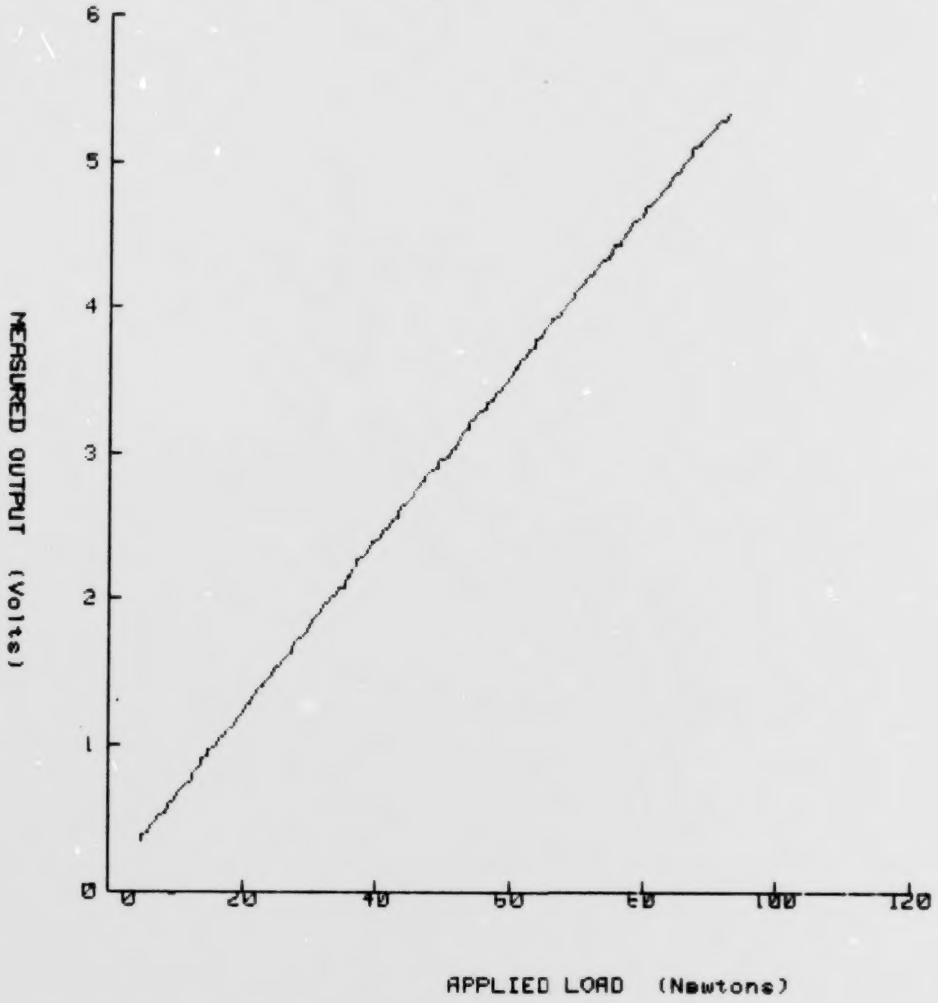

EXCITATION = 5.00 Volts
GAIN = 2000 Volts/Volts

SENSITIVITY= .5714 mV/V @ 100 Newtons

REGRESSION ANALYSIS :
SLOPE = .0571 Volts/Newton
INTERCEPT = .1056 Volts
CORRELATION COEFF. = .9999

CALIBRATION = 17.50 Newtons/Volt

TRANSDUCER S/N: 107

JUL-08-83

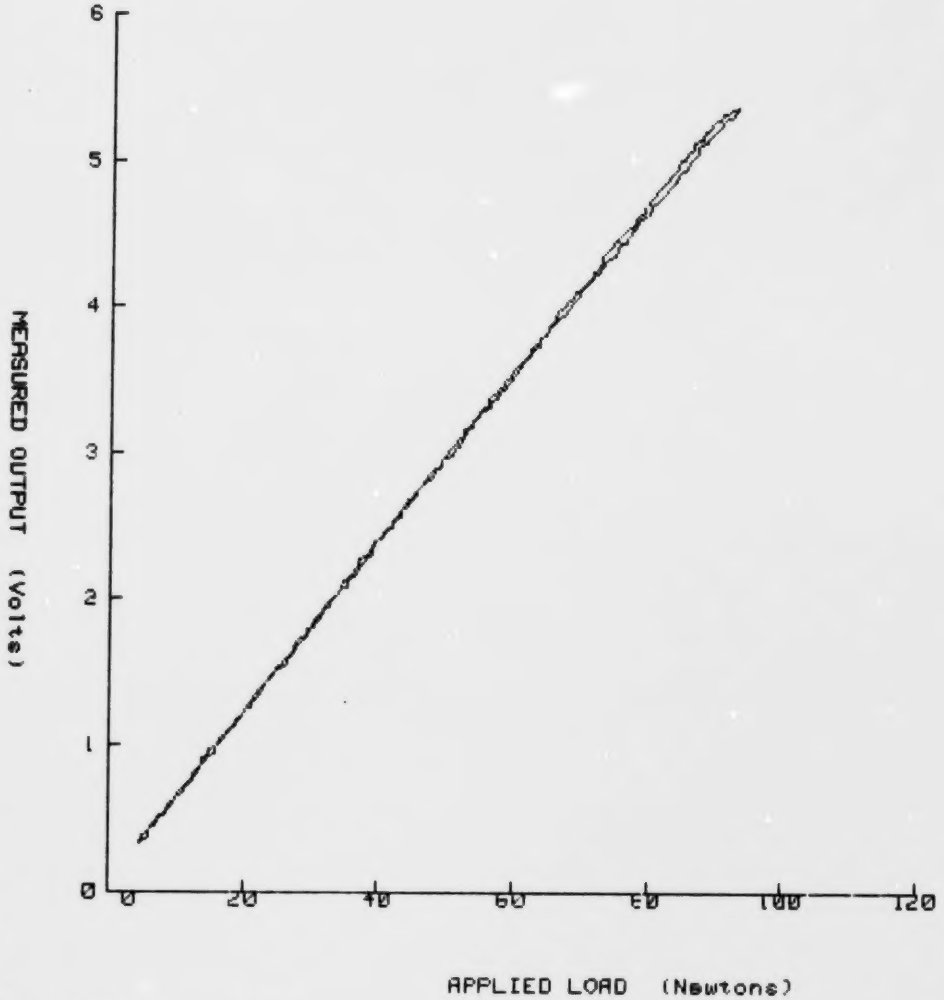

```
EXCITATION = 5.00 Volts
      GAIN = 2000 Volts/Volts

  SENSITIVITY= .5767 mV/V @ 100 Newtons
NON-LINEARITY= 1.6211 %
   HYSTERESIS= 1.6459 %

REGRESSION ANALYSIS :
            SLOPE  = .0577  Volts/Newton
        INTERCEPT  = .0869  Volts
 CORRELATION COEFF. = .9998

      CALIBRATION  = 17.34  Newtons/Volt
```

TRANSDUCER S/N: 108 JUL-09-83

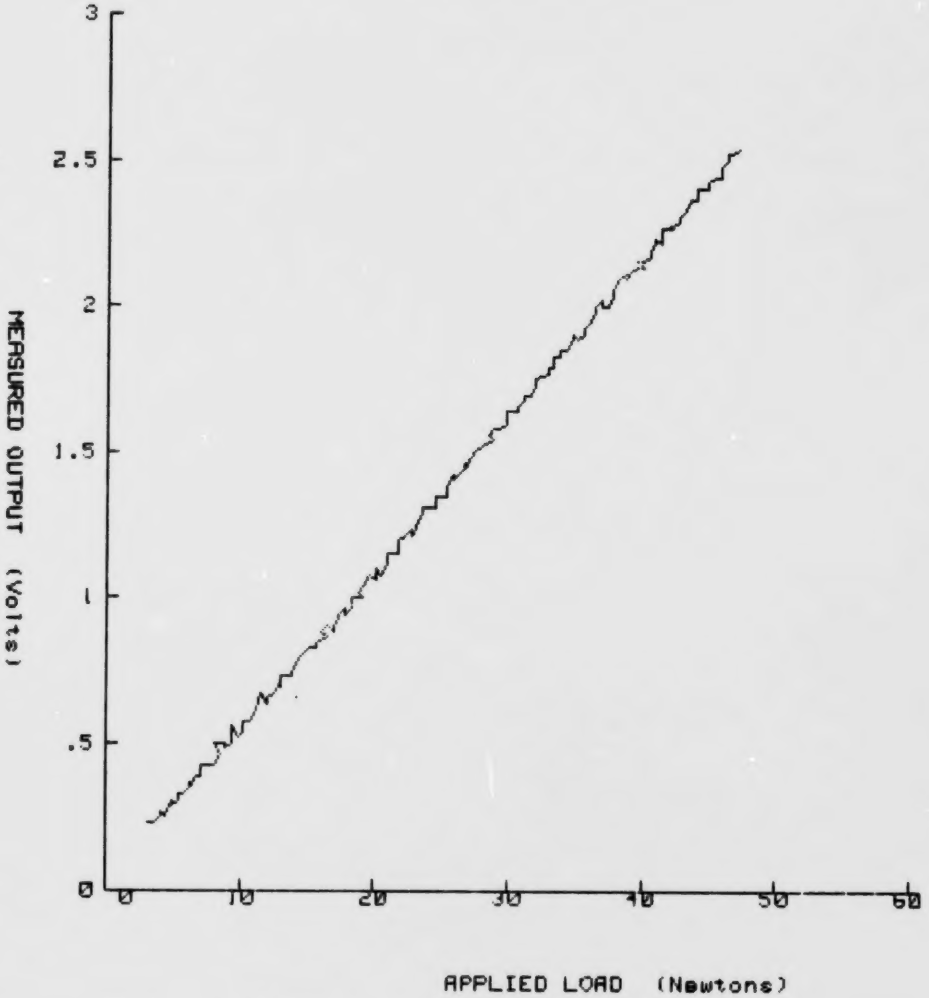

```
EXCITATION = 5.00 Volts
      GAIN = 2000 Volts/Volts

  SENSITIVITY= .2681 mV/V @ 50 Newtons

REGRESSION ANALYSIS :
             SLOPE   = .0536  Volts/Newton
         INTERCEPT   = .0178  Volts
 CORRELATION COEFF.  = .9997

       CALIBRATION   = 18.65  Newtons/Volt
```

TRANSDUCER S/N: 108

JUL-09-83

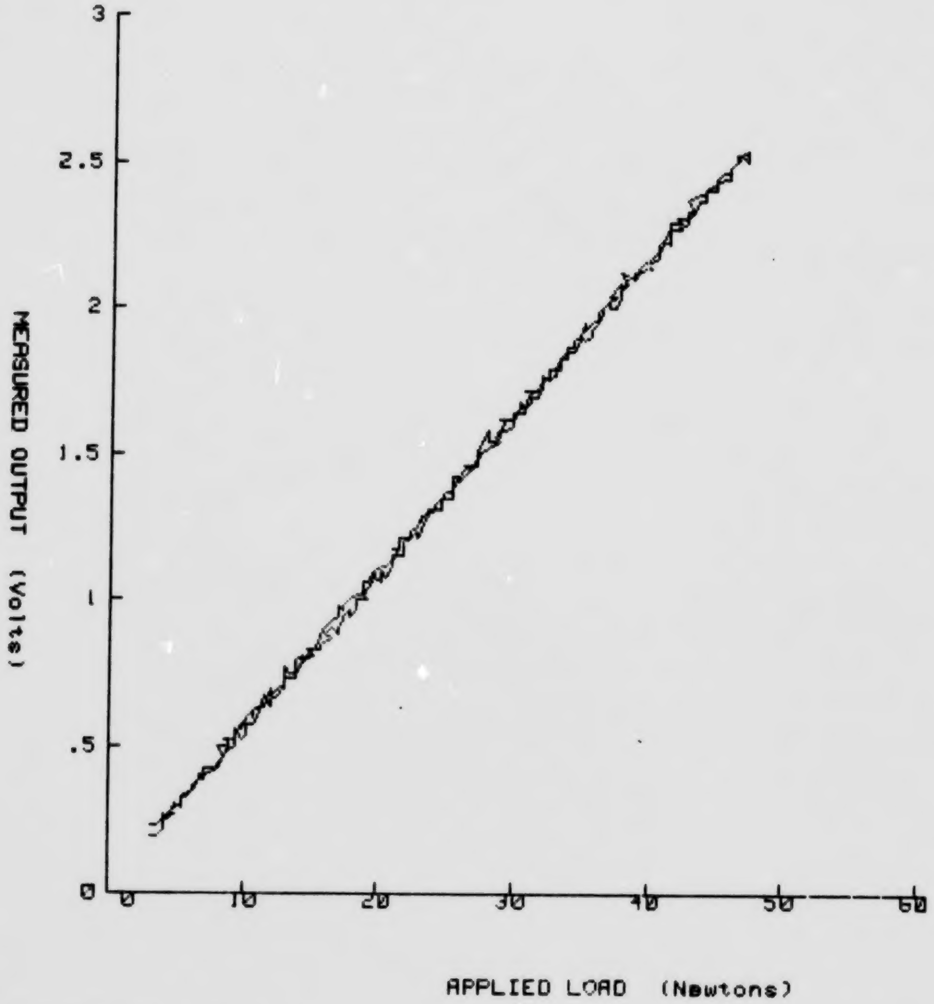

EXCITATION = 5.00 Volts
GAIN = 2000 Volts/Volts

SENSITIVITY= .2685 mV/V @ 50 Newtons
NON-LINEARITY= 1.7384 %
HYSTERESIS= 2.8447 %

REGRESSION ANALYSIS :
SLOPE = .0537 Volts/Newton
INTERCEPT = .0244 Volts
CORRELATION COEFF. = .9996

CALIBRATION = 18.62 Newtons/Volt

TRANSDUCER S/N: 109 JUL-09-83

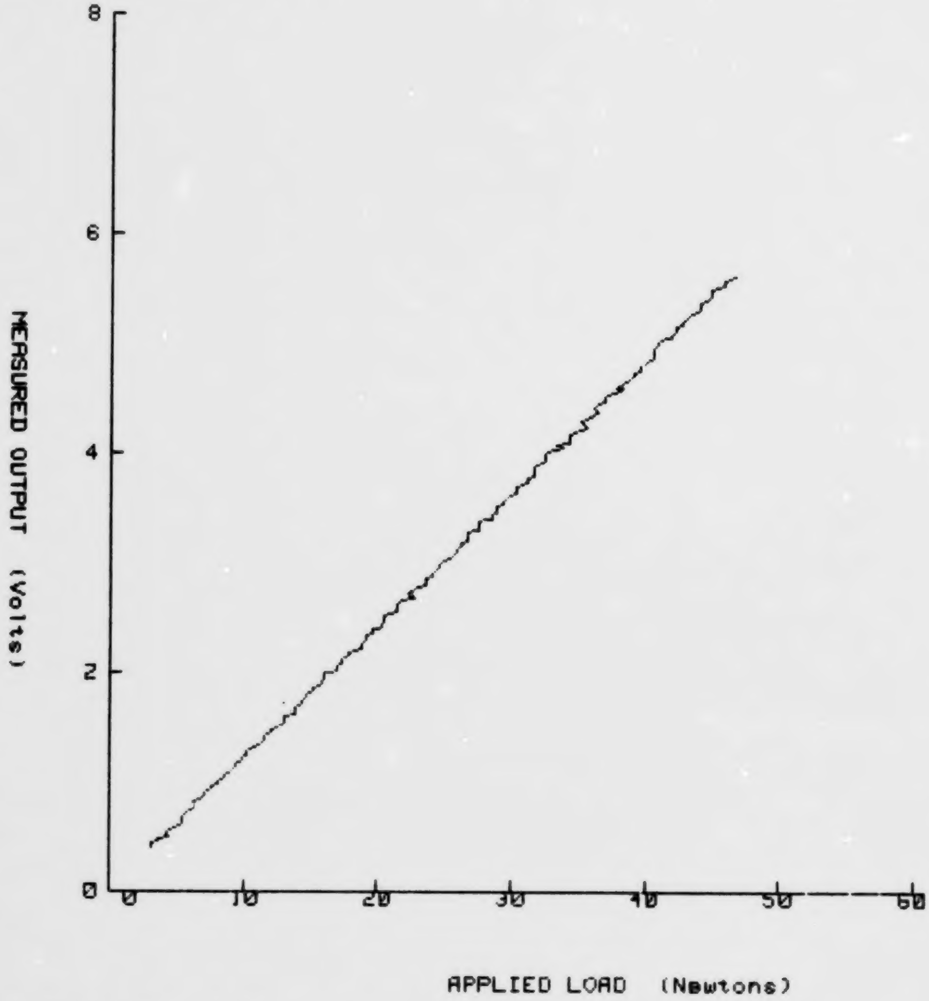

EXCITATION = 5.00 Volts
GAIN = 2000 Volts/Volts

SENSITIVITY= .6058 mV/V @ 50 Newtons

REGRESSION ANALYSIS :
SLOPE = .1212 Volts/Newton
INTERCEPT = .0005 Volts
CORRELATION COEFF. = .9998

CALIBRATION = 8.25 Newtons/Volt

TRANSDUCER S/N: 109 JUL-09-83

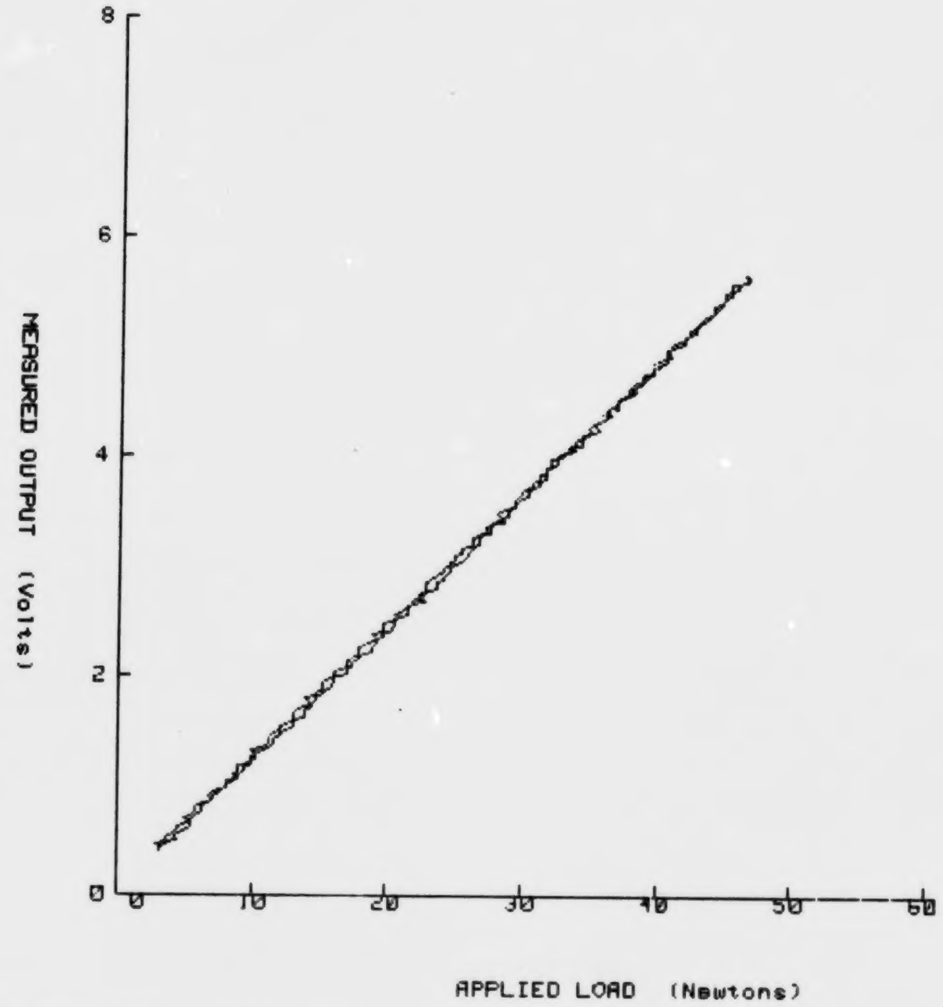

EXCITATION = 5.00 Volts
GAIN = 2000 Volts/Volts

SENSITIVITY= .6018 mV/V @ 50 Newtons
NON-LINEARITY= 1.4477 %
HYSTERESIS= 1.7513 %

REGRESSION ANALYSIS :
SLOPE = .1204 Volts/Newton
INTERCEPT = .0401 Volts
CORRELATION COEFF. = .9997

CALIBRATION = 8.31 Newtons/Volt

TRANSDUCER S/N: 110 JUL-08-83

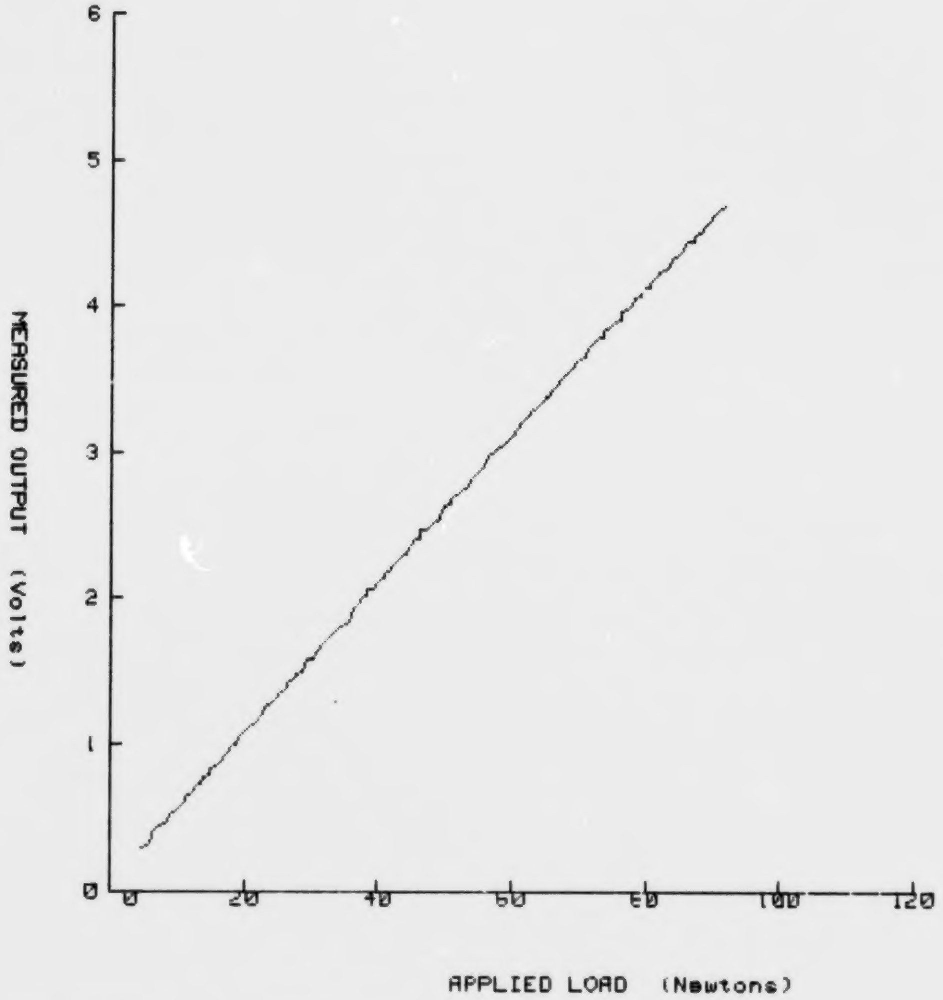

```
EXCITATION = 5.00 Volts
      GAIN = 2000 Volts/Volts

  SENSITIVITY= .5090 mV/V @ 100 Newtons

REGRESSION ANALYSIS :
             SLOPE   = .0509  Volts/Newton
         INTERCEPT   = .0685  Volts
 CORRELATION COEFF. = .9999

       CALIBRATION  = 19.64  Newtons/Volt
```

TRANSDUCER S/N: 110 JUL-08-83

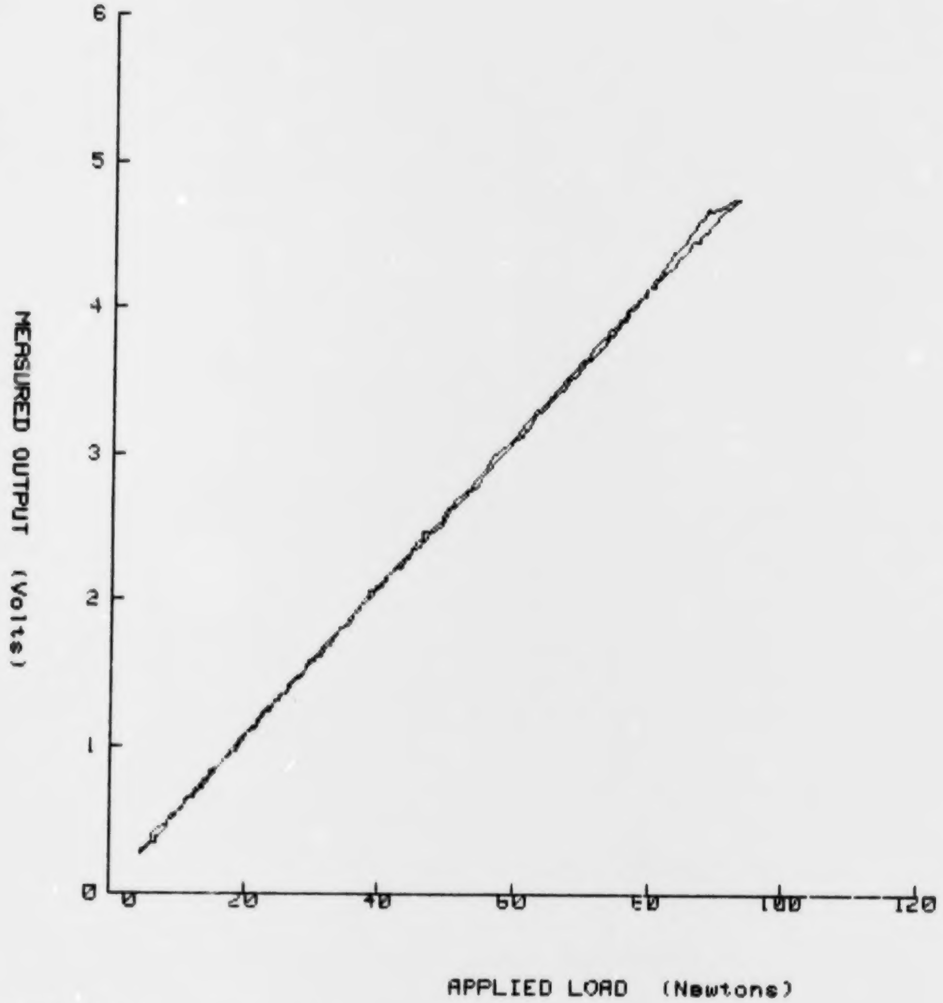

```
EXCITATION = 5.00 Volts
      GAIN = 2000 Volts/Volts

  SENSITIVITY= .5121 mV/V @ 100 Newtons
NON-LINEARITY= 1.6915 %
   HYSTERESIS= 2.7094 %

REGRESSION ANALYSIS :
              SLOPE  = .0512  Volts/Newton
          INTERCEPT  = .0495  Volts
 CORRELATION COEFF. = .9998

       CALIBRATION  = 19.53  Newtons/Volt
```

TRANSDUCER S/N: 111

JUL-11-83

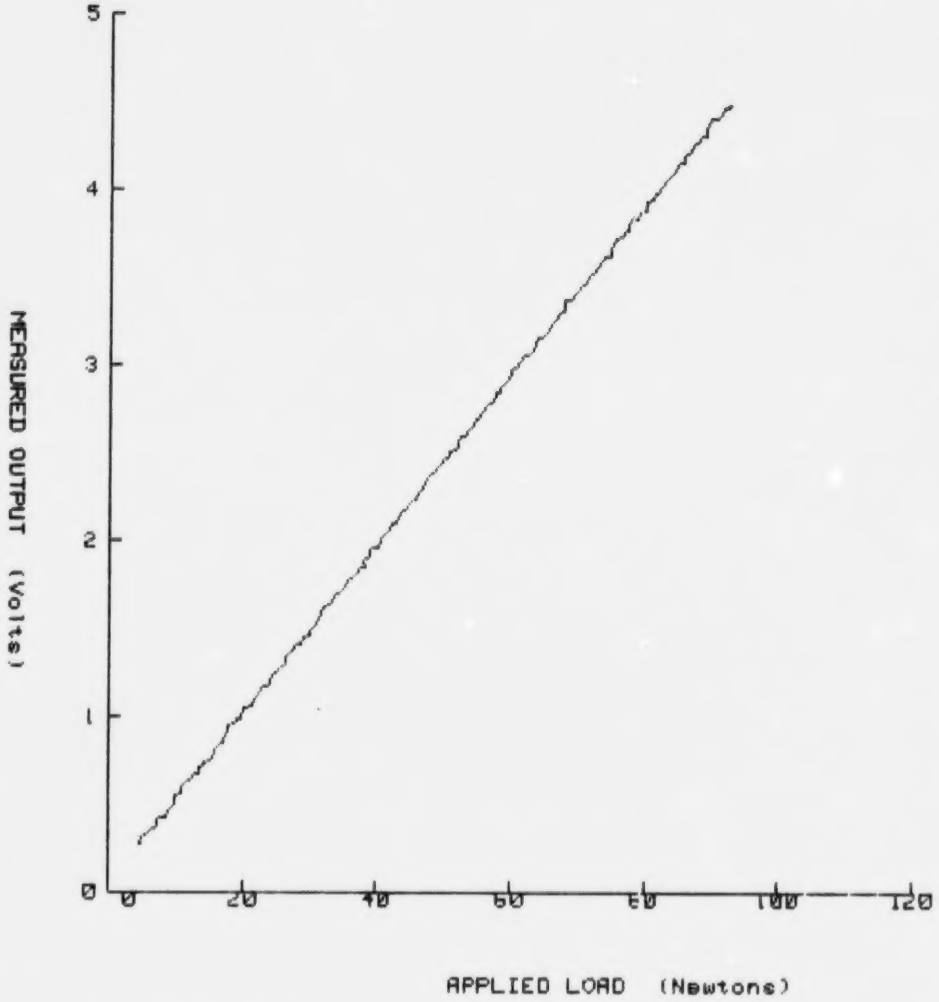

EXCITATION = 5.00 Volts
GAIN = 2000 Volts/Volts

SENSITIVITY= .4825 mV/V @ 100 Newtons

REGRESSION ANALYSIS :
SLOPE = .0482 Volts/Newton
INTERCEPT = .0488 Volts
CORRELATION COEFF. = .9999

CALIBRATION = 20.73 Newtons/Volt

TRANSDUCER S/N: 111 JUL-11-83

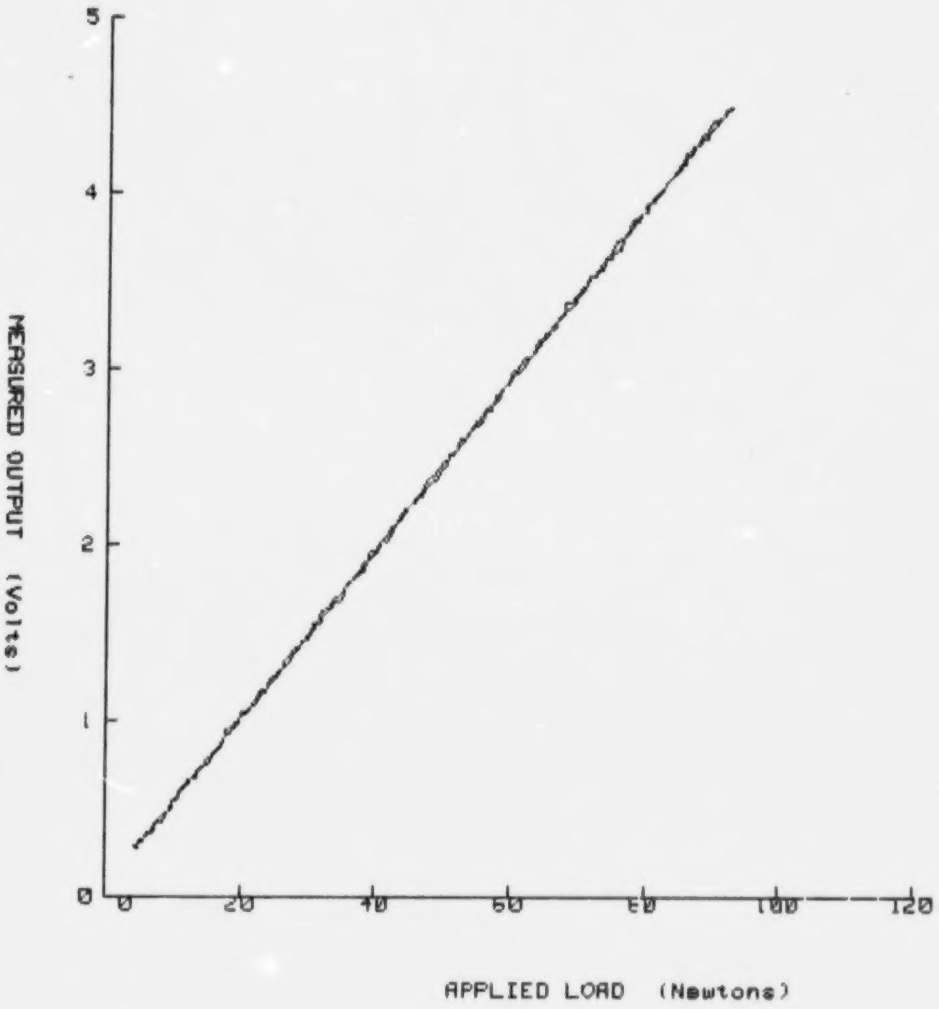

EXCITATION = 5.00 Volts
GAIN = 2000 Volts/Volts

SENSITIVITY= .4824 mV/V @ 100 Newtons
NON-LINEARITY= 1.2238 %
HYSTERESIS= .8515 %

REGRESSION ANALYSIS :
SLOPE = .0482 Volts/Newton
INTERCEPT = .0449 Volts
CORRELATION COEFF. = .9999

CALIBRATION = 20.73 Newtons/Volt

```
TRANSDUCER S/N: 112                                                  JUL-08-83
```

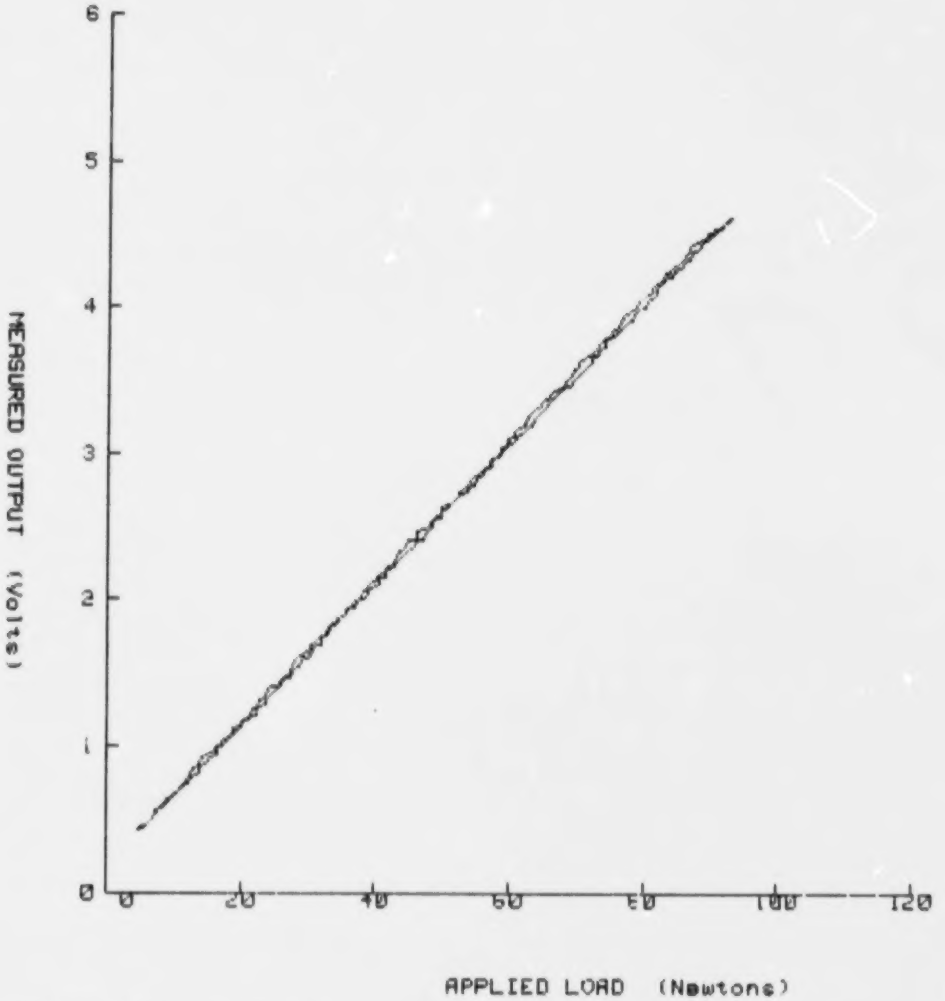

```
EXCITATION = 5.00 Volts
      GAIN = 2000 Volts/Volts

  SENSITIVITY= .4807 mV/V @ 100 Newtons
NON-LINEARITY= 1.1397 %
   HYSTERESIS= 1.5404 %

REGRESSION ANALYSIS :
             SLOPE   = .0481  Volts/Newton
         INTERCEPT   = .1968  Volts
 CORRELATION COEFF.  = .9998

       CALIBRATION   = 20.80  Newtons/Volt
```

TRANSDUCER S/N: 112 JUL-08-83

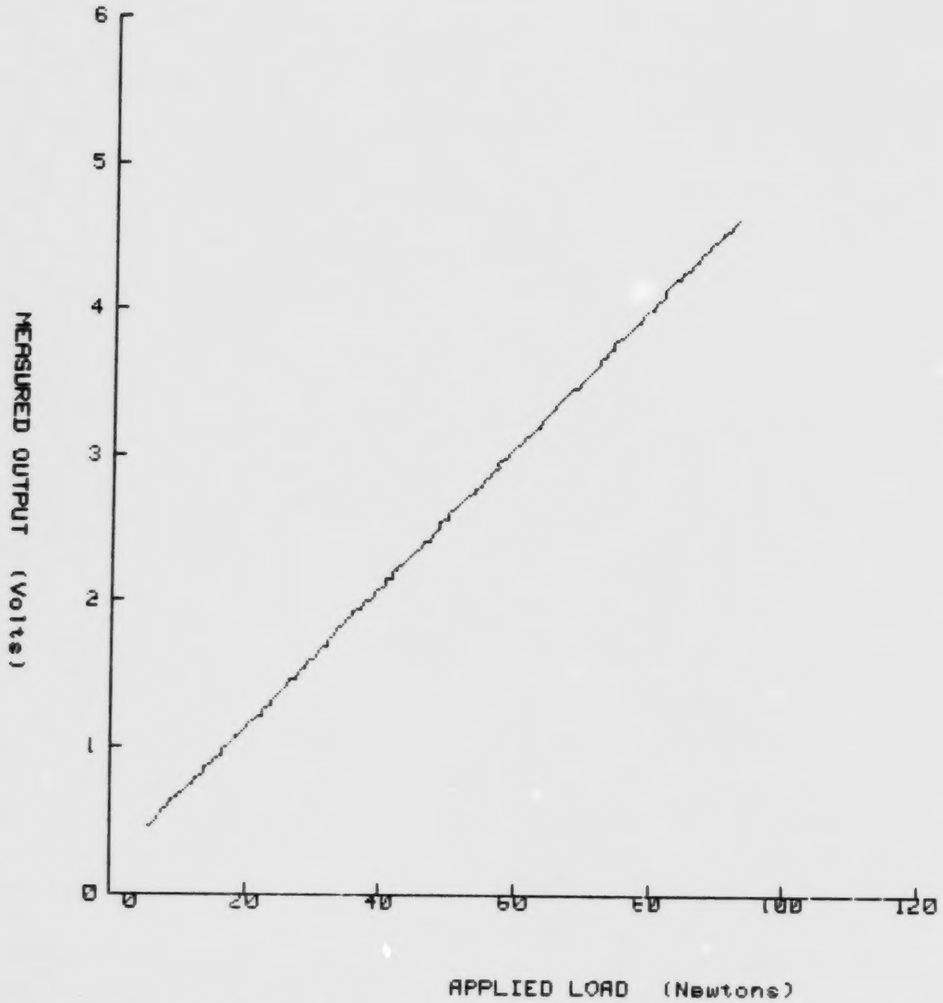

```
EXCITATION = 5.00 Volts
      GAIN = 2000 Volts/Volts

  SENSITIVITY= .4794 mV/V @ 100 Newtons

REGRESSION ANALYSIS :
             SLOPE  = .0479  Volts/Newton
         INTERCEPT  = .1868  Volts
 CORRELATION COEFF. = .9999

       CALIBRATION  = 20.86  Newtons/Volt
```

TRANSDUCER S/N: 113 JUL-09-83

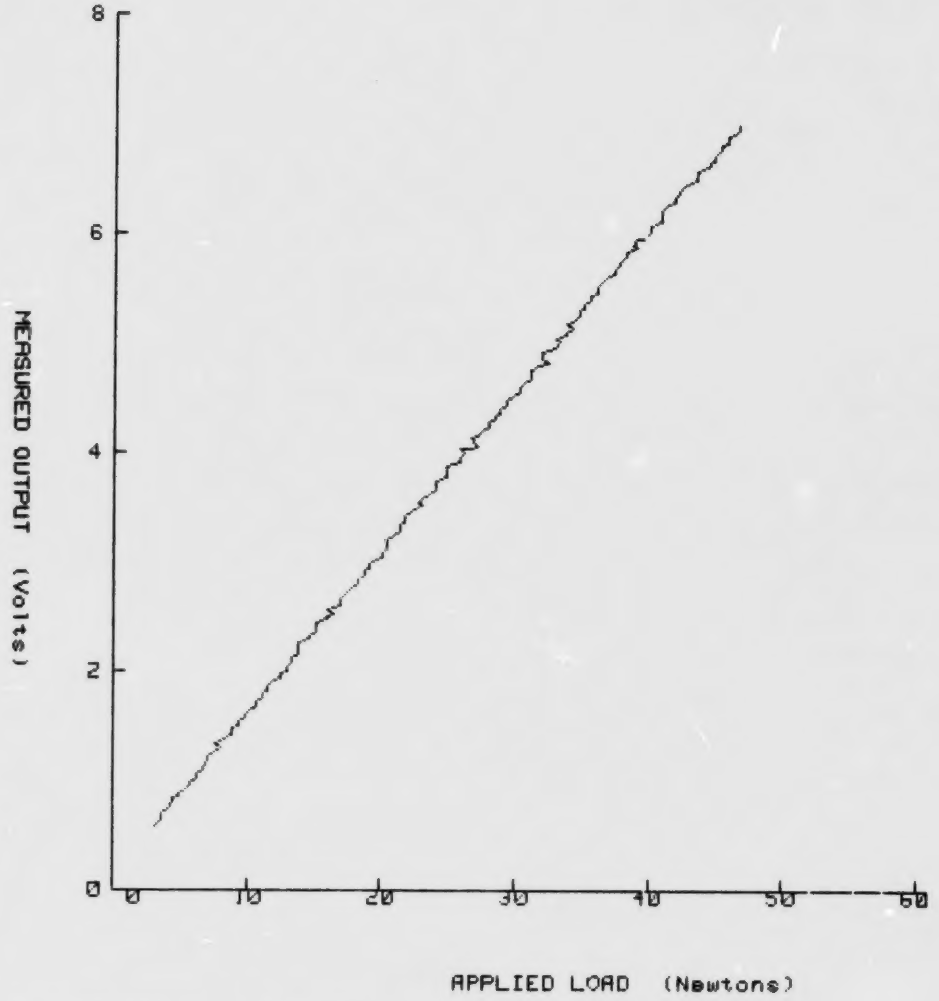

EXCITATION = 5.00 Volts
GAIN = 2000 Volts/Volts

SENSITIVITY= .7362 mV/V @ 50 Newtons

REGRESSION ANALYSIS :
SLOPE = .1472 Volts/Newton
INTERCEPT = .1417 Volts
CORRELATION COEFF. = .9998

CALIBRATION = 6.79 Newtons/Volt

TRANSDUCER S/N: 113 JUL-09-83

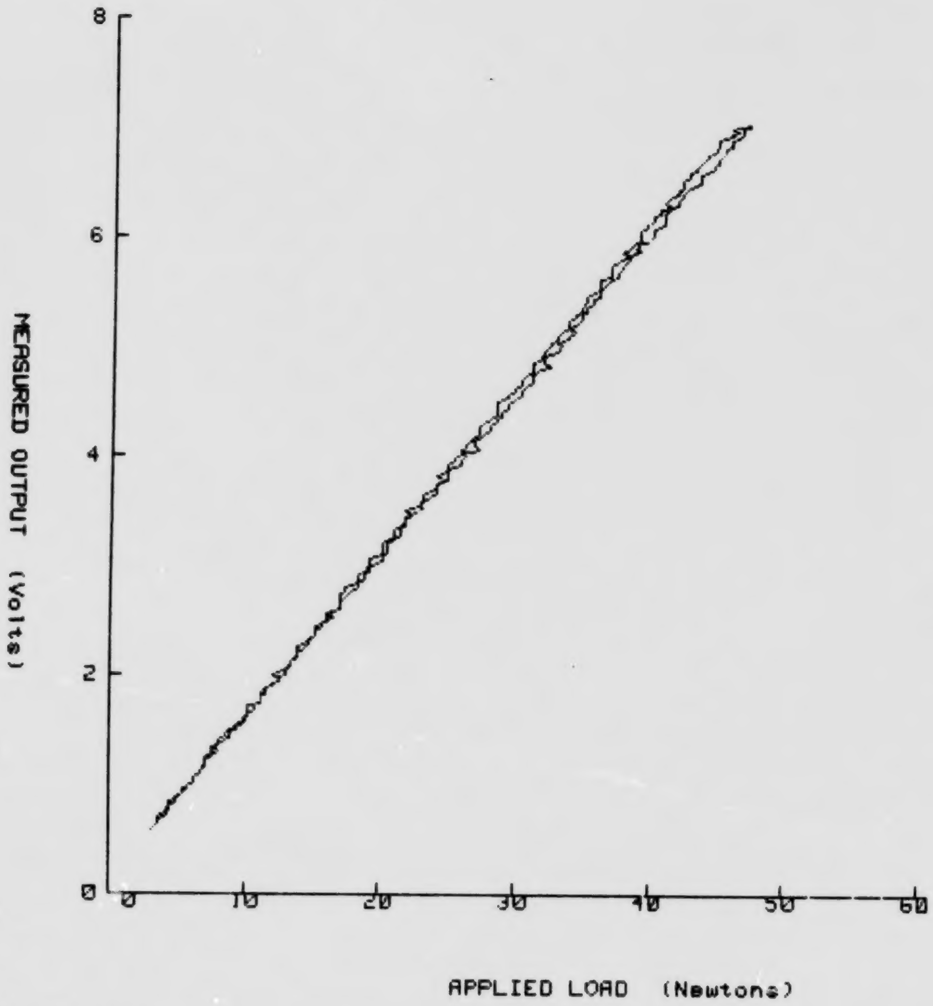

```
EXCITATION = 5.00 Volts
      GAIN = 2000 Volts/Volts

  SENSITIVITY= .7436 mV/V @ 50 Newtons
NON-LINEARITY= 1.5840 %
   HYSTERESIS= 2.0959 %

REGRESSION ANALYSIS :
             SLOPE   = .1487  Volts/Newton
         INTERCEPT   = .1358  Volts
 CORRELATION COEFF.  = .9996

       CALIBRATION   = 6.72  Newtons/Volt
```

TRANSDUCER S/N: 114 JUL-07-83

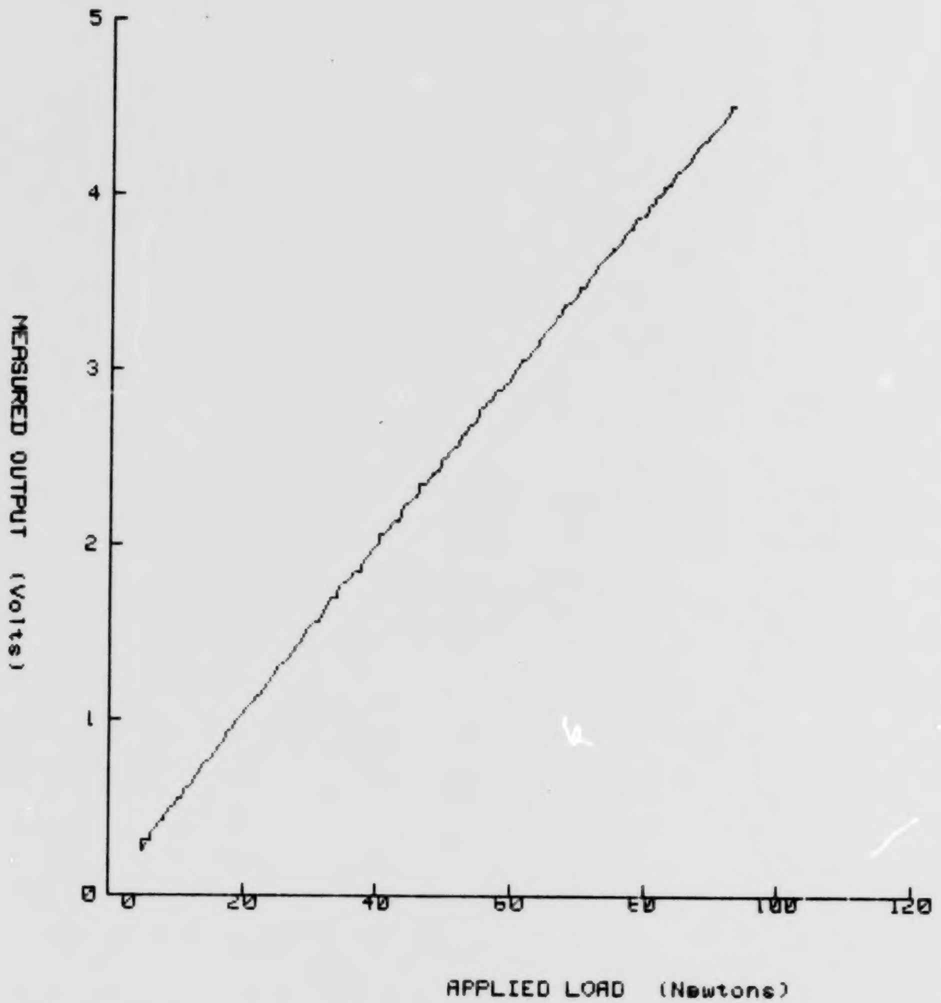

```
EXCITATION = 5.00 Volts
      GAIN = 2000 Volts/Volts

  SENSITIVITY= .4805 mV/V @ 100 Newtons

REGRESSION ANALYSIS :
            SLOPE   = .0480  Volts/Newton
        INTERCEPT   = .0743  Volts
 CORRELATION COEFF. = .9998

      CALIBRATION   = 20.81  Newtons/Volt
```

TRANSDUCER S/N: 114 JUL-07-83

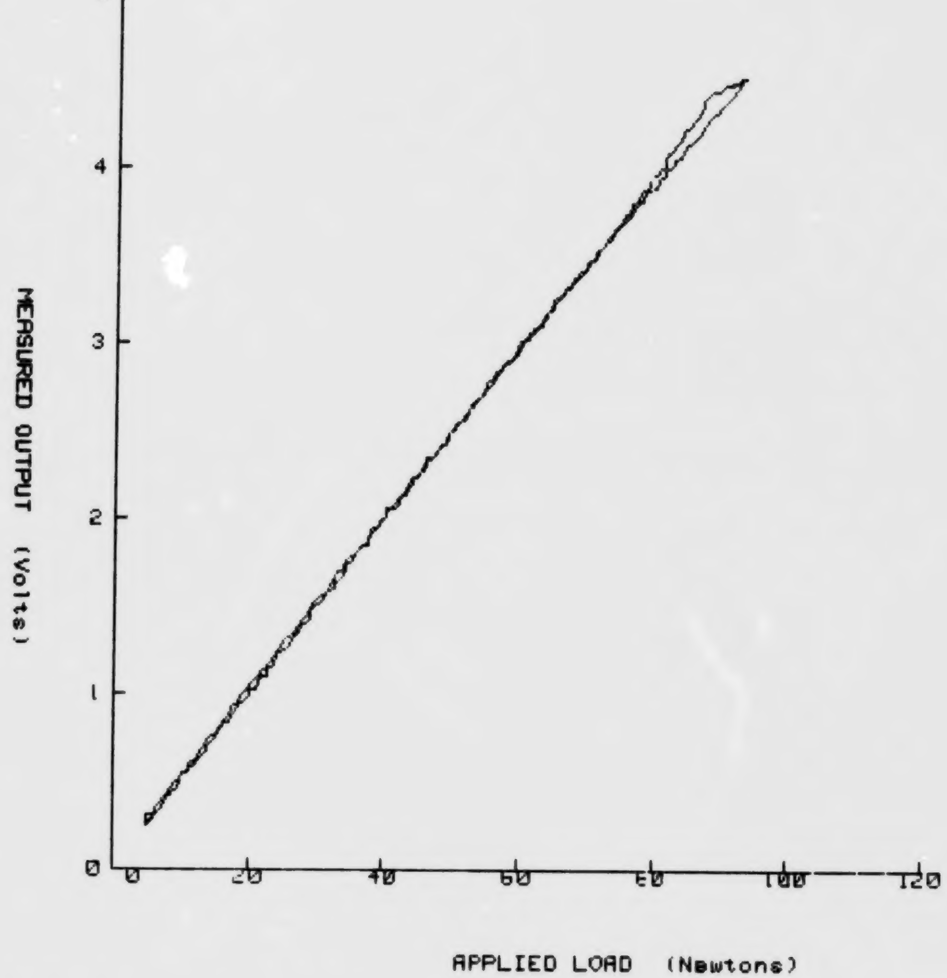

```
EXCITATION = 5.00 Volts
      GAIN = 2000 Volts/Volts

  SENSITIVITY= .4867 mV/V @ 100 Newtons
NON-LINEARITY= 2.5103 %
   HYSTERESIS= 2.7452 %

REGRESSION ANALYSIS :
             SLOPE  = .0487  Volts/Newton
         INTERCEPT  = .0472  Volts
 CORRELATION COEFF. = .9997

       CALIBRATION  = 20.55  Newtons/Volt
```

TRANSDUCER S/N: 115 JUL-07-83

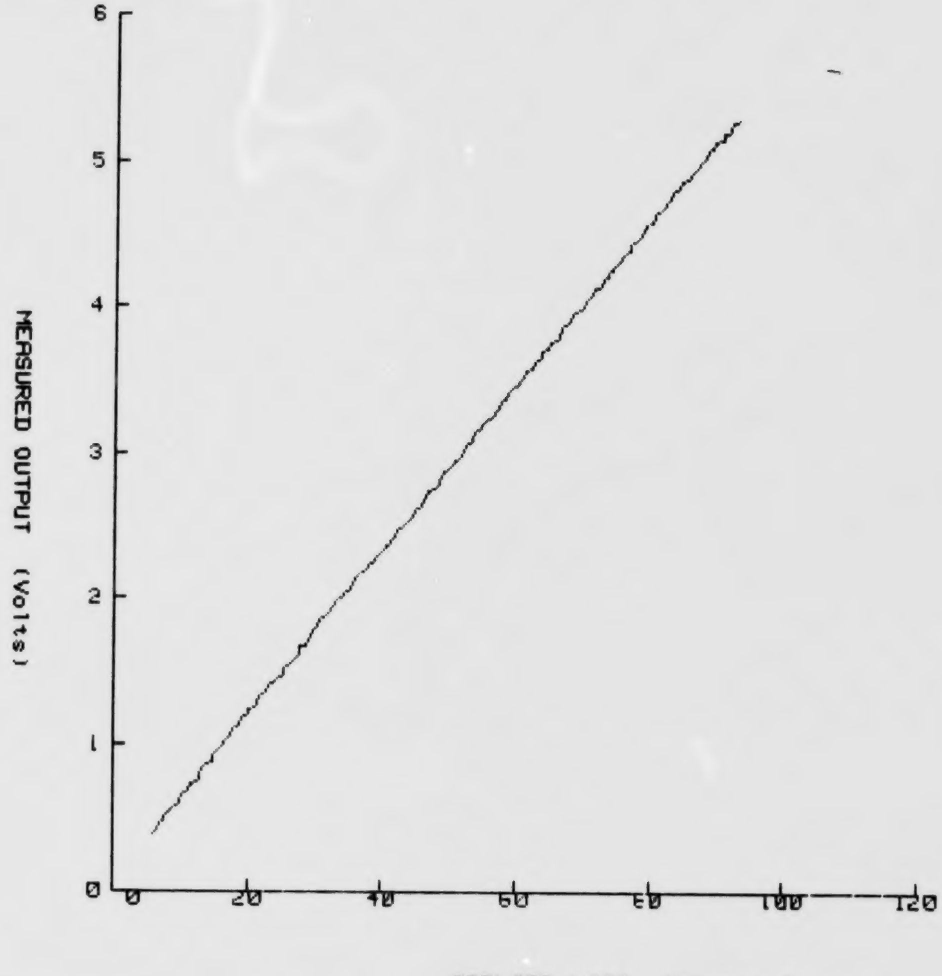

```
EXCITATION = 5.00 Volts
      GAIN = 2000 Volts/Volts

  SENSITIVITY= .5644 mV/V @ 100 Newtons

REGRESSION ANALYSIS :
             SLOPE  = .0564  Volts/Newton
         INTERCEPT  = .0816  Volts
 CORRELATION COEFF. = .9999

       CALIBRATION  = 17.72  Newtons/Volt
```

TRANSDUCER S/N: 115 JUL-07-83

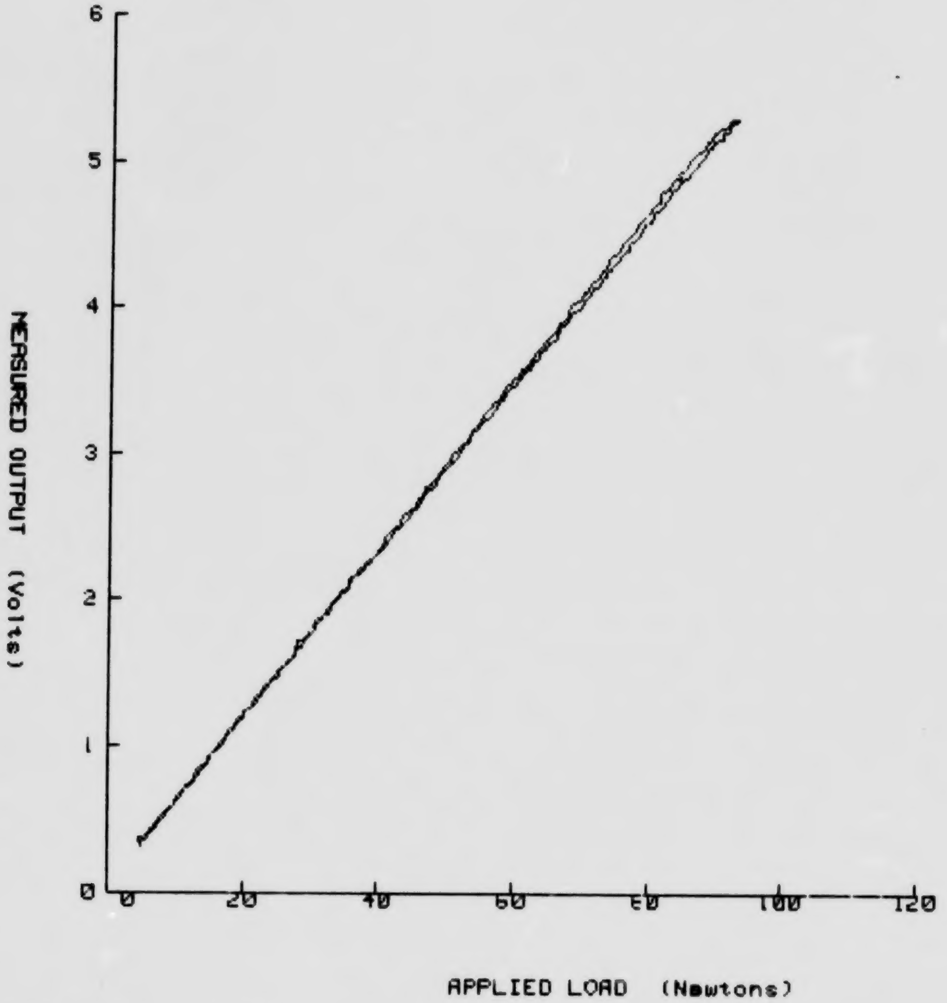

```
EXCITATION = 5.00 Volts
      GAIN = 2000 Volts/Volts

  SENSITIVITY= .5698 mV/V @ 100 Newtons
NON-LINEARITY= 1.2606 %
   HYSTERESIS= 1.4471 %

REGRESSION ANALYSIS :
            SLOPE   = .0570  Volts/Newton
        INTERCEPT   = .0673  Volts
 CORRELATION COEFF. = .9998

       CALIBRATION  = 17.55  Newtons/Volt
```

TRANSDUCER S/N: 116

JUL-11-83

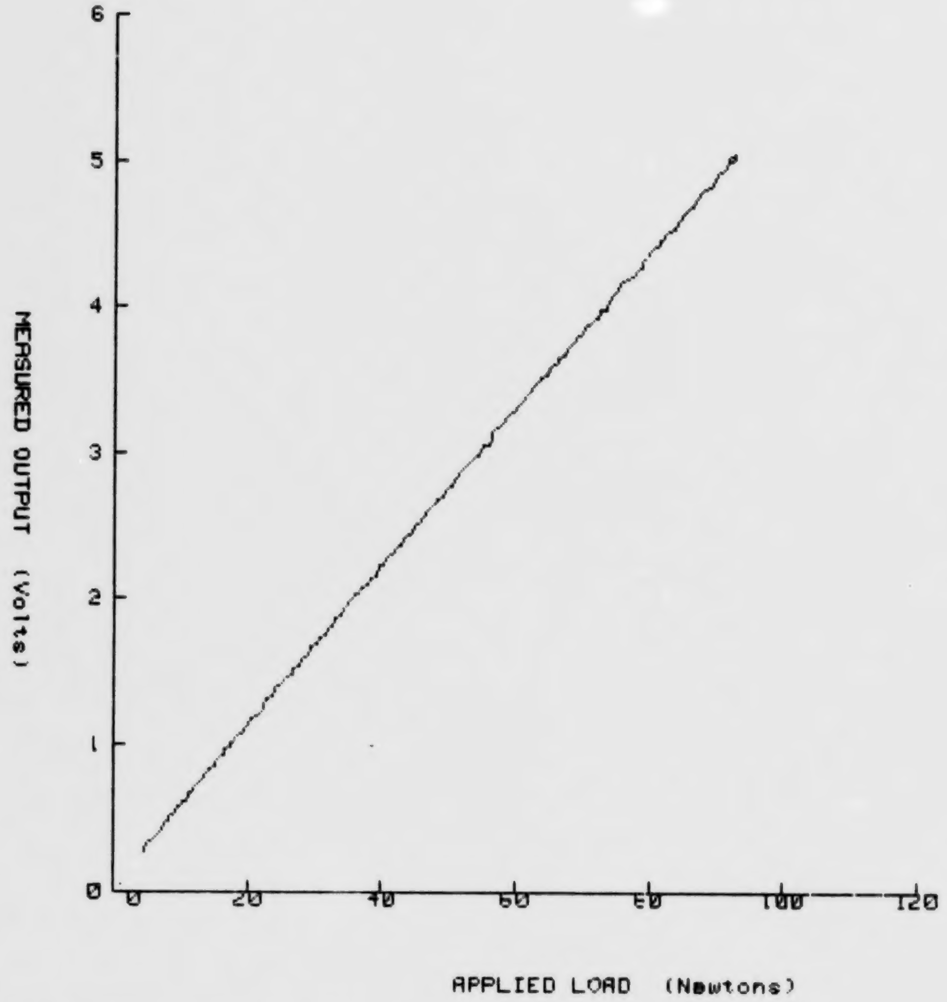

EXCITATION = 5.00 Volts
GAIN = 2000 Volts/Volts

SENSITIVITY= .5392 mV/V @ 100 Newtons

REGRESSION ANALYSIS :
SLOPE = .0539 Volts/Newton
INTERCEPT = .0657 Volts
CORRELATION COEFF. = .9999

CALIBRATION = 18.55 Newtons/Volt

TRANSDUCER S/N: 116 JUL-11-83

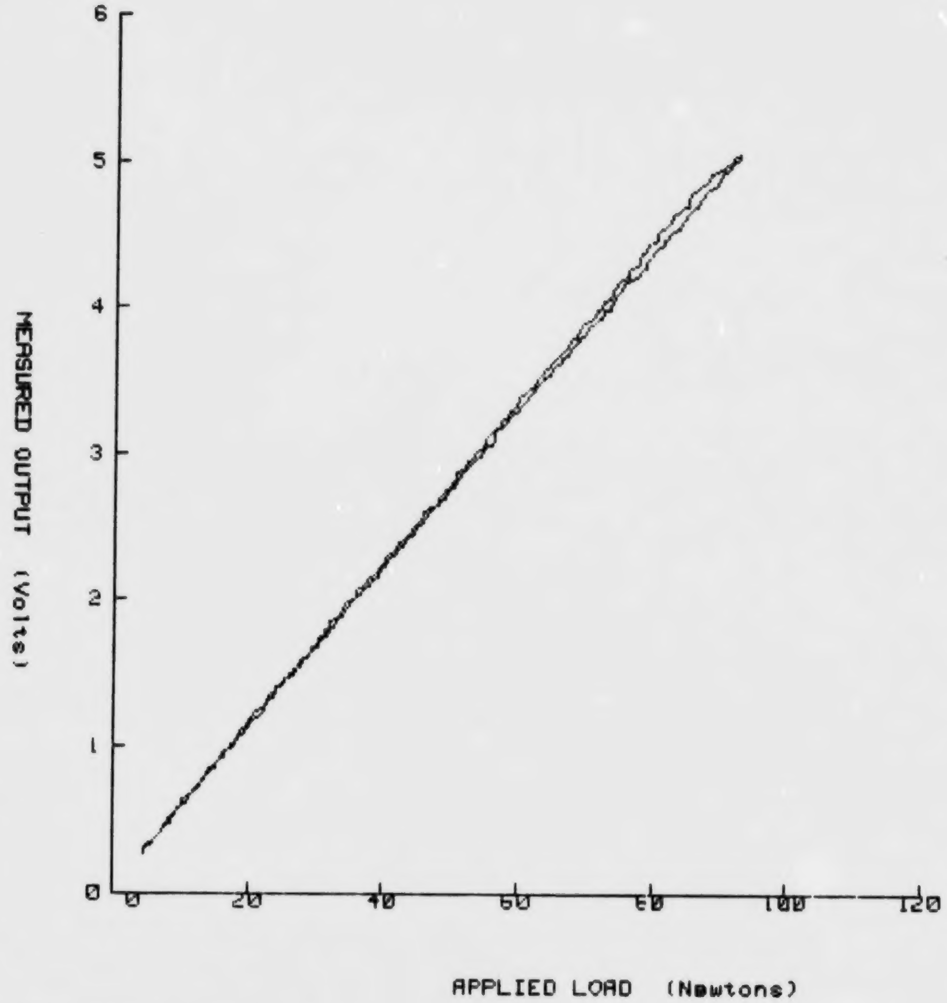

```
EXCITATION = 5.00 Volts
      GAIN = 2000 Volts/Volts

  SENSITIVITY= .5439 mV/V @ 100 Newtons
NON-LINEARITY= 1.3138 %
   HYSTERESIS= 2.1650 %

REGRESSION ANALYSIS :
            SLOPE    = .0544  Volts/Newton
        INTERCEPT    = .0618  Volts
 CORRELATION COEFF.  = .9998

       CALIBRATION   = 18.39  Newtons/Volt
```

TRANSDUCER S/N: 117

JUL-09-83

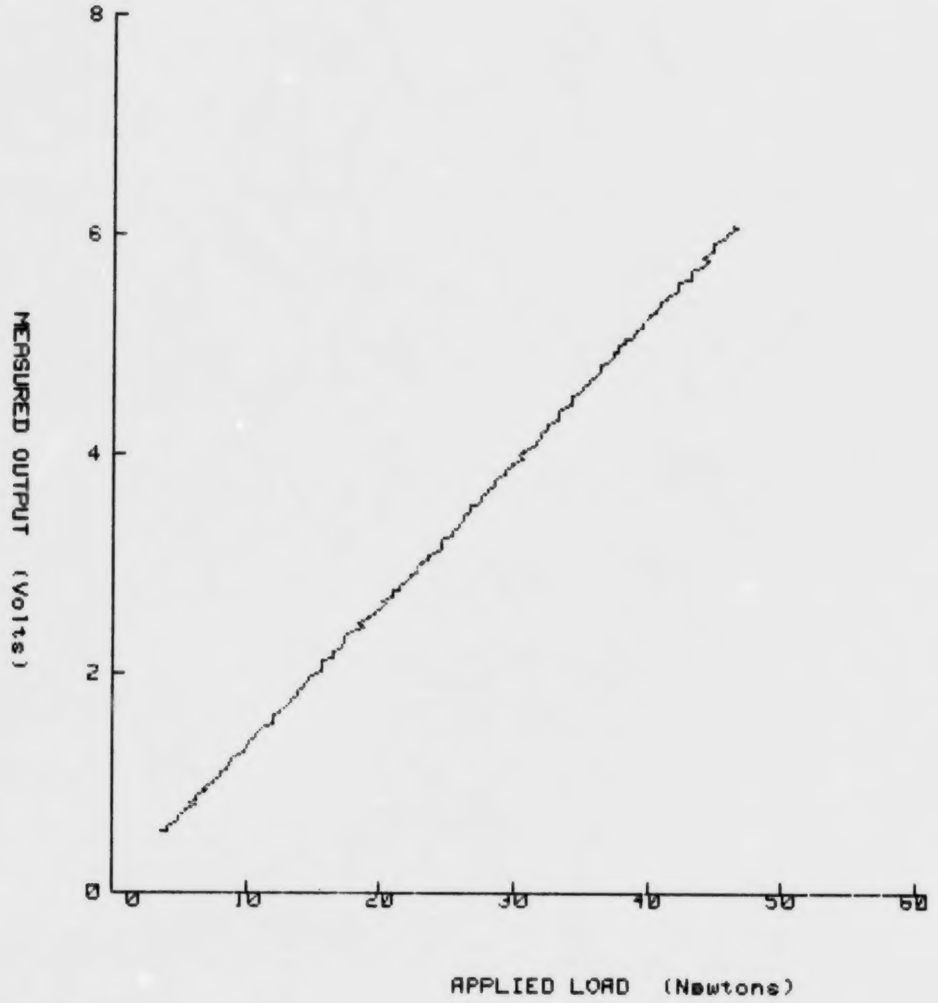

EXCITATION = 5.00 Volts
GAIN = 2000 Volts/Volts

SENSITIVITY= .6514 mV/V @ 50 Newtons

REGRESSION ANALYSIS :
SLOPE = .1303 Volts/Newton
INTERCEPT = .0200 Volts
CORRELATION COEFF. = .9998

CALIBRATION = 7.68 Newtons/Volt

TRANSDUCER S/N: 117

JUL-09-83

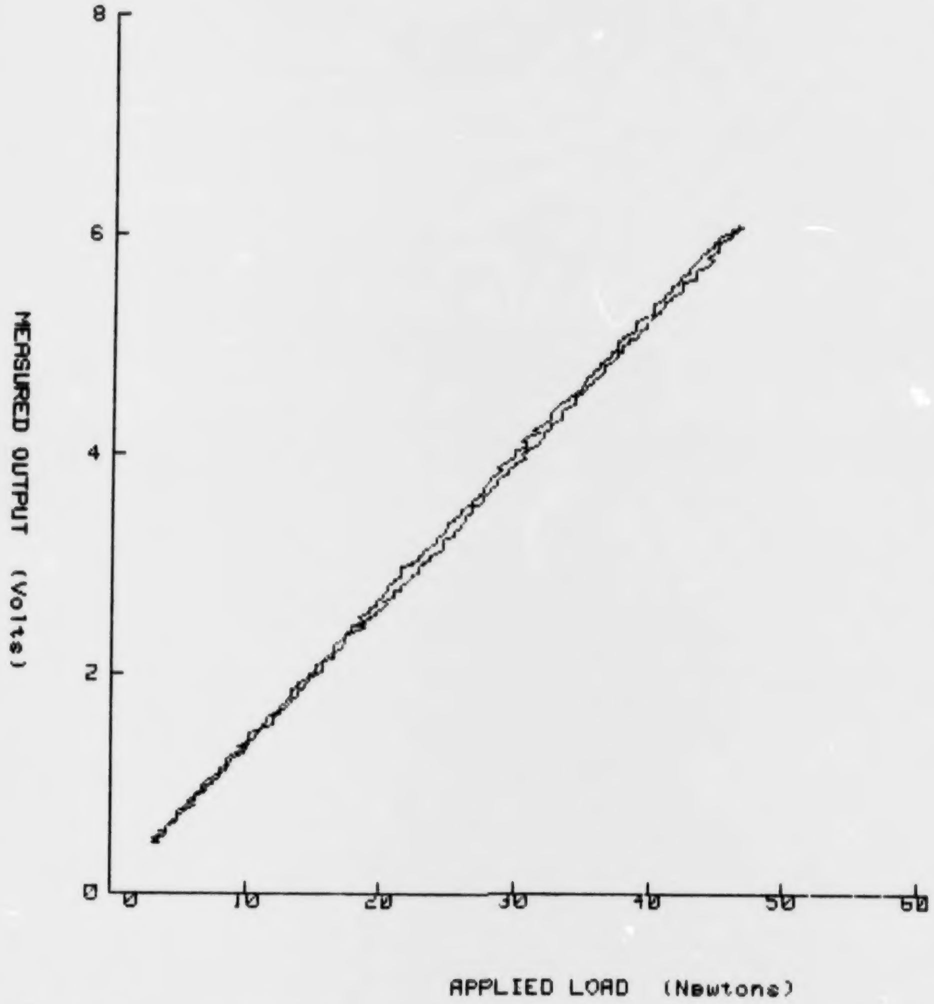

EXCITATION = 5.00 Volts
GAIN = 2000 Volts/Volts

SENSITIVITY= .6545 mV/V @ 50 Newtons
NON-LINEARITY= 1.7642 %
HYSTERESIS= 2.1576 %

REGRESSION ANALYSIS :
SLOPE = .1309 Volts/Newton
INTERCEPT = .0430 Volts
CORRELATION COEFF. = .9996

CALIBRATION = 7.64 Newtons/Volt

TRANSDUCER S/N: 118 JUL-09-83

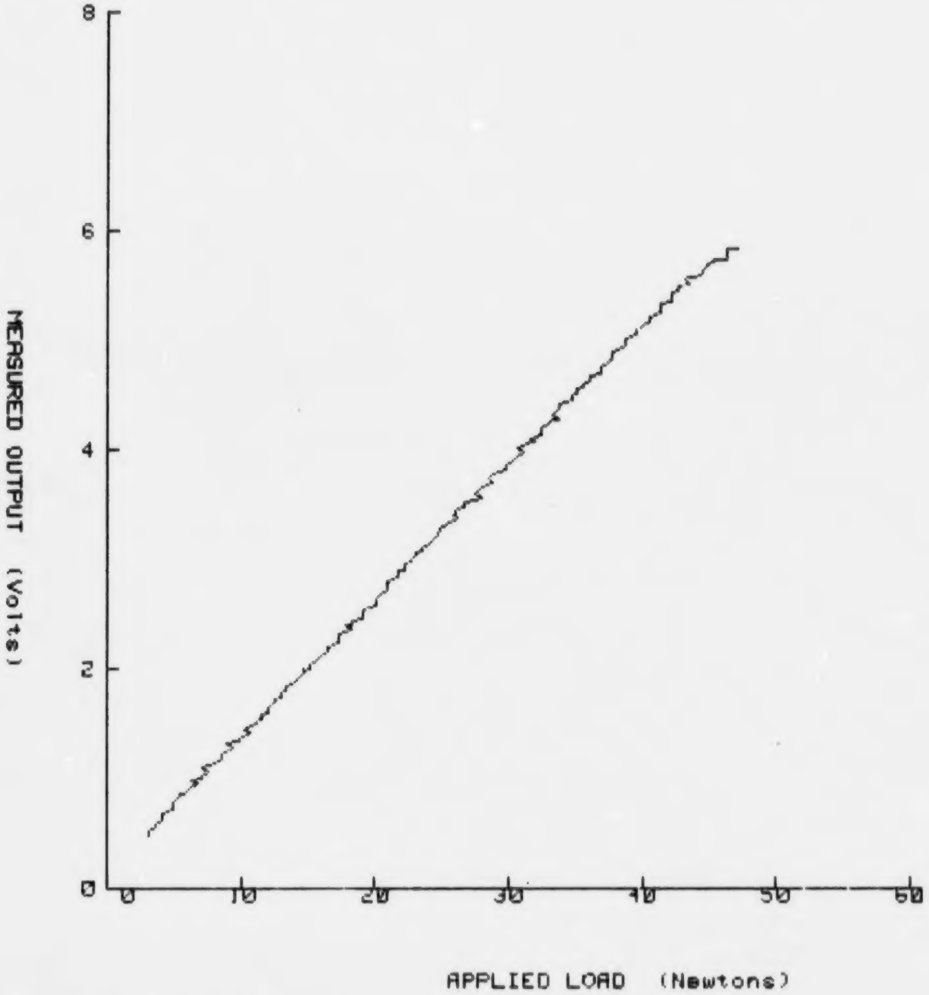

EXCITATION = 5.00 Volts
GAIN = 2000 Volts/Volts

SENSITIVITY= .6195 mV/V @ 50 Newtons

REGRESSION ANALYSIS :
SLOPE = .1239 Volts/Newton
INTERCEPT = .1490 Volts
CORRELATION COEFF. = .9997

CALIBRATION = 8.07 Newtons/Volt

TRANSDUCER S/N: 118 JUL-09-83

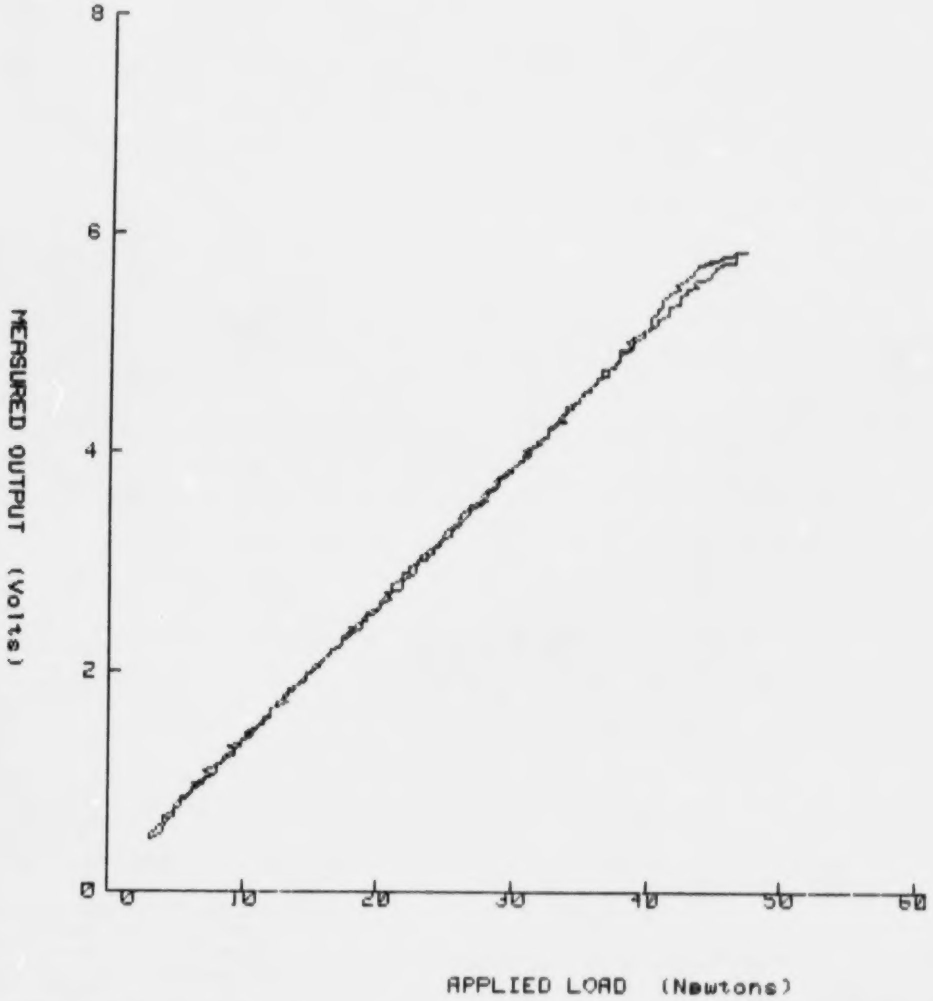

EXCITATION = 5.00 Volts
GAIN = 2000 Volts/Volts

SENSITIVITY= .6281 mV/V @ 50 Newtons
NON-LINEARITY= 2.0985 %
HYSTERESIS= 2.9615 %

REGRESSION ANALYSIS :
SLOPE = .1256 Volts/Newton
INTERCEPT = .1093 Volts
CORRELATION COEFF. = .9996

CALIBRATION = 7.96 Newtons/Volt

TRANSDUCER S/N: 120 JUL-09-83

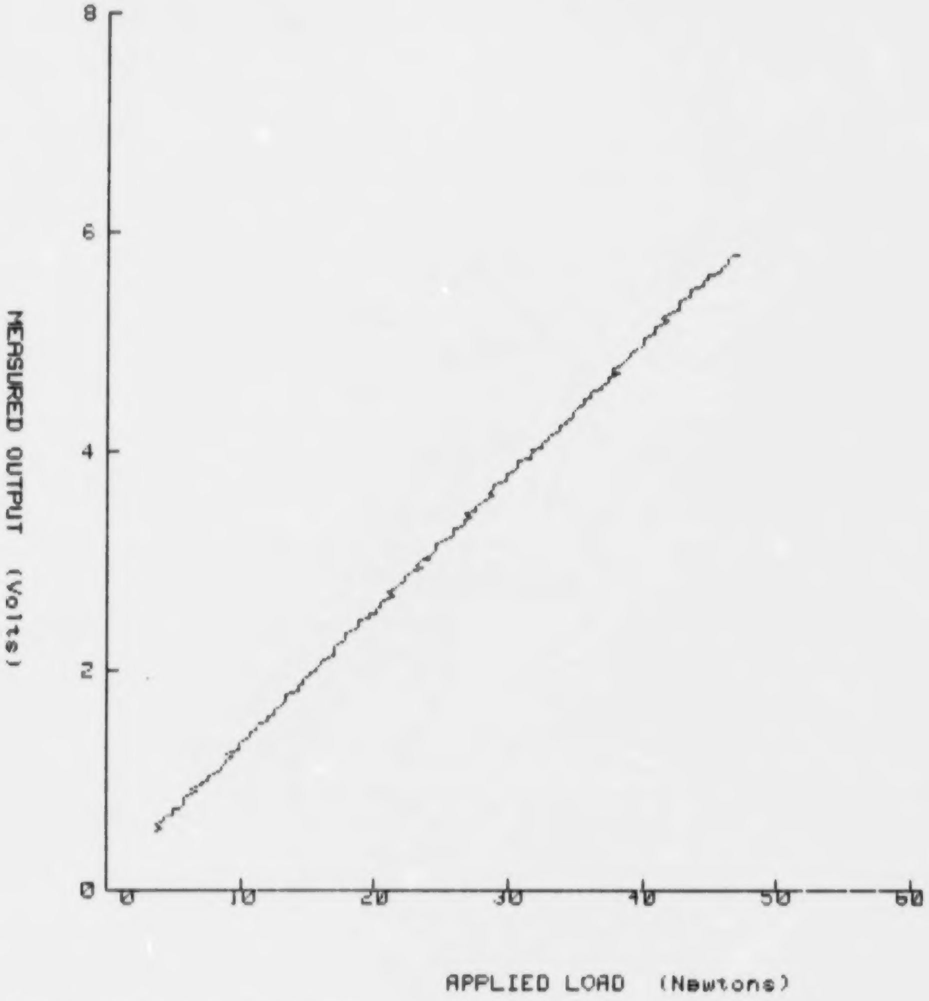

```
EXCITATION = 5.00 Volts
      GAIN = 2000 Volts/Volts

  SENSITIVITY= .6106 mV/V @ 50 Newtons

REGRESSION ANALYSIS :
             SLOPE  = .1221  Volts/Newton
         INTERCEPT  = .1061  Volts
 CORRELATION COEFF. = .9999

       CALIBRATION  = 8.19  Newtons/Volt
```

TRANSDUCER S/N: 120 JUL-09-83

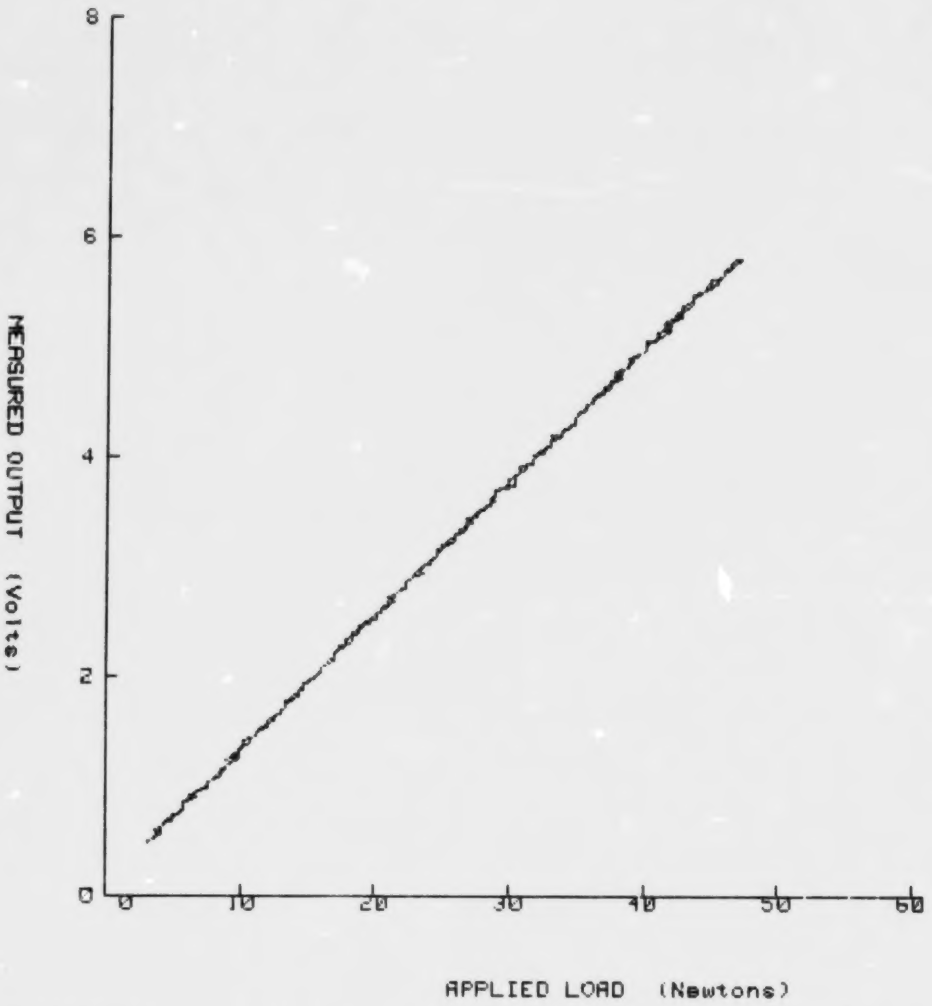

```
EXCITATION = 5.00 Volts
      GAIN = 2000 Volts/Volts

  SENSITIVITY= .6097 mV/V @ 50 Newtons
NON-LINEARITY= 1.8558 %
   HYSTERESIS= 1.2414 %

REGRESSION ANALYSIS :
             SLOPE  = .1219  Volts/Newton
         INTERCEPT  = .1121  Volts
 CORRELATION COEFF. = .9999

       CALIBRATION  = 8.20  Newtons/Volt
```

# APPENDIX B

# CALIBRATION OF SEGMENTS

## B.1 Overview

Each segment of the model was supported by a number of load cells and tension wires. Ideally the system should perform in an elastic manner and the load should be distributed among the load points as calculated by the data reduction algorithms discussed in Chapter 4 of the main report. However, defects in the assembly of the segments and other inaccuracies could result in deviations from the calculated response, the extent of these deviations must be determined experimentally.

This can be done by in-water calibration of the segments after the model is ballasted to the test waterline. Attempts to conduct such a calibration on the free floating model were not successful and was realized that a special loading arrangement would be necessary to apply the load properly without hydrodynamic disturbance and in a known direction with respect to the hull.

When the model was later removed from water it was possible to conduct a dry calibration at room temperature where the model was raised on a working platform.

## B.2 Dry Calibration Procedure and Results

Following the second ice test, it became apparent that the measured load did not correspond to expected loads, a calibration check of all load cells was performed (as described in Appendix A) followed by a segment calibration. The segment calibration was performed with the model out of the water, with the pretension wires properly adjusted, and with each load cell properly preloaded. At each calibration location, five loads were applied with a hand held spring scale in increments of 8.9 Newtons (2.0 lb). While the loads were applied, the measured output from each load cell was recorded. Figure B.1 shows the profile of the CCGS PIERRE RADISSON with the segments outlined and the location of each calibration point marked with a diamond.

For each calibration, the applied normal load was divided into x, y and z components by determining the direction cosines of the model surface at each location. These x, y and z force components were then compared to the sum of the actual load cell measurements for each direction. The ratio between the measured reaction and calculated reaction is plotted versus applied load for each segment in Figures B.2, B.3 and B.4. The raw calibration data for each segment are tabulated at the end of this section.

Figures B.2, B.3 and B.4 illustrate the variation of force ratios versus the applied load which are defined as follows:

> °Applied load in Newtons is the external calibration load applied in the normal direction to the surface at the calibration locations defined in Figure B.1.

FIGURE B.1

DRY CALIBRATION LOCATIONS

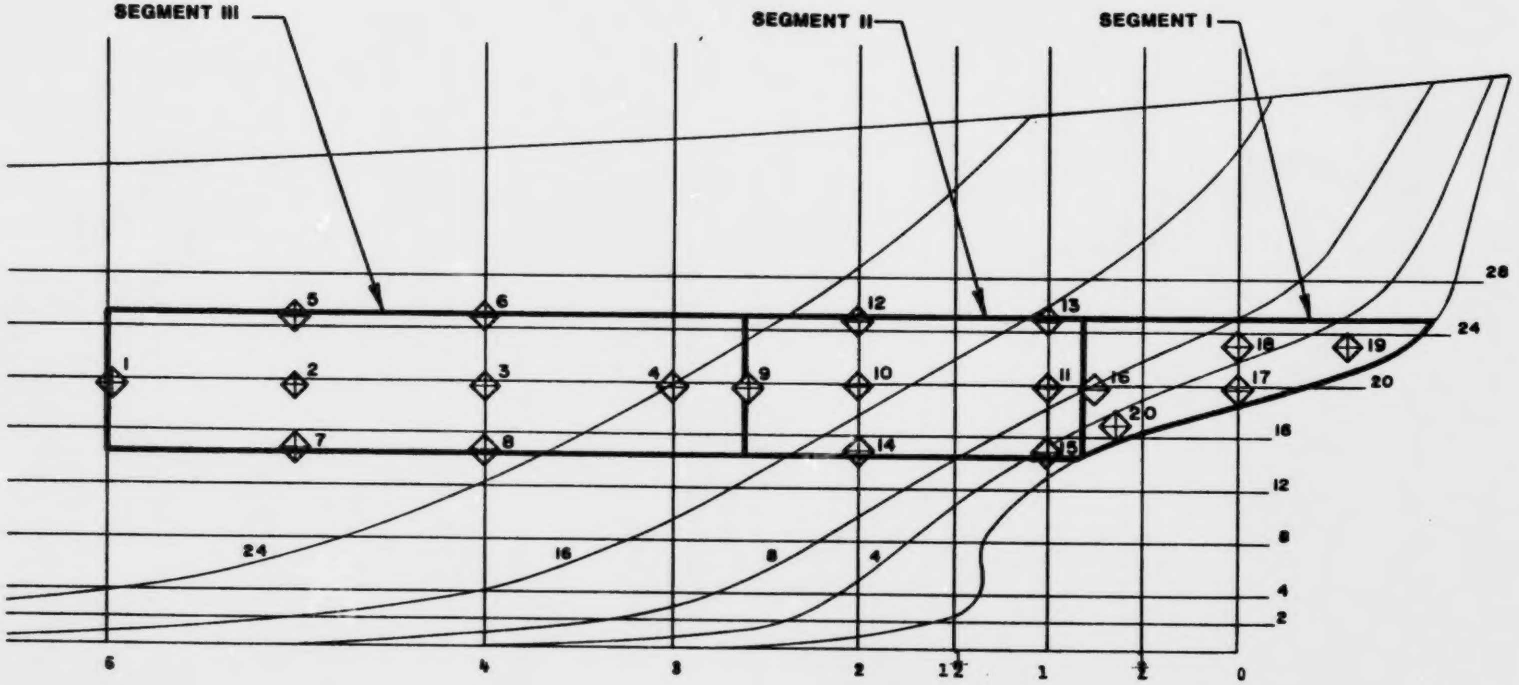
SEGMENT III
SEGMENT II
SEGMENT I
1
2
3
4
5
6
7
8
9
10
11
12
13
14
15
16
17
18
19
20
28
24
20
16
12
8
4
2
24
16
8
4
6
4
3
2
1½
1
½
0

**FIGURE B.2 DRY CALIBRATIONS of SEGMENT 1**

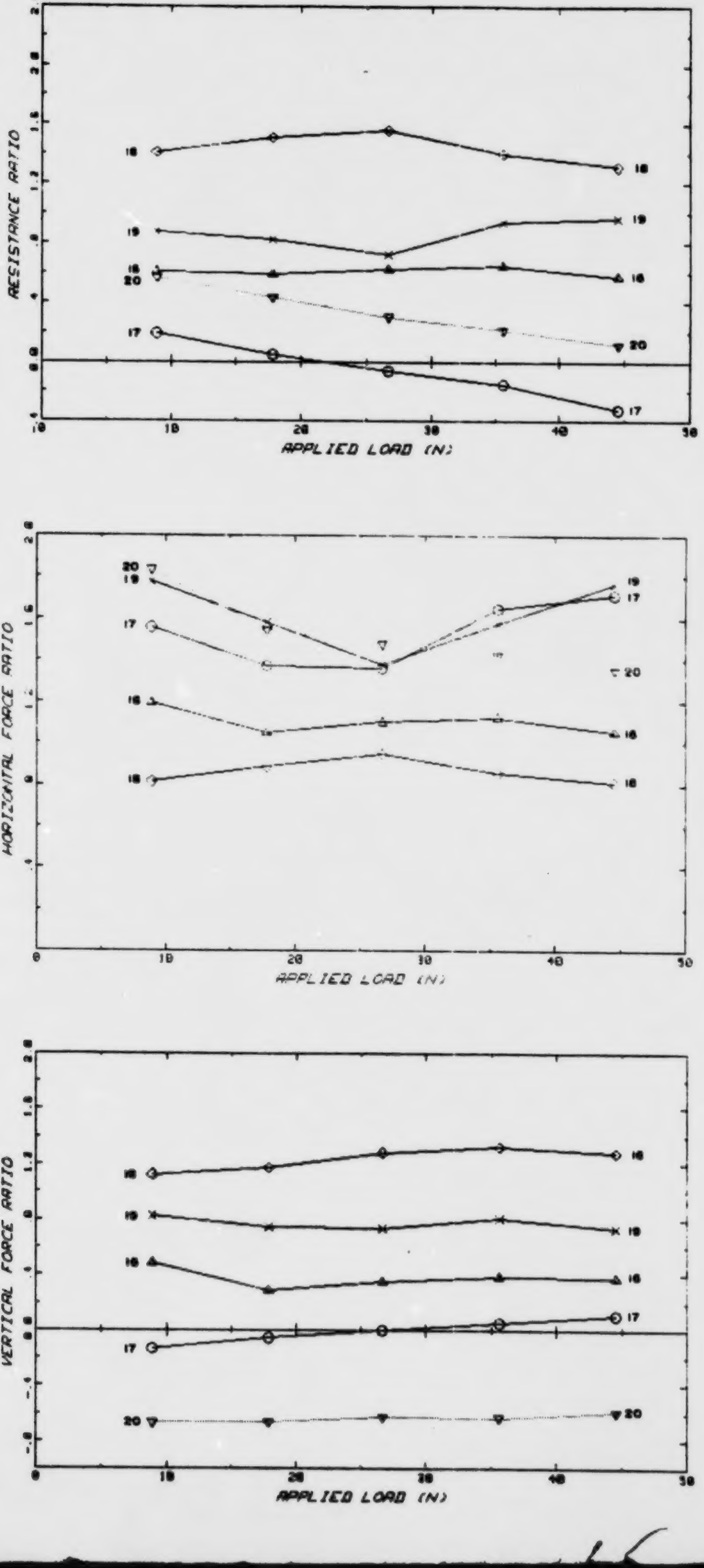

**FIGURE B.3 DRY CALIBRATIONS of SEGMENT 2**

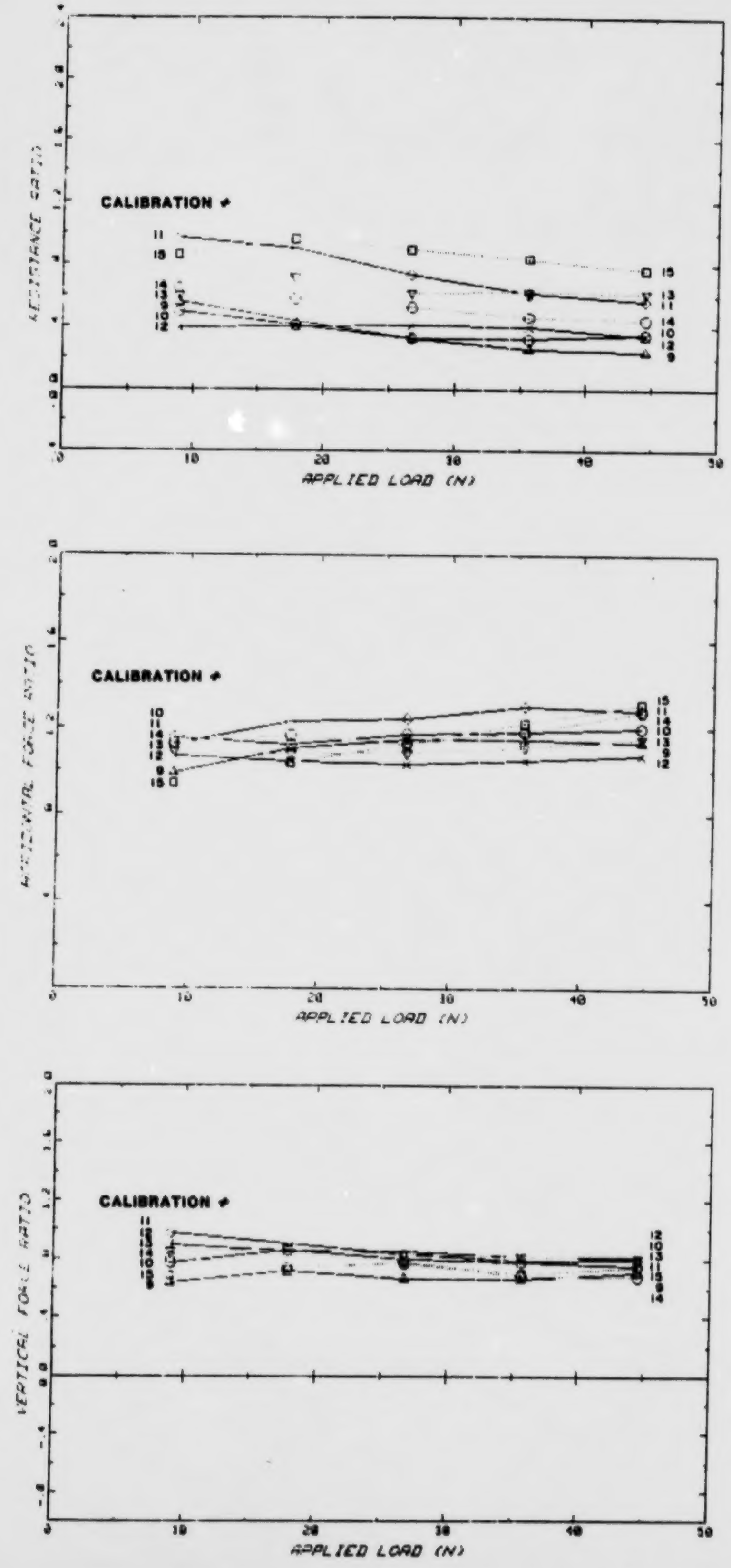

**FIGURE B.4 DRY CALIBRATIONS of SEGMENT 3**

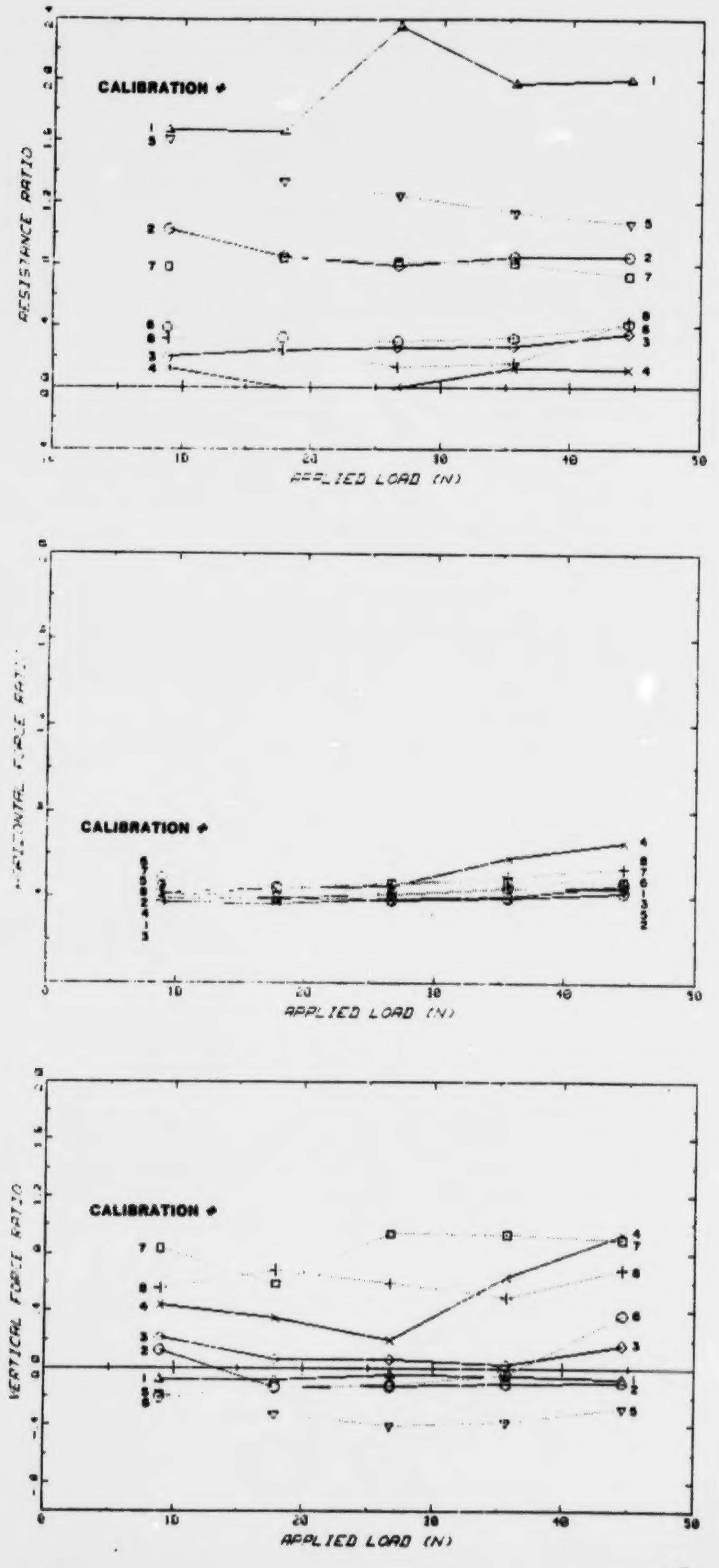

°Resistance ratio is the dimensionless ratio of the measured resistance force (R - load cell) in any segment divided by the resolved component of the applied load in the resistance direction (x - direction), or $F_x$.

°Horizontal force ratio is the dimensionless ratio of the sum of the two measured horizontal (transverse) forces or the H - load cells in any segment divided by the resolved component of the applied load in the horizontal (transverse) direction (y - direction) or $F_y$.

°Vertical force ratio is the dimensionless ratio of the sum of all measured vertical reaction forces or the V - load cells in any segment divided by the resolved component of the applied load in the vertical direction or $F_z$.

Therefore ratios greater or smaller than unity indicate over- or under-registration of the measuring system, respectively.

The results offered the needed explanation for the observed anomalies in data interpretation of the first two tests. However, specific observations and comments can be made:

a) Most scatter in results is associated with segment No.1. This scatter indicates that the response of the segment load cells is more dependent on the position of the applied load. The resistance component for instance can be over- or under-estimated depending on the load position. Some load positions would result in unloading of the resistance or vertical load cells and hence produce a response which is close to zero.

b) The most consistant load cell measurements are those obtained by the horizontal load cells. The measured horizontal component ranges between 0.8 and 1.8 of the actual component. The high values are associated with significant load reduction for the other components, eg. 0.5 for the resistance load cell and -0.6 for the vertical component (the negative sign means loss of preload).

c) For segment #1 the interpretation of the measured loads should be made with due care in determining the load position.

d) The second segment is actually the best segment in terms of consistency of the measurements obtained for the horizontal and vertical components. The horizontal force ratio ranges between 1.0 and 1.3 while the vertical and resistance force ratio ranges betwen 0.65 and 0.95, and 0.25 and 0.95, respectively.

e) In segment #2 there is some observed dependency on location of load but this dependency varies within a narrower range.

f) For segment #3, the best signals are those of the horizontal force component and greater variations were observed in the other components including the unloading effects and signifying the application of preload in these cases.

Two major conclusions may be made as a result of this dry calibration:

1) The horizontal load cell measurements which will be used in identifying load position (Chapter 4) are the most consistent and reliable. Once the load position is identified some correction factors may be applied to adjust the measured load components. They may serve as an interim solution until a more comprehensive in-water calibration is performed.

2) The performance of in-water calibration is necessary to provide a better calibration of the model segments. The dry calibration demonstrates this necessity for the wet calibration will be done under conditions of neutrally buoyant segments, and hence, lower pretension to support them. Some of the response we have observed in the dry calibration is due to specific factors such as segment suspension, increased friction forces, lack of water lubrication, etc. Therefore, the discrepancies observed here may be ameliorated in the wet calibration of the segments.

In order to better understand the response of the segments, it was decided to model Segment #2 using the finite element method. This analysis and results may be found in Appendix G.

The results of the dry in-situ calibration runs for all positions illustrated in Figure B.1 are listed in the following pages.

## 566C DRY INSITU CALIBRATION

Segment Number: 3 Calibration Number: 1
Cal. Location:@ Station 7.00 @19.50 Ft. Waterline
Comments: Load Applied in `Y´ Direction (assuning small angle)

| | APPLIED LOAD (N) | | | | |
|---|---|---|---|---|---|
| | 8.90 | 17.80 | 26.70 | 35.60 | 44.50 |
| R1 (N) | .64 | 1.27 | 2.70 | 3.02 | 3.82 |
| H1 (N) | -.42 | -.83 | -1.25 | -1.67 | -2.08 |
| H2 (N) | 3.82 | 7.64 | 12.15 | 17.01 | 21.52 |
| V1 (N) | 0.00 | 0.00 | .37 | .37 | .37 |
| V2 (N) | 0.00 | 0.00 | -.17 | -.17 | -.17 |
| V3 (N) | 0.00 | 0.00 | 0.00 | 0.00 | 0.00 |
| V4 (N) | -.14 | -.29 | -.43 | -.57 | -.86 |
| Fx (N) | .38 | .77 | 1.15 | 1.53 | 1.91 |
| Fy (N) | 8.73 | 17.46 | 26.19 | 34.92 | 43.65 |
| Fz (N) | 1.70 | 3.40 | 5.10 | 6.80 | 8.50 |
| Sum R | .64 | 1.27 | 2.70 | 3.02 | 3.82 |
| Sum H | 3.40 | 6.81 | 10.90 | 15.34 | 19.44 |
| Sum V | -.14 | -.29 | -.23 | -.37 | -.66 |
| R ratio | 1.672 | 1.659 | 2.352 | 1.973 | 1.996 |
| H ratio | .389 | .390 | .416 | .439 | .445 |
| V ratio | -.082 | -.085 | -.045 | -.054 | -.078 |

## 566C DRY INSITU CALIBRATION

Segment Number: 3 Calibration Number: 2
Cal. Location:@ Station 7.50 @19.50 Ft. Waterline
Comments: Load Applied in `Y´ Direction (assuning small angle)

| | APPLIED LOAD (N) | | | | |
|---|---|---|---|---|---|
| | 8.90 | 17.80 | 26.70 | 35.60 | 44.50 |
| R1 (N) | .96 | 1.59 | 2.23 | 3.18 | 3.98 |
| H1 (N) | .42 | .83 | .83 | 1.67 | 2.92 |
| H2 (N) | 3.12 | 5.90 | 9.02 | 11.80 | 14.93 |
| V1 (N) | -.37 | -.74 | -.74 | -.74 | -1.12 |
| V2 (N) | .66 | .33 | .33 | .33 | .33 |
| V3 (N) | .31 | .15 | 0.00 | 0.00 | .15 |
| V4 (N) | -.29 | -.43 | -.57 | -.71 | -.57 |
| Fx (N) | .93 | 1.87 | 2.80 | 3.74 | 4.67 |
| Fy (N) | 8.48 | 16.96 | 25.45 | 33.93 | 42.41 |
| Fz (N) | 2.51 | 5.02 | 7.53 | 10.04 | 12.55 |
| Sum R | .96 | 1.59 | 2.23 | 3.18 | 3.98 |
| Sum H | 3.54 | 6.73 | 9.85 | 13.47 | 17.85 |
| Sum V | .31 | -.69 | -.98 | -1.12 | -1.21 |
| R ratio | 1.027 | .851 | .795 | .851 | .852 |
| H ratio | .417 | .397 | .387 | .397 | .421 |
| V ratio | .124 | -.137 | -.130 | -.112 | -.096 |

## 566C DRY INSITU CALIBRATION

Segment Number: 3 Calibration Number: 3
Cal. Location:@ Station 8.00 @19.50 Ft. Waterline
Comments: Load Applied in 'Y' Direction (assuning small angle)

| | APPLIED LOAD (N) | | | | |
|---|---|---|---|---|---|
| | 8.90 | 17.80 | 26.70 | 35.60 | 44.50 |
| R1 (N) | .32 | .80 | 1.27 | 1.75 | 2.87 |
| H1 (N) | 1.25 | 2.08 | 4.17 | 5.84 | 8.75 |
| H2 (N) | 1.74 | 3.82 | 5.21 | 6.94 | 9.37 |
| V1 (N) | -.74 | -1.12 | -1.12 | -1.12 | -2.23 |
| V2 (N) | 1.16 | 1.49 | 1.66 | 1.66 | 4.32 |
| V3 (N) | .92 | 1.22 | 1.53 | 1.53 | 3.82 |
| V4 (N) | -.57 | -1.14 | -1.43 | -1.71 | -3.00 |
| Fx (N) | 1.66 | 3.31 | 4.97 | 6.62 | 8.28 |
| Fy (N) | 7.99 | 15.98 | 23.98 | 31.97 | 39.96 |
| Fz (N) | 3.56 | 7.12 | 10.68 | 14.24 | 17.80 |
| Sum R | .32 | .80 | 1.27 | 1.75 | 2.87 |
| Sum H | 2.99 | 5.90 | 9.38 | 12.78 | 18.12 |
| Sum V | .77 | .45 | .64 | .36 | 2.91 |
| R ratio | .193 | .242 | .256 | .264 | .347 |
| H ratio | .374 | .369 | .391 | .400 | .453 |
| V ratio | .216 | .063 | .060 | .025 | .163 |

## 566C DRY INSITU CALIBRATION

Segment Number: 3 Calibration Number: 4
Cal. Location:@ Station 8.50 @19.50 Ft. Waterline
Comments: Load Applied in 'Y' Direction (assuning small angle)

| | APPLIED LOAD (N) | | | | |
|---|---|---|---|---|---|
| | 8.90 | 17.80 | 26.70 | 35.60 | 44.50 |
| R1 (N) | .32 | 0.00 | 0.00 | 1.27 | 1.43 |
| H1 (N) | 2.92 | 5.84 | 9.17 | 15.42 | 22.51 |
| H2 (N) | .35 | 1.04 | 1.39 | 2.78 | 3.12 |
| V1 (N) | 0.00 | -.74 | -1.49 | 0.00 | .37 |
| V2 (N) | 2.49 | 4.48 | 5.32 | 13.79 | 23.42 |
| V3 (N) | .92 | 1.68 | 2.29 | 4.59 | 6.88 |
| V4 (N) | -1.43 | -2.28 | -3.43 | -6.85 | -9.57 |
| Fx (N) | 2.59 | 5.18 | 7.77 | 10.36 | 12.95 |
| Fy (N) | 7.84 | 15.68 | 23.52 | 31.36 | 39.20 |
| Fz (N) | 4.51 | 9.02 | 13.54 | 18.05 | 22.56 |
| Sum R | .32 | 0.00 | 0.00 | 1.27 | 1.43 |
| Sum H | 3.27 | 6.88 | 10.56 | 18.20 | 25.63 |
| Sum V | 1.98 | 3.14 | 2.69 | 11.53 | 21.10 |
| R ratio | .124 | 0.000 | 0.000 | .123 | .110 |
| H ratio | .417 | .439 | .449 | .580 | .654 |
| V ratio | .439 | .348 | .199 | .639 | .935 |

## 566C DRY INSITU CALIBRATION

Segment Number: 3 Calibration Number: 5
Cal. Location:@ Station 7.50 @24.80 Ft. Waterline
Comments: Load Applied in ‘Y’ Direction (assuning small angle)

| | APPLIED LOAD (N) 8.90 | 17.80 | 26.70 | 35.60 | 44.50 |
|---|---|---|---|---|---|
| R1 (N) | .96 | 1.59 | 2.23 | 2.71 | 3.18 |
| H1 (N) | .42 | 1.25 | 1.67 | 2.92 | 4.17 |
| H2 (N) | 3.47 | 5.90 | 9.02 | 12.50 | 14.93 |
| V1 (N) | -.74 | -1.86 | -2.98 | -3.72 | -4.46 |
| V2 (N) | 1.16 | 1.83 | 2.66 | 3.49 | 4.32 |
| V3 (N) | .61 | 1.22 | 1.83 | 2.29 | 3.21 |
| V4 (N) | -1.29 | -2.14 | -3.28 | -4.28 | -5.14 |
| Fx (N) | .[illegible] | 1.19 | 1.79 | 2.39 | 2.98 |
| Fy (N) | 8.[illegible] | 17.52 | 26.27 | 35.03 | 43.79 |
| Fz (N) | 1.[illegible] | 2.94 | 4.41 | 5.87 | 7.34 |
| Sum R | .96 | 1.59 | 2.23 | 2.71 | 3.18 |
| Sum H | 3.89 | 7.15 | 10.69 | 15.42 | 19.10 |
| Sum V | -.26 | -.95 | -1.77 | -2.22 | -2.07 |
| R ratio | 1.610 | 1.333 | 1.247 | 1.136 | 1.067 |
| H ratio | .444 | .408 | .407 | .440 | .436 |
| V ratio | -.177 | -.323 | -.402 | -.378 | -.282 |

## 566C DRY INSITU CALIBRATION

Segment Number: 3 Calibration Number: 6
Cal. Location:@ Station 8.00 @24.80 Ft. Waterline
Comments: Load Applied in ‘Y’ Direction (assuning small angle)

| | APPLIED LOAD (N) 8.90 | 17.80 | 26.70 | 35.60 | 44.50 |
|---|---|---|---|---|---|
| R1 (N) | .48 | .80 | 1.11 | 1.59 | 2.55 |
| H1 (N) | 2.08 | 3.75 | 5.42 | 7.92 | 10.42 |
| H2 (N) | 2.08 | 3.82 | 5.21 | 7.29 | 9.37 |
| V1 (N) | -1.12 | -2.23 | -3.35 | -4.09 | -5.95 |
| V2 (N) | 1.00 | 2.66 | 3.82 | 5.15 | 9.80 |
| V3 (N) | 1.22 | 1.68 | 2.60 | 3.67 | 7.65 |
| V4 (N) | -1.57 | -2.71 | -3.86 | -5.14 | -7.28 |
| Fx (N) | 1.25 | 2.49 | 3.74 | 4.98 | 6.23 |
| Fy (N) | 8.51 | 17.02 | 25.53 | 34.03 | 42.54 |
| Fz (N) | 2.28 | 4.56 | 6.84 | 9.11 | 11.39 |
| Sum R | .48 | .80 | 1.11 | 1.59 | 2.55 |
| Sum H | 4.16 | 7.57 | 10.63 | 15.21 | 19.79 |
| Sum V | -.47 | -.60 | -.79 | -.41 | 4.22 |
| R ratio | .385 | .321 | .297 | .319 | .409 |
| H ratio | .489 | .445 | .416 | .447 | .465 |
| V ratio | -.206 | -.132 | -.116 | -.045 | .370 |

## 566C DRY INSITU CALIBRATION

Segment Number: 3 Calibration Number: 7
Cal. Location:@ Station 7.50 @14.90 Ft. Waterline
Comments: Load Applied in `Y' Direction (assuning small angle)

| | APPLIED LOAD (N) | | | | |
|---|---|---|---|---|---|
| | 8.90 | 17.80 | 26.70 | 35.60 | 44.50 |
| R1 (N) | .96 | 2.07 | 3.02 | 3.98 | 4.46 |
| H1 (N) | 0.00 | .42 | .83 | 1.25 | 2.08 |
| H2 (N) | 3.82 | 6.94 | 10.76 | 14.58 | 17.70 |
| V1 (N) | 0.00 | 0.00 | -.74 | -1.12 | -1.12 |
| V2 (N) | .50 | .33 | 1.66 | 2.33 | 2.33 |
| V3 (N) | 1.53 | 1.83 | 5.35 | 7.03 | 8.56 |
| V4 (N) | .43 | 1.29 | 2.00 | 2.71 | 3.43 |
| Fx (N) | 1.23 | 2.46 | 3.68 | 4.91 | 6.14 |
| Fy (N) | 8.31 | 16.63 | 24.94 | 33.25 | 41.56 |
| Fz (N) | 2.95 | 5.89 | 8.84 | 11.78 | 14.73 |
| Sum R | .96 | 2.07 | 3.02 | 3.98 | 4.46 |
| Sum H | 3.82 | 7.36 | 11.59 | 15.83 | 19.78 |
| Sum V | 2.46 | 3.45 | 8.27 | 10.95 | 13.20 |
| R ratio | .782 | .843 | .820 | .810 | .726 |
| H ratio | .460 | .443 | .465 | .476 | .476 |
| V ratio | .835 | .586 | .936 | .929 | .896 |

## 566C DRY INSITU CALIBRATION

Segment Number: 3 Calibration Number: 8
Cal. Location:@ Station 8.00 @14.90 Ft. Waterline
Comments: Load Applied in `Y' Direction (assuning small angle)

| | APPLIED LOAD (N) | | | | |
|---|---|---|---|---|---|
| | 8.90 | 17.80 | 26.70 | 35.60 | 44.50 |
| R1 (N) | .64 | .96 | .80 | 1.27 | 4.30 |
| H1 (N) | 1.25 | 2.92 | 5.42 | 7.92 | 9.59 |
| H2 (N) | 2.08 | 3.82 | 5.21 | 7.29 | 10.76 |
| V1 (N) | 0.00 | .37 | .74 | 1.12 | .74 |
| V2 (N) | 1.33 | 3.16 | 3.82 | 3.65 | 7.14 |
| V3 (N) | 1.22 | 2.60 | 3.21 | 3.52 | 7.19 |
| V4 (N) | -.29 | -.57 | -.57 | -.29 | -1.14 |
| Fx (N) | 2.01 | 4.02 | 6.03 | 8.05 | 10.06 |
| Fy (N) | 7.65 | 15.31 | 22.96 | 30.62 | 38.27 |
| Fz (N) | 4.07 | 8.13 | 12.20 | 16.27 | 20.34 |
| Sum R | .64 | .96 | .80 | 1.27 | 4.30 |
| Sum H | 3.33 | 6.74 | 10.63 | 15.21 | 20.35 |
| Sum V | 2.26 | 5.56 | 7.20 | 8.00 | 13.93 |
| R ratio | .318 | .239 | .133 | .158 | .428 |
| H ratio | .435 | .440 | .463 | .497 | .532 |
| V ratio | .556 | .684 | .590 | .492 | .685 |

## 566C DRY INSITU CALIBRATION

Segment Number: 2 Calibration Number: 9
Cal. Location:@ Station 8.69 @19.50 Ft. Waterline
Comments: Calibration is NORMAL to Surface

| | APPLIED LOAD (N) | | | | |
|---|---|---|---|---|---|
| | 8.90 | 17.80 | 26.70 | 35.60 | 44.50 |
| R1 (N) | 1.60 | 2.50 | 2.80 | 3.00 | 3.50 |
| H1 (N) | -1.90 | -2.60 | -3.00 | -3.90 | -5.20 |
| H2 (N) | 8.80 | 18.00 | 27.00 | 35.80 | 44.70 |
| V1 (N) | -.20 | -.30 | -.50 | -.70 | -.70 |
| V2 (N) | -.40 | -.70 | -1.10 | -1.40 | -1.40 |
| V3 (N) | 3.60 | 7.70 | 11.00 | 14.50 | 18.80 |
| V4 (N) | 0.00 | 0.00 | 0.00 | 0.00 | 0.00 |
| Fx (N) | 2.89 | 5.79 | 8.68 | 11.57 | 14.46 |
| Fy (N) | 6.98 | 13.96 | 20.93 | 27.91 | 34.89 |
| Fz (N) | 4.71 | 9.42 | 14.12 | 18.83 | 23.54 |
| Sum R | 1.60 | 2.50 | 2.80 | 3.00 | 3.50 |
| Sum H | 6.90 | 15.40 | 24.00 | 31.90 | 39.50 |
| Sum V | 3.00 | 6.70 | 9.40 | 12.40 | 16.70 |
| R ratio | .553 | .432 | .323 | .259 | .242 |
| H ratio | .989 | 1.104 | 1.147 | 1.143 | 1.132 |
| V ratio | .637 | .712 | .666 | .658 | .709 |

## 566C DRY INSITU CALIBRATION

Segment Number: 2 Calibration Number: 10
Cal. Location:@ Station 9.00 @19.50 Ft. Waterline
Comments: Calibration is NORMAL to Surface

| | APPLIED LOAD (N) | | | | |
|---|---|---|---|---|---|
| | 8.90 | 17.80 | 26.70 | 35.60 | 44.50 |
| R1 (N) | 1.58 | 2.62 | 3.15 | 4.10 | 5.61 |
| H1 (N) | 1.49 | 2.61 | 4.48 | 5.97 | 7.46 |
| H2 (N) | 5.59 | 11.18 | 17.17 | 23.16 | 29.54 |
| V1 (N) | .17 | .27 | .40 | .50 | .67 |
| V2 (N) | 1.44 | 3.96 | 4.90 | 6.27 | 7.21 |
| V3 (N) | 2.89 | 5.86 | 8.60 | 11.28 | 14.10 |
| V4 (N) | -.23 | -.52 | -.61 | -.73 | -1.02 |
| Fx (N) | 3.21 | 6.43 | 9.64 | 12.85 | 16.06 |
| Fy (N) | 6.17 | 12.34 | 18.50 | 24.67 | 30.84 |
| Fz (N) | 5.55 | 11.11 | 16.66 | 22.21 | 27.77 |
| Sum R | 1.58 | 2.62 | 3.15 | 4.10 | 5.61 |
| Sum H | 7.08 | 13.79 | 21.65 | 29.13 | 37.00 |
| Sum V | 4.27 | 9.57 | 13.29 | 17.32 | 20.96 |
| R ratio | .492 | .408 | .327 | .319 | .349 |
| H ratio | 1.148 | 1.118 | 1.170 | 1.181 | 1.200 |
| V ratio | .769 | .862 | .798 | .780 | .755 |

```
                      566C DRY INSITU CALIBRATION

Segment Number: 2                             Calibration Number: 11
Cal. Location:@ Station  9.50                 @19.50 Ft. Waterline
Comments: Calibration is NORMAL to Surface

---------------------------------------------------------------------
|          |                  APPLIED LOAD (N)                      |
|          |   8.90   |  17.80   |  26.70   |  35.60   |   44.50    |
|----------|----------|----------|----------|----------|----------  |
|  R1 (N)  |   3.15   |   5.83   |   7.16   |   7.95   |    9.15    |
|  H1 (N)  |   4.92   |  11.19   |  17.24   |  24.10   |   29.85    |
|  H2 (N)  |    .80   |   1.36   |   1.76   |   2.40   |    2.79    |
|  V1 (N)  |   1.23   |   2.33   |   3.33   |   4.00   |    5.00    |
|  V2 (N)  |   5.12   |   9.37   |  12.68   |  16.21   |   20.18    |
|  V3 (N)  |   0.00   |   0.00   |   0.00   |   0.00   |    0.00    |
|  V4 (N)  |    .03   |    .09   |    .23   |    .47   |     .73    |
|          |          |          |          |          |            |
|  Fx (N)  |   3.25   |   6.50   |   9.75   |  12.99   |   16.24    |
|  Fy (N)  |   5.10   |  10.20   |  15.30   |  20.40   |   25.50    |
|  Fz (N)  |   6.53   |  13.07   |  19.60   |  26.13   |   32.66    |
|          |          |          |          |          |            |
|  Sum R   |   3.15   |   5.83   |   7.16   |   7.95   |    9.15    |
|  Sum H   |   5.72   |  12.55   |  19.00   |  26.50   |   32.64    |
|  Sum V   |   6.38   |  11.79   |  16.24   |  20.68   |   25.91    |
|  R ratio |    .970  |    .897  |    .735  |    .612  |     .563   |
|  H ratio |   1.122  |   1.230  |   1.242  |   1.299  |    1.280   |
|  V ratio |    .977  |    .902  |    .829  |    .791  |     .793   |
|----------|----------|----------|----------|----------|----------  |
```

```
                      566C DRY INSITU CALIBRATION

Segment Number: 2                             Calibration Number: 12
Cal. Location:@ Station  9.00                 @24.80 Ft. Waterline
Comments: Calibration is NORMAL to Surface

---------------------------------------------------------------------
|          |                  APPLIED LOAD (N)                      |
|          |   8.90   |  17.80   |  26.70   |  35.60   |   44.50    |
|----------|----------|----------|----------|----------|----------  |
|  R1 (N)  |   1.17   |   2.37   |   3.63   |   4.73   |    5.05    |
|  H1 (N)  |    .85   |   1.77   |   2.69   |   3.68   |    4.95    |
|  H2 (N)  |   6.79   |  13.17   |  19.56   |  26.35   |   33.54    |
|  V1 (N)  |  -1.03   |  -2.17   |  -3.33   |  -4.50   |   -5.40    |
|  V2 (N)  |   3.60   |   6.85   |  10.45   |  13.47   |   16.21    |
|  V3 (N)  |   3.62   |   7.23   |  10.85   |  14.46   |   18.22    |
|  V4 (N)  |  -2.33   |  -4.54   |  -6.99   |  -9.32   |  -11.36    |
|          |          |          |          |          |            |
|  Fx (N)  |   2.99   |   5.98   |   8.97   |  11.96   |   14.95    |
|  Fy (N)  |   7.18   |  14.36   |  21.55   |  28.73   |   35.91    |
|  Fz (N)  |   4.32   |   8.63   |  12.95   |  17.27   |   21.58    |
|          |          |          |          |          |            |
|  Sum R   |   1.17   |   2.37   |   3.63   |   4.73   |    5.05    |
|  Sum H   |   7.64   |  14.94   |  22.25   |  30.03   |   38.49    |
|  Sum V   |   3.86   |   7.37   |  10.98   |  14.11   |   17.67    |
|  R ratio |    .391  |    .396  |    .405  |    .395  |     .338   |
|  H ratio |   1.064  |   1.040  |   1.033  |   1.045  |    1.072   |
|  V ratio |    .894  |    .854  |    .848  |    .817  |     .819   |
|----------|----------|----------|----------|----------|----------  |
```

## 566C DRY INSITU CALIBRATION

Segment Number: 2 Calibration Number: 13
Cal. Location:@ Station 9.50 @24.80 Ft. Waterline
Comments: Calibration is NORMAL to Surface

| | APPLIED LOAD (N) | | | | |
|---|---|---|---|---|---|
| | 8.90 | 17.80 | 26.70 | 35.60 | 44.50 |
| R1 (N) | 1.89 | 4.54 | 5.83 | 7.88 | 9.78 |
| H1 (N) | 6.02 | 11.68 | 17.34 | 23.71 | 30.78 |
| H2 (N) | .88 | 2.00 | 3.19 | 4.39 | 5.67 |
| V1 (N) | -.67 | -1.40 | -2.17 | -3.23 | -4.00 |
| V2 (N) | 6.49 | 13.11 | 18.45 | 24.50 | 29.98 |
| V3 (N) | 1.08 | 2.31 | 3.76 | 5.06 | 6.58 |
| V4 (N) | -2.33 | -4.66 | -6.56 | -8.74 | -10.78 |
| Fx (N) | 3.16 | 6.32 | 9.48 | 12.64 | 15.80 |
| Fy (N) | 6.33 | 12.66 | 18.98 | 25.31 | 31.64 |
| Fz (N) | 5.40 | 10.80 | 16.21 | 21.61 | 27.01 |
| Sum R | 1.89 | 4.54 | 5.83 | 7.88 | 9.78 |
| Sum H | 6.90 | 13.68 | 20.53 | 28.10 | 36.45 |
| Sum V | 4.57 | 9.36 | 13.48 | 17.59 | 21.78 |
| R ratio | .598 | .718 | .615 | .624 | .619 |
| H ratio | 1.090 | 1.081 | 1.081 | 1.110 | 1.152 |
| V ratio | .846 | .866 | .832 | .814 | .806 |

## 566C DRY INSITU CALIBRATION

Segment Number: 2 Calibration Number: 14
Cal. Location:@ Station 9.00 @14.90 Ft. Waterline
Comments: Calibration is NORMAL to Surface

| | APPLIED LOAD (N) | | | | |
|---|---|---|---|---|---|
| | 8.90 | 17.80 | 26.70 | 35.60 | 44.50 |
| R1 (N) | 2.21 | 3.94 | 5.36 | 6.31 | 7.57 |
| H1 (N) | 1.06 | 2.12 | 3.33 | 4.95 | 7.43 |
| H2 (N) | 5.19 | 10.78 | 15.41 | 21.16 | 27.95 |
| V1 (N) | 1.37 | 2.67 | 4.07 | 5.17 | 6.83 |
| V2 (N) | -1.08 | -2.16 | -2.95 | -3.96 | -5.40 |
| V3 (N) | 2.39 | 4.19 | 6.44 | 7.09 | 8.10 |
| V4 (N) | 2.19 | 4.25 | 6.41 | 8.16 | 11.07 |
| Fx (N) | 3.43 | 6.85 | 10.28 | 13.71 | 17.13 |
| Fy (N) | 5.54 | 11.09 | 16.63 | 22.18 | 27.72 |
| Fz (N) | 6.05 | 12.10 | 18.16 | 24.21 | 30.26 |
| Sum R | 2.21 | 3.94 | 5.36 | 6.31 | 7.57 |
| Sum H | 6.25 | 12.90 | 18.74 | 26.11 | 35.38 |
| Sum V | 4.87 | 8.95 | 13.97 | 16.46 | 20.60 |
| R ratio | .645 | .575 | .521 | .460 | .442 |
| H ratio | 1.127 | 1.163 | 1.127 | 1.177 | 1.276 |
| V ratio | .805 | .739 | .769 | .680 | .681 |

# 566C DRY INSITU CALIBRATION

Segment Number: 2 Calibration Number: 15
Cal. Location:@ Station 9.50 @14.90 ft. Waterline
Comments: Calibration is NORMAL to Surface

| | APPLIED LOAD (N) | | | | |
|---|---|---|---|---|---|
| | 8.90 | 17.80 | 26.70 | 35.60 | 44.50 |
| R1 (N) | 2.90 | 6.47 | 8.99 | 11.29 | 12.93 |
| H1 (N) | 5.31 | 10.62 | 16.63 | 23.35 | 30.43 |
| H2 (N) | -1.20 | -1.60 | -1.92 | -2.00 | -1.84 |
| V1 (N) | 3.17 | 6.33 | 9.33 | 12.00 | 15.33 |
| V2 (N) | 1.73 | 3.46 | 5.04 | 5.04 | 6.85 |
| V3 (N) | -2.60 | -4.70 | -6.15 | -7.95 | -9.76 |
| V4 (N) | 2.48 | 5.10 | 8.01 | 10.49 | 13.40 |
| Fx (N) | 3.37 | 6.75 | 10.12 | 13.49 | 16.87 |
| Fy (N) | 4.36 | 8.72 | 13.08 | 17.44 | 21.81 |
| Fz (N) | 6.99 | 13.97 | 20.96 | 27.95 | 34.93 |
| Sum R | 2.90 | 6.47 | 8.99 | 11.29 | 12.93 |
| Sum H | 4.11 | 9.02 | 14.71 | 21.35 | 28.59 |
| Sum V | 4.78 | 10.19 | 16.23 | 19.58 | 25.82 |
| R ratio | .860 | .959 | .888 | .837 | .767 |
| H ratio | .942 | 1.034 | 1.124 | 1.224 | 1.311 |
| V ratio | .684 | .729 | .774 | .701 | .739 |

## 566C DRY INSITU CALIBRATION

Segment Number: 1 Calibration Number: 16
Cal. Location:@ Station 9.63 @19.50 Ft. Waterline
Comments: Calibration is NORMAL to Surface

| | APPLIED LOAD (N) | | | | |
|---|---|---|---|---|---|
| | 8.90 | 17.80 | 26.70 | 35.60 | 44.50 |
| R1 (N) | 2.02 | 3.90 | 6.18 | 8.60 | 9.54 |
| H1 (N) | -1.64 | -3.28 | -4.51 | -6.51 | -6.97 |
| H2 (N) | 7.36 | 13.32 | 20.33 | 28.05 | 32.26 |
| V1 (N) | -1.56 | -3.90 | -5.85 | -7.41 | -8.19 |
| V2 (N) | 4.80 | 7.76 | 12.93 | 17.73 | 20.69 |
| V3 (N) | - | - | - | - | - |
| V4 (N) | - | - | - | - | - |
| Fx (N) | 3.32 | 6.64 | 9.96 | 13.28 | 16.60 |
| Fy (N) | 4.80 | 9.59 | 14.39 | 19.19 | 23.99 |
| Fz (N) | 6.72 | 13.44 | 20.16 | 26.88 | 33.60 |
| Sum R | 2.02 | 3.90 | 6.18 | 8.60 | 9.54 |
| Sum H | 5.72 | 10.04 | 15.82 | 21.54 | 25.29 |
| Sum V | 3.24 | 3.86 | 7.08 | 10.32 | 12.50 |
| R ratio | .608 | .587 | .621 | .648 | .575 |
| H ratio | 1.192 | 1.046 | 1.099 | 1.123 | 1.054 |
| V ratio | .482 | .287 | .351 | .384 | .372 |

## 566C DRY INSITU CALIBRATION

Segment Number: 1 Calibration Number: 17
Cal. Location:@ Station 10.00 @19.50 Ft. Waterline
Comments: Calibration is NORMAL to Surface

| | APPLIED LOAD (N) | | | | |
|---|---|---|---|---|---|
| | 8.90 | 17.80 | 26.70 | 35.60 | 44.50 |
| R1 (N) | .54 | .27 | -.54 | -1.75 | -4.70 |
| H1 (N) | 5.33 | 8.20 | 12.31 | 18.87 | 23.38 |
| H2 (N) | .70 | 2.45 | 3.51 | 6.66 | 9.82 |
| V1 (N) | 1.95 | 4.29 | 6.63 | 9.76 | 12.10 |
| V2 (N) | -2.96 | -5.17 | -6.65 | -8.13 | -8.13 |
| V3 (N) | - | - | - | - | - |
| V4 (N) | - | - | - | - | - |
| Fx (N) | 2.91 | 5.82 | 8.73 | 11.64 | 14.55 |
| Fy (N) | 3.88 | 7.76 | 11.64 | 15.52 | 19.40 |
| Fz (N) | 7.46 | 14.92 | 22.37 | 29.83 | 37.29 |
| Sum R | .54 | .27 | -.54 | -1.75 | -4.70 |
| Sum H | 6.03 | 10.65 | 15.82 | 25.53 | 33.20 |
| Sum V | -1.01 | -.88 | -.02 | 1.63 | 3.97 |
| R ratio | .186 | .046 | -.062 | -.150 | -.323 |
| H ratio | 1.554 | 1.372 | 1.359 | 1.645 | 1.711 |
| V ratio | -.135 | -.059 | -.001 | .055 | .106 |

## 566C DRY INSITU CALIBRATION

Segment Number: 1 Calibration Number: 18
Cal. Location:@ Station 10.00 @23.00 ft. Waterline
Comments: Calibration is NORMAL to Surface

| | APPLIED LOAD (N) | | | | |
|---|---|---|---|---|---|
| | 8.90 | 17.80 | 26.70 | 35.60 | 44.50 |
| R1 (N) | 3.90 | 8.33 | 12.90 | 15.46 | 18.14 |
| H1 (N) | -1.64 | -3.28 | -5.74 | -8.20 | -10.67 |
| H2 (N) | 5.61 | 11.92 | 19.63 | 24.89 | 30.50 |
| V1 (N) | 0.00 | 0.00 | .39 | .39 | -.78 |
| V2 (N) | 7.76 | 16.25 | 26.23 | 36.20 | 45.07 |
| V3 (N) | - | - | - | - | - |
| V4 (N) | - | - | - | - | - |
| Fx (N) | 2.76 | 5.52 | 8.28 | 11.04 | 13.80 |
| Fy (N) | 4.89 | 9.77 | 14.66 | 19.54 | 24.43 |
| Fz (N) | 6.91 | 13.81 | 20.72 | 27.63 | 34.53 |
| Sum R | 3.90 | 8.33 | 12.90 | 15.46 | 18.14 |
| Sum H | 3.97 | 8.64 | 13.89 | 16.69 | 19.83 |
| Sum V | 7.76 | 16.25 | 26.62 | 36.59 | 44.29 |
| R ratio | 1.414 | 1.510 | 1.559 | 1.401 | 1.315 |
| H ratio | .813 | .884 | .948 | .854 | .812 |
| V ratio | 1.124 | 1.176 | 1.285 | 1.324 | 1.283 |

## 566C DRY INSITU CALIBRATION

Segment Number: 1 Calibration Number: 19
Cal. Location:@ Station 10.29 @23.00 ft. Waterline
Comments: Calibration is NORMAL to Surface

| | APPLIED LOAD (N) | | | | |
|---|---|---|---|---|---|
| | 8.90 | 17.80 | 26.70 | 35.60 | 44.50 |
| R1 (N) | 2.28 | 4.30 | 5.64 | 9.81 | 12.63 |
| H1 (N) | 11.90 | 21.33 | 27.48 | 37.33 | 48.81 |
| H2 (N) | -3.86 | -7.01 | -8.77 | -8.77 | -8.77 |
| V1 (N) | 7.41 | 13.66 | 19.51 | 26.14 | 30.05 |
| V2 (N) | -1.48 | -2.96 | -3.69 | -2.96 | -3.69 |
| V3 (N) | - | - | - | - | - |
| V4 (N) | - | - | - | - | - |
| Fx (N) | 2.61 | 5.22 | 7.82 | 10.43 | 13.04 |
| Fy (N) | 4.53 | 9.06 | 13.59 | 18.12 | 22.65 |
| Fz (N) | 7.20 | 14.40 | 21.60 | 28.80 | 36.00 |
| Sum R | 2.28 | 4.30 | 5.64 | 9.81 | 12.63 |
| Sum H | 8.04 | 14.32 | 18.71 | 28.56 | 40.04 |
| Sum V | 5.93 | 10.70 | 15.82 | 23.18 | 26.36 |
| R ratio | .874 | .824 | .721 | .940 | .969 |
| H ratio | 1.775 | 1.581 | 1.377 | 1.576 | 1.768 |
| V ratio | .824 | .743 | .732 | .805 | .732 |

# 566C DRY INSITU CALIBRATION

Segment Number: 1 Calibration Number: 20
Cal. Location:@ Station 9.68 @16.90 ft. Waterline
Comments: Calibration is NORMAL to Surface

| | APPLIED LOAD (N) | | | | |
|---|---|---|---|---|---|
| | 8.90 | 17.80 | 26.70 | 35.60 | 44.50 |
| R1 (N) | 2.02 | 3.09 | 3.23 | 3.09 | 2.02 |
| H1 (N) | .41 | .82 | 1.23 | 2.05 | 1.64 |
| H2 (N) | 7.36 | 12.27 | 17.53 | 22.09 | 27.00 |
| V1 (N) | -4.29 | -7.41 | -9.76 | -12.88 | -15.61 |
| V2 (N) | -.37 | -1.85 | -3.32 | -4.80 | -5.17 |
| V3 (N) | - | - | - | - | - |
| V4 (N) | - | - | - | - | - |
| Fx (N) | 3.57 | 7.14 | 10.71 | 14.28 | 17.84 |
| Fy (N) | 4.24 | 8.47 | 12.71 | 16.95 | 21.18 |
| Fz (N) | 6.97 | 13.94 | 20.91 | 27.87 | 34.84 |
| Sum R | 2.02 | 3.09 | 3.23 | 3.09 | 2.02 |
| Sum H | 7.77 | 13.09 | 18.76 | 24.14 | 28.64 |
| Sum V | -4.66 | -9.26 | -13.08 | -17.68 | -20.78 |
| R ratio | .566 | .433 | .302 | .216 | .113 |
| H ratio | 1.834 | 1.545 | 1.476 | 1.425 | 1.352 |
| V ratio | -.669 | -.664 | -.626 | -.634 | -.596 |

# APPENDIX C

# SYSTEM RESPONSE TO MODEL MOTION

## C.1 Measuring System Response to Ship Motion

During the model ice tests the model was free to roll, pitch and heave, thus causing the question to arise as to the effect of these motions on measured segment loads (particularly vertical loads). One solution to reduce any affect the ship's motion may have on segment loads is to restrain the model from moving. However experience has shown that when the model is restrained, higher ice resistance is measured. Therefore, if ice resistance is affected when the model is restrained, it could be possible that both the horizontal and vertical forces may also be affected. Since the purpose of these tests was to determine the magnitude of the segment loads, it was decided to perform the model tests with as much model freedom as practical. Due to the fact that this model required being towed from the stern half of the ship (due to space limitations in the segmented half) it was necessary to restrain the model in both sway and yaw. Thus the model was permitted to roll, pitch and heave for all tests with the exception of the fourth ice sheet. During the fourth ice sheet, heave was also restrained.

To determine the effect model motion has on measured segment loads, a series of open water tests were performed. These tests began by properly adjusting and preloading each segment as done during the ice tests. The model was then subjected to a hydrodynamic load while recording the signal from all nineteen load cells, the model resistance, acceleration, roll, pitch and speed. As well, three LVDT's were installed on the model to measure vertical displacement. The first LVDT was placed on the heavestaff. The second LVDT was placed on the port gunnel a distance of 0.45 m from the midship plane. The second LVDT was approximately 0.10 m aft of the heavestaff. The third LVDT was placed in the midship plane on the stern gunnel a distance of 1.95 m from the heavestaff. (Note: the heave LVDT measures a positive displacement as up whereas the port and stern LVDT's measure a positive displacement as down).

The first four open water tests performed consisted of towing the segmented model down the length of the basin while permitting the model to either roll or pitch. The fifth open water test was performed with the model stationary. Initially three different weights were added in steps to the heavestaff to determine the effect on the segment when the model heaves. In the next series of tests the model was ballasted along the gunnel to determine the effect on the segments when the model rolls. Finally the model was ballasted at the bow followed by the stern to determine the effect when the model pitches. The final open water tests were a repeat of the fourth open water test with the heavestaff free to heave. Table C.1 lists the mean transducer readings for tests OW-1, OW-2, OW-3, OW-4 and OW-6. Table C.2 lists the results of the heave, roll and pitch tests of OW-5. The raw digitized data is plotted for each test as well at the end of this appendix.

Examining the results of Table C.1, maximum hydrodynamic segment load during open water resistance tests occurred in the vertical direction. Both $V_{11}$ and $V_{22}$ recorded a mean load of above 1 Newton. Also, a significant number of load cells recorded a signal of less than 0.1 Newtons (of the order of noise). A total of 53.3% of all resistance

## TABLE C.1
## RESULTS OF OPEN WATER RESISTANCE TESTS

| TRANSDUCER | OW-1 | OW-2 | OW-3 | OW-4 | OW-6 |
|---|---|---|---|---|---|
| $R_{11}$ | -.1332 N | -.0190 N | -.0249 N | .9910 N | +.0280 N |
| $H_{11}$ | -.4130 N | -.1732 N | -.1391 N | .2679 N | -.3930 N |
| $H_{12}$ | -.4790 N | -.2514 N | -.2380 N | .1650 N | -.7090 N |
| $V_{11}$ | -.1424 N | -.0986 N | -.3057 N | -1.0400 N | -1.2300 N |
| $V_{12}$ | -.01258 N | -.0970 N | -.2137 N | -.5420 N | -.7870 N |
| $R_{21}$ | +.7690 N | +.1665 N | +.0616 N | -.2973 N | -.6370 N |
| $H_{21}$ | +.1302 N | +.0519 N | +.0418 N | +.0548 N | +.0110 N |
| $H_{22}$ | -.0125 N | +.0125 N | -.0214 N | +.0060 N | -.0812 N |
| $V_{21}$ | -.2058 N | -.1032 N | -.1949 N | -.5650 N | -.5900 N |
| $V_{22}$ | +.0626 N | -.1444 N | -.3097 N | -.9050 N | -1.3600 N |
| $V_{23}$ | +.7450 N | +.8330 N | -.2848 N | -.4870 N | -.8510 N |
| $V_{24}$ | +.0093 N | +.0015 N | +.0091 N | +.0022 N | +.0019 N |
| $R_{31}$ | -.1471 N | +.0338 N | -.0034 N | +.0256 N | -.0004 N |
| $H_{31}$ | -.1616 N | -.0149 N | +.0891 N | +.1052 N | -.0569 N |
| $H_{32}$ | +.0173 N | +.1447 N | +.1592 N | +.4450 N | +.9600 N |
| $V_{31}$ | +.0846 N | -.0133 N | -.0084 N | +.2252 N | -.0113 N |
| $V_{32}$ | +.1550 N | +.1312 N | +.2986 N | +.8920 N | +.7470 N |
| $V_{33}$ | -.1064 N | +.0615 N | -.0192 N | +.5380 N | -.2302 N |
| $V_{34}$ | +.1346 N | +.0129 N | +.0137 N | +.0754 N | -.3035 N |
| Res | -.3630 N | -.7260 N | -2.2900 N | -2.8700 N | -8.2030 N |
| $\ddot{X}$ accl.(m/s²) | -.000321 | -.000283 | -.000301 | -.0001225 | -.000503 |
| Pitch(Trim) | +.0721° | +.1702° | +.0385° | -.1936° | -.0895° |
| Roll (Heel) | +.0920° | +.0849° | -.0030° | -.0540° | -.0160° |
| Heave LVDT | -.013 mm | -.013 mm | -.006 mm | -.024 mm | -1.870 mm |
| Port LVDT | -.044 mm | -.140 mm | -.072 mm | -.662 mm | -1.354 mm |
| Speed | +.1276 m/s | .1980 m/s | .3101 m/s | .5770 m/s | .5670 m/s |

load cells were less than 0.1 Newtons. Similarly, 43.3% and 36.0% of all horizontal and vertical load cells respectively were less than 0.1 Newtons. Therefore, it appears that the higher hydrodynamic loads occurred in the vertical direction, but the magnitude of hydrodynamic loading due to these open water resistance tests was still relatively low.

Examining the results of Table C.2, it was observed that severe model movements cause the load cells to respond in different ways. As may be expected the resistance component was the least affected by heave, roll or pitch tests. Meanwhile, both horizontal and vertical components were affected due to changes in segment buoyancy forces and resulting loads on the load support points due to these changes. However, significant responses were associated with vertical load cells as can be noted in the table. It should be noted, however, that these changes are still small on an absolute scale (10N load is only 1 kg) and they should be interpreted in terms of the readings of the load cells. For instance if a load cell reads 5N and the pitch and roll correction amounts to 5N that is a significant correction which must be included. On the other hand if a cell reads 50N and the effect of pitch and roll amounts to 1N this is less significant and may or may not be used to correct the measurement.

It has been noted that 62.5% of all vertical measurements during the open water static tests exceeded 1.0 Newtons with a maximum of 13 Newtons occurring during the roll test on Segment 3. It was also noted that Segment 3 had the largest vertical response but was comparable in both resistance and horizontal direction. Comparing the pitch test with the bow down to the pitch tests with the stern down, there was considerably more effect on the vertical segment loads when the bow was submerged, i.e. when the segments were submerged. The comparative response of Segment 3 reflects its heavy weight compared to Segments 1 and 2. The magnitudes observed suggest that measured ship motions be used to apply some correction of the vertical load cell measurements of Segment 3.

The detailed results of open water tests are given in the following pages, preceded by a summary of test conditions given in Table C.3.

## TABLE C.2

## RESULTS OF OPEN WATER STATIC TESTS

| TRANSDUCER | HEAVE TEST HEAVESTAFF DOWN | ROLL TEST PORT DOWN | PITCH TEST | |
|---|---|---|---|---|
| | | | BOW DOWN | STERN DOWN |
| $R_{11}$ | -.05 N | -0.05 N | -0.07 | -0.07 |
| $H_{11}$ | +3.3 N | +0.2 N | +0.3 | 0 |
| $H_{12}$ | +0.2 N | +0.2 N | +0.6 | - .1 |
| $V_{11}$ | -1.2 N | -0.5 N | -1.8 | + .7 |
| $V_{12}$ | -0.7 N | -0.7 N | -1.0 | + .3 |
| $R_{21}$ | -0.2 N | +0.25 N | +1.0 | + .4 |
| $H_{21}$ | +0.1 N | +0.1 N | +0.1 | +0.1 |
| $H_{22}$ | +0.2 N | 0 N | -0.8 | +0.5 |
| $V_{21}$ | -1.2 N | -1.2 N | -0.6 | +0.05 |
| $V_{22}$ | -1.2 N | -2.9 N | -4.8 | +1.5 |
| $V_{23}$ | -3.2 N | -5.0 N | -2.0 | +0.8 |
| $V_{24}$ | +0.04 N | + .04 N | +0.04 | +0.04 |
| $R_{31}$ | -0.25 N | 0 N | 0 | 0 |
| $H_{31}$ | -0.35 N | -0.35 N | +.5 | +1.5 |
| $H_{32}$ | +1.0 N | +1.0 N | +1.0 | +1.2 |
| $V_{31}$ | -3.7 N | - 5 N | -3.5 | 0 |
| $V_{32}$ | -3.0 N | - 9 N | -7.2 | -1.5 |
| $V_{33}$ | -8.0 N | -13 N | -6 | 0 |
| $V_{34}$ | -3.3 N | -4.5 N | -6 | -1.2 |
| Pitch | - .02° | 0° | 0° | - .25° |
| Roll | 0° | 3.7° | 0° | 0° |
| Heave LVDT | -17 mm | -7.5 mm | -6 mm | -8 mm |
| Port LVDT | +14 mm | +32.5 mm | +6 mm | +8 mm |
| Stern LVDT | +16 mm | + 9.0 mm | -2.5 mm | +15 mm |

- Peak Measurements During Test
- Heave LVDT: up +ve, down -ve
- Port LVDT: up -ve, down +ve
- Stern LVDT: up -ve, down +ve
- +ve roll angle: port down, segments submerged
- -ve roll angle: port up, segments lifted
- +ve pitch angle: bow down, segments submerged
- -ve pitch angle: bow up, segments lifted

## TABLE C.3
## TEST CONDITIONS OF OPEN WATER TESTS

| CONDITIONS | TEST NUMBERS | | | | | |
|---|---|---|---|---|---|---|
| | 1 | 2 | 3 | 4 | 5 | 6 |
| Model Speed, m/s | 0.127 | 0.198 | 0.310 | 0.577 | 0 | 0.567 |
| Motions Restricted | | | | | | |
| Surge | Y | Y | Y | Y | Y | Y |
| Heave | Y | Y | Y | Y | N | N |
| Sway | Y | Y | Y | Y | Y | Y |
| Yaw | Y | Y | Y | Y | Y | Y |
| Pitch | N | N | N | N | N | N |
| Roll | N | N | N | N | N | N |
| Output Runs[1] | J1<br>K1<br>L1<br>M1 | J2<br>K2<br>L2<br>M2 | J3<br>K3<br>L3<br>M3 | J4<br>K4<br>L4<br>M4 | A5<br>B5<br>C5<br>D5<br>E5<br>F5<br>G5<br>H5<br>I5 | J6<br>K6<br>L6<br>M6 |

(1) Output runs are designated by a single letter followed by a digit. The digit denotes the test number while the letter is only used to specify a set of plots. For instance, the J-grouping includes H11, H12, V11, V12 plots and interval statistics. This grouping is identical for any run number. Another example is the H-grouping which includes pitch, roll, velocity and heave without interval statistics.

SEGMENTED MODEL TESTS *** 566C
TEST OW RUN J1

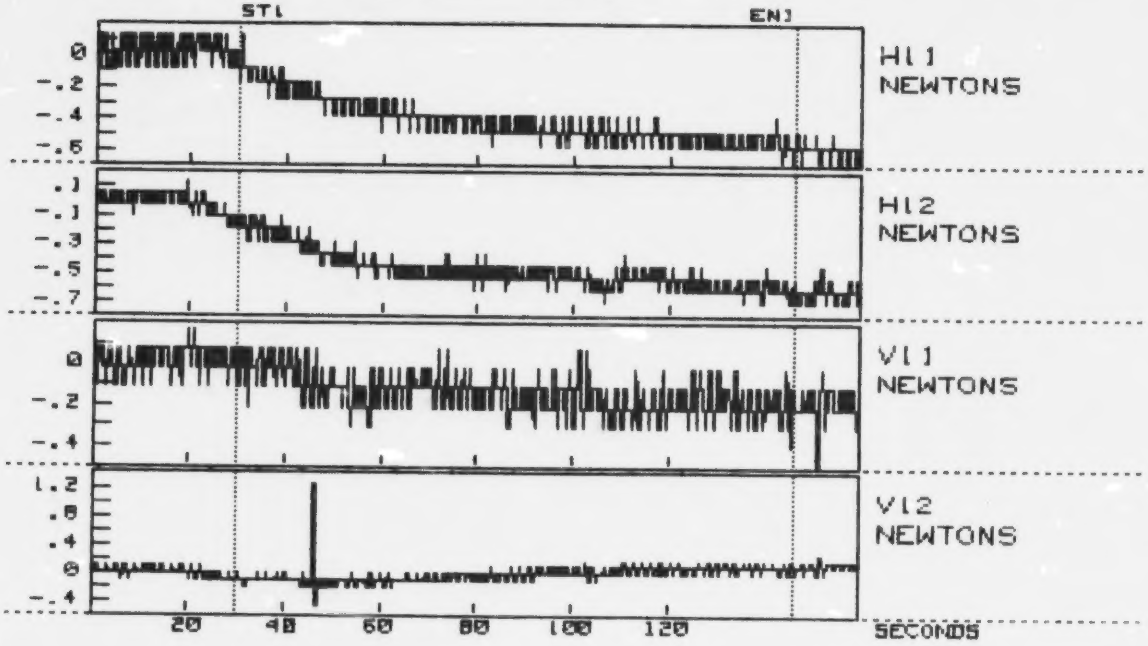

DATA DIGITIZED ON: 31 AUG 1983
DIGITIZING RATE: 32 Hz/CHANNEL
FILTER FREQUENCY: 1 HZ

INTERVAL STATISTICS

INTERVAL 1 START: 29.84375 END: 146.1875

| CHANNEL | MINIMUM | MAXIMUM | MEAN VALUE | STAN. DEV. |
|---|---|---|---|---|
| H11 | -.68 | .1214 | -.413 | .1261 |
| H12 | -.709 | -.1101 | -.479 | .1199 |
| V11 | -.402 | .07419 | -.1424 | .08593 |
| V12 | -.46 | 1.25 | -.012584 | .1142 |

SEGMENTED MODEL TESTS *** 566C
TEST OW RUN J1

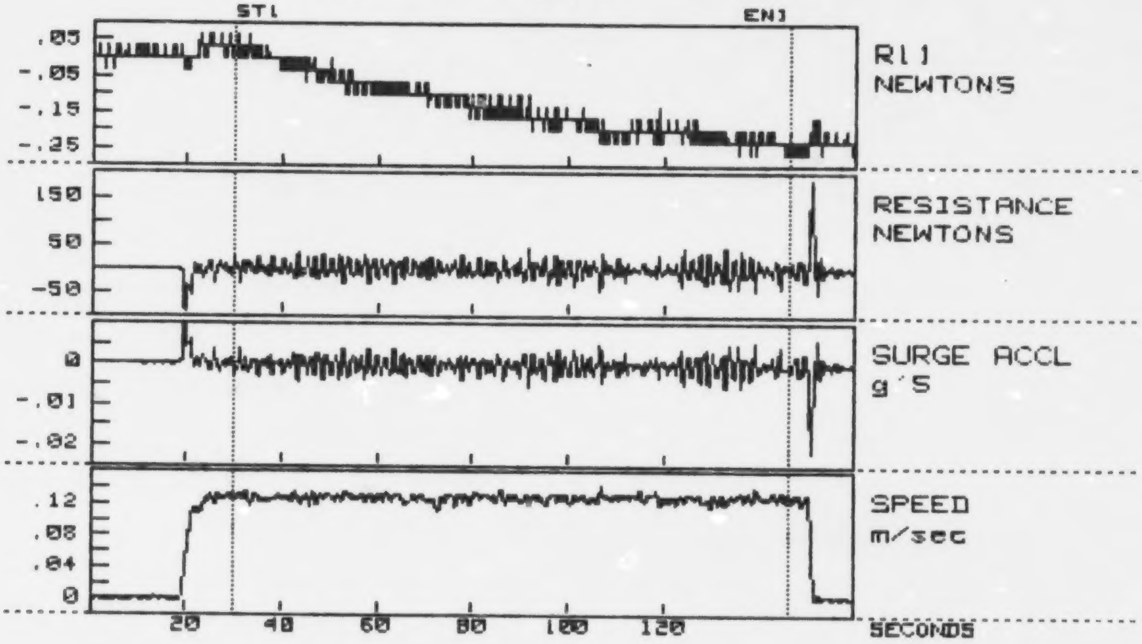

DATA DIGITIZED ON: 31 AUG 1983
DIGITIZING RATE: 32 Hz/CHANNEL
FILTER FREQUENCY: 1 HZ

INTERVAL STATISTICS

INTERVAL 1 START: 29.84375 END: 146.1875

| CHANNEL | MINIMUM | MAXIMUM | MEAN VALUE | STAN. DEV. |
|---|---|---|---|---|
| R11 | -.2644 | .0638 | -.1332 | .07714 |
| RESISTANCE | -47.287 | 45.525 | -.363 | 14.74 |
| SURGE ACCL | -.0056837 | .0053026 | -.000320983 | .00177413 |
| SPEED | .1109 | .1427 | .1276 | .0039907 |

SEGMENTED MODEL TESTS *** 566C
TEST OW RUN K1

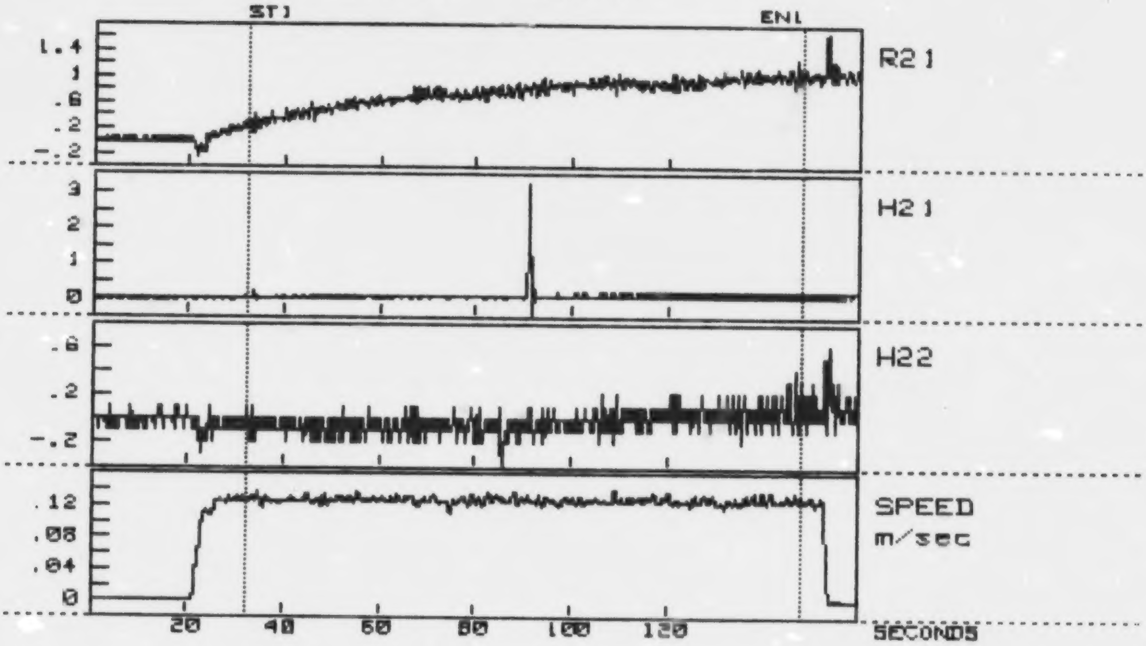

DATA DIGITIZED ON: 01 SEP 1983
DIGITIZING RATE: 32 Hz/CHANNEL
FILTER FREQUENCY: 1 HZ

INTERVAL STATISTICS

INTERVAL 1 START: 31.9375 END: 148.375

| CHANNEL | MINIMUM | MAXIMUM | MEAN VALUE | STAN. DEV. |
|---|---|---|---|---|
| R21 | .1167 | 1.28 | .769 | .2209 |
| H21 | -.44 | 3.293 | .1302 | .1848 |
| H22 | -.392 | .419 | -.01245 | .09494 |
| SPEED | .1098 | .1416 | .1277 | .0039905 |

SEGMENTED MODEL TESTS *** 566C
TEST OW RUN K1

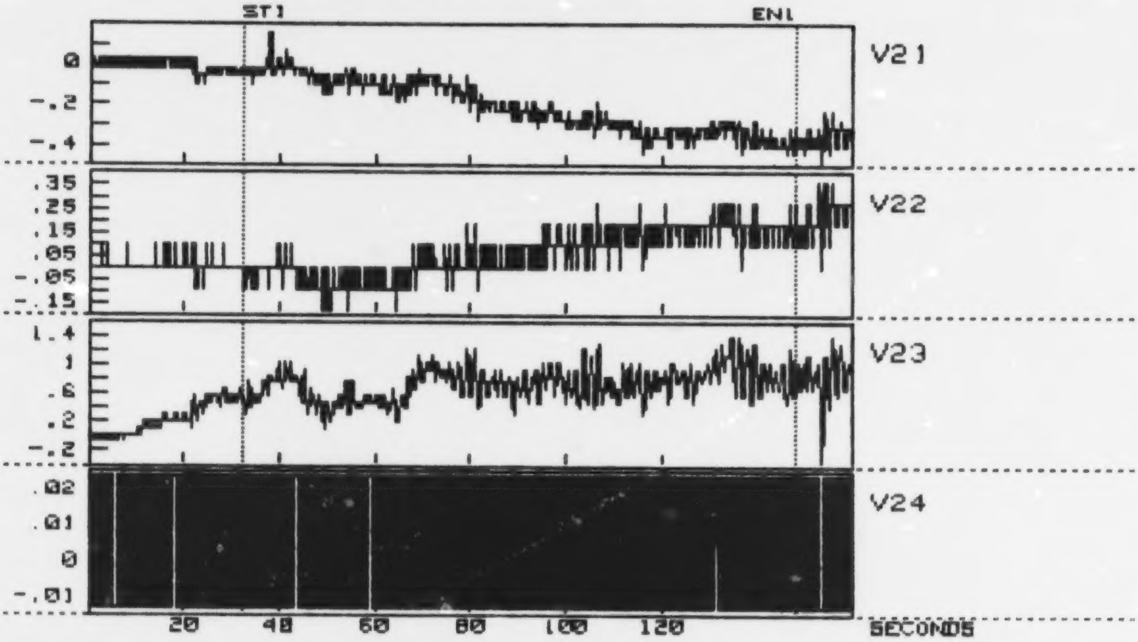

```
DATA DIGITIZED ON:  01 SEP 1983
  DIGITIZING RATE:  32  Hz/CHANNEL
 FILTER FREQUENCY:   1  HZ

                    INTERVAL STATISTICS

INTERVAL 1      START: 31.9375     END: 148.375

CHANNEL         MINIMUM        MAXIMUM        MEAN VALUE       STAN. DEV.
V21             -.44            .152          -.2058           .1238
V22             -.181           .2764          .06255          .09976
V23              .1187         1.4             .745            .2269
V24             -.013136        .023852        .0092532        .018079
```

## SEGMENTED MODEL TESTS *** 566C
## TEST OW RUN L1

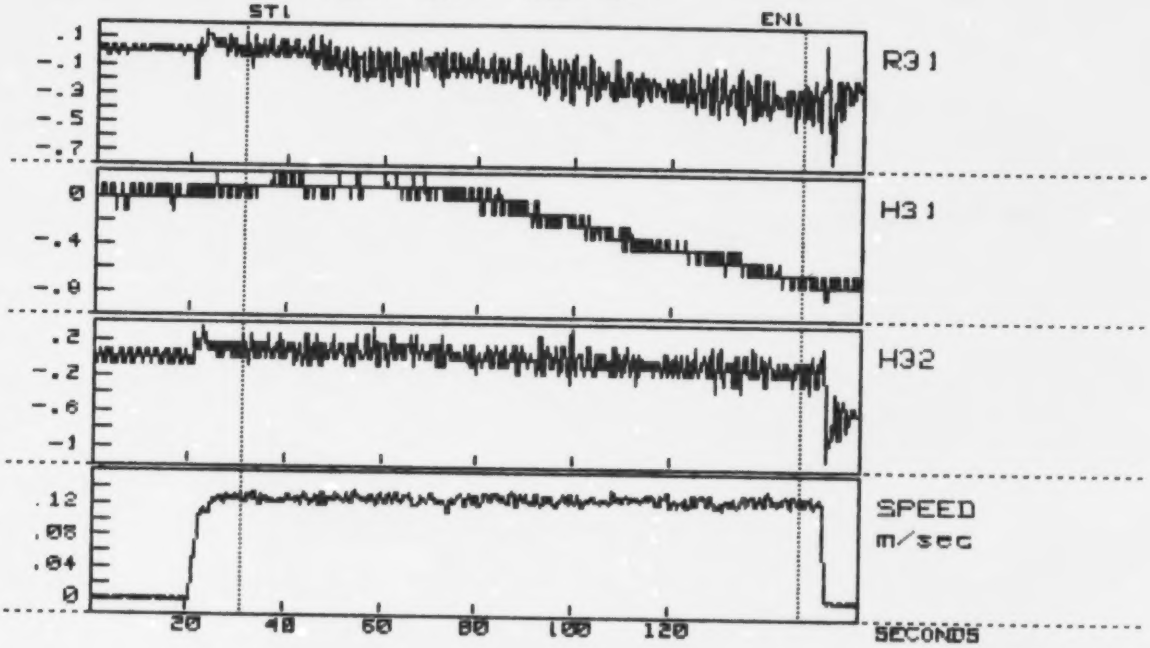

DATA DIGITIZED ON: 02 SEP 1983
DIGITIZING RATE: 32 Hz/CHANNEL
FILTER FREQUENCY: 1 HZ

### INTERVAL STATISTICS

INTERVAL 1 START: 31.15625 END: 147.625

| CHANNEL | MINIMUM | MAXIMUM | MEAN VALUE | STAN. DEV. |
|---|---|---|---|---|
| R31 | -.507 | .1147 | -.1471 | .1178 |
| H31 | -.73 | .1861 | -.1616 | .2554 |
| H32 | -.336 | .342 | .01728 | .1096 |
| SPEED | .1113 | .1406 | .1275 | .0039848 |

## SEGMENTED MODEL TESTS *** 566C
## TEST OW RUN L1

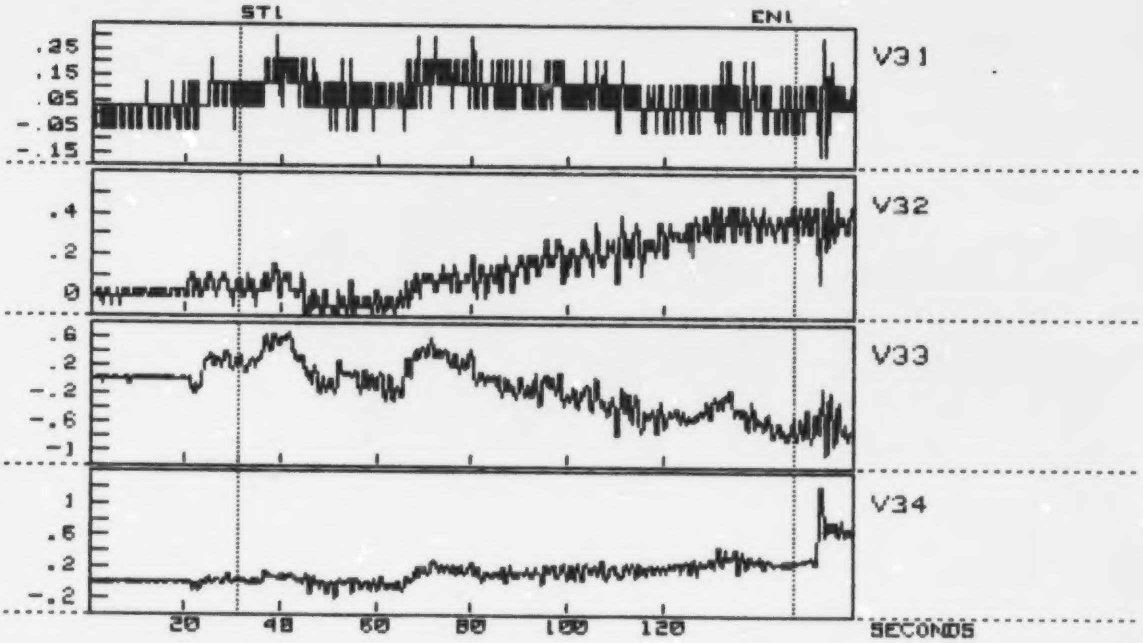

DATA DIGITIZED ON: 02 SEP 1983
DIGITIZING RATE: 32 Hz/CHANNEL
FILTER FREQUENCY: 1 HZ

### INTERVAL STATISTICS

INTERVAL 1 START: 31.15625 END: 147.625

| CHANNEL | MINIMUM | MAXIMUM | MEAN VALUE | STAN. DEV. |
|---|---|---|---|---|
| V31 | -.06055 | .3027 | .0846 | .06606 |
| V32 | -.08929 | .438 | .155 | .1414 |
| V33 | -.828 | .665 | -.1064 | .351 |
| V34 | -.2002 | .462 | .1346 | .1145 |

## SEGMENTED MODEL TESTS *** 566C
## TEST OW RUN M1

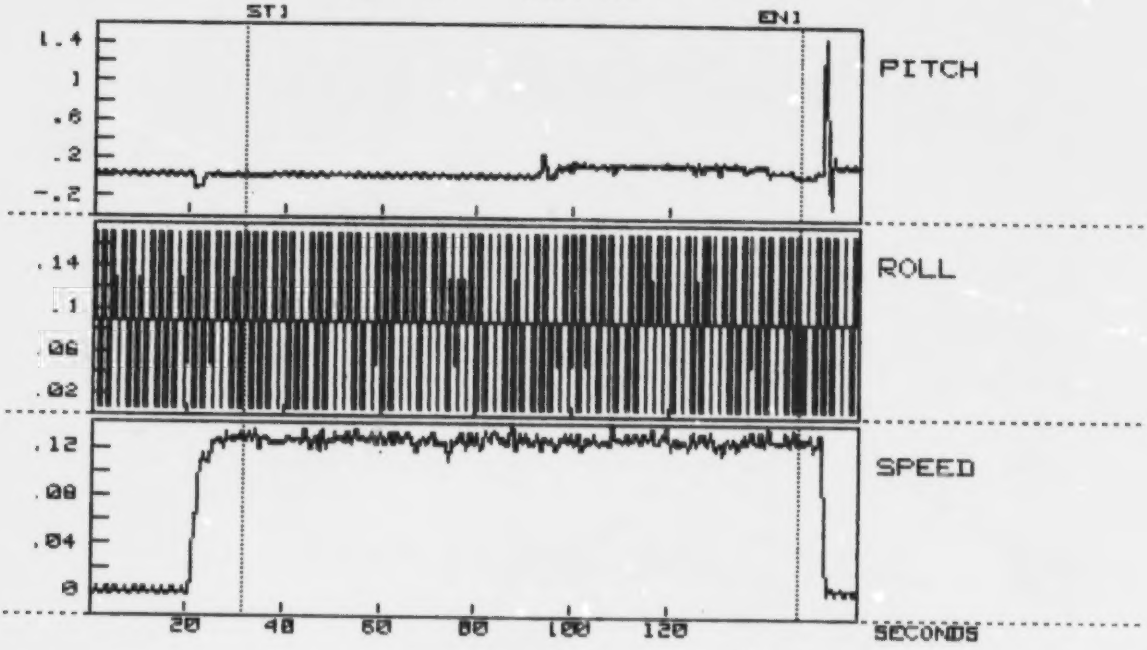

DATA DIGITIZED ON: 02 SEP 1983
DIGITIZING RATE: 32 Hz/CHANNEL
FILTER FREQUENCY: 1 HZ

### INTERVAL STATISTICS

INTERVAL 1 START: 31.34375 END: 147.8125

| CHANNEL | MINIMUM | MAXIMUM | MEAN VALUE | STAN. DEV. |
|---|---|---|---|---|
| PITCH | .0053118 | .2611 | .0721 | .05753 |
| ROLL | .0078867 | .1712 | .09198 | .04503 |
| SPEED | .1102 | .1395 | .1272 | .00403 |

SEGMENTED MODEL TESTS *** 566C
TEST OW RUN M1

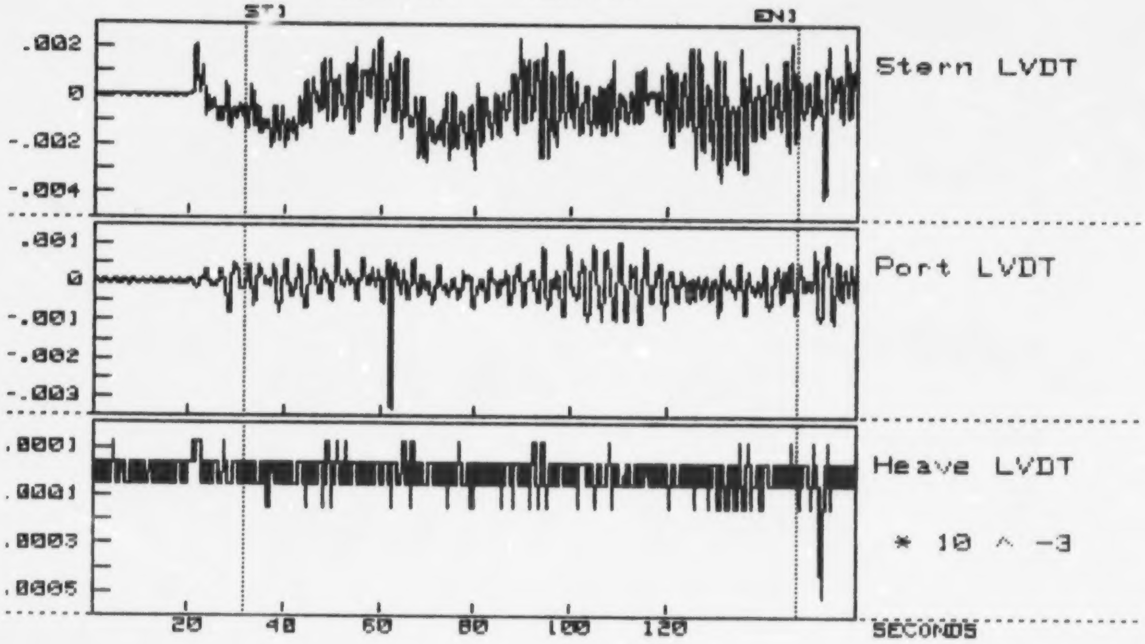

```
DATA DIGITIZED ON:  02 SEP 1983
  DIGITIZING RATE:  32  Hz/CHANNEL
 FILTER FREQUENCY:   1  HZ
```

INTERVAL STATISTICS

```
INTERVAL 1      START: 31.34375     END: 147.8125

CHANNEL          MINIMUM           MAXIMUM          MEAN VALUE         STAN. DEV.
Stern LVDT       -.0034364          .00237919       -.000416946        .00107636
Port LVDT        -.003293           .00106337       -4.417132E-5       .000415381
Heave LVDT       -.0001485425       .0001286792     -1.3005249E-5      5.443951E-5
```

## SEGMENTED MODEL TESTS *** 566C
## TEST OW RUN J2

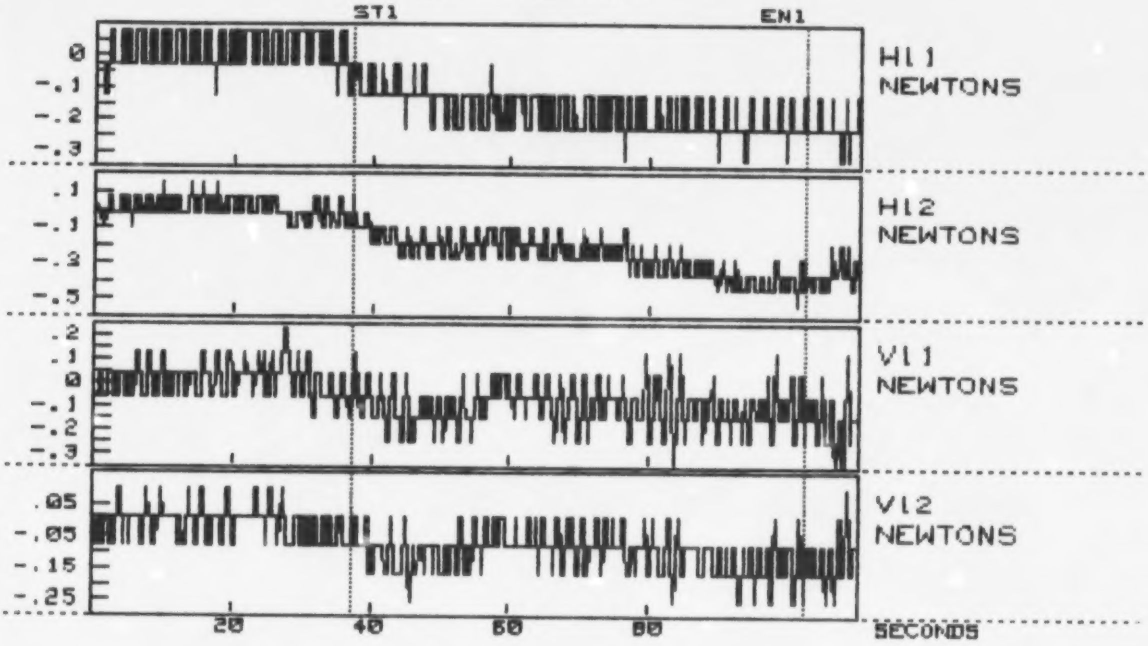

DATA DIGITIZED ON: 31 AUG 1983
DIGITIZING RATE: 32 Hz/CHANNEL
FILTER FREQUENCY: 1 HZ

### INTERVAL STATISTICS

INTERVAL 1 START: 37.21875 END: 102.21875

| CHANNEL | MINIMUM | MAXIMUM | MEAN VALUE | STAN. DEV. |
|---|---|---|---|---|
| H11 | -.325 | -.024647 | -.1732 | .05889 |
| H12 | -.529 | .07066 | -.2514 | .1053 |
| V11 | -.342 | .1347 | -.09864 | .08251 |
| V12 | -.2574 | .013205 | -.09696 | .05774 |

SEGMENTED MODEL TESTS *** 566C
TEST OW RUN J2

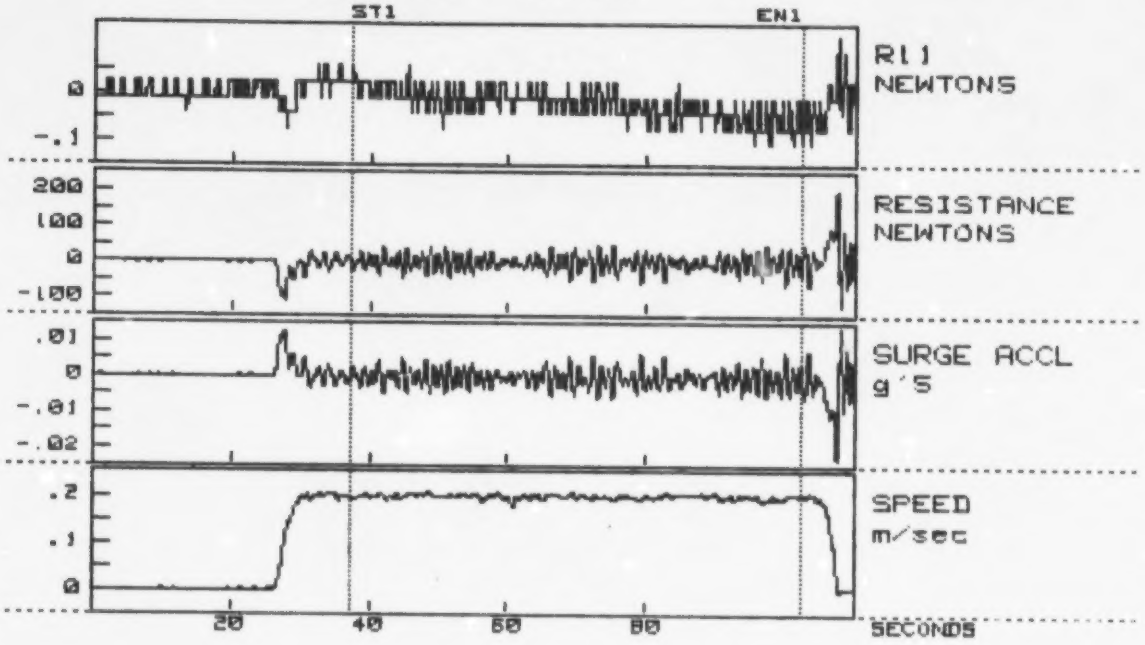

DATA DIGITIZED ON: 31 AUG 1983
DIGITIZING RATE: 32 Hz/CHANNEL
FILTER FREQUENCY: 1 HZ

INTERVAL STATISTICS

INTERVAL 1 START: 37.21875 END: 102.21875

| CHANNEL | MINIMUM | MAXIMUM | MEAN VALUE | STAN. DEV. |
|---|---|---|---|---|
| R11 | -.1054 | .05869 | -.019003 | .029644 |
| RESISTANCE | -63.296 | 50.545 | -.726 | 21.47 |
| SURGE ACCL | -.0062602 | .0069234 | -.0002830284 | .00248065 |
| SPEED | .176 | .2102 | .198 | .0046971 |

SEGMENTED MODEL TESTS *** 566C
TEST OW   RUN K2

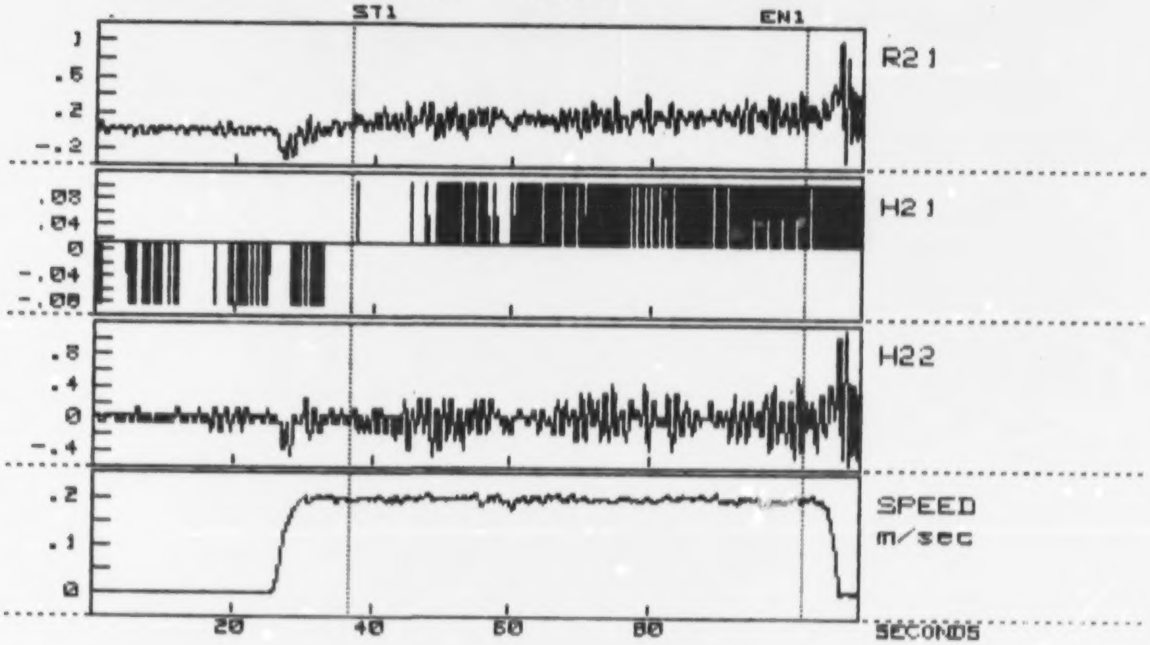

DATA DIGITIZED ON: 01 SEP 1983
DIGITIZING RATE: 32 Hz/CHANNEL
FILTER FREQUENCY: 1 HZ

INTERVAL STATISTICS

INTERVAL 1   START: 36.75   END: 101.84375

| CHANNEL | MINIMUM | MAXIMUM | MEAN VALUE | STAN. DEV. |
|---|---|---|---|---|
| R21 | -.07908 | .481 | .1665 | .09438 |
| H21 | .012209 | .1055 | .05192 | .04614 |
| H22 | -.468 | .546 | .012478 | .1615 |
| SPEED | .1751 | .2117 | .1982 | .0047764 |

SEGMENTED MODEL TESTS *** 566C
TEST OW   RUN K2

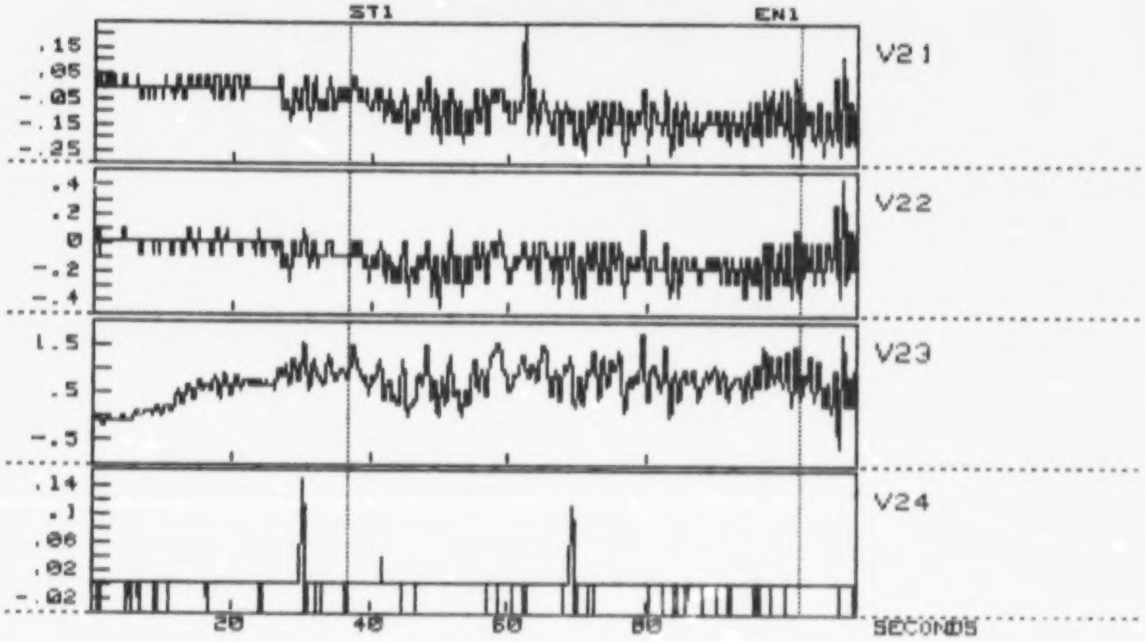

```
DATA DIGITIZED ON:   01 SEP 1983
  DIGITIZING RATE:   32  Hz/CHANNEL
 FILTER FREQUENCY:    1  HZ


                     INTERVAL STATISTICS

INTERVAL 1      START: 36.75     END: 101.84375

CHANNEL              MINIMUM           MAXIMUM         MEAN VALUE        STAN. DEV.
V21                  -.2598             .2479          -.1032            .06598
V22                  -.452              .09661         -.1444            .09692
V23                   .010009          1.75             .833             .332
V24                  -.03537            .1126           .00152441        .010595
```

SEGMENTED MODEL TESTS *** 56BC
TEST OW RUN L2

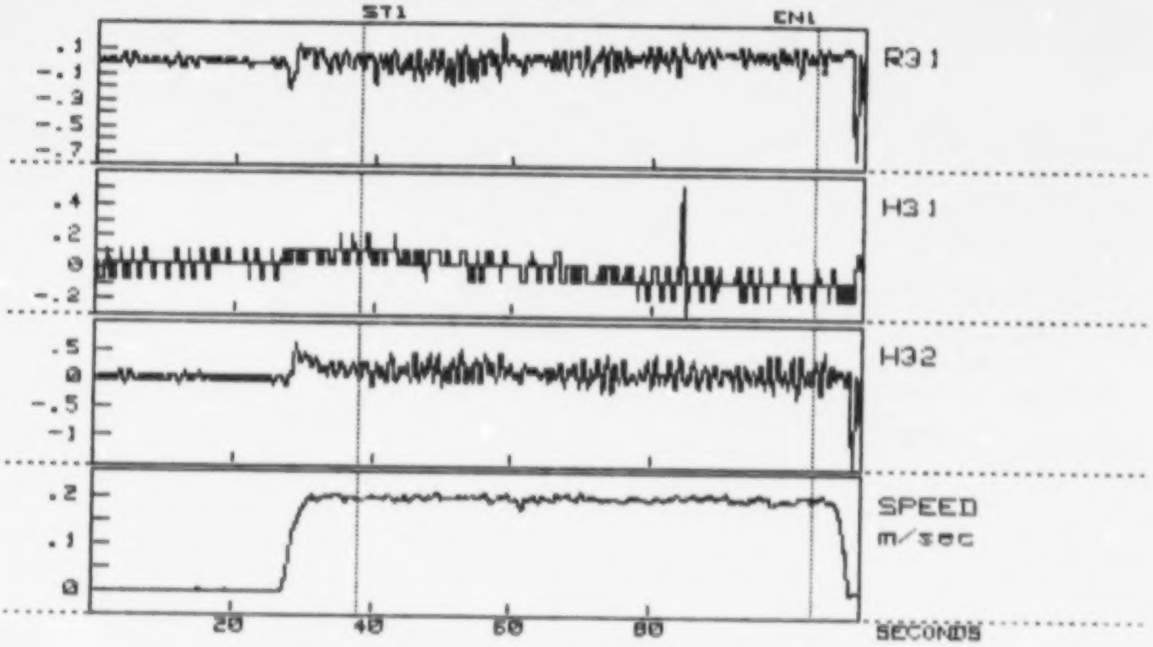

```
DATA DIGITIZED ON:  02 SEP 1983
  DIGITIZING RATE:  32  Hz/CHANNEL
 FILTER FREQUENCY:   1  HZ

                     INTERVAL STATISTICS

INTERVAL 1      START: 38.03125    END: 103.09375

CHANNEL         MINIMUM          MAXIMUM          MEAN VALUE       STAN. DEV.
R31             -.1701            .2186            .03381          .06853
H31             -.2853            .529            -.014861         .08938
H32             -.2952            .552             .1447           .1444
SPEED            .1741            .2107            .1978           .0047722
```

SEGMENTED MODEL TESTS *** 566C
TEST OW   RUN L2

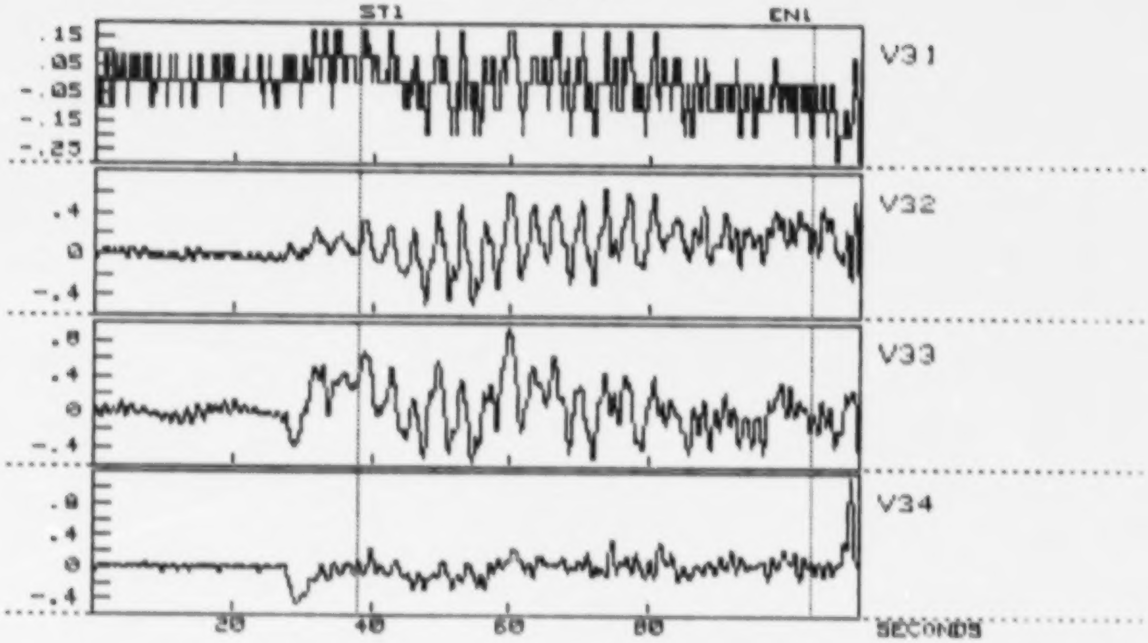

DATA DIGITIZED ON: 02 SEP 1983
DIGITIZING RATE: 32 Hz/CHANNEL
FILTER FREQUENCY: 1 HZ

INTERVAL STATISTICS

INTERVAL 1   START: 38.03125   END: 103.09375

| CHANNEL | MINIMUM | MAXIMUM | MEAN VALUE | STAN. DEV. |
|---|---|---|---|---|
| V31 | -.1924 | .1709 | -.01328 | .08321 |
| V32 | -.485 | .65 | .1312 | .2257 |
| V33 | -.556 | .937 | .0615 | .2837 |
| V34 | -.2623 | .365 | .012935 | .1078 |

SEGMENTED MODEL TESTS *** 56BC
TEST OW RUN M2

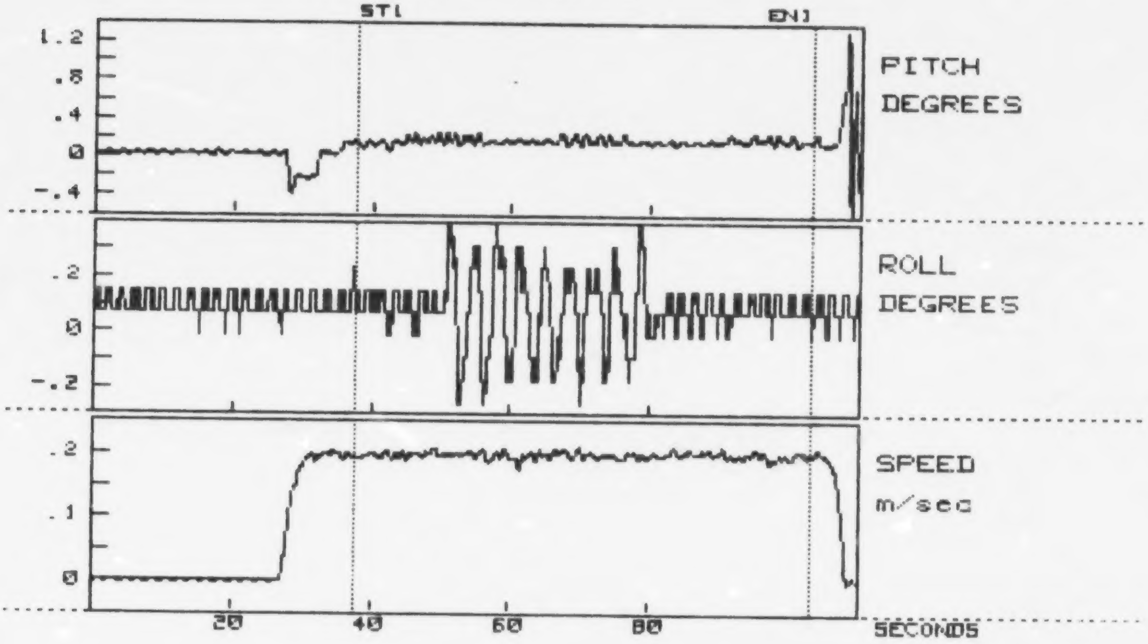

DATA DIGITIZED ON: 02 SEP 1983
DIGITIZING RATE: 32 Hz/CHANNEL
FILTER FREQUENCY: 1 HZ

INTERVAL STATISTICS

INTERVAL 1 START: 37.78125 END: 102.875

| CHANNEL | MINIMUM | MAXIMUM | MEAN VALUE | STAN. DEV. |
|---|---|---|---|---|
| PITCH | .04462 | .2578 | .1702 | .03086 |
| ROLL | -.2592 | .394 | .08493 | .1221 |
| SPEED | .1739 | .2106 | .1978 | .0047708 |

SEGMENTED MODEL TESTS *** 56BC
TEST OW RUN M2

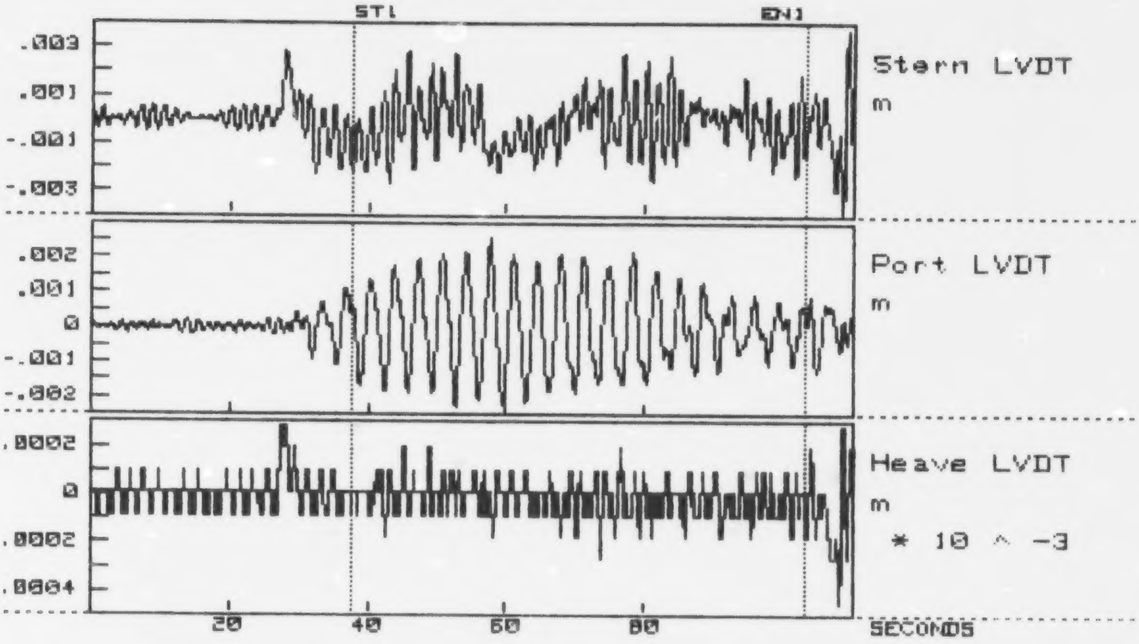

DATA DIGITIZED ON: 02 SEP 1983
DIGITIZING RATE: 32 Hz/CHANNEL
FILTER FREQUENCY: 1 HZ

INTERVAL STATISTICS

INTERVAL 1 START: 37.78125 END: 102.875

| CHANNEL | MINIMUM | MAXIMUM | MEAN VALUE | STAN. DEV. |
|---|---|---|---|---|
| Stern LVDT | -.00268795 | .00279997 | -.0001398414 | .00111405 |
| Port LVDT | -.00230601 | .00254219 | 1.1717859E-5 | .00112935 |
| Heave LVDT | -.0002688734 | .0001931628 | -1.2802474E-5 | 6.470599E-5 |

## SEGMENTED MODEL TESTS *** 566C
## TEST OW RUN J3

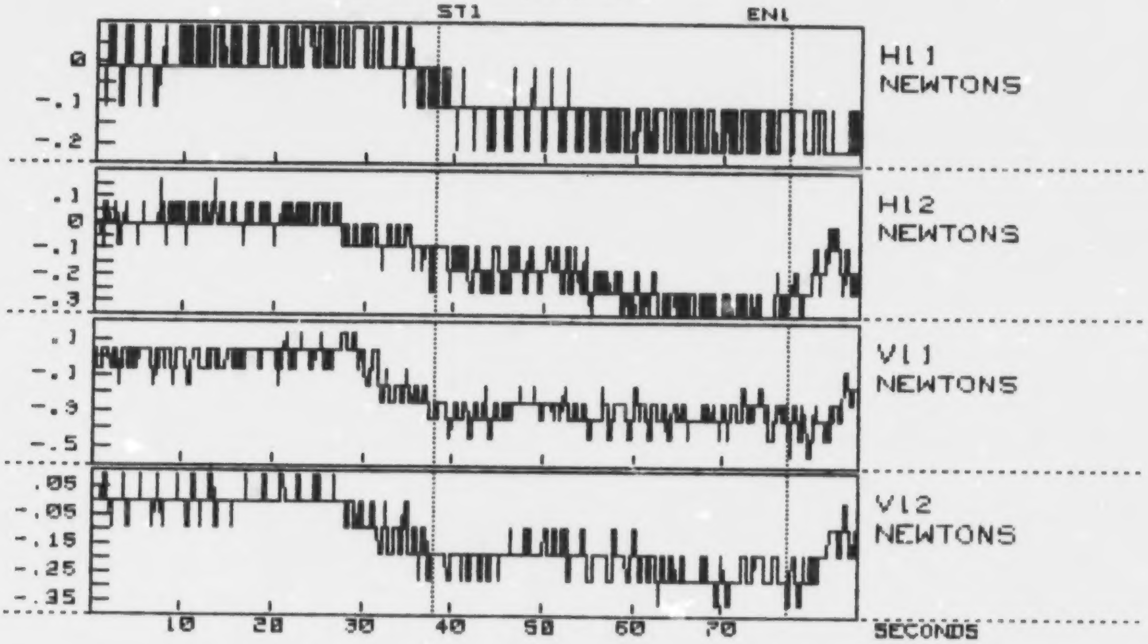

DATA DIGITIZED ON: 31 AUG 1983
DIGITIZING RATE: 32 Hz/CHANNEL
FILTER FREQUENCY: 1 HZ

### INTERVAL STATISTICS

INTERVAL 1 START: 37.875 END: 77.25

| CHANNEL | MINIMUM | MAXIMUM | MEAN VALUE | STAN. DEV. |
|---|---|---|---|---|
| H11 | -.2109 | -.010607 | -.1391 | .04965 |
| H12 | -.348 | -.09093 | -.238 | .08512 |
| V11 | -.442 | -.1561 | -.3057 | .06555 |
| V12 | -.362 | -.09131 | -.2137 | .05502 |

SEGMENTED MODEL TESTS *** 566C
TEST OW RUN J3

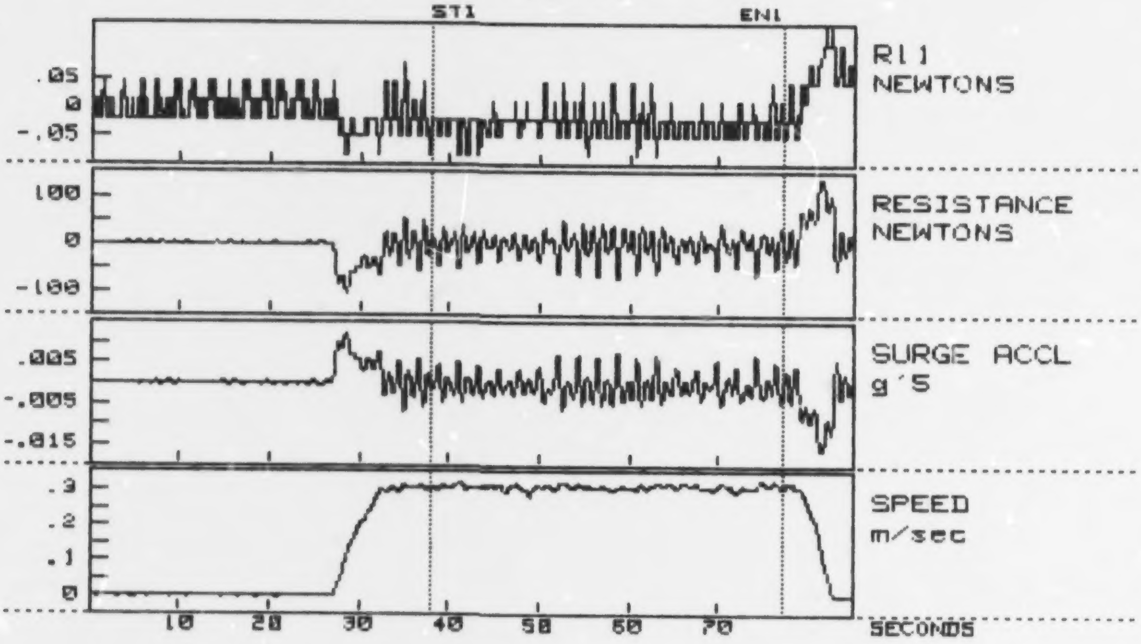

DATA DIGITIZED ON: 31 AUG 1983
DIGITIZING RATE: 32 Hz/CHANNEL
FILTER FREQUENCY: 1 HZ

## INTERVAL STATISTICS

INTERVAL 1 START: 37.875 END: 77.25

| CHANNEL | MINIMUM | MAXIMUM | MEAN VALUE | STAN. DEV. |
|---|---|---|---|---|
| R11 | -.08344 | .04785 | -.024871 | .023877 |
| RESISTANCE | -70.56 | 49.081 | -2.29 | 24.3 |
| SURGE ACCL | -.0062343 | .0074375 | -.0003011925 | .00275597 |
| SPEED | .2834 | .325 | .3101 | .0064001 |

SEGMENTED MODEL TESTS *** 566C
TEST OW    RUN K3

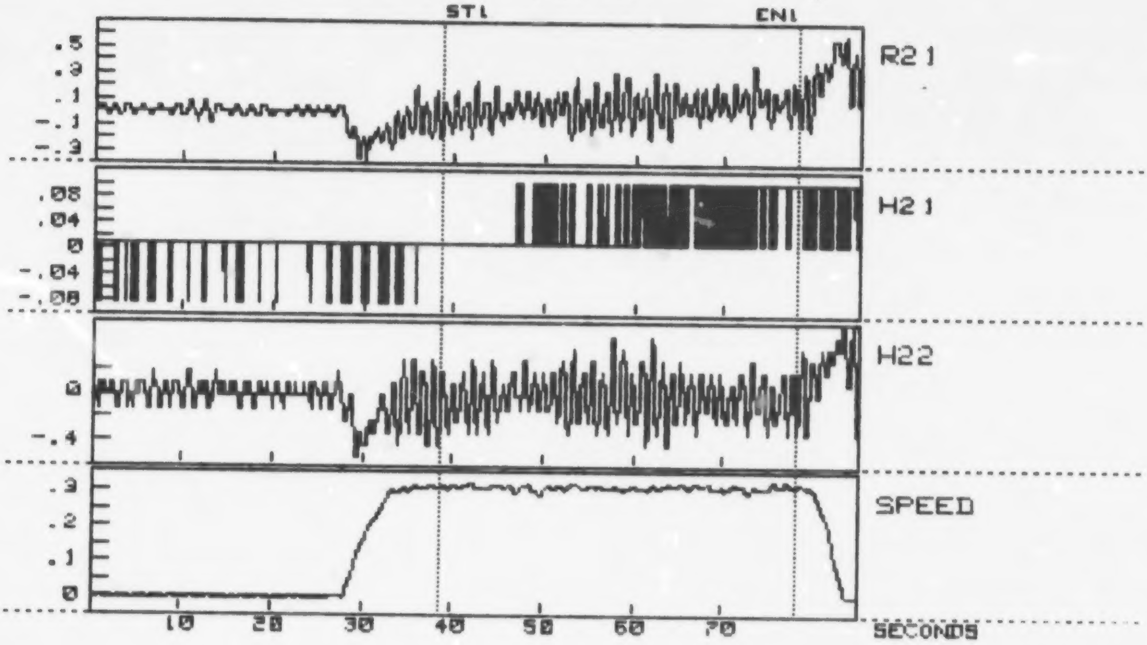

DATA DIGITIZED ON: 02 SEP 1983
DIGITIZING RATE: 32 Hz/CHANNEL
FILTER FREQUENCY: 1 HZ

INTERVAL STATISTICS

INTERVAL 1    START: 38.65625    END: 78.125

| CHANNEL | MINIMUM | MAXIMUM | MEAN VALUE | STAN. DEV. |
|---|---|---|---|---|
| R21 | -.1971 | .363 | .06162 | .108 |
| H21 | .010465 | .1038 | .04177 | .04406 |
| H22 | -.43 | .482 | -.021418 | .1727 |
| SPEED | .2845 | .326 | .3102 | .0063925 |

SEGMENTED MODEL TESTS *** 56BC
TEST OW RUN K3

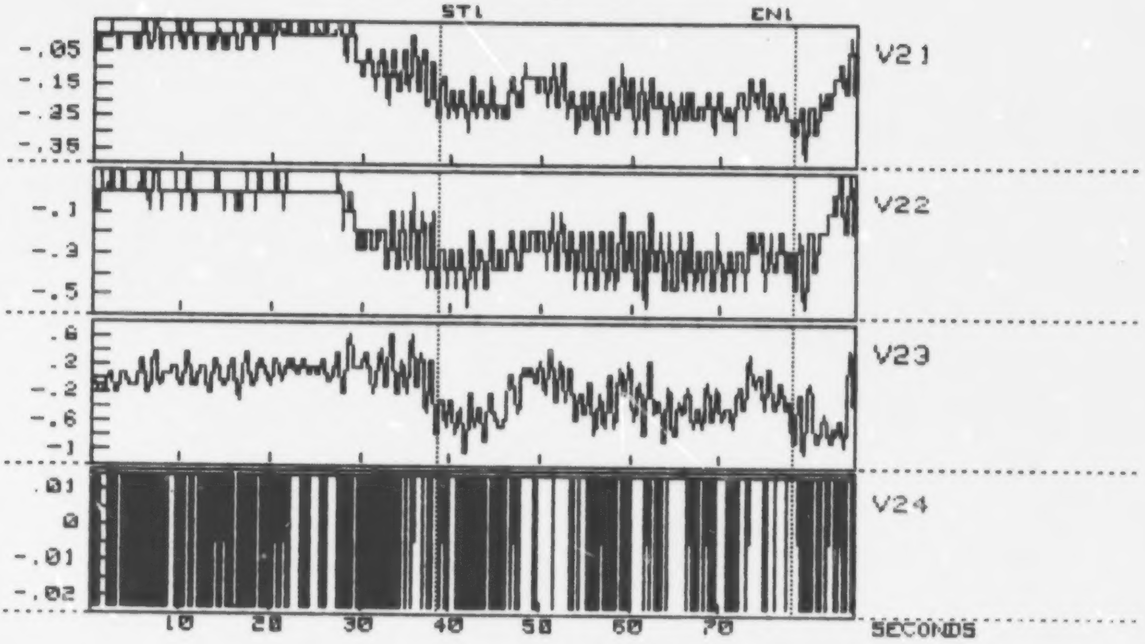

DATA DIGITIZED ON: 02 SEP 1983
DIGITIZING RATE: 32 Hz/CHANNEL
FILTER FREQUENCY: 1 HZ

INTERVAL STATISTICS

INTERVAL 1 START: 38.65625 END: 78.125

| CHANNEL | MINIMUM | MAXIMUM | MEAN VALUE | STAN. DEV. |
|---|---|---|---|---|
| V21 | -.2922 | -.08066 | -.1949 | .04745 |
| V22 | -.553 | -.09518 | -.3097 | .09001 |
| V23 | -1.02 | .447 | -.2848 | .2846 |
| V24 | -.022699 | .014288 | .0090793 | .012866 |

SEGMENTED MODEL TESTS *** 566C
TEST OW RUN L3

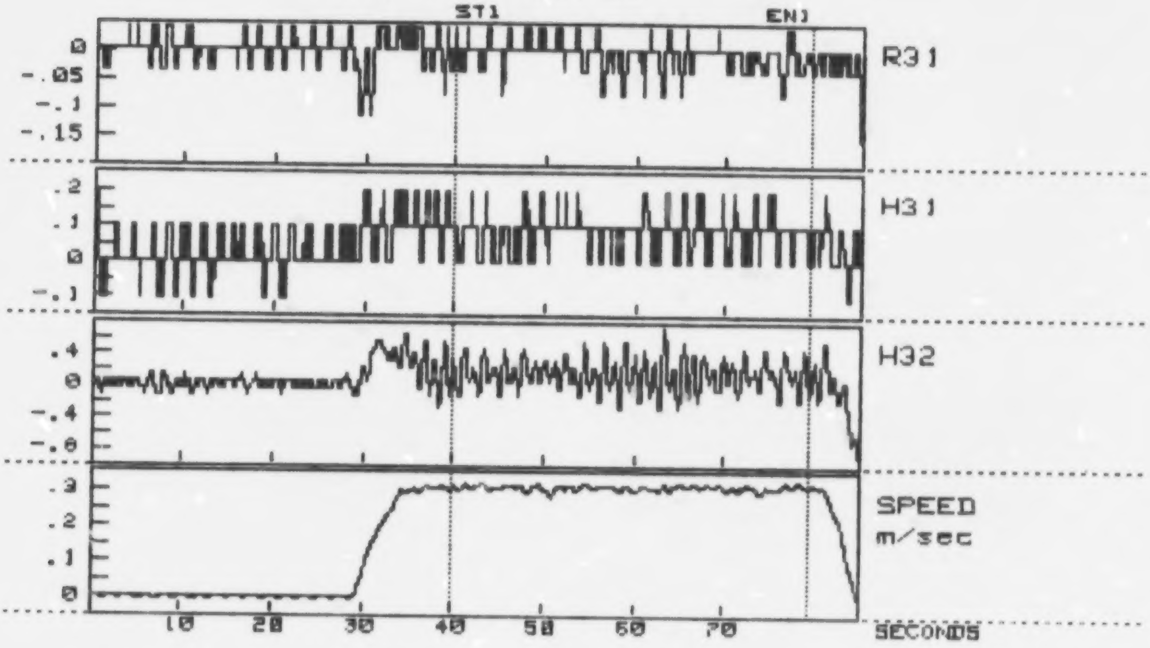

DATA DIGITIZED ON: 02 SEP 1983
DIGITIZING RATE: 32 Hz/CHANNEL
FILTER FREQUENCY: 1 HZ

INTERVAL STATISTICS

INTERVAL 1 START: 39.8125 END: 79.25

| CHANNEL | MINIMUM | MAXIMUM | MEAN VALUE | STAN. DEV. |
|---|---|---|---|---|
| R31 | -.07386 | .04274 | -.0034188 | .022902 |
| H31 | -.00126807 | .2023 | .08905 | .0496 |
| H32 | -.2798 | .737 | .1592 | .178 |
| SPEED | .2838 | .325 | .31 | .0065684 |

## SEGMENTED MODEL TESTS *** 566C
## TEST OW RUN L3

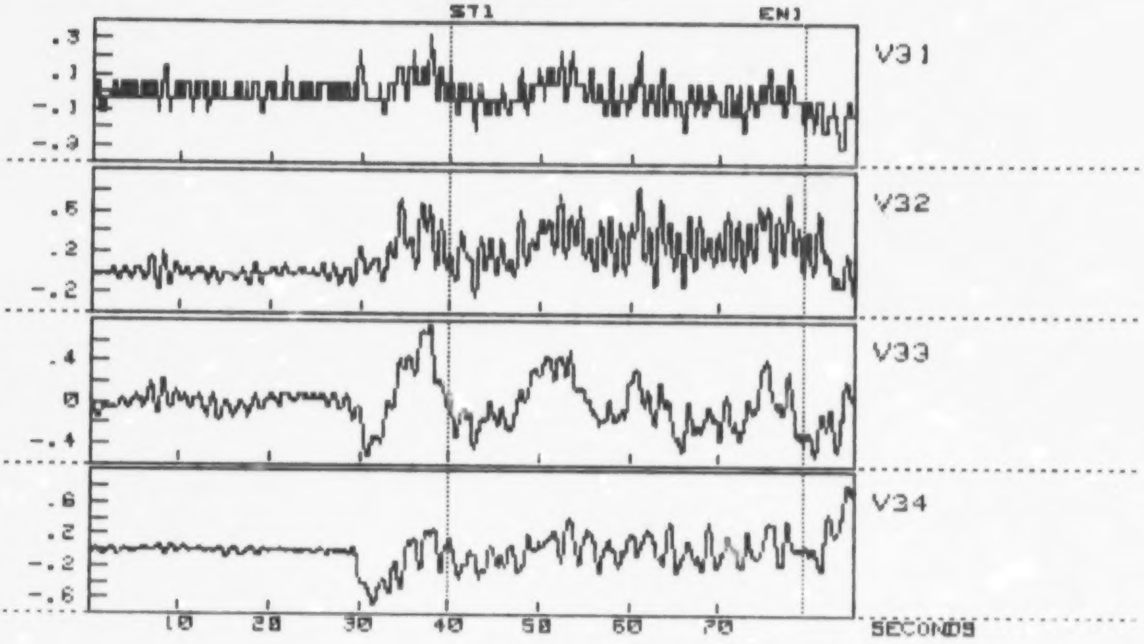

DATA DIGITIZED ON: 02 SEP 1983
DIGITIZING RATE: 32 Hz/CHANNEL
FILTER FREQUENCY: 1 HZ

### INTERVAL STATISTICS

INTERVAL 1 START: 39.8125 END: 79.25

| CHANNEL | MINIMUM | MAXIMUM | MEAN VALUE | STAN. DEV. |
|---|---|---|---|---|
| V31 | -.2142 | .2399 | -.0084476 | .08154 |
| V32 | -.2398 | .855 | .2986 | .2017 |
| V33 | -.477 | .53 | -.019244 | .2217 |
| V34 | -.343 | .424 | .013651 | .1667 |

SEGMENTED MODEL TESTS *** 56BC
TEST OW RUN M3

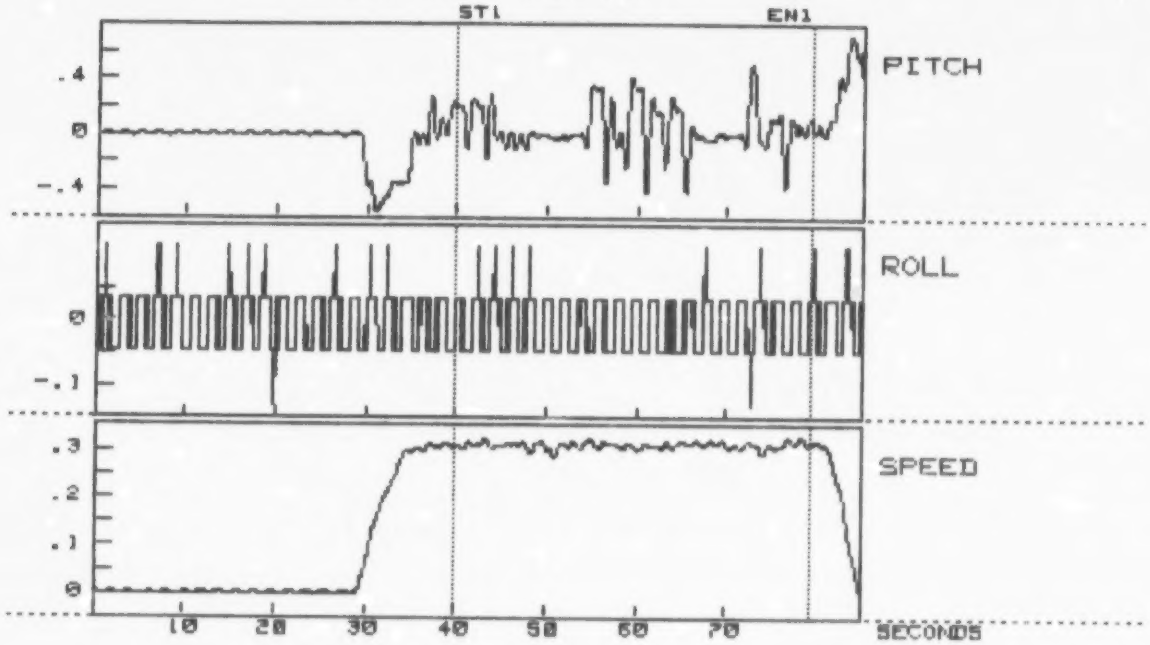

DATA DIGITIZED ON: 06 SEP 1983
DIGITIZING RATE: 32 Hz/CHANNEL
FILTER FREQUENCY: 1 HZ

INTERVAL STATISTICS

INTERVAL 1 START: 39.875 END: 79.3125

| CHANNEL | MINIMUM | MAXIMUM | MEAN VALUE | STAN. DEV. |
|---|---|---|---|---|
| PITCH | -.412 | .504 | .03852 | .1583 |
| ROLL | -.1289 | .1161 | -.00298545 | .04197 |
| SPEED | .2851 | .327 | .3105 | .0066242 |

SEGMENTED MODEL TESTS *** 56BC
TEST OW RUN M3

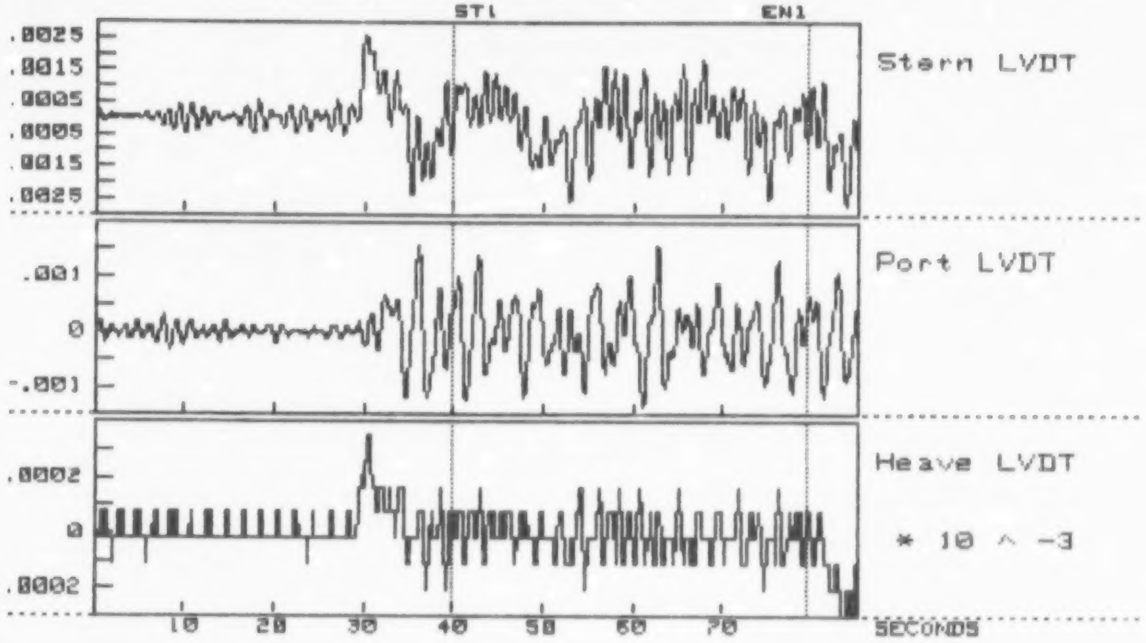

DATA DIGITIZED ON: 06 SEP 1983
DIGITIZING RATE: 32 Hz/CHANNEL
FILTER FREQUENCY: 1 HZ

INTERVAL STATISTICS

INTERVAL 1 START: 39.875 END: 79.3125

| CHANNEL | MINIMUM | MAXIMUM | MEAN VALUE | STAN. DEV. |
|---|---|---|---|---|
| Stern LVDT | -.00257809 | .001845 | -7.178727E-5 | .000876424 |
| Port LVDT | -.00137651 | .00157456 | -1.3572036E-5 | .000573682 |
| Heave LVDT | -.0002030071 | .0001666218 | -5.8278103E-6 | 6.752408E-5 |

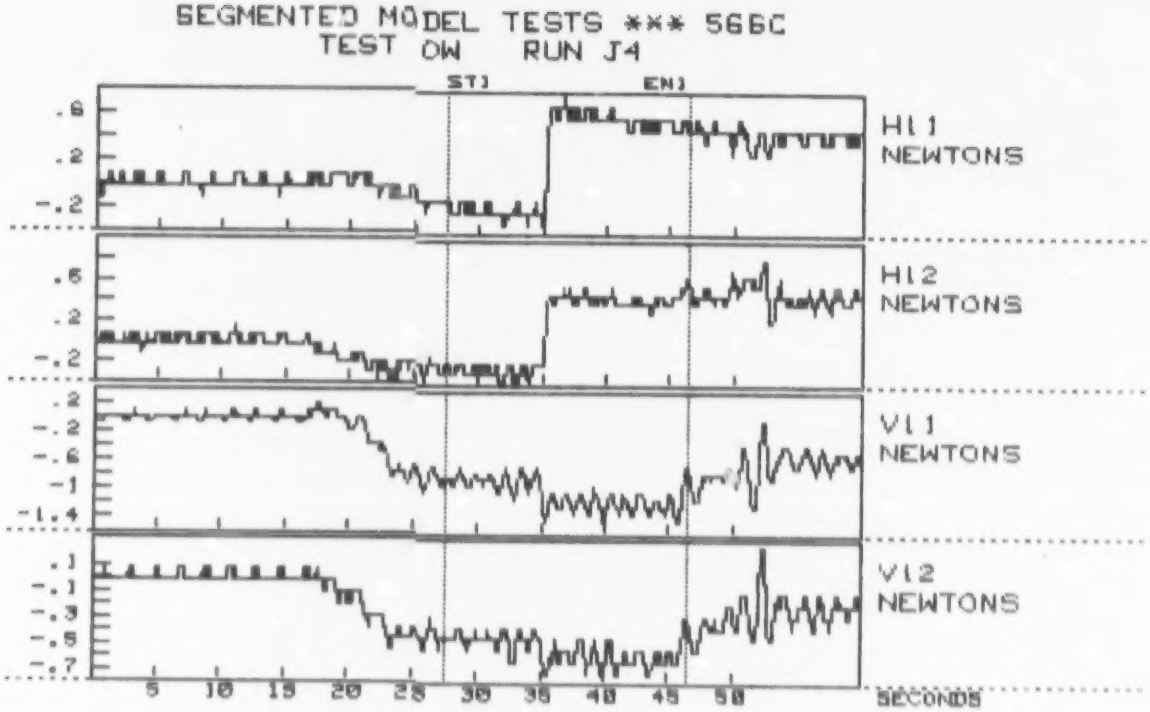

DATA DIGITIZED ON: 31 AUG 1983
DIGITIZING RATE: 32 Hz/CHANNEL
FILTER FREQUENCY: 1 HZ

INTERVAL STATISTICS

INTERVAL 1 START: 27.40625 END: 46.375

| CHANNEL | MINIMUM | MAXIMUM | MEAN VALUE | STAN. DEV. |
|---|---|---|---|---|
| H11 | -.3129 | .789 | .2679 | .389 |
| H12 | -.371 | .657 | .165 | .352 |
| V11 | -1.41 | -.649 | -1.04 | .2 |
| V12 | -.733 | -.2824 | -.542 | .1019 |

SEGMENTED MODEL TESTS *** 566C
TEST OW RUN J4

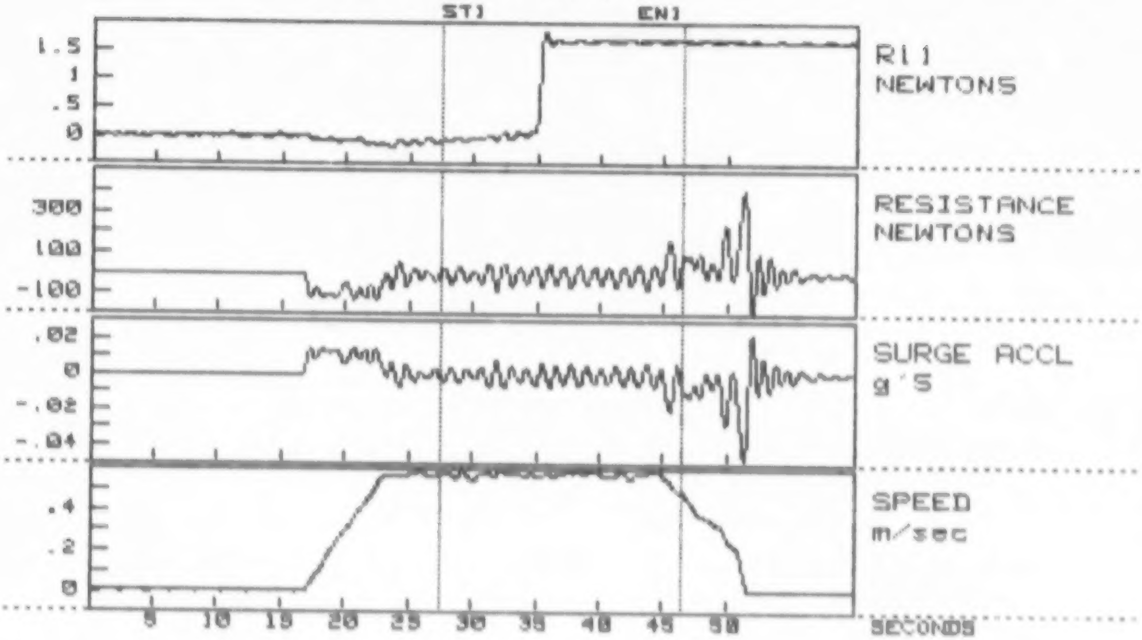

DATA DIGITIZED ON: 31 AUG 1983
DIGITIZING RATE: 32 Hz/CHANNEL
FILTER FREQUENCY: 1 HZ

INTERVAL STATISTICS

INTERVAL 1 START: 27.40625 END: 46.375

| CHANNEL | MINIMUM | MAXIMUM | MEAN VALUE | STAN. DEV. |
|---|---|---|---|---|
| R11 | -.08681 | 1.82 | .991 | .817 |
| RESISTANCE | -80.057 | 157.78 | -2.87 | 40.598 |
| SURGE ACCL | -.019854 | .0077342 | -.00122516 | .0046517 |
| SPEED | .493 | .598 | .577 | .018881 |

SEGMENTED MODEL TESTS *** 566C
TEST OW    RUN K4

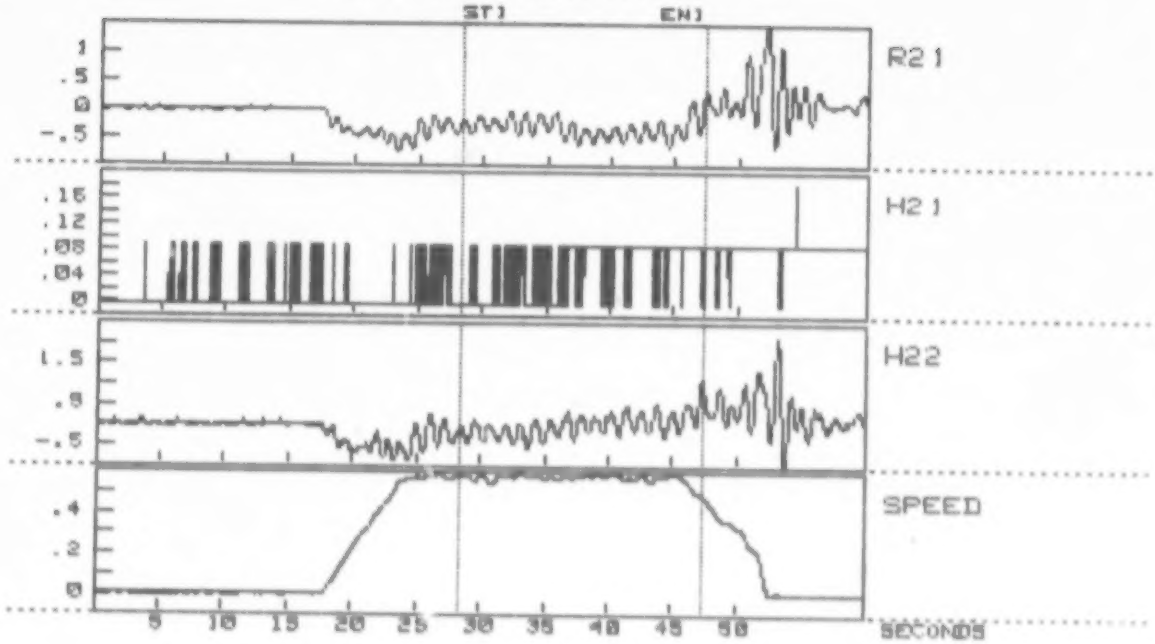

DATA DIGITIZED ON: 02 SEP 1983
DIGITIZING RATE: 32 Hz/CHANNEL
FILTER FREQUENCY: 1 HZ

INTERVAL STATISTICS

INTERVAL 1    START: 28.25    END: 47.25

| CHANNEL | MINIMUM | MAXIMUM | MEAN VALUE | STAN. DEV. |
|---|---|---|---|---|
| R21 | -.665 | .336 | -.2973 | .1695 |
| H21 | -.00261618 | .09069 | .05484 | .04539 |
| H22 | -.568 | 1.05 | .0059657 | .2702 |
| SPEED | .494 | .599 | .576 | .019128 |

SEGMENTED MODEL TESTS *** 566C
TEST OW RUN K4

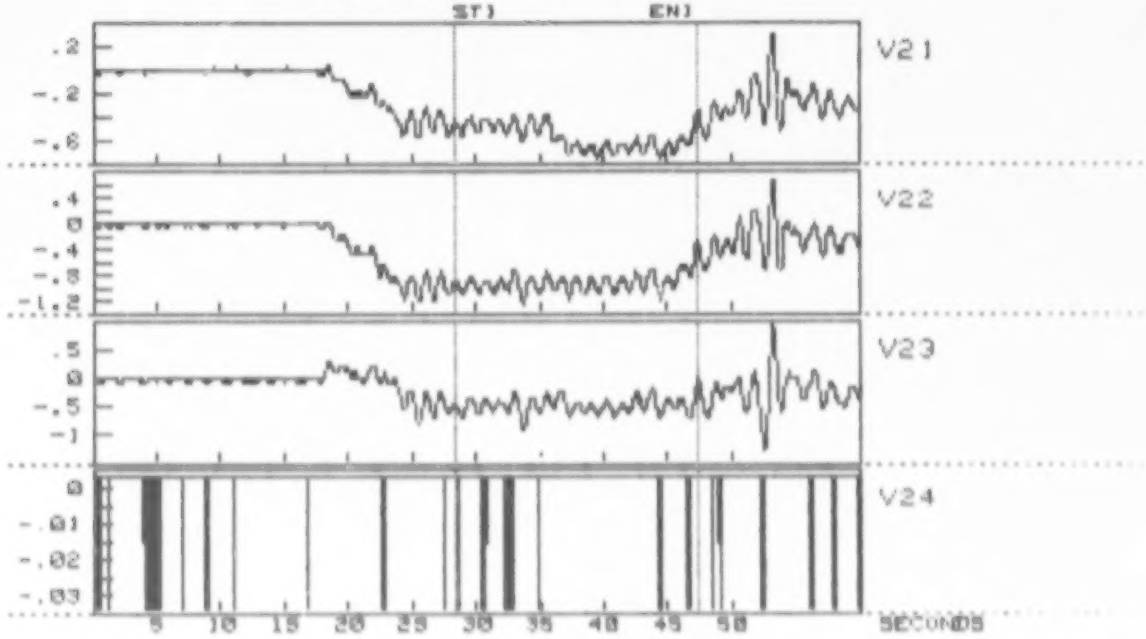

DATA DIGITIZED ON: 02 SEP 1983
DIGITIZING RATE: 32 Hz/CHANNEL
FILTER FREQUENCY: 1 HZ

INTERVAL STATISTICS

INTERVAL 1 START: 28.25 END: 47.25

| CHANNEL | MINIMUM | MAXIMUM | MEAN VALUE | STAN. DEV. |
|---|---|---|---|---|
| V21 | -.76 | -.337 | -.565 | .1049 |
| V22 | -1.26 | -.2556 | -.905 | .1373 |
| V23 | -.896 | -.06949 | -.487 | .137 |
| V24 | -.03342 | .003572 | .00223582 | .0069019 |

SEGMENTED MODEL TESTS *** 566C
TEST OW RUN L4

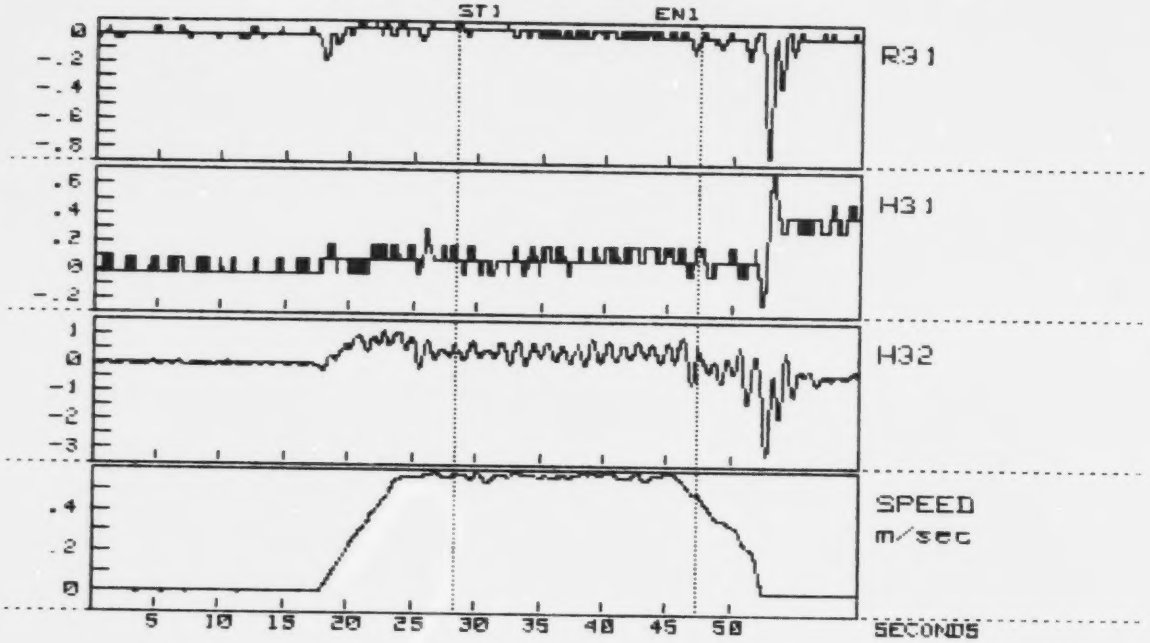

DATA DIGITIZED ON: 02 SEP 1983
DIGITIZING RATE: 32 Hz/CHANNEL
FILTER FREQUENCY: 1 HZ

INTERVAL STATISTICS

INTERVAL 1 START: 28.28125 END: 47.28125

| CHANNEL | MINIMUM | MAXIMUM | MEAN VALUE | STAN. DEV. |
|---|---|---|---|---|
| R31 | -.1118 | .08258 | .025649 | .025566 |
| H31 | -.017436 | .1861 | .1052 | .05909 |
| H32 | -.641 | .969 | .445 | .2513 |
| SPEED | .493 | .598 | .576 | .019156 |

SEGMENTED MODEL TESTS *** 566C
TEST OW RUN L4

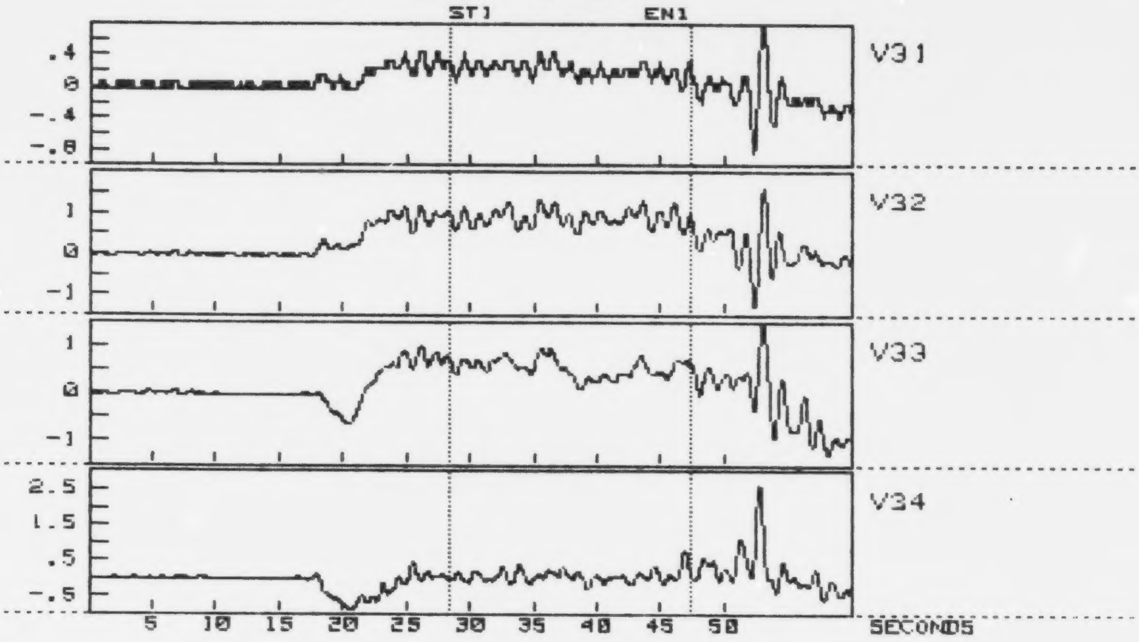

DATA DIGITIZED ON: 02 SEP 1983
DIGITIZING RATE: 32 Hz/CHANNEL
FILTER FREQUENCY: 1 HZ

INTERVAL STATISTICS

INTERVAL 1 START: 28.28125 END: 47.28125

| CHANNEL | MINIMUM | MAXIMUM | MEAN VALUE | STAN. DEV. |
|---|---|---|---|---|
| V31 | -.027727 | .426 | .2252 | .09081 |
| V32 | .498 | 1.35 | .892 | .198 |
| V33 | .1289 | .95 | .538 | .1907 |
| V34 | -.2759 | .805 | .0754 | .1671 |

SEGMENTED MODEL TESTS *** 566C
TEST OW RUN M4

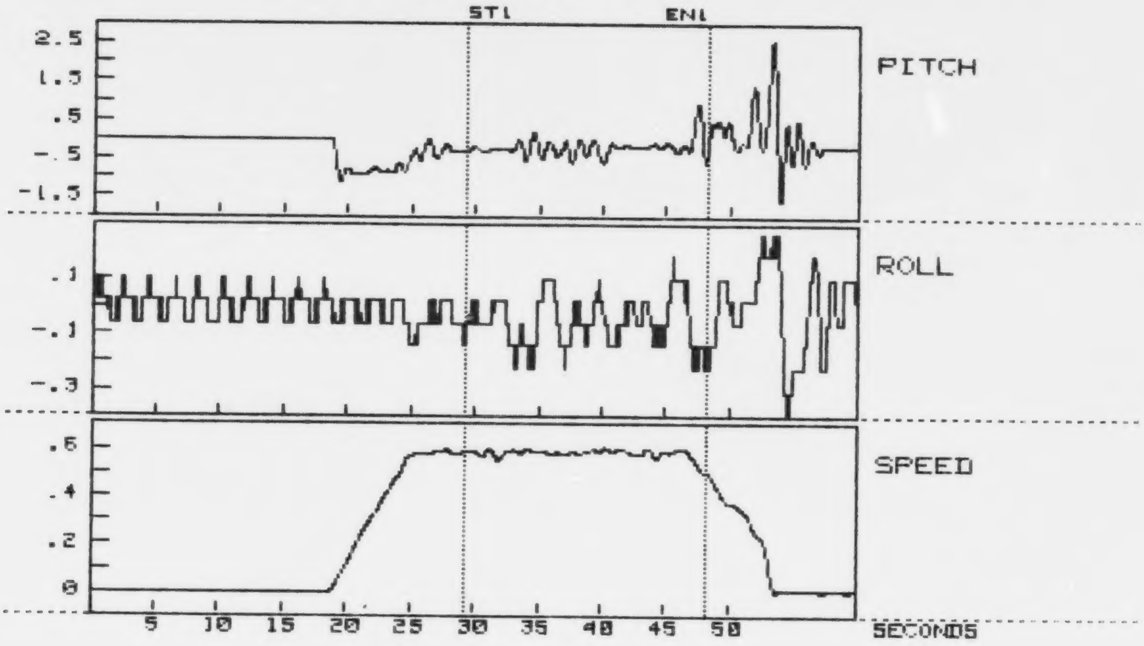

DATA DIGITIZED ON: 06 SEP 1983
DIGITIZING RATE: 32 Hz/CHANNEL
FILTER FREQUENCY: 1 HZ

## INTERVAL STATISTICS

INTERVAL 1 START: 29.28125 END: 48.28125

| CHANNEL | MINIMUM | MAXIMUM | MEAN VALUE | STAN. DEV. |
|---|---|---|---|---|
| PITCH | -.619 | .937 | -.1936 | .2301 |
| ROLL | -.2259 | .1825 | -.05099 | .08767 |
| SPEED | .495 | .6 | .578 | .019146 |

SEGMENTED MODEL TESTS *** 566C
TEST OW RUN M4

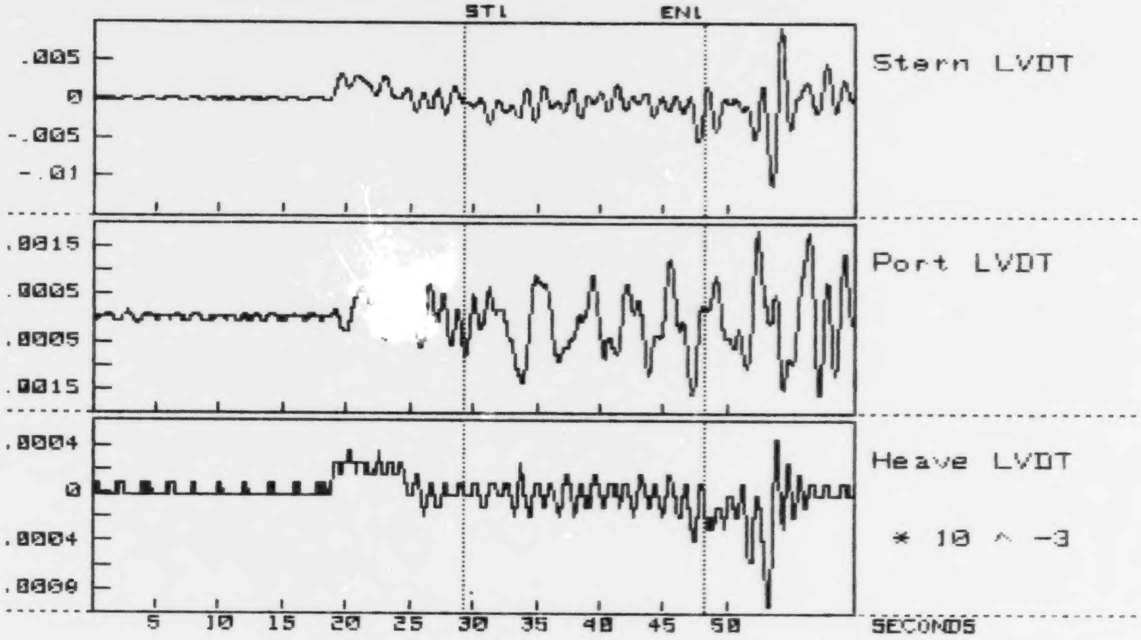

DATA DIGITIZED ON: 06 SEP 1983
DIGITIZING RATE: 32 Hz/CHANNEL
FILTER FREQUENCY: 1 HZ

INTERVAL STATISTICS

INTERVAL 1 START: 29.28125 END: 48.28125

| CHANNEL | MINIMUM | MAXIMUM | MEAN VALUE | STAN. DEV. |
|---|---|---|---|---|
| Stern LVDT | -.0054572 | .00199654 | -.000662486 | .00127027 |
| Port LVDT | -.00161123 | .00126958 | -.0001377735 | .000620313 |
| Heave LVDT | -.000388977 | .0002578739 | -2.4203315E-5 | .0001081591 |

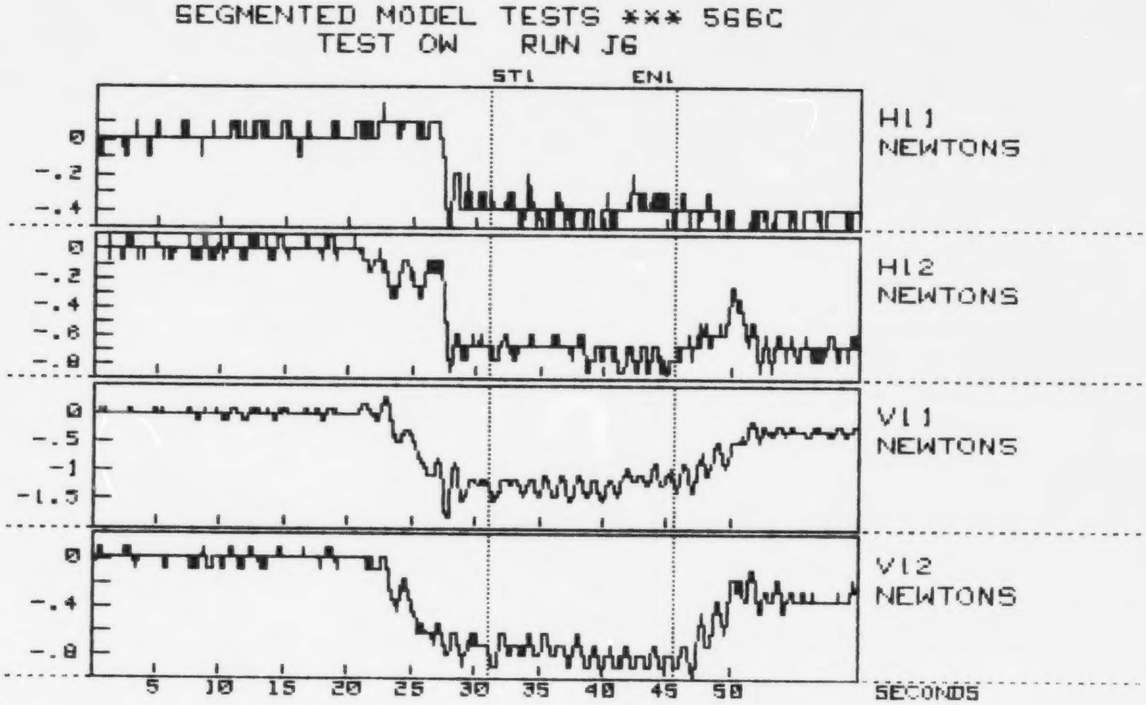

DATA DIGITIZED ON: 31 AUG 1983
DIGITIZING RATE: 32 Hz/CHANNEL
FILTER FREQUENCY: 1 HZ

## INTERVAL STATISTICS

INTERVAL 1 START: 31.0625 END: 45.5625

| CHANNEL | MINIMUM | MAXIMUM | MEAN VALUE | STAN. DEV. |
|---|---|---|---|---|
| H11 | -.495 | -.1947 | -.393 | .05704 |
| H12 | -.847 | -.591 | -.709 | .06371 |
| V11 | -1.53 | -.865 | -1.23 | .1454 |
| V12 | -.896 | -.625 | -.787 | .08212 |

SEGMENTED MODEL TESTS *** 566C
TEST OW RUN J6

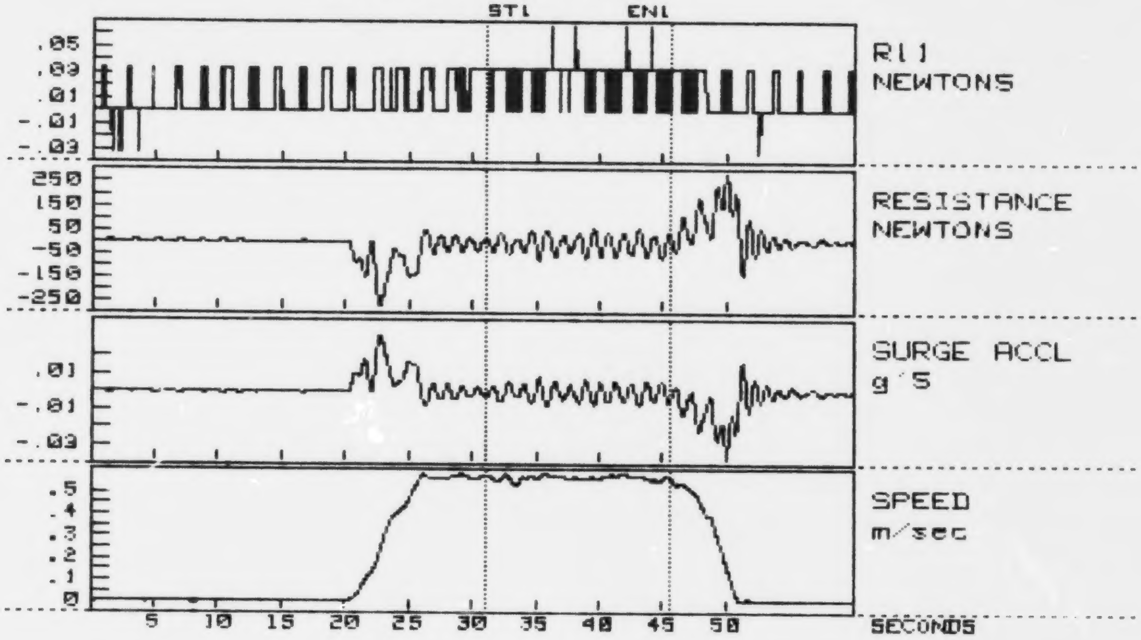

DATA DIGITIZED ON: 31 AUG 1983
DIGITIZING RATE: 32 Hz/CHANNEL
FILTER FREQUENCY: 1 HZ

INTERVAL STATISTICS

INTERVAL 1 START: 31.0625 END: 45.5625

| CHANNEL | MINIMUM | MAXIMUM | MEAN VALUE | STAN. DEV. |
|---|---|---|---|---|
| R11 | .00132925 | .06697 | .028011 | .013505 |
| RESISTANCE | -79.718 | 52.975 | -8.203 | 35.133 |
| SURGE ACCL | -.0075524 | .0075843 | -.000503286 | .0039689 |
| SPEED | .532 | .586 | .567 | .0095768 |

SEGMENTED MODEL TESTS *** 566C
TEST OW RUN K6

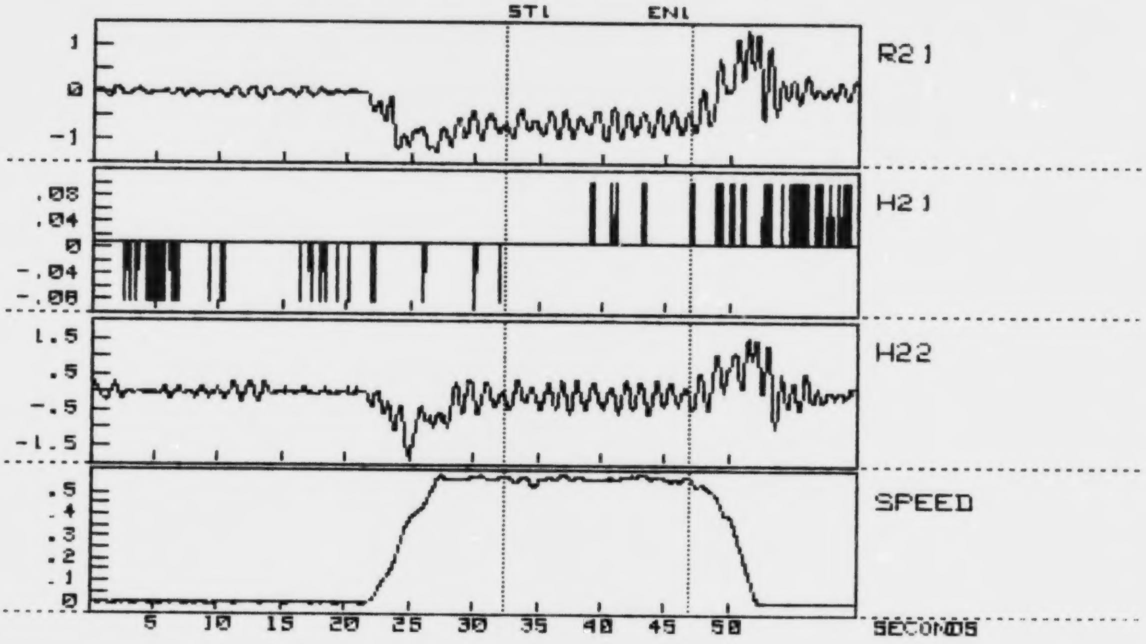

DATA DIGITIZED ON: 02 SEP 1983
DIGITIZING RATE: 32 Hz/CHANNEL
FILTER FREQUENCY: 1 HZ

INTERVAL STATISTICS

INTERVAL 1 START: 32.40625 END: 46.90625

| CHANNEL | MINIMUM | MAXIMUM | MEAN VALUE | STAN. DEV. |
|---|---|---|---|---|
| R21 | -.993 | -.3128 | -.637 | .1833 |
| H21 | .0075927 | .1029 | .010997 | .011362 |
| H22 | -.561 | .351 | -.08123 | .2454 |
| SPEED | .533 | .587 | .567 | .009649 |

SEGMENTED MODEL TESTS *** 56SC
TEST OW RUN K6

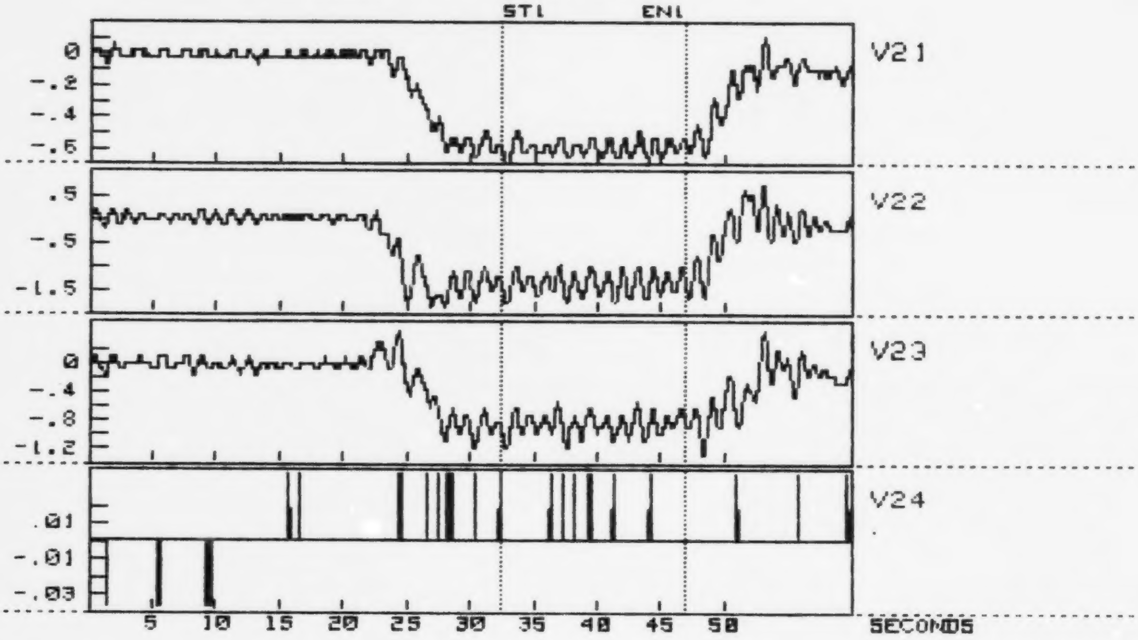

DATA DIGITIZED ON: 02 SEP 1983
DIGITIZING RATE: 32 Hz/CHANNEL
FILTER FREQUENCY: 1 HZ

INTERVAL STATISTICS

INTERVAL 1 START: 32.40625 END: 46.90625

| CHANNEL | MINIMUM | MAXIMUM | MEAN VALUE | STAN. DEV. |
|---|---|---|---|---|
| V21 | -.697 | -.486 | -.59 | .04867 |
| V22 | -1.77 | -.943 | -1.36 | .2135 |
| V23 | -1.18 | -.534 | -.851 | .1437 |
| V24 | .00103703 | .03802 | .001912 | .0056211 |

SEGMENTED MODEL TESTS *** 566C
TEST OW   RUN L6

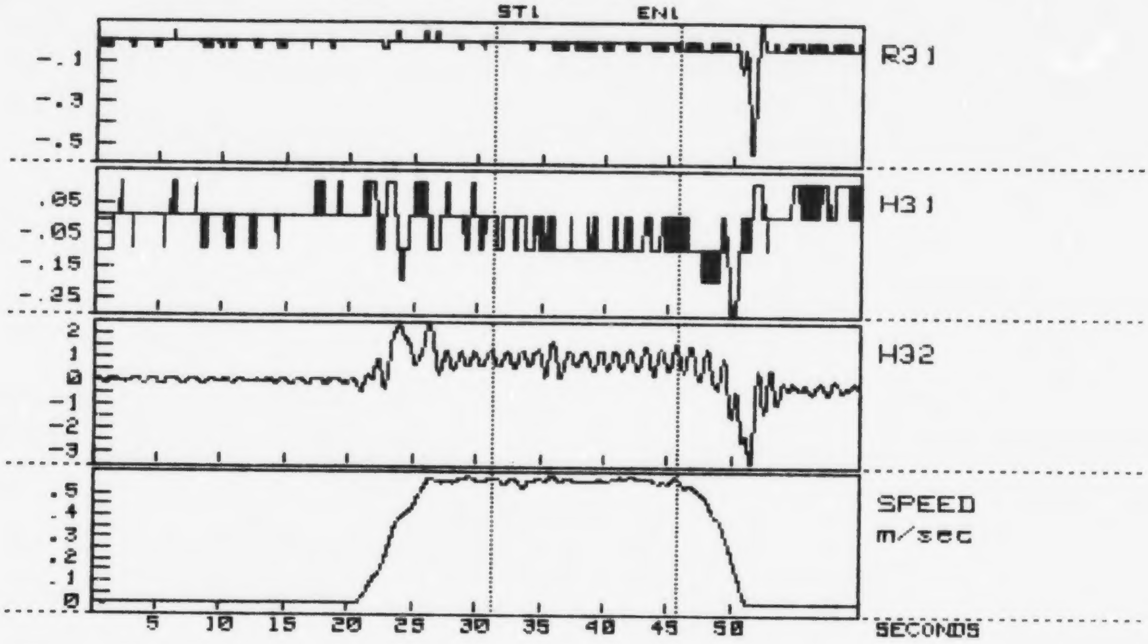

DATA DIGITIZED ON: 02 SEP 1983
DIGITIZING RATE: 32 Hz/CHANNEL
FILTER FREQUENCY: 1 HZ

INTERVAL STATISTICS

INTERVAL 1    START: 31.28125    END: 45.8125

| CHANNEL | MINIMUM | MAXIMUM | MEAN VALUE | STAN. DEV. |
|---|---|---|---|---|
| R31 | -.031118 | .0077492 | -.000424565 | .015839 |
| H31 | -.09035 | .011413 | -.05694 | .04779 |
| H32 | .2439 | 1.68 | .96 | .34 |
| SPEED | .532 | .586 | .567 | .0095407 |

SEGMENTED MODEL TESTS *** 566C
TEST OW RUN L6

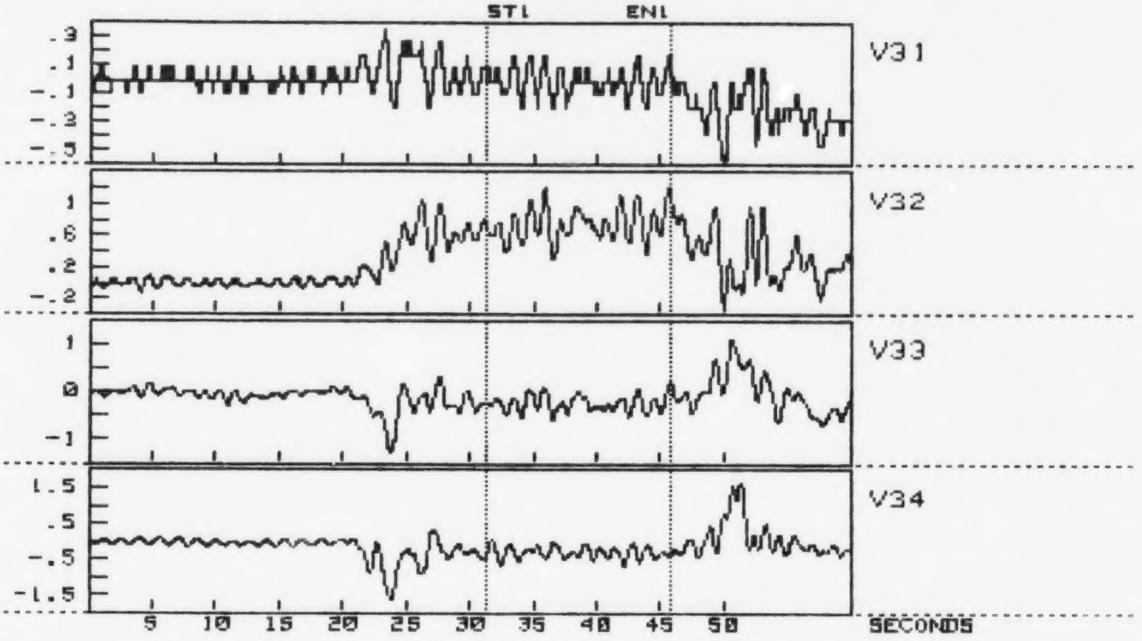

DATA DIGITIZED ON: 02 SEP 1983
DIGITIZING RATE: 32 Hz/CHANNEL
FILTER FREQUENCY: 1 HZ

INTERVAL STATISTICS

INTERVAL 1 START: 31.28125 END: 45.8125

| CHANNEL | MINIMUM | MAXIMUM | MEAN VALUE | STAN. DEV. |
|---|---|---|---|---|
| V31 | -.191 | .1723 | -.011286 | .09177 |
| V32 | .318 | 1.21 | .747 | .2022 |
| V33 | -.601 | .2201 | -.2302 | .1679 |
| V34 | -.685 | .04746 | -.3035 | .1592 |

SEGMENTED MODEL TESTS *** 566C
TEST OW     RUN M6

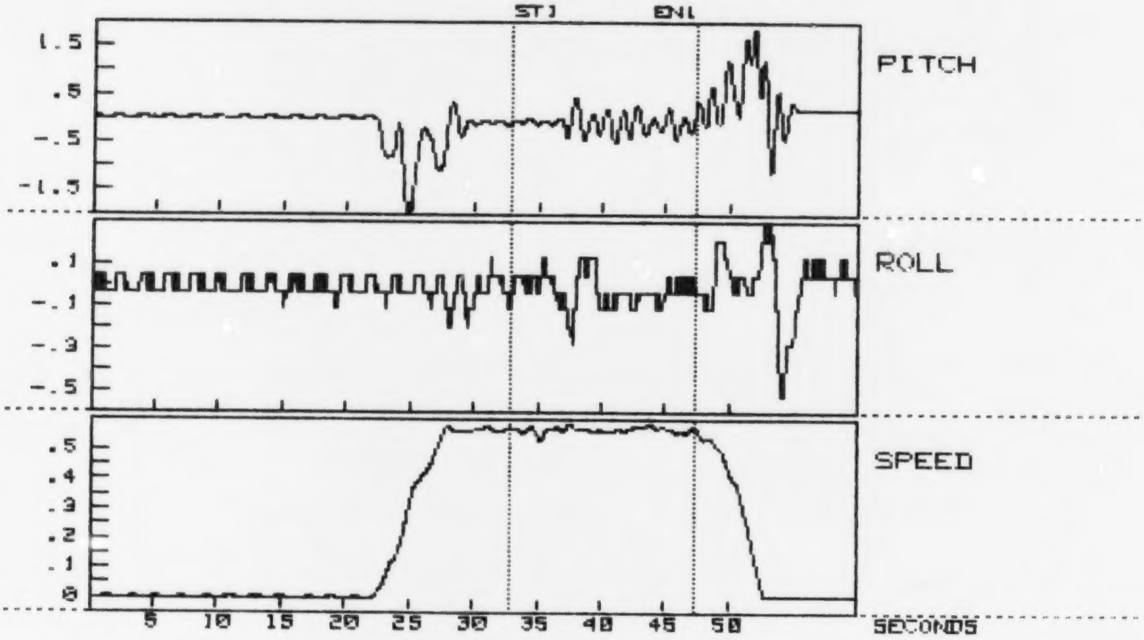

DATA DIGITIZED ON:   06 SEP 1983
DIGITIZING RATE:   32  Hz/CHANNEL
FILTER FREQUENCY:   1  HZ

INTERVAL STATISTICS

INTERVAL 1     START: 32.90625     END: 47.40625

| CHANNEL | MINIMUM | MAXIMUM | MEAN VALUE | STAN. DEV. |
|---|---|---|---|---|
| PITCH | -.52 | .418 | -.08949 | .1892 |
| ROLL | -.2794 | .1289 | -.016012 | .07773 |
| SPEED | .534 | .588 | .568 | .0096552 |

SEGMENTED MODEL TESTS *** 566C
TEST OW RUN M6

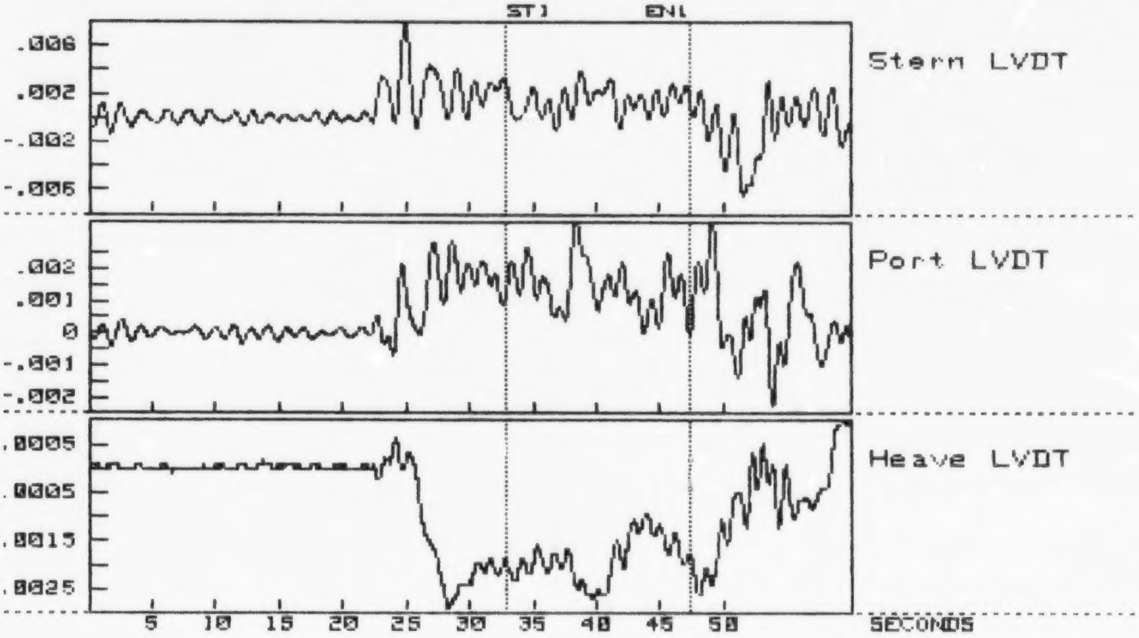

DATA DIGITIZED ON: 06 SEP 1983
DIGITIZING RATE: 32 Hz/CHANNEL
FILTER FREQUENCY: 1 HZ

INTERVAL STATISTICS

INTERVAL 1 START: 32.90625 END: 47.40625

| CHANNEL | MINIMUM | MAXIMUM | MEAN VALUE | STAN. DEV. |
|---|---|---|---|---|
| Stern LVDT | -.000937092 | .0038955 | .00133407 | .00107484 |
| Port LVDT | -.0001310857 | .0034524 | .00144781 | .000766741 |
| Heave LVDT | -.00270089 | -.000945153 | -.00186962 | .0004613 |

SEGMENTED MODEL TESTS *** 566C
TEST OW   RUN A5

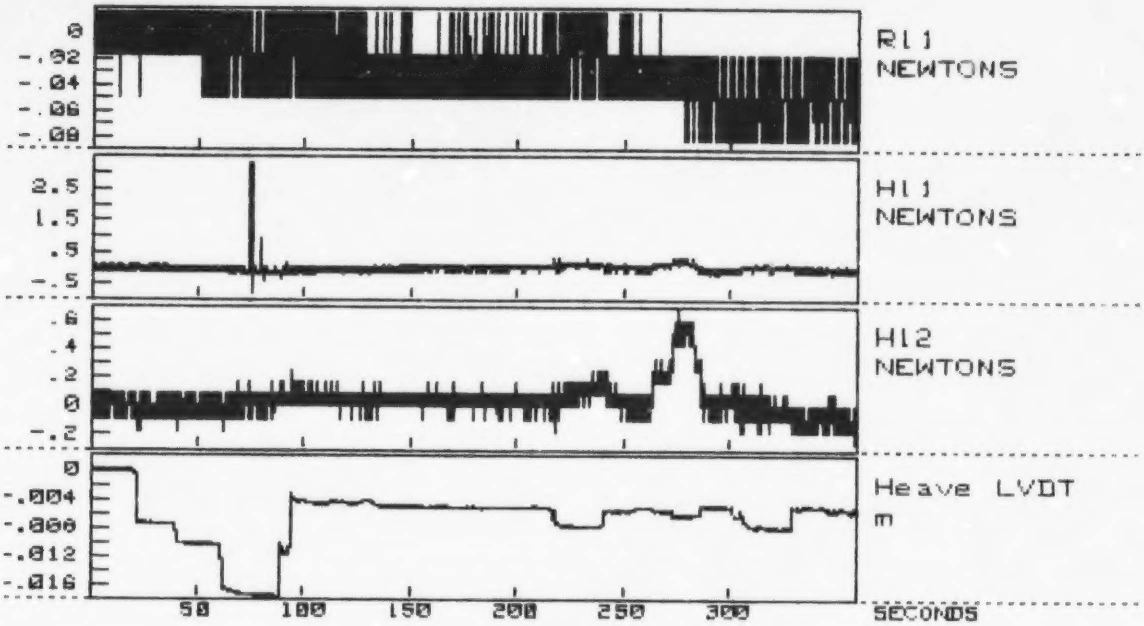

DATA DIGITIZED ON: 06 SEP 1983
DIGITIZING RATE: 32 Hz/CHANNEL
FILTER FREQUENCY: 1 HZ

INTERVAL STATISTICS

SEGMENTED MODEL TESTS *** 566C
TEST OW RUN B5

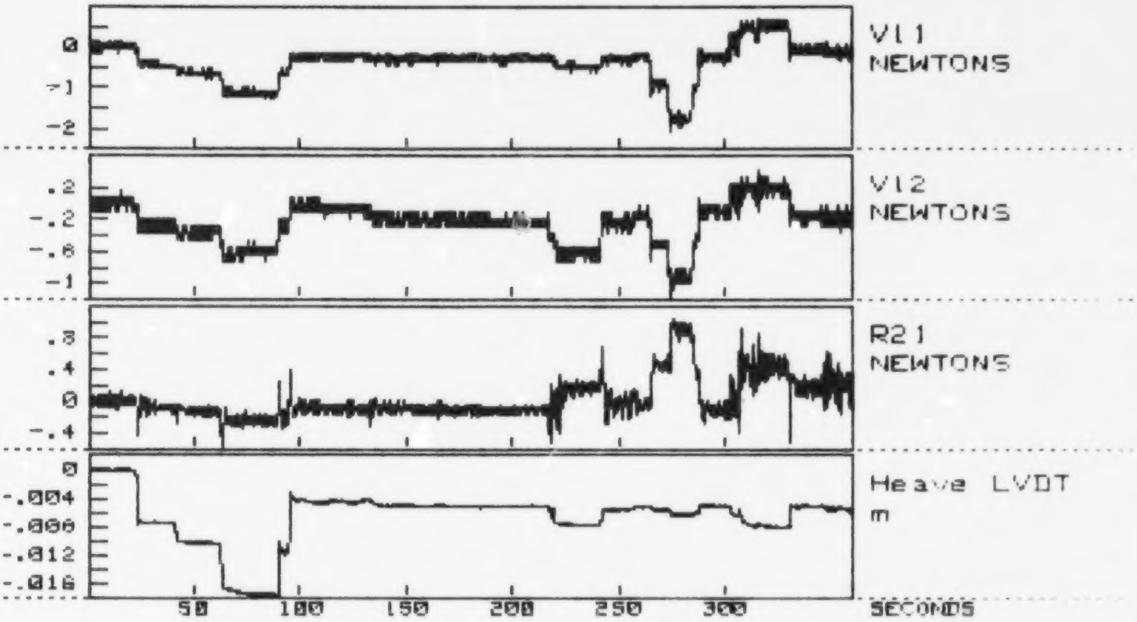

DATA DIGITIZED ON: 06 SEP 1983
DIGITIZING RATE: 32 Hz/CHANNEL
FILTER FREQUENCY: 1 HZ

INTERVAL STATISTICS

SEGMENTED MODEL TESTS *** 566C
TEST OW RUN C5

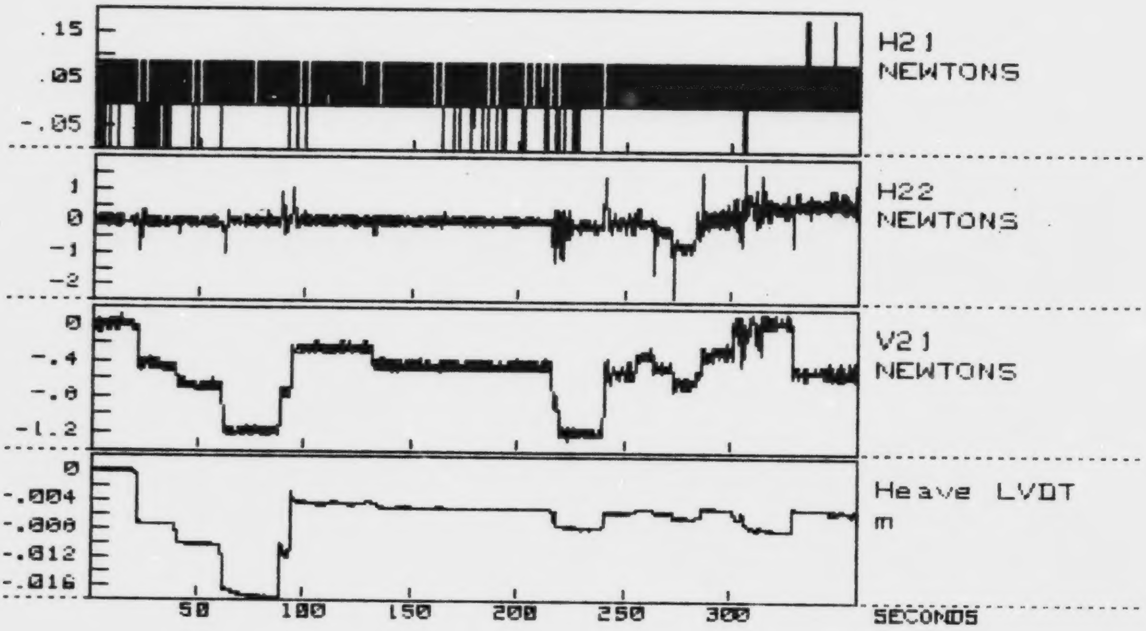

DATA DIGITIZED ON: 06 SEP 1983
DIGITIZING RATE: 32 Hz/CHANNEL
FILTER FREQUENCY: 1 HZ

INTERVAL STATISTICS

SEGMENTED MODEL TESTS *** 566C
TEST OW RUN DS

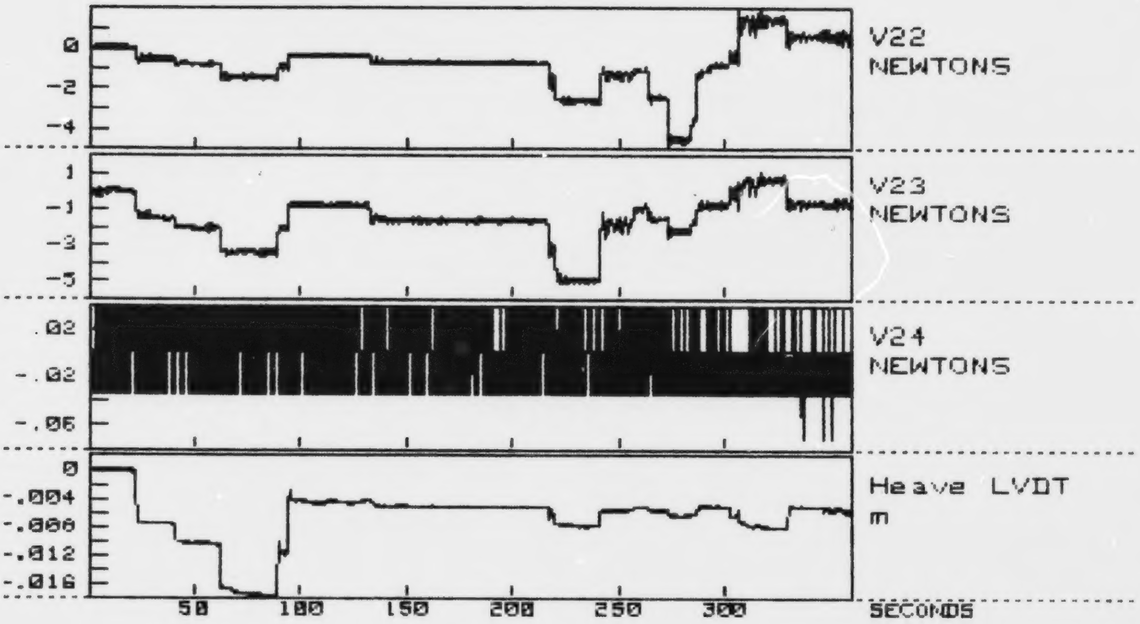

DATA DIGITIZED ON: 06 SEP 1983
DIGITIZING RATE: 32 Hz/CHANNEL
FILTER FREQUENCY: 1 HZ

INTERVAL STATISTICS

SEGMENTED MODEL TESTS *** 566C
TEST OW RUN E5

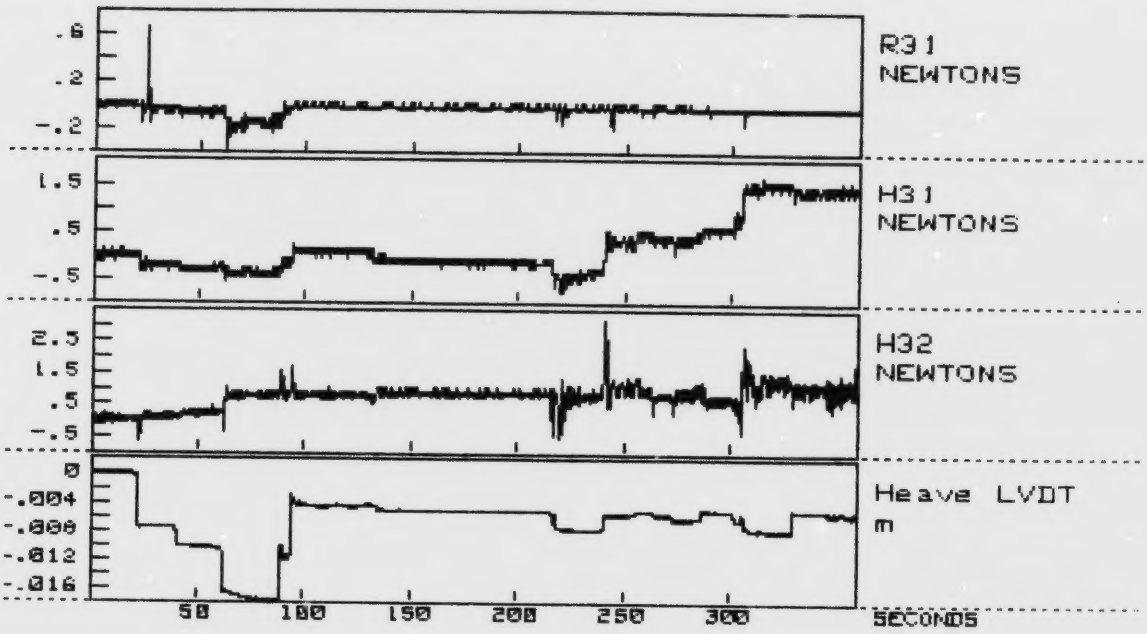

DATA DIGITIZED ON: 07 SEP 1983
DIGITIZING RATE: 32 Hz/CHANNEL
FILTER FREQUENCY: 1 HZ

INTERVAL STATISTICS

SEGMENTED MODEL TESTS *** 566C
TEST OW   RUN F5

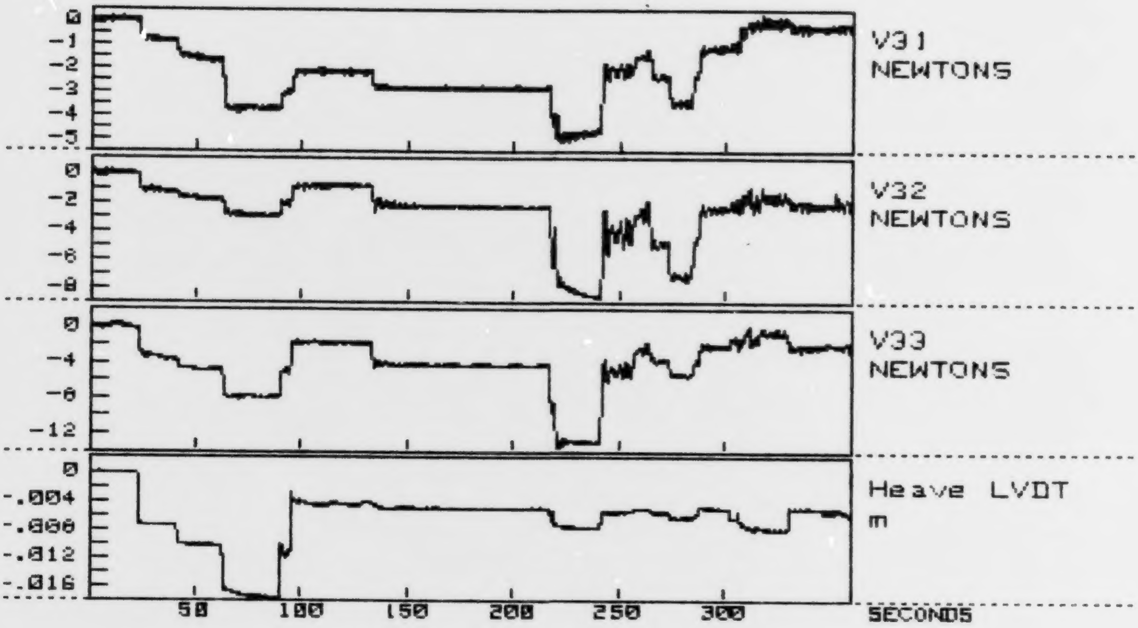

DATA DIGITIZED ON: 07 SEP 1983
DIGITIZING RATE: 32 Hz/CHANNEL
FILTER FREQUENCY: 1 HZ

INTERVAL STATISTICS

SEGMENTED MODEL TESTS *** 566C
TEST OW RUN G5

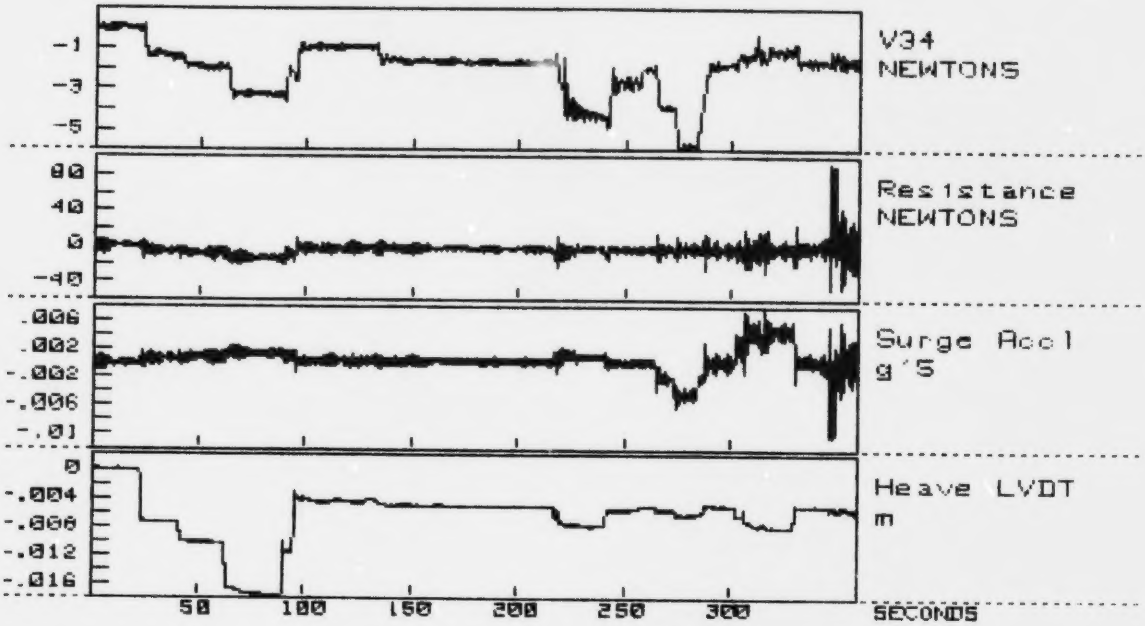

DATA DIGITIZED ON: 07 SEP 1983
DIGITIZING RATE: 32 Hz/CHANNEL
FILTER FREQUENCY: 1 HZ

INTERVAL STATISTICS

SEGMENTED MODEL TESTS *** 566C
TEST OW RUN H5

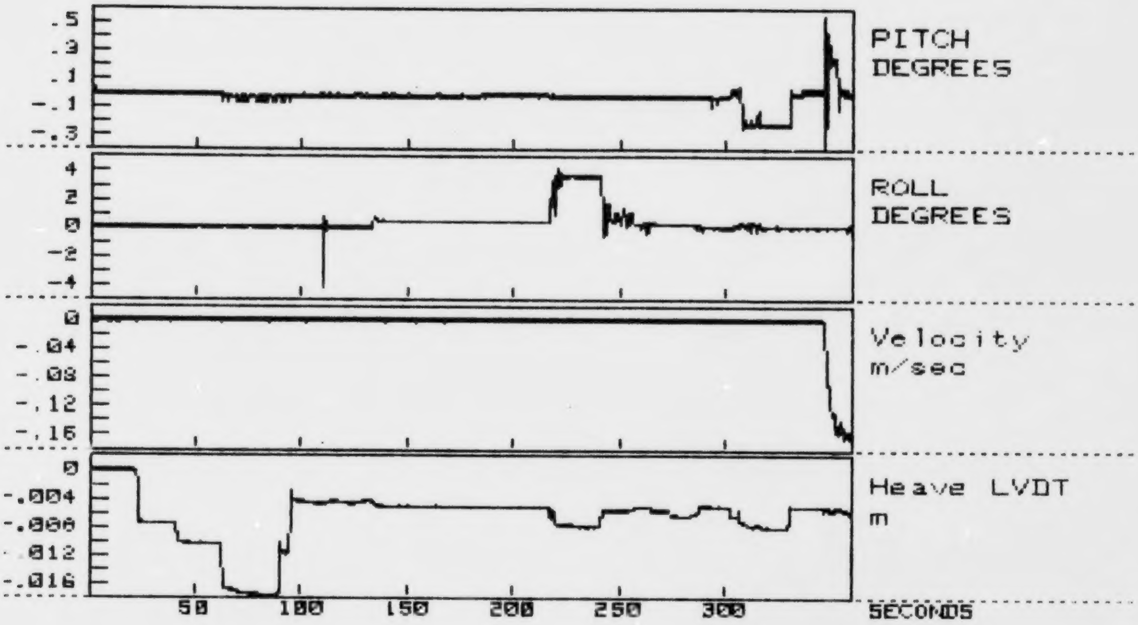

DATA DIGITIZED ON: 07 SEP 1983
DIGITIZING RATE: 32 Hz/CHANNEL
FILTER FREQUENCY: 1 HZ

INTERVAL STATISTICS

SEGMENTED MODEL TESTS *** 566C
TEST OW RUN I5

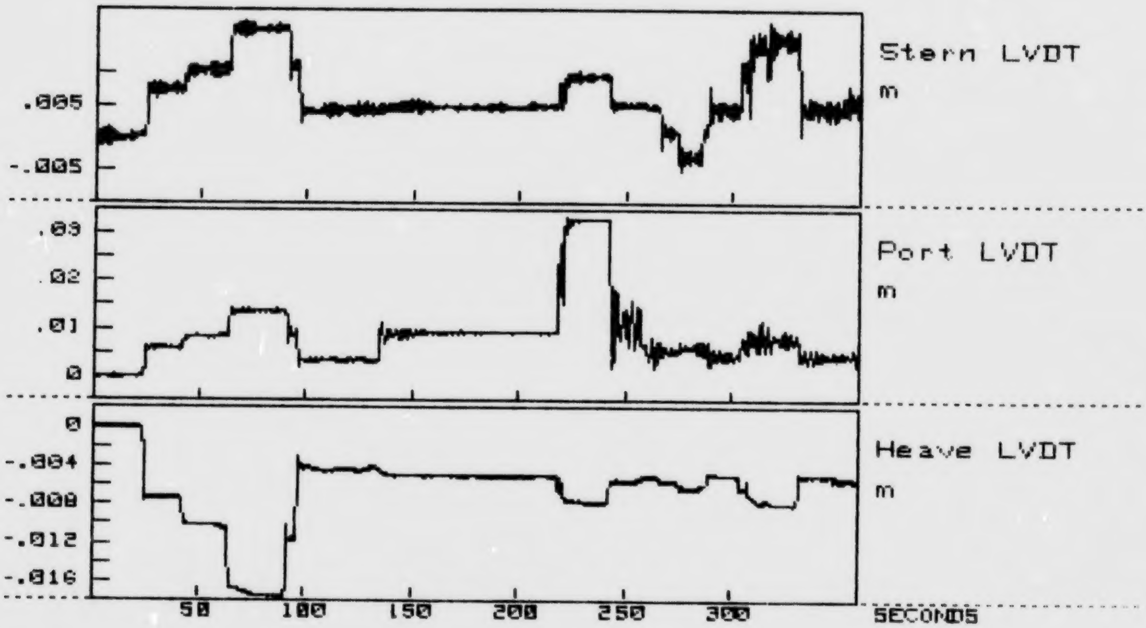

DATA DIGITIZED ON: 07 SEP 1983
DIGITIZING RATE: 32 Hz/CHANNEL
FILTER FREQUENCY: 1 HZ

INTERVAL STATISTICS

# APPENDIX D

# MISCELLANEOUS TRANSDUCER CALIBRATIONS

## D.1 Miscellaneous Transducer Calibrations

The remaining transducers were calibrated using standard laboratory calibration techniques. Both the resistance force block and the ice strength load ring were calibrated through identical instrumentation with dead weights. Since both transducers are in frequent use, these calibrations were also checked with a number of previous calibrations.

For both the pitch and roll pendulum pots these calibrations were performed by rolling the instrument in discrete angular increments and measuring the voltage output.

The carriage position is determined from resistance pots mounted to the carriage drive drum. Therefore, each distinct carriage position has a distinct resistance. By applying a set voltage across the resistance pot, each distinct position produces a distinct voltage which is periodically checked. The carriage velocity is calculated by differentiating the carriage position which is also periodically checked.

Both the accelerometers and yaw rate gyros were calibrated by the manufacturer.

Table D.1 lists the above calibrations.

## TABLE D.1

## TRANSDUCER CALIBRATIONS

| TRANSDUCER NAME | TRANSDUCER NUMBER | VISHAY GAIN | VISHAY EXCITATION (volts) | CALIBRATION |
|---|---|---|---|---|
| Resistance | FB #4 | 2000 | 10.00 | 297.0 N/volt |
| Ice Strength | LR #1 | 1366 | 5.00 | 9.533 N/volt |
| X accel. | - | - | - | 0.10 g/volt |
| Pitch | - | - | - | 8.73 deg/volt |
| Roll | - | - | - | 33.45 deg/volt |
| Yaw Rate | - | - | - | 6.0 deg/sec-volt |
| Carriage Position | - | - | - | 20.377 m/volt |
| Carriage Speed | - | - | - | 1.000 m/sec-volt |

# APPENDIX E

# MODEL ICE PROPERTIES MEASUREMENT

## E.1 Elastic Modulus of Ice Sheets

The elastic modulus of the ice is determined by applying a load and simultaneously measuring the deflection of the ice. The load is applied in discrete increments using a small dead weight set, while the deflection measurement is obtained using a dial gauge. Although a dial gauge does apply a varying load to the ice sheet, the error associated with the load is of the order of 1% for a 30 mm ice sheet and will be smaller for thicker ice. To prevent errors caused by "creep" while loading the ice, the load should be applied and removed in less than thirty seconds, recording the load, the maximum ice deflection and the deflection following the removal of the load (this latter measurement is to measure the amount of creep which does occur). A number of different loads are applied and the data regressed to give the mean load to deflection ratio. This ratio is then used in Wyman's theory for an infinite free floating plate on an elastic foundation to produce the elastic modulus. The distance "r" between the applied load and the deflection measuring point is kept between 0.3 and 0.5 $l_c$.

$$2\pi\rho_w g r^2 \left(\frac{\delta(r)}{p}\right) = \left(\frac{r}{l_c}\right)^2 \left[\mathrm{kei}\ (r/l_c)\right] \qquad (E.1)$$

Note: The value of "kei" must either be solved numerically or looked up in tables. Listings of "kei" can be found in most mathematical handbooks.

Equation E.1 is calculated iteratively until an exact value for the characteristic length is found. Once the characteristic length is determined, then the elastic modulus is calculated as follows:

$$E = \frac{12\rho_w\, g(1-\nu^2) l_c^4}{h^3} \qquad (E.2)$$

where $\nu$ = Poisson's Ratio (assumed = 0.33).

## E.2 Flexural Strength Measurements

The flexural strength is determined by the cantilever beam test. The cantilever beam test is performed by cutting three of the four sides of a rectangular shape beam and then loading its free end until failure occurs. The beam is cut to the appropriate size using an ice saw, leaving sufficient clearance on all three sides of the beam so as not to restrict its deflection. The beam is broken using a hand held instrumented load ring at a speed of approximately 0.010 m/sec, and then carefully removed to measure the exact dimensions of the failed beam. The target beam dimensions are: $L = 5\ h$; $B = 1.5\ h$.

Using these dimensions it is possible to neglect the effect of having the beam supported on an elastic foundation, as well the three dimensional effect, permitting the use of 'classical beam theory'. The error caused by using simple beam theory is less than 5% if these target dimensions are achieved. The flexural strength can be calculated as follows:

$$\sigma_f = \frac{6PL}{Bh^2} \tag{E.3}$$

## E.3 Ice Thickness and Channel Width Measurements

Both ice thickness and channel width measurements are made following the completion of the model test. Ice thickness is measured using a standard vernier caliper, with measurements taken and recorded in one metre intervals along both sides of the broken channel. At the same time as thickness measurements are obtained, the channel width is measured using a 'metre-stick', again in one metre intervals. This data will be averaged over the length of each run to give the mean and standard deviation for each test.

# APPENDIX F

# DETAILED TEST RESULTS

## F.1 Standard Format

The test results listed in Section F.2 have been prepared in a standard format. Each test is presented in five standard calculation runs which include the following time series:

a) Run E:

- resistance components R11, R21, R31, in Newtons
- total resistance in Newtons
- Model position in metres
- Model speed in m/s
- Event marker (which identifies the beginning and end of the test run)
- Model surge acceleration in g's (1g = 9.81 $m/s^2$)

b) Run F:

- Event marker and position
- Model Roll angle, deg.
- Model Pitch angle, deg.
- 1st segment loads: R11, H11, H12, V11 and V12 in Newtons.

c) Run G:

- 2nd Segment loads: R21, H21, H22, in Newton
- Event
- Vertical segment loads: V11, V12, V13, V14, in Newton
- Model position, in metres

d) Run H:

- 3rd Segment loads: R31, H31, H32 in Newtons
- Event marker
- Vertical segment loads: V31, V32, V33, V34 in Newtons
- Model position, in Newtons

Each run contains interval statistics which give the exact start and finish times for the calculation interval (the length of the run). The statistics calculated for each variable with the interval include; the minimum, maximum and mean values and the standard deviation.

The scaling was performed automatically for each signal, and therefore, the signal is spread over the entire available space. While this permits a better examination of the signal it does not allow overlaying signals due to differences in scales. All signals were filtered at 1 Hz and digitized at 32 Hz. The selection of the filtering frequency was done after examination of the results of filtering at 4, 2, 1 and 0.5 Hz. While 4 Hz was not effective in reducing the noise levels, the 0.5 Hz resulted in heavy masking of the data. As shown in the following pages, the 1 Hz frequency offered the best compromise.

## SEGMENTED MODEL TESTS
## TEST 02 RUN 02

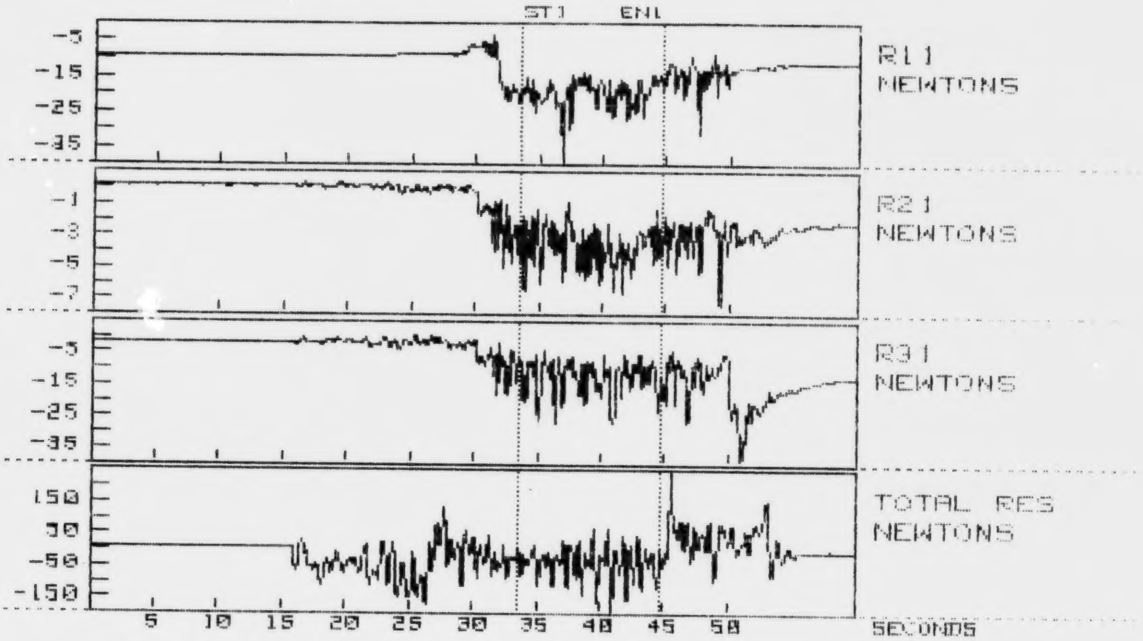

DATA DIGITIZED ON: 28 JUN 1983
DIGITIZING RATE: 32 Hz/CHANNEL
FILTER FREQUENCY: 4 HZ

### INTERVAL STATISTICS

INTERVAL 1 START: 33.5625 END: 44.6875

| CHANNEL | MINIMUM | MAXIMUM | MEAN VALUE | STAN. DEV. |
|---|---|---|---|---|
| R11 | -39.001 | -13.89 | -19.66 | 3.65 |
| R21 | -6.648 | -.939 | -3.62 | 1.14 |
| R31 | -27.06 | -3.916 | -12.51 | 5.097 |
| TOTAL RES | -191.3 | 70.159 | -38.15 | 45.986 |

SEGMENTED MODEL TESTS
TEST 02 RUN 02

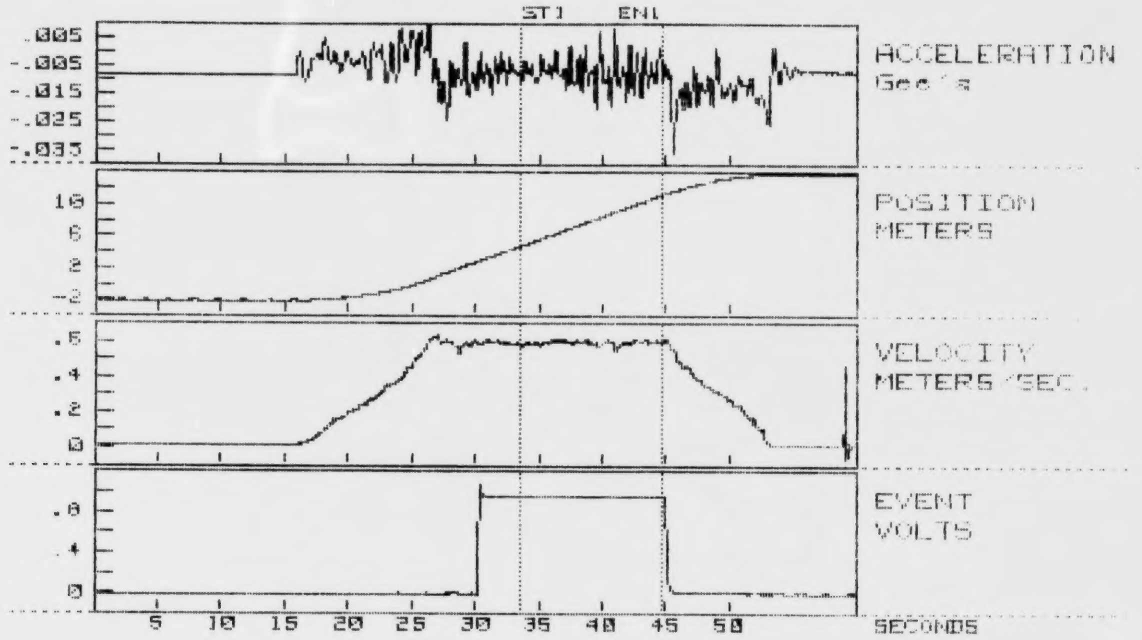

DATA DIGITIZED ON: 28 JUN 1983
DIGITIZING RATE: 32 Hz/CHANNEL
FILTER FREQUENCY: 4 HZ

INTERVAL STATISTICS

INTERVAL 1 START: 33.5625 END: 44.6875

| CHANNEL | MINIMUM | MAXIMUM | MEAN VALUE | STAN. DEV. |
|---|---|---|---|---|
| ACCELERATION | -.020868 | .007941 | -.0069707 | .0050691 |
| POSITION | 4.827 | 11.29 | 8.026 | 1.88 |
| VELOCITY | .541 | .612 | .59 | .011886 |

## SEGMENTED MODEL TESTS
## TEST 02 RUN 22

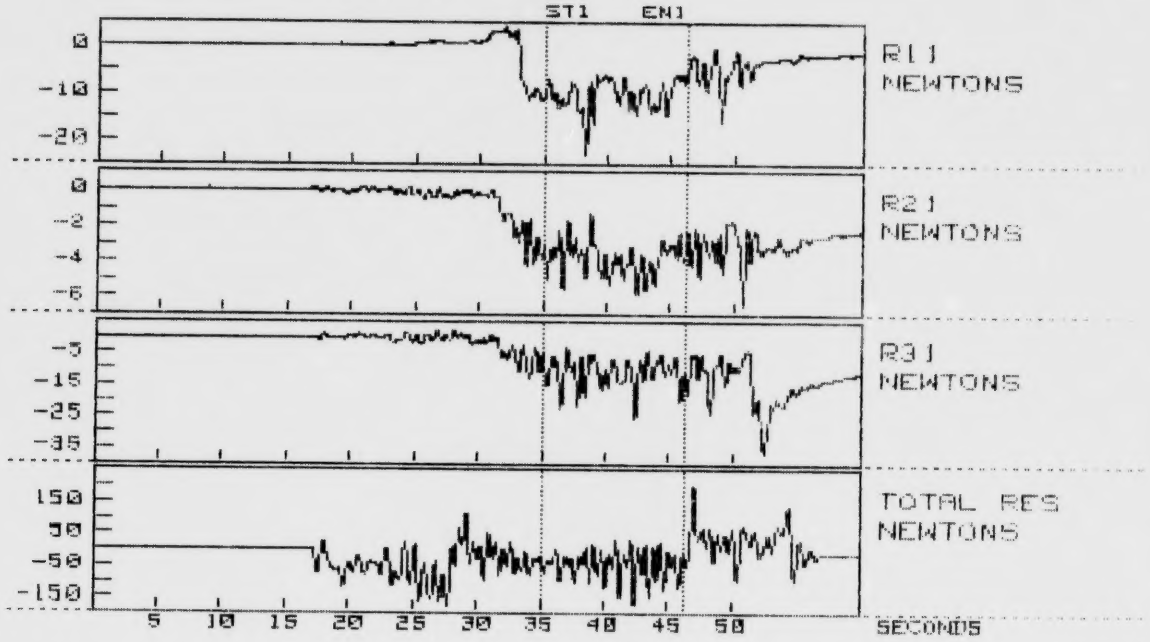

DATA DIGITIZED ON: 28 JUN 1983
DIGITIZING RATE: 32 Hz/CHANNEL
FILTER FREQUENCY: 2 HZ

### INTERVAL STATISTICS

INTERVAL 1 START: 35 END: 46.125

| CHANNEL | MINIMUM | MAXIMUM | MEAN VALUE | STAN. DEV. |
|---|---|---|---|---|
| R11 | -22.92 | -5.903 | -10.1 | 3.11 |
| R21 | -5.833 | -1.36 | -3.778 | .888 |
| R31 | -25.72 | -3.407 | -11.04 | 4.518 |
| TOTAL RES | -172.47 | 33.908 | -46.369 | 40.47 |

## SEGMENTED MODEL TESTS
## TEST 02 RUN 22

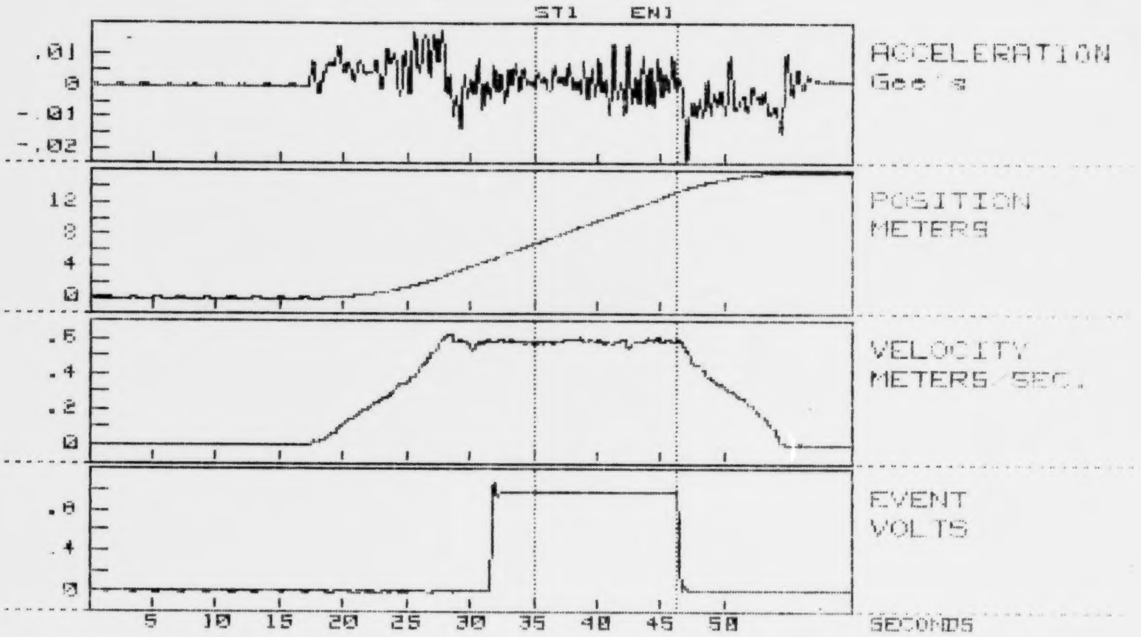

DATA DIGITIZED ON: 28 JUN 1983
DIGITIZING RATE: 32 Hz/CHANNEL
FILTER FREQUENCY: 2 HZ

### INTERVAL STATISTICS

INTERVAL 1 START: 35 END: 46.125

| CHANNEL | MINIMUM | MAXIMUM | MEAN VALUE | STAN. DEV. |
|---|---|---|---|---|
| ACCELERATION | -.0093032 | .013158 | .00137744 | .0043231 |
| POSITION | 6.834 | 13.35 | 10.08 | 1.88 |
| VELOCITY | .54 | .603 | .583 | .011306 |

## SEGMENTED MODEL TESTS
## TEST 02 RUN 12

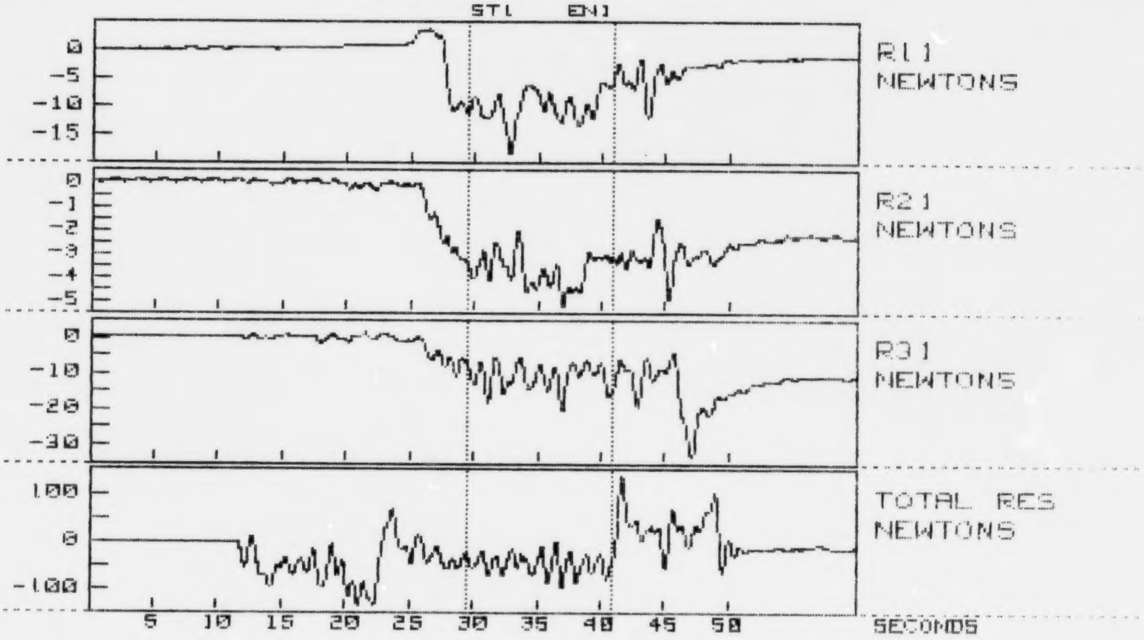

DATA DIGITIZED ON: 28 JUN 1983
DIGITIZING RATE: 32 Hz/CHANNEL
FILTER FREQUENCY: 1 HZ

### INTERVAL STATISTICS

INTERVAL 1 START: 29.53125 END: 40.75

| CHANNEL | MINIMUM | MAXIMUM | MEAN VALUE | STAN. DEV. |
|---|---|---|---|---|
| R11 | -18.09 | -5.63 | -9.958 | 2.66 |
| R21 | -5.188 | -2.03 | -3.692 | .686 |
| R31 | -20.37 | -5.397 | -10.79 | 3.332 |
| TOTAL RES | -96.904 | -2.16 | -46.98 | 19.56 |

## SEGMENTED MODEL TESTS
## TEST 02    RUN 12

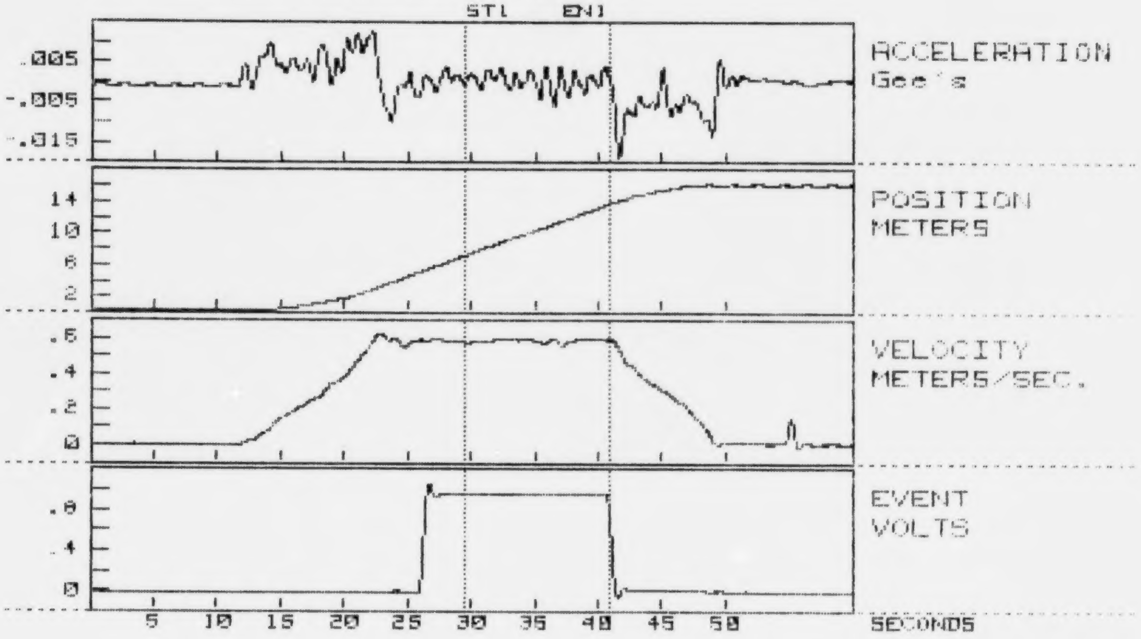

DATA DIGITIZED ON: 28 JUN 1983
DIGITIZING RATE: 32 Hz/CHANNEL
FILTER FREQUENCY: 1 HZ

### INTERVAL STATISTICS

INTERVAL 1    START: 29.53125    END: 40.75

| CHANNEL | MINIMUM | MAXIMUM | MEAN VALUE | STAN. DEV. |
|---|---|---|---|---|
| ACCELERATION | -.0060297 | .0042242 | .000324697 | .00212688 |
| POSITION | 7.234 | 13.75 | 10.46 | 1.39 |
| VELOCITY | .553 | .6 | .586 | .010024 |

SEGMENTED MODEL TESTS
TEST 02    RUN _2

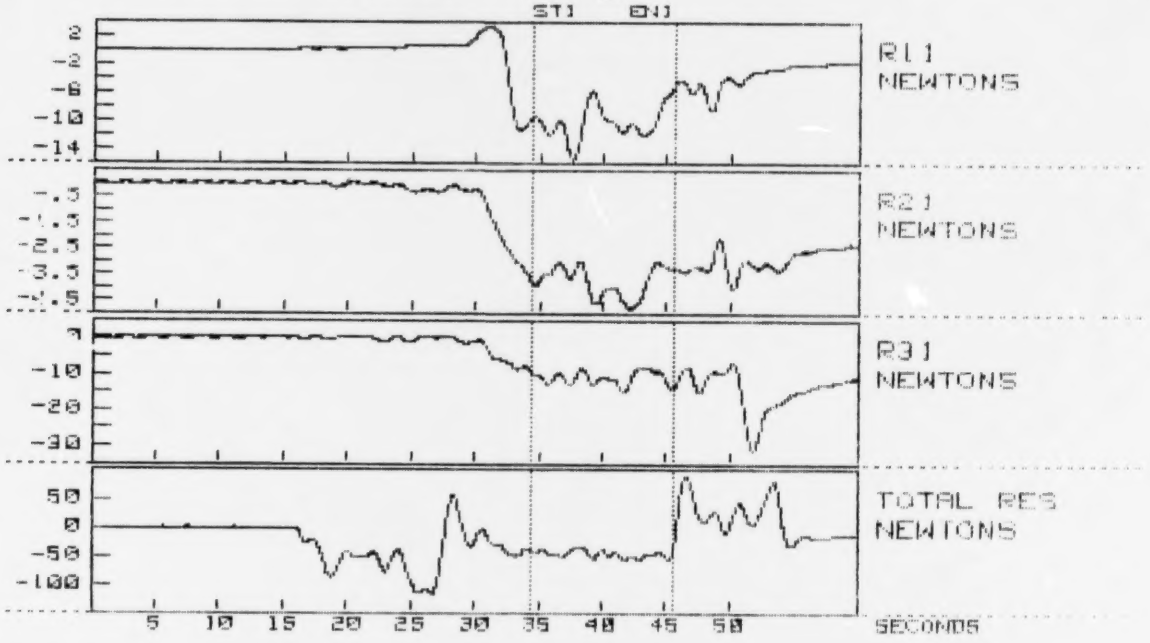

DATA DIGITIZED ON:   28 JUN 1983
DIGITIZING RATE:   32  Hz/CHANNEL
FILTER FREQUENCY:   .5  HZ

INTERVAL STATISTICS

INTERVAL 1     START: 34.3125     END: 45.4375

| CHANNEL | MINIMUM | MAXIMUM | MEAN VALUE | STAN. DEV. |
|---|---|---|---|---|
| R11 | -15.38 | -5.258 | -10.09 | 2.3 |
| R21 | -4.815 | -2.96 | -3.762 | .557 |
| R31 | -15.03 | -7.994 | -10.98 | 1.8 |
| TOTAL RES | -55.614 | -32.847 | -45.812 | 5.795 |

## SEGMENTED MODEL TESTS
## TEST 02 RUN _2

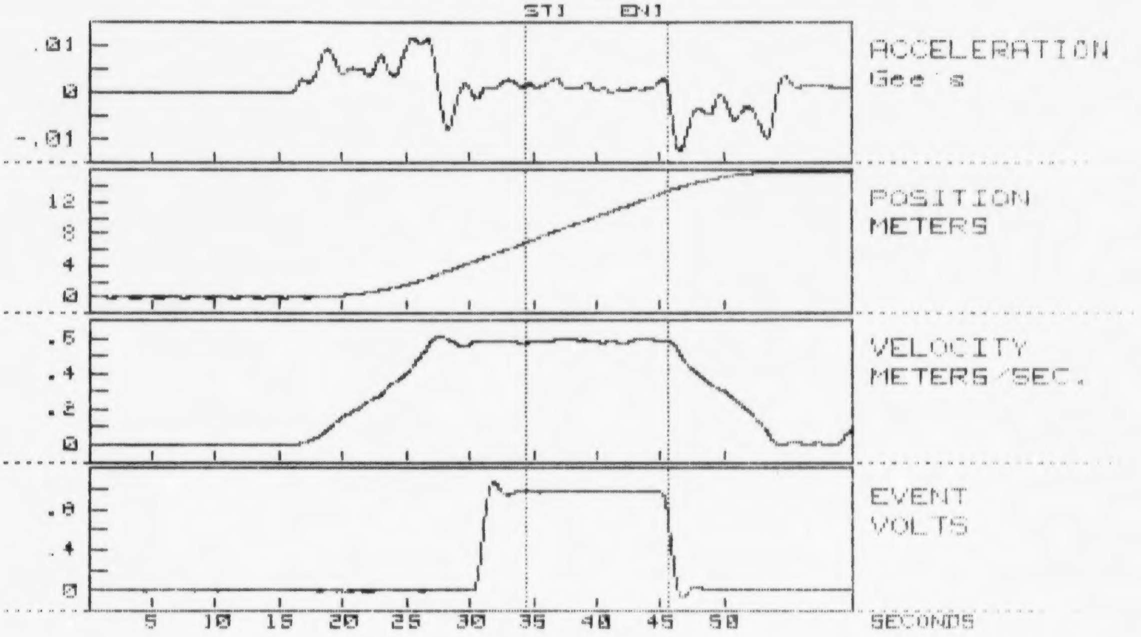

```
DATA DIGITIZED ON:  28 JUN 1983
  DIGITIZING RATE:  32  Hz/CHANNEL
 FILTER FREQUENCY:   .5  HZ

                         INTERVAL STATISTICS

INTERVAL 1      START: 34.3125     END: 45.4375

CHANNEL          MINIMUM           MAXIMUM          MEAN VALUE       STAN. DEV.
ACCELERATION     -.0001505914       .00302324        .00132177       .000839254
POSITION          6.908             13.38            10.11            1.88
VELOCITY          .565              .597             .583             .0080383
```

## F.2 Data Sheets

The calibration constants used in conversion of measured signals into engineering units are listed in Table F.1 for all tests. Some changes have taken place due to recalibration and rewiring of some of the load cells (as noted in the table) after the first four tests.

The results from all runs are listed in the following pages.

Each test is designated by two numbers, e.g. 3 - 2. The first digit is the ice sheet number and the second is the test number which can be either 1 or 2 (since only two tests were conducted in each ice sheet). The run designation letters (E, F, G or H), as described in Section F.1, refer to the standardized groupings of plots of measured variables and interval statistics.

It should be noted that the letter designations for Test 4-1 are given as A, B, C, D and I which are identical to the designations E, F, G and H except for F where the roll and pitch data are excluded and printed as grouping I. The format of the results of Test 4-2 are similar to 4-1.

TABLE F.1 CALIBRATION CONSTANTS IN UNITS PER VOLT DURING PHASE I TEST SERIES

| VARIABLE | | UNITS | 1-1 17 JUL 83 | 1-2 17 JUL 83 | 2-1 19 JUL 83 | 2-2 19 JUL 83 | 3-1 9 AUG 83 | 3-2 9 AUG 83 | 4-1 12 AUG 83 | 4-2 12 AUG 83 |
|---|---|---|---|---|---|---|---|---|---|---|
| Event Marker | | - | 1 | ✓ | ✓ | ✓ | ✓ | ✓ | ✓ | ✓ |
| Motions | Position | m | -20.38 | ✓ | ✓ | ✓ | ✓ | ✓ | ✓ | ✓ |
| | Speed | m/s | -1 | ✓ | ✓ | ✓ | ✓ | ✓ | ✓ | ✓ |
| | Acceleration | g's | 0.1 | ✓ | ✓ | ✓ | ✓ | ✓ | ✓ | ✓ |
| | Pitch | deg | 8.73 | ✓ | ✓ | ✓ | ✓ | ✓ | ✓ | ✓ |
| | Roll | deg | 33.45 | ✓ | ✓ | ✓ | ✓ | ✓ | ✓ | ✓ |
| Total Resistance | | N | 297 | ✓ | ✓ | ✓ | ✓ | ✓ | ✓ | ✓ |
| Segment 1 | R11 | N | -13.44 | ✓ | ✓ | ✓ | ✓ | ✓ | ✓ | ✓ |
| | H11 | N | -41.02 | ✓ | ✓ | ✓ | -38.06 | ✓ | ✓ | ✓ |
| | H12 | N | -35.06 | ✓ | ✓ | ✓ | ✓ | ✓ | ✓ | ✓ |
| | V11 | N | -39.02 | ✓ | ✓ | ✓ | ✓ | ✓ | ✓ | ✓ |
| | V12 | N | -36.94 | ✓ | ✓ | ✓ | ✓ | ✓ | ✓ | ✓ |
| Segment 2 | R21 | N | -31.60 | ✓ | ✓ | ✓ | -16.40 | ✓ | ✓ | ✓ |
| | R21 | N | -70.91 | ✓ | ✓ | ✓ | -36.80 | ✓ | -38.22 | ✓ |
| | H22 | N | -80.01 | ✓ | ✓ | ✓ | -41.52 | ✓ | ✓ | ✓ |
| | V21 | N | -33.40 | ✓ | ✓ | ✓ | -17.33 | ✓ | ✓ | ✓ |
| | V22 | N | -72.21 | ✓ | ✓ | ✓ | -37.47 | ✓ | ✓ | ✓ |
| | V23 | N | -37.60 | ✓ | ✓ | ✓ | ✓ | ✓ | ✓ | ✓ |
| | V24 | N | -15.15 | ✓ | ✓ | ✓ | ✓ | ✓ | ✓ | ✓ |
| Segment 3 | R31 | N | -15.92 | ✓ | ✓ | ✓ | ✓ | ✓ | ✓ | ✓ |
| | H31 | N | -41.68 | ✓ | ✓ | ✓ | ✓ | ✓ | ✓ | ✓ |
| | H32 | N | -34.71 | ✓ | ✓ | ✓ | ✓ | ✓ | ✓ | ✓ |
| | V31 | N | -37.20 | ✓ | ✓ | ✓ | ✓ | ✓ | ✓ | ✓ |
| | V32 | N | -16.61 | ✓ | ✓ | ✓ | ✓ | ✓ | ✓ | ✓ |
| | V33 | N | -15.29 | ✓ | ✓ | ✓ | ✓ | ✓ | ✓ | ✓ |
| | V34 | N | -14.28 | ✓ | ✓ | ✓ | ✓ | ✓ | ✓ | ✓ |

✓ No change of previous value

## SEGMENTED MODEL *** 566C
## TEST 01 RUN E1.

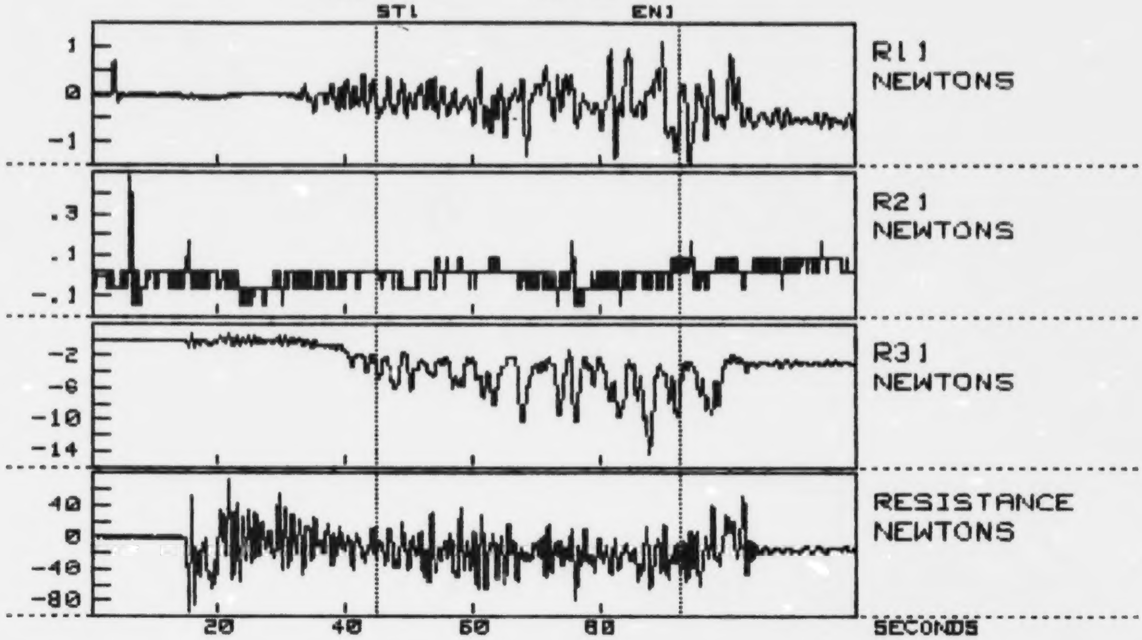

DATA DIGITIZED ON: 18 AUG 1983
DIGITIZING RATE: 32 Hz/CHANNEL
FILTER FREQUENCY: 1 HZ

### INTERVAL STATISTICS

INTERVAL 1 START: 44.78125 END: 92.28125

| CHANNEL | MINIMUM | MAXIMUM | MEAN VALUE | STAN. DEV. |
|---|---|---|---|---|
| R11 | -1.33 | 1.1 | -.1467 | .393 |
| R21 | -.1375 | .1711 | -.0057482 | .04365 |
| R31 | -14.49 | -1.35 | -4.871 | 2.4 |
| RESISTANCE | -78.017 | 37.274 | -20.82 | 18.38 |

SEGMENTED MODEL *** 566C
TEST 01 RUN E1

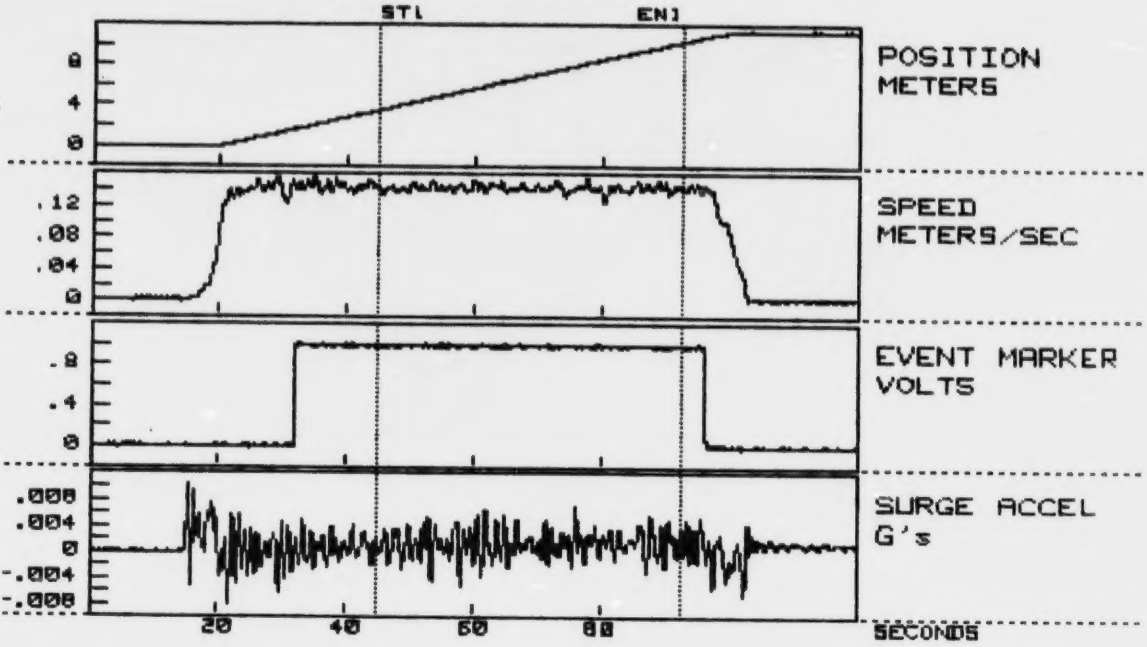

DATA DIGITIZED ON: 18 AUG 1983
DIGITIZING RATE: 32 Hz/CHANNEL
FILTER FREQUENCY: 1 HZ

INTERVAL STATISTICS

INTERVAL 1 START: 44.78125 END: 92.28125

| CHANNEL | MINIMUM | MAXIMUM | MEAN VALUE | STAN. DEV. |
|---|---|---|---|---|
| POSITION | 3.597 | 10.31 | 6.921 | 1.94 |
| SPEED | .1245 | .1538 | .1434 | .0043549 |
| EVENT MARKER | .97 | 1.01 | .989 | .0059815 |
| SURGE ACCEL | -.0054137 | .0070375 | .00137105 | .0020116 |

SEGMENTED MODEL TESTS *** 56BC
TEST 01 RUN F1

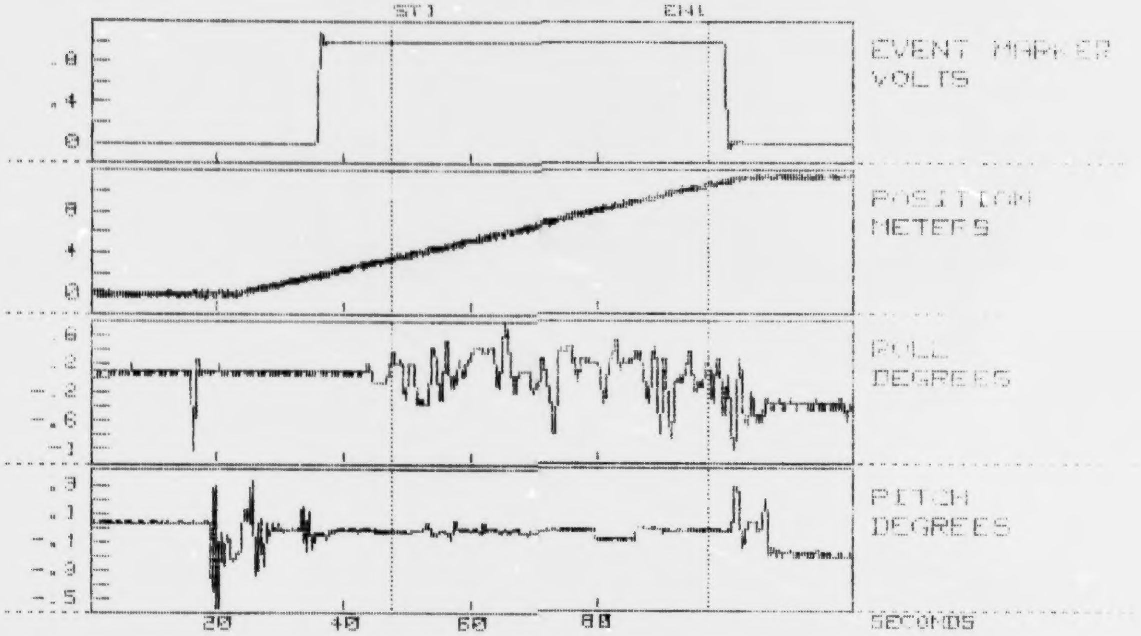

DATA DIGITIZED ON: 22 AUG 1983
DIGITIZING RATE: 32 Hz/CHANNEL
FILTER FREQUENCY: 1 HZ

INTERVAL STATISTICS

INTERVAL 1 START: 47.5 END: 97.375

| CHANNEL | MINIMUM | MAXIMUM | MEAN VALUE | STD. DEV. |
|---|---|---|---|---|
| EVENT MARKER | .983 | .988 | .985 | [illegible] |
| POSITION | 3.403 | 10.77 | 7.047 | [illegible] |
| ROLL | -.861 | .772 | .09263 | [illegible] |
| PITCH | -.1048 | .04442 | -.03421 | [illegible] |

SEGMENTED MODEL TESTS *** 56GC
TEST 01 RUN F1

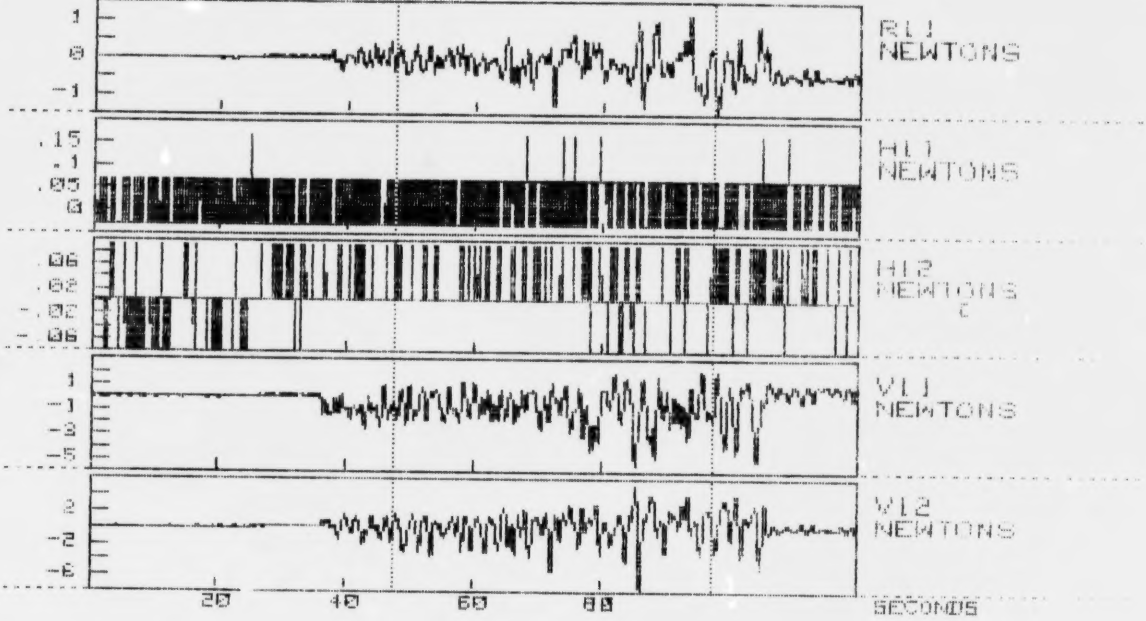

DATA DIGITIZED ON: 22 AUG 1983
DIGITIZING RATE: 32 Hz/CHANNEL
FILTER FREQUENCY: 1 HZ

INTERVAL STATISTICS

INTERVAL 1 START: 47.5 END: 97.375

| CHANNEL | MINIMUM | MAXIMUM | MEAN VALUE | STAN. DEV |
|---|---|---|---|---|
| R11 | -1.31 | 1.12 | -.1121 | .389 |
| H11 | -.03245 | .1678 | .026312 | .04982 |
| H12 | -,07973 | .09146 | .009511 | .020888 |
| V11 | -5.411 | 2.21 | -.77 | [illegible] |
| V12 | -7.662 | 5.055 | .1338 | 1.54 |

SEGMENTED MODEL TESTS *** 566C
TEST 01 RUN G1

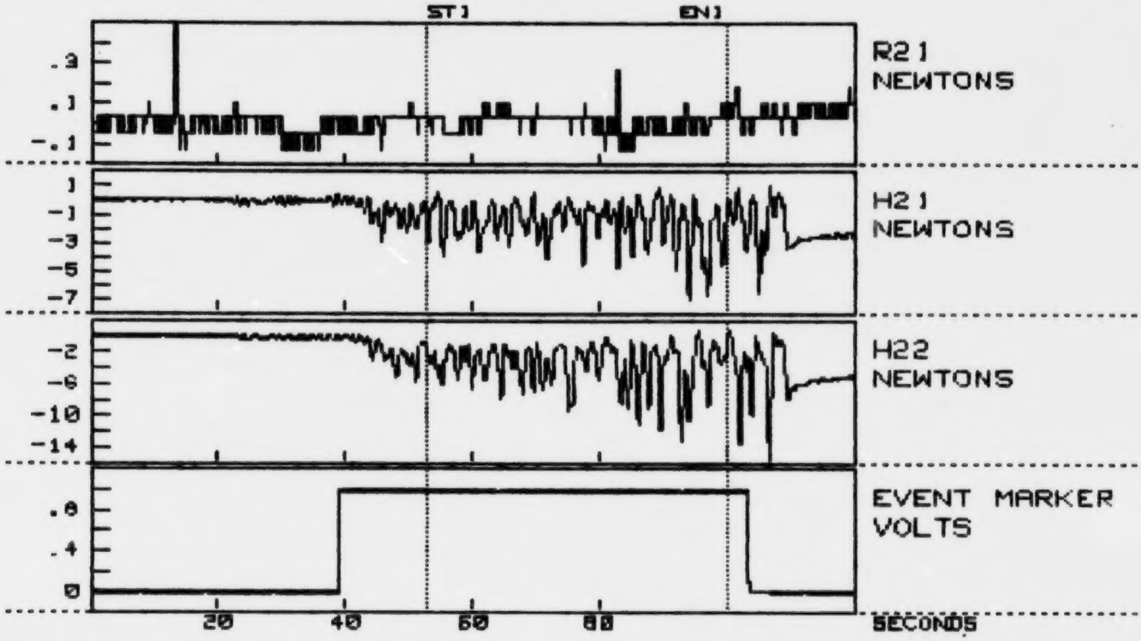

DATA DIGITIZED ON: 23 AUG 1983
DIGITIZING RATE: 32 Hz/CHANNEL
FILTER FREQUENCY: 1 HZ

INTERVAL STATISTICS

INTERVAL 1 START: 52.875 END: 99.71875

| CHANNEL | MINIMUM | MAXIMUM | MEAN VALUE | STAN. DEV. |
|---|---|---|---|---|
| R21 | -.1207 | .2651 | .013539 | .04802 |
| H21 | -7.061 | .903 | -1.53 | 1.39 |
| H22 | -13.16 | .905 | -3.511 | 2.57 |
| EVENT MARKER | .972 | 1.01 | .989 | .0058422 |

## SEGMENTED MODEL TESTS *** 566C
## TEST 01 RUN G1

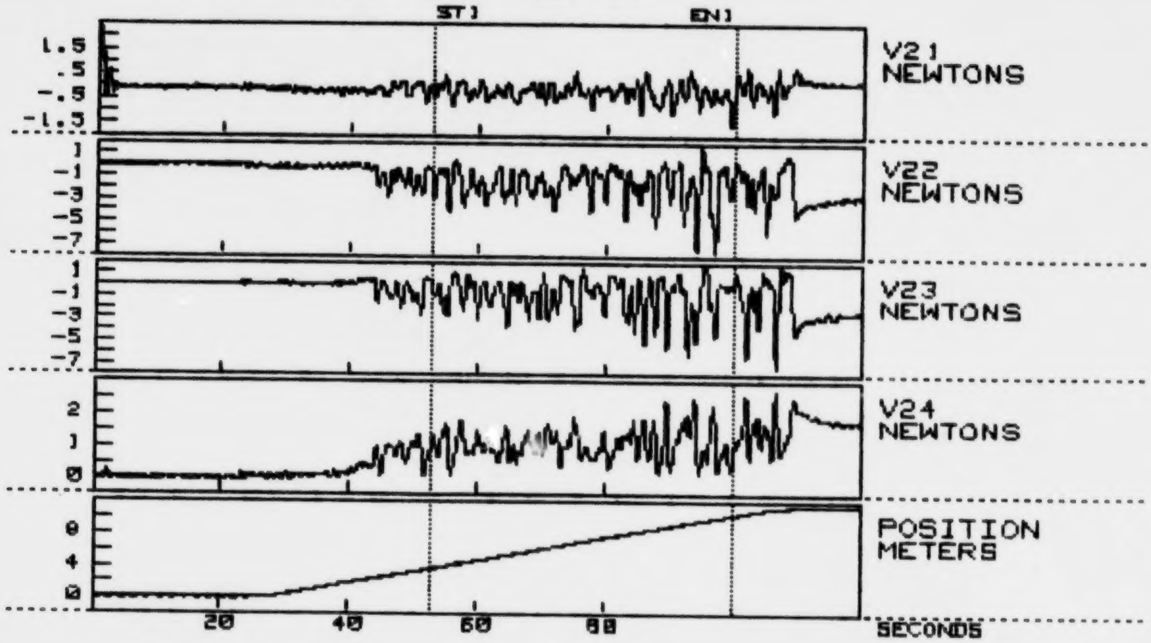

DATA DIGITIZED ON: 23 AUG 1983
DIGITIZING RATE: 32 Hz/CHANNEL
FILTER FREQUENCY: 1 HZ

### INTERVAL STATISTICS

INTERVAL 1 START: 52.875 END: 99.71875

| CHANNEL | MINIMUM | MAXIMUM | MEAN VALUE | STAN. DEV. |
|---|---|---|---|---|
| V21 | -1.53 | .67 | -.2387 | .344 |
| V22 | -7.687 | 1.66 | -1.65 | 1.47 |
| V23 | -6.218 | 1.95 | -.935 | 1.53 |
| V24 | .08319 | 2.52 | 1.07 | .445 |
| POSITION | 3.712 | 10.38 | 7.015 | 1.92 |

SEGMENTED MODEL TESTS *** 566C
TEST 01 RUN H1

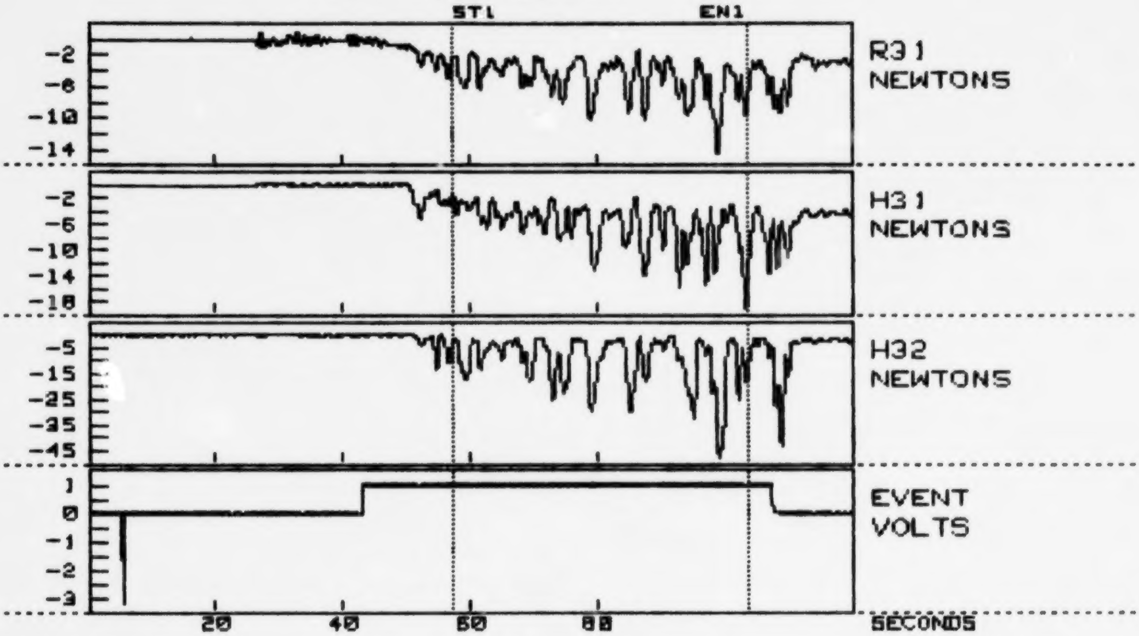

DATA DIGITIZED ON: 23 AUG 1983
DIGITIZING RATE: 32 Hz/CHANNEL
FILTER FREQUENCY: 1 HZ

INTERVAL STATISTICS

INTERVAL 1 START: 57.25 END: 103.5

| CHANNEL | MINIMUM | MAXIMUM | MEAN VALUE | STAN. DEV. |
|---|---|---|---|---|
| R31 | -14.53 | -1.35 | -4.897 | 2.43 |
| H31 | -18.77 | -1.36 | -6.015 | 3.307 |
| H32 | -47.535 | -.501 | -9.855 | 9.37 |
| EVENT | .977 | 1.02 | 1 | .0060906 |

## SEGMENTED MODEL TESTS *** 566C
## TEST 01 RUN H1

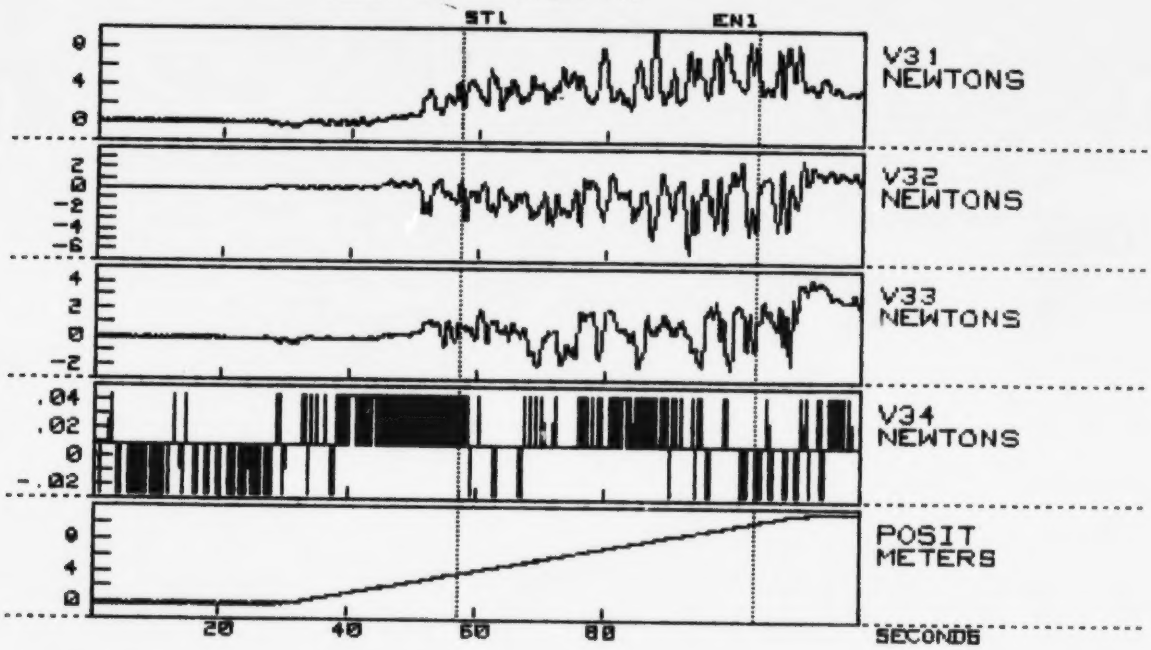

DATA DIGITIZED ON: 23 AUG 1983
DIGITIZING RATE: 32 Hz/CHANNEL
FILTER FREQUENCY: 1 HZ

### INTERVAL STATISTICS

INTERVAL 1 START: 57.25 END: 103.5

| CHANNEL | MINIMUM | MAXIMUM | MEAN VALUE | STAN. DEV. |
|---|---|---|---|---|
| V31 | 1.53 | 9.794 | 4.251 | 1.74 |
| V32 | -6.218 | 2.78 | -1.06 | 1.52 |
| V33 | -2.03 | 2.68 | .432 | 1.11 |
| V34 | -.025957 | .04377 | .012413 | .013253 |
| POSIT | 3.734 | 10.3 | 7.014 | 1.9 |

SEGMENTED MODEL *** 566C
TEST 01 RUN E2

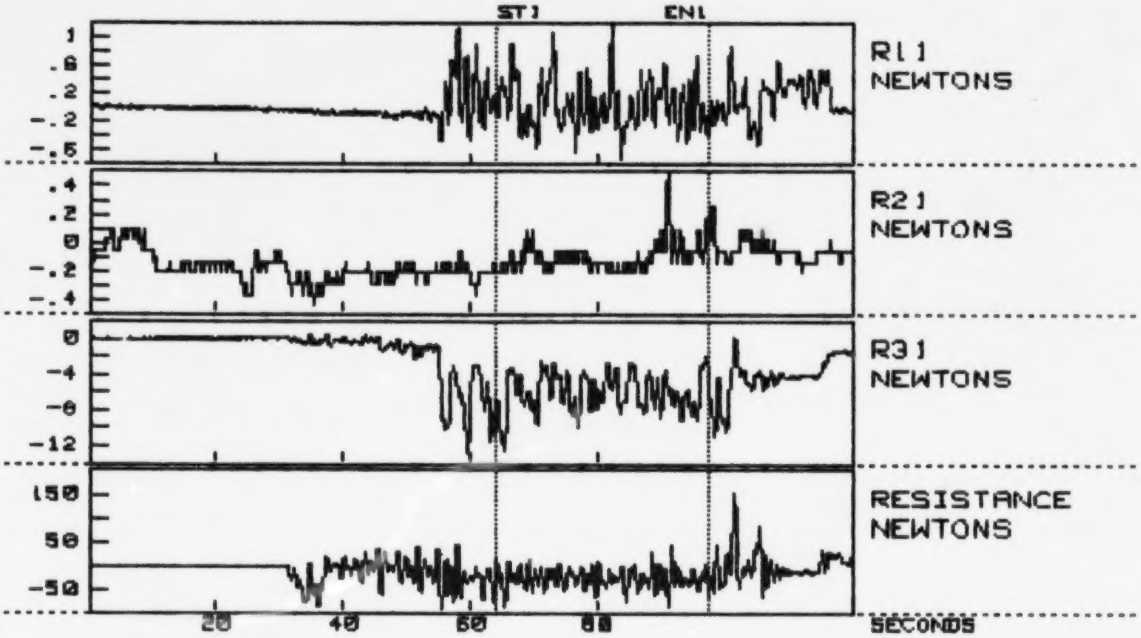

DATA DIGITIZED ON: 18 AUG 1983
DIGITIZING RATE: 32 Hz/CHANNEL
FILTER FREQUENCY: 1 HZ

## INTERVAL STATISTICS

INTERVAL 1 START: 64.03125 END: 97.34375

| CHANNEL | MINIMUM | MAXIMUM | MEAN VALUE | STAN. DEV. |
|---|---|---|---|---|
| R11 | -.719 | 1.15 | .04939 | .332 |
| R21 | -.2084 | .486 | -.09147 | .1023 |
| R31 | -12.56 | -2.06 | -5.93 | 2.07 |
| RESISTANCE | -83.434 | 42.733 | -24.79 | 19.74 |

SEGMENTED MODEL *** 566C
TEST 01 RUN E2

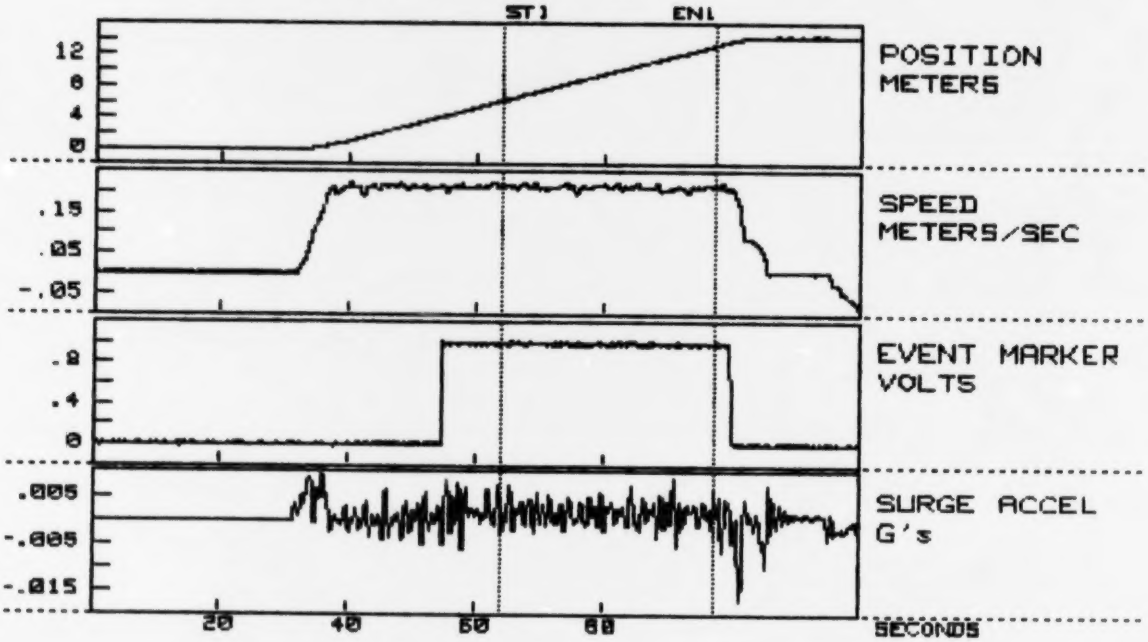

DATA DIGITIZED ON: 18 AUG 1983
DIGITIZING RATE: 32 Hz/CHANNEL
FILTER FREQUENCY: 1 HZ

INTERVAL STATISTICS

INTERVAL 1 START: 64.03125 END: 97.34375

| CHANNEL | MINIMUM | MAXIMUM | MEAN VALUE | STAN. DEV. |
|---|---|---|---|---|
| POSITION | 6.251 | 13.27 | 9.741 | 2.03 |
| SPEED | .1972 | .2241 | .2135 | .0050925 |
| EVENT MARKER | .966 | 1.01 | .989 | .0061594 |
| SURGE ACCEL | -.0056076 | .0087967 | .00158136 | .00219216 |

SEGMENTED MODEL TESTS *** 566C
TEST 01 RUN F2

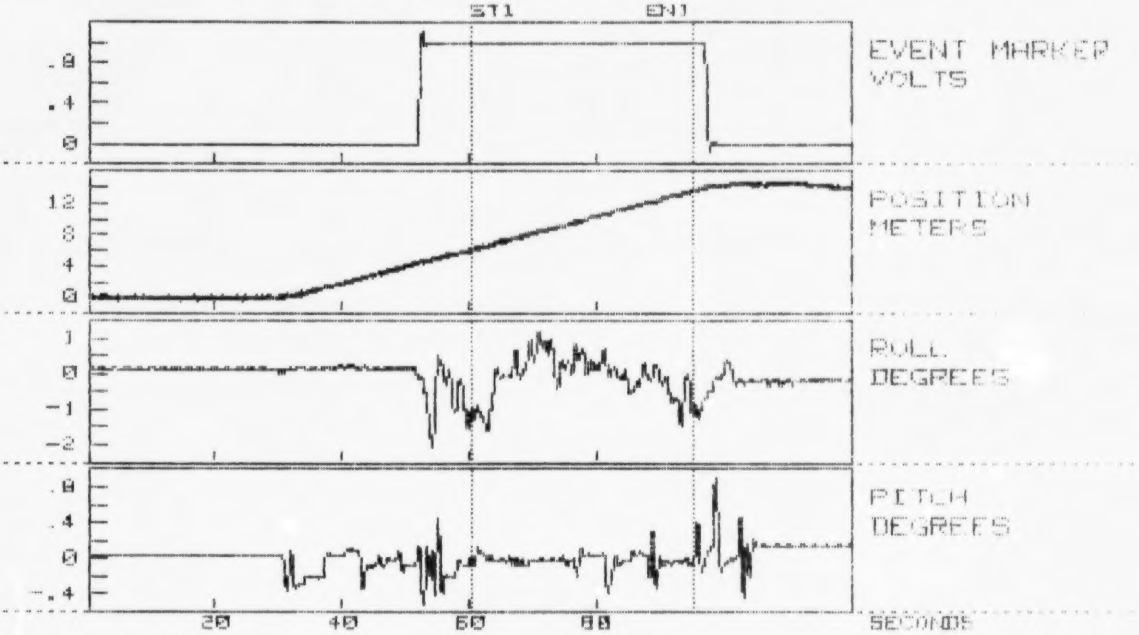

DATA DIGITIZED ON: 23 AUG 1983
DIGITIZING RATE: 32 Hz/CHANNEL
FILTER FREQUENCY: 1 HZ

INTERVAL STATISTICS

INTERVAL 1 START: 60.1875 END: 94.875

| CHANNEL | MINIMUM | MAXIMUM | MEAN VALUE | STAN. DEV. |
|---|---|---|---|---|
| EVENT MARKER | .984 | .986 | .985 | .00116459 |
| POSITION | 6.05 | 13.66 | 9.847 | 2.17 |
| ROLL | -1.64 | 1.14 | -.06057 | .503 |
| PITCH | -.381 | .3006 | -.019468 | .07995 |

## SEGMENTED MODEL TESTS *** 56BC
### TEST 01 RUN F2

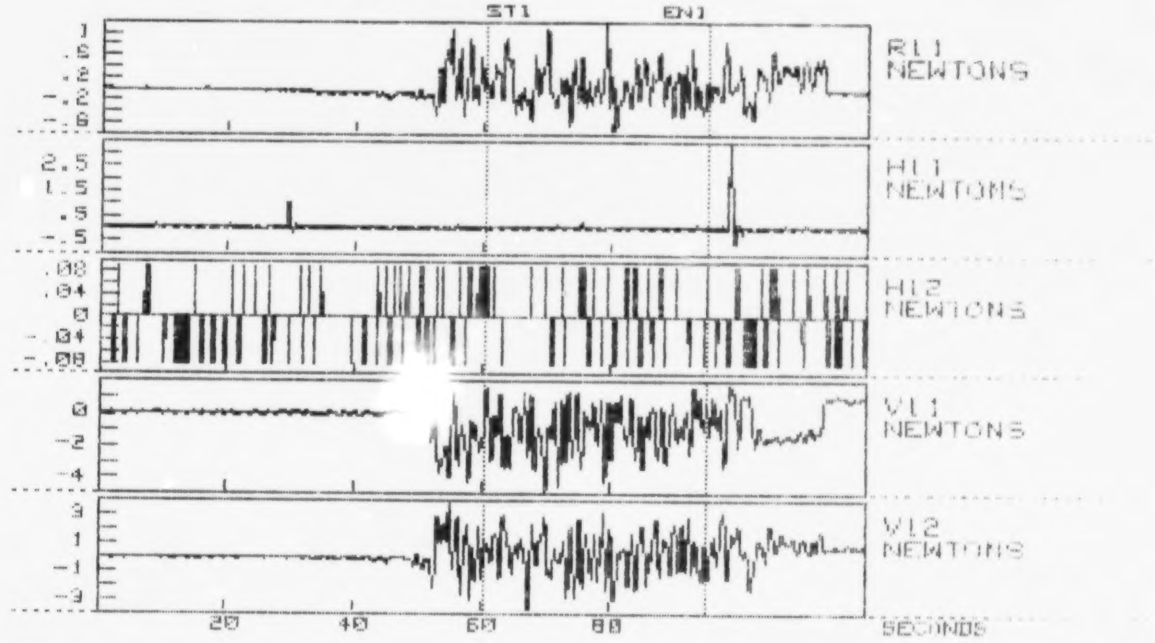

DATA DIGITIZED ON: 23 AUG 1983
DIGITIZING RATE: 32 Hz/CHANNEL
FILTER FREQUENCY: 1 HZ

### INTERVAL STATISTICS

INTERVAL 1 START: 60.1875 END: 94.875

| CHANNEL | MINIMUM | MAXIMUM | MEAN VALUE | STAN. DEV. |
|---|---|---|---|---|
| R11 | -.722 | 1.15 | .04804 | .729 |
| H11 | -.05429 | .2462 | .018188 | .04883 |
| H12 | -.08346 | .08773 | .00221027 | .01829 |
| V11 | -4.942 | 1.63 | -.97 | [illegible] |
| V12 | -3.694 | 3.16 | .2427 | 1.79 |

SEGMENTED MODEL TESTS *** 566C
TEST 01 RUN G2

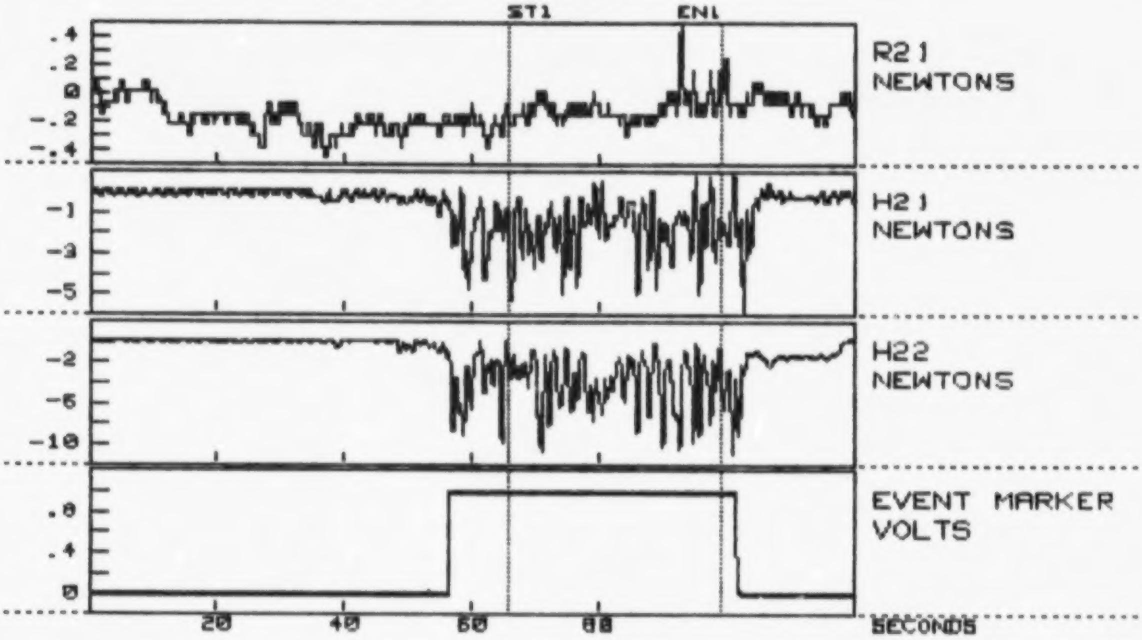

DATA DIGITIZED ON: 23 AUG 1983
DIGITIZING RATE: 32 Hz/CHANNEL
FILTER FREQUENCY: 1 HZ

INTERVAL STATISTICS

INTERVAL 1 START: 65.5625 END: 99.125

| CHANNEL | MINIMUM | MAXIMUM | MEAN VALUE | STAN. DEV. |
|---|---|---|---|---|
| R21 | -.2966 | .475 | -.09923 | .09993 |
| H21 | -5.255 | .804 | -1.74 | 1.22 |
| H22 | -10.69 | -.1467 | -3.936 | 2.43 |
| EVENT MARKER | .971 | 1.01 | .989 | .0063611 |

## SEGMENTED MODEL TESTS *** 566C
## TEST 01 RUN G2

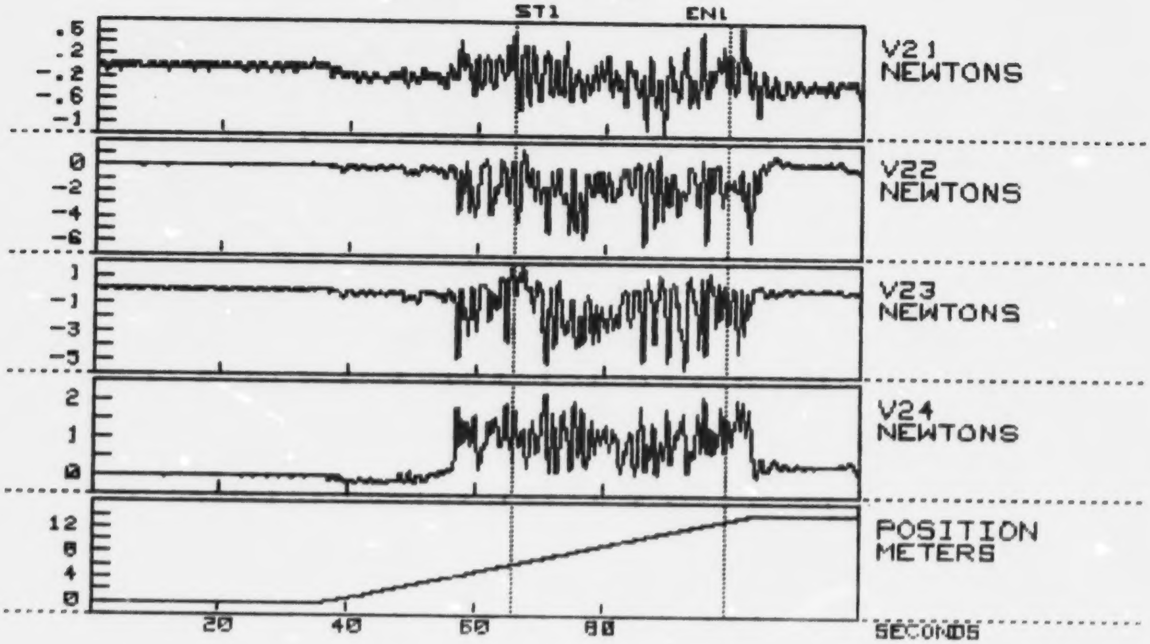

DATA DIGITIZED ON: 23 AUG 1983
DIGITIZING RATE: 32 Hz/CHANNEL
FILTER FREQUENCY: 1 HZ

### INTERVAL STATISTICS

INTERVAL 1 START: 65.5625 END: 99.125

| CHANNEL | MINIMUM | MAXIMUM | MEAN VALUE | STAN. DEV. |
|---|---|---|---|---|
| V21 | -1.17 | .621 | -.2004 | .31 |
| V22 | -6.195 | 1.39 | -1.67 | 1.46 |
| V23 | -5.474 | 1.69 | -1.22 | 1.57 |
| V24 | .06383 | 2.21 | .993 | .467 |
| POSITION | 6.186 | 13.3 | 9.737 | 2.05 |

SEGMENTED MODEL TESTS *** 56BC
TEST 01 RUN H2

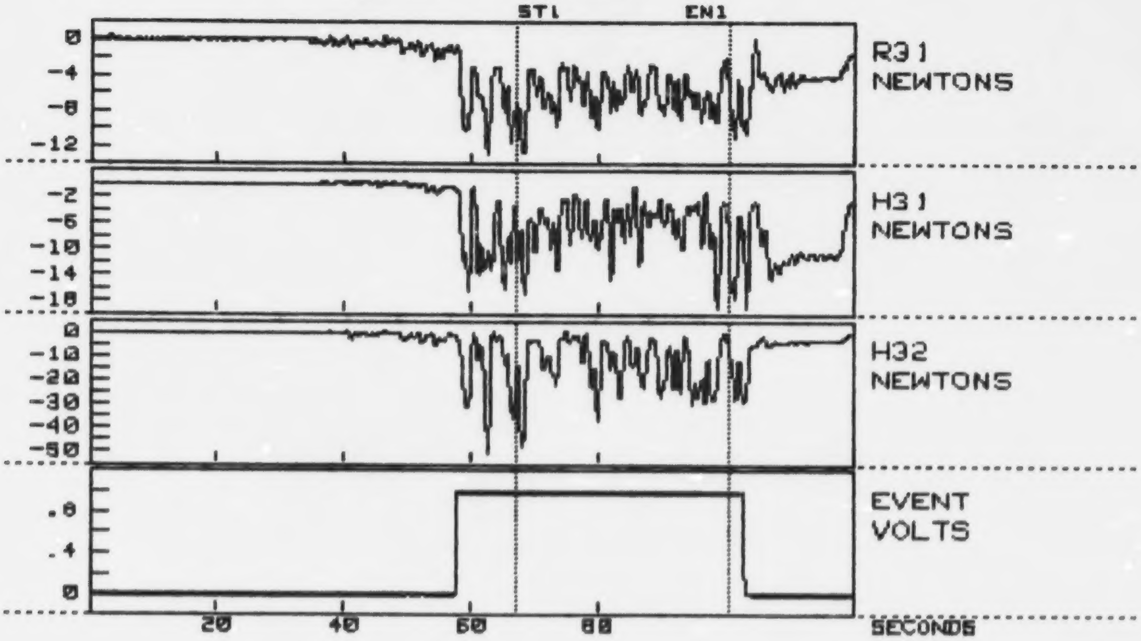

```
DATA DIGITIZED ON:   23 AUG 1983
  DIGITIZING RATE:   32  Hz/CHANNEL
 FILTER FREQUENCY:    1  HZ
```

```
                              INTERVAL STATISTICS

INTERVAL 1      START: 66.96875    END: 100.40625

CHANNEL          MINIMUM          MAXIMUM          MEAN VALUE          STAN. DEV.
R31              -12.61           -2.08            -5.963              2.07
H31              -18.86           -.344            -6.154              3.361
H32              -47.849           .796            -12.95              10.08
EVENT             .969            1.01              .99                .0065325
```

## SEGMENTED MODEL TESTS *** 566C
## TEST 01 RUN H2

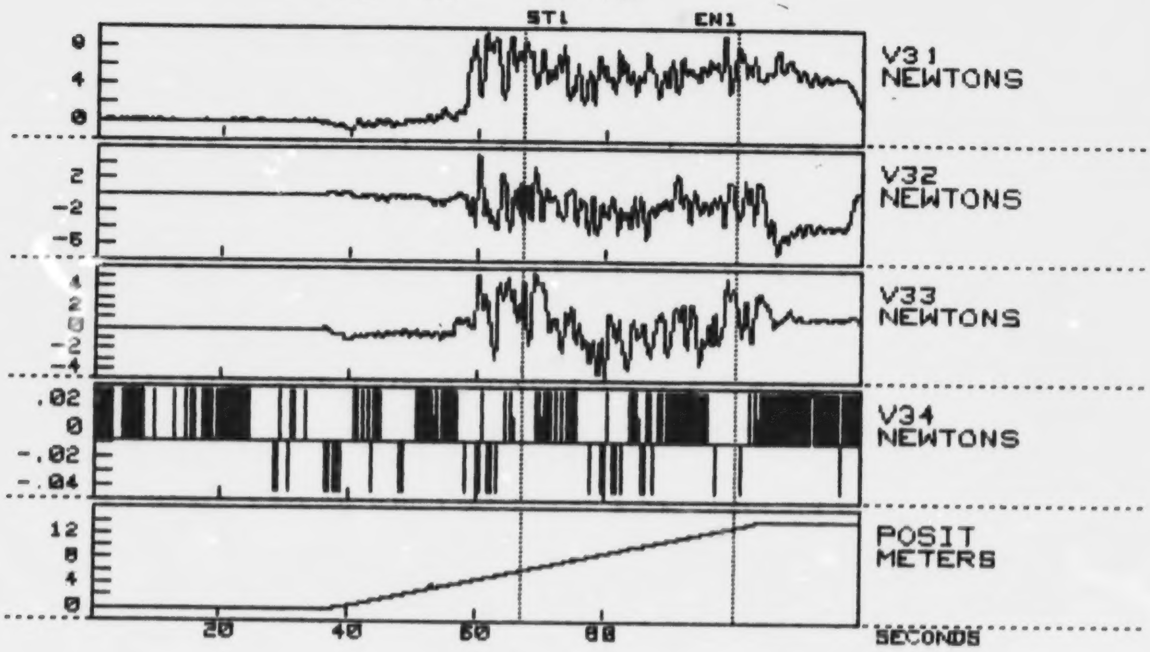

DATA DIGITIZED ON: 23 AUG 1983
DIGITIZING RATE: 32 Hz/CHANNEL
FILTER FREQUENCY: 1 HZ

### INTERVAL STATISTICS

INTERVAL 1 START: 66.96875 END: 100.40625

| CHANNEL | MINIMUM | MAXIMUM | MEAN VALUE | STAN. DEV. |
|---|---|---|---|---|
| V31 | 2.07 | 9.334 | 5.25 | 1.44 |
| V32 | -5.107 | 3.691 | -1.1 | 1.61 |
| V33 | -4.298 | 5.479 | .2242 | 2.13 |
| V34 | -.04257 | .027152 | -.0051396 | .012294 |
| POSIT | 6.247 | 13.26 | 9.757 | 2.04 |

SEGMENTED MODEL *** 566C
TEST 02 RUN E1

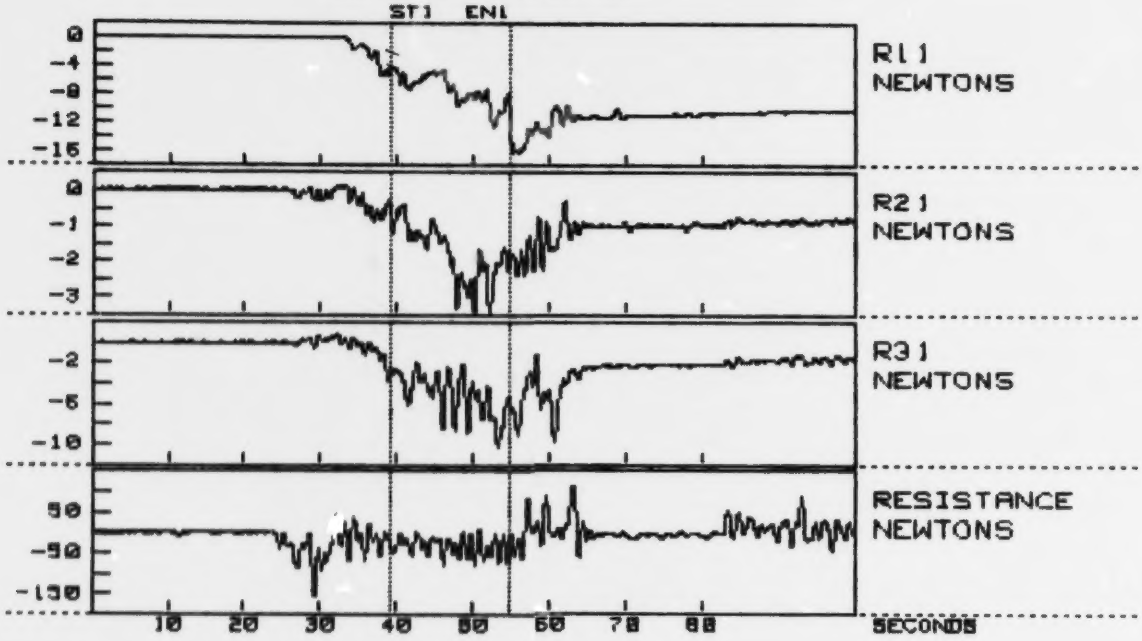

DATA DIGITIZED ON: 18 AUG 1983
DIGITIZING RATE: 32 Hz/CHANNEL
FILTER FREQUENCY: 1 HZ

INTERVAL STATISTICS

INTERVAL 1 START: 38.90625 END: 54.71875

| CHANNEL | MINIMUM | MAXIMUM | MEAN VALUE | STAN. DEV. |
|---|---|---|---|---|
| R11 | -12.89 | -4.165 | -7.34 | 2.13 |
| R21 | -3.407 | -.321 | -1.76 | .79 |
| R31 | -10.18 | -1.83 | -5.062 | 2.06 |
| RESISTANCE | -78.785 | 9.677 | -31.641 | 20.64 |

## SEGMENTED MODEL *** 566C
## TEST 02 RUN E1

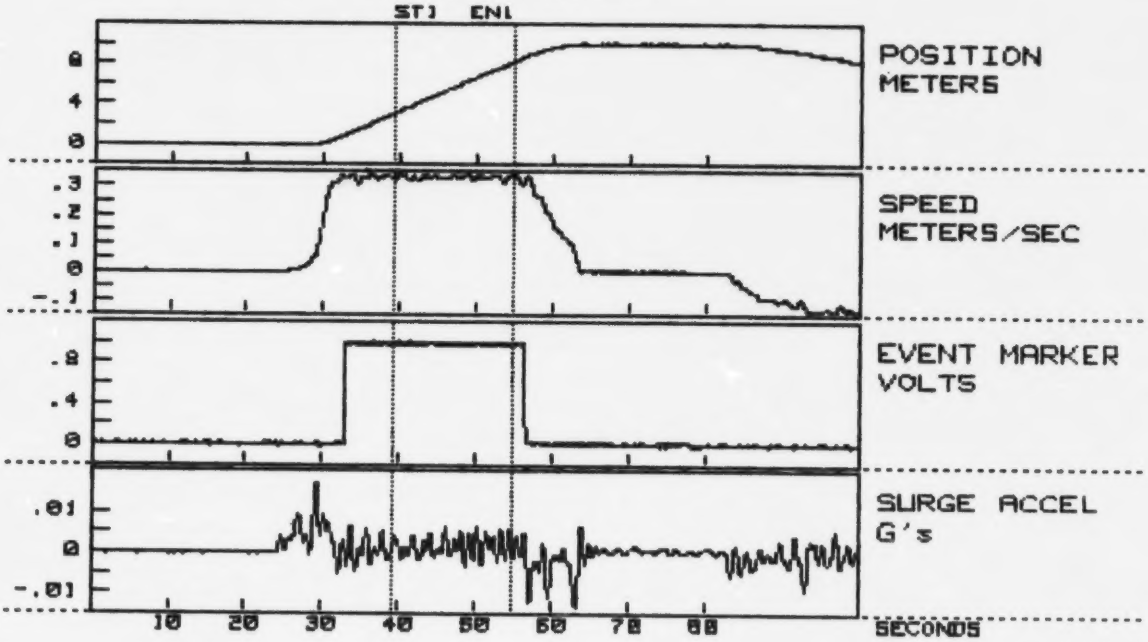

DATA DIGITIZED ON: 18 AUG 1983
DIGITIZING RATE: 32 Hz/CHANNEL
FILTER FREQUENCY: 1 HZ

### INTERVAL STATISTICS

INTERVAL 1 START: 38.90625 END: 54.71875

| CHANNEL | MINIMUM | MAXIMUM | MEAN VALUE | STAN. DEV. |
|---|---|---|---|---|
| POSITION | 3.05 | 8.228 | 5.637 | 1.51 |
| SPEED | .3115 | .343 | .331 | .0061234 |
| EVENT MARKER | .969 | 1 | .985 | .0059035 |
| SURGE ACCEL | -.0032195 | .0065462 | .0015786 | .00219571 |

SEGMENTED MODEL TESTS *** 566C
TEST 02 RUN F1

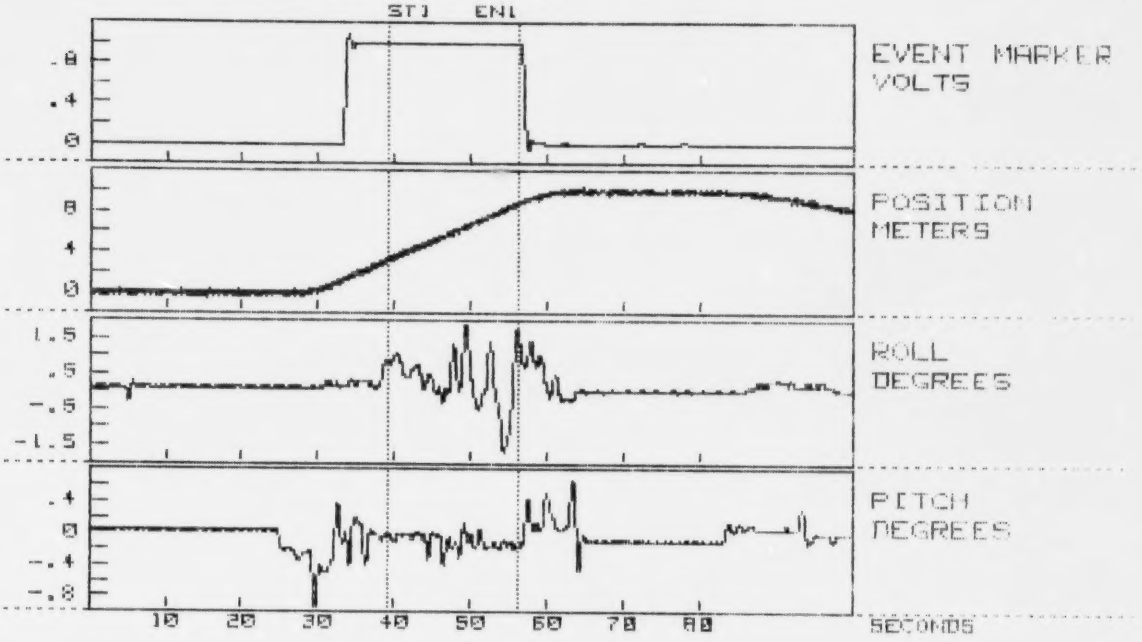

DATA DIGITIZED ON: 23 AUG 1983
DIGITIZING RATE: 32 Hz/CHANNEL
FILTER FREQUENCY: 1 HZ

## INTERVAL STATISTICS

INTERVAL 1 START: 38.9375 END: 56.25

| CHANNEL | MINIMUM | MAXIMUM | MEAN VALUE | STAN. DEV. |
|---|---|---|---|---|
| EVENT MARKER | .981 | .986 | .983 | .000967365 |
| POSITION | 2.99 | 8.963 | 5.994 | 1.66 |
| ROLL | -1.71 | 1.88 | .33 | .739 |
| PITCH | -.416 | .117 | -.1003 | .08889 |

SEGMENTED MODEL TESTS *** 566C
TEST 02 RUN F1

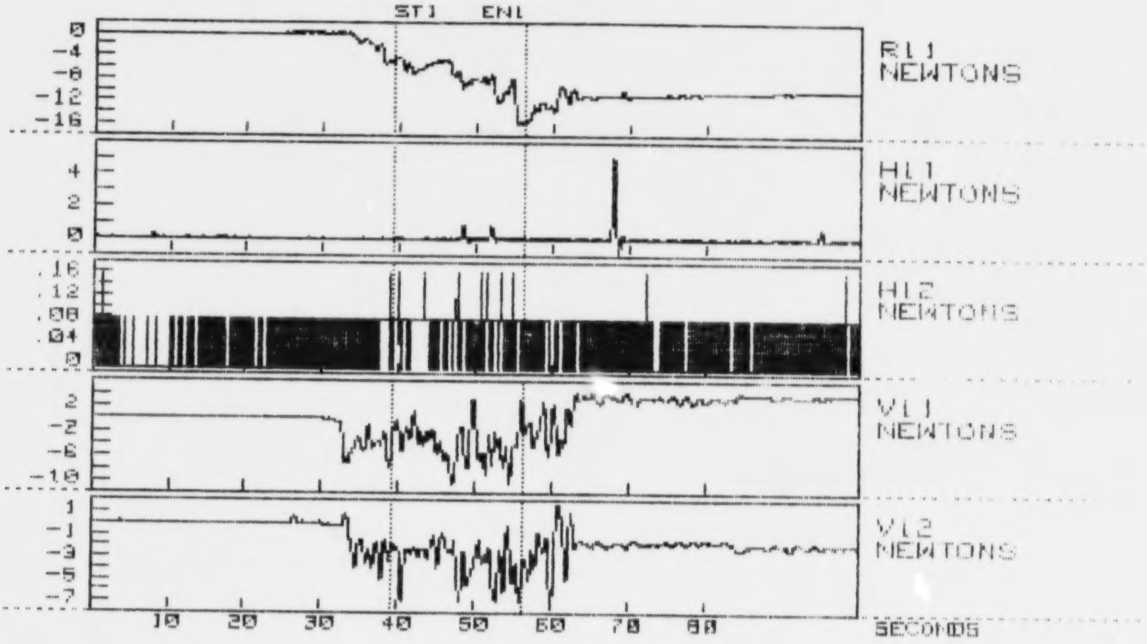

DATA DIGITIZED ON: 23 AUG 1983
DIGITIZING RATE: 32 Hz/CHANNEL
FILTER FREQUENCY: 1 HZ

INTERVAL STATISTICS

INTERVAL 1 START: 38.9375 END: 56.25

| CHANNEL | MINIMUM | MAXIMUM | MEAN VALUE | STAN. DEV. |
|---|---|---|---|---|
| R11 | -16.15 | -4.165 | -7.977 | 3.05 |
| H11 | -.2093 | .892 | .05086 | .1685 |
| H12 | -.0087996 | .1624 | .06631 | .031185 |
| V11 | -10.36 | 3.08 | -3.928 | 2.93 |
| V12 | -7.023 | -.35 | -3.31 | 1.57 |

SEGMENTED MODEL TESTS *** 56BC
TEST 02 RUN G1

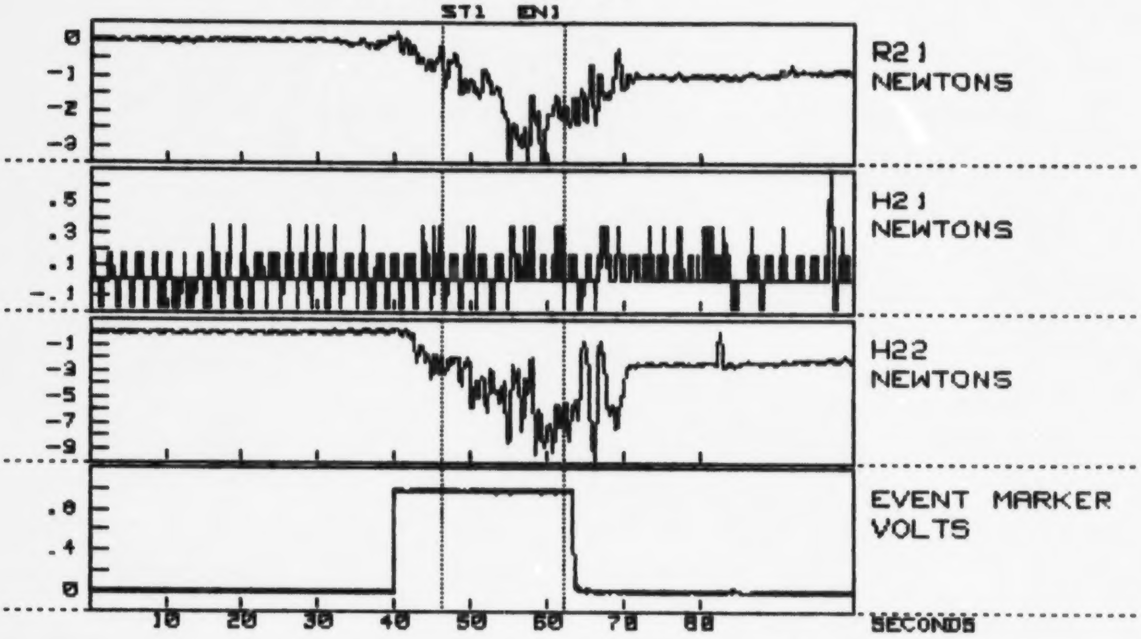

DATA DIGITIZED ON: 23 AUG 1983
DIGITIZING RATE: 32 Hz/CHANNEL
FILTER FREQUENCY: 1 HZ

INTERVAL STATISTICS

INTERVAL 1 START: 46.0625 END: 61.9375

| CHANNEL | MINIMUM | MAXIMUM | MEAN VALUE | STAN. DEV. |
|---|---|---|---|---|
| R21 | -3.421 | -.2577 | -1.78 | .79 |
| H21 | -.1699 | .349 | .05426 | .0964 |
| H22 | -9.287 | -1.86 | -4.703 | 2.06 |
| EVENT MARKER | .966 | 1 | .987 | .0060947 |

## SEGMENTED MODEL TESTS *** 566C
## TEST 02    RUN G1

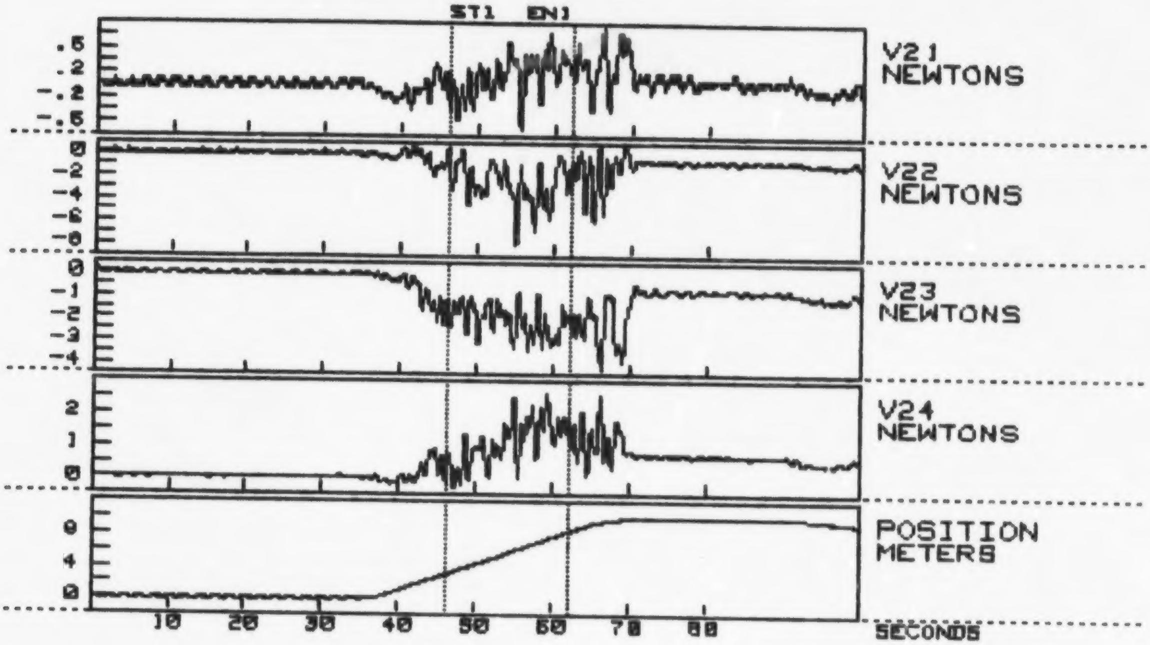

DATA DIGITIZED ON: 23 AUG 1983
DIGITIZING RATE: 32 Hz/CHANNEL
FILTER FREQUENCY: 1 HZ

### INTERVAL STATISTICS

INTERVAL 1    START: 46.0625    END: 61.9375

| CHANNEL | MINIMUM | MAXIMUM | MEAN VALUE | STAN. DEV. |
|---|---|---|---|---|
| V21 | -.707 | .842 | .1544 | .317 |
| V22 | -8.007 | .2779 | -2.59 | 1.69 |
| V23 | -3.427 | -.765 | -2.04 | .666 |
| V24 | -.3017 | 2.66 | 1.12 | .707 |
| POSITION | 3.07 | 8.247 | 5.66 | 1.52 |

SEGMENTED MODEL TESTS *** 566C
TEST 02 RUN H1

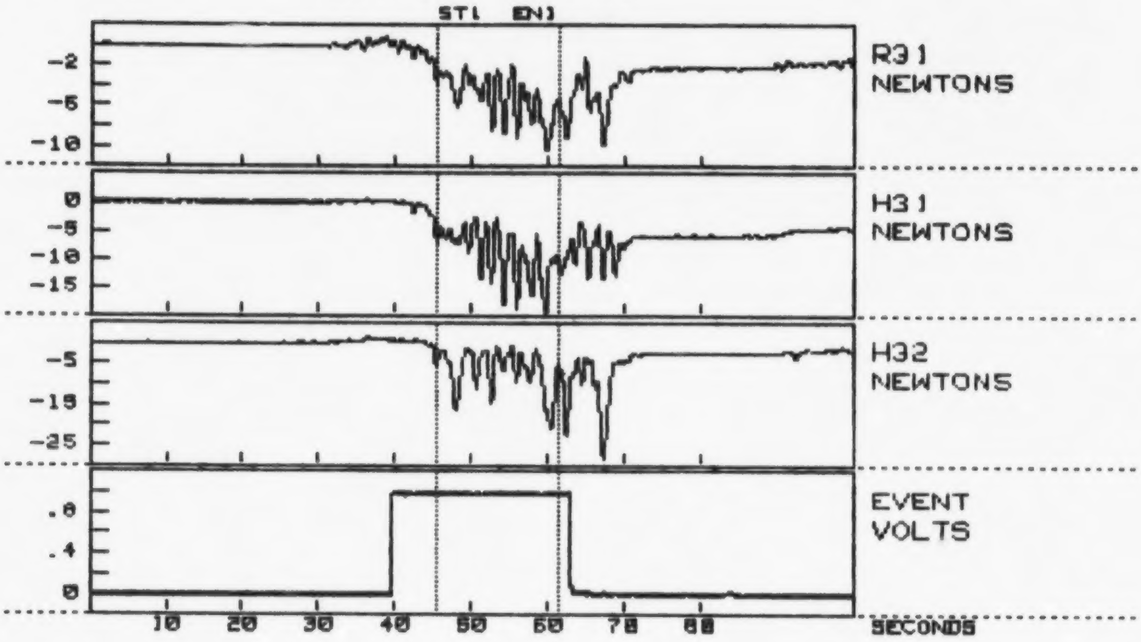

DATA DIGITIZED ON: 23 AUG 1983
DIGITIZING RATE: 32 Hz/CHANNEL
FILTER FREQUENCY: 1 HZ

INTERVAL STATISTICS

INTERVAL 1 START: 45.375 END: 61.21875

| CHANNEL | MINIMUM | MAXIMUM | MEAN VALUE | STAN. DEV. |
|---|---|---|---|---|
| R31 | -10.26 | -1.87 | -5.097 | 2.07 |
| H31 | -19.72 | -2.72 | -8.999 | 4.255 |
| H32 | -20.91 | -.744 | -6.559 | 5.034 |
| EVENT | .973 | 1.01 | .987 | .0058465 |

## SEGMENTED MODEL TESTS *** 566C
## TEST 02 RUN H1

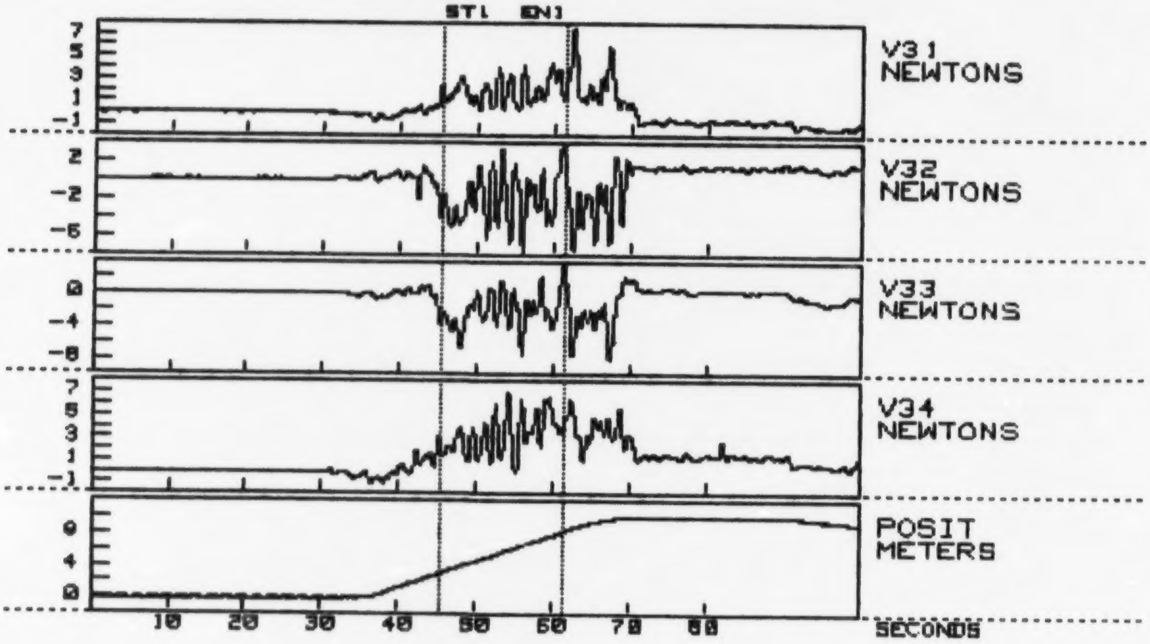

DATA DIGITIZED ON: 23 AUG 1983
DIGITIZING RATE: 32 Hz/CHANNEL
FILTER FREQUENCY: 1 HZ

### INTERVAL STATISTICS

INTERVAL 1 START: 45.375 END: 61.21875

| CHANNEL | MINIMUM | MAXIMUM | MEAN VALUE | STAN. DEV. |
|---|---|---|---|---|
| V31 | .1726 | 4.35 | 1.9 | 1.08 |
| V32 | -7.815 | 3.577 | -1.97 | 2.53 |
| V33 | -7.448 | 3.411 | -2.13 | 2.08 |
| V34 | -.05018 | 7.027 | 3.268 | 1.69 |
| POSIT | 3.03 | 8.205 | 5.615 | 1.51 |

!!

SEGMENTED MODEL *** 566C
TEST 02 RUN E2

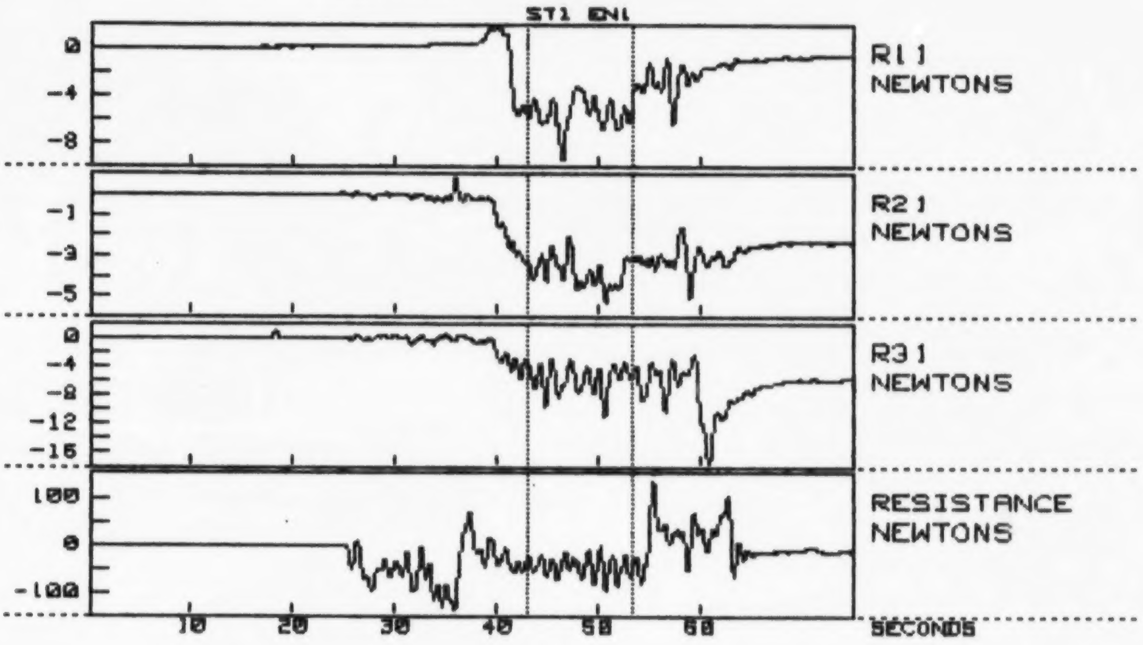

DATA DIGITIZED ON: 22 AUG 1983
DIGITIZING RATE: 32 Hz/CHANNEL
FILTER FREQUENCY: 1 HZ

INTERVAL STATISTICS

INTERVAL 1 START: 42.90625 END: 53.40625

| CHANNEL | MINIMUM | MAXIMUM | MEAN VALUE | STAN. DEV. |
|---|---|---|---|---|
| R11 | -9.406 | -3.11 | -5.384 | 1.27 |
| R21 | -5.282 | -2.12 | -3.78 | .678 |
| R31 | -10.74 | -2.93 | -5.633 | 1.71 |
| RESISTANCE | -94.163 | -1.35 | -44.519 | 19.18 |

SEGMENTED MODEL *** 566C
TEST 02 RUN E2

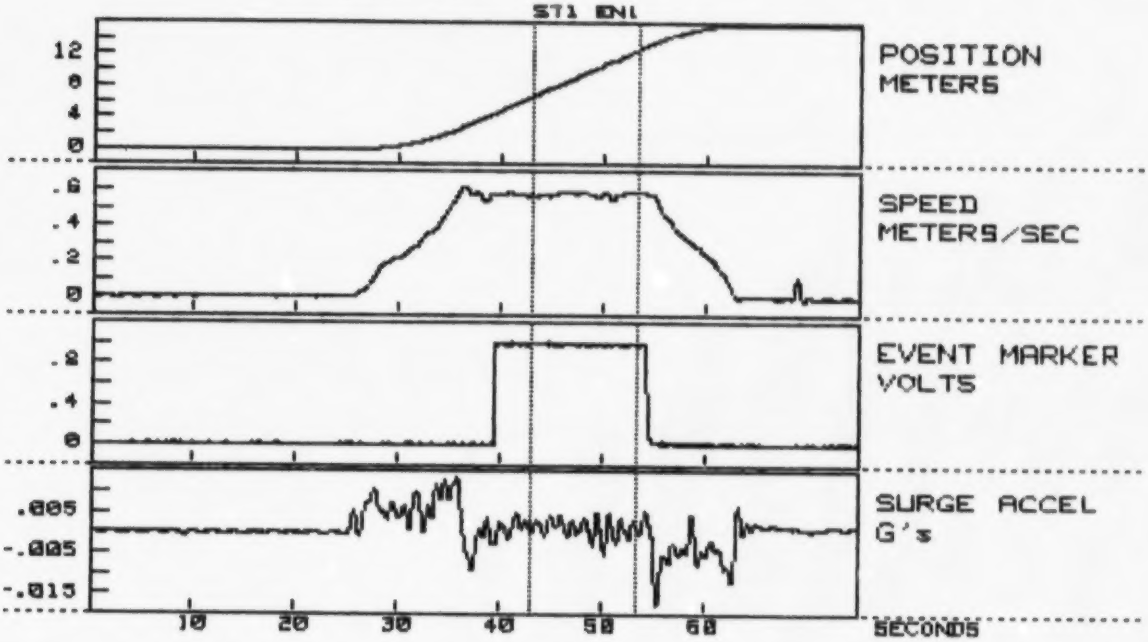

DATA DIGITIZED ON: 22 AUG 1983
DIGITIZING RATE: 32 Hz/CHANNEL
FILTER FREQUENCY: 1 HZ

INTERVAL STATISTICS

INTERVAL 1 START: 42.90625 END: 53.40625

| CHANNEL | MINIMUM | MAXIMUM | MEAN VALUE | STAN. DEV. |
|---|---|---|---|---|
| POSITION | 6.63 | 12.65 | 9.656 | 1.75 |
| SPEED | .543 | .591 | .576 | .010638 |
| EVENT MARKER | .972 | 1 | .987 | .0061895 |
| SURGE ACCEL | -.0052981 | .0049558 | .0011894 | .00208583 |

## G.1 Introduction

As discussed earlier in Appendix B, the dry calibration of segments have produced unexpected errors which warranted further investigation. During calibration the load was applied at some points and the expected reactions at the various load support points were calculated. The sums of the three principal components as measured were different from the calculated components indicating a deviation which may have been caused by unknown deficiencies in the physical model.

In order to examine such possibilities, a finite element model was built for Segment 2. The reason for selecting segment 2 was mainly that it produced the best response in terms of quantity and quality. The purpose of the model was two-fold:

a) To study the effect of elastic support points (pretension) on the reactions measured at load support points (load cells).

b) To investigate possible reasons for the observed deviation of the experimental measurements and provide a tool which can be used effectively to identify the sources of error and ways of correcting such errors.

## G.2 The Finite Element Model

Segment 2 was considered as a 3-D rigid body supported by a number of elastic supports in space. Figure G.1(a) is an isometric view of the segment and load cell positions as well as points of elastic support identified by S1 and S2. Figure G.1(b, c and d) are three projections of the hull lines of the PIERRE RADISSON showing both the outlines of segment 2 as well as the beam elements connecting the selected nodal points and forming an idealized rigid segment model.

It was only necessary for the finite element model to contain:

- ° nodes corresponding to the load cell, which were the reaction points.
- ° nodes corresponding to the points of load application on the hull.
- ° correct spring stiffness at the reaction points.

It was not necessary to model the results of the segment itself. The model, in fact, only contained the points of interest, and joined those points with very stiff beams.

## FIGURE G.1 FINITE ELEMENT MODEL GEOMETRY

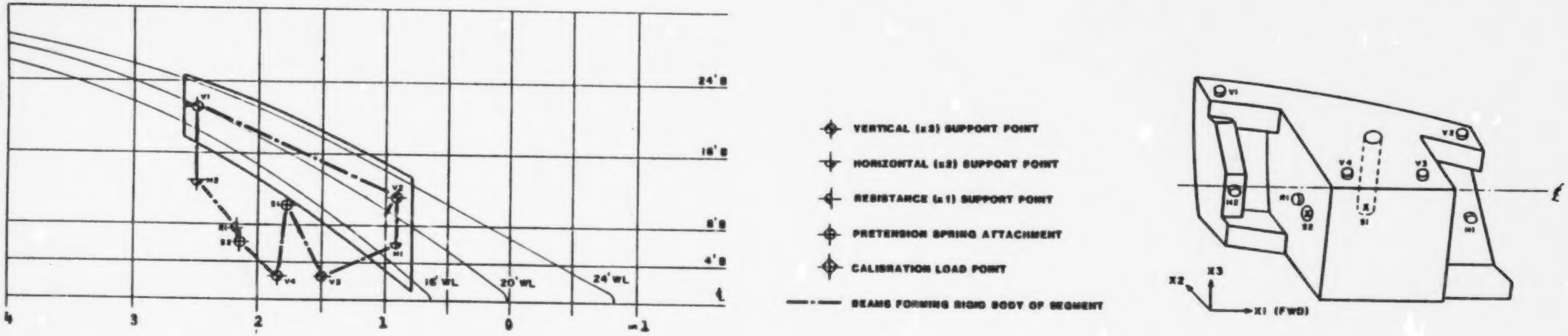
24'B
16'B
8'B
4'B
℄
16'WL
20'WL
24'WL
4
3
2
1
0
-1
V1
H2
R1
S2
S1
V4
V3
V2
H1
VERTICAL (x3) SUPPORT POINT
HORIZONTAL (x2) SUPPORT POINT
RESISTANCE (x1) SUPPORT POINT
PRETENSION SPRING ATTACHMENT
CALIBRATION LOAD POINT
BEAMS FORMING RIGID BODY OF SEGMENT
X2
X3
X1 (FWD)

(b) WATERLINES of THE RADISSON SHOWING THE OUTLINE of SEGMENT No. 2
LOADCELL POSITIONS SHOWN

(a) ISOMETRIC VIEW of LOADCELL POSITIONS on SEGMENT No. 2

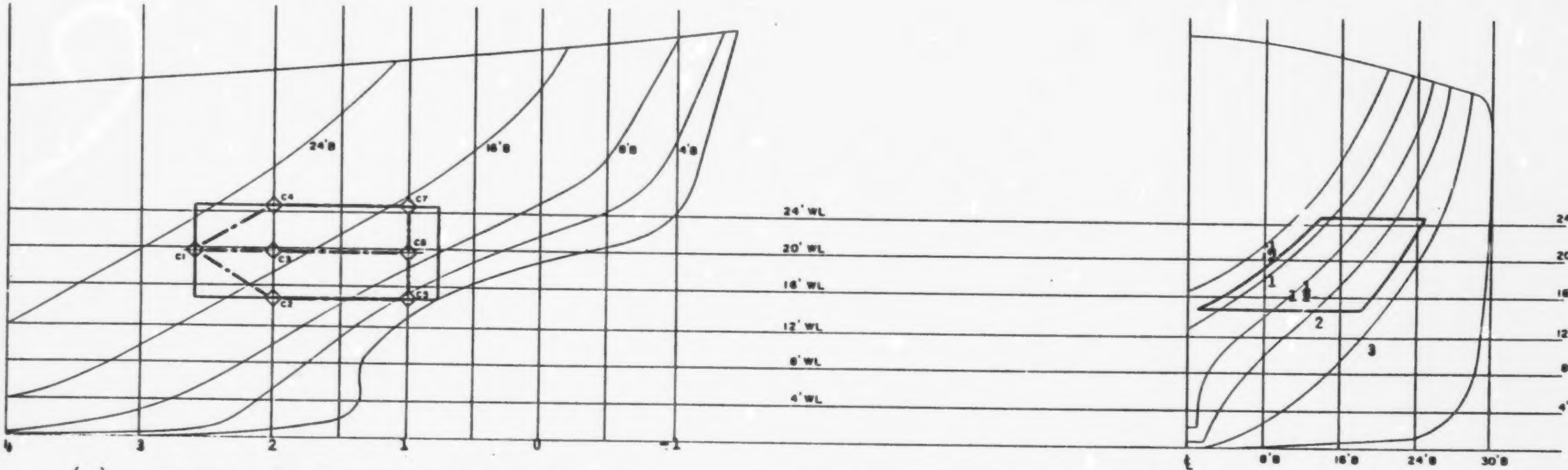
24'B
16'B
8'B
4'B
C1
C2
C3
C4
C5
C6
C7
24'WL
20'WL
16'WL
12'WL
8'WL
4'WL
4
3
2
1
0
-1
℄
8'B
16'B
24'B
30'B
1
2
3

(c) BUTTOCKS of RADISSON SHOWING THE OUTLINE OF SEGMENT No. 2
CALIBRATION LOADING POINTS SHOWN

(d) BODY PLAN of RADISSON SHOWING OUTLINE of SEGMENT No. 2

The stiffness of the load cells (spring supports) were determined by the stiffnesss of a plate with fixed edge. The circular dimensions of the load cell diaphragm were used in the equations to determine the stiffness of the cell:

For a circular plate -

$$K = \frac{W}{Y} = \frac{\text{load}}{\text{deflection}}$$

The deflection of the center due to a point load;

$$Y = \frac{-Wr^2}{16\pi D}$$

where $D = \frac{Et^3}{12(1-\nu^2)}$

therefore $K = \frac{-16\pi D}{r^2}$

There were two plate thicknesses:

$$t_1 = .001 \text{ m}$$
$$t_2 = .0007 \text{ m}$$

which resulted in two stiffnesses:

$$K_1 = 2.36 \times 10^7 \text{ N/m}$$
$$K_2 = 8.115 \times 10^6 \text{ N/m}$$

where:
$W$ = load (N)
$Y$ = deflection (m)
$r$ = radius of plate (m)
$E$ = Young's modulus ($=2.06 \times 10^{11}$ N/m$^2$)
$\nu$ = Poissons ratio (=.3)
$t$ = plate thickness (m)
$K$ = stiffness of plate (N/m)

With the model thus constructed, loads were applied to seven points on the shell at the same locations as in the physical calibration as shown in Figure A.1(c). The finite element results are by definition linear (i.e. if the load is doubled, all responses will be doubled, exactly). It is therefore only of interest to compare the results to the physical calibration at one load level.

Two finite element models were used. In the first model all support points were assumed to react only in the normal direction to the segment along their appropriate axis. This would represent the ideal simulation where no physical deficiencies exist. However, when the model was applied, the calculation algorithms were verified and it was clear that some physical inaccuracies were behind the observed experimental errors. This prompted the modification of the first model to examine possible sources of deviation.

In the second finite element model, a modification was introduced by assuming that the seats of the load cells were not perfectly normal. Thus, a lateral obstruction would be produced resulting in what may be termed wedging action. Proper scrutinization of the physical model indicated that support H2 had an off normal angle of approximately 11.5° in the vertical plane. This was incorporated into the modified model by including two additional stiffnesses:

$K_{12} = \cos 11.5° \times K_{22}$

$K_{11} = (\cos 11.5°) \times K_{22}$

where $K_{22}$ = spring constant of H2 load cell

## G.3 Results and Discussions

The results obtained from exercising the two finite element models for the seven calibration cases are given in Tables G.1 through G.7. The following observations may be made:

a) The response of the horizontal, vertical and resistance load cells in the finite element model is similar to calculated response.

b) The ratios of measured to finite element components are, therefore, similar to those reported in Appendix B for the same applied load.

c) While the finite element response is linear, the measured quantities are non-linearly variable with applied load.

d) The effect of defective seat as simulated in load cell position H2 brings the finite element predictions much closer to experimental measurements. The ratio of experimental to finite element resistance changed as follows:

|  |  |  |
|---|---|---|
| °First model:<br>(ideal) | average prediction<br>standard deviation | 0.543<br>0.214 (39.4% of mean) |
| °Second model:<br>(w/defect) | average prediction<br>standard deviation | 0.736<br>0.125 (17.0% of mean) |

This means that if the defect observed in the physical model is modelled properly in the finite element model, the latter becomes more capable of predicting experimental results (35.5% better) and explaining the observed scatter (reduced by 56.9%).

TABLE G.1

CALIBRATION: NO.1 SEGMENT: NO.2
STATION: 8.69 WATERLINE: 19.5 FT

DIRECTION COSINES

$\ell = .325 \quad m = .784 \quad n = .529$

Applied load (Normal) = 26.7 N

REACTION (N)

| LOAD CELL | MEASURED | 1ST FINITE ELEMENT MODEL | MODIFIED FINITE ELEMENT MODEL |
|---|---|---|---|
| R1 | 2.8 | 8.7 | 3.3 |
| H1 | -3.0 | -6.3 | -5.7 |
| H2 | 27.0 | 27.9 | 26.6 |
| V1 | -0.5 | -0.4 | -0.4 |
| V2 | -1.1 | -1.0 | -1.0 |
| V3 | 11.0 | 15.0 | 15.0 |
| V4 | 0.0 | 0.5 | 0.5 |
| | $\Sigma R_M/\Sigma R_{FE}$ | .32 | .85 |
| | $\Sigma H_M/\Sigma H_{FE}$ | 1.11 | 1.15 |
| | $\Sigma V_M/\Sigma V_{FE}$ | .66 | .66 |

## TABLE G.2

CALIBRATION: NO. 2 SEGMENT: NO.2
STATION: 9.0 WATERLINE: 14.9 FT

DIRECTION COSINES

$\ell = .385$ $m = .623$ $n = .680$

Applied load (Normal) = 26.7 N

| LOAD CELL | REACTION | | |
|---|---|---|---|
| | MEASURED | 1ST FINITE ELEMENT MODEL | MODIFIED FINITE ELEMENT MODEL |
| R1 | 5.4 | 10.3 | 7.6 |
| H1 | 3.3 | 2.5 | 3.1 |
| H2 | 15.4 | 14.2 | 13.5 |
| V1 | 4.1 | 5.8 | 5.8 |
| V2 | -2.9 | -3.2 | -3.2 |
| V3 | 6.4 | 8.0 | 8.0 |
| V4 | 6.4 | 7.6 | 7.6 |
| | $\Sigma R_M/\Sigma R_{FE}$ | .52 | .71 |
| | $\Sigma H_M/\Sigma H_{FE}$ | 1.12 | 1.13 |
| | $\Sigma V_M/\Sigma V_{FE}$ | .77 | .77 |

## TABLE G.3

CALIBRATION: NO. 3 SEGMENT: NO.2
STATION: 9.0 WATERLINE: 19.5 FT

DIRECTION COSINES

$\ell = .361$ $m = .623$ $n = .624$

Applied load (Normal) = 26.7 N

| | REACTION | | |
|---|---|---|---|
| LOAD CELL | MEASURED | 1ST FINITE ELEMENT MODEL | MODIFIED FINITE ELEMENT MODEL |
| R1 | 3.2 | 9.6 | 6.3 |
| H1 | 4.5 | 1.2 | 2.0 |
| H2 | 17.2 | 17.3 | 16.5 |
| V1 | 0.4 | .2 | .2 |
| V2 | 4.9 | 4.9 | 4.9 |
| V3 | 8.6 | 11.4 | 11.4 |
| V4 | -.6 | .2 | .2 |
| | $\Sigma R_M/\Sigma R_{FE}$ | .33 | .51 |
| | $\Sigma H_M/\Sigma H_{FE}$ | 1.18 | 1.18 |
| | $\Sigma V_M/\Sigma V_{FE}$ | .80 | .80 |

## TABLE G.4

CALIBRATION: NO. 4 SEGMENT: NO. 2
STATION: 9.0 WATERLINE: 24.8 FT

DIRECTION COSINES

$\ell = .336$ $m = .807$ $n = .485$

Applied load (Normal) = 26.7 N

| LOAD CELL | REACTION (N) | | |
|---|---|---|---|
| | MEASURED | 1ST FINITE ELEMENT MODEL | MODIFIED FINITE ELEMENT MODEL |
| R1 | 3.6 | 8.9 | 5.0 |
| H1 | 2.7 | .9 | 1.9 |
| H2 | 19.6 | 20.7 | 19.7 |
| V1 | -3.3 | -5.5 | -5.5 |
| V2 | 10.5 | 12.3 | 12.3 |
| V3 | 10.8 | 13.3 | 13.3 |
| V4 | -7.0 | -7.2 | -7.2 |

| | 1ST FINITE ELEMENT MODEL | MODIFIED FINITE ELEMENT MODEL |
|---|---|---|
| $\Sigma R_M/\Sigma R_{FE}$ | .40 | .72 |
| $\Sigma H_M/\Sigma H_{FE}$ | 1.03 | 1.03 |
| $\Sigma V_M/\Sigma V_{FE}$ | .85 | .85 |

## TABLE G.5

CALIBRATION: NO.5 SEGMENT: NO.2
STATION: 9.5 WATERLINE: 14.9 FT

DIRECTION COSINES

$\ell$ = .379 m = .490 n = .785

Applied load (Normal) = 26.7 N

| LOAD CELL | REACTION (N) | | |
|---|---|---|---|
| | MEASURED | 1ST FINITE ELEMENT MODEL | MODIFIED FINITE ELEMENT MODEL |
| R1 | 9.0 | 10.1 | 10.3 |
| H1 | 16.6 | 14.1 | 14.1 |
| H2 | -1.9 | -1.1 | -1.0 |
| V1 | 9.3 | 9.8 | 9.8 |
| V2 | 5.0 | 7.6 | 7.6 |
| V3 | -6.2 | -5.9 | -5.9 |
| V4 | 8.0 | 9.4 | 9.4 |

| | | |
|---|---|---|
| $\Sigma R_M/\Sigma R_{FE}$ | .89 | .87 |
| $\Sigma H_M/\Sigma H_{FE}$ | 1.13 | 1.12 |
| $\Sigma V_M/\Sigma V_{FE}$ | .77 | .77 |

## TABLE G.6

CALIBRATION: NO.6 SEGMENT: NO.2
STATION: 9.5 WATERLINE: 19.5 FT

DIRECTION COSINES

$\ell$ =.365 m = .573 n = .73

Applied load (Normal) = 26.7 N

| | REACTION (N) | | |
|---|---|---|---|
| LOAD CELL | MEASURED | 1ST FINITE ELEMENT MODEL | MODIFIED FINITE ELEMENT MODEL |
| R1 | 7.2 | 9.8 | 8.8 |
| H1 | 17.2 | 10.3 | 10.5 |
| H2 | 1.8 | 5.0 | 4.7 |
| V1 | 3.3 | 2.0 | 2.0 |
| V2 | 12.7 | 13.8 | 13.8 |
| V3 | 0.0 | 2.9 | 2.9 |
| V4 | 0.2 | 0.9 | 0.9 |
| | $\Sigma R_M/\Sigma R_{FE}$ | .73 | .82 |
| | $\Sigma H_M/\Sigma H_{FE}$ | 1.24 | 1.25 |
| | $\Sigma V_M/\Sigma V_{FE}$ | .82 | .82 |

## TABLE G.7

CALIBRATION: NO.7 SEGMENT: NO.2
STATION: 9.5 WATERLINE: 24.8 FT

DIRECTION COSINES

$\ell = .355$ $m = .711$ $n = .607$

Applied load (Normal) = 26.7 N

| | REACTION (N) | | |
|---|---|---|---|
| LOAD CELL | MEASURED | 1ST FINITE ELEMENT MODEL | MODIFIED FINITE ELEMENT MODEL |
| R1 | 5.8 | 9.5 | 8.6 |
| H1 | 17.3 | 14.4 | 14.5 |
| H2 | 3.2 | 4.6 | 4.4 |
| V1 | -2.2 | -4.4 | -4.4 |
| V2 | 18.4 | 23.2 | 23.2 |
| V3 | 3.8 | 5.2 | 5.2 |
| V4 | -6.6 | -7.7 | -7.7 |
| | $\Sigma R_M/\Sigma R_{FE}$ | .61 | .67 |
| | $\Sigma H_M/\Sigma H_{FE}$ | 1.08 | 1.08 |
| | $\Sigma V_M/\Sigma V_{FE}$ | .82 | .82 |

e) The largest scatter in experimental results is associated with the resistance direction of measurement. Comparison with other directions is made below:

| | Average | Std. deviation | % of mean |
|---|---|---|---|
| R | 0.543 | 0.214 | 39.4% |
| H | 1.127 | 0.068 | 6.0% |
| V | 0.784 | 0.062 | 7.9% |

This corroborates our earlier conclusion (Appendix B) that the horizontal measurements were the most consistent and closest to what was expected.

FEB 1995
Canada

f) The trend of response in the modified finite element model is such that all deviations observed in the experimental measurements may be explained by a set of modelled defects in the physical model. This points out to the need for upgrading the load support points squareness using proper metrological instruments.

g) Two possible ways exist for correcting the existing database. The first is by applying segment correction factors to the measured loads to increase or decrease such to the appropriate levels. Such correction factors will be obtained as an overall average for the segment from measurements. The second method would be to first define the proximity of the load point and approximate value of the load then correct the measured value according to experimental measurements reported in Appendix B.

## G.4 Conclusions

In conclusion, the work conducted and reported in this appendix confirmed that the experimental results of segment calibration can be explained. The finite element results demonstrate that the presence of some physical deficiencies, which may not be evident at first, can cause large departures and high scatter of measurements. The elimination of such deficiencies will improve the physical model as may be expected, and the experimental response will then resemble the ideal solution obtained by the first finite element model.

There are a number of points which were not dealt with in this analysis and may be included in future work. Such points include the effect of high pretension of the segments, additional pretension wires, misalignment and frictional effects. In the present study the pretension did not appear to influence the predicted load levels.

It should be borne in mind, however, that the present experimental results reported in Appendix B are subject to experimental error which can significantly be reduced if a proper calibration rig is built to conduct in-water calibration runs.